ISSN 0021-9673

VOL. 671 NOS. 1 + 2 JUNE 10, 1994
COMPLETE IN ONE ISSUE

Int. Ion Chromatography Symp. 1993
Baltimore, MD, September 12–15, 1993

JOURNAL OF CHROMATOGRAPHY A

INCLUDING ELECTROPHORESIS AND OTHER SEPARATION METHODS

SYMPOSIUM VOLUMES

ELSEVIER

JOURNAL OF CHROMATOGRAPHY A

INCLUDING ELECTROPHORESIS AND OTHER SEPARATION METHODS

Scope. The *Journal of Chromatography A* publishes papers on all aspects of **chromatography, electrophoresis** and related methods. Contributions consist mainly of research papers dealing with chromatographic theory, instrumental developments and their applications. In the *Symposium volumes*, which are under separate editorship, proceedings of symposia on chromatography, electrophoresis and related methods are published. *Journal of Chromatography B: Biomedical Applications* —This journal, which is under separate editorship, deals with the following aspects: developments in and applications of chromatographic and electrophoretic techniques related to clinical diagnosis or alterations during medical treatment; screening and profiling of body fluids or tissues related to the analysis of active substances and to metabolic disorders; drug level monitoring and pharmacokinetic studies; clinical toxicology; forensic medicine; veterinary medicine; occupational medicine; results from basic medical research with direct consequences in clinical practice.

Submission of Papers. The preferred medium of submission is on disk with accompanying manuscript (see *Electronic manuscripts* in the Instructions to Authors, which can be obtained from the publisher, Elsevier Science B.V., P.O. Box 330, 1000 AH Amsterdam, Netherlands). Manuscripts (in English; *four* copies are required) should be submitted to: Editorial Office of *Journal of Chromatography A*, P.O. Box 681, 1000 AR Amsterdam, Netherlands, Telefax (+31-20) 5862 304, or to: The Editor of *Journal of Chromatography B: Biomedical Applications*, P.O. Box 681, 1000 AR Amsterdam, Netherlands. Review articles are invited or proposed in writing to the Editors who welcome suggestions for subjects. An outline of the proposed review should first be forwarded to the Editors for preliminary discussion prior to preparation. Submission of an article is understood to imply that the article is original and unpublished and is not being considered for publication elsewhere. For copyright regulations, see below.

Publication information. *Journal of Chromatography A* (ISSN 0021-9673): for 1994 Vols. 652–682 are scheduled for publication. *Journal of Chromatography B: Biomedical Applications* (ISSN 0378-4347): for 1994 Vols. 652–662 are scheduled for publication. Subscription prices for *Journal of Chromatography A*, *Journal of Chromatography B: Biomedical Applications* or a combined subscription are available upon request from the publisher. Subscriptions are accepted on a prepaid basis only and are entered on a calendar year basis. Issues are sent by surface mail except to the following countries where air delivery via SAL is ensured: Argentina, Australia, Brazil, Canada, China, Hong Kong, India, Israel, Japan, Malaysia, Mexico, New Zealand, Pakistan, Singapore, South Africa, South Korea, Taiwan, Thailand, USA. For all other countries airmail rates are available upon request. Claims for missing issues must be made within six months of our publication (mailing) date. Please address all your requests regarding orders and subscription queries to: Elsevier Science B.V., Journal Department, P.O. Box 211, 1000 AE Amsterdam, Netherlands. Tel.: (+31-20) 5803 642; Fax: (+31-20) 5803 598. Customers in the USA and Canada wishing information on this and other Elsevier journals, please contact Journal Information Center, Elsevier Science Inc., 655 Avenue of the Americas, New York, NY 10010, USA, Tel. (+1-212) 633 3750, Telefax (+1-212) 633 3764.

Abstracts/Contents Lists published in Analytical Abstracts, Biochemical Abstracts, Biological Abstracts, Chemical Abstracts, Chemical Titles, Chromatography Abstracts, Current Awareness in Biological Sciences (CABS), Current Contents/Life Sciences, Current Contents/Physical, Chemical & Earth Sciences, Deep-Sea Research/Part B: Oceanographic Literature Review, Excerpta Medica, Index Medicus, Mass Spectrometry Bulletin, PASCAL-CNRS, Referativnyi Zhurnal, Research Alert and Science Citation Index.

US Mailing Notice. *Journal of Chromatography A* (ISSN 0021-9673) is published weekly (total 52 issues) by Elsevier Science B.V., (Sara Burgerhartstraat 25, P.O. Box 211, 1000 AE Amsterdam, Netherlands). Annual subscription price in the USA US$ 4994.00 (US$ price valid in North, Central and South America only) including air speed delivery. Second class postage paid at Jamaica, NY 11431. **USA POSTMASTERS**: Send address changes to *Journal of Chromatography A*, Publications Expediting, Inc., 200 Meacham Avenue, Elmont, NY 11003. Airfreight and mailing in the USA by Publications Expediting.

See inside back cover for Publication Schedule, Information for Authors and information on Advertisements.

0021-9673/94/$07.00

Printed in the Netherlands

For Contents see p. VII.

Membrane-based Sample Prep Device for Ion Analysis

Alltech's Novo-Clean™ IC Disk

- Solid-Phase Membrane Eliminates IC and CE Matrix Interferences
- Impregnated PTFE Membrane Eliminates Bed Channeling
- High Cross-Sectional Area Increases Extraction Speed

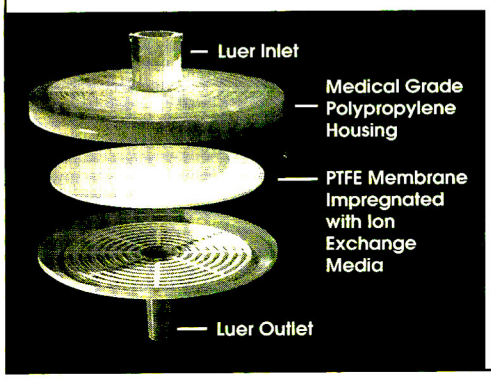

Anions in Battery Electrolyte (KOH)

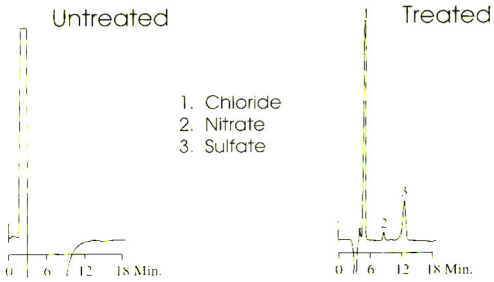

Request Bulletin #289 for More Information ☐

Suppressor-Based and SCIC in One Convenient System

Alltech's Universal Ion Chromatograph!

- Analyze Anions, Cations, Organic Acids, Metals and More!
- Compatible with all IC Methods - No More Compromises
- Modular Design for Maximum Flexibility

EPA Method 300.0 with Suppressor-based IC

- Meets EPA Method 300.0 Requirements
- SPCS™* Eliminates Regeneration

1. Fluoride
2. Chloride
3. Nitrite
4. Bromide
5. Nitrate
6. Phosphate
7. Sulfate

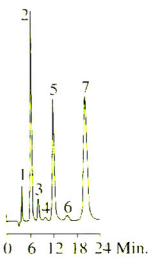

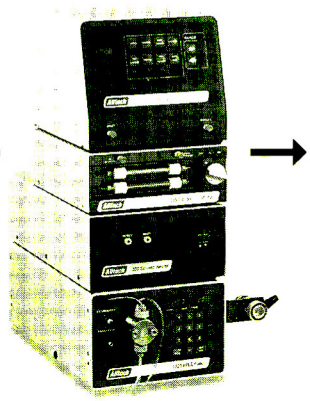

SCIC is the Best Method for Analyzing Cations

- Low ppb Detection Limits
- Simple, Less Expensive to Operate

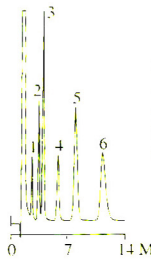

1. Lithium
2. Sodium
3. Ammonium
4. Potassium
5. Magnesium
6. Calcium

*Solid-Phase Chemical Suppressor

Request Bulletin #277 for More Information ☐

FAX THIS PAGE!

To receive information on the products mentioned on this page, please check the appropriate boxes and fax to: Alltech (USA) 1-708-948-1078

☐ **Please Send me Alltech's General Chromatography Catalog**

☐ **Please Add My Name to the Alltech Mailing List**

Name		
Title		
Company		
Address		
City	**State**	**Zip**
Country	**Phone**	

Please Indicate Your Areas of Interest:

☐ GC[05] ☐ LC[03] ☐ IC[07] ☐ TLC[04] ☐ Sample Prep[04]

Alltech

In the USA
Alltech Associates, Inc.•2051 Waukegn Rd.
Deerfield, IL 60015•Tel: 708-948-8600

In Europe
Alltech Associates, Inc.•Provinciebaan 144
9270 Laarne Belgium•Tel: 091-66 03 00

Announcing...

International Ion Chromatography Symposium 1994

19-22 September , 1994
Turin, Italy

Program Chairman:
Corrado Sarzanini
Analytical Chemistry
University of Turin
Via Giuria 5
I - 10125 Turin, Italy
Telephone: +39-11-670-7628
Fax: +39-11-670-7615

Session Topics

- Separation Selectivity and Column Technology
- Developments in Separation Methodology
- Advances in Detection
- Special Sample Treatment Procedures
- Novel Applications
- Process Monitoring and Control
- Separation of Metal Ions
- Pharmaceutical Applications
- Environmental Applications
- Ion analysis in the Electrical Generating Industry
- Standard Methods and Data Processing

For more information, contact:

Century International, Inc.
P.O.Box 493 • 25 Lee Road
Medfield, MA 02052-0493 USA
508/359-8777 • 508/359-8778 (FAX)

JOURNAL OF CHROMATOGRAPHY A

VOL. 671 (1994)

JOURNAL OF CHROMATOGRAPHY A

INCLUDING ELECTROPHORESIS AND OTHER SEPARATION METHODS

SYMPOSIUM VOLUMES

ELSEVIER

AMSTERDAM — LAUSANNE — NEW YORK — OXFORD — SHANNON — TOKYO

J. Chromatogr. A, Vol. 671 (1994)

0021-9673/94/$07.00

SYMPOSIUM VOLUME

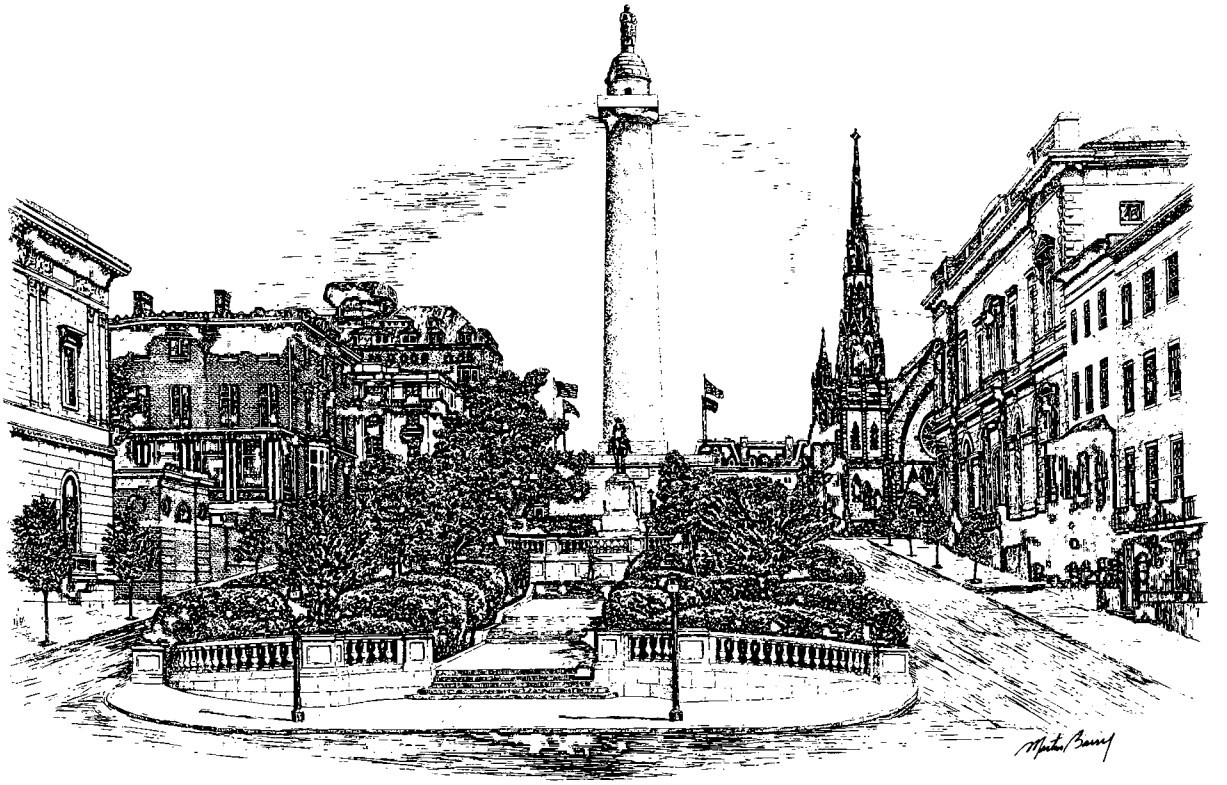

INTERNATIONAL ION CHROMATOGRAPHY SYMPOSIUM 1993

Baltimore, MD (USA), September 12–15, 1993

Guest Editor

R.M. CASSIDY

(Saskatoon, Canada)

VOL. 671, NOS. 1 + 2 JOURNAL OF CHROMATOGRAPHY A JUNE 10, 1994

CONTENTS

Miscellaneous applications

CAPILLARY ELECTROPHORESIS

ELSEVIER

Journal of Chromatography A, 671 (1994) 1

JOURNAL OF CHROMATOGRAPHY A

Foreword

The *6th International Ion Chromatography Symposium* was held at the Inner Harbour in Baltimore, MD, September 12–15, 1993. Over 230 scientists from 21 countries participated in the meeting, which featured special symposia on pharmaceutical applications, process monitoring and control, carbohydrate separations, forensic applications, and ion analysis in the electrical generating industry. Several other topics were also addressed, and interaction between participants was encouraged via the introduction of workshop/discussion sessions and evening poster/social sessions. A highlight of the meeting was the opening plenary address by Dan Lee, who was the 1993 recipient of the Ion Chromatography Achievement Award, an award given annually to a person who has made significant contributions to the field of ion chromatography (IC). In his award address Dan outlined his past work in the development of polymers for IC applications. This presentation was followed by a plenary lecture by Chris Pohl, who outlined the experimental and theoretical factors that must be considered in the design of new stationary phases for IC.

An important trend at these IC meetings has been the significant increase in the number of papers dealing with the development and application of capillary electrophoresis (CE). In just three years the CE content of this meeting has increased from 0 to over 30%, and most of the CE papers have dealt with analytical problems that would previously have been considered to be areas for IC. The Scientific Committee will monitor this development, but the focus of the meeting will remain the separation and determination of species that have been traditionally separated by IC methods.

The success of this meeting was to a large extent due to the cooperation from all commercial equipment manufacturers who contributed high-quality scientific papers where emphasis was placed on new approaches and procedures rather than on new commercial equipment. In addition, the financial and organizational support from Dionex Corporation and the Waters Chromatography Division of Millipore is gratefully acknowledged. Recognition must also be made of the contributions of the Scientific Committee (Wolfgang Buchberger, James Fritz, Douglas Gjerde, Paul Haddad, William Jones, John Lamb, Donald Pietrzyk, Corrado Sarzanini, Gabriella Schmuckler, Hamish Small and John Stillian) and the Organizing Committee (Betsy Baer, Mike Bedford, Rosemary Gaffney, Kelly Hargadon, Robert Kelly, Jay Nair, and Costas Stathakis). Specific thanks must also be given to Costas Stathakis, who organized the workshop sessions, and to Janet Strimaitis of Century International for her excellent organizational skills.

The Chair of the 1994 meeting, Professor Corrado Sarzanini, at the University of Turin, has organized an exciting program for the next meeting, September 19–22, 1994. This meeting will be held in the new Incontra Congress Centre, Turin, Italy, and we look forward to seeing you there.

Saskatoon, Canada R.M. Cassidy

SSDI 0021-9673(94)00240-A

ELSEVIER

Journal of Chromatography A, 671 (1994) 3–9

JOURNAL OF CHROMATOGRAPHY A

Factors affecting retention of basic solutes in ion-exclusion chromatography using an anion-exchange column

Paul R. Haddad*[,a], Fuping Hao[a], Bronislaw K. Glod[b]

[a]*Department of Chemistry, University of Tasmania, GPO Box 252C, Hobart, Tasmania 7001, Australia*
[b]*Institute of Physical Chemistry, Polish Academy of Sciences, Kasprzaka 44/52, 01-224 Warsaw, Poland*

Abstract

Retention volumes have been measured for a variety of inorganic and organic (both aliphatic and aromatic) bases on a quaternary ammonium functionalized styrene–divinylbenzene stationary phase using dilute sodium hydroxide as eluent. The retention behaviour of the inorganic bases and some of the aliphatic bases could be explained on the basis of ion-exclusion effects alone, with strong bases (which are cationic at the eluent pH) being co-eluted at the column void volume and very weak bases (which are neutral at the eluent pH) being co-eluted at the sum of the column void and inner volumes. Solutes intermediate between these extremes were eluted in order of increasing pK_{b1} and their retention could be varied by changing the eluent pH. A mixed retention mechanism involving hydrophobic adsorption and steric effects was observed for other aliphatic amines. Aromatic amines were found to be retained almost solely by a reversed-phase mechanism involving interaction of the solute with the unfunctionalized regions of the stationary phase. For such solutes, retention could be manipulated most easily by addition of acetonitrile to the eluent.

1. Introduction

Ion-exclusion chromatography, first introduced by Wheaton and Bauman in 1953 [1], has been used predominantly for the separation of organic acids and some inorganic weak acid anions using a sulphonate-type cation-exchange stationary phase (usually in the hydrogen form) with an eluent comprising a dilute solution of a mineral acid. Several studies [2–7] have been devoted to the elucidation of the mechanism of ion-exclusion chromatography under these conditions. Tanaka *et al.* [3] found that the retention volume of an acidic solute was dependent primarily on the first acid dissociation constant (pK_{a1}) of the solute. They showed that the dependence between the sample retention volume and its pK_{a1} value could be explained, at least to a first approximation, by the magnitude of the charge on the solute. That is, all solutes which were fully ionized at the eluent pH were unretained by virtue of their repulsion by the anionic functional groups of the stationary phase and were eluted at the column void volume. On the other hand, solutes which were neutral were all co-eluted at a retention volume equal to the sum of the void and inner volumes of the column since they are able to partition freely between the eluent and the inner volume (that is, the occluded liquid trapped within the pores of the stationary phase). Solutes having intermediate charge exhibited retention volumes which fell between the above extremes.

This behaviour considers only the effects of

* Corresponding author.

0021-9673/94/$07.00
SSDI 0021-9673(93)E0073-4

solute charge and has been described quantitatively by Glod and co-workers [4,5]. Further studies [2,4,6,7] have identified other factors which can influence the solute retention, including hydrophobic adsorption of the solute on the underivatized regions of the stationary phase resin and a size-exclusion effect which mediates the ability of the solute to penetrate the pores of the stationary phase. The magnitude of the effects of these factors depends on such solute parameters as the length of the molecular chain, molecular mass, solubility in water, etc. A comprehensive review of these effects may be found elsewhere [2]. The existence of these factors results in significant departures from the retention behaviour predicted on the basis of solute charge alone. For example, some neutral solutes show retention volumes which are much greater than expected due to the additional retention caused by hydrophobic adsorption.

Ion-exclusion chromatography may also be used for the separation of basic compounds using a quaternary ammonium anion-exchange resin and an alkaline eluent [8]. In this case, a dependence between the retention volume and the pK_{b1} value of the solute would be anticipated, along similar lines to those observed for acidic solutes. To our knowledge, no detailed study of the retention behaviour of basic solutes has been reported and the aim of the present paper has been to examine the factors contributing to the retention of such solutes. These factors included solute characteristics such as the pK_{b1} value, length of aliphatic chain, presence of aromatic groups, and degree of substitution, together with eluent characteristics such as concentration, pH, and presence of organic modifiers.

2. Experimental

2.1. Instrumentation

The chromatographic instrumentation comprised a Millipore–Waters (Milford, MA, USA) Model 510 chromatographic pump, Model U6K universal injection valve, Model 430 conductivity detector and Model TCM temperature-control module. A Shimadzu (Kyoto, Japan) model SPD-6AV UV–Vis photoabsorbance detector was also used in tandem with the conductivity detector and was operated at either 214 nm (for aliphatic amines) or 254 nm (for aromatic amines). The ion-exclusion column used was a Bio-Rad (Richmond, CA, USA) Model HPX-72-O, 300 × 7.8 mm I.D., packed with 11-μm particles of polystyrene–divinylbenzene co-polymer (8% cross-linking) derivatized with quaternary ammonium groups. Chromatograms were recorded using a Goerz–Metrawatt (Vienna, Austria) SE-120 dual-pen chart recorder.

2.2. Reagents

The mobile phase comprised water with varying concentrations of analytical reagent-grade sodium hydroxide (BDH, Port Fairy, UK) and HPLC-grade acetonitrile (Millipore–Waters). The aliphatic amines were obtained from Sigma (St. Louis, MO, USA) and aromatic amines, pyridines and inorganic bases were from Fluka (Buchs, Switzerland) or from Ega-Chemie (Steinheim, Germany). All reagents were of analytical-reagent grade and were used without any further purification.

2.3. Procedures

Water was triply distilled and was passed through a Millipore (Bedford, MA, USA) Milli-Q water purification apparatus. Eluents were filtered through a 0.45-μm membrane filter and were degassed in an ultrasonic bath, boiled and purged with nitrogen prior to use. Eluent reservoirs were fitted with a sodium hydroxide trap to exclude carbon dioxide from the air. All experiments were performed using an eluent flow-rate of 1 ml/min. The column was conditioned with the mobile phase for 30 min prior to the recording of chromatographic data and the column temperature was maintained at 25°C.

Stock solutions of solute bases were prepared as 10 mM solutions in Milli-Q water and diluted to the required concentrations before use. Injections (20 μl) of sample solutions were made using a 100-μl syringe (Hamilton, Reno, NV,

USA), and chromatograms were recorded simultaneously on the conductivity and UV-absorbance detectors.

The void and the inner column volumes for the Bio-Rad column were determined by the method described [3] and were found to be 3.8 and 6.5 ml, respectively.

3. Results and discussion

3.1. Ion-exclusion effect

Retention data for a wide variety of organic (both aliphatic and aromatic) and inorganic bases using 10 m*M* sodium hydroxide as eluent are listed in Table 1, together with the pK_{b1} value for each solute. It can be seen that the strong inorganic bases were eluted at or close to the column void volume (3.8 ml) since they are excluded from the resin by electrostatic repulsion from the positively charged quaternary ammonium functional groups. Very weak aliphatic bases which are neutral at the eluent pH, together with methanol which was used as a neutral marker compound, can partition freely into the inner volume of the resin and were eluted at or close to a retention volume equal to the sum of the dead and the inner column volumes (10.3 ml). Most of the other aliphatic amines were eluted between these boundaries, with the exception of higher alkylamines, di-

Table 1
Retention data for basic compounds

Solute	pK_{b1}	V_R (ml)	K_d	Solute	pK_{b1}	V_R (ml)	K_d
Inorganic bases				*Aromatic amines*			
KOH	−10.00	3.90	0.02	Pyridine	8.79	22.40	2.86
NaOH	−5.00	3.90	0.02	2-Picoline	8.08	33.10	4.51
$Ca(OH)_2$	2.43	4.00	0.03	3-Picoline	8.48	41.78	5.84
$Zn(OH)_2$	3.02	3.80	0.01	4-Picoline	7.92	39.36	5.47
$Pb(OH)_2$	3.02	4.00	0.03	2,3-Lutidine	7.43	66.92	9.71
AgOH	3.96	3.80	0.01	2,4-Lutidine	7.01	66.40	9.63
$As(OH)_3$	3.96	3.95	0.02	2,6-Lutidine	7.28	51.36	7.32
NH_4OH	4.75	6.96	0.49	3,4-Lutidine	7.51	81.76	11.99
				3,5-Lutidine	7.85	90.40	13.32
Organic bases				3-Aminopyridine	7.97	27.40	3.63
Hydrazine	5.77	6.20	0.37	4-Aminopyridine	4.89	35.16	4.82
Hydroxylamine	7.97	10.40	1.02	Aniline	9.39	114.00	16.95
Urea	13.82	10.32	1.00	2-Methylaniline	9.56	206.70	31.22
Thiourea	14.26	10.40	1.02	3-Methylaniline	9.30	223.20	33.75
$(CH_3)_4NOH$	−15.00	3.80	0.00	4-Methylaniline	8.89	200.88	30.32
Methylamine	3.34	6.60	0.43	2,4-Dimethylaniline	9.11	394.30	60.08
Ethylamine	3.30	7.15	0.52	3,5-Dimethylaniline	9.09	456.20	69.60
Propylamine	3.40	8.00	0.65	2-Aminoaniline	9.51	70.80	10.31
Butylamine	3.37	14.56	1.66	4-Aminoaniline	7.84	19.56	2.42
Pentylamine	3.37	28.00	3.72	Benzylamine	4.67	49.06	6.96
Hexylamine	3.36	62.70	9.06	4-Methylbenzylamine	4.64	104.92	15.56
Trimethylamine	4.19	7.36	0.55	2-Phenylbenzylamine	4.16	84.56	12.42
Diethylamine	2.96	8.60	0.74	2-Methylbenzylamine	4.81	87.12	12.82
Triethylamine	3.00	16.70	1.98				
Dibutylamine	2.99	81.42	11.94				
Triethanolamine	6.24	7.00	0.49				
Ethylenediamine	4.07	5.30	0.23				
Methanol	15.00	10.30	1.00				

A Bio-Rad HPX-72-O column (300 × 7.8 mm I.D.) was used with 0.01 *M* NaOH as mobile phase. K_d = Distribution coefficient.

butylamine and triethylamine which, together with the aromatic bases, were eluted at retention volumes greater than 10.4 ml.

Values of the distribution coefficient for each solute were calculated from the retention volumes and are presented in Table 1. The strong bases are characterised by a distribution coefficient close to zero, whilst the very weak bases show a distribution coefficient close to unity. Since we are considering the distribution of the solutes between two phases with the same chemical composition, the largest theoretical value that the distribution coefficient can attain is unity; that is, when an equal solute concentration exists in both phases. When the distribution coefficient exceeds unity (as is the case, for example, for the aromatic bases), this indicates that a retention mechanism other than ion exclusion is in operation.

Fig. 1 shows a plot of pK_{b1} *vs.* retention volume for the inorganic and aliphatic solutes shown in the left-hand column of Table 1. Many of the data points (those represented as open circles in Fig. 1) can be joined by three straight lines characteristic of ion-exclusion behaviour in which the retention volume can be predicted from the pK_{b1} of the solute. This part of Fig. 1 is identical to a plot of pK_a *vs.* retention volume obtained previously for aliphatic carboxylic acids [3]. The remaining data points do not follow the ion-exclusion model. Linear alkylamines (△) and the secondary and tertiary amines (□) show greater retention than expected, whilst triethanolamine and hydrazine (○) show less retention than expected. The retention behaviour of these species will be rationalised below.

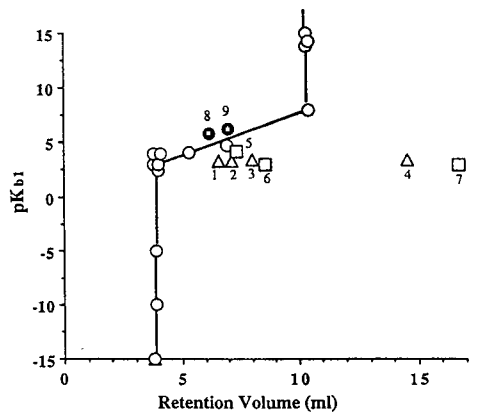

Fig. 1. Plot of pK_{b1} *versus* retention volume for the inorganic and aliphatic organic bases listed in Table 1. A 10 m*M* sodium hydroxide eluent was used with a Bio-Rad HPX-72O ion-exclusion column. Solutes: 1 = methylamine; 2 = ethylamine; 3 = propylamine; 4 = butylamine; 5 = trimethylamine; 6 = diethylamine; 7 = triethylamine; 8 = hydrazine; 9 = triethanolamine.

Apart from the general shape of Fig. 1, the existence of an ion-exclusion mechanism for those data points falling on the lines can be confirmed by the influence of other factors which affect the degree of ionization of the solute. When water alone was used as the eluent, the retention volume was found to decrease when the amount of injected solute was decreased. This behaviour can be attributed to increased ionization of the solute at low concentration, in accordance with theoretical prediction [5], and results in the appearance of fronted peaks. The dependence of retention volume on the amount of solute injected is eliminated when sodium hydroxide is used as eluent since the degree of solute dissociation is maintained at a constant value regardless of solute concentration. Symmetrical peaks are also obtained with this eluent. Solute dissociation can also be manipulated by changing the concentration (and hence the pH) of the sodium hydroxide eluent, with an increase in retention volume being observed with an increase of eluent concentration. Other alkaline buffers such as carbonate buffers might be used as well but have not been investigated during this study.

3.2. Hydrophobic interaction between solute and stationary phase

The retention volumes for the linear alkylamines and the secondary and tertiary amines in Fig. 1 are larger than those predicted on the basis of their pK_{b1} values alone. Retention volumes increase steadily for the homologous series of alkylamines as the alkyl chain length increases, despite the fact that all have very similar pK_{b1} values. Similarly, triethylamine has a much greater retention volume

than diethylamine, without any significant change in pK_{b1}. As mentioned previously, hydrophobic interaction between the solute and the stationary phase has been observed in ion-exclusion chromatography of carboxylic acids [4,6,7] and is clearly also a factor in ion-exclusion chromatography of aliphatic bases.

This effect is even more pronounced for aromatic amines, as seen from their anomalously large distribution coefficients listed in Table 1 and can be attributed to strong π-electron interaction with the aromatic rings of the solute and the resin. In order to determine whether such hydrophobic adsorption effects were the predominant cause of solute retention, two further experiments were performed. First, the dependence between the logarithm of the solute capacity factor and the number of the carbon atoms in the solute molecule was determined and is shown in Fig. 2. A linear dependence was observed for higher (propyl to hexyl) aliphatic amines and is indicative of hydrophobic adsorption, but was not observed for the lower aliphatic amines (methyl and ethyl), suggesting that the retention of these latter species occurs through a mixed retention mechanism combining ion-exclusion and hydrophobic adsorption.

The second experiment involved measurement of retention volumes after addition of an organic solvent to the eluent. Organic solvents are usually characterised by a smaller dielectric constant than water so that, if one considers only the ion-exclusion mechanism, an increase in the retention volume might be anticipated as the percentage of organic modifier in the eluent increases. The observed relationship between the logarithm of capacity factor of some aromatic amines and the concentration of acetonitrile in the eluent is given in Fig. 3, from which it can be seen that the addition of acetonitrile caused solute retention to decrease. This fact, together with the linearity of the plots, is again indicative of reversed-phase behaviour wherein the hydrophobic interaction of the solute with the stationary phase is diminished as the percentage of acetonitrile is increased. Separation of aromatic amines in ion-exclusion chromatography can therefore be manipulated most conveniently by adjusting the percentage of organic modifier in the eluent and the magnitude of this effect is illustrated in Fig. 4 which shows chromatograms obtained with 1 m*M* sodium hydroxide made up in water and in 30% acetonitrile.

3.3. Other factors influencing retention

Fig. 1 reveals that some solutes (*e.g.* triethanolamine) show retention volumes which are somewhat smaller than those predicted from

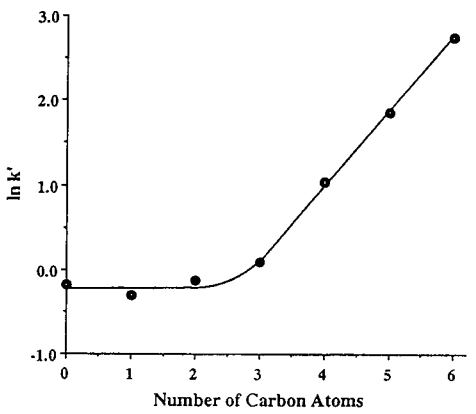

Fig. 2. Effect of the number of carbon atoms on retention volume for aliphatic amines. Chromatographic conditions as in Fig. 1.

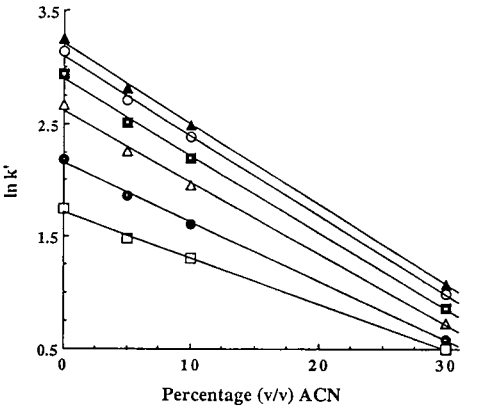

Fig. 3. Dependence of the logarithm of capacity factor on percentage of acetonitrile (ACN) in the eluent for some aromatic amines. Chromatographic conditions as in Fig. 1, but with the indicated percentages of acetonitrile added to the eluent. ▲ = 3,5-Lutidine; ○ = 3,4-lutidine; ■ = 2,3-lutidine; △ = 2,6-lutidine; ● = 2-picoline; □ = pyridine.

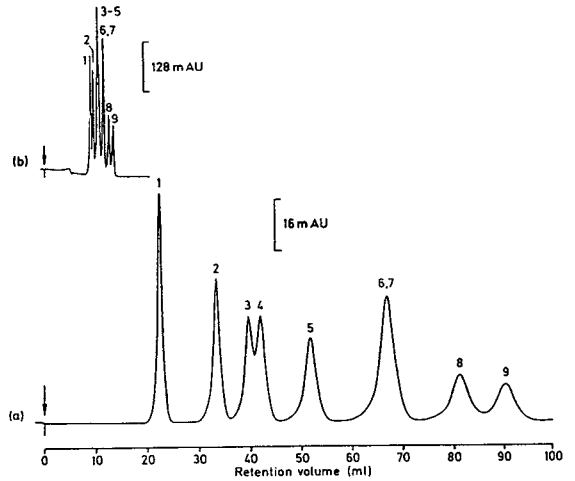

Fig. 4. Chromatograms showing the effect of acetonitrile added to the eluent on the separation of some pyridine derivatives. Eluent: (a) 1 m*M* sodium hydroxide, (b) 1 m*M* sodium hydroxide containing 30% (v/v) acetonitrile. Detection was by UV absorbance at 254 nm. Solutes: 1 = pyridine; 2 = 2-picoline; 3 = 4-picoline; 4 = 3-picoline; 5 = 2,6-lutidine; 6 = 2,4-lutidine; 7 = 2,3-lutidine; 8 = 3,4-lutidine; 9 = 3,5-lutidine. Other conditions as in Fig. 1.

consideration of the ion-exclusion mechanism alone. In the case of organic acids, this behaviour has been attributed to size-exclusion effects [3] and this appears to also be a factor in ion-exclusion chromatography of bases. Triethanolamine is a relatively large molecule in comparison to other solutes in Fig. 1 and can be partially excluded from the pores of the stationary phase through size-exclusion effects. This effect occurs in competition with enhanced hydrophobic adsorption anticipated as the size of the solute molecule is increased. However, a decrease in retention is apparent for triethanolamine since it is quite hydrophilic and would show little reversed-phase adsorption.

A second factor which could be considered in the prediction of retention volume is the effective charge of the solute. Only the first ionization constant has been plotted in Fig. 1 and where the solute has more than one amine functionality it might be necessary to consider further ionization steps if these are significant at the eluent pH. In the case of ethylenediamine ($pK_{b1} = 4.3$, $pK_{b2} = 6.8$, $V_R = 5.3$ ml) the retention volume is predictable from consideration of pK_{b1} alone since the second ionization does not occur under the conditions used.

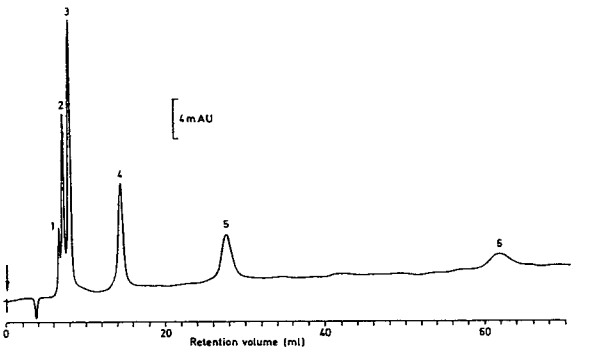

Fig. 5. Separation of aliphatic amines by ion-exclusion chromatography. Chromatographic conditions as in Fig. 1. Solutes: 1 = methylamine; 2 = ethylamine; 3 = propylamine; 4 = butylamine; 5 = pentylamine; 6 = hexylamine.

3.4. Separation of amines

The above-mentioned factors which have been shown to contribute to the retention of bases in ion-exclusion chromatography can be applied to their separation. Two examples of such separations are presented in Fig. 5 (aliphatic amines with different chain lengths) and Fig. 6

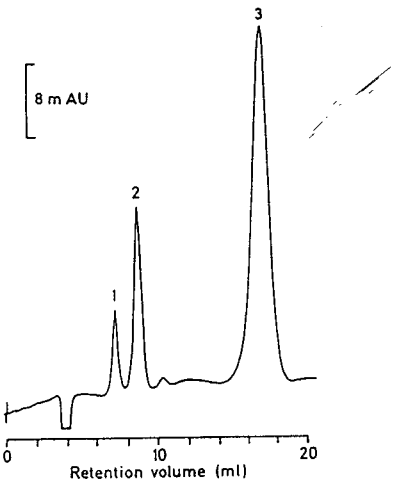

Fig. 6. Separation of ethylamines by ion-exclusion chromatography. Conditions as in Fig. 1. Solutes: 1 = ethylamine; 2 = diethylamine; 3 = triethylamine.

(ethylamines) and these chromatograms show that symmetrical peaks are observed.

4. Conclusions

The relationship between the retention volume and the pK_{b1} value of the solute using sodium hydroxide as eluent and a quaternary ammonium functionalized styrene–divinylbenzene stationary phase has been found for inorganic and some aliphatic amines to be analogous to the previously reported behaviour exhibited by carboxylic acids. This dependence made it possible to establish the dead volume and the inner column volumes and permitted prediction of retention volume for many amines on the basis of their pK_{b1} values. Solute retention increased with an increase in the concentration of sodium hydroxide in the eluent due to decreased ionization of the solute, enabling penetration into the resin network. Again, this effect was similar to that observed for acidic compounds separated using acidic buffers.

As the hydrophobicity of the solute was increased, retention volume also increased such that the retention behaviour no longer fitted the ion-exclusion model. This increased retention was due to hydrophobic interaction (adsorption) of the solute on the underivatized portions of the stationary phase resin. For the aliphatic amines, retention increased with the length of the alkyl chain and with the number of alkyl groups connected to the amine nitrogen. Very large retention volumes were observed for aromatic amines and were attributed to π-electron interactions between the solute and the stationary phase. The existence of reversed-phase behaviour for both longer chain aliphatic amines and aromatic amines has been confirmed. The magnitude of this hydrophobic adsorption effect for aromatic solutes was such that ion-exclusion played very little part in the retention process for these solutes. Some compounds were eluted earlier than predicted from their pK_{b1} value and this was attributed to size-exclusion (or steric) effects.

5. References

[1] R.M. Wheaton and W.C. Bauman, *Ind. Eng. Chem.*, 45 (1953) 228.
[2] P.R. Haddad and P.E. Jackson, *Ion Chromatography: Principles and Applications*, Elsevier, Amsterdam, 1990, pp. 195–220.
[3] K. Tanaka, T. Ishizuka and H. Sunahara, *J. Chromatogr.*, 174 (1979) 153.
[4] B.K. Glod and W. Kemula, *J. Chromatogr.*, 366 (1986) 39.
[5] B.K. Glod, A.K. Piasecki and J. Stafiej, *J. Chromatogr.*, 457 (1988) 43.
[6] K. Kihara, S. Rokushika and H. Hatano, *J. Chromatogr.*, 410 (1987) 103.
[7] B.K. Glod and R. Nowakowski, in preparation.
[8] *HPLC Columns, Methods and Applications*, Bio-Rad Labs., Richmond, CA, 1989.

ELSEVIER

Journal of Chromatography A, 671 (1994) 11–14

JOURNAL OF CHROMATOGRAPHY A

"Heart-cut" column switching techniques for the determination of an aliphatic amine in an organic matrix and for low levels of sulfate in an anion matrix

Steven R. Villaseñor

Mallinckrodt Specialty Chemicals Company, 3600 N. Second Street, St. Louis, MO 63147, USA

Abstract

A "dilute-and-shoot" approach to ion chromatographic analysis employing "heart-cut" column switching techniques has been demonstrated to be a powerful tool to solve a variety of analytical problems. This paper describes various refinements of this technology for a cationic "slice" method for the determination of an aliphatic amine in an organic matrix and an unprecedented example of low level anion analysis in an anion matrix: sulfate analysis in sodium phosphate.

1. Introduction

The "heart-cut" technique and its application as a tool for dealing with matrix interferences has been previously described [1,2]. This paper describes some refinements to this basic technology in an attempt to make the technique more user-friendly. The most significant problems encountered include determining retention times of the analyte on the "pre-column" in the sample matrix and dealing with the dramatic pressure changes for the analytical pump during column switching. A systematic automated approach to attaining optimal retention time parameters has been developed. The latter complication, pressure changes, is dealt with by toggling the pump off and on. It should be noted that these column switching systems may take as much as two days to fully equilibrate and analysis times can be as long as an hour; however, this technique is a powerful tool to deal with matrix interference problems and in some instances affords results that would otherwise be impossible to attain with conventional ion chromatography (IC), as well as other analytical techniques.

2. Experimental

The IC system used for the analyses was a Dionex 4500i dual channel chromatograph with an automated sampler and a pulsed electrochemical detector (PED), utilized in the conductivity mode. The aliphatic amine analyses were conducted employing three CS-3 cation-exchange columns (Dionex) with a 0.3 m*M* 2,3-diaminopropionic acid (DAP) in 10 m*M* HCl eluent at 1 ml/min. Two CS-3 columns constituted the pre-column. A single CS-3 column served as the separator column. Instrumental details of the "heart-cut" technique are described in ref. 1. The rest of the system consisted of a 200-μl loop and a CMMS Dionex suppressor with 50 m*M* tetrabutylammonium hydroxide, TBA-OH, regenerant at 3 ml/min.

The sulfate analysis in sodium phosphate was

0021-9673/94/$07.00
SSDI 0021-9673(93)E1244-T

conducted using four AS-4A (Dionex) anion-exchange columns with a 2.0 m*M* sodium carbonate–0.75 m*M* sodium bicarbonate eluent at 1 ml/min. The pre-column and separator column were each comprised of two AS-4A columns. The rest of the system consisted of a 50-μl loop and an AMMS Dionex suppressor with 50 m*M* sulfuric acid at 3 ml/min.

2.1. Chemicals

All chemicals were Mallinckrodt AR and the water that was used was polished (deionized water further purified through a Millipore Milli-Q filtration system). The sample for the amine analysis was a large organic compound. The sample for the sulfate analysis was sodium phosphate dibasic (ACS grade).

2.2. Sample preparation

Amine sample preparation

About 1 g of sample was accurately weighed into a 100-ml volumetric flask, vigorously mixed and sonicated in about 95 ml of eluent to dissolve. The solution was allowed to cool to room temperature then diluted to volume with eluent.

Sulfate sample preparation

About 10 g of sample was accurately weighed into a 100-ml volumetric flask, vigorously mixed and sonicated in about 95 ml of water. The solution was allowed to cool to room temperature then diluted to volume with water.

3. Results and discussion

The valve configuration for the IC "heart-cut" system was previously described for sulfite analysis in food and drug items [1,2]. Fig. 1 shows the time events program for the "heart-cut" analysis. The initial configuration of the valves consists of Valve A ON, Valve B OFF. The "heart-cut" itself occurs at 5.8 min, Valve B ON. Note that the gradient pump is toggled off and back on in concert with the "heart-cut" to accommodate the

```
Step  Time        Description
-------------------------------------------------------
     Init      CDM-2 AutoOffset ON
     Init      CDM-2  Recorder  Mark  OFF
     Init      CDM-2 Temp.  Comp.  =  1.7 / Deg C
     Init      CDM-2 Recorder Range = 1.00 us
     Init      CDM-2  Cell  ON
     Init      CHA Heater  =  25  Deg.  C
     Init      Valve A ON
     Init      Valve B OFF
     Init      Inject Valve OFF
     Init      ACI  ASM  OFF
     Init      ACI  HLD/RS OFF
     Init      ACI  PGM+L  OFF
     Init      ACI  ON/OFF  ON
     Init      ACI  TTL  OFF
     Init      ACI  Regen ON
     Init      GPM  Start
     Init      GPM  Hold  Gradient  Clock
     Init      GPM  Reset ON
      1   0.0  ACI  ASM ON
      1   0.0  GPM  Reset  OFF
      2   0.1  ACI  ASM  OFF
      3   2.2  Inject Valve ON
      4   5.7  GPM Stop
      5   5.8  Valve B ON
      5   5.8  GPM Start
      6   7.7  GPM Run Gradient clock
      7   7.8  Valve  A  OFF
      7   7.8  Valve  B  OFF
      7   7.8  Start Sampling
      8   9.9  CDM-2 AutoOffset Off
      9  10.0  CDM-2 AutoOffset ON
```

Fig. 1. Time events program for sulfite heart-cut analysis.

dramatic change in pressure experienced by the gradient pump. The final configuration, Valve A OFF and Valve B OFF, which occurs at 7.8 min, by-passes the pre-column and completes the analysis. The system is very reproducible and works quite well once it's set up and fully equilibrated; however, good analytical results are generally not attained immediately after setting up the system. Due to minor differences in eluent or when using different columns, the parameters for the timing of the "heart-cut" will need to be optimized. The optimization process can be automated through repeated analysis with varying retention time windows of a sample with a reasonably high analyte content or a spiked sample. The optimum parameters are evaluated based on maximum peak area with minimum interference.

A "slice" analysis consists of a "heart-cut" analysis minus the last step, late eluters to waste. The chromatograms in Fig. 2 show the effect of varying the "slice" parameters. The variable slice parameters analyses were conducted using a spiked reference sample. Fig. 3 and Table 1 show a standard additions analysis of an actual production sample using the optimized system. Attempts to develop GC or LC procedures for

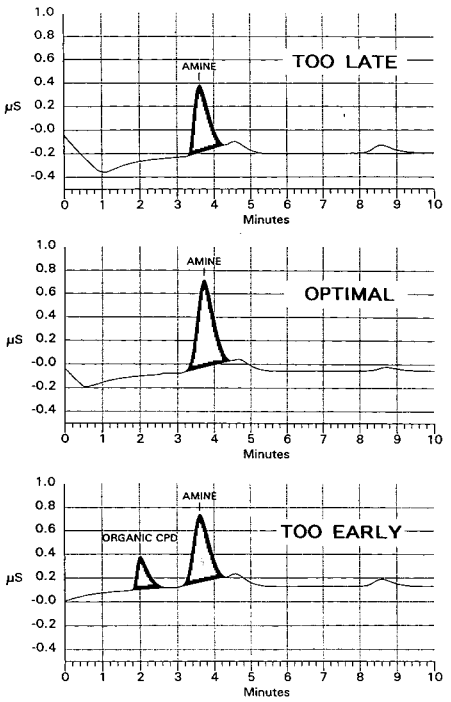

Fig. 2. Effect of varying slice parameter.

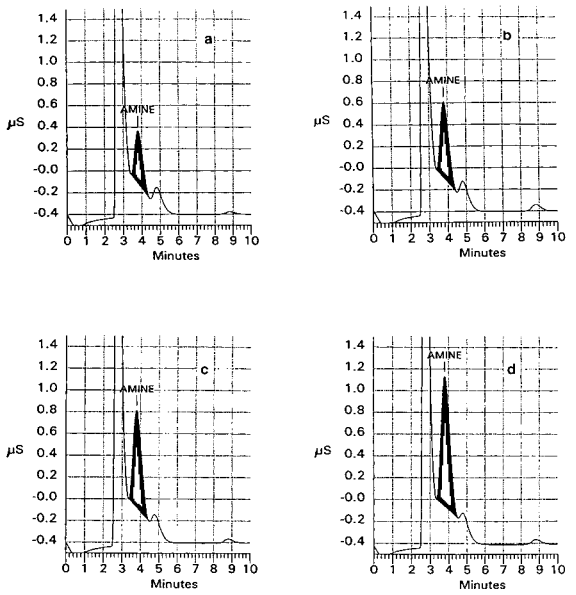

Fig. 3. Amine spikes in organic compound. (a) Unspiked; (b) 50 ppm; (c) 100 ppm; (d) 200 ppm.

Table 1
Standard additions analysis of amine in organic compound

	Spike (ppm)			
	0	50	100	200
	105	166	210	287
	104	167	209	290
	102	158	205	286
	106	165	205	282
	108	163	210	283
Average	105	164	208	286
S.D.	2.32	3.82	2.67	3.03
R.S.D. (%)	2.21	2.33	1.28	1.06

this analysis proved unsuccessful, as did a conventional IC approach.

ACS-grade sodium phosphate dibasic has a limit of 50 mg/kg sulfate maximum [3]. The recommended ACS test involves preparing an acidic 10% solution, adding barium chloride, digesting on a steam bath overnight, and filtering to weigh back any precipitate formed. The usual complications of gravimetric sulfate determination are further exacerbated by the limited solubility of barium phosphate. Copious amounts of precipitate are frequently formed during the filtration step. An alternative IC method was developed in response to the need for another means of analysis to referee borderline results.

An IC approach to analyze for a low level anion in an anion matrix presents a formidable analytical challenge, considering that a selective chemical pretreatment scheme to reduce the phosphate content without affecting the sulfate level has yet to be realized. A "dilute-and-shoot", mechanical, on-line sample preparation approach using "heart-cut" column switching techniques was developed in response to this challenge.

A 10% solution was chromatographed using a pre-column and a separator column, each of which was comprised of two anion-exchange columns. The bulk of the phosphate was diverted to waste. Fig. 4 shows a standard addition analysis. The chromatograms also show two upsets at about 22 and 32 min. The upsets are associated with the column switching. The first

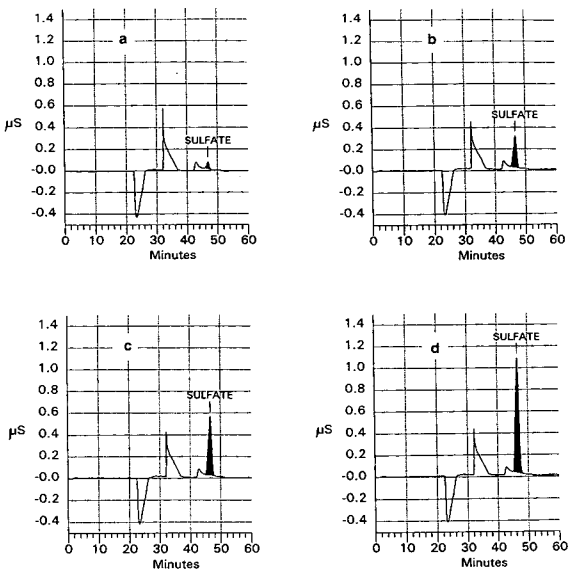

Fig. 4. Sulfate spikes in sodium phosphate. (a) Unspiked; (b) 25 ppm; (c) 50 ppm; (d) 100 ppm.

40 min of the analysis would normally not be recorded; however, the entire chromatogram was shown here to demonstrate the effect of column switching on the conductivity detector.

4. Conclusions

Our column switching technique has been demonstrated for a cationic system, namely amine analysis. Previously, only anion examples were published. The optimization of the "heart-cut" or "slice" parameters can be automated; however, the system may require a couple of days to fully equilibrate prior to optimization. A series of methods in which the retention time window of the "heart-cut" or "slice" was the only variable was used to analyze a given sample with a relatively high level of analyte present. Typically, the analyses were set-up for an overnight schedule of runs. The following day the timing of the requisite parameters were finalized and the requisite analyses begun.

The aforementioned column switching techniques for IC have been utilized to address some very difficult analytical problems. Column switching does possess some disadvantages, in particular the complexity of the system and lengthy equilibration and analysis times. These shortcomings must be weighed against alternative means of analysis, which in some cases may be non-existent.

5. Acknowledgements

Permission to publish and all funding of this work was granted by Mallinckrodt Specialty Chemicals Company. J. Kendall Killgore prepared the figures and proofread the manuscript.

6. References

[1] S.R. Villaseñor, *Anal. Chem.*, 63 (1991) 1362–1366.
[2] S.R. Villaseñor, *J. Chromatogr.*, 602 (1992) 155–161.
[3] *Reagent Chemicals*, American Chemical Society, Washington, DC, 8th ed., 1993, pp. 696–698.

ELSEVIER

Journal of Chromatography A, 671 (1994) 15–22

JOURNAL OF CHROMATOGRAPHY A

Determination of anions at the ng/l level by means of switching valves to eliminate the water-dip interference

Hiroki Kumagai*, Tetsushi Sakai, Kyouji Matsumoto, Yuzuru Hanaoka

Yokogawa Analytical Systems, Inc., R&D Section, Naka-cho 2-11-19, Musashino-shi, Tokyo 180, Japan

Abstract

It is well known that anions, such as chloride, nitrate and sulphate can be determined relatively easily at the μg/l level using an on-line concentrator column. In recent years, however, ultra-pure water containing only ng/l levels of anions or cations is demanded by the most advanced semiconductor factories or power generation plants. For the determination of anions and cations at the ng/l level in such ultra-pure water, higher sensitivity is required. To achieve this, it is necessary to eliminate the water-dip which interferes with the determination of chloride at the ng/l level. We developed and tested a water-dip cutting system consisting of switching valves and a water-dip cutting column. When we combined this with an on-line concentration system, we were able to determine chloride, nitrite, bromide, nitrate, phosphate and sulphate at the ng/l level.

1. Introduction

Ion chromatography (IC) is a popular method for ion analysis (especially anions) for several reasons. First, many anions can be determined quickly with high precision. Second, since IC is a chromatographic technique, many anions or cations can be determined simultaneously, and different chemical species of same element (*e.g.* chlorite, chlorate and chloride) can be separated. Third, low level ion analysis can be done relatively easily [1–5]. This third feature is important for semiconductor factories and power generation plants that use ultra-pure water in manufacturing process and heat transfer systems [6].

In recent years, these industries have demanded even purer water, allowing only ng/l levels of anions and cations. There are two approaches to achieve the levels of sensitivity required. The first is to improve the signal-to-noise (S/N) ratio, and the second is the use of an on-line concentration column, which increases the amount of ions introduced into the separation column, a widely used technique for μg/l-level ion analysis [1–3]. Unfortunately, both techniques are sometimes insufficient to determine ng/l-level anions, because the large negative water peak (water-dip) interferes with the determination of ng/l levels of fluoride and chloride. Since ng/l levels of chloride are especially important in semiconductor factories and power-generation plants, the development of a method to avoid water-dip interference is particularly significant. Some methods for avoiding water-dip interference have been already reported [7–9], but they are not satisfactory for the determination of ng/l-level chloride or polyvalent anions, such as phosphate or sulphate.

This paper describes the development of a new method for avoiding water-dip interference to determine ng/l-level chloride and other anions eluted after chloride. The method uses a system

* Corresponding author.

0021-9673/94/$07.00
SSDI 0021-9673(93)E1153-Q

consisting of a water-dip cutting column and two column-switching valves. Using this system coupled with the well-known on-line concentration technique, ng/l levels of chloride were determined.

2. Experimental

2.1. Instrumentation

A Model IC7000 ion chromatographic analyzer (Yokogawa Analytical Systems, Tokyo, Japan) with a conductivity detector and automatic switching high-pressure six-port valves was used in all experiments. A Model WS 7000 data station (Yokogawa Analytical Systems) was used for data acquisition. The columns used were an Excelpak ICS-A44 (polystyrene based, 150 mm × 4.9 mm I.D.) as a separation column, and an Excelpak ICS-ANC (polyvinyl alcohol based, 20 mm × 4.6 mm I.D.) as an on-line concentration column. The water-dip cutting column (75 mm × 4.9 mm I.D.) was packed with the same anion-exchange resin as the Excelpak ICS-A44. HPS-SA1, which was made from Nafion tube, was used as a suppressor. The separation column, the cutting column and the suppressor were kept at 40°C. The eluent and the regenerator were degassed by an on-line vacuum degassing unit. All columns and the suppressor were manufactured by Yokogawa Analytical Systems.

2.2. Reagents

Sodium carbonate (Japan Industrial Standards primary standard-grade, Asahi Glass, Tokyo, Japan) was used for preparing the eluent, and sulphuric acid (reagent-grade, Wako Pure Chemicals, Osaka, Japan) was used to regenerate the suppressor. Highly purified sodium carbonate is necessary for determining ng/l levels of anions, because inorganic contaminants interfere with the determination of samples. For example, when a sample contains a smaller amount of chloride than the eluent, a negative peak appears at the same retention time as chloride.

Standard stock solutions of chloride, nitrite, bromide, nitrate, and sulphate were prepared by dissolving appropriate amounts of sodium salts (IC grade, Kanto Chemical, Tokyo, Japan) in water. Samples were prepared by diluting stock solutions with purified water. Water used in the analysis was purified with a Millipore (Bedford, MA, USA) Milli-Q water purification system.

All samples and the eluent were prepared in aged vessels made of polyethylene or polypropylene. The Vessels were aged by soaking them in ultra-pure water for 3 days, and replacing ultra-pure water every day.

2.3. Eluent and regenerator

The eluent, 4.0 m*M* Na_2CO_3–4.0 m*M* $NaHCO_3$, was prepared daily and filtered before use. The flow-rate was 1.0 ml/min. The regenerator 15 m*M* H_2SO_4, was used at a flow-rate of 1.0 ml/min.

2.4. Procedure

The sample was passed by the sampling pump into the concentration column, where anions were concentrated. During this step, the posi-

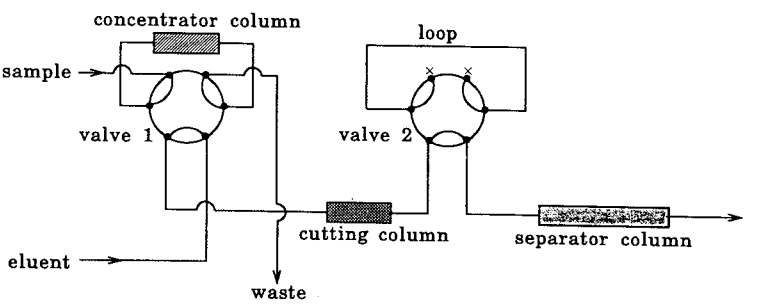

Fig. 1. Sample concentration and water-dip cutting procedure: concentration of sample on the concentration column.

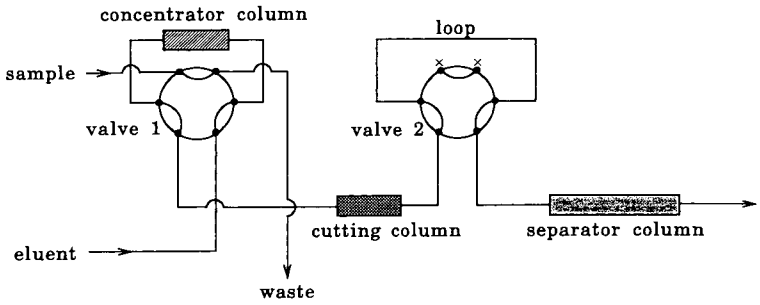

Fig. 2. Sample concentration and waster-dip cutting procedure: the water-dip cutting process. Separation of chloride and other anions from water and early-eluting anions.

tions of valve 1 and valve 2 were as shown in Fig. 1.

After a concentration period of normally 5–20 min, the positions of valve 1 and valve 2 were changed, as in Fig. 2. The eluent flowed through the concentration column, and anions were eluted from this column to the cutting column. On the cutting column, water and anions eluting before chloride were separated from chloride and anions eluting after chloride.

Water and the early-eluting anions were carried to the loop, and the position of valve 2 was then changed as in Fig. 3 (normally 1.5 min after the switching of valves 1 and 2 in Fig. 2). Then chloride and the anions eluting after chloride were carried to the separation column. On this column, chloride and the other anions were separated from each other, and detected by the conductivity detector. After this determination, positions of valve 1 and valve 2 were changed as in Fig. 2, and the water and early-eluting anions were carried to separation column from the loop and discharged.

3. Results and discussion

3.1. Effects of the water-dip cutting column

A typical chromatogram of anions obtained using a common on-line concentration system is shown in Fig. 4. This shows that the water-dip clearly interferes with the determination of chloride and nitrite. The volume of the water-dip depends on the volume of the sample introduced into the separation column. The most effective way of reducing the volume of the water-dip is to reduce the volume of the concentration column. There is a limit to this, however, because it reduces the loading capacity of the concentration column. Increasing the sample volume increases the peak signal, but, because the volume of the water-dip does not change, the quantifiability of

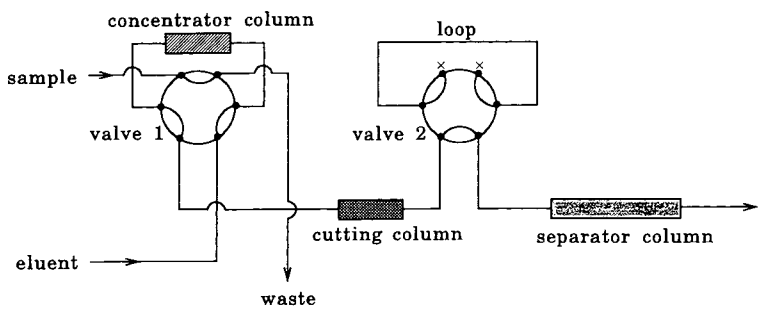

Fig. 3. Sample concentration and water-dip cutting procedure: determination of chloride and anions eluted after chloride.

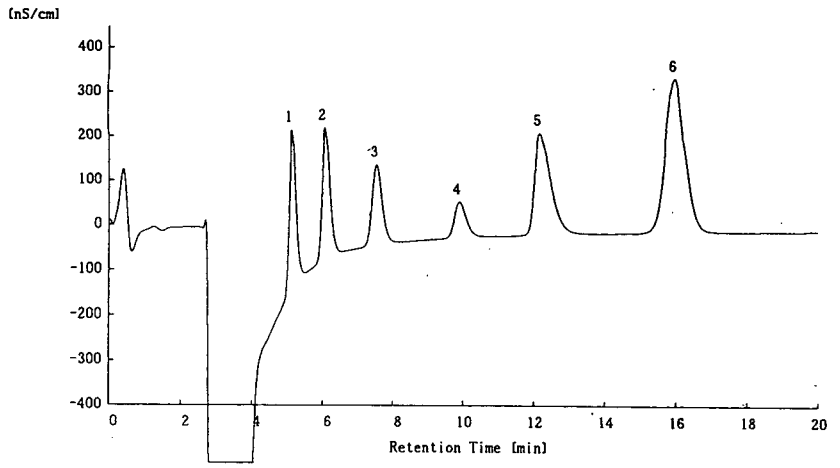

Fig. 4. Chromatogram of low-level anions obtained using an on-line concentration method. Analytical conditions were as in Experimental. The concentration time was 10 min at a sample flow-rate of 2.0 ml/min. Peaks: 1 = chloride (0.5 μg/l); 2 = nitrite (0.75 μg/l); 3 = phosphate (1.5 μg/l); 4 = bromide (0.5 μg/l); 5 = nitrate (1.5 μg/l); 6 = sulphate (2.0 μg/l).

chloride is not improved. In addition, a very long pre-concentration time is required. Using a separation column with a large ion-exchange capacity, or controlling the anion retention time by adding a modifier to the eluent, will separate chloride from the water-dip, but these changes would result in such a long analysis time that phosphate would not elute [5]. It follows, therefore, that the most effective way to remove the water-dip is to prevent the introduction of water into the separation column.

A chromatogram obtained using the water-dip cutting column and the on-line concentration column is shown in Fig. 5. The sample was as same as in Fig. 4. In this system (see Figs. 1–3), water and fluoride are separated in the cutting column from chloride and the anions eluting after it. After this cutting step, chloride and the

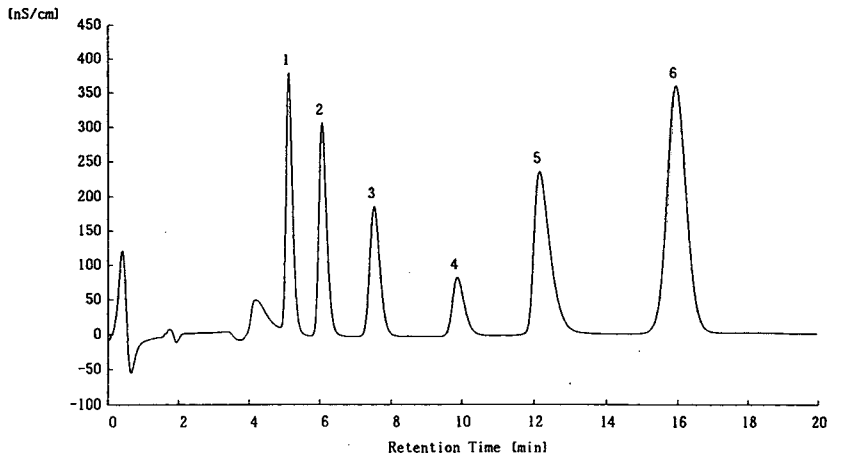

Fig. 5. Chromatogram of low-level anions obtained using the water-dip cutting system and on-line concentration method. The analytical conditions were the same as for Fig. 4, with the addition of the water-dip cutting column. Peaks: 1 = chloride; 2 = nitrite; 3 = phosphate; 4 = bromide; 5 = nitrate; 6 = sulphate; the concentrations of all the ions were same as in Fig. 4.

anions eluting after it are carried to the separation column.

When using a concentration column with a large volume (producing a large water-dip), adjustment of the cutting time (valve-switching time) is all that is required to eliminate the water-dip.

3.2. Sampling and sample preparation

Sampling and sample preparation techniques are important when determining anions at the ng/l level, because contamination at the μg/l level may frequently occur from the atmosphere [1] and the measurement system. Contamination from the system can be prevented by using pumps equipped with a self-washing mechanism, which automatically washes the plunger and plunger seal with ultra-pure water. On the other hand, preventing contamination from the atmosphere is very difficult. On-line sampling is the best solution for this problem, but on-line preparation of calibration samples is not easy. It is necessary, though, to use samples immediately after preparation to minimize the contamination from the atmosphere.

Another important consideration when preparing calibration samples is how to prepare the zero concentration sample. Very small amounts of contamination from water is unavoidable, thus a zero concentration sample cannot be prepared, but this contamination is serious problem when determining anions at the ng/l level. Therefore, water for ng/l-level anion analysis must be contaminant certified. External contamination for the "blank" was minimized by direct connection of a Milli-Q water purification system to the pre-concentration sampling pump.

Good linearity was obtained for chloride (0.1–1.0 μg/l) and sulphate (0.1–1.0 μg/l) using calibration samples prepared as described above. The R^2 value of the calibration curves were 0.998 (chloride, peak height) and 0.992 (sulphate, peak height). Under the conditions of Fig. 5, the detection limit for chloride was 2 ng/l at a signal-to-noise ratio of 3.

The coefficients of variation for 0.5 μg/l of chloride was 1.2% (peak area) and 0.8% (peak height); those for 1 μg/l of sulphate were 1.0% (peak area) and 0.7% (peak height). Thus this system can be regarded as having good reproducibility.

3.3. Life of the cutting column

In this system, water is separated from chloride by the cutting column, which is packed with anion-exchange resin. Thus, if the anion-exchange capacity changes within a short period, it is necessary to change the time-sequence programme of the switching-valve positions. This becomes a problem for continuous measurement in industrial applications. However, because the samples and the eluent contain very low levels of anions, the reduction of the anion-exchange capacity of the cutting column was negligible. The cutting column could be used for a minimum of three months without any significant deterioration.

3.4. Determination of anions in some actual samples

The chromatogram of anions in the recycling water of a boiler system in a thermal power (Fig. 6) shows that ng/l levels of chloride, nitrite, nitrate and sulphate were detected. The large negative peak that appeared just before chloride was due to ammonium hydroxide, an additive in recycling water. In this case, chloride could not be determined without a water-dip cutting system.

Fig. 7 is a chromatogram of a semiconductor water rinse. In this chromatogram, the concentration of nitrite was relatively high. It is speculated that this is due to atmospheric contamination during the rinse process. Nitrite is a typical air contaminant. Because nitrite increases directly with increasing exposure of the sample to air, the sampling method is of importance when determining low levels of nitrite.

Fig. 8 shows a chromatogram of anions in the washing water of the inner surface of pipes for an ultra-pure water delivery system. By measuring chloride and several anions at the ng/l level, it is possible to estimate the cleanliness of the

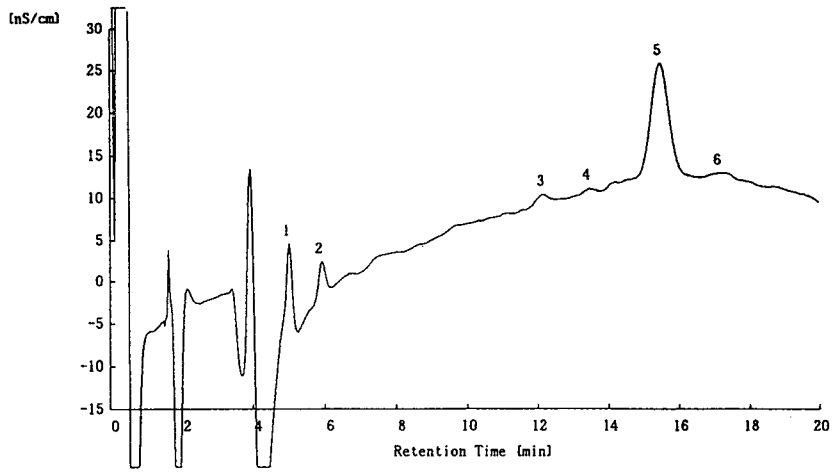

Fig. 6. Chromatogram of anions in the recycling water of the boiler system in a thermal power-generation plant. The analytical conditions were the same as for Fig. 5. Peaks: 1 = chloride (70 ng/l); 2 = nitrite (30 ng/l); 3 = nitrate (20 ng/l); 4 = unknown; 5 = sulphate (25 ng/l); 6 = unknown.

pipes. Chloride, nitrite, phosphate, bromide, nitrate and sulphate were determined at the sub-μg/l or ng/l level. By controlling the anion elution time, it is possible to separate chloride from the water-dip, but then sulphate or phosphate take a long time to elute or are not eluted at all. However, by using this water-dip cutting system, monovalent anions and polyvalent anions, such as sulphate or phosphate, can be determined simultaneously.

Fig. 9 shows the measurement of anions in CO_2 gas used in the electronics industry. The

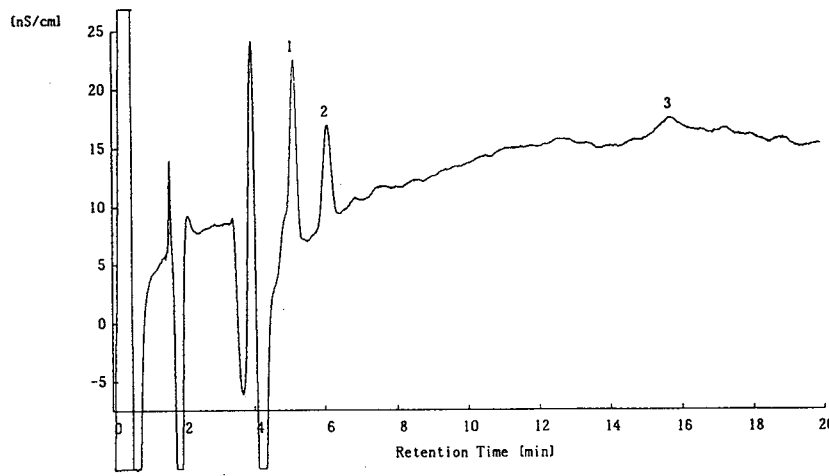

Fig. 7. chromatogram of the anions in the washing water of a semiconductor. The analytical conditions were the same as for Fig. 5. Peaks: 1 = chloride (16 ng/l); 2 = nitrite (22 ng/l); 3 = sulphate (8 ng/l).

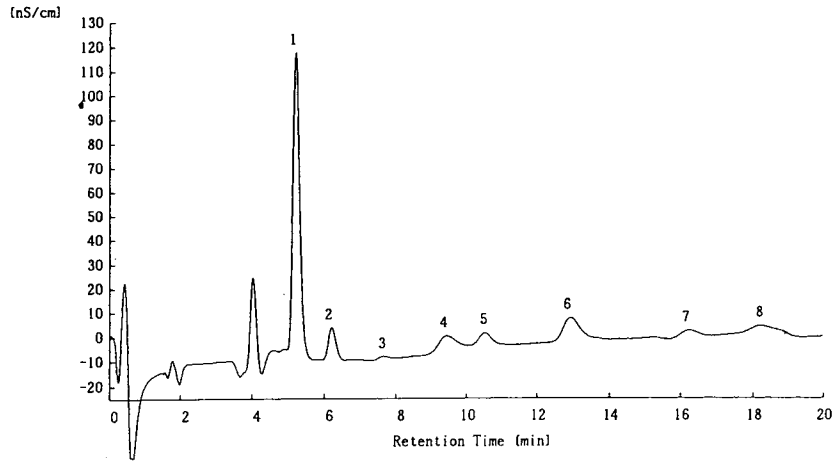

Fig. 8. Chromatogram of anions in the rinsing water of the inner surface of a stainless steel pipe. The analytical conditions were the same as for Fig. 5. Peaks; 1 = chloride (150 ng/l); 2 = nitrite (30 ng/l); 3 = phosphate (10 ng/l); 4 = unknown; 5 = bromide (50 ng/l); 6 = nitrate (50 ng/l); 7 = sulphate (10 ng/l); 8 = unknown.

sample was prepared by bubbling CO_2 into ultra-pure water, therefore very large amounts of carbonate and hydrogencarbonate are found in this sample. These ions interfere with the determination of chloride, in the same way as water. The water-dip cutting system can be used to prevent the interference of carbonate and bicarbonate. This example shows that the water-dip cutting system is also useful for avoiding the influence of sample matrixes.

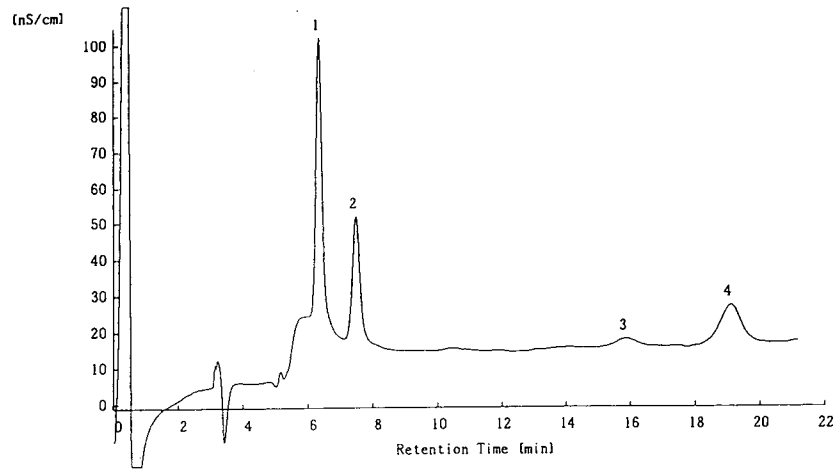

Fig. 9. Chromatogram of the anions in CO_2 gas. The analytical conditions were the same as for Fig. 5. The sample was prepared by bubbling CO_2 into ultra-pure water. Peaks: 1 = chloride (240 ng/l); 2 = nitrite (180 ng/l); 3 = nitrate (50 ng/l); 4 = sulphate (150 ng/l).

4. Conclusions

Using a water-dip cutting column and an on-line concentration column, connected by automatic-switching valves, chloride and the anions eluting it were determined at the ng/l level with good precision. This system was useful for determining chloride and the anions eluting after it in ultra-pure water, such as that used in semiconductor factories or power-generation plants. This system is also useful for eliminating the influence of sample matrixes.

5. References

[1] R.A. Wetzel, C.L. Anderson, H. Schleicher and G.D. Crook, *Anal. Chem.*, 51 (19790 1532.

[2] R.M. Robert, D.J. Gjerde and J.S. Fritz, *Anal. Chem.*, 53 (1981) 1691.

[3] P.E. Jackson and P.R. Hadadd, *J. Chromatogr.*, 439 (1988) 37.

[4] A.L. Heckenberg and P.R. Hadadd, *J. Chromatogr.*, 299 (1984) 301.

[5] T. Okada and T. Kuwamoto, *J. Chromatogr.*, 350 (1985) 317.

[6] T.B. Willhite, S.G. Sawochka and W.L. Pearl, *ASTM Spec. Tech. Publ.*, 742 (1981) 83.

[7] Y. Hanaoka, T. Murayama, S. Muramoto, T. Matsuura and A. Nanba, *Proceedings of the 43rd Symposium of Analytical Chemistry, June, 1982, Yamagata*, Japan Society of Analytical Chemistry, Tokyo, 1982, p. 229.

[8] T. Murayama, T. Matsuura, A. Nanba, H. Miyajima, Y. Kobayasi and Y. Hanaoka, *Proceedings of the 44th Symposium of Analytical Chemistry, June, 1983, Nagasaki*, Japan Society of Analytical Chemistry, Tokyo, 1983, p. 411.

[9] H. Tretter, G. Paul, F. Blum and H. Schreck, *Fresenius' Z. Anal. Chem.*, 321 (1985) 650.

ELSEVIER

Journal of Chromatography A, 671 (1994) 23–28

JOURNAL OF CHROMATOGRAPHY A

Low-pressure ion chromatography

Xinshen Zhang*, Xiaoping Jiang

Leather Department, Chengdu University of Science and Technology, Chengdu 610065, Sichuan, China

Abstract

This paper describes the series of studies on low-pressure ion chromatography (LPIC), including its operating principle, distinguishing feature, Technology Index, and its application in analysis of acid rain, blood, oil field water and medicines etc.

1. Introduction

Ion chromatography (IC) first appeared in the mid-1970s [1] and has become highly developed in the last 10 years. At present, IC is operated with a high-pressure system, using a high-pressure pump to make the mobile phase flow through the separation column. The trend in IC has been a steady increase in the operating pressure (OP), *e.g.*, the Dionex Model 14 with OP 800 p.s.i. (1 p.s.i. = 6894.76 Pa), the 2000i series in the mid-1980s with OP 2000 p.s.i. and the present 4000i and 5000i series with OP 4000 and 5000 p.s.i., respectively.

We began to study IC in 1979 and devised low-pressure IC (LPIC) in 1985 [2]. Two kinds of instrument, "low-pressure fast analysis ion chromatograph" (LPFAIC) and "low-pressure transition metal ion chromatograph" (LPTMIC), were developed in 1988 and 1992, respectively. Both of them can be operated at a low pressure of $1.96 \cdot 10^5$–$2.94 \cdot 10^5$ Pa (30–40 p.s.i.).

When a conductivity detector is used, the former can measure Li^+, Na^+, NH_4^+, K^+, Rb^+, Cs^+, Mg^{2+}, Ca^{2+}, Sr^{2+} and Ba^{2+} cations, inorganic anions such as haloides, NO_3^-, PO_4^{3-}, SO_4^{2-} and CO_3^{2-} and numerous organic acid ions. When combined with an optical detector, the latter can measure metal ions such as Fe^{3+}, Cu^{2+}, Ni^{2+}, Zn^{2+}, Co^{2+}, Pb^{2+}, Fe^{2+}, Cd^{2+}, Mn^{2+}, Cr^{3+}, Cr^{6+}, Al^{3+} and Zr^{3+} and SiO_3^{2-}, S^{2-}, $H_2PO_4^-$, phenol, salicylate, etc. Detailed studies of LPIC are described in this paper.

2. Experimental

2.1. Instrumentation

The ion chromatographs used in this work were a ZJ-1 LPFAIC and a ZJ-2 LPTMIC.

Figs. 1 and 2 show the flow systems of the LFAIC with a conductivity detector and the LPTMIC with an optical detector, respectively.

Instead of the separation column 4 shown in Fig. 2, a 30 mm × 0.5 mm I.D. PTFE tube is used to allow flow-injection analysis to be carried out. Placement of a concentration column at the position of the injection loop will permit on-line concentration and analyses for ultra-trace element components. Elution pump 2 and reaction

* Corresponding author.

0021-9673/94/$07.00
SSDI 0021-9673(93)E1193-4

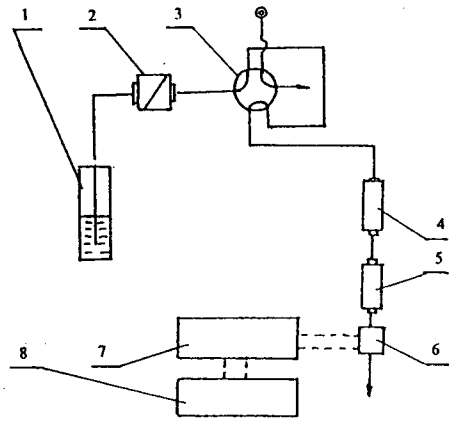

Fig. 1. Schematic diagram of the flow system of the LPFAIC. 1 = Eluent; 2 = low-pressure pump; 3 = injection valve; 4 = separation column; 5 = suppressor column; 6 = conductivity cell; 7 = detector; 8 = computer.

pump 6 shown in Fig. 2 can be replaced with a two-way low-pressure pump.

2.2. Reagents

Dilute nitric acid solutions were prepared from analytical-reagent grade concentrated nitric acid. Sodium carbonate solutions were prepared from analytical-reagent grade Na_2CO_3. Distilled, deionized water was used throughout.

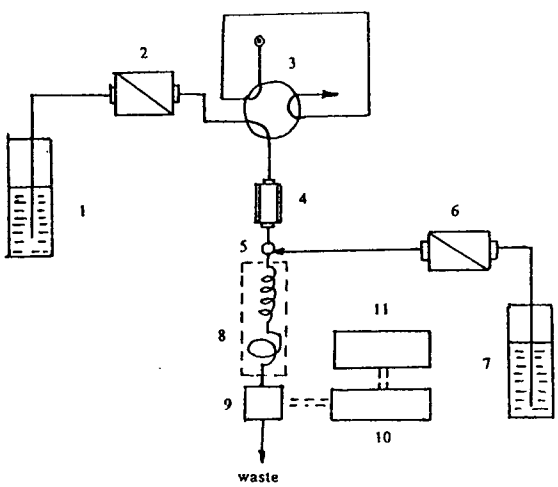

Fig. 2. Schematic diagram of the flow system of the LPTMIC. 1 = Eluent; 2,6 = low-pressure pumps; 3 = injection valve; 4 = separation column; 5 = mixer; 7 = chromogenic reagent; 8 = reaction coil; 9 = flow cell; 10 = optical detector; 11 = computer.

2.3. Main chromatographic conditions

The conditions were as follows: for the determination of alkali metals and NH_4^+, eluent $1.44 \cdot 10^{-3}$ mol/l HNO_3, column C_1 (30 mm × 5 mm I.D.), flow-rate 0.8–1.0 ml/min, conductivity detector and single-column system; for the determination of alkaline earth metals, eluent $6.0 \cdot 10^{-4}$ mol/l ethylenediamine–8.0×10^{-4} mol/l citric acid, column C_2 (30 mm × 5 mm I.D.), flow-rate 0.8–1.0 ml/min, conductivity detection and single-column system; for the determination of anions, eluent $2.0 \cdot 10^{-3}$ mol/l Na_2CO_3, low-pressure anionic column (60 mm × 6 mm I.D.), flow rate 1.0 ml/min, conductivity detection and double-column system; for the determination of organic acids, eluent $1.0 \cdot 10^{-4}$ –$7.2 \cdot 10^{-4}$ mol/l HNO_3, low-pressure organic acid column (100 mm × 6 mm I.D.), flow-rate 0.4–0.6 ml/min, conductivity detection and single-column system; for the determination of Cu^{2+}, Ni^{2+}, Zn^{2+}, Co^{2+}, Pb^{2+} and Fe^{2+}, eluent 0.02 mol/l oxalic acid–0.02 mol/l citric acid, column C_3 (40 mm × 5 mm I.D.), optical detection at 520 nm and postcolumn reaction system; and for the determination of Zn^{2+}, Pb^{2+}, Fe^{2+}, Cd^{2+}, Mn^{2+}, eluent tartaric acid–citric acid, column C_3 (40 mm × 5 mm I.D.), optical detection at 520 nm and postcolumn reaction system.

3. Results and discussion

3.1. Operating principle

Instead of a high-pressure pump, a low-pressure pump is adopted to transmit the eluent. After the ions to be measured have passed through the low-pressure column at a low pressure of $1.96 \cdot 10^5$–$2.94 \cdot 10^5$ Pa they are separated efficiently by ion-exchange equilibrium. The detection and determination of alkali metal, alkaline earth metal and inorganic anions and other numerous organic ions can be achieved using a conductivity detector with a unique, jet-

formed structure conductivity cell. For the measurement of transition metal ions, postcolumn derivatization is helpful to allow the ions to react with coloured material in the postcolumn mixer and the reaction coli. An optical detector can then be used for the determination.

The separation principle of the LPIC column is mainly based on rapid ion exchange (organic acid based on ion exclusion) on the surface of the resin particles. The principle of the dynamics is membrane broadening and that of conductivity detection is based on the formation of ions of the ionic material in the aqueous solution to produce conductivity. Changes in ion concentration are converted into conductivity signals, which are recorded by a computer or a recorder.

With visual photometric detection, after separation in the column, the ions to be measured enter the postcolumn mixer and mixed with a postcolumn chromogenic reagent, resulting in the formation of a coloured chelate, the concentration and absorbance of which are linearly related. The concentration of the metal ions can thus be measured.

3.2. Investigation of the technique

The replacement of the high-pressure pump with a low-pressure one decreases the problems of leakage and blockage, etc., and results in high performance at low pressure. To establish why LPIC can be carried out at such a low pressure as 30–40 p.s.i. with excellent efficiency we consider mainly the following aspects.

A series of packings for low-pressure use were developed through several years of investigation. The technique for making these special packings is different from that for packings for high-pressure IC. An LPIC packing has the advantages of low capacity, excellent dynamic performance and rapid mass-transfer ability.

The packing for the cation-exchange separation column in LPIC consists of round-shaped particles of ion exchanger. There is a very thin covering of ion exchanger with an inert nucleus in the centre. The exchange capacity is 0.012 mequiv./g. The packing of the anion-exchange separation column for LPIC is also a sort of round ion exchanger with exchange capacity 0.015 mequiv./g.

The LPIC columns used in the separation of organic acids employ an H^+ cation exchanger as packing material, with a particle diameter of 15–20 μm and an exchange capacity of 4 mequiv./g.

Very short columns are used, the length being only 30 mm, whereas that of a high-pressure IC column is 250–500 mm. The effusive conductivity cell, of novel design, has an electrode at the solution entry end. The ions to be measured are effused directly to the opposite electrodes, so a much higher sensitivity can be achieved. The dead volume is only 1 μl which is much less than that of HPIC conductivity cells (usually 5 μl). It also has the advantages of no dead-angle, easy air removal, low interference of the flow stream and low baseline drift and noise. Fig. 3 shows the construction of the LPIC conductivity cell.

3.3. Development of LPIC postcolumn reaction system

In the postcolumn system in high-pressure IC, a steel nitrogen bottle is needed to provide pressure to transport the reaction solution. In our method, only a two-way pump is used, without the requirement for any all-plastic high-pressure pump, a large-volume steel nitrogen bottle, a pressure-reducing value, a one-way valve or a buffer valve.

In addition to its use in IC analysis, LPIC can also be applied with flow-injection analysis, whereas high-pressure IC cannot.

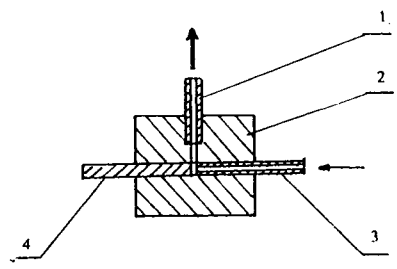

Fig. 3. Construction of LPIC conductivity cell 1 = Exit of solution; 2 = cell body; 3 = entry of solution (an electrode); 4 = second electrode.

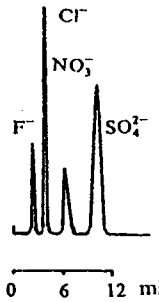

Fig. 4. Analysis of acid rain.

The detection limit for each ion is generally $\leq 10^{-9}$ g/ml. Both the baseline noise and drift are very low. LPIC also has the merits of small volume, low mass (one tenth of that in high-pressure IC), low cost and easy maintenance.

3.4. Application of LPIC

Chromatograms obtained in the analysis of various types of samples are shown in Figs. 4–9. Details of some analyses are given below.

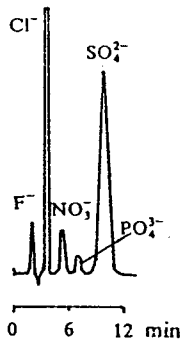

Fig. 5. Analysis of Chengdu tannery waste water.

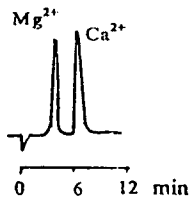

Fig. 6. Analysis of river water.

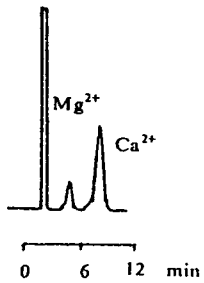

Fig. 7. Analysis of acid rain. Concentrations: Mg^{2+} 0.4 μg/ml and Ca^{2+} 1.0 μg/ml.

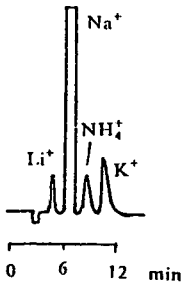

Fig. 8. Analysis of oilfield water.

Analysis acid rain

Standard US EPA (Environmental Protection Agency) samples prepared for the WMO (World Meteorological Organization) were analysed and the results were compared with the stated values (which were not known to us prior to the analyses).

The results agreed well (Table 1). A comparison made by the Atmospheric Laboratory of the Chinese Academy of Meteorology Science with statistical data from the 7th International

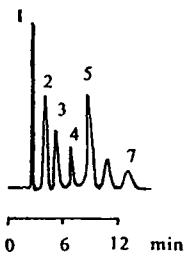

Fig. 9. Analysis of tobacco. Peaks: 1 = inorganic acid; 2 = lactic acid; 3 = formic acid; 4 = succinc acid; 5 = acetic acid; 6 = propionic acid; 7 = butyric acid.

Table 1
Comparison of US EPA values and LPIC results

Ion	Series No.	EPA value (μg/ml)	LPIC result (μg/ml)
Na^+	1313	0.185	0.18
	2026	0.241	0.29
	3286	0.490	0.49
NH_4^+ (as N)	1313	0.083	0.084
	2026	0.627	0.613
	3286	0.798	0.761
K^+	1313	0.066	0.08
	2026	0.094	0.10
	3286	0 094	0.10

Rainfall Chemistry Analysis Results of the 38 Laboratories of BAPMoN (Background Air Pollution Monitor Net of WMO) confirmed that the accuracy of the LPIC analyses corresponded to the average accuracy obtained by the 38 international laboratories.

Analysis of blood [3]

Measurement of Na^+, K^+ and Cl^- in fourteen samples of human serum provided by the Medical University of West China by LPIC gave results very close to those obtained using a Beckman E4A instrument with ion selective electrodes. One of the fourteen samples was injected successively twelve times to determine the accuracy of the LPIC method and the relative standard deviation was 1.2%. The results indicate that LPIC has a high sensitivity and with its easy operation it can be widely used in clinical medicine.

Measurement of oilfield water

The results for the determination of Fe^{2+}, Zn^{2+} and Mn^{2+} in oilfield water are given in Table 2 and compared with those obtained using a Jarrell-Ash ICAP9000 (N + M) inductively coupled plasma atomic emission spectrometer.

The results given by the two methods agreed well. Recovery experiments showed that the

Table 2
Comparison of LPIC and ICP results for oilfield water

Series No.	Methods	Fe^{2+} (μg/ml)	Zn^{2+} (μg/ml)	Mn^{2+} (μg/ml)
18	ICP	0.59	9.14	5.17
	LPIC	0.60	9.21	5.00
80	ICP	0.31	10.7	5.59
	LPIC	0.36	10.5	5.50
46	ICP	1.16	7.70	3.70
	LPIC	1.10	7.53	3.90
9	ICP	0.30	–	0.025
	LPIC	0.50	–	0.030
36	ICP	0.92	–	0.020
	LPIC	0.83	–	0.030

recoveries of Fe^{2+}, Zn^{2+} and Mn^{2+} in oilfield water by LPIC are between 94 and 105%.

Analysis of medicines

Using LPIC, samples provided by the Medicines Institute of the Medical University of West China were analysed as follows: measurement of the content of nitrate and sulphate in the inorganic medical carbon, magnesium silicate and the organic medical methoxyestrone (OPC-8212) and measurement of the content of related elements in the medical Li_2CO_3 and KCl which contain lithium, fluorine and chlorine. The results were similar to the data in the Chinese Pharmacopoeia.

The following medicines were also analysed by LPIC: measurement of trace Zn^{2+} in insulin, providing results in agreement with the Chinese Pharmacopoeia but much faster and more easily way than by the stipulated method; and measurement of zinc gluconate content, giving a result close to that obtained with by the standard method of the National Hygiene Department.

Measurement of zinc gluconate particulate reagent in abundant blood syrup (a blood tonic made in China) gave a recovery between 96 and 105.3%. Owing to the high sensitivity and small injection volume with LPIC, the sample need not be pretreated. Also, there is no interference with the measurement from the matrix.

4. Acknowledgement

We thank National Natural Science Foundation of China for its support.

5. References

[1] H. Small, T.S. Stevens and W.C. Bauman, *Anal. Chem.*, 47 (1975) 1801.
[2] X.-S. Zhang, *Ion Chromatography Analysis and Application*, Sichuan Science and Technology Publishing House, Chengdu, 1986.
[3] X.-S. Zhang, *Chin. J. Chromatogr.*, 8 (1990) 128.

ELSEVIER

Journal of Chromatography A, 671 (1994) 29–32

JOURNAL OF CHROMATOGRAPHY A

Application of a dynamically coated sorbent and conductimetric and UV detectors to the determination of alkaline earth and transition metal cations

M.L. Litvina*, I.N. Voloschik, B.A. Rudenko

V.I. Vernadsky Institute of Geochemistry and Analytical Chemistry, Russian Academy of Science, 19 Kosygin Street, 117975 Moscow, Russian Federation

Abstract

The separation of alkaline earth and transition metal cations was performed on the reversed-phase sorbent Silasorb C_{18} modified under static conditions with dodecylbenzenesulphonic acid and cetyltrimethylammonium bromide. Mixtures of ethylenediamine, citric acid and tartric acid without addition of an ion-pair reagent and of dipicolinic and oxalic acid with an ion-pair reagent were used as eluents. The selective separation of twelve cations (Fe^{3+}, Cu^{2+}, Ni^{2+}, Zn^{2+}, Pb^{2+}, Co^{2+}, Cd^{2+}, Fe^{2+}, Mg^{2+}, Ca^{2+}, Sr^{2+} and Ba^{2+}) in 15 min was obtained. The lifetime of this dynamically coated column was found to exceed that of a column packed with silica gel with sulphonic functional groups.

1. Introduction

The determination of alkaline earth and transition metals is an important part of the determination of the ionogenic content of natural and waste waters. Ion chromatography (IC) is successfully applied for this purpose and can compete with inductively coupled plasma and atomic absorption spectrometric methods for the determination of alkaline earth and transition metals [1]. Conventional reversed-phase columns and LC instruments have been increasingly used to separate metal ions [2–4].

In this paper, we propose techniques for the determination of alkaline earth and transition metal cations using ion-pair and ion-interaction chromatography.

2. Experimental

The separation column for ion-interaction chromatography was prepared as follows. The reversed-phase sorbent Silasorb C_{18} (7.5 μm) (Tessek, Prague, Czech Republic) was treated with an excess of aqueous dodecylbenzenesulphonic acid solution under static conditions. The column was filled with the resulting aqueous suspension of the sorbent with a column packing device. The column packing efficiency was evaluated by determining the number of theoretical plates per metre for the K^+ peak in suppressed IC. The eluent contained 5 m*M* HNO_3 and 0.2

* Corresponding author.

0021-9673/94/$07.00
SSDI 0021-9673(94)00202-K

m*M* dodecylbenzenesulphonic acid. The efficiency of a well packed 100 × 3 mm I.D. column was about 30 000 theoretical plates per metre. This column has been applied to the determination of alkaline earth and transition metal cations [5].

The determination of anionic complexes of transition and alkaline earth metals by ion-pair and ion-interaction chromatography was performed on a standard glass column (100 × 3 mm I.D.) containing Silasorb C_{18} (7.5 μm). The ion-pair reagents used included tetrabutylammonium hydroxide, sodium iodide and cetyltrimethylammonium bromide.

3. Results and discussion

The method for determining transition and rare earth metal cations proposed initially by Cassidy and co-workers [2,3] requires post-column reaction with 4-(2-pyridylazo)resorcinol (PAR) or Arsenazo-III and UV–Vis spectrophotometric detection. In addition, relatively high-concentration solutions of sodium tartrate, citrate and oxalate (pH 3–4) are used as the eluent. This does not permit the use of conductimetric detection and does not allow the determination of the transition and the alkaline earth metals simultaneously.

We used solutions of ethylenediamine with tartric, citric and oxalic acid as eluents. Because of the strong eluting ability of ethylenediamine, the eluent concentration can be considerably decreased. Analogous eluents are used for the separation of metal cations on functionalized sulphonic cation exchangers. In this way the background conductivity is sufficiently low for conductimetric detection to be practicable. The alkaline earth and transition metal cations were separated on the 100 × 3 mm I.D. column packed with the dynamically coated sorbent described.

With the use of the ethylenediamine-containing eluent comes the column stability is of concern. It was demonstrated experimentally that the column lifetime is more than 300 sample injections. The column's operational stability was evaluated by the separation efficiency of the metals and by the theoretical plate number for Ca^{2+}. The sufficiently long column lifetime can be explained by assuming that one ethylenediamine cation is sorbed by two molecules of dodecylbenzenesulphonic acid via an ion-exchange mechanism. The associate produced is strongly sorbed by the hydrophobic surface of the reversed-phase sorbent. The addition of dodecylbenzenesulphonic acid to eluent is not helpful, because its ethylenediamine salts are hardly soluble.

The addition of small amounts of 0.05 m*M* sodium dodecyl sulphate to the eluent and the use of guard and precolumns increases the analytical column lifetime. The precolumn filled with reversed-phase sorbent is placed between the pump and the injector for elimination of eluent contamination. The guard column is placed between the injector and the analytical column. It protects the analytical column from sample contaminants and is packed with the same sorbent.

The optimum conditions for the determination of the alkaline earth and transition metal cations on the dynamically coated sorbent were established from the results of the experimental work. A mixture of Fe^{3+}, Cu^{2+}, Ni^{2+}, Zn^{2+}, Pb^{2+}, Cd^{2+}, Co^{2+}, Fe^{2+}, Mg^{2+}, Ca^{2+}, Sr^{2+} and Ba^{2+} was selectively separated using an eluent consisting of 2.5 m*M* ethylenediamine–2.5 m*M* citric acid–2.5 m*M* tartric acid (Fig. 1). The most rapid separation of alkaline earth metals was obtained with 1.5 m*M* ethylenediamine–1.5 m*M* oxalic acid. Fig. 2 shows the separation of a mixture of Be^{2+}, Mg^{2+}, Ca^{2+}, Sr^{2+} and Ba^{2+}. The detection limit for all of the alkaline earth and transition metals using conductimetric detection is *ca.* 0.5 mg/l.

The technique developed for the determination of alkaline earth and transition metal cations on the dynamically coated column using indirect UV detection might be of interest. A 1 m*M* $Ce(NO_3)_3$ solution was used as the eluent and UV detection at 254 nm was applied. The analysis time for a mixture of Mg^{2+}, Ca^{2+}, Sr^{2+} and Ba^{2+} under these conditions did not exceed 5 min. This technique for the determination of

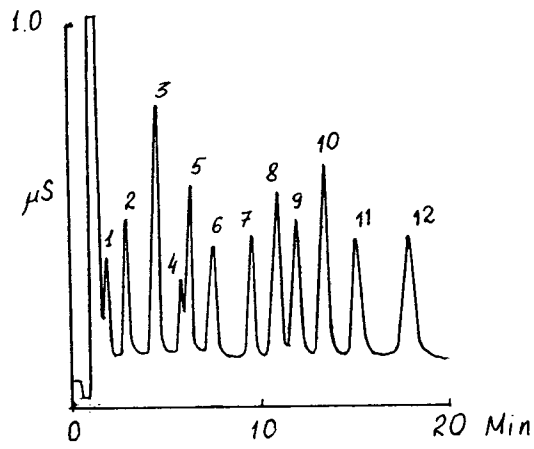

Fig. 1. Separation of transition metal ions on a dynamically coated column. Column, 100 × 3 mm I.D., packed with Silasorb C_{18}, coated with dodecylbenzenesulphonic acid; eluent, 2.5 m*M* ethylenediamine–2.5 m*M* citric acid–2.5 m*M* tartric acid (pH 3.2); flow-rate, 1 ml/min; detection, conductimetric. Peaks: 1 = Fe^{3+}; 2 = Cu^{2+}; 3 = Ni^{2+}; 4 = Pb^{2+}; 5 = Zn^{2+}; 6 = Co^{2+}; 7 = Fe^{2+}; 8 = Mg^{2+}; 9 = Cd^{2+}; 10 = Ca^{2+}; 11 = Sr^{2+}; 12 = Ba^{2+}. Metals concentrations, 1–10 mg/l.

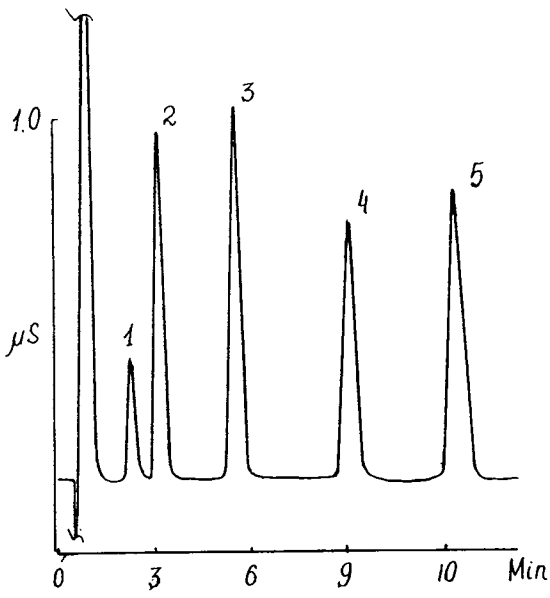

Fig. 2. Separation of alkaline earth metal ions on a dynamically coated column. Eluent, 2.5 m*M* ethylenediamine–3.5 m*M* oxalic acid (pH 3.4); other conditions as in Fig. 1. Peaks: 1 = Be^{2+}; 2 = Mg^{2+}; 3 = Ca^{2+}; 4 = Sr^{2+}; 5 = Ba^{2+}.

alkaline earth metals is more sensitive than that with conductimetric detection. The determination limit of alkaline earth metal cations is 0.01 mg/l. Unfortunately, the determination of transition metals by this technique is not possible, as the selectivity of the separation of these cations is low when a $Ce(NO_3)_3$-containing eluent is used.

A technique for determining transition metals in the form of their anionic complexes was worked out. The separation is carried out on the standard reversed-phase Silasorb C_{18} column. The eluent used permits the production of the anionic metal complexes in the analytical column and these complexes can be detected by direct UV methods. An analogous technique has been proposed for the determination of metals in the form of their cyanide complexes with UV detection at 214 nm [6]. We used an eluent consisting

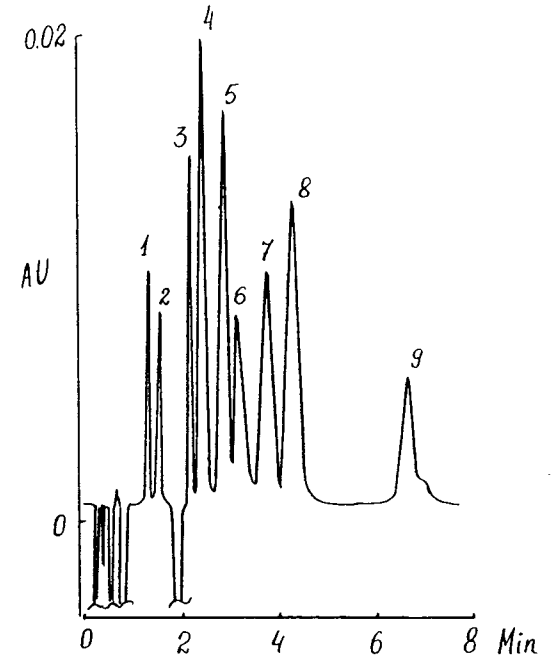

Fig. 3. Separation of transition metals by ion-pair chromatography. Column, 100 × 3 mm I.D., packed with Silasorb C_{18}; eluent, 5 m*M* sodium oxalate–0.3 m*M* pyridinedicarboxylic acid–1 m*M* tetrabutylammonium hydroxide (pH 5.5); flow-rate, 0.5 ml/min; detection, UV at 254 nm. Peaks: 1 = Pb^{2+}; 2 = Fe^{3+}; 3 = Cu^{2+}; 4 = Ni^{2+}; 5 = Zn^{2+}; 6 = Co^{2+}; 7 = Mn^{2+}; 8 = Cd^{2+}; 9 = Hg^{2+}.

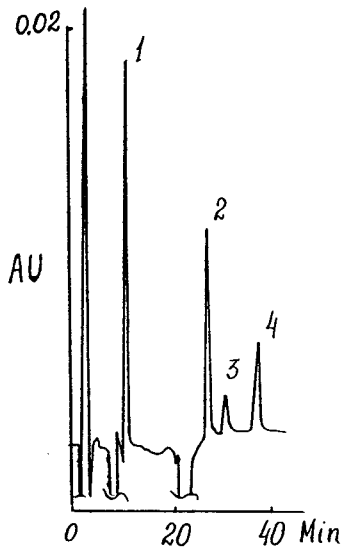

Fig. 4. Chromatogram of Moscow drinking water obtained by direct sample injection. Column, 100 × 3 mm I.D., packed with Silasorb C_{18}, dynamically coated with cetyltrimethylammonium iodide; eluent, 2 m*M* sodium oxalate–0.2 m*M* pyridinedicarboxylic acid–1 m*M* tetrabutylammonium iodide (pH 5.2); flow-rate, 0.5 ml/min; detection, UV at 254 nm. Peaks: 1 = Fe^{3+} (0.2 mg/l); 2 = Cu^{2+} (0.04 mg/l); 3 = Ni^{2+} (0.02 mg/l); 4 = Zn^{2+} (0.1 mg/l).

of 2 m*M* sodium oxalate–0.2 m*M* dipicolinic acid–1 m*M* tetrabutylammonium hydroxide. Dipicolinic acid has been shown to be a convenient eluent for the separation of heavy and transition metals with postcolumn PAR reaction detection [7]. The eluent used in this technique permits direct UV detection at 254 nm. The limit of determination of the transition metals is 0.005 mg/l.

Fig. 3 shows the separation of a mixture of transition metal cations obtained by ion-pair chromatography. The selective separation of Pb^{2+}, Fe^{3+}, Mn^{2+}, Cu^{2+}, Ni^{2+}, Zn^{2+}, Co^{2+}, Cd^{2+} and Hg^{2+} was achieved. All the inorganic ions were eluted before the system peak caused by the sorption of dipicolinic acid. The high sensitivity of the technique makes it possible to perform the determination of some transition metals in natural water samples without preconcentration. Fig. 4 shows a chromatogram for Moscow drinking water obtained by direct sample injection. This separation was carried out on the Silasorb C_{18} column treated with cetyltrimethylammonium bromide.

Ion-pair and ion-interaction chromatography are practical methods for determining cations of metals and their anionic complexes. The technique described can be successfully used in routine analyses for heavy, transition and alkaline earth metal cations and also for investigations of unknown samples. The developed techniques utilize direct and indirect conductimetric and UV detection. The ability to use all of these detection modes enhances the usefulness of LC for the determination of cations in environmental samples.

References

[1] J. Weiss, *Lab Prax.*, 12 (1988) 54.
[2] R.M. Cassidy and S. Elchuk, *Anal. Chem.*, 54 (1982) 1558.
[3] D.J. Barkley, M. Blanchette, R.M. Cassidy and S. Elchuk, *Anal. Chem.*, 58 (1986) 2222.
[4] P.R. Haddad and R.C. Foley, *J. Chromatogr.*, 500 (1990) 301.
[5] I.N. Voloschik, in *Abstracts of the VIth Symposium on Ion Exchange, Budapest, 1990*, p. 98.
[6] D.F. Hilton and P.R. Haddad, *J. Chromatogr.*, 361 (1986) 141.
[7] G.O. Frankin, *Am. Lab.*, 17 (1985) 65.

ELSEVIER

Journal of Chromatography A, 671 (1994) 33–41

JOURNAL OF CHROMATOGRAPHY A

Centrally localized ion exchangers as separating sorbents for ion chromatography Theory and application

Anatoly M. Dolgonosov

V.I. Vernadsky Institute of Geochemistry and Analytical Chemistry of the RAS, 117975 Moscow, Russian Federation

Abstract

The possibility of applying differen separation sorbents to those traditionally used in ion chromatography, having the structure of surface-layer ion exchangers, is considered. The theoretical possibility of using a new class of separation sorbents having the structure of centrally localized ion exchangers for highly efficient ion chromatographic separations is shown. The principles of the synthesis of centrally localized ion exchangers and the properties of representative materials, KanK sorbents, are outlined. Examples of the application of KanK sorbents to the analysis of mixtures of anions, metals and ammonium are presented.

1. Introduction

The rapid progress of ion chromatography in analytical chemistry is largely based on successful syntheses and applications of special ion exchangers as packings in separation columns. As a rule, they are fine-grained, narrow-fraction polymeric or silica gel materials, with granules having a thin ion-exchanging surface layer [1]. Such a structure of the separating sorbent grains confers two very important chromatographic properties on the sorbent: a low capacity and rapid kinetics of ion exchange.

The first property permits rapid analysis and the second makes chromatographic separation highly efficient. The separation selectivity is completely determined by the chemistry of the ion-exchange process: by the nature of the functional groups and by the elution power of the mobile phase, which is in no way connected with the special structure of the sorbent particles.

2. Theoretical aspects of selection of separation sorbents

In deciding on a separation sorbent, the basic question is whether the above-mentioned structure of the grains of the so-called surface-layer ion exchanger (SLIE) is necessary for making chromatographic separations rapid and efficient or whether there are alternative ways of achieving these purposes. For example, can the fairly fine fraction of a uniformly localized ion exchanger (ULIE), which finds extensive application in technology, be used or not? Calculations based on the sorption dynamics theory [2] have shown that the nature of the relationships between the packing capacity, its grain size and the efficiency of columns filled with it is such that in order to obtain the necessary characteristics of chromatographic separation of an ordinary series of inorganic anions, a pressure differential of several hundred bars builds up in the separation

0021-9673/94/$07.00
SSDI 0021-9673(94)00023-3

columns. Such a pressure destroys polymeric ion exchangers. A decrease in the density of the ULIE functional groups does not change the result because of the proportional decrease in the specific efficiency of the packing (it should be noted that the ULIE capacity can be decreased only to a lower limit of 0.1 mequiv./ml as the further decreases in functional group density generally lead to deterioration of the ion-exchange selectivity [3]). In our opinion, the only way to use ULIE for ion chromatographic purposes is the proposal of Small *et al.* [4] to mix ULIE sub-micrometre particles with large (tens of micronmetres) grains of an inert material. It was thus required that the ULIE particles be firmly bonded to the grain surface (Fig. 1). However, can such a packing be considered to be structureless?; it cannot. It has the SLIE structure and this fact considerably lowers the requirements both for the separation system and for the separation conditions needed to obtain the necessary results. Hence our conclusion is not unexpected: the ULIE does not make an efficient separation medium for ion chromatography.

The example cited does not cover all alternatives to separation sorbents of the SLIE type. Let us consider a sorbent characterized by a non-uniform distribution of functional groups located, in contrast to SLIE, not on the surface

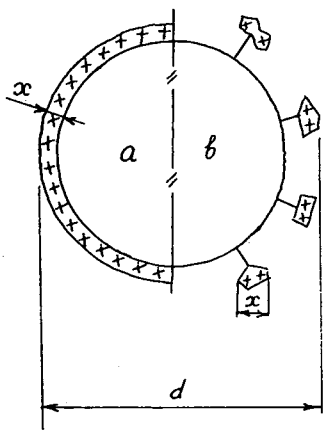

Fig. 1. Structure of surface-layer ion exchangers. (a) Surface-functionalized anion exchanger; (b) agglomerated anion exchanger [4].

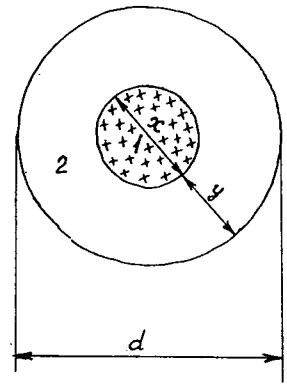

Fig. 2. Structure of centrally localized ion exchangers. 1 = Ion-exchanging nucleus; 2 = inert envelope.

but in the centre of the grains; let us call such a sorbent a centrally localized ion exchanger (CLIE) (Fig. 2). Needless to say, the CLIE inert envelope will be permeable to separated ions and it is desirable that their diffusion through the CLIE envelope be as rapid as possible. In ion chromatography, this sorbent has the general advantage over the ULIE that by decreasing the size of the CLIE ion-exchanging nucleus, it is possible to minimize the ion-exchange capacity and diffusion resistance area in the CLIE grains (it is common knowledge that in ion-exchange materials the diffusion coefficients of ions are several orders of magnitude smaller than in non-ion-exchanging materials having the same porosity [5]). Obviously, a change in the CLIE nucleus size has no effect on the hydrodynamic characteristics of the packing. In other words, conceiving CLIE as an enveloped ULIE nucleus makes it possible to see that CLIE has virtually the same equilibrium and kinetic characteristics at a much lower pressure in the column bed.

The properties of SLIE and CLIE used as packings in separation columns for ion chromatography can be evaluated quantitatively [2]. Based on the structure geometry, for the capacity of these sorbents we have

$$a_{0\,\mathrm{SLIE}} = 6Ax/d \qquad (1)$$

$$a_{0\,\mathrm{CLIE}} = Ax^3/d^3 \qquad (2)$$

where x is the size of the grain area saturated

with functional groups, A is its local capacity and d is the diameter of a grain. Chromatography uses low concentrations of the sample components compared with those of the eluent. In this area, the ion-exchange isotherms are approximately linear and characterized by constant ion distribution factors Γ_i, which depend on the structural parameters of the grains, similar to the capacity in Eqs. 1 and 2.

To determine which kinetic stage is the slowest and limits the speed of ion exchange in the sorbent grain, the criterion H equal to the ratio of the characteristic times of particle and film diffusion is used:

$$H = \beta_i d^2/(60 D_i \Gamma_i) \quad (3)$$

where D_i and β_i are particle diffusion coefficient and film diffusion factor, respectively. To large H values there correspond particle diffusion kinetics and to $H \ll 1$ there correspond film diffusion kinetics. In the area of hydrodynamics characteristic for ion chromatography, the film diffusion factor is expressed in terms of ion kinetic constants, α_i, and the linear velocity of the mobile phase, v:

$$\beta_i = \alpha_i v^{0.5}/d^{1.5} \quad (4)$$

where α_i is the well known function of ion charges and equivalent conductivities (ref. 2, p. 28).

Let us find in which kinetic area the SLIE and CLIE work. Assuming that the factor of particle diffusion in Eq. 3 relates only to the size x and the distribution factor is subject to the laws in Eqs. 1 and 2, we obtain from Eqs. 3 and 4 that the criterion H is proportional to the expression $xv^{0.5}/Dd^{0.5}$ for SLIE and to $d^{1.5}v^{0.5}/Dx$ for CLIE. To decrease the capacity, investigators usually try to lower the ratio x/d. For example, for SLIE it is usually ≤ 0.01. Therefore, film diffusion is characteristic for SLIE and particle diffusion for CLIE. According to this conclusion, the SLIE packed column efficiency (the number of theoretical plates) can be expressed by

$$N_{Bi,SLIE} = 0.5\alpha_i l/d^{1.5} v^{0.5} \quad (5)$$

and the CLIE packed column efficiency is

$$N_{Bi,CLIE} = 30 D_i \Gamma_i' l x/d^3 v \quad (6)$$

where Γ_i' is the local distribution factor of the ith ion in the CLIE nucleus, which does not depend on the structural parameters of the grain, l is the separating column length and B and i are indexes.

Analysis of Eqs. 5 and 6 shows that by decreasing d at a fixed x/d it is easier to improve the efficiency for CLIE (the proportionality d^{-2}) than for SLIE (the proportionality $d^{-1.5}$). However, a more detailed analysis of the kinetic dispersion of ion zones in ion chromatography leads to the conclusion about the existence of areas of the chromatographic separation conditions where one or another type of separation sorbent structure has advantages with regard to separation efficiency [2]. In Eq. 6, the efficiency as a function of x/d [at a fixed value of the envelope thickness: $y = (d - x)/2 \neq 0$; Fig. 3] has the maximum at $d = 3x$, which is equal to

$$\max\{N_{Bi,CLIE}\} = 1.11 D_i \Gamma_i' l/x^2 v \quad (7)$$

[$N = 0$ for $x/d = 1$ only when x and $d \gg y$, but this does not mean that ULIE sorbents (with $x/d = 1$) have $N = 0$ because they have $y = 0$). According to Eq. 2, at this point the capacity is 1/27th of the functional groups density in the CLIE nucleus (A).

The fraction of the feedstock that is chemically modified into SLIE or CLIE is usually made up of particles of various sizes. The functional group

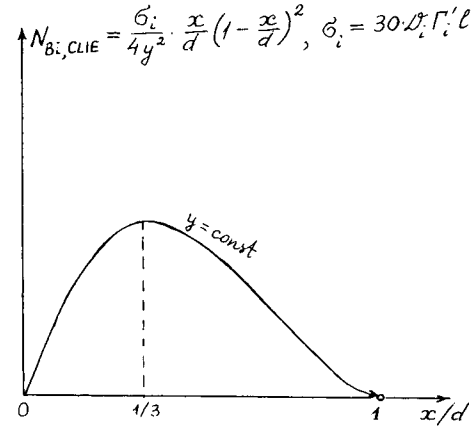

Fig. 3. Efficiency of CLIE bed as a function of x/d [with fixed $y = (d - x)/2$].

bonding required to produce SLIE or CLIE is carried out under the same conditions for the variously sized particles of the feedstock fraction, so the particles of the sorbents synthesized acquire envelopes of equal thickness which, according to Eqs. 1 and 2, results in the individual values of the capacities of the particles being dependent on their diameters (Fig. 4). For SLIE this dependence is a decreasing one and for CLIE it is an increasing one. It has been shown [6] that such dependencies lead to an additional dispersion of chromatographic peaks, which increases with increasing sorbent fraction width. In CLIE this effect is more pronounced. Taking this so-called capacity broadening into account, we obtain the following expression for the efficiency of the separation column:

$$N_{Ai} = N_{Bi}/(1 + \delta a\sqrt{N_{Bi}d/l})^2 \quad (8)$$

where

$$\delta a = |a_0(d_{max}) - a_0(d_{min})|/[a_0(d_{max}) + a_0(d_{min})]$$

and d_{min} and d_{max} are the values of the fraction limits obtained by approximating the particle size distribution by rectangles with height and area corresponding to the distribution. N_{Bi} is determined from Eqns. 6 and 7.

The dependences illustrated in Fig. 4 can be used to identify the sorbent structure and determine the structural parameters of grains. We have used this approach to study the structure of a strongly basic anion-exchanger sulphonation

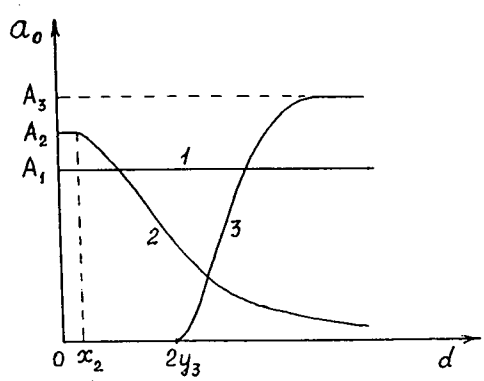

Fig. 4. Dependence of capacity of individual particles on diameter for the various kinds of ion exchangers. 1 = ULIE; 2 = SLIE (x = constant); 3 = CLIE (y = constant).

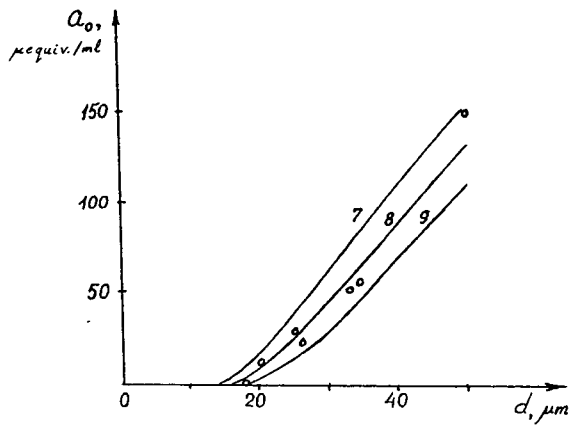

Fig. 5. Dependence of capacity of individual particles on diameter for SAV sorbent. ○ = experimental points; lines = theoretical curves for y = 7, 8 and 9 μm.

product (Sulfirovanniy Anionit Vysokoosnovniy, SAV; Fig. 5). Comparison of the experimental data with Eq. 2 indicated that the experimental conditions permit the production of CLIE characterized by grains not smaller than 16 μm and an envelope thickness of 8 ± 1 μm.

3. Synthesis of centrally localized ion exchangers

As has been pointed out above, the CLIE grain has, in its centre, a nucleus with ion-exchanging groups, enveloped with a layer of a material inert to the ions being exchanged. The main function of such a layer is, first, to impart to the grain the necessary rigidity and make it sufficiently large to prevent a high pressure build-up in columns; second, to ensure rapid transport of ions to the ion-exchanging nucleus and to distribute uniformly the ionic flow on the boundary between the envelope and nucleus; and third, to decrease the sorbent capacity to the necessary level. The first and third properties develop automatically if the particle of ion exchanger is covered with a polymeric or another, sufficiently strong layer of the necessary thickness, and has no affinity for the ions being separated. To possess the second property, the inert envelope should be a porous hydrophilic membrane. One of the candidates for the CLIE

envelope material is an ion exchanger with polarity opposite to that of the functional groups of the nucleus. For example, if the nucleus is an anion exchanger, a macroporous cation exchanger may be used as the envelope. Obviously, the selectivity of such a bipolar sorbent has two components, the anion-exchanging selectivity of the nucleus and the cation-exchanging selectivity of the envelope. In further discussion of the selectivity of CLIE as an ion-chromatographic separation sorbent, we mean the former component.

In our opinion, the most acceptable of the great variety of ways to synthesize chromatographic sorbents is chemical treatment of the grain surface layer. For example, it is possible to prepare CLIE by taking as the starting material an ion exchanger whose properties allow it to be used as the nucleus and whose grains are of the size necessary for the product and removing the functional groups from the surface layer through the required depth. It should be remembered that the envelope should have the above-mentioned properties.

In developing the CLIE preparation method, we were guided not only by the foregoing considerations, but also by the following facts: (1) strongly basic ion exchangers prepared from a styrene–divinylbenzene (SDVB) copolymer partially lose their capacity with time at temperatures around 100°C; (2) in this temperature range it is possible to sulphonate SDVB with concentrated sulphuric acid; (3) the sulphuric acid neutralizes the quaternary ammonium base split off from the anion-exchanger. In addition, the high viscosity, high boiling temperature and weak dissociation of sulphuric acid in the concentrated state promote the formation of a sharp front of the reaction. The sulphonation reaction front makes a boundary between the nucleus and envelope of CLIE, and therefore the ratio of the nucleus size to the envelope size depends on when the reaction front was stopped.

All the necessary parameters of the product (SAV) synthesis and the means of controlling its properties were found experimentally [7]. On the basis of the procedure for SAV preparation used in this Institute, a series of sorbents (KanK) for ion chromatography were developed. These sorbents are manufactured by the Sojuz Lyubertsi Research and Production Association (Lyubertsi, Moscow Region, Russian Federation). Russian ion chromatographs (TSVET-3006, KHPI-1: DOKBA, Dzerzhinsk, Nizhny Novgorod Region, Russian Federation) have utilized KanK sorbents since 1989.

4. Applications of KanK centrally localized ion exchangers

4.1. Conventional applications

The KanK sorbents come in three modifications: KanK-ASt, KanK-ASR and KanK-BP. The fraction size varies from 10 to 16 μm and the fraction dispersion is 20–40%. Each of the sorbent modifications is oriented to its own group of ionic mixtures. Thus, KanK-ASt is intended for ion chromatographic analyses of mixtures of medium-retained anions (F^-, Cl^-, Br^-, NO_2^-, NO_3^-, SO_3^{2-}, SO_4^{2-}, $S_2O_3^{2-}$, CrO_4^{2-}, PO_4^{3-}, $HCOO^-$, $C_2O_4^{2-}$, etc.). Examples of separations of various mixtures of these anions are given in Figs. 6 and 7. The KanK-ASt

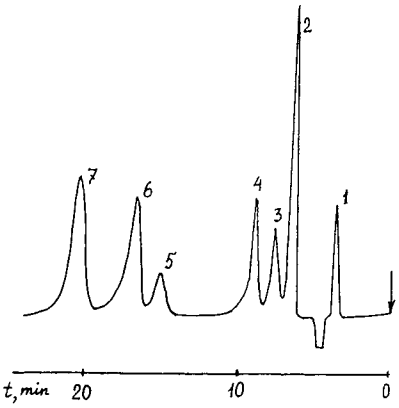

Fig. 6. Typical chromatogram for the separation of an anion mixture. 1 = F^-; 2 = Cl^-; 3 = NO_2^-; 4 = HPO_4^{2-}; 5 = Br^-; 6 = NO_3^-; 7 = SO_4^{2-} (several mg/l of each). Conditions: separation column, 120 × 5 mm I.D. containing KanK-ASt (15 μm); suppressor column, 200 × 6 mm I.D. containing Dowex 50-×8 (H^+ form); eluent, 2.4 m*M* Na_2CO_3–3.0 m*M* $NaHCO_3$–4.0 μ*M* KCNS; flow-rate, 2.3 ml/min.

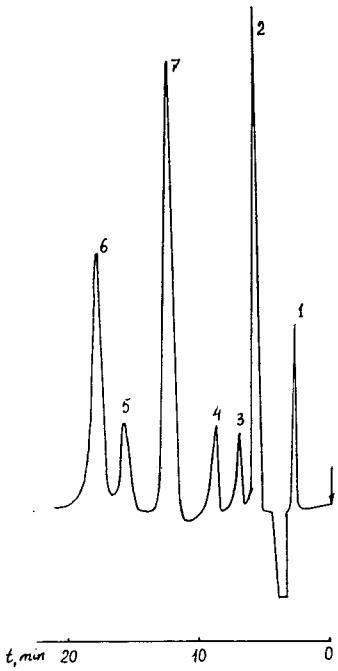

Fig. 7. Reversed separation of the same mixture as in Fig. 6. Conditions as in Fig. 6 except eluent, 9.0 m*M* Na_2CO_3–4.0 m*M* NaOH–5.0 μM KCNS; flow-rate, 1.7 ml/min.

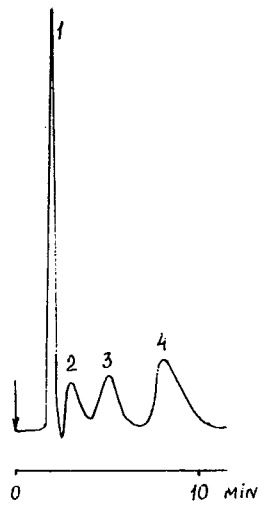

Fig. 8. Typical chromatogram for the separation of a strongly retained anion mixture. 1 = CrO_4^{2-}; 2 = WO_4^{2-}; 3 = I^-; 4 = CNS^- (10 mg/l of each). Conditions: separation column, 120 × 5 mm I.D. containing KanK-ASR (15 μm); suppressor column, 200 × 6 mm I.D. containing Dowex 50-X8 (H^+ form); eluent, 3.0 m*M* Na_2CO_3–3.0 m*M* $NaHCO_3$; flow-rate, 1.7 ml/min.

capacity is 5–20 μequiv./ml. KanK-ASR sorbent is intended for the analysis of mixtures of strongly retained anions (I^-, SCN^-, ClO_4^-, $S_2O_3^{2-}$, CrO_4^{2-}, WO_4^{2-} etc.) (Fig. 8); its capacity is 0.05–1 μequiv./ml. KanK-BP sorbent, featuring an increased anion-exchange capacity (100–300 μequiv./ml), is intended for the analysis of mixtures of weakly retained anions ($HCOO^-$, CH_3COO^-, etc. (Fig. 9).

4.2. New applications

Recently, we have developed highly selective methods for the simultaneous ion chromatographic determination of anions and cations, based on the bipolarity of the KanK sorbents. The methods are based on executing selective reactions in two-column anion chromatographic experiments, which convert the cations under study into either non-conducting substances or anions.

The technique of ammonium ion determina-

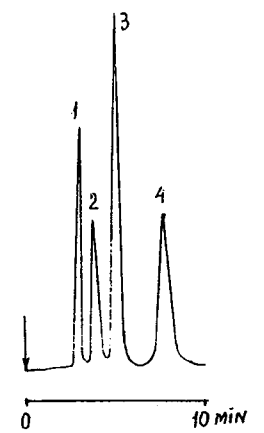

Fig. 9. Typical chromatogram for the separation of a weakly retained anion mixture. 1 = F^-; 2 = CH_3COO^-; 3 = $HCOO^-$; 4 = Cl^- (several mg/l of each). Conditions: separation column 120 × 5 mm I.D. containing KanK-BP (15 μm); suppressor column, 200 × 6 mm I.D. containing Dowex 50-×8 (H^+ form); eluent, 1.0 m*M* Na_2CO_3; flow-rate, 2.0 ml/min.

tion uses a selective reaction between ammonium and nitrous acid, forming nitrogen and water molecules [8], and is executed using the H^+ form of the suppressing sorbent. The eluent is selected so that the retention of ammonium ion of the cation-exchanges layer of the KanK-BP separation sorbent and on the sodium form of the Dowex 50 suppressing sorbent was insignificant, but sufficient for resolving the ammonium peak from the water peak. The eluent contains both hydroxide ions to convert most of the ammonium ions into molecular ammonia and nitrite ions to execute the above reaction. Thus, in this technique the suppressing column serves as a postcolumn reactor for ammonium ions. On the basis that the system is anion exchanging, it is also possible to determine the weakly and medium-retained anions (Fig. 10). To perform the rapid routine determination of ammonium ions, sample anions can be separated by ion exchange, which decreases the time of analysis to 2–3 min and permits an analysis selectivity with respect to the other cations of about 100 and an ammonia detection limit of about 0.1 mg/l.

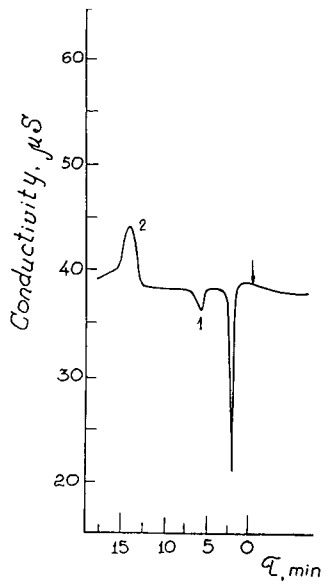

Fig. 10. Chromatogram for highly selective ammonium determination. $1 = NH_4^+$ (0.2 m*M*); $2 = Cl^-$. Conditions as in Fig. 9, except eluent, 1.0 m*M* $NaNO_2$–4.0 m*M* NaOH–0.03% formaldehyde; flow-rate, 1.0 ml/min.

Two other techniques are used to increase considerably the selectivity and sensitivity of the determination of metal ions. They may be defined as methods of anion chromatography using controlled on-column conversion of the analyte cations into anions.

The principles on which the methods are based are as follows:

(1) separation of ions according to the charge sign: stopping of cations and elution of anions;

(2) injection of a reactant that converts metal cations into anions, in an amount necessary for effecting quantitative conversion of the components under analysis;

(3) elution of the resultant anions after the sample anions.

The properties that the system must have are as follows:

(1) the separation sorbent should be bipolar and be highly efficients as regards the separation of anions;

(2) under the conditions maintained in the separation system, the injected reactants should either form strong anion complexes or oxidize the metal ions to the corresponding oxoanions;

(3) the eluent should efficiently separate anions and not given rise to rapid metal hydrolysis.

Let us consider the first method, the controlled on-column formation of anionic complexes of metals [9]. One of the most widespread universal complexing agents having a multiply charged ligand, ethylenediaminetetraacetic acid (EDTA), can be used as the reactant. EDTA and transition metals (M^{2+}), such as Pb, Cd, Zn and Cu, form strong doubly charged anionic complexes, $MEDTA^{2-}$. When an excess amount of EDTA is injected into the system, quantitative conversion of metal cations, pre-stopped in the starting layer of the separation column, into anionic complexes occurs. To elute the anions thus produced, and also accompanying sample anions, a carbonate eluent is used. It is distinguished from the usual eluents by containing ammonium ions, which hinder metal hydrolysis (Fig. 11a).

The principle just considered permits the highly sensitive and selective determination of transition metals, which is clearly demonstrated by the

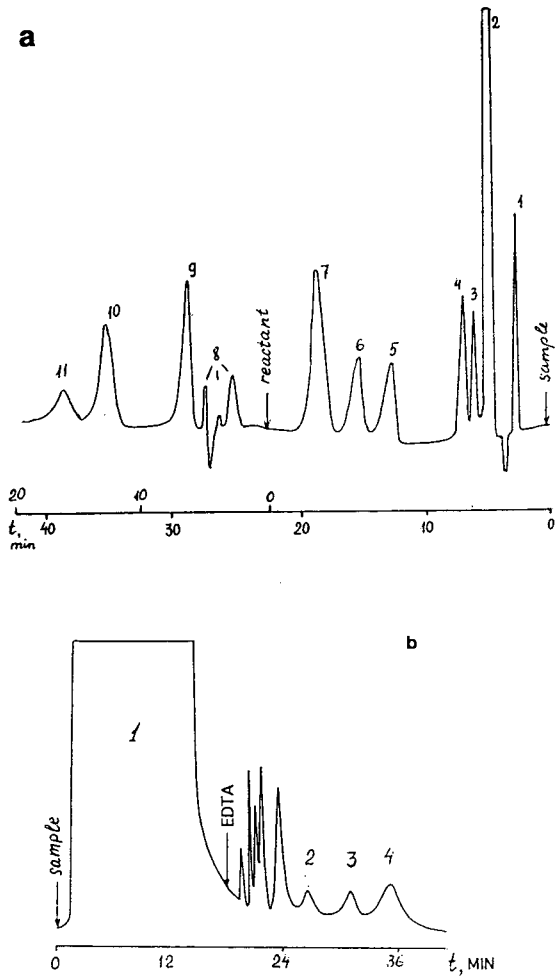

Fig. 11. Simultaneous determination of anions and metal ions. (a) Separation of anion and metal ion mixture. Mixture: $1 = F^-$; $2 = Cl^-$; $3 = NO_2^-$; $4 = HPO_4^{2-}$; $5 = Br^-$; $6 = NO_3^-$; $7 = SO_4^{2-}$; 8 = EDTA; $9 = CdEDTA^{2-}$; $10 = ZnEDTA^{2-}$; $11 = CuEDTA^{2-}$. (b) Black Sea water analysis. 1 = Sample anions; 2 = Cd + Pd (<2.0 μM); 3 = Zn (<5.0 μM); 4 = Cu (<4.0 μM). Conditions: separation column, 120 × 5 mm I.D. containing KanK-ASt; suppressor column, 200 × 6 mm I.D. containing Dowex 50-×8 (H^+ form); eluent, 3.3 mM Na_2CO_3–1.5 mM NH_4HCO_3–4.0 μM KCNS; flow-rate, 2.0 ml/min; reactant, 5.0 mM Na_2EDTA; injection volume, 30 μl.

example of a Black Sea water analysis shown in Fig. 11b.

The second method involves controlled on-column oxidation of transition metals to the corresponding oxoanions. Hydrogen peroxide can be used as the reactant; under basic conditions, it has an oxidation potential of −0.88 V, which, in some instances, is sufficient for oxidizing transition metal cations to oxoanions. For example, the oxidation–reduction potential of the reaction

$$Cr(OH)_3 + 5OH^- \rightleftharpoons CrO_4^{2-} + 4H_2O + 3e^-$$

is 0.13, which makes it possible to use the above reagent to oxidize Cr(III) to Cr(VI) in a basic eluent. When 20–40% hydrogen peroxide is injected into the eluent flow, the quantitative conversion of pre-stopped chromium cations into chromate ions occurs. To elute the chromate ions, and also accompanying anions in the solution under analysis, a carbonate eluent of approximately double strength containing a small amount of a weak oxidant is used to neutralize the reducing potential of the separation column. It is convenient to use iodate ion as the oxidant additive.

The difficult task of the separate determination of jointly present forms of chromium can be simply solved with the aid of the proposed method. A sample containing both chromium forms is injected unchanged into a flow of the eluent described above. The ion chromatographic system includes a separation column packed with KanK-ASt bipolar sorbent and a suppressing column packed with Dowex 50 in the H^+ form. The chromium cations are detained by the starting layer of the separation sorbent and the anions, including chromate ions, participate in the chromatographic separation process and their peaks are recorded on the chromatogram. After all the anions have been eluted and the baseline established, the oxidant is injected into the system and quantitatively converts the pre-stopped chromium cations into chromate ions, the peak of which is well resolved from the oxidant anion peaks and is registered together with appropriate retention time counted from the time of injection of the oxidant (Fig. 12). The described method has very good sensitivity and selectivity for the determination of chromium forms in various water solutions.

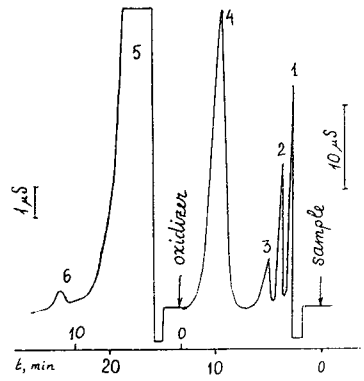

Fig. 12. Determination of different forms of chromium. Mixture: 1 = Cl^-; 2 = SO_4^{2-}; 3 = NO_3^-; 4 = CrO_4^{2-} (12 mg/l); 5 = system peak; 6 = Cr^{3+} (0.5 mg/l). Conditions: separation column, 100 × 3 mm I.D. containing KanK-ASt; suppressor column, 120 × 5 mm I.D. containing Dowex 50-X8 (H^+ form); eluent, 5.0 m*M* Na_2CO_3–0.22 m*M* KIO_3; flow-rate, 0.9 ml/min; reactant, 20% H_2O_2; injection volume, 30 μl. The time scales are plotted with a shift in accordance with injections.

5. Acknowledgement

This work was financially supported by the Russian Foundation for Fundamental Research (Grant No. 93-03-4565).

6. References

[1] P.R. Haddad and P.E. Jackson, *Ion Chromatography —Principles and Applications (Journal of Chromatography Library*, Vol. 46), Elsevier, Amsterdam, 1990, Ch. 3, p. 29.
[2] A.M. Dolgonosov, M.M. Senjavin and I.N. Voloschik, *Ionniy Obmen i Ionnaja Khromatografija (Ion Exchange and Ion Chromatography)*, Nauka, Moscow, 1993 (in Russian).
[3] S. Lindenbaum, C.F. Jumper and G.E. Boyd, *J. Phys. Chem.*, 63 (1959) 1924.
[4] H. Small, T.S. Stevens and W.C. Bauman, *Anal. Chem.*, 47 (1975) 1801.
[5] F. Helfferich, *Ionenaustauscher*, Band 1, Verlag Chemie, Weinheim, 1959, Ch. 8, 3b.
[6] A.M. Dolgonosov, *Zh. Fiz. Khim.*, 60 (1986) 3074.
[7] A.M. Dolgonosov, *Russ. Pat.*, 1 161 513 (1992) [Copyright Certificate SU 1161513 A; *Byull. Izobret.*, No. 22 (1985)].
[8] A.M. Dolgonosov and A.N. Krachak, *J. Chromatogr.*, 640 (1993) 351.
[9] A.M. Dolgonosov, *React. Polym.*, 17 (1992) 95.

ELSEVIER

Journal of Chromatography A, 671 (1994) 43–49

JOURNAL OF CHROMATOGRAPHY A

Ion chromatographic separation of transition metals on a polybutadiene maleic acid-coated stationary phase

Lakshmy M. Nair,* Raaidah Saari-Nordhaus, James M. Anderson, Jr.

Alltech Associates, 2051 Waukegan Road, Deerfield, IL 60015, USA

Abstract

Transition metals are traditionally analyzed by cation-exchange or ion-pair chromatography. Divalent metal ions are separated on sulfonic acid cation stationary phase using various eluents along with conductivity detection. An alternative method is reversed-phase ion-pair chromatography coupled with conductivity detection. This method of detection is not very sensitive for transition metals. For better separation and sensitivity, UV–Vis detection along with pre- or post-column derivatization with an absorbing ligand is the most common method applied. This method is messy and complicated.

This paper describes the separation of transition metals on a polybutadiene maleic acid stationary phase. This cation-exchange stationary phase has been successfully applied for the simultaneous separation of mono- and divalent cations. Several cations including group I and group II cations along with transition metals can be analyzed using complexing acid eluents. Detection limits and the effect of different eluent concentrations are discussed.

1. Introduction

Traditional ion chromatography techniques for the determination of transition metals are based on ion-pair chromatography, cation-exchange chromatography or coordination chromatography. Reversed-phase ion interaction chromatography or ion-pair chromatography is the most common method used for the determination of transition metals [1]. The transition metals are separated on a reversed-phase stationary phase using an eluent containing an ion-pairing reagent and detected by conductivity or post-column derivatization and UV–Vis detection. Conductivity detection provides detection sensitivity for transition metals in the ppm (mg/l) range. Post-column derivatization along with UV–Vis detection is free of interferences and is more sensitive. A light-absorbing chelating reagent such as pyridilazoresorcinol (PAR) is used to complex the metal ions which are then detected at 520 nm. However this method requires messy reagents and complicated instrumentation.

Cation-exchange chromatography along with conductivity detection is another method used for the determination of transition metals. Divalent metal ions including heavy metal ions are separated on conventional sulfonic acid columns and detected by conductivity detection. For effective elution of divalent metal ions, an eluent containing a divalent cation is required. For example an eluent containing ethylenediammonium tartrate is used to separate several divalent metal ions on the conventional sulfonic acid columns [2]. Usage of such a complexing eluent along with the addition of a complexing reagent to the sample has also been reported [2]. For example, ethylenediamine tetraacetic acid

* Corresponding author.

0021-9673/94/$07.00
SSDI 0021-9673(94)00037-A

(EDTA) and nitrotriacetic acid (NTA) are added to the sample to improve the separation [2]. Cation exchange separation along with post-column UV detection is another common method used to determine transition metals [3]. Even though this method improves the sensitivity of metal ions as mentioned earlier, requirement of stringent instrumentation and messy post column reagents makes it less desirable.

A convenient and frequently used method for the determination of metal ions is by coordination chromatography. Metal ions are separated on a stationary phase made of resin or silica material in which a suitable ligand is immobilized. One of the most common chelating stationary phase is a silica-based imminodiacetic acid (IDA) stationary phase, which exhibits different complexing abilities towards different transition metals [4]. A weak carboxylic acid is the functional group on this stationary phase. The retention of cations are controlled by the concentration of the complexing agent and the pH of the eluent. Weak complexing acids such as citric acid, tartaric acid or strong complexing acids such as pyridine-2,6-dicarboxylic acid or nitrilotriacetic acid are used for the separation.

This paper describes the application of an alternative stationary phase made of polybutadiene maleic acid (PBDMA) coated on silica material for the determination of transition metals. The column has been successfully used for the simultaneous separation of mono and divalent cations. This report focuses on the separation of several transition metal ions on this stationary phase using a mixture of two different complexing acids. By changing the eluent concentrations, different metal ions can be separated along with mono and divalent cations.

2. Experimental

The Alltech modular ion chromatography system (Alltech Associates, Deerfield, IL, USA) which includes Model 325 HPLC pump, Model 320 conductivity detector, Model 330 column heater and Model 9125 injection valve was used for all applications. The temperature of the column and the detector cell were maintained at 35°C. All data were recorded by a Model SP 4400 chromjet integrator (Spectra-Physics, Santa Clara, CA, USA). A column packed with PBDMA coated on silica material (Alltech Universal Cation Column, 100 mm × 4.6 mm) was used for the separation of metal ions.

All eluents and standards were prepared from reagent grade chemicals (Aldrich, Milwaukee, WI, USA) and deionized (18 MΩ) water. Stock solutions of 100 m*M* tartaric and oxalic acids were prepared and these solutions were diluted to prepare mixtures of tartaric and oxalic acid eluents.

2.1. Sample preparation

The fermentation broth and cooling tower water samples were diluted with deionized water before injection. To prepare the plant material for ion chromatographic analysis, 1 g of bean leaves was ashed at 600°C for 6 h and 0.1 g of this sample was dissolved in 100 ml of deionized water containing 0.2 ml of 12 *M* hydrochloric acid. This sample was then diluted five times and injected on the ion chromatograph. The brass ferrule was dissolved in concentrated nitric acid and 0.5 ml of this sample was diluted in 50 ml of deionized water before injection.

3. Results and discussion

Separation of mono- and divalent cations on the PBDMA stationary phase using various eluents and electrical conductivity detection has been reported by several authors. Some of these eluents are organic complexing acids such as citric acid, tartaric acid, phthalic acid, salicyclic acid and pyridine- 2,6-dicarboxylic acid and mineral acid eluents such as hydrochloric acid [5]. Mineral acid eluents are not suitable for transition metal analysis because many transition metals do not form complexes with chloride or nitrate and will not be eluted from the stationary phase. Organic acid eluents such as citric, tartaric or phthalic acid eluents can separate a few

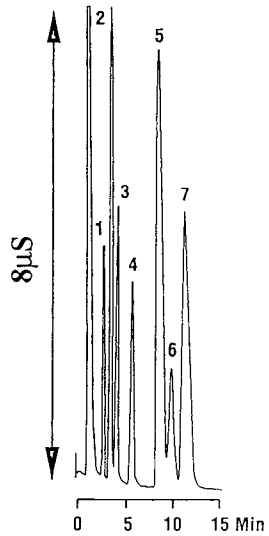

Fig. 1. Citric acid eluent on PBDMA stationary phase. Peaks: 1 = lithium (0.2 mg/l); 2 = sodium (1.5 mg/l); 3 = ammonium (1.5 mg/l); 4 = potassium (2.5 mg/l); 5 = magnesium (2 mg/l); 6 = iron(II) (5 mg/l); 7 = calcium (2 mg/l). Column: Universal Cation (100 mm × 4.6 mm); eluent: 7 m*M* citric acid; flow-rate: 1 ml/min; detector: conductivity; injection volume: 100 μl.

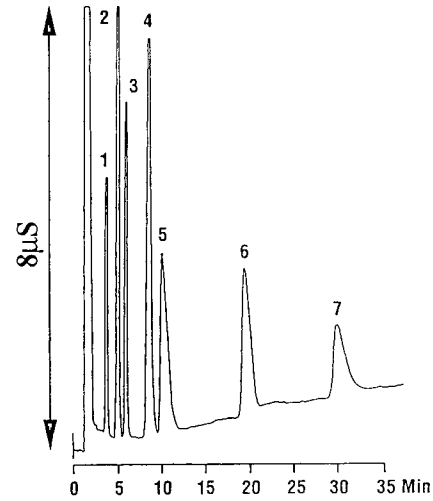

Fig. 2. Oxalic acid eluent on PBDMA stationary phase. Peaks: 1 = lithium (0.2 ppm); 2 = sodium (1.5 mg/l); 3 = ammonium (1.5 mg/l); 4 = zinc, nickel, cobalt; 5 = potassium (2.5 mg/l); 6 = magnesium (2 mg/l); 7 = calcium (2 mg/l). Column: Universal Cation (100 mm × 4.6 mm); eluent: 2 m*M* oxalic acid; flow-rate: 1 ml/min; detector: conductivity; injection volume: 100 μl.

transition metals on the PBDMA stationary phase.

Fig. 1 shows the separation of iron(II) on the PBDMA stationary phase using 7 m*M* citric acid. With this eluent, iron(II) is eluted between magnesium and calcium. If other transition metals such as zinc, manganese, cobalt or nickel were present in the sample they all will be eluted at the same retention time as iron(II). The same results were obtained with tartaric, phthalic or salicyclic acid eluents. These organic acids exhibit similar properties hence changing the eluents from citric to tartaric, phthalic or salicylic acids did not affect the retention time of the metal ions [6].

Oxalic acid was also investigated as an eluent for the separation of transition metals on the PBDMA stationary phase. Fig. 2 shows the separation of transition metals along with mono-/divalent cations using oxalic acid eluent on the PBDMA stationary phase. Under these conditions the transition metals eluted before the divalent cations and some are co-eluting with the monovalent cations. The metal complexes of oxalic acid are more stable than those of divalent cations and hence they elute first [7]. Another drawback with this eluent is that the retention time of divalent cations is too long.

A mixture of tartaric and oxalic acids was investigated as a possible eluent for the separation. Fig. 3a shows the separation of transition metals on the PBDMA stationary phase using a combination of 2 m*M* tartaric acid and 1 m*M* oxalic acid. Fig. 3b shows the separation of mono- and divalent cations using the same conditions. If the above sample had manganese or cadmium they will co-elute with magnesium and calcium, respectively. However, the separation of lithium, sodium, ammonium, potassium, nickel, zinc, cobalt, magnesium and calcium is very good.

To solve the co-elution problem of manganese and cadmium with divalent cations a different type of eluent was developed. By adding pyridine-2,6-dicarboxylic acid (PDCA) to tartaric acid, a change in selectivity for the divalent cations was found as shown in Fig. 4. Under

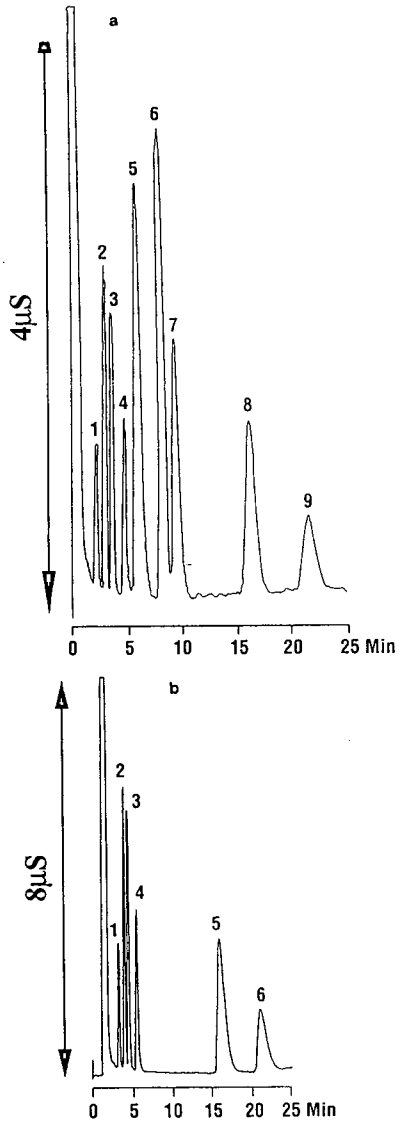

Fig. 3. (a) Separation of transition metals using a mixture of tartaric and oxalic acid eluent. Peaks: 1 = lithium (0.1 ppm); 2 = sodium (0.75 mg/l); 3 = ammonium (0.75 mg/l); 4 = potassium (1.3 mg/l); 5 = nickel (5 mg/l); 6 = zinc (5 mg/l); 7 = cobalt (5 ppm); 8 = manganese (5 mg/l); 9 = cadmium (5 mg/l). Column: Universal Cation (100 mm × 4.6 mm); eluent: 2 m*M* tartaric acid–1 m*M* oxalic acid; flow-rate: 1 ml/min; detector: conductivity; injection volume: 100 μl. (b) Mono- and divalent cation analysis using a mixture of tartaric and oxalic acid eluent. Peaks: 1 = lithium (0.2 ppm); 2 = sodium (1.5 mg/l); 3 = ammonium (1.5 mg/l); 4 = potassium (2.5 mg/l); 5 = magnesium (2 ppm); 6 = calcium (2 ppm). Column: Universal Cation (100 mm × 4.6 mm); eluent: 2 m*M* tartaric acid–1 m*M* oxalic acid; flow-rate: 1 ml/min; detector: conductivity; injection volume: 100 μl.

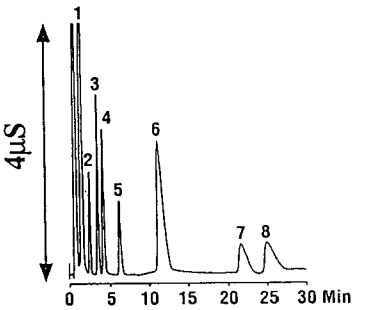

Fig. 4. Separation of cadmium and manganese on PBDMA stationary phase peaks: 1 = cadmium (10 mg/l); 2 = lithium (0.2 ppm); 3 = sodium (1.5 mg/l); 4 = ammonium (1.5 mg/l); 5 = potassium (2.5 mg/l); 6 = manganese (10 mg/l); 7 = calcium (2 mg/l); 8 = magnesium (2 ppm). Column: Universal Cation (100 mm × 4.6 mm); eluent: 3m*M* tartaric acid–0.5 m*M* PDCA; flow-rate: 1.5 ml/min; detector: conductivity; injection volume: 100 μl.

these conditions, calcium eluted before magnesium. This is due to the formation of strong complexes of Ca–PDCA which is much more stable than Mg–PDCA [8]. Magnesium and manganese can be separated by this eluent. The same eluent is useful for the separation of cadmium which elutes before lithium as shown in Fig. 4. If the sample contain other transition metals they may co-elute with cadmium.

By changing the concentrations of tartaric and oxalic acids different transition metals can be separated on the PBDMA column. For example, Fig. 5 shows the separation of copper, sodium, ammonium, potassium, zinc, cobalt, magnesium, calcium and lead with an eluent containing 1.5 m*M* tartaric and 1 m*M* oxalic acids. Under these conditions retention time for lead is excessive. A combination of 3 m*M* tartaric–2 m*M* oxalic acid eluent was found suitable for the determination of lead. Fig. 6 shows the separation of copper, sodium, ammonium, potassium, zinc, magnesium, calcium and lead. Under these conditions retention time for lead is reduced to 25 min.

The separation and retention of metal ions on the PBDMA stationary phase is greatly influenced by various eluent concentrations. The elution ability of the organic acids in the eluent dependent upon their dissociation and complex-

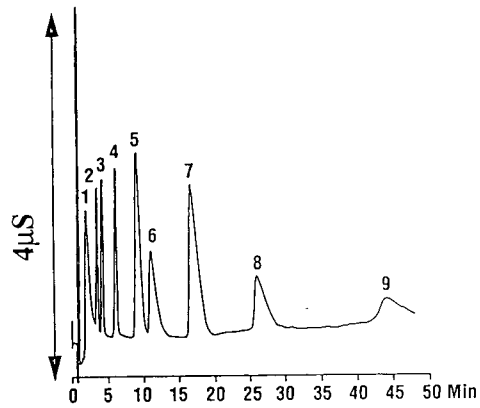

Fig. 5. Separation of transition metals using tartaric and oxalic acid eluent. Peaks: 1 = copper (10 mg/l); 2 = sodium (0.75 mg/l); 3 = ammonium (0.75 mg/l); 4 = potassium (1.3 mg/l); 5 = zinc (10 mg/l); 6 = cobalt (10 mg/l); 7 = magnesium (2 mg/l); 8 = calcium (2 mg/l); 9 = lead (10 mg/l). Column: Universal Cation (100 mm × 4.6 mm); eluent: 1.5 m*M* tartaric acid–1 m*M* oxalic acid; flow-rate: 1.5 ml/min; detector: conductivity; injection volume: 100 μl.

ing stability constants as well as the concentrations used. The eluent pH also affect the retention of metal ions on the PBDMA stationary phase. An increase in pH dramatically decreases the retention time for transition metals and other cations. When the eluent pH was increased from 2.4 (eluent pH unadjusted) to 3.4, all transition metal ions and other cations were co-eluted with each other. This may be due to the strong complex formation of metal ions at a higher pH which causes the metal ions to move rapidly through the column. For complete separation of metal ions, the eluent pH should be kept low so the complexation is only partial [8].

The detection limits (calculated as a signal-to-noise ratio of 3) obtained for transition metals using tartaric acid–oxalic acid eluent, based on a 100 μl injection are shown in Table 1. The detection limits vary from 45 to 410 μg/l. Even though post-column derivatization is more sensitive for the determination of transition metals, the simplicity of the methods described here are much more desirable. The plots of peak area *vs.* concentrations of zinc and cadmium gave linear calibration curves over two orders of magnitude. Correlation coefficients (*r*) for peak area response against ionic concentrations for zinc and cadmium ions were 0.999 and 0.998, respectively.

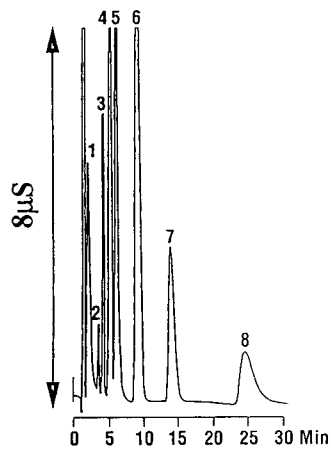

Fig. 6. Effect of higher eluent concentration on PBDMA column: Peaks: 1 = copper (10 mg/l); 2 = sodium (0.75 mg/l); 3 = ammonium (0.75 mg/l); 4 = potassium (1.3 mg/l); 5 = zinc (10 mg/l); 6 = magnesium (2 mg/l); 7 = calcium (2 mg/l); 8 = lead (10 mg/l). Column: Universal Cation (100 mm × 4.6 mm); eluent: 3 m*M* tartaric acid–2 m*M* oxalic acid; flow-rate: 1.5 ml/min; detector: conductivity; injection volume: 100 μl.

3.1. Applications

Many samples contain transition metals and mono-/divalent cations and by choosing optimum conditions, PBDMA stationary phase can

Table 1
Method detection limits for transition metals

Transition metals	Method detection limit[a] (mg/l)
Zinc	0.045
Cobalt	0.120
Manganese	0.040
Copper	0.150
Cadmium	0.035
Lead	0.410
Nickel	0.150
Iron(II)	0.060

[a] Injection volume 100 μl; calculated as 3 × signal-to-noise ratio.

separate these species simultaneously. Some examples of applications are given here. Fig. 7a shows the ion chromatographic separation of sodium, potassium, zinc, magnesium and calcium in cooling tower water. Separation of copper and zinc in brass ferrule is shown in Fig. 7b. Figs. 7c and d show chromatograms of plant extract and fermentation broth, respectively.

4. Conclusions

PBDMA stationary phase provides a simple ion chromatographic method for the separation of transition metals. By using a mixture of two complexing acids, tartaric and oxalic acids, various metal ions can be separated along with mono- and divalent cations. The method is

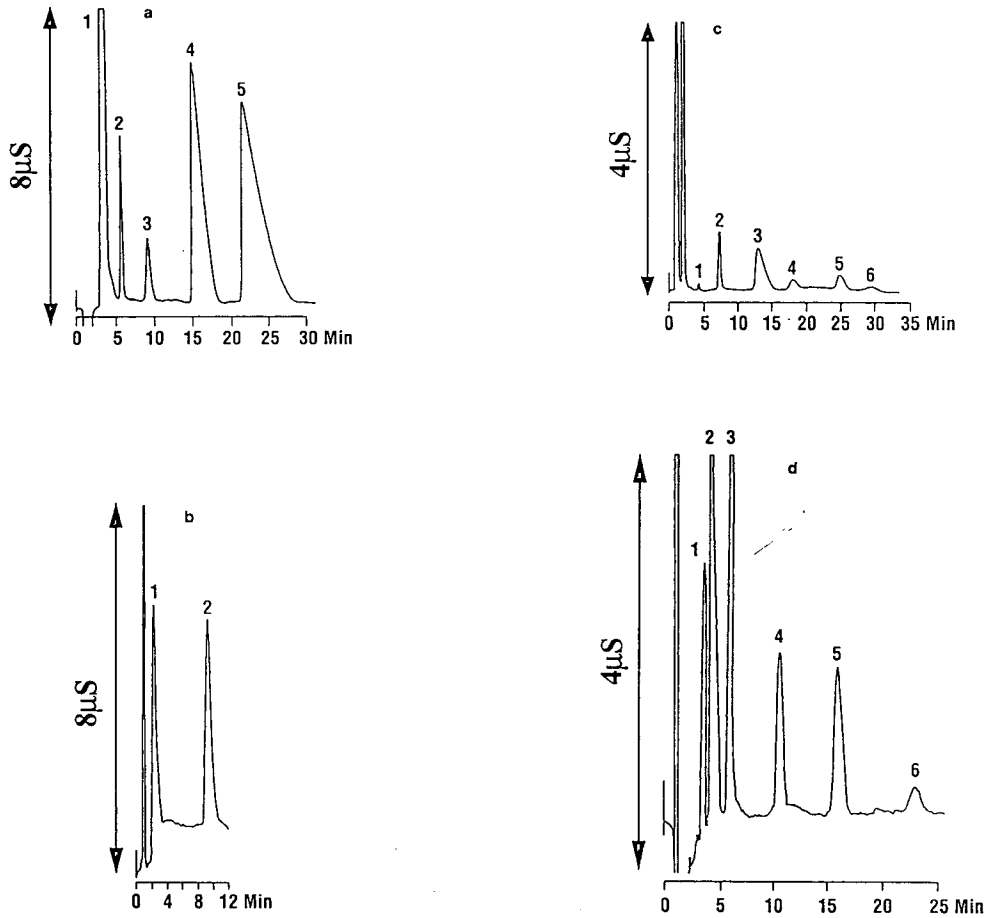

Fig. 7. (a) Cooling tower water. Peaks: 1 = sodium; 2 = potassium; 3 = zinc; 4 = magnesium; 5 = calcium. Column: Universal Cation (100 mm × 4.6 mm); eluent: 1.5 m*M* tartaric acid–1 m*M* oxalic acid; flow-rate: 1.5 ml/min; detector: conductivity; injection volume: 100 μl. (b) Brass ferrule. Peaks: 1 = copper; 2 = zinc. Column: Universal Cation (100 mm × 4.6 mm); eluent: 3 m*M* tartaric acid–2 m*M* oxalic acid; flow-rate: 1.5 ml/min; detector: conductivity; injection volume: 100 μl. (c) Manganese in soybean leaves. Peaks: 1 = sodium; 2 = potassium; 3 = manganese; 4 = unknown; 5 = calcium; 6 = magnesium. Column: Universal Cation (100 mm × 4.6 mm); eluent: 3 m*M* tartaric acid–0.5 m*M* PDCA; flow-rate: 1 ml/min; detector: conductivity; injection volume: 100 μl. (d) Fermentation broth. Peaks: 1 = sodium; 2 = ammonium; 3 = potassium; 4 = magnesium; 5 = calcium; 6 = lead. Column: Universal Cation (100 × mm × 4.6 mm); eluent: 3 m*M* tartaric acid–2 m*M* oxalic acid; flow-rate: 1.5 ml/min; detector: conductivity; injection volume: 100 μl.

simple and less complicated compared to many existing methods. The detection limits for transition metals are in the μg/l range. The ability of PBDMA stationary phase to separate transition metals from mono-/divalent cations is useful for routine analysis of many samples.

References

[1] Cassidy and Elchuk, *Anal. Chem.*, 54 (1982) 1558.
[2] D.T. Gerde and J.S. Fritz, *Ion Chromatography*, Hüthig, New York, 2nd ed., 1987, Ch. 9.
[3] P.R. Haddad and P.E. Jackson, *Ion Chromatography —Principles and Applications*, Elsevier, Amsterdam, 1990, Ch. 4.
[4] G. Bonn, S. Reiffenstuhl and P. Jandik, *J. Chromatogr.*, 499 (1990) 669.
[5] L.M. Nair, R. Saari-Nordhaus and James M. Anderson, Jr., *J. Chromatogr.*, 640 (1993) 41.
[6] G. Schomburg, P. Kolla and M.W. Laubli, *Am. Lab.*, 21 (1989) 92.
[7] D. Yan and G. Schwedt, *Anal. Chim Acta*, 178 (1985) 347.
[8] D. Yan and G. Schwedt, *Anal. Chem.*, 338 (1990) 149.

ELSEVIER

Journal of Chromatography A, 671 (1994) 51–54

JOURNAL OF CHROMATOGRAPHY A

Separation of transition and heavy metals on an amidoxime complexing sorbent

I.N. Voloschik*, M.L. Litvina, B.A. Rudenko

V.I. Vernadsky Institute of Geochemistry and Analytical Chemistry, Russian Academy of Science, 19 Kosygin Street, 117975 Moscow, Russian Federation

Abstract

A silica gel-based sorbent with chemically bonded amidoxime functional groups was applied to the determination of transition and heavy metals. The sorbent has both complexing and anion-exchanging properties. The separation of transition and heavy metals showed high selectivity. Solutions of complexing acids (oxalic and dipicolinic) were used as eluents. The dependence of metal retention on pH and the concentration and nature of the complexing agents was studied. For Mn^{2+}, Cd^{2+}, Pb^{2+}, Co^{2+}, Ni^{2+}, Zn^{2+}, Cu^{2+} and Hg^{2+} selective separation was achieved by gradient elution with oxalic acid as the eluent on a 100 × 3 mm I.D. column in 10 min. The interference of Fe^{3+} was completely eliminated, as this metal is very strongly retained on the sorbent. UV detection with postcolumn reaction with 4-(2-pyridylazo)resorcinol was used.

1. Introduction

The use of complexing sorbents in ion-exchange chromatography has led to considerable progress in the analysis of transition and heavy metals. Sorbents with iminodiacetic [1–3] and dithiocarbamate [4] functional groups have been successfully used for metal separations. In this work, a silica gel-based sorbent with chemically bonded amidoxime functional groups was applied to the determination of transition and heavy metals. The sorbent structure is

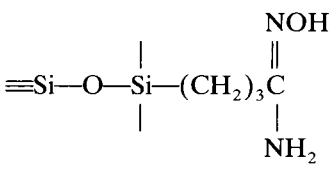

Previously this sorbent was used only for the sorbent was used only for the sorption and separation of Fe^{3+}, V^{5+}, Cu^{2+} and Mo^{5+} cations [5–7]. The amidoxime NH_2 groups are responsible for both the sorbent's anion-exchange and complexing ability. An amidoxime complexing sorbent can be applied to the selective ion chromatographic (IC) determination in waters of Mn^{2+}, Pb^{2+}, Cd^{2+}, Co^{2+}, Ni^{2+}, Zn^{2+}, Cu^{2+} and Hg^{2+}.

2. Experimental

The chromatographic system consisted of a double-piston pump (Dokba, Russian Federation), a reagent-delivery module for postcolumn derivatization and a UV–Vis detector (LCD 2563; Prague, Czech Republic). Sample injection was carried out with a Rheodyne (Berkeley, CA,

* Corresponding author.

0021-9673/94/$07.00
SSDI 0021-9673(94)00201-J

USA) Model 7125 valve equipped with a 100-μl loop. The separation was carried out on 50 × 3 mm I.D. and 100 × 3 mm I.D. stainless-steel columns packed with Amidoxim (Elsiko, Russian Federation) amidoxime-based sorbent.

Solutions of 5 m*M* oxalic acid with several pH values, solutions of 5–15 m*M* oxalic acid and a solution of 8 m*M* oxalic acid–0.5 m*M* dipicolinic acid were used as eluents. The pH of the oxalic acid solutions was adjusted by the addition of sodium hydroxide. The eluent flow-rate was maintained at 1.0 ml/min. After leaving the analytical column, the eluate stream was mixed with a postcolumn reagent, which was delivered by nitrogen pressure providing of flow-rate of 0.3 ml/min. The postcolumn reagent contained 0.5 m*M* sodium 4-(2-pyridylazo)resorcinol (PAR) in 3 *M* ammonia solution and 1 *M* acetic acid. The coloured complexes of metal ions were monitored for absorption at 540 nm. All solvents were of analytical-reagent grade.

3. Results and discussion

Solutions of tartaric, citric, oxalic and dipicolinic acid were tried as eluents. It was found that tartaric and citric acid did not provide a good simultaneous separation of the transition metal cations. The low selectivity of separation with these eluents is analogous to that obtained with 3 m*M* HNO_3 (Fig. 1). As can be seen, only Cu^{2+} cations show sufficiently strong retention on this sorbent; Zn^{2+}, Ni^{2+}, Co^{2+}, Cd^{2+} and Pb^{2+} are weakly retained on the amidoxime sorbent under these conditions. However, all these metals are separated on the amidoxime sorbent-packed column using an eluent containing 5 m*M* oxalic acid or a mixture of 8 m*M* oxalic and 0.5 m*M* dipicolinic acid. This presumably occurs because of the higher stability of the anionic metal complexes produced by these acids in the eluent than the stability of such complexes in the case of tartaric and citric acid. The anionic metal complexes are sorbed by the amidoxime basic groups and are separated (Fig. 2). The eluent pH exerts affects the degree of separation and the order of elution.

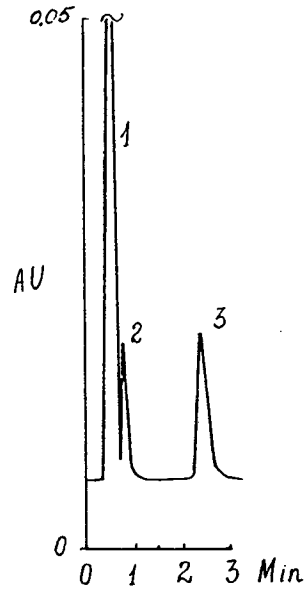

Fig. 1. Chromatogram of transition metals on the Amidoxim column with nitric acid as eluent. Column, 50 × 3 mm I.D. packed with Amidoxim sorbent; eluent, 3 m*M* HNO_3 (pH 2.5); flow-rate, 1 ml/min; detection, UV–Vis; postcolumn reaction with PAR. Peaks: 1 = Cd^{2+}, Ni^{2+}, Co^{2+}, Pb^{2+}; 2 = Zn^{2+}; 3 = Cu^{2+}.

The graphs for the dependence of some transition metal retention times on oxalic acid eluent pH value are shown in Fig. 3. The sorbent's chelating properties and its anion-exchange properties contribute to the retention of the metals. With a decrease in pH, the chelating ability of the sorbent and oxalate also decreases, which leads to a decrease in the metal retention times. With an increase in pH, the anion-exchange capacity of the sorbent decreases and the eluting ability of oxalate increases, which also leads to a decrease in the metal retention times. These facts explain the presence of maxima on the curves (Fig. 3).

The eluent pH exerts a very strong influence on the retention time of Cu^{2+}, which may be due to the especially powerful complexing ability of Cu^{2+}. As Fig. 3 shows, the best and fastest separation of the metals is achieved using an eluent of pH 3.6. The separation under these conditions is shown in Fig. 4. An increase in eluent concentration produces a decrease in the

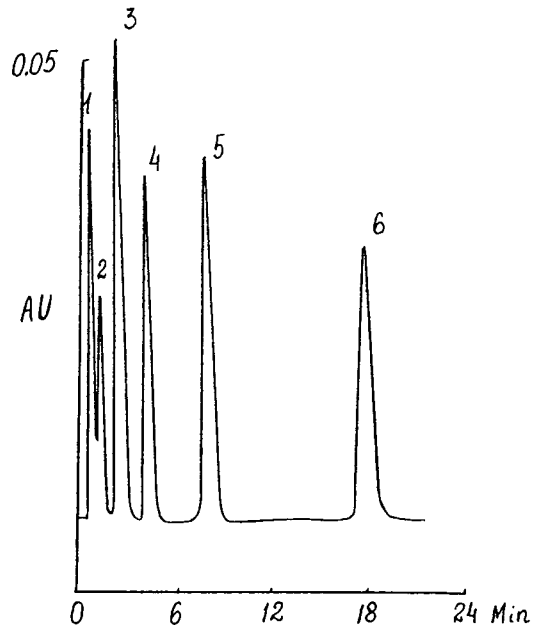

Fig. 2. Separation of transition metal ions on the Amidoxim column using oxalic acid as eluent. Eluent, 5 m*M* oxalic acid (pH 2.2); other conditions as in Fig. 1. Peaks: 1 = Cd^{2+}; 2 = Pb^{2+}; 3 = Co^{2+}; 4 = Zn^{2+}; 5 = Ni^{2+}; 6 = Cu^{2+}.

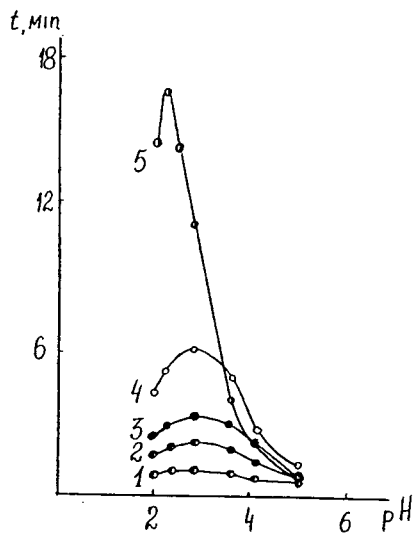

Fig. 3. Graphs of retention time *versus* oxalic acid eluent pH for some transition metals. Column, 50 × 3 mm I.D. packed with Amidoxim sorbent; eluent, 5 m*M* oxalic acid with various pH values; flow-rate, 1 ml/min; detection, UV–Vis; postcolumn reaction with PAR. 1 = Cd^{2+}; 2 = Co^{2+}; 3 = Zn^{2+}; 4 = Ni^{2+}; 5 = Cu^{2+}.

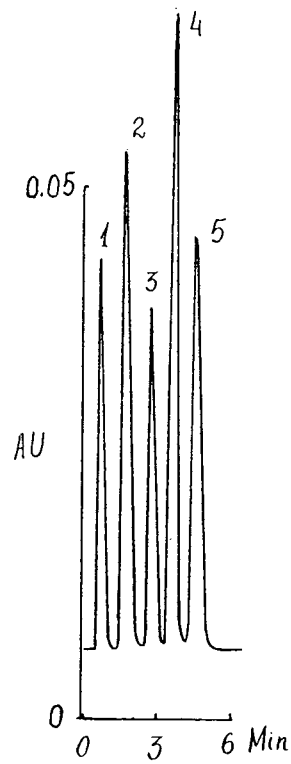

Fig. 4. Separation of transition metals on the Amidoxim column with sodium oxalate as eluent. Eluent, 5 m*M* sodium oxalate (pH 3.6); other conditions as in Fig. 1. Peaks: 1 = Cd^{2+}; 2 = Co^{2+}; 3 = Zn^{2+}; 4 = Cu^{2+}; 5 = Ni^{2+}.

retention times of the anionic metal complexes. For this reason, on acceptable retention time for the Hg^{2+} cation, which is very strongly retained on the amidoxime sorbent, can be obtained (Fig. 5).

The application of gradient elution noticeably decreases the analysis time, preserving the multicomponent character of the analysis.

One of the specific features of the amidoxime sorbent is the weak affinity to Mg and Ca and the very strong affinity to Fe. This makes it possible to eliminate their interference in the determination of Zn^{2+}, Co^{2+}, Ni^{2+}, Cu^{2+} and Hg^{2+}.

The amidoxime sorbent-filled column has a long lifetime. The degree of separation on the amidoxime column increases on adding dipicolinic acid to the oxalic eluent, as more stable

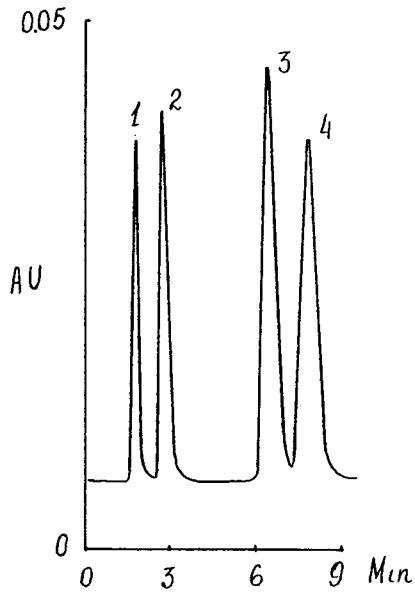

Fig. 5. Determination of Hg^{2+} on the Amidoxim column with oxalic acid as eluent. Eluent, 15 m*M* oxalic acid (pH 1.8); other conditions as in Fig. 1. Peaks: 1 = Zn^{2+}; 2 = Ni^{2+}; 3 = Cu^{2+}; 4 = Hg^{2+}.

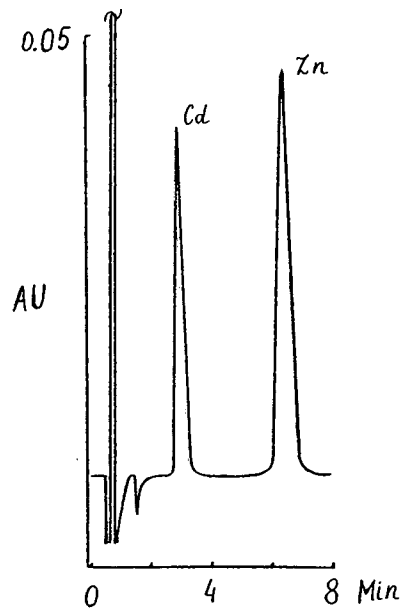

Fig. 6. Determination of Cd^{2+} and Zn^{2+} on the Amidoxim column using oxalic acid–dipicolinic acid as eluent. Eluent, 4 m*M* oxalic acid–4 m*M* sodium oxalate–0.5 m*M* dipicolinic acid (pH 3.4); detection, UV at 254 nm; other conditions as in Fig. 1.

and strongly retained metal dipicolinic complexes are formed. In this instance direct UV detection of the separated metal complexes at 254 nm was applied (Fig. 6).

The elution conditions developed may be used for quantitative analysis. For example, the results for Cu^{2+} determination were certified value 5.0 ppm and found (mean ± S.D.) 5.1 ± 0.1 ppm ($n = 5$). Chromatographic conditions for the rapid separation and determination of Zn^{2+}, Co^{2+}, Pb^{2+}, Cd^{2+}, Hg^{2+} and Cu^{2+} in water samples were established. The technique involves the application of standard spectrophotometric conditions for the detection of metals with postcolumn reaction with PAR.

References

[1] E.M. Moyers and J.S. Fritz, *Anal. Chem.*, 49 (1977) 418.
[2] G. Bonn, S. Reiffenstuhl and P. Jandik, *J. Chromatogr.*, 499 (1990) 669.
[3] G. Bonn, S. Nathakarnikitkool and P. Jandik, in P. Jandik and R.M. Cassidy (Editors), *Advances in Ion Chromatography*, Vol. 1, Century International, Medfield, MA, 1991, p. 197.
[4] R. Raja, *Am. Lab.*, 14 (1982) 35.
[5] C.H. Risner and J.R. Jezorek, *Anal. Chim. Acta*, 186 (1986) 233.
[6] I.B. Yuferova, G.V. Kudriavtsev, T.I. Tihomirova and V.N. Fadeeva, *Zn. Anal. Khim.*, 43 (1988) 1643.
[7] P.N. Nesterenko, T.I. Tihomirova, V.N. Fadeeva, I.B. Yuferova and Q.V. Kudriavtsev, *Zh. Anal. Khim.*, 46 (1991) 1108.

ELSEVIER

Journal of Chromatography A, 671 (1994) 55–62

JOURNAL OF CHROMATOGRAPHY A

Anion separations on columns based on transition metal–macrocycle complex exchange sites

John D. Lamb*, Robert G. Smith, Randal C. Anderson, Max K. Mortensen

Department of Chemistry, Brigham Young University, Provo, UT 84602, USA

Abstract

Macrocycle-based ion chromatographic columns can provide fast and effective separations of inorganic anions. Chromatographic columns based on nitrogen-containing macrocycles such as cryptand decyl-2.2.2 (D222) and didecyl-diaza-18-crown-6 (DD22) have high affinities for transition metal cations. This work compares the chromatographic separation of anions using transition metal cation eluents in columns based on the macrocyclic ligands DD22 and D222 adsorbed on two different polystyrene resins, MPIC and AS10 (Dionex). When a transition metal ion, *e.g.* Cu^{2+}, Ni^{2+}, or Co^{2+}, was present in the mobile phase flowing through an MPIC column loaded with didecyl-diaza-18-crown-6, anion separations of differing selectivities were obtained. Separations of anions were achieved with these columns even when only a cation that has low affinity for the macrocycles, such as Li^{+}, was included in the mobile phase. This is due to protonation of the nitrogen atoms in the macrocycles. Columns based on the AS10 type resin produced much higher efficiency and shorter retention times than did columns based on the MPIC resin.

1. Introduction

The unique selectivity of crown ethers and cryptands has been widely used in performing many types of separations including chromatographic separations [1–5]. Anions as well as cations can be separated on macrocycle-based columns. Because most macrocycles are uncharged, anion separator columns can be generated when macrocycle-cation complexes form on the column and serve as anion exchange sites. Anions must be associated with the positively charged complexes to maintain electrical neutrality on the column. Since macrocycles are generally hydrophobic and are associated with the hydrophobic environment of the column, the more hydrophobic anions are retained most strongly [6–9].

In our laboratory, we have developed a macrocycle-based anion separation system that involves an ion-exchange mechanism (as opposed to a ligand-exchange mechanism, described below) by the inclusion of an alkali metal hydroxide in the eluent [10–13]. Eluent alkali metal cations form cationic complexes with the neutral column macrocycles. Gradient separations of anions have been performed by changing the eluent alkali metal cation from one with a high affinity for the column macrocycle to one of lower affinity. In such a gradient system, the column anion exchange capacity decreases during the course of the separation [11–13].

Transition metal cation–macrocycle complexes

* Corresponding author.

0021-9673/94/$07.00
SSDI 0021-9673(93)E1152-P

have the potential to function in this type of ion chromatographic system not only by an ion exchange mode, but also by a ligand-exchange mechanism. This latter mechanism involves the temporary association of sample anions with the inner coordination sphere of the bound transition metal. Since these interactions involve more specific coordination than simple charge–charge interactions, variations in selectivity from one transition metal cation to another might be expected. The ligands didecyl-diaza-18-crown-6 (DD22) and cryptand decyl-2.2.2 (D222) (shown in Fig. 1) have an affinity for transition metals and are sufficiently hydrophobic to remain adsorbed indefinitely on reversed-phase columns. In this research we have studied the use of DD22 and D222 for anion separations in this way, when loaded onto one of two different polystyrene-based reversed-phase columns, namely MPIC or AS10 (Dionex).

One goal of this research was to determine the extent to which macrocycle-based separations using transition metal ions involve a ligand-exchange mechanism. When this mechanism prevails, a change in selectivity is expected when compared to separations achieved with alkali metal cations, reported earlier [10–13]. The performance of such systems in separating anions was examined in three ways:

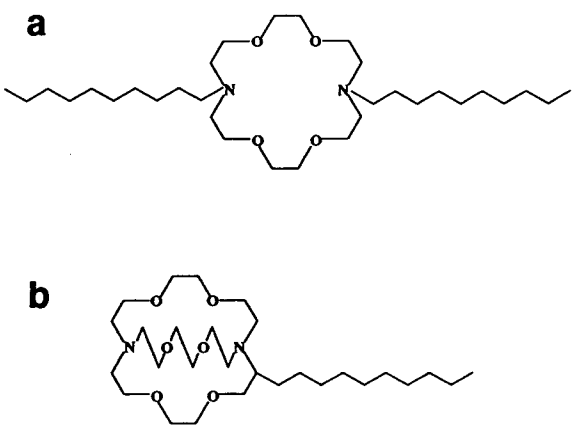

Fig. 1. Structures of (a) didecyl-diaza-18-crown-6 (DD22) and (b) decyl-2.2.2. (D222).

(1) changing the eluent cation, (2) changing the macrocycle adsorbed to the column, and (3) changing the type of reversed-phase resin. In the following sections we report anion separations with transition metal eluents on columns packed with MPIC and AS10 resin loaded with DD22 or with D222.

2. Experimental

2.1. Materials

DD22 was obtained from Parish Chemical (Provo, UT, USA). D222 was obtained from EM Science (Gibbstown, NJ, USA). All chemicals used for eluent preparation were reagent grade. The eluents were made with water purified to 18 MΩ resistivity with a Milli-Q water purification system (Millipore). Each eluent was degassed by sparging with helium.

2.2. Instrumentation

A Dionex 4000i series ion chromatograph was used in all chromatographic separations. A Shimadzu variable wavelength UV–vis detector was used for anion detection at 214 nm. The chromatograph was controlled and the data collected on a personal computer using the Dionex AI400 control software.

2.3. Column preparation

The MPIC column loaded with DD22 or D222 was prepared as previously described [10,11] by recirculating the ligand in a methanol–water (60:40 v/v) solution through the column for a period of 12 h. The AS10 resin loaded with DD22 or D222 was prepared by slurrying the appropriated macrocycle with the resin in a MeOH–water (60:40) solution and then evaporating off the methanol. The resin thus prepared was then packed into chromatographic columns.

3. Results and discussion

The purpose of this research was to explore the possibility of employing transition metal containing eluents to perform anion separations in macrocycle-based ion chromatography. Three different parameters were studied for their effect on the separation of anions: the type of macrocycle adsorbed onto the column; the identity of the eluent cation; and the type of reversed-phase resin substrate. Each of these parameters was evaluated on the basis of column capacity, selectivity, and efficiency.

3.1. Effect of macrocycle type

Macrocycles have been noted since their discovery for their ability to selectively complex metal ions. The selectivity of cation-macrocycle complexation is often determined by the ability of the metal ion to fit into the macrocyclic cavity. Cations that fit more closely are often bound more strongly than cations that do not fit as well.

The selectivity of cation binding by macrocycles is also a function of the types of heteroatoms in the macrocyclic ring. Oxygen-only crown ethers show affinity for alkali metal and alkaline earth cations, but little interaction with transition metal cations. Nitrogen-containing macrocycles show much higher affinities for transition metals than for alkali metal and alkaline earth cations. The binding of transition metal cations by 2.2.2 and dimethyl-diaza-18-crown-6 ($Me_2$2.2), the water soluble parent macrocycles analogous to those employed in this study, but without the hydrophobic aliphatic substituent groups, is shown in Fig. 2, in which the log of the aqueous binding constant is plotted *versus* metal ion. These nitrogen containing crown ethers show very high affinity for copper ions among the transition metal ions studied.

The bicyclic cryptand 2.2.2 shows slightly higher affinity for the metal ions than the monocyclic crown ether derivative dimethyl-2.2 ($Me_2$2.2). For this reason, columns incorporating cryptands have higher capacities than columns containing crown ethers due to the ability

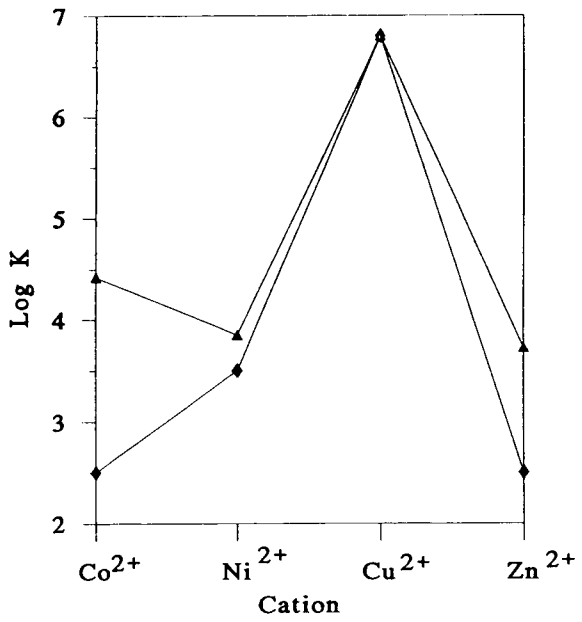

Fig. 2. Aqueous binding constants of selected transition metal cations by $Me_2$2.2 (▲) and 2.2.2 (◆) (from refs. 14 and 15).

of the cryptands to form more stable cation complexes [13].

The effect of macrocycle type on anion separations using $NiSO_4$ eluent is shown in Fig. 3. The same amount of each macrocycle was loaded onto separate MPIC columns. The separation of an 8 anion standard is shown using a 1 m*M* $NiSO_4$ eluent on each of these columns. The column loaded with D222 shows higher capacity than the column loaded with DD22. Specifically, with the D222 column the separation took 70 min; with the DD22 column, 45 min were required to elute all species. This effect can be attributed to the higher affinity of the cryptand column for eluent metal ions, yielding a column of higher capacity. Similar results were obtained with eluents containing copper, zinc, and cobalt — in all cases retention of anions on the D222 column was greater than on the DD22 column.

The selectivity among anions was observed to be a function of the column macrocycle type, as

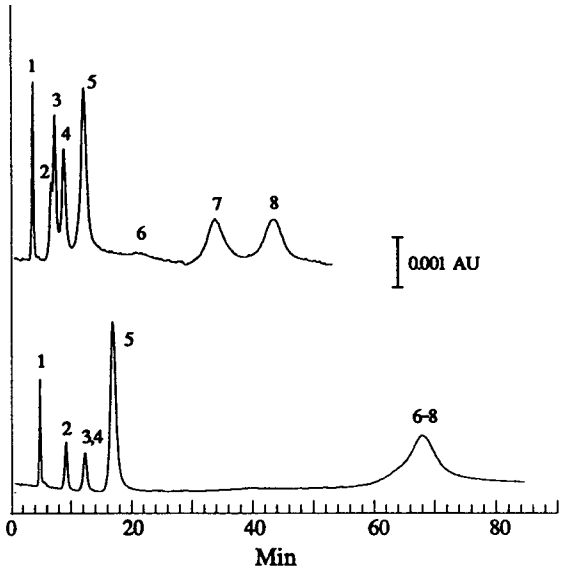

Fig. 3. Effect of macrocycle on anion separations with 1 m*M* $NiSO_4$ (pH = 7.8) eluent. Columns: MPIC columns loaded with DD22 (top chromatogram), D222 (bottom chromatogram). Peaks 1 = IO_3^-, 25 ppm (w/w); 2 = BrO_3^-, 50 ppm; 3 = NO_2^-, 5 ppm; 4 = Br^-, 25 ppm; 5 = NO_3^-, 10 ppm; 6 = $Cr_2O_7^{2-}$, 50 ppm; 7 = MoO_4^{2-}, 25 ppm; 8 = I^-, 10 ppm.

evidenced by Fig. 3. The DD22 column provided greater selectivity and resolution than the D222 column, with at least partial resolution of all 8 anions in the standard. In contrast, with the D222 column there was coelution of nitrite and bromide, and of dichromate, molybdate and iodide. The elution order was the same with both of these macrocycle-based columns. Improved resolution of anions was also observed in the DD22 column as compared with the D222 column when comparable cobalt or zinc eluents were used.

An important criterion in the evaluation of a separation is column efficiency. The efficiencies measured for several anions on both the DD22 and D222 columns using $NiSO_4$ eluent are listed in Table 1. The efficiency of the D222-based column is generally double that of the DD22 column. Specifically, an average efficiency of 2200 theoretical plates was obtained for the four anions listed using the D222 column as compared to 1300 for the DD22-based MPIC column. The higher efficiency of the D222 column is probably

Table 1
Effect of macrocycle and column substrate on efficiency of anion separations using 1 m*M* $NiSO_4$ eluent

Anion	Column efficiency (Theoretical plates)		
	MPIC–DD22	MPIC–D222	AS10–DD22
IO_3^-	1380	2460	7360
NO_2^-	1150	2220	10 870
Br^-	1470	2220	11 110
NO_3^-	1100	1900	10 870

due to the structures of the macrocycles themselves. DD22 is tethered to the resin surface by two hydrophobic side chains on either side of the ring. Thus, it probably sits very close to the hydrophobic resin surface, so that the mass transfer of anions into and out of the stationary phase is hindered. D222, on the other hand, is tethered by only one side chain. Thus, it is probably not as closely bound to the resin surface, resulting in faster mass transfer and higher efficiency.

3.2. *Effect of eluent cation*

As shown in Fig. 2, the nitrogen containing macrocycles DD22 and D222 have affinity for transition metal cations. Since the stationary phase macrocycles contain nitrogen in the ring, they also can be protonated under the proper pH conditions. This is an additional way positively charged anion exchange sites may be generated. The p*K* values for these nitrogens are 10.0 and 7.5 for 2.2.2 and 9.5 and 7.5 for $Me_2$2.2, the water soluble parent compounds of the macrocycles used in this study. Thus at the neutral pH employed with these eluents, the macrocycles can have a +1 or +2 charge due to the protonation of the nitrogens in the macrocyclic ring. The effect of macrocycle protonation is demonstrated by the observation that anions are separated even in the presence of a lithium sulfate eluent (the top chromatogram in Fig. 4). Li^+ ion has very little affinity for either of the ligands and hence little column anion capacity can result from the formation of metal ion-macrocycle

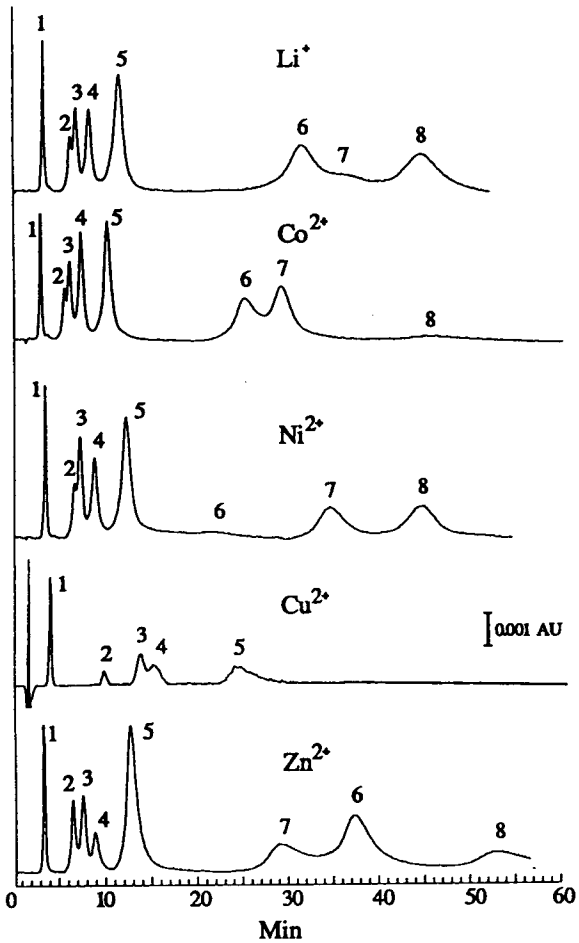

Fig. 4. Effect of eluent cation on anion separation on MPIC–DD22 column. Eluents (from top to bottom): Li_2SO_4 (pH 7.2), $CoSO_4$ (pH 6.9), $NiSO_4$ (pH 7.8), $CuSO_4$ (pH 7.8), $ZnSO_4$ (pH 7.5); each 1 m*M*. Peaks as in Fig. 3.

complexes. Yet with the Li^+ containing eluent, significant retention of anions was observed. This column capacity must be due to the protonation of the macrocycle nitrogens. Since the binding of metal ions by the macrocycle occurs in competition with the protonation reaction, we must consider the degree to which protonation occurs.

The reactions that can take place in the column to form anion exchange sites are (1) the protonation of each of the macrocyclic nitrogens and (2) the binding of a metal ion. These reactions can be written as:

$$H^+_{aq} + L_s \rightleftarrows HL^+_s$$

$$H^+_{aq} + HL^+_s \rightleftarrows H_2L^{2+}_s$$

$$M^{2+}_{aq} + L_s \rightleftarrows ML^{2+}_s$$

where L_s denotes the macrocyclic ligand adsorbed on the resin and M^{2+}_{aq} is the eluent cation. Each of these reactions has a corresponding expression for the equilibrium constant that can be written:

$$K_1 + \frac{[HL^+_s]}{[L_{f,s}][H^+_{aq}]}$$

$$K_2 = \frac{[H_2L^{2+}_s]}{[HL^+_s][H^+_{aq}]}$$

$$K_M = \frac{[ML^{2+}_s]}{[L_{f,s}][M^{2+}_{aq}]}$$

where K_1 and K_2 are the first and second protonation constants, K_M the equilibrium constant for the binding of the metal ion by the macrocycle, and $L_{f,s}$ the amount of free ligand on the stationary phase. The extent to which the macrocycles are bound to metal ions can be found by combining these three equilibrium expressions:

$$[ML^{2+}_s] = \frac{K_M[L_{T,s}][M^{2+}_{aq}]}{1 + K_1[H^+_{aq}] + K_1K_2[H^+_{aq}]^2 + K_M[M^{2+}_{aq}]}$$

where $L_{T,s}$ is the total amount of ligand adsorbed on the column. The protonation constants and the binding constants of a variety of metal ions in homogeneous aqueous solution with the parent compounds of these ligands have been tabulated [14,15]. Calculations using these values can be made as an indirect method to determine the relative population of complex and protonated species if the water soluble parent compounds were used. Although not directly applicable to our system, this exercise may be useful in explaining some of the trends in our results. Indeed, extraction equilbria often follow patterns similar to those observed in homogeneous solution data, although the absolute values of the association constants differ. For $Me_2$2.2, with a 1

m*M* $CuSO_4$ eluent at a pH of 7.8, the majority (approximately 98%) of the macrocycles would contain Cu^{2+} ions. 2.2.2, which also has high affinity for Cu^{2+}, would be bound to a similar degree by Cu^{2+} ions. The other transition metals have lower affinities for both $Me_2$2.2 and 2.2.2, and would be bound to a much lower degree relative to protons. For example, with a 1 m*M* Ni^{2+} (pH 7.8) eluent, only 9% of the $Me_2$2.2 and 3% of 2.2.2 macrocycles would contain a metal ion. Zinc and cobalt would be bound even less, with 2.4% and 1.3% of $Me_2$2.2 macrocycles containing a metal ion for 1 m*M* Zn^{2+} (pH 7.5) and Co^{2+} (pH 6.9) eluents, respectively. For 2.2.2, the degree of binding of Zn^{2+} and Co^{2+} ought to be even lower, with 0.2% of 2.2.2 macrocycles containing metal ions for either of these ions at a concentration of 1m*M*. The degree of complexation could be increased by raising the eluent pH, but this approach is not feasible due to the precipitation of the metal ion hydroxide at pH values greater than 7. To the extent that these solution data can be used to predict species distributions in our multiphase system, one would expect Cu^{2+} to be the transition metal ion most likely to yield the highest number of stationary phase complexes.

When comparing eluents with different metal ions, two effects on retention were observed in our experiments. The first was the increase in retention of all the anions with eluents containing cations with higher affinity for the column macrocycle. This effect is shown in Fig. 4. Cu^{2+}, which has a much higher affinity for both DD22 and D222, showed the longest retention, with only 5 of the anions eluting within 1 h. The other transition metal cations exhibited only small differences in affinities for the macrocycles. Eluents containing Co^{2+}, Ni^{2+} and Zn^{2+} all showed similar capacities, as expected by their binding constants and by the likelihood that many of the column macrocycles contain protons rather than metal cations.

The second effect of transition metal-containing eluents involves differences in anion selectivity, due to complexation interactions between the metal ion and the analyte anion. This effect is illustrated by changes in the retention of MoO_4^{2-} and I^- with the Cu^{2+} eluent. Specifically, the retention times of these two anions increased dramatically over the other anions. One possible explanation for this increased retention is inner sphere complex formation between MoO_4^{2-} or I^- and the Cu^{2+}–macrocycle complex. These ligands are known to form complexes with copper(II) [16]. With the Zn^{2+} eluent there was also a change in selectivity, with molybdate eluting before dichromate. For other anions the overall separations were very similar, with some slight variations. This is not unexpected since it is likely that many of the column macrocycles contain protons rather than metal ions with the Zn^{2+} eluent.

The effect of the eluent cation on the separation of anions can also be examined by comparison to separations achieved with alkali metal cations. DD22 has little affinity for alkali metal cations, and thus little retention was observed with these ions under alkaline conditions. On the other hand, D222 has a high affinity for alkali metal ions, and we have reported excellent separations of anions on D222 columns with alkali metal hydroxide eluents. The separation of anions on the D222 column using a NaOH eluent is similar to the separation observed with the LI_2SO_4 eluent in this work. We have concluded that the separation using Li_2SO_4 eluent resulted from retention of anions by the protonated cryptand, as shown in Fig. 5. With both the protonated macrocycle and the alkali metal cation–macrocycle complex, separation is postulated to occur by purely electrostatic interaction between the anion and the positively charged stationary phase complex. In contrast, with Ni^{2+} eluent, a noticeable effect on the selectivity of anion retention was observed, particularly with the retention of iodide and molybdate. Similar variations were seen with Co^{2+} and Zn^{2+} eluents. In addition, the copper eluent showed a dramatic increase in retention, with only five of the eight anions eluting within 90 min.

3.3. *Effect of column substrate*

Two different polymeric substrates were used in this research, both based on a polystyrene–divinylbenzene copolymer. The Dionex MPIC resin is designed to perform ion-pairing and

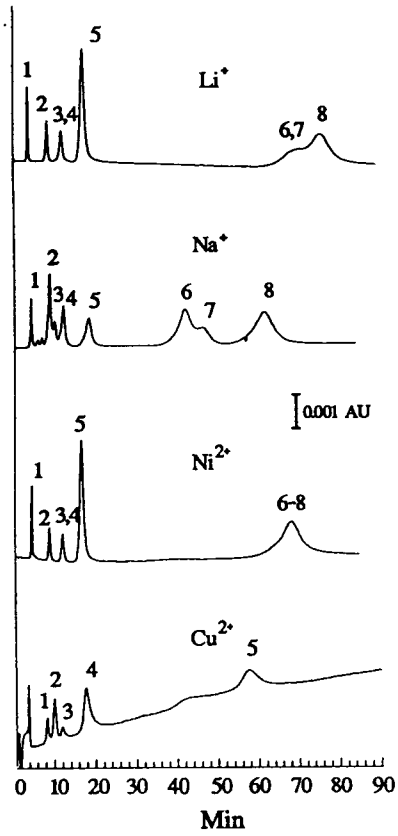

Fig. 5. Effect of eluent cation on separation of anions on MPIC–D222 column. Eluents (from top to bottom): Li_2SO_4 (pH 7.2), NaOH, $NiSO_4$ (pH 7.8), $CuSO_4$ (pH 7.8); each 1 m*M* except NaOH (20 m*M*). Peaks as in Fig. 3.

reversed-phase HPLC separations. The MPIC resin is a macroporous, high surface area resin with a particle size of 10 μm. The AS10 resin used in this study is the resin used to make for Dionex AS10 anion separator columns, but which has not yet been derivatized to introduce the ionic functionality. This resin is also a reversed-phase macroporous resin, but of a much lower surface area than the MPIC resin. The average particle size of the AS10 resin is 8.5 μm.

The effect of the column packing substrate is shown in Fig. 6. The same amount of DD22 was loaded onto each of the columns, and the separation was performed with a 1 m*M* $NiSO_4$ eluent in both cases. The AS10 based column provided much higher efficiency than the similar separation performed on the MPIC-based column. For

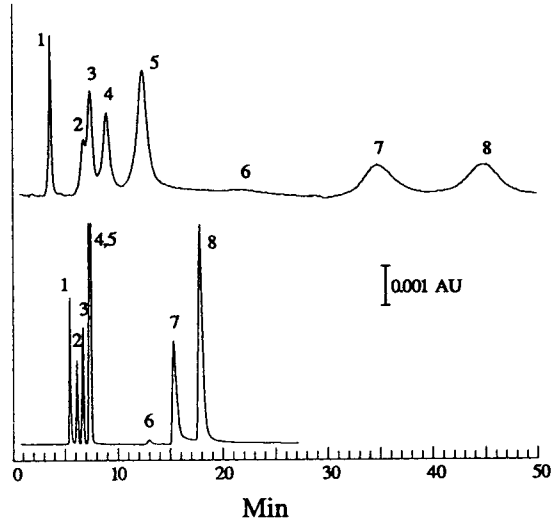

Fig. 6. Separation of anions on MPIC (top) and AS10 (bottom) columns, each loaded with DD22 and 1 m*M* $NiSO_4$ (pH 7.8) eluent. Peaks as in Fig. 3.

example, the peak for nitrate on the MPIC resin has a measured efficiency of 1100 theoretical plates, while the same peak on the AS10 column shows a separation efficiency of 10 870 theoretical plates, an increase in efficiency by more than a factor of almost ten.

While the efficiency of the separation is greatly improved with the AS10 resin, the column capacity is also significantly decreased. This is evident from the fact that the retention times of all of the analytes are significantly lower on the AS10 column, with all 8 anions eluting in 20 min on the AS10 column, as compared to 45 min on the MPIC-based system. Similar results are seen with the D222-based system, with an increase in column efficiency and decrease in analysis time. This effect may be due to crowding since the same amount of ligand was loaded onto each column and the AS10 resin has a much lower surface area.

4. Conclusions

The use of transition metal containing eluents in conjunction with macrocycle-based columns can impart an extra selectivity on anion separations. The retention of MoO_4^{2-} and I^- is greatly

increased with Cu^{2+} eluents. However, in cases where the column may be largely protonated rather than bound with metal cations, no major changes in selectivity were observed, indicating that the ion-exchange mechanism is the predominant retention mechanism. The column substrate can play an important part in the efficiency of the separations, even among similar polystyrene-based resins. The use of AS10 resin, a reversed-phase resin intended for anion separator columns that has not yet been derivatized to introduce the ion exchange functionality, greatly improves the efficiency of separations of anions in macrocycle-based ion chromatography.

5. Acknowledgement

The authors thank Dionex Corporation for graciously providing funding for this research.

References

[1] K. Kimura, H. Harino, E. Hayata and T. Shono, *Anal. Chem.*, 58 (1986) 2233.
[2] M. Lauth and P. Gramain, *J. Chromatogr.*, 395 (1987) 153.
[3] E. Blasius and K.P. Janzen, *Top. Curr. Chem.*, 98 (1981) 163.
[4] M. Nakajima, K. Kimura, E. Hayata and T. Shono, *J. Liq. Chromatogr.*, 7 (1984) 2115.
[5] T. Iwachido, H. Naito, F. Samukawa and K. Ishimaru, *Bull. Chem. Soc. Jpn.*, 59 (1986) 1475.
[6] M. Nakajima, K. Kimura and T. Shono, *Bull. Chem. Soc. Jpn.*, 56 (1983) 3052.
[7] Y. Frere and P. Gramain, *Makromol. Chem.*, 183 (1982) 2163.
[8] E. Blasius, K.P. Janzen, W. Klein, H. Klotz, V.B. Nguyen, T. Nguyen-Tien, R. Pfieffer, G. Scholten, H. Simon, H. Stockemer and A. Toussaint, *J. Chromatogr.*, 201 (1980) 147.
[9] M. Takagi and H. Nakamura, *J. Coord. Chem.*, 15 (1986) 53.
[10] J.D. Lamb and P.A. Drake, *J. Chromatogr.*, 482 (1989) 367.
[11] J.D. Lamb, P.A. Drake and K. Woolley, in P. Jandik and R.M. Cassidy (Editors), *Advances in Ion Chromatography*, Vol. 2, Century International, Medfield, MA, 1990, p. 197.
[12] J.D. Lamb and R.G. Smith, *Talanta*, 39 (1992) 923.
[13] J.D. Lamb, R.G. Smith and J. Jagodzinski, *J. Chromatogr.*, 640 (1993) 33.
[14] R.M. Izatt, J.S. Bradshaw, S.A. Nielsen, J.D. Lamb and J.J. Christensen, *Chem. Rev.*, 85 (1985) 271.
[15] R.M. Izatt, K. Pawlak, J.S. Bradshaw and R.L. Bruening, *Chem. Rev.*, 91 (1991) 1721.
[16] E. Hogfeldt and A.E. Martell, *Stability Constants of Metal–Ion Complexes, Supplement No. 1.*, Burlington House, London, 1971, p. 75.

ELSEVIER

Journal of Chromatography A, 671 (1994) 63–71

JOURNAL OF CHROMATOGRAPHY A

Practical aspects on the use of organic solvents in ion chromatography

Steve Rabin*, John Stillian

Dionex Corporation, 1228 Titan Way, Sunnyvale, CA 94088, USA

Abstract

Organic solvents play an important role in ion chromatography. The advent of solvent-compatible ion-exchange stationary phases permit all proportions of organic eluents to be employed. Selectivity mediation for the ion-exchange process is the most important usage of solvents. Changing the retention characteristics of the column packing toward the analyte permits the analyst to alter retention order, peak efficiency and resolution to optimize the separation. Column clean-up of organic molecules is also dramatically enhanced by addition of solvent. Several examples are offered to describe the utility of organic solvents in modern ion chromatography.

1. Introduction

Ion chromatography (IC) has made great advances since the early days of the technique when it was used as a method of determining chloride and sulfate. The modern ion chromatographer has a variety of detectors and separation modes to perform analyses of inorganic and organic ions in a broad range of matrices. Ion-exchange separations followed by suppressed conductivity detection is still the mainstay of IC, and it remains a very powerful and versatile technique.

The advent of chemically suppressed conductance made IC practical. Beginning with the packed-bed suppressor developed by Small *et al.* [1] and proceeding through several generations to the current state-of-the-art device, an electrochemical suppressor that generates its own regenerant *in situ* from water in the detector cell effluent [2], suppression has advanced to the point where it is essentially invisible, can suppress very strong eluent concentrations including solvent-containing eluents, and creates very quiet baselines to further lower detection limits.

Ion-exchange column packings have also improved over the years since the inception of IC. Higher-capacity, higher-efficiency and faster columns have been developed [3], often in tandem with increased capacity and efficiency of the suppression devices. Stationary phases for IC have also become organic solvent compatible through development of highly cross-linked substrate beads which minimize swelling.

Solvents can play an important role in the modern day practice of IC. Column clean-up, sample solubility and selectivity optimization may all be enhanced through addition of solvents to the aqueous phase. This paper will discuss the use of solvents in IC, including description of the ion-exchange process as mediated by organic

* Corresponding author.

0021-9673/94/$07.00
SSDI 0021-9673(94)00002-Q

solvents, column clean up techniques and several examples of separation optimization.

2. Experimental

2.1. Chromatography systems

The chromatography systems used in this study were Dionex DX-300 and System 4500i ion chromatographs. The DX-300 uses a Dionex AGP quaternary gradient pump fitted with pistons to generate flow-rates compatible with either 2 or 4 mm I.D. columns. The System 4500i is equipped with Dionex GPM-2 quaternary gradient pump. Detectors for these systems were a Dionex CDM-II conductivity detector and a Dionex PED pulsed electrochemical detector operating in the conductivity mode. All data were collected and processed on Dionex AI-450 software.

2.2. Columns

Separation columns used in this study included the Dionex IonPac CS14 for cation determinations, and the Dionex IonPac AS4A-SC, AS5A, AS11, OmniPac PAX-500 and OmniPac PAX-100 for anion determinations. Mobile phase ion chromatography (MPIC) separations were performed with the Dionex IonPac NS1 column. Suppressors for this work included the Dionex CSRS, ASRS (both operating with external water feed for regeneration) and AMMS-II (with sulfuric acid regeneration).

2.3. Reagents

Methanesulfonic acid (MSA) eluents for cation determinations were prepared from the 99 + % puriss. acid (Fluka, Ronkonkoma, NY, USA). Sodium hydroxide eluents for anion separations were prepared by dilution from the certified grade 50% solution (Fisher, Pittsburgh, PA, USA). Tetrabutylammonium hydroxide (TBAOH; Dionex, Sunnyvale, CA, USA) was diluted from the MPIC-grade 0.10 *M* solution. Acetonitrile and methanol (both Optima grade, Fisher, Pittsburgh, PA, USA) were used as received. Deionized water (18 MΩ) was obtained from a Millipore (Bedford, MA, USA) Milli-Q water purifier.

Note: Non-spectral-grade acetonitrile (Burdick & Jackson, suitable for GC and pesticide analysis) was found to be unsuitable for IC. This solvent contained ionic impurities that caused poor separations and intolerably high backgrounds in the conductivity traces.

3. Results and discussion

3.1. Stationary phase development

In the early days of IC, stationary phases were not solvent compatible. The polymer beads that formed the substrate to which the ion-exchange latex were attached was lightly cross-linked ($<5\%$) polystyrene–divinylbenzene. The consequence of this was that the polymer beads would swell dramatically in the presence of even small amounts of organic solvent, creating high backpressure on the column and also creating headspace when the column had water pumped through it after use with the solvent. To produce a more solvent-tolerant resin, *i.e.* with reduced swelling characteristics, the degree of cross-linking had to increase. Today, advances in polymer chemistry yields greater than 50% cross-linked substrate beads that are 100% compatible with all common HPLC solvents [4]. Columns produced with these substrates exhibit very little swelling when exposed to solvents. These advances now allow the use of solvents for various purposes with IC.

3.2. Uses of solvents with IC

Selectivity mediation

Perhaps the most important usage of organic solvents for IC is mediation of the ion-exchange selectivity of a column. Changing the retention characteristics of a particular column may be important in separating otherwise co-eluting species, reducing the overall run time of the

chromatogram, or helping to reduce peak asymmetry and increase efficiency.

Ion exchange is a very complex process. Adding solvents to the eluent greatly increases this complexity as there are several competing effects that govern the overall retention. This section will discuss the major constituents that mediate ion exchange in the presence of organic solvents.

Solvents are commonly used to alter retention characteristics of ion-pair chromatography, where they have a long history [5]. While the use of organic modifiers to alter ion-exchange selectivity for IC is relatively new, it was not unknown before the advent of solvent-compatible stationary phases. Some ion chromatographers were willing to tolerate the high backpressures and swelling to get the advantages that solvent mediation had to offer [6]. With solvent-compatible columns, swelling is minimized, allowing the full use of solvents up to 100% concentration.

In solution, ions are surrounded by a solvation sphere, that is, a relatively ordered group of solvent molecules oriented around the ions in equilibrium with the bulk solvent phase [7]. In aqueous solution, ions are surrounded by water molecules (hydration). In a mixed aqueous–organic solvent system, however, the organic molecules can disrupt this hydration sphere, allowing intrusion of the organic solvent molecules in the solvation matrix. The degree of this intrusion is based upon several factors, most notably hydrophobicity, ability of the solvent to hydrogen bond to the ion, and polarizability of the ion [8]. This solvation sphere determines the ability of the ion to move in solution, as it must tow these molecules along with it. As the nature of the solvent sphere changes, so changes the movement of the ion in solution. For an ion to adsorb on an ion-exchange site, it must first rearrange and eventually, partially shed its solvation sphere to allow close approach to the ion-exchange site. The greater the degree of shedding, the closer the ion can approach the site; the closer it can approach, the more tightly bound it becomes. Likewise, the ion-exchange site must reorient its solvation sphere (it is essentially a permanently bound ion) to permit the ion to approach. Therefore, the ability of an ion to shed a part of its solvation sphere plays an important role in the ion-exchange process [9]. Combining these concepts leads to the notion of selectivity mediation. The degree of solvation and ability of an ion to remove the surrounding solvent molecules would then alter the affinity that ion has for the ion-exchange site, a significant part of the overall selectivity. Another related factor is the affinity that the eluting ion exhibits toward the stationary phase. These eluting ions are also solvated, and subject to the same effects that govern retention of the analyte. In essence, observed selectivity is a competition of relative affinities of the analyte and eluent ions for the ion-exchange sites, *i.e.* how easily can the eluent elute the analyte and *vice versa*.

Selectivity mediation is influenced by several factors, including choice of solvent mediator, concentration of solvent, and nature of the analyte. All of these factors can be exploited to enhance the IC separation.

The choice of solvent can be an important parameter when performing a separation. Solvating power and hydrophobicity of the solvent can influence the retention mechanism. Stillian and Pohl [4] have looked at different solvent types on the separation of various inorganic anions with a hydroxide eluent on a Dionex OmniPac PAX-100 column. They concluded that if a longer chromatogram with improved resolution is desired, a methanol-containing eluent should be used. The highly hydrated hydroxide ion would tend to lose waters of hydration less readily than the stationary phase or the analyte in the presence of methanol, thus decreasing the selectivity of the ion-exchange sites for hydroxide. For shorter retention times, acetonitrile can be used. They contend that swelling of the latex containing the ion-exchange sites is greater in acetonitrile, therefore creating a lower effective cross-link of the latex, which would spread out the ion-exchange sites, effectively reducing the number of these sites per unit area of ion-exchange polymer. To a much lesser degree, acetonitrile mediates the ion-exchange process due to a decrease in dielectric constant of the bulk solvent relative to water; this phenomenon is

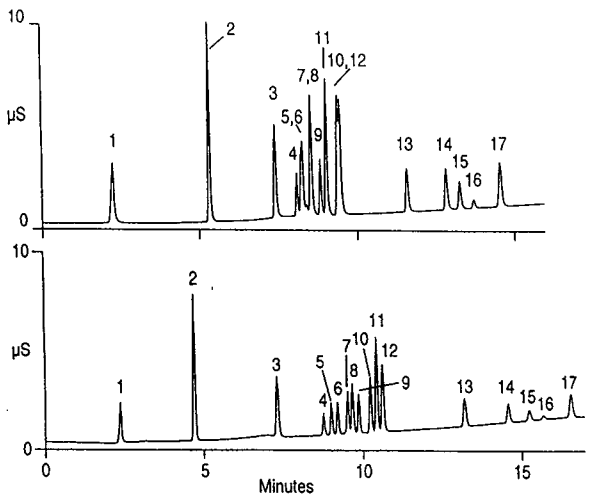

Fig. 1. Effect of methanol on retention on an IonPac AS11 column. Eluent: NaOH gradient: 0.5 to 5 m*M* in 5 min, to 38 m*M* in 15 min. Flow-rate: 2.0 ml/min. Detection: suppressed conductivity, ASRS suppressor. Peaks: 1 = acetate; 2 = chloride; 3 = nitrate; 4 = glutarate; 5 = succinate; 6 = malate; 7 = malonate; 8 = tartrate; 9 = maleate; 10 = fumarate; 11 = sulfate; 12 = oxalate; 13 = phosphate; 14 = citrate; 15 = isocitrate; 16 = *cis*-aconitate; 17 = *trans*-aconitate. Top: NaOH gradient with aqueous eluent; bottom: NaOH gradient with eluent containing 16% methanol.

more pronounced in longer-chain solvents such as isopropanol.

These effects are demonstrated in Figs. 1 and 2. Fig. 1 is a separation of various organic and inorganic anions on an IonPac AS11 column with a NaOH gradient. The top chromatogram does not contain methanol, while the bottom chromatogram contains 16% methanol. A longer retention time results with addition of methanol, yielding better resolution of closely eluting ions. In Fig. 2, various inorganic anions are eluted off of an OmniPac PAX-100 column. The first chromatogram contains 5% acetonitrile, the second 20%, and the third has 40% acetonitrile, all with 40 m*M* NaOH. As the acetonitrile concentration increases, the retention time decreases.

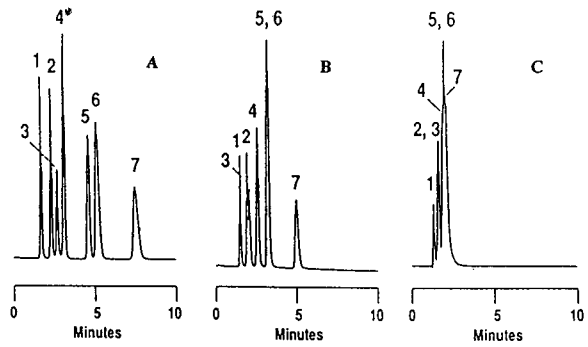

Fig. 2. Effect of acetonitrile on retention on an OmniPac PAX-100 column. All chromatograms contain 40 m*M* NaOH. (A) 5% MeCN; (B) 20% MeCN; (C) 40% MeCN. Flow-rate: 1.0 ml/min. Detection: suppressed conductivity, AMMS-II suppressor. Peaks: 1 = fluoride; 2 = chloride; 3 = nitrite; 4 = sulfate; 5 = bromide; 6 = nitrate; 7 = phosphate.

One thing to beware of when performing anion chromatography with a hydroxide eluent and acetonitrile is eluent decomposition. In the presence of base, acetonitrile slowly hydrolyzes to acetate and ammonia [10]. Acetate in particular is troublesome as it causes higher background conductivity and changes eluent composition; if running a gradient, acetate could build up on the column, then elute causing a large baseline disturbance. Therefore, to avoid eluent degradation, it is best to keep hydroxide and acetonitrile in separate bottles and proportion them together in the desired ratio(s) rather than mixing them together.

Other solvents can be used to enhance anion separations. Ethanol and isopropanol can be used as alternatives. The longer-chain, more hydrophobic alcohols such as isopropanol would tend to swell the matrix polymer to a greater degree than methanol. It has been reported [4] that addition of isopropanol to hydroxide eluents increases the k' for many ions at low alcohol concentrations, and then decreases k' as the isopropanol concentration increases. At low concentrations, isopropanol is more like methanol in its ion-exchange mediation properties, and at higher concentrations, it becomes a swelling solvent as is acetonitrile. Ethanol has properties midway between methanol and isopropanol. As depicted in Fig. 3, addition of ethanol to sodium hydroxide gives a shorter run time chromatogram than adding methanol. This can be explained in terms of solvation and dielectric constant effects. The dielectric constant for ethanol is significantly lower than methanol [11], therefore a solution of ethanol in water would be

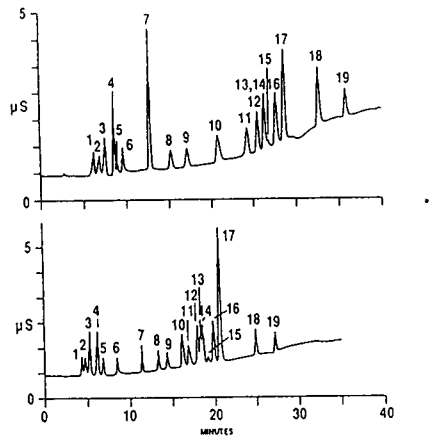

Fig. 3. Effect of solvent type on retention. Column: OmniPac PAX-500. Eluent: NaOH gradient–isocratic solvent; (top) 30% methanol, (bottom) 27% ethanol. Flow-rate: 1.0 ml/min. Detection: suppressed conductivity, AMMS-II suppressor. Peaks: 1 = fluoride; 2 = acetate; 3 = lactate; 4 = glycolate; 5 = formate; 6 = gluconate; 7 = chloride; 8 = galacturonate; 9 = glucuronate; 10 = nitrate; 11 = succinate; 12 = malate; 13 = sulfite; 14 = maleate; 15 = carbonate; 16 = tartrate; 17 = sulfate; 18 = phosphate; 19 = citrate.

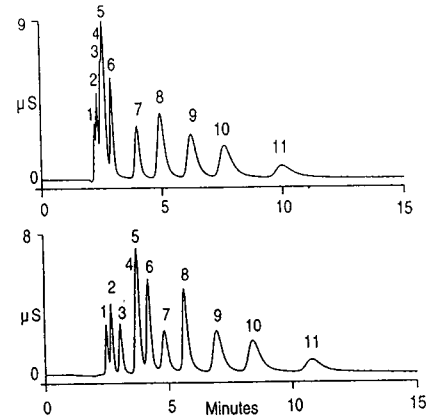

Fig. 4. Effect of solvent on separation of cations. Column: IonPac CS14. (Top) Eluent A: 40 m*M* MSA. (Bottom) Eluent B: 20 m*M* MSA + 1% acetonitrile. Flow-rate: 1.0 ml/min. Detection: suppressed conductivity, CSRS suppressor. Peaks: 1 = lithium; 2 = sodium; 3 = ammonium; 4 = potassium; 5 = magnesium; 6 = calcium; 7 = propylamine; 8 = *tert.*-butylamine; 9 = *sec.*-butylamine; 10 = isobutylamine; 11 = *n*-butylamine.

less polar than an equivalent methanolic solution, which in turn affects the degree of solvation and ability of ions to exchange.

The selectivity of cation chromatography can also be mediated by addition of organic solvents, for much the same reason as for anions. Fig. 4 shows two separations on a Dionex CS14 cation-exchange column. The top chromatogram contains no solvent, the bottom has half the acid concentration plus 1% acetonitrile. The retention times are nearly the same, yet peak resolution of the early eluting ions and tailing of the organic amines is greatly enhanced in the bottom chromatogram.

Cation-exchange columns with carboxylate functionality such as the Dionex IonPac CS12 and CS14 are difficult to use with alcohols. This is because the ion-exchange sites esterify in the presence of alcohol. This process is reversible, however it makes the use of alcohols impractical with this type of columns. Acetonitrile is the recommended solvent to use with carboxylate-functionalized resins.

There are some other effects of solvents on ion-exchange columns that play a small part in the mediation process. While solvent-compatible columns exhibit greatly reduced swelling relative to their lightly cross-linked predecessors, they still do swell to some degree, which would cause a slight increase in retention time as the ion-exchange sites are spaced further away.

Selection of column types in combination with solvents is dependent upon the type of analysis to be performed. As a general rule, hydrophilic ions are better separated on hydrophilic column packings, and hydrophobic analytes are better on hydrophobic packings. Ion-exchange capacity also can play an important role. For example, in a high-ionic-strength matrix, use of a high-ion-exchange-capacity column for overload prevention is desirable.

Column clean-up

Another important use of organic solvents with IC is for column clean-up. Many compounds, both ionic and non-ionic, can adsorb strongly on the ion-exchange sites and polymer backbone, respectively. These materials can cause loss of resolution and capacity, thus having a deleterious effect on the separation. While

pre-removal of these species through filtration or adsorption is always preferable, sometimes this is not possible and they find their way onto the column packing.

Before the days of solvent-compatible stationary phases, once the column became fouled, little could be done to recover it. High concentrations of acid or base could be used, sometimes with a small amount of organic modifier, but these often did not work, particularly if the fouling material was a bulky organic molecule. The use of solvents, however, allows another dimension in column clean-up as a combination of high ionic strength and organic modifier can often elute the fouling species from the stationary phase.

Humic acids have long presented a difficult analytical problem for IC because the acids adsorb strongly onto the ion-exchange stationary phases, gradually causing a loss of efficiency and capacity due to fouling of the ion-exchange sites. An example of this is shown in Fig. 5. Chromatogram A shows an injection of seven anions on an AS4A-SC column. After fouling with humic acid, chromatogram B demonstrates that the retention time and efficiency have dramatically decreased. After the first clean up step, some of the capacity has been recovered as shown on chromatogram C. Treatment with the final clean-up step gives nearly 100% recovery of both efficiency and retention time as depicted in chromatogram D.

Suppressed conductivity detection with solvents

Chemical suppression for IC serves three purposes: it increases the conductivity signal due to the analyte while reducing the background noise, thus it dramatically increases the signal-to-noise ratio to enhance sensitivity, as well as removing counterions, which serves to improve the resolution of early-eluting species. Until the advent of flat membrane suppressors such as the MicroMembrane Suppressor [12], solvent compatibility of suppressors was not possible due to solvent swelling effects encountered with the older devices. Today, modern suppressors are solvent compatible, allowing the combination of benefits that solvents have to offer regarding selectivity mediation with signal-to-noise enhancement of suppression.

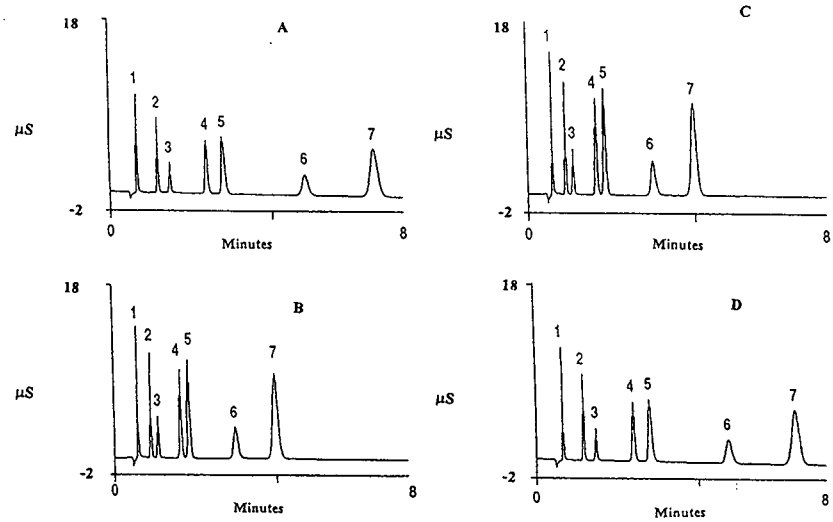

Fig. 5. Humic acid fouling and clean-up. Column: IonPac AS4A-SC. Eluent: 1.8 m*M* Na_2CO_3, 1.7 m*M* $NaHCO_3$. Flow-rate: 2.0 ml/min. Detection: suppressed conductivity, AMMS-II suppressor. Peaks: 1 = fluoride; 2 = chloride; 3 = nitrite; 4 = bromide; 5 = nitrate; 6 = phosphate; 7 = sulfate. Detection: suppressed conductivity. Clean-up steps: (1) 12 m*M* HCl, 50% acetonitrile for 1 h; (2) 200 m*M* HCl, 80% tetrahydrofuran for 1 h. Chromatograms: (A) before fouling; (B) after fouling; (C) after clean up step 1; (D) after clean up step 2.

The state-of-the-art suppression device, the Self Regenerating Suppressor (SRS), produces its own regenerant ions *in situ* from the electrolysis of water. The original design of the unit prevented use of organic solvents with electrochemical operation [13]. Design improvements now permit the use of all commonly employed IC solvents in all proportions while taking advantage of the ease of use of water electrolysis.

To operate the SRS when using solvents, a sufficient supply of water must be delivered to the suppressor to ensure good hydration of the membranes. To do this, an external supply of water must be supplied to the unit at flow-rates of 5–10 ml/min either by a pressure bottle, pump, or connection directly to a deionized water source. The other operational mode of the SRS, where the conductivity cell effluent is recycled back to the suppressor as the water source for electrolysis cannot be used with solvent-containing eluents. A sufficient supply of water must be available for the electrolytic reaction; addition of solvent to eluent reduces the bulk water concentration. Methanol is able to oxidize electrolytically, so the presence of this species in the electrolysis chambers would have a deleterious effect on suppression.

Following are several examples of separations using organic containing eluents and electrolytic suppression. Polarizable anions such as thiosulfate and perchlorate have long been a difficult separation problem due to their strong affinities for ion-exchange sites. Addition of methanol to a sodium hydroxide eluent on an IonPac AS11 allows easy separation of these species as shown in Fig. 6. Without addition of methanol, the more polarizable ions would have long run times and would exhibit greatly increased peak tailing. Kraft black liquor samples contain a substantial amount of thiosulfate. A separation shown in Fig. 7 demonstrates elution of thiosulfate in less than 10 min with good resolution of other oxyanions and chloride.

Ion-pair or mobile phase ion chromatography (MPIC) can also benefit from solvent gradients and electrolytic suppression. In the past, membrane suppression for anion MPIC separations required a specialized suppressor, the AMMS-

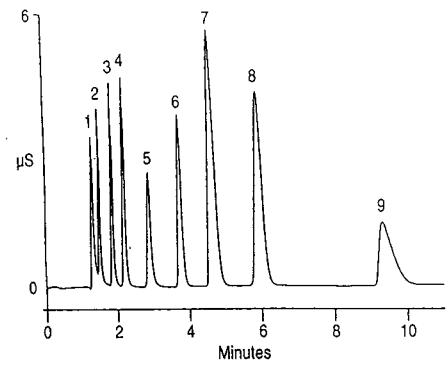

Fig. 6. Separation of polarizable anions. Column: IonPac AS11. Eluent: 45 m*M* NaOH, 40% methanol. Flow-rate: 1.0 ml/min. Detection: suppressed conductivity, ASRS suppressor. Peaks: 1 = fluoride; 2 = chloride; 3 = nitrate; 5 = phosphate; 6 = iodide; 7 = thiocyanate; 8 = thiosulfate; 9 = perchlorate.

MPIC. With the introduction of a solvent-compatible ASRS, MPIC can now be performed with the same device used for anion-exchange determinations. A demonstration of this is shown in Fig. 8. An acetonitrile gradient is used to elute various alkanesulfonic acids from C_3 to C_8 in less than 25 min. An ASRS is used in electrolytic mode with external water delivery to suppress the TBAOH eluent.

Organic solvents can aid cation determinations as well. Morpholine is a common additive to power plant waters to increase pH. The presence of morpholine often creates problems for determining other trace cations as it can coelute with ions of similar retention times, as well as exhibiting substantial band broadening and tail-

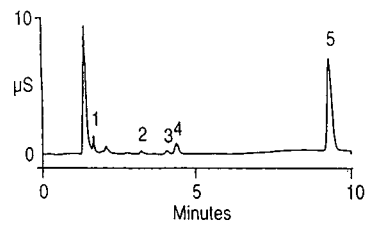

Fig. 7. Analysis of Kraft black liquor. Column: IonPac AS11. Eluent: 30 m*M* NaOH in 40% methanol for 3 min; gradient to 60 m*M* NaOH in 40% methanol at 5 min. Flow-rate: 1.0 ml/min. Detection: suppressed conductivity, ASRS suppressor. Peaks: 1 = chloride; 2 = sulfite; 3 = oxalate; 4 = sulfate; 5 = thiosulfate.

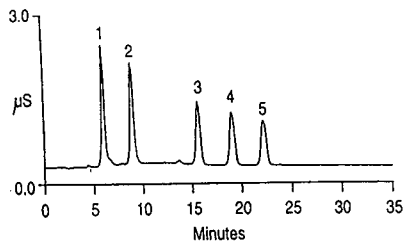

Fig. 8. Separation of sulfonic acids by MPIC with electrolytic suppression. Column: IonPac NS1. Eluent: 10 m*M* TBAOH, 20% acetonitrile to 40% acetonitrile in 20 min. Flow-rate: 1.0 ml/min. Detection: suppressed conductivity, ASRS suppressor. Peaks: 1 = 2-propanesulfonic acid; 2 = 1-butanesulfonic acid; 3 = hexanesulfonic acid; 4 = heptanesulfonic acid; 5 = octanesulfonic acid.

ing. The use of 5% acetonitrile in a methanesulfonic acid eluent can reduce the peak width and tailing to the point where determination of the other analytes is greatly simplified (see Fig. 9).

One thing to keep in mind when using conductivity detection with solvent-containing eluents is that peak response for ions will decrease somewhat as the solvent concentration increases. This is a function of the reduction of the dielectric constant of the overall solvent mixture. As the dielectric constant of the solvent system decreases, the resistance of the bulk solution increases [7], hence the specific conductivity of this solution decreases. Signal reduction is more pronounced in weak acids or bases, where the presence of solvent suppresses the dissociation of the ions relative to that of pure water. The decrease in peak response is offset somewhat by lower detector noise; unfortunately, however, sensitivity will suffer somewhat when using substantial amounts of organic solvent in IC eluents.

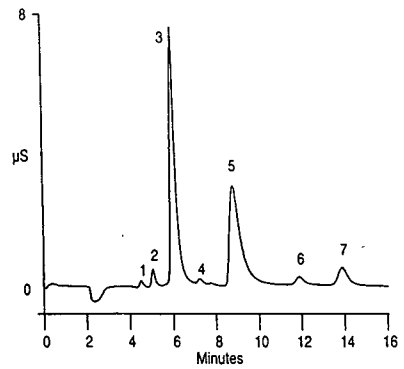

Fig. 9. Determination of trace cations in morpholine-treated power water. Columns: IonPac CG14, CS14 (2 mm). Eluent: 8 m*M* MSA, 5% acetonitrile. Flow-rate: 0.25 ml/min. Injection volume: 1.0 ml concentrated on a CG14 (2 mm) column. Suppressor: CSRS, external water supply. Peaks: 1 = lithium (0.5 μg/l); 2 = sodium (2.0 μg/l); 3 = ammonium (150 μg/l); 4 = potassium (2.0 μg/l); 5 = morpholine (2000 μg/l); 6 = magnesium (2.0 μg/l); 7 = calcium (10 μg/l).

4. Conclusions

Organic solvents are an important addition to one's IC "toolbox". Using solvent to mediate selectivity allows one to get maximal value from just a few columns. Through reduction of secondary effects, organic solvents also serve to improve chromatographic performance by decreasing tailing and peak broadening. Coupled with suppressed conductance, they provide a powerful problem-solving tool for the modern ion chromatographer.

5. Acknowledgement

The authors wish to thank Ruthann Kiser, John Statler, Charanjit Saini, Maria Rey, Rosanne Slingsby and Chris Pohl of Dionex for their helpful discussions and data collection.

6. References

[1] H. Small, T.S. Stevens and W.C. Bauman, *Anal. Chem.*, 47 (1975) 1801.
[2] A. Henshall, S. Rabin, J. Statler and J. Stillian, *Am. Lab.*, 24 (1992) 20R.
[3] P.K. Dasgupta, *Anal. Chem.*, 64 (1992) 775A.
[4] J. Stillian and C. Pohl, *J. Chromatogr.*, 499 (1990) 249.
[5] L.R. Snyder, J.L. Glach and J.J. Kirkland, *Practical HPLC Method Development*, Wiley-Interscience, New York, 1988.
[6] R. Buechele and D. Reutter, *J. Chromatogr.*, 240 (1982) 502.

[7] J. Bockris and A. Reddy, *Modern Electrochemistry*, Vol. 1, Plenum, New York, 1970.
[8] B. Karger, J. LePage and N. Tanaka, in Cs. Horváth (Editor), *High-Performance Liquid Chromatography —Advances and Perspectives*, Vol. 1, Academic Press, New York, 1980, pp. 126–128.
[9] Y. Marcus, in J. Marinsky and Y. Marcus (Editors), *Ion Exchange and Solvent Extraction*, Vol. 4, Marcel Dekker, New York, 1973, p. 47.
[10] J. March, *Advanced Organic Chemistry: Reactions, Mechanisms, and Structure*, McGraw-Hill, New York, 1968.
[11] J. Dean (Editor), *Lange's Handbook of Chemistry*, McGraw-Hill, New York, 11th ed., 1973.
[12] J. Stillian, *LC Mag.*, 3 (1985) 802.
[13] S. Rabin, J. Stillian, V. Barreto, K. Friedman and M. Toofan, *J. Chromatogr.*, 640 (1993) 97.

ELSEVIER

Journal of Chromatography A, 671 (1994) 73–82

JOURNAL OF CHROMATOGRAPHY A

Reversed phase liquid chromatographic separation of linear alkylbenzenesulfonates Effect of mobile phase ionic strength

Suhe Chen, Donald J. Pietrzyk*

Department of Chemistry, University of Iowa, Iowa City, IA 52242, USA

Abstract

Linear alkylbenzenesulfonate (LAS) homologues and positional isomers are separated on C_{18} and polystyrene–divinylbenzene reversed stationary phases using an acetonitrile–water + sodium chloride mobile phase. Retention of the LAS surfactants and separation selectivity, efficiency, and resolution are enhanced according to the mobile phase ionic strength and the ionic strength electrolyte cation. The enhanced column performance is due to Stern–Gouy–Chapman double layer interactions at the reversed stationary phase surface. The optimum mobile phase cations of those studied are Na^+, Mg^{2+} and Ba^{2+}. Isocratic or gradient elution can be used with detection by either UV absorbance (2.5 pmol detection limit at signal-to-noise ratio of 3) or by conductance following postcolumn anionic micromembrane suppression (130 pmol detection limit at signal-to-noise ratio of 3). Resolution of the LAS positional isomers is most favorable by using a gradient where acetonitrile increases and sodium chloride decreases simultaneously in an acetonitrile–water + sodium chloride mobile phase.

1. Introduction

Anionic surfactants, such as branched and linear alkylbenzenesulfonates (LASs), alkane-sulfonates (RSO_3^-) and alkyl sulfates ($ROSO_3^-$) are used industrially and in consumer products in large quantities because of their detergent action. Thus, sensitive analytical procedures for their determination are essential to these applications. In addition the anionic surfactants are often discharged into the environment and there is growing concern about their residue levels in plants, foods, and river and waste water. Identification and determination of anionic surfactants in these samples are particularly difficult because the surfactants are present at trace levels in a complex sample matrix.

Traditional methods [1] for the determination of anionic surfactants, such as precipitation and color formation and quenching procedures, are not applicable to these more complex samples for two major reasons. First, the sample matrix causes significant interference. And second, these methods provide poor selectivity. That is, they will not distinguish between different types of anionic surfactants, between members of a homologous series of a surfactant family, or between isomeric anionic surfactants. Modern separation techniques, such as gas chromatography (GC), high-performance liquid chromatography (LC), and capillary electrophoresis (CE), are powerful discriminating techniques for

* Corresponding author.

0021-9673/94/$07.00
SSDI 0021-9673(94)00128-V

separating anionic surfactants. They often provide low detection limits and permit anionic surfactants to be determined and identified at a trace level in a complex sample matrix. This is particularly true when the separation procedure can be combined with mass spectrometric (MS) detection.

Anionic surfactants have low volatility and GC procedures require surfactants to be converted into volatile hydrocarbons through desulfonation [2,3] or conversion into volatile compounds, such as sulfonyl chlorides, sulfonyl fluorides or methyl esters [4–10]. Interfacing GC with MS significantly enhances identification of anionic surfactants particularly in complex matrices [5,6,11].

LC has been widely used to separate RSO_3^-, $ROSO_3^-$, LASs and related anionic surfactants. LC procedures for the separation and determination of RSO_3^- and $ROSO_3^-$ surfactants, which are reviewed elsewhere [12–14], do not require precolumn derivatization, however, postcolumn derivatization, postcolumn anionic suppression, or indirect detection strategies are required to obtain the lowest detection limits. Since LAS surfactants contain a benzene chromophore, they are readily detected at favorable detection limits by UV absorption and fluorescence.

LAS surfactants are commonly used as mixtures of alkyl homologues and alkyl phenyl positional isomers over the alkyl chain length range of C_9 to C_{14}, although in some applications the chain length can be extended to C_{24}. LC procedures for the separation and determination of LAS surfactants employ reversed-phase chromatography usually with C_8 or C_{18} columns and organic–water mobile phases often containing an electrolyte [12,14–26], anion exchangers [27], or reversed stationary phases in combination with mobile phases containing ion interaction reagents such as quaternary ammonium salts [28–34]. Solid-phase extraction, for example by a reversed stationary phase [12,18,19] or an anion exchanger [12,23], to isolate and concentrate LAS surfactants prior to LC separation has been successfully used for environmental type samples, particularly for waste, river and treated water. Mobile phase conditions are optimized in most studies to yield resolution of LAS homologues, however, partial resolution of isomeric LAS surfactants is possible by reversed-phase chromatography, particularly when an electrolyte [15–19] or an ion interaction reagent [28–31,34], are in the mobile phase. Interfacing LC to MS for LAS surfactant identification and analyses has also been successful [33].

LAS homologues can be separated rapidly and with high efficiency by CE strategies [35–37]. CE separations with an acetonitrile–aqueous boric acid-borate, pH 9 buffer were compared to micellar electrokinetic chromatography (MEKC) by including sodium dodecyl sulfate in the buffer [36]. When different mono- and divalent cations (Mg^{2+} is optimum) are added to a pH 7 phosphate buffer the CE resolution of the LAS surfactant homologues is significantly enhanced because the cation decreases the electroosmotic flow [37]. However, resolution of LAS structural isomers by CE is not improved [36,37] even in the presence of the cation electroosmotic flow modifier and MEKC [36] appears to be the better strategy for separating LAS positional isomers.

Recent studies [13] demonstrated that a high mobile phase ionic strength and the ionic strength electrolyte cation (Li^+ and Mg^{2+} are optimum) significantly enhance the retention, column efficiency, and resolution for the reversed-phase separation of RSO_3^- and $ROSO_3^-$ surfactants. By using a postcolumn anionic micromembrane suppressor and a conductance detector the detection limit was 0.3 nmol of injected anionic surfactant. For a mobile phase gradient where CH_3CN concentration increases and the LiOH ionic strength electrolyte concentration decreases in the CH_3CN–water mobile phase solvent, multicomponent mixtures of even-numbered RSO_3^- and $ROSO_3^-$ surfactants from C_2 to C_{18} are baseline resolved. This report establishes how mobile phase ionic strength and the ionic strength electrolyte cation influences retention of LAS surfactants on reversed stationary phases. When these parameters and mobile phase solvent composi-

tion are optimized, resolution of complex mixtures of LAS surfactant homologues and positional isomers is significantly improved.

2. Experimental

2.1. Reagents and instrumentation

Sodium salts of 2-nonyl-, 2-decyl-, 2-tetradecyl- and 2-pentadecyl-benzenesulfonate were obtained as pure samples from Procter & Gamble. The absence of other positional isomers was verified by LC and the samples were used as standards. The C_{12} and C_{13} LAS surfactants were obtained from Chem Service and Aldrich and were shown to contain positional isomers by LC. These samples were used as received. Commercial LAS mixtures composed of C_{10} to C_{14} homologues and positional isomers were supplied by Procter & Gamble, Vista Chemical, and Pilot Co. and were used as received. Acetonitrile (EM Science) was LC grade and all inorganic salts and acids were analytical-reagent grade. LC water was obtained by passing water distilled in our laboratory through a Millipore Milli-Q Plus water-treatment system. All reversed stationary phases were purchased as prepacked columns. PRP-1, a polystyrene–divinylbenzene copolymer stationary phase, was obtained from Hamilton as a 10 μm, 150 mm × 4.1 mm column while Zorbax ODS, a silica-bonded phase, was obtained from Mac Mod Analytical, as 6 μm, 150 mm or 250 mm × 4.6 mm columns.

The LC system consisted of two Beckman 110A pumps, a Beckman 332 gradient controller, a Rheodyne 7125 injector with a 20-μl fixed sample loop, and either a Spectra-Physics Model SP 8450 variable-wavelength detector or a Dionex AMMS-12 anionic micromembrane suppressor coupled to a Waters 430 conductivity detector. Chromatograms and all related data were collected and handled with a Spectra-Physics 4270 integrator and computer loaded with Spectra-Physics WINner chromatographic software.

2.2. Procedures

Analyte solutions of LAS standards were prepared by dissolving a known quantity of LAS in LC water at a concentration of 0.01 to 0.1 mg/ml. Known mixtures of LAS homologues were similarly prepared to contain each analyte within this range. Mobile phases were made by combining known volumes of CH_3CN and LC water with a known mass of electrolyte and diluting to volume with solvent mixture to yield the desired composition. Solvent composition is expressed in % (v/v). All mobile phases were degassed by water aspiration for about 5 min prior to use. Columns were conditioned by passing 100 to 150 ml of the mobile phase prior to sample injection. Sample aliquots of 5 to 10 μl were injected with a 10-μl syringe. Column performance was determined during the study with a benzene and toluene test sample and a CH_3CN–water (9:1) mobile phase. A new column was used when column efficiency and capacity factor for the two analytes deteriorated with respect to manufacture certification and our initial column evaluation.

Retention time, capacity factor, and other column performance data determined in the presence of the electrolyte were the average of three or more measurements. Retention order and peak identity were established by comparison of unknown retention times to those for the injection of single, known LAS standards except where noted. Calibration curve data were obtained by using samples prepared by dilution of a standard LAS solution. Peak areas were determined and an average of at least three measurements were used to establish each data point. Linear regression was performed with Slide Write software. Flow-rate was 1.0 ml/min, ambient temperature was 25°C, inlet pressure was 700 to 900 p.s.i. (1 p.s.i. = 6894.76 Pa), and column void volume (determined by a KNO_3 sample) was 0.9 to 1.0 ml depending on the column and mobile phase. Absorbance detection was at 225 nm. For conductivity detection the anion micromembrane suppressor was regenerated with 25 m*M* H_2SO_4 at 1.0 ml/min.

3. Results and discussion

3.1. Effect of solvent

LAS surfactants, which contain both a hydrophobic and an anionic center, are retained on both reversed-phase and anion exchange columns. Retention on the former follows reversed-phase interactions in that the LAS surfactant retention decreases as the mobile phase organic modifier concentration increases and increases as the hydrophobicity or the alkyl chain length in the LAS homologue increases. This is illustrated in Fig. 1 where the capacity factor for the retention of 2-positional C_9 and C_{10} LAS standards on a Zorbax ODS column is plotted as a function of the CH_3CN–water mobile phase composition.

3.2. Effect of ionic strength electrolyte

The $-SO_3^-$ group reduces LAS retention on a reversed stationary phase compared to the corresponding hydrocarbon and also causes LAS retention to be sensitive to mobile phase ionic strength [13,38]. This is illustrated in Fig. 2 where capacity factors for 2-positional C_9 and C_{10} LAS standards are shown to increase as NaCl concentration increases in a CH_3CN–water (35:65) mobile phase. The effect of ionic strength is consistent with a double-layer-type interaction [38,39].

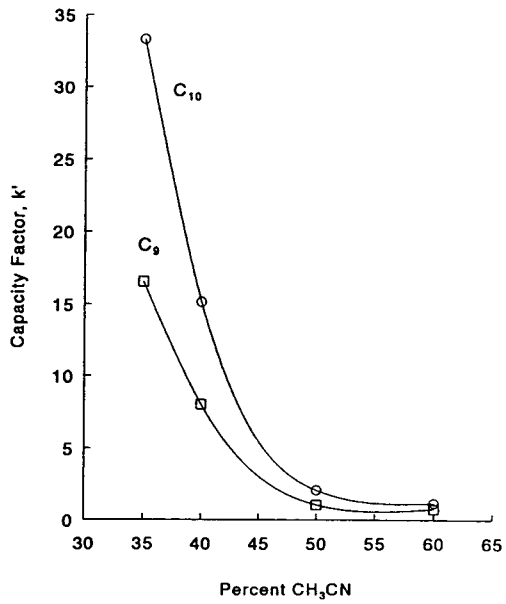

Fig. 1. Effect of CH_3CN–water composition on the retention of LAS surfactants on a Zorbax ODS column.

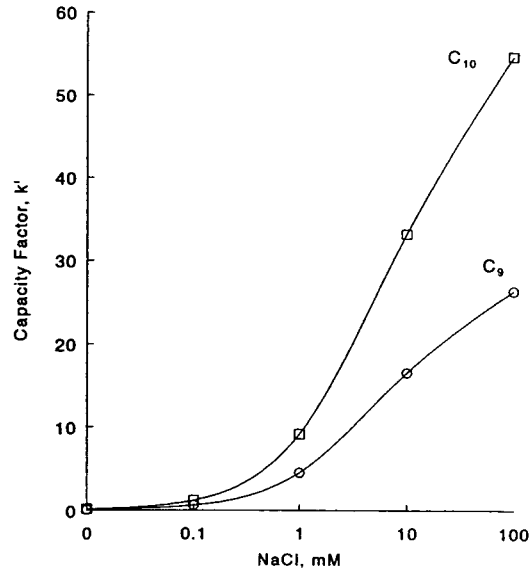

Fig. 2. Effect of mobile phase electrolyte concentration on the retention of LAS surfactants on a Zorbax ODS column. A CH_3CN–water (35:65) + NaCl mobile phase at 1.0 ml/min.

When electrolytes that differ only in the cation are used in the mobile phase at identical mobile phase ionic strength, LAS retention changes depending on the cation provided by the ionic strength electrolyte. This is illustrated in Table 1 where capacity factors for the 2-positional C_9 and C_{10} LAS standards are listed for both the PRP-1 and Zorbax ODS stationary phases in the presence of monovalent and multivalent charged cations. Ionic strengths of the different mobile phases are identical assuming that the electrolytes are completely dissociated. A similar cation dependence was observed in previous studies using RSO_3^- and $ROSO_3^-$ surfactant analytes [13].

The enhancement in retention on the two reversed stationary phases due to the cation (see Table 1) follows the order: $Al^{3+} > Ba^{2+} > Mg^{2+}$

Table 1
Effect of mobile phase cations on LAS retention on reversed stationary phases

Electrolyte	Capacity factor, k'			
	PRP-1		Zorbax ODS	
	C_9	C_{10}	C_9	C_{10}
LiCl	4.51	7.78	2.87	5.88
NaCl	5.54	9.54	4.49	9.15
NH_4Cl	5.75	9.59	4.67	9.62
$(CH_3)_4NBr$	5.70	9.97	5.52	11.2
$MgCl_2$	6.47	11.1	7.70	15.5
$BaCl_2$	8.02	13.7	7.89	16.0
$AlCl_3$	9.46	16.1	9.64	19.4

CH_3CN–water (35:65) mobile phase containing electrolyte at 0.0010 *M* ionic strength at 1.0 ml/min, 2-positional C_9 and C_{10} LAS standards as analytes, and 150 mm × 4.6 mm Zorbax ODS column.

$> (CH_3)_4N^+ > NH_4^+ > Na^+ > Li^+$. In general, the trivalent cation has the largest effect while the monovalent cation has the least effect on enhancing LAS retention. The increase in the enhancement correlates linearly to the ratio, cation hydrated radius to cation charge. As this value decreases LAS analyte retention increases according to the equation $k' = -4.72$ (cation hydrated radius/cation charge) + 31.44 with a correlation coefficient of 0.9827.

Enhanced column efficiency, resolution, and selectivity for LAS surfactant retention are also dependent on the mobile phase electrolyte cation and its concentration. As mobile phase NaCl concentration increases, column efficiency increases. This is illustrated in Fig. 3 using a 2-positional C_9 LAS standard and both the Zorbax ODS (solid line) and the PRP-1 (dashed line) columns. The enhanced efficiency, which was also determined with other LAS standards, is much greater on the Zorbax ODS column by a factor of about 3. Selectivity, for example for the separation of a mixture of C_{10}/C_9 2-positional LAS standards, undergoes only a small increase on both columns and does not contribute appreciably to the improved resolution. Thus, the sharp increase in resolution as NaCl concentration increases, which is shown in Fig. 3 only

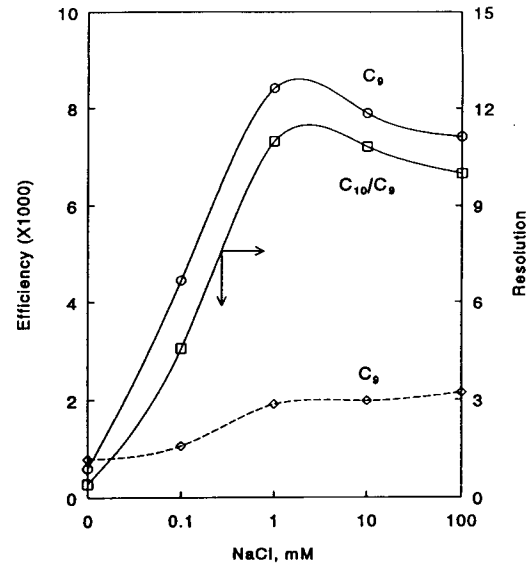

Fig. 3. Effect of mobile phase electrolyte concentration on efficiency and resolution. Conditions as in Fig. 2; solid lines = Zorbax ODS column; dotted line = PRP-1 column; analytes are 2-positional C_9 and C_{10} LAS standards.

for the separation of a mixture of C_{10}/C_9 2-positional standards and the Zorbax ODS column, occurs because of the significant peak narrowing.

Enhanced column efficiency, resolution, and selectivity are cation dependent. Table 2 surveys

Table 2
Effect of different cations on efficiency, resolution and selectivity for a Zorbax ODS column

Electrolyte[a]	Efficiency[b]	Resolution[c]	Selectivity[c]
None	590	0.41	1.89
LiCl	7040	9.52	2.05
NaCl	8420	11.0	2.04
NH_4Cl	7640	10.8	2.06
$(CH_4)_4NBr$	8370	10.8	2.03
$MgCl_2$	7790	10.7	2.01
$BaCl_2$	7670	10.8	2.03
$AlCl_3$	3940	7.30	2.01

[a] A CH_3CN–water (35:65), 0.0010 *M* ionic strength mobile phase.
[b] The analyte was a 2-positional C_9 LAS standard; efficiency is expressed as plates/column.
[c] Data are for separation of 2-positional C_{10}/C_9 LAS standards.

how individual cations enhance these three key column properties for the Zorbax ODS column. In Table 2 the mobile phase solvent is CH_3CN–water (35:65) and each electrolyte as the chloride salt, except for the tetramethylammonium cation which was used as the bromide salt, provides an ionic strength of 0.0010 *M* assuming the electrolytes are completely dissociated. Efficiency data are for a 2-positional C_9 LAS standard and selectivity and resolution data are for the separation of a mixture of C_{10}/C_9 2-positional LAS standards. The mobile phase cation also enhances efficiency, resolution, and selectivity on the PRP-1 column, but to a much lesser extent compared to the Zorbax ODS column. For example, PRP-1 column efficiency was lower by a factor of three to four, resolution was less by two to three, and selectivity was lower by about 10% depending on the cation.

3.3. Role of the cation

Retention of the LAS surfactants on the reversed stationary phase follows the Stern–Gouy–Chapman electric double layer model [38,39]. The LAS anions are retained on the stationary phase surface through a hydrophobic interaction between the alkyl chain of the anionic surfactant and the stationary phase. This creates a negatively charged primary layer at the stationary phase surface and a secondary diffuse layer of cations to maintain electrical neutrality. This is shown in Eq. 1

$$\begin{aligned} &SP + R\text{–phenyl–}SO_3^- + M^+ \rightarrow \\ &SP\cdots R\text{–phenyl–}SO_3^-M^+ \rightarrow \\ &SP\cdots R\text{–phenyl–}SO_3M \end{aligned} \quad (1)$$

where SP is the reversed stationary phase. As mobile phase ionic strength increases, the interaction between the cation and the retained LAS increases which decreases the diffuse nature of the cation. This reduces the anionic character of the LAS surfactant anionic group, thus increasing the interaction between the LAS surfactant and the stationary phase.

The influence of different cations provided by the ionic strength electrolyte on anionic surfactant retention and the linear correlation between the hydrated radius of the cation and retention of the LAS surfactant can be explained by considering the change in the surface charge density. Because the hydrated cations have a finite size, they cannot approach the charged surface any closer than the hydrated radius. The plane of closest approach of cations in the double layer is the Outer Helmholz Plane (OHP) (see ref. 39) and the region between the charged surface and the OHP is a compact layer. The compact layer can be treated as a capacitor consisting of the LAS anion and the cation. The surface charge density, σ°, is related to the capacitance, c, of the compact layer by:

$$\sigma^\circ = C(\Psi_0 - \Psi_{OHP}) \quad (2)$$

where Ψ_0 is the potential difference between the stationary phase surface and the bulk solution and Ψ_{OHP} is the potential difference between the OHP plane and the bulk solution. As the hydrated radius of the hydrated cation decreases, the capacitance of the compact layer increases, thus σ° increases. Since the surface charge is due to the LAS anions, there would be more LAS anions retained on the stationary phase surface and a longer retention time would occur.

When an inert electrolyte such as NaCl is added to the mobile phase, both surfactant anions and electrolyte anions will be adsorbed on the stationary phase surface as potential determining ions and they are responsible for the potential difference, Ψ_{OHP}, between the stationary phase surface and the bulk solution. Since the concentration of the added electrolyte is high, the electrolyte anions are largely responsible for establishing Ψ_{OHP}. As a result, Ψ_{OHP} is independent of anionic surfactant concentration and the equilibrium constant for the retention of the surfactant anion is constant and a linear adsorption isotherm is obtained. Thus, under these conditions of high ionic strength, chromatographic peaks are more symmetrical and well defined which results in a sharply improved column efficiency and resolution.

3.4. Separations

Comparison of the data included here and elsewhere [40] indicates that the Zorbax ODS

column provides a significantly improved column performance, particularly in column efficiency, over the PRP-1 column. Since the better detection limit is obtained by UV absorption over postcolumn anionic micromembrane suppression and conductivity detection, a basic mobile phase is not required for the lowest detection limit [13], thus, this also favors the C_{18} column over the PRP-1 column and increases the flexibility in optimizing the mobile phase conditions. For these reasons separation examples shown here focus only on the Zorbax ODS column. No attempt was made to study other C_{18} columns of similar or microbore diameters.

Tables 1, 2 and other data [40] demonstrate that Na^+, Mg^{2+} and Ba^{2+} are the optimum cations of those studied while Figs. 1–3 indicate the optimum mobile phase and cation concentration to use to separate LAS mixtures efficiently and effectively at a reasonable analysis time. Since a potential solubility problem may occur between Mg^{2+} or Ba^{2+} and the higher-alkyl-chain LAS analytes, Na^+ was selected as the optimum cation and NaCl was used as the electrolyte to provide both the cation and the mobile phase ionic strength.

Mixtures of homologous LAS analytes are readily separated by isocratic elution when the benzenesulfonate is located at the same position on the alkyl chain and the alkyl chain covers a small range of carbon chain lengths. Fig. 4 illustrates the separation of 2-positional C_9, C_{10}, C_{14} and C_{15} LAS standards from an isomeric C_{12}

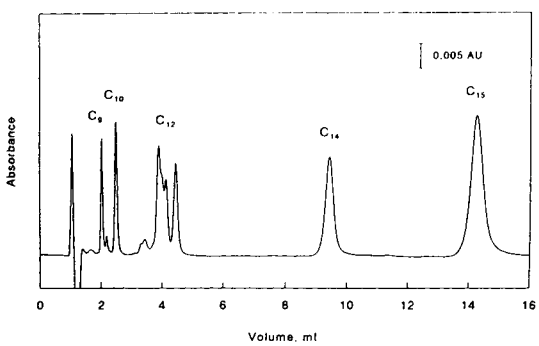

Fig. 4. Isocratic separation of an isomeric mixture of C_{12} LAS and 2-positional C_9, C_{10}, C_{14} and C_{15} LAS standards. CH_3CN–water (3:2) + 100 m*M* NaCl mobile phase at 1.0 ml/min and 150 mm × 4.6 mm Zorbax ODS column.

LAS sample using an isocratic CH_3CN–water (3:2) + 100 m*M* NaCl mobile phase and a Zorbax ODS column. For the conditions reported in Fig. 4 a linear correlation was found between log k' and alkyl chain carbon number for the 2-positional C_9, C_{10}, C_{14} and C_{15}, LAS standards and corresponds to the equation log k' = 0.190 (alkyl chain carbon number) − 1.71 with a correlation coefficient of 0.9991. When these chromatographic data for each 2-positional LAS standard were compared to the chromatographic data for the separation of the corresponding isomeric mixture of each LAS, the 2-positional isomer peak occurred at the longest retention time. Based on these studies and others [30] it is concluded that the peak of highest retention in the C_{12} isomeric peak region in Fig. 4 contains or is the 2-positional C_{12} isomer. Other positional LAS standards where not available, however, it is expected that other positional isomer homologues should also yield linear log k'–carbon number retention–structure correlations.

More complex mixtures of LAS surfactants and/or resolution of isomeric LAS homologues in a favorable analysis time require a gradient elution. Three gradient strategies examined when using the Zorbax ODS column were: (1) a solvent gradient where CH_3CN concentration increases in a CH_3CN–water + constant NaCl mobile phase, (2) an electrolyte gradient where NaCl concentration decreases in a NaCl + constant CH_3CN–water mobile phase, and (3) a combined solvent and electrolyte gradient where CH_3CN increases and NaCl decreases simultaneously in a CH_3CN–water + NaCl mobile phase. Preliminary studies demonstrated that the combined solvent, electrolyte gradient was optimum for the separation of a complex mixture of homologues and positional isomers. In addition the combined gradient provided a minimum absorbance background change during the course of the gradient and this yielded the best detection limit for the LAS peaks. The background changes for the three gradients and the Zorbax ODS column are shown in Fig. 5. For the solvent gradient (Fig. 5A), at fixed NaCl the absorbance increases with an increase in CH_3CN concentration while for the NaCl gradient (Fig. 5C), at fixed CH_3CN–water, absorbance de-

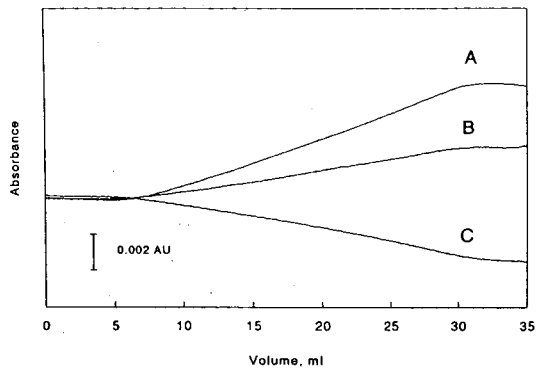

Fig. 5. Effect of gradient change on absorbance background. A = A solvent gradient where solvent 2 of CH_3CN–water (60:40) is added to solvent 1 of CH_3CN–water (40:60). B = A solvent and electrolyte gradient where solvent 2 of CH_3CN–water (60:40) is added to solvent 2 of CH_3CN–water (40:60) + 100 m*M* NaCl. C = An electrolyte gradient where solvent 2 of CH_3CN–water (40:60) is added to solvent 1 of CH_3CN–water (40:60) + 100 m*M* NaCl. In all cases the gradient is 0 to 90% solvent 2 in 25 min at 1.0 ml/min and a 150 mm × 4.6 mm Zorbax ODS column was used.

creases as the NaCl concentration decreases. When the combined NaCl + solvent gradient was employed with the UV detector used in these studies, the two opposing effects partially cancel and provide a more favorable, small background absorbance change (see Fig. 5B).

Several industrial-grade LAS mixtures were separated on the more efficient Zorbax ODS column. Fig. 6 illustrates the effectiveness of adding an electrolyte to the mobile phase. In the absence of the electrolyte and elution by a CH_3CN–water mobile phase (Fig. 6A), bands are broader, resolution is less complete, and positional isomers are poorly resolved. In the presence of NaCl and elution by a combined solvent and electrolyte gradient similar to that used in Fig. 5B, retention, efficiency and resolution of the LAS homologues and positional isomers are significantly improved as shown in Fig. 6B. Fig. 7 illustrates the separation of two other industrial LAS surfactant mixtures that differ in homologue ratio on the 150 mm × 4.6 mm Zorbax ODS column. In Fig. 7A the longer alkyl chain homologues are in the majority while in Fig. 7B the shorter homologues dominate. A combined solvent and electrolyte gradient was used for both separations in Fig. 7. For Fig. 7A the gradient was the same as Fig. 5B while for Fig. 7B the gradient change to 85% solvent 2 occurred over 30 min. The peaks for the C_{10}, C_{12} and C_{14} LASs were identified by comparison to

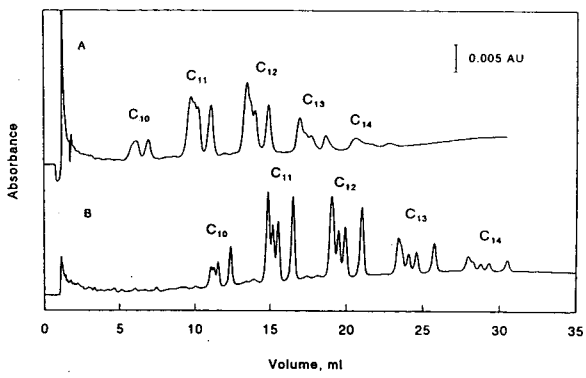

Fig. 6. Effect of mobile phase electrolyte on resolution of a commercial LAS mixture. In (A) the gradient free of electrolyte listed in Fig. 5A was used while for (B) the gradient listed in Fig. 5B was used. Flow-rate was 1.0 ml/min and a 150 mm × 4.6 mm Zorbax column was used.

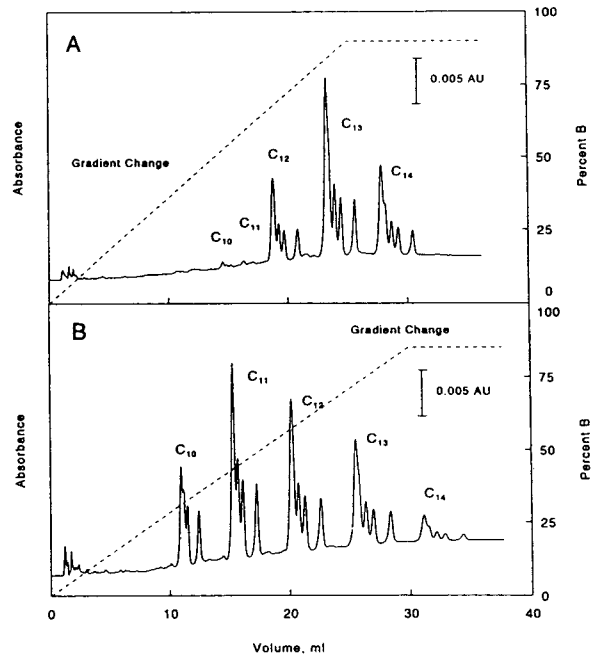

Fig. 7. Separation of two different commercial LAS mixtures. The gradient and column used in A and B are the same as listed in Fig. 5B except in B the change is 0 to 85% solvent 2 in 30 min.

2-positional LAS standards while C_{11} and C_{13} isomeric peaks were predicted based on hydrophobic considerations of the LAS derivatives. In both Figs. 6 and 7 the LAS sample solution was made by dissolving 0.5 mg of the commercial LAS mixture per ml of CH_3CN–water (2:3) and was injected as a 5-μl aliquot. When the column length was increased from 150 mm (see Fig. 6B) to 250 mm (see Fig. 8), resolution of the positional isomers is increased. For these separations the peak of highest retention for each homologue was shown to be the 2-positional isomer by comparison to retention data determined for 2-positional C_9, C_{10}, C_{14} and C_{15} LAS standards. Based on hydrophobic considerations the other homologue isomeric peaks are believed to correspond to shorter retention times as the benzenesulfonate group is positioned towards the center of the alkyl chain. Standards, however, were not available to confirm this prediction.

Calibration curves were prepared for 2-positional C_{10} and C_{14} LAS standards using detection by UV absorbance at 225 nm and by conductance following postcolumn anionic micromembrane suppression. The former, which provides the better detection limit was established using the gradient outlined in Fig. 6B while in the latter the elution was isocratic at a CH_3CN–water (45:55) + 10 m*M* $Mg(OAc)_2$ mobile phase. The linear calibration curve for the C_{10} LAS standard and the absorbance detection corresponded to the equation peak area = $1.1 \cdot 10^3$ (pmol LAS) $- 9.8 \cdot 10^2$ with a correlation coefficient of 0.9995 and provided a detection limit (at a signal-to-noise ratio 3) of 2.5 pmol of injected C_{10} LAS standard in a 10-μl aliquot while for conductance detection the linear calibration curve corresponded to peak area = $1.25 \cdot 10^2$ (pmol LAS) $- 5.46 \cdot 10^3$ with a correlation coefficient of 0.9995 and yielded a detection limit of 130 pmol for the same injection and signal-to-noise ratio. Similar results were also obtained with a C_{14} LAS standard.

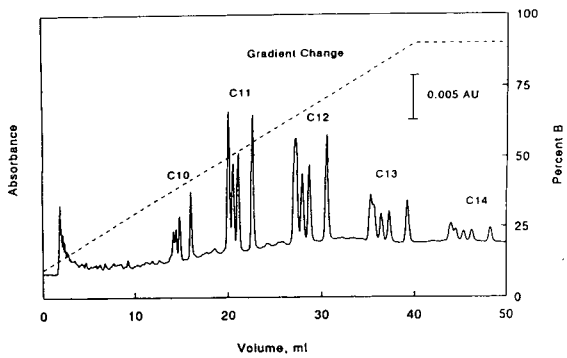

Fig. 8. Separation of a commercial LAS mixture from Fig. 7 on a 250 mm Zorbax column. The gradient is the same as Fig. 5B except the gradient change from 0 to 90% solvent 2 occurred over 40 min.

4. Conclusions

Retention of LAS surfactants increases on reversed stationary phases according to mobile phase ionic strength and ionic strength electrolyte cation. A major improvement in efficiency and resolution is also ionic strength and cation dependent while selectivity is only modestly increased. The optimum mobile phase cations are Na^+, Mg^{2+} and Ba^{2+} with Na^+ being the most convenient to use. LAS homologues are resolved conveniently by isocratic elution while resolution of LAS positional isomers requires a mobile phase gradient. The most favorable gradient is one where the CH_3CN concentration increases and the NaCl concentration decreases simultaneously in a CH_3CN–water solvent mixture.

5. Acknowledgements

The authors are grateful to Procter & Gamble, Vista Chemical and Pilot Co. for providing the commercial LAS samples. Special thanks are due to Procter & Gamble for supplying the pure 2-positional LAS standards.

6. References

[1] J. Cross (Editor), *Chemical Surfactants – Chemical Analysis*, Vol. 8, Marcel Dekker, New York, 1977.
[2] Q.W. Osburn, *J. Am. Oil Chem. Soc.*, 63 (1986) 257–263.

[3] I. Zeman, *Tenside Deterg.*, 19 (1982) 353–356.
[4] E.L. Sones, J.L. Hoyt and A.J. Sooter, *J. Am. Oil Chem. Soc.*, 56 (1979) 689–700.
[5] H. Hon-Nami and T. Hanya, *J. Chromatogr.*, 161 (1978) 205–212.
[6] M.L. Trehy, W.E. Gledhill and R.G. Orth, *Anal. Chem.*, 62 (1990) 2581–2586.
[7] J.J. Kirkland, *Anal. Chem.*, 32 (1960) 1388–1393.
[8] J. McEvoy and W. Giger, *Environ. Sci. Technol.*, 20 (1986) 376–378.
[9] J.S. Parsons, *J. Gas Chromatogr.*, 5 (1967) 254–256.
[10] P. Sandra and F. David, *J. High Resolut. Chromatogr.*, 13 (1990) 414–417.
[11] R.E.A. Escott and D.W. Chandler, *J. Chromatogr. Sci.*, 27 (1989) 134–138.
[12] M.A. Castles, B.L. Moore and S.R. Ward, *Anal. Chem.*, 61 (1989) 2534–2540.
[13] D. Zhou and D.J. Pietrzyk, *Anal. Chem.*, 64 (1992) 1003–1008.
[14] P. MacCarthy, R.W. Klusman, S.W. Cowling and J.A. Rice, *Anal. Chem.*, 65 (1993) 244R–292R.
[15] A. Nakae and K. Kunihiro, *J. Chromatogr.*, 152 (1978) 137–144.
[16] P. Jandera and J. Churàček, *J. Chromatogr.*, 197 (1980) 181–187.
[17] F. Smedes, J.C. Kraak, C.F. Werkhoven-Goewie, U.A.Th. Brinkman and R.W. Frei, *J. Chromatogr.*, 247 (1982) 123–132.
[18] M. Kikuchi, A. Tokai and T. Yoshida, *Water Res.*, 20 (1986) 643–650.
[19] A. Marcomini, S. Capri and W. Giger, *J. Chromatogr.*, 403 (1987) 243–252.
[20] E. Mathijs and H. DeHenau, *Tenside Surfactants, Deterg.*, 24 (1987) 193–199.
[21] A. Marcomini and W. Giger, *Anal. Chem.*, 59 (1987) 1709–1715.
[22] K. Inaba and K. Amano, *Int. J. Environ. Anal. Chem.*, 34 (1988) 203–213.
[23] Y. Yokayama and H. Sato, *J. Chromatogr.*, 555 (1991) 155–162.
[24] I. Fujita, Y. Ozasa, T. Tobino and T. Sugimura, *Chem. Pharm. Bull.*, 38 (1990) 1425–1428.
[25] T. Bán, E. Papp and J. Inczédy, *J. Chromatogr.*, 593 (1992) 227–231.
[26] A. Marcomini, A. DiCorcia, R. Samperi and S. Capri, *J. Chromatogr.*, 644 (1993) 59–71.
[27] Y. Yokoyama, M. Kondo and H. Sato, *J. Chromatogr.*, 643 (1993) 169–172.
[28] P.W. Taylor and G. Nickless, *J. Chromatogr.*, 178 (1979) 259–269.
[29] A. Nakae, K. Tsuji and M. Yamanaka, *Anal. Chem.*, 52 (1980) 2275–2277.
[30] A. Nakae, K. Tsuji and M. Yamanaka, *Anal. Chem.*, 53 (1981) 1818–1821.
[31] G.R. Bear, *J. Chromatogr.*, 371 (1986) 387–402.
[32] R.H. Schreuder and A. Martin, *J. Chromatogr.*, 435 (1988) 73–82.
[33] J.J. Conboy, J.D. Henion, M.W. Martin and J.A. Zweigenbaum, *Anal. Chem.*, 62 (1990) 800–807.
[34] A. DiCorcia, M. Marchetti, R. Samperi and A. Marcomini, *Anal. Chem.*, 63 (1991) 1179–1182.
[35] W.C. Brumley, *J. Chromatogr.*, 603 (1992) 267–272.
[36] P.L. Desbène, C. Rony, B. Desmazières and J.C. Jacquier, *J. Chromatogr.*, 608 (1992) 375–383.
[37] S. Chen and D.J. Pietrzyk, *Anal. Chem.*, 65 (1993) 2770–2775.
[38] T.D. Rotsch, W.R. Cahill, Jr., D.J. Pietrzyk and F.F. Cantwell, *Can. J. Chem.*, 59 (1981) 2179–2183.
[39] F.F. Cantwell, in J.A. Marinsky and J.A. Marcus (Editors), *Advances in Ion Exchange and Solvent Extraction*, Vol. 9, Marcel Dekker, New York, 1985, Ch. 6.
[40] S. Chen, *Ph.D. Thesis*, University of Iowa, Iowa City, IA, August 1993.

ELSEVIER

Journal of Chromatography A, 671 (1994) 83–88

JOURNAL OF CHROMATOGRAPHY A

Use of combined sodium hydroxide and carbonate–bicarbonate eluents with various anion-exchange columns

L.E. Vanatta

Texas Instruments, P.O. Box 655012, MS 301, Dallas, TX 75265, USA

Abstract

Retention characteristics of various anion-exchange columns were studied, using combinations of sodium hydroxide and carbonate–bicarbonate as eluents. A Dionex 4000i unit was utilized for this work. Dionex AS4A and AS11 columns for determining inorganic anions were evaluated, both using suppressed conductivity detection. Also investigated were CarboPac PA1/AS6 columns, which are used with pulsed amperometric detection to separate saccharides. Eluent components were proportioned via the mixing capabilities of the gradient pumps.

1. Introduction

Dionex anion-exchange columns are used with a variety of eluents, including sodium hydroxide and sodium carbonate–sodium bicarbonate. The AS11 and CarboPac PA1/AS6 columns are designed primarily for use with the first solution, while the AS4A often is used with the second. When sodium hydroxide is used, it is traditionally kept free of carbonates, as they act as "pushers" [1,2]. Any leakage of carbon dioxide into the eluent will lead to irreproducible retention times and altered resolution of analytes.

Some chromatographers have separated anions on the AS4A using mixtures of these three solutions. To optimize chromatography of various samples, Gros and Gorenc [3] studied a wide range of carbonate–bicarbonate eluents, but they never introduced hydroxide. Balconi and Sigon [4] combined sodium hydroxide and sodium bicarbonate, but their main goal was to separate chloride from the "water dip", while eluting sulfate in ten minutes or less. Talmage and Biemer [5] used a specific ratio of sodium hydroxide and sodium carbonate to optimize resolution of fluoride, nitrate, monofluorophosphate, sulfate, and phosphate in toothpaste samples. None attempted to determine the general behavior of the column under a wide range of eluent mixes. For the AS11 and PA1/AS6 columns, no evidence was found to suggest that these mixed eluents have been tried at all.

The goal of this work was to determine if controlled mixing of the above eluents could give desirable retention characteristics on these columns (*e.g.*, faster run times, better resolution). Parameters monitored were: (1) retention time, (2) retention order, and (3) peak shape. Also, the ability to remove carbonate from the columns was tested.

2. Experimental

2.1. Materials

The chemicals used in preparing standard solutions and eluents were obtained from various

0021-9673/94/$07.00
SSDI 0021-9673(94)00025-5

suppliers. Sodium hydroxide was purchased in carbonate-free solution form from Fisher Scientific (Pittsburgh, PA, USA); all other chemicals were the highest purity available. All water was from the in-house system, available at a resistivity of 18 MΩ. In varying concentrations as needed, separate solutions of sodium hydroxide, sodium carbonate, and sodium bicarbonate were prepared for use as eluents. Water for eluents was sparged with helium before solutions were prepared; sparging continued for the life of the mixtures. Analyte solutions were prepared in concentrations that provided an adequate response on the chromatogram. For the conductivity work, values ranged from 1 to 6 ppm (w/w); sugars were made up at 50 ppm each.

2.2. Apparatus and columns

A Dionex (Sunnyvale, CA, USA) Series 4000i ion chromatograph was utilized for all work. All columns were from Dionex and were 4 mm I.D. In analyses of inorganic anions, post-column eluent suppression was accomplished with a Dionex Anion Self-Regenerating Suppressor (ASRS-I); detection was via a Dionex CDM-2 conductivity detector at an output range of 1 μS. Column sets employed were: (1) IonPac AG11 guard and AS11 analytical, and (2) IonPac AG4A guard and AS4A analytical columns. In both cases, the eluent flow-rate was 2.0 ml/min. A 50-μl sample loop was used.

Sugar separations were effected using: (1) HPIC-AG6 guard and HPIC-AS6 analytical, or (2) CarboPac PA1 guard and PA1 analytical column sets. In both cases, the flow-rate for the mobile phase was 1.0 ml/min. A Dionex PAD-2 pulsed amperometric detector with a gold electrode was used at an output range of 30 000 nA; applied potentials were 0.05 V for 420 ms, 0.80 V for 180 ms, and −0.10 V for 360 ms. Sample loop size was 10 μl.

To remove carbonate–bicarbonate from the columns, 500 m*M* sodium hydroxide was pumped through (bypassing any suppressor and the detector) for 30 min, followed by deionized water for 30 min. Flow-rates were the same as for the applicable eluent. For all work, instrument control and data collection were performed with a personal computer and the Dionex AI-450 software.

3. Results and discussion

3.1. CarboPac PA1 (formerly AS6)

This research centered on lactose and sucrose, two of the saccharides this column was designed to separate (see Table 1 for a summary of retention times *vs.* eluent composition). With the typically used eluent of 100 m*M* sodium hydroxide, lactose eluted before sucrose (the "normal" order), with a run time of 17 min (Fig. 1a). Hydroxide mobile phases between 100 and 500 m*M* were tried, and all gave this same sequence. When the eluent concentration was dropped below 100 m*M*, retention times lengthened, as expected. By 60 m*M*, though, the two sugars essentially coeluted in around 20 min. A further reduction to 40 m*M* resolved the pair again, but in *reverse* order. However, sucrose and lactose were retained for 25 and 28 min, respectively.

Carbonate solutions of 0.5 and 1.0 m*M* were

Table 1
Retention times *vs.* eluent composition for the PA1 column

Eluent composition		Retention times (min)	
NaOH (m*M*)	Na_2CO_3 (m*M*)	Lactose	Sucrose
100	–	13.8	16.0
80	–	15.2	16.6
60	–	19.6	19.6
40	–	28.0	24.7
100	0.5	6.7	7.4
80	0.5	6.6	6.8
60	0.5	5.9	5.8
40	0.5	4.9	4.4
100	1.0	5.2	5.7
80	1.0	5.0	5.2
60	1.0	4.6	4.6
40	1.0	3.7	3.4

Experimental conditions are those detailed in the Experimental section.

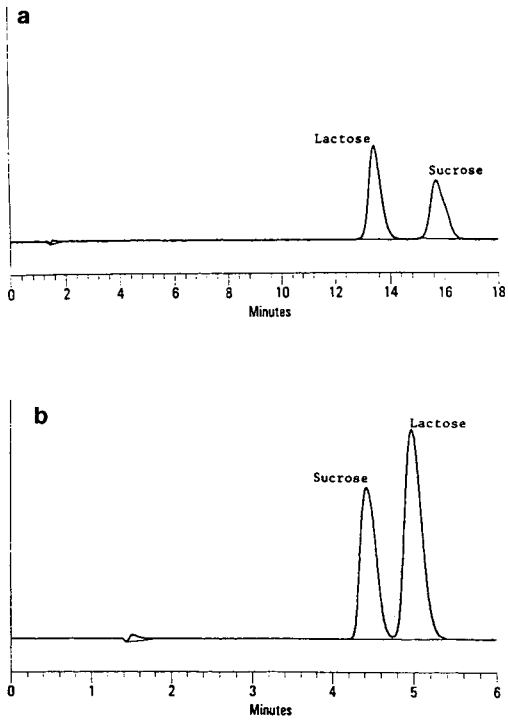

Fig. 1. (a) shows the normal retention order of lactose and sucrose (both at 50 ppm, w/w) on the CarboPac PA1 or AS6 column, using 100 m*M* NaOH as the eluent. In (b), the order is reversed with a mobile phase of 40 m*M* NaOH–0.5 m*M* Na_2CO_3. This sequence was seen for pure 40 m*M* NaOH as well, but run times were about 30 min.

added to various levels of sodium hydroxide (between 40 and 100 m*M*). The retention order was always the same as seen for the sodium hydroxide alone, but the retention times were reduced. (Fig. 1b illustrates the results for 0.5 m*M* sodium carbonate with 40 m*M* sodium hydroxide.) In addition, the resolution often was not altered significantly. For a given concentration of carbonate, though, the retention times increased as the sodium hydroxide molarity increased, presumably because less carbonate "pusher" could remain on the column with higher amounts of hydroxide.

When carbonate–bicarbonate eluents were tried in various ratios (total molarity: 1.5 to 5.5 m*M*), the two sugars coeluted in approximately 1.5 min. Also, the response was poor, since the PAD requires a high pH for maximum sensitivity [6].

3.2. AS11 and AS4A

Ten anions were chromatographed on the AS11. They always eluted in the order: fluoride (off first), acetate, formate, chlorite, bromate, chloride, nitrite, bromide, nitrate, and chlorate. The first seven of these were tested on the AS4A; elution order was the same. All reported concentration values for eluents are net of the reaction: $NaOH + NaHCO_3 \rightarrow Na_2CO_3 + H_2O$. This process appeared to be essentially instantaneous and complete in the gradient pump.

AS11

Typically, a sodium hydroxide gradient [7] is used with this column. The above ten anions are well resolved within 9 min. However, a gradient pump is required and reequilibration time (5 to 10 min) is necessary. In this work, isocratic eluent mixtures of hydroxide and carbonate were tested to see if similar chromatography could be achieved (see Table 2). When 0.48 m*M* sodium hydroxide was tried, all ten ions were resolved quite nicely (Fig. 2a), but chlorate eluted only after 29.5 min. An increase to 1.1 m*M* gave run times similar to the gradient run, but fluoride and acetate essentially coeluted. However, when a hydroxide–carbonate ratio of 0.43 m*M*:0.05 m*M* was used, chlorate's retention time was 14.9 min; separation of fluoride and acetate suffered somewhat (Fig. 2b). Further reductions in the eluent ratio continued to decrease retention times, but at the expense of resolution (fluoride and acetate, bromate and chloride). Also, a "water dip" eventually appeared right before fluoride.

Bicarbonate–carbonate eluents alone were not able to achieve the chromatography shown in Fig. 2b. As seen in Fig. 2c, an eluent ratio of 0.12 m*M*:0.36 m*M* (bicarbonate–carbonate) could not resolve fluoride and acetate, or bromate and chloride. Ratios of 0.24 m*M*:0.24 m*M* and 0.36 m*M*:0.12 m*M* did not improve resolution, even though retention times lengthened.

Table 2
Retention times *vs.* eluent composition for the AS11 column

Eluent composition			Retention times of peaks[a] (min)									
NaOH (m*M*)	$NaHCO_3$ (m*M*)	Na_2CO_3 (m*M*)	1	2	3	4	5	6	7	8	9	10
[b]			2.2	2.4	3.3	4.6	5.7	5.9	6.4	8.2	8.3	8.5
0.48	–	–	2.1	2.4	3.1	4.4	7.6	8.6	11.4	24.8	27.0	29.5
1.10	–	–	1.4	1.4	1.8	2.4	3.7	4.2	5.4	11.1	12.0	13.1
0.43	–	0.05	1.4	1.6	1.9	2.5	4.1	4.4	5.9	12.2	13.5	14.9
0.33	–	0.10	1.3	1.4	1.7	2.2	3.6	3.8	5.1	10.4	11.5	12.7
0.24	–	0.24	1.2	1.2	1.4	1.8	2.9	2.9	3.8	7.6	8.4	9.3
–	0.12	0.36	1.1	1.1	1.4	1.8	2.8	2.8	3.6	7.1	7.9	8.7
–	0.24	0.24	1.2	1.2	1.5	2.0	3.1	3.1	4.2	8.1	9.1	10.2
–	0.36	0.12	1.4	1.5	1.8	2.4	4.0	4.0	5.5	10.5	13.0	14.1
–	0.48	–	2.7	3.0	4.3	6.8	12.2	12.2	17.6	36.6	41.0	46.3
–	–	0.48	1.1	1.1	1.3	1.7	2.6	2.6	3.3	6.4	7.0	7.8

Experimental conditions are those detailed in the Experimental section.
[a] Peak identification: 1 = fluoride, 2 = acetate, 3 = formate, 4 = chlorite, 5 = bromate, 6 = chloride, 7 = nitrite, 8 = bromide, 9 = nitrate, and 10 = chlorate.
[b] These retention times are for the typical eluent scheme (a sodium hydroxide gradient) on this column; see Ref. 7 for gradient details.

In addition, peak shapes for bromide, nitrate, and chlorate often were poor. Similarly poor chromatography was seen with either 0.48 m*M* carbonate or 0.48 m*M* bicarbonate eluents.

Eluents with total molarity less than 0.3 m*M* gave excellent separations in most cases, but retention times became quite long (*e.g.*, chlorite did not elute for at least 9 or 10 min). Once the total concentration exceeded 0.5 m*M*, retention times became very short for all species and coelution was a problem (fluoride with acetate, chloride with bromate).

AS4A

The standard eluent conditions on this column are 1.7 m*M* sodium bicarbonate–1.8 m*M* sodium carbonate. The run time for the first seven anions listed above was only two min, but fluoride and acetate coeluted and were not resolved from the "water dip" (see Table 3). When 0.48 m*M* sodium hydroxide was used, chromatography was excellent, but nitrite did not elute until 22.2 min (Fig. 3a). However, if 0.05 m*M* sodium carbonate was added to 0.43 m*M* sodium hydroxide, resolution remained high and nitrite eluted in 7.1 min (Fig. 3b). In neither case was the "water dip" a problem.

Mixing carbonate and bicarbonate (each at 0.24 m*M*) shortened nitrite's retention time to 4 min, but at the expense of resolution of the first four peaks. Pure carbonate produced a poor separation as well. Bicarbonate alone could resolve all seven ions, but the last one remained on the column for 15.7 min.

It should be noted that with the pure sodium hydroxide (Fig. 3a), two to three days were needed to bring the retention times to equilibrium. Seven hours after the system was changed from the post-cleaning rinse to the hydroxide eluent, nitrite still was being retained for 40 min. By equilibrium, though, the anion was eluting in half that time.

As with the AS11, long retention times were seen with eluents totalling less than 0.3 m*M* (nitrite at 10 min or greater). Coelution (fluoride

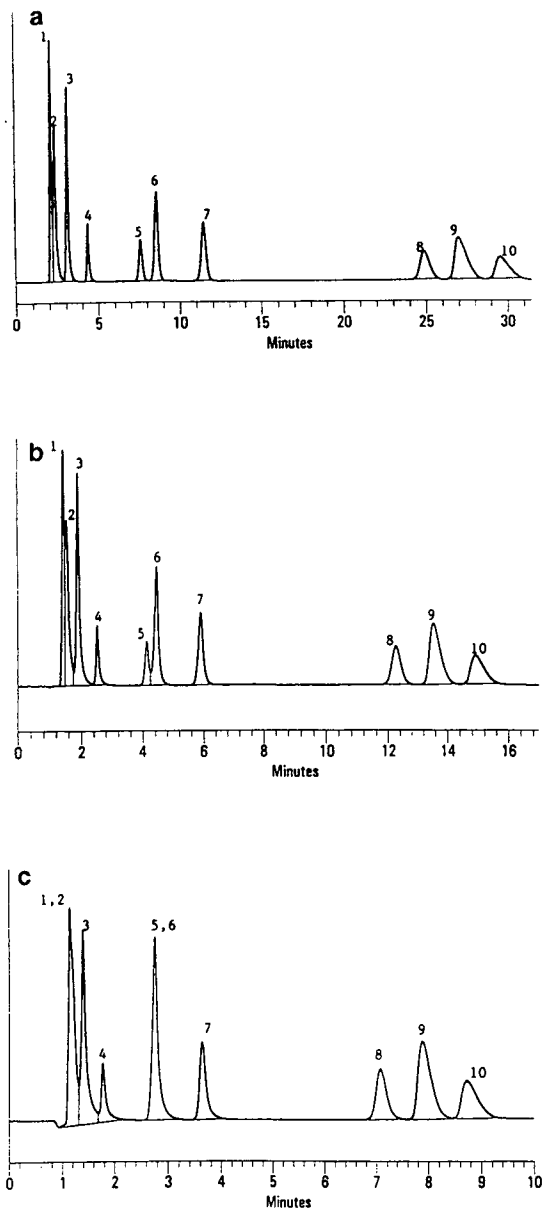

Fig. 2. Chromatograms showing the retention characteristics of inorganic anions on the AS11 column, using mixtures of NaOH (A), $NaHCO_3$ (B), and Na_2CO_3 (C) as the mobile phase. Eluent ratios (A–B–C, all values in m*M*) are: (a) 0.48:0:0; (b) 0.43:0:0.05; (c) 0:0.12:0.36. Peaks: 1 = fluoride, 1 ppm; 2 = acetate, 5 ppm; 3 = formate, 6 ppm; 4 = chlorite, 2 ppm; 5 = bromate, 3 ppm; 6 = chloride, 1 ppm; 7 = nitrite, 2 ppm; 8 = bromide, 3 ppm; 9 = nitrate, 4 ppm; and 10 = chlorate, 4 ppm (all ppm values are w/w ratios).

with acetate) again was a factor if total molarity was above 1.0 m*M*.

4. Conclusions and summary

On all three columns, results show that *controlled* proportioning of hydroxide, carbonate, and bicarbonate mobile phases can affect retention characteristics beneficially. Retention times are stable and reproducible for any given eluent mix. Also, run times can be reduced, usually without sacrificing resolution.

Elution order of the inorganic anions remains unchanged with these mixes. However, on the AS11, mixing of carbonate and hydroxide offers the possibility of isocratically separating early-eluting anions in reasonable lengths of time. It also permits broader application of the widely used AS4A. With proper ratios on this latter column, fluoride can be resolved completely from both the "water dip" and from acetate, an achievement impossible with the standard carbonate–bicarbonate eluent.

Lactose and sucrose *can* be eluted in reverse order, depending on the sodium hydroxide concentration. However, with pure hydroxide, having sucrose first requires a run time of 30 min. Adding between 0.5 and 1.0 m*M* carbonate maintains separation, but reduces retention times to around 4 min. This phenomenon will be beneficial in cases where one sugar is present in much greater concentration than the other. By controlling the eluent mix, the minor constituent can be eluted first and thereby be resolved from the large peak that follows. Also, retention times can be adjusted as desired.

Carbonate can be removed easily from all exchangers by using strong sodium hydroxide, thereby restoring original selectivity. However, if any formerly used mixture then is reintroduced, the previously seen chromatography again is obtainable. All of the above results indicate that combining carbonate and hydroxide in specific proportions gives the chromatographer another useful means of managing his separations.

Table 3
Retention times *vs.* eluent composition for the AS4A column

Eluent composition			Retention times of peaks[a] (min)						
NaOH (m*M*)	$NaHCO_3$ (m*M*)	Na_2CO_3 (m*M*)	1	2	3	4	5	6	7
–	1.7	1.8	1.0	1.0	1.1	1.2	1.4	1.6	1.9
0.48	–	–	5.0	5.8	7.6	9.4	13.6	15.9	22.2
0.43	–	0.05	2.0	2.3	2.8	3.3	4.5	5.2	7.1
–	0.24	0.24	1.4	1.6	1.8	2.0	2.7	3.1	4.0
–	–	0.48	1.3	1.4	1.6	1.8	2.3	2.6	3.3
–	0.48	–	3.7	4.2	5.4	6.7	9.6	11.2	15.7

Experimental conditions are those detailed in the Experimental section.
[a] Peak identification: 1 = fluoride, 2 = acetate, 3 = formate, 4 = chlorite, 5 = bromate, 6 = chloride, and 7 = nitrite.

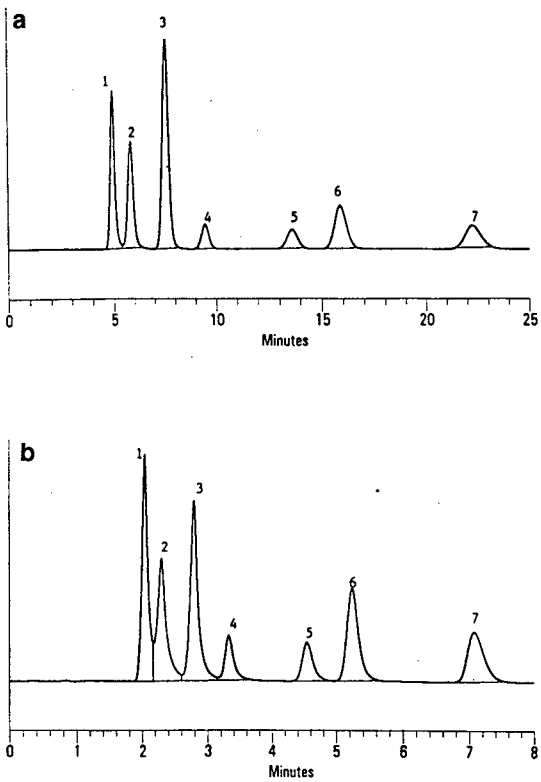

Fig. 3. Chromatograms showing the retention characteristics of inorganic anions on the AS4A column, using mixtures of NaOH (A), $NaHCO_3$ (B), and Na_2CO_3 (C) as the mobile phase. Eluent ratios (A–B–C, all values in m*M*) are: (a) 0.48:0:0; (b) 0.43:0:0.05. Peaks: 1 = fluoride, 1 ppm; 2 = acetate, 5 ppm; 3 = formate, 6 ppm; 4 = chlorite, 2 ppm; 5 = bromate, 3 ppm; 6 = chloride, 1 ppm; and 7 = nitrite, 2 ppm (all ppm values are w/w ratios).

5. Acknowledgement

The author would like to thank Rosanne Slingsby of Dionex Corporation for her helpful comments concerning this manuscript.

6. References

[1] *Technical Note No. 20*, Dionex, Sunnyvale, CA, 1989, p. 6.
[2] C.A. Pohl and E.L. Johnson, *J. Chromatogr. Sci.*, 18 (1980) 442.
[3] N. Gros and B. Gorenc, *J. Chromatogr.*, 552 (1991) 475.
[4] M.L. Balconi and F. Sigon, *Anal. Chim. Acta*, 191 (1986) 299.
[5] J.M. Talmage and T.A. Biemer, *J. Chromatogr.*, 410 (1987) 494.
[6] L.E. Welch, D.A. Mead, Jr. and D.C. Johnson, *Anal. Chim. Acta*, 204 (1988) 323.
[7] *Document No. 034791*, Dionex, Sunnyvale, CA, 1992, p. 24.

ELSEVIER

Journal of Chromatography A, 671 (1994) 89–94

JOURNAL OF CHROMATOGRAPHY A

Use of step gradients on different polymeric substrates in the separation of anions by macrocycle-based ion chromatography

Robert G. Smith, John D. Lamb*

Department of Chemistry, Brigham Young University, Provo, UT 84602, USA

Abstract

Macrocycle-based ion-exchange columns have been used in our laboratory for the separation of anions. Column anion capacity is determined by the degree to which column macrocycles are bound with mobile phase cations. Capacity gradient separations have previously been performed by gradually changing the eluent cation from one with a high affinity for the macrocycle to one with a lower affinity over the course of the separation. In this work, we demonstrate that gradient separations can also be performed in step rather than linear fashion by switching eluent cations at the start of the separation and allowing the more strongly bound cation to slowly bleed from the column, reducing the column capacity during the separation. The column capacity is reduced at a rate determined by the rate of loss of the first cation from the column. Two different substrates were used as the basis for the macrocycle-based columns, Dionex MPIC and unsulfonated AS10 resins. The MPIC-based column showed retention characteristics similar to those that we have previously described with ramp gradients, while the AS10-based systems showed improved column efficiencies. Separations achieved with step gradients on these two substrates are comparable to linear gradients achieved with the same chemical systems, eliminating the need for pumps with gradient capabilities. Fourteen anions of widely varying character were separated on the AS10-based D222 column using a step gradient from NaOH to LiOH in just over 10 min.

1. Introduction

Until recently, gradient elution anion chromatography was considered incompatible with conductivity detection, which is the most common mode of detection in ion chromatography. The changes in eluent strength required to elute strongly retained anions caused severe changes in the baseline. With improvements in column and suppressor technology, gradient separations have become more feasible. Salts of weak acids have been used to perform gradient anion separations, and protonated cations of weak bases or amino acids have been used as eluents in cation gradients [1,2]. Gradients in unsuppressed ion chromatography have been performed using a concentration gradient between two isoconductive eluents [3]. Improvements in suppressor technology have allowed gradient separations with hydroxide eluents. All of the above types of gradients are based on an increase in eluent strength (gradient elution). This increase in eluent strength can cause baseline disturbances with conductivity detection.

In our laboratory we have performed gradient separations of anions by changing the column capacity rather than the eluent strength during the course of the separation (gradient capacity). These gradients employ macrocycle-based ion-exchange columns [4–7]. Macrocycle-based col-

* Corresponding author.

0021-9673/94/$07.00
SSDI 0021-9673(93)E1253-V

umns have been used to separate cations with purely aqueous mobile phases based on the ability of macrocycles to selectively complex cations. Cations that are more tightly bound by the macrocycle are retained longer on the column [8–10]. Anions have also been separated on macrocycle-based columns with water as eluent. In this case, anions that facilitate closer interaction between the cation and the macrocycle are retained longer than other anions [11–14].

In our laboratory we have separated anions by an ion-exchange rather than a ligand-exchange mechanism using an alkali metal hydroxide in the eluent. The metal ion undergoes complexation with the neutral macrocycle on the stationary phase, creating a positively charged anion-exchange site. The hydroxide ions serve to elute the anions from the column. The number of ion-exchange sites is dependent on the degree to which the macrocycle complexes the eluent cation. Thus, eluent cations that are more strongly bound by the macrocycle generate higher column capacities than cations that are less tightly bound.

Capacity gradient separations have been performed based on the effect of eluent cation on column anion-exchange capacity. This effect is accomplished in macrocycle-based systems by changing the eluent cation from one with a high affinity for the macrocycle to one of a lower affinity during the separation. Column capacity decreases as the number of exchange sites diminishes due to loss of the strongly bound cation from the column [10–12]. The eluent ionic strength remains more or less constant as only the identity, rather than the concentration, of the eluent cation is changed. Resulting gradient separations show the ability to elute a wide variety of anions with little or no change in baseline.

In the past, capacity gradients of the type described have been performed by gradually changing from one cation to another over a period of time in a linear mode, with the column capacity changing slowly. In this work we describe gradient separations performed in a step mode, which requires no gradient programming with its associated hardware. Excellent separations were achieved with these step gradients.

The type of column polymer substrate plays an important role in the type of separation achieved in the systems we have developed. All of our previous work has been done using Dionex MPIC columns, which contain a polystyrene–divinylbenzene polymeric resin. We recently began using columns based on the resin used in Dionex AS10 anion separator columns, but which has not yet been derivatized to produce the anion-exchange functionalities. Macrocycle columns made using this resin show better efficiency and faster separations than the MPIC resin-based columns used previously.

2. Experimental

2.1. Materials

Cryptand *n*-decyl-2.2.2 (D222), whose structure is shown in Fig. 1, was obtained from EM Science (Gibbstown, NJ, USA). All compounds used in making eluents and standards were reagent grade or better. Water used in making eluents was purified to 18 MΩ resistivity using a Milli-Q purification system and was degassed by sparging with helium. Eluent purity and degassing is crucial to prevent baseline disturbances in gradient separations. Underivatized AS10 type resin was obtained from Dionex. Both the MPIC and AS10 substrates are macroporous, ethylvinylbenzene–divinylbenzene copolymeric resins with 55% cross-linking. The AS10 resin differs from the MPIC resin in particle size (8.5 μm versus 10 μm) and that it has a much lower surface area (100 m^2/g compared to 300 m^2/g) due to increased pore size.

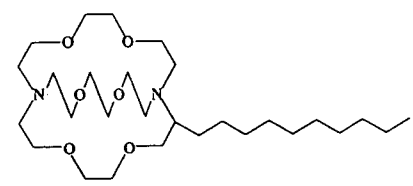

Fig. 1. Structure of the cryptand D222.

2.2. Apparatus

A Dionex 4000i series ion chromatograph was used in conjunction with Dionex anion micromembrane suppressors (AMMS) prior to conductivity detection with a Dionex CDM-2 conductivity detector. The suppressant was 12.5 m*M* H_2SO_4 flowing at 3–5 ml/min. Prepacked columns used were Dionex NS-1 MPIC columns.

2.3. Column preparation

Two different methods were employed to prepare macrocycle-based columns. Columns based on MPIC resin were prepared in the manner described previously [9] by circulation of a methanol–water (60:40) solution containing the appropriate amount of cryptand through the column for a period of 12 h.

Columns based on the underivatized AS10 resin were prepared by slurrying a methanol–water (60:40) solution containing the cryptand with the resin, also in a methanol–water mixture. The methanol was evaporated, and the resulting resin was packed into a 25 cm × 0.4 cm column.

3. Results and discussion

3.1. Macrocycle-based separation system

In macrocycle-based anion chromatography, the cation in the eluent has a great influence on the column capacity, and hence anion retention, as shown in Fig. 2. With the cryptand D222, lithium hydroxide eluent shows little retention of anions; all fourteen anions elute within 5 min. With a sodium hydroxide eluent at the same concentration, a high capacity results with only eight anions eluting in 60 min. This change in column capacity results from the much higher affinity of the Na^+ cation for the cryptand. The effect of the eluent cation on anion retention has been used to perform linear gradient separations by changing from an eluent that displays high capacity at the beginning of the separation, such as sodium, to an eluent cation that shows lower capacity, such as lithium, during the course of the separation [5,7].

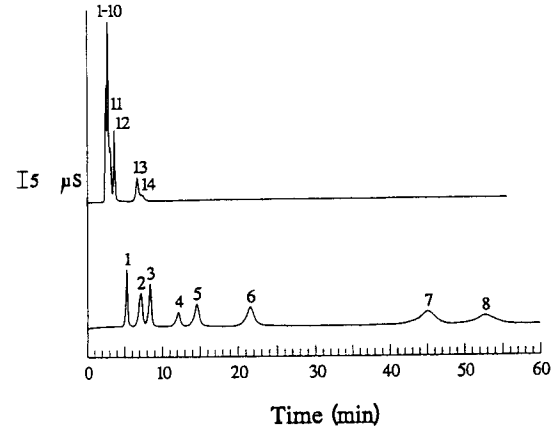

Fig. 2. Separation of 14 anion standard on D222-MPIC based column. Eluent: top chromatogram: 30 m*M* LiOH; bottom chromatogram: 30 m*M* NaOH; both at 1.0 ml/min. Peaks: 1 = F^-, 1.5 ppm (w/w); 2 = acetate, 10 ppm; 3 = Cl^-, 3 ppm; 4 = NO_2^-, 10 ppm; 5 = Br^-, 10 ppm; 6 = NO_3^-, 10 ppm; 7 = SO_4^{2-}, 10 ppm; 8 = oxalate, 10 ppm; 9 = CrO_4^{2-}, 10 ppm; 10 = I^-, 10 ppm; 11 = PO_4^{3-}, 10 ppm; 12 = phthalate, 10 ppm; 13 = citrate, 10 ppm; 14 = SCN^-, 10 ppm. From ref. 5.

3.2. Step gradients

Gradient separations of anions have been performed using linear gradients between two different eluents over a period of time to gradually increase eluent strength while lowering column capacity and provide separations of anions with widely varying affinities for the stationary phase. Such gradients require pumps that are capable of proportioning different eluent concentrations over the course of the separation. This need for high-pressure pumps with the capability to proportion eluents increases the cost and complexity of separations.

Step gradients have been reported for the separation of cations with widely different affinities for the stationary phases used in cation exchange chromatography, such as the separation of alkali metal and alkaline earth cations [15,16]. Anion selectivities do not show the same grouping of behavior as do the group I and II

cations. Rather, selectivities vary more smoothly between mono- and divalent anions. Hence, little has been reported on the use of step gradients in anion separations due to the need to more gently increase the eluent strength in order to provide optimum resolution of anions.

Capacity gradient separations with macrocycle-based ion chromatography are possible due to the bleeding from the column of the strongly bound cation employed at the beginning of the separation as the cation with lower affinity is introduced into the column. Since the strongly bound cation slowly bleeds from the column, step gradients in which the capacity of the column changes slowly are possible. Such a gradient is shown in Fig. 3, where a corresponding linear gradient is shown for comparison. The top chromatogram shows the separation of a fourteen-anion standard with a linear gradient between sodium and lithium hydroxides, each 30 m*M*, over the first 20 min of the separation. Good separation of the early eluting anions is achieved, with strongly retained anions eluting in a reasonable period of time. The lower chromatogram shows a step gradient between the same two eluents, but with the eluent switched from sodium to lithium at the time of injection. The resulting separation strongly resembles the linear gradient, with only minor differences in elution times, and some improvement in overall analysis time.

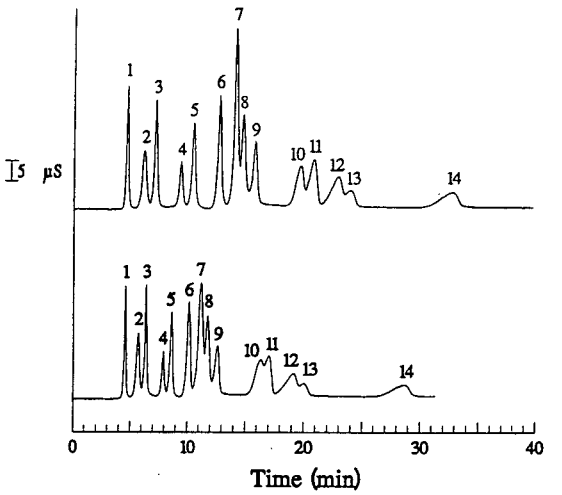

Fig. 3. Gradient separations of 14 anion standard on MPIC column loaded with D222. Gradient conditions: top chromatogram: linear gradient from 30 m*M* NaOH to 30 m*M* LiOH from 0 to 20 min; bottom chromatogram: step gradient from 30 m*M* NaOH to 30 m*M* LiOH at time of injection. Peaks as in Fig. 2.

3.3. *Effect of column substrate*

To date, we have reported cryptand stationary phases based on Dionex MPIC resin, a cross-linked, polystyrene–divinylbenzene substrate used for ion-pairing separations. In order to increase column efficiency, we have recently employed a new type of substrate for cryptand-based columns. This substrate is the underivatized resin used by Dionex as the basis for AS10 anion separator columns. This resin, while chemically similar to MPIC resin, differs in particle porosity and surface area. The resin is normally sulfonated and agglomerated with aminated latex to form AS10 anion separators. The underivatized resin, containing no ion-exchange sites, was combined in a slurry with the cryptand, and the resulting resin was packed into columns.

The effect of the column substrate on the separation of a seven-anion standard is shown in Fig. 4. The top chromatogram shows the seven-anion standard separated on the MPIC-based

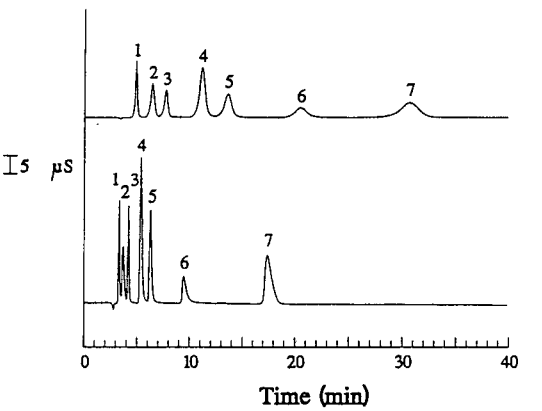

Fig. 4. Comparison of D222 on (top) MPIC resin and (bottom) AS10 resin. Eluent: 30 m*M* NaOH at 1.0 ml/min. Peaks: 1 = F^-, 1.5 ppm; 2 = acetate, 10 ppm; 3 = Cl^-, 3 ppm; 4 = NO_2^-, 10 ppm; 5 = Br^-, 10 ppm; 6 = NO_3^-, 10 ppm; 7 = SO_4^{2-}, 10 ppm.

D222 column used in the previously mentioned separations with a 30 m*M* NaOH eluent. The lower chromatogram shows the separation of the same standard on the AS10-based D222 column with the same 30 m*M* NaOH eluent. The AS10-based system shows higher efficiency and a shorter separation time (10 min as compared to more than 20 min for the MPIC-based resin).

3.4. Gradients on AS10 resin macrocycle columns

Gradients, both linear and step mode, can be performed on the AS10 based column. Fig. 5 shows the separation of a fourteen-anion standard on the AS10–D222 column. The top chromatogram shows a linear gradient between 30 m*M* NaOH and 30 m*M* LiOH over the first 10 min of the separation, with good resolution of all fourteen anions in less than 20 min. The step gradient performed between these two eluents, with the eluents switched at the time of injection, is shown in the bottom chromatogram. All fourteen anions are resolved in just over 10 min, a factor of four times faster than similar separations on the MPIC based systems such as those shown in Fig. 3.

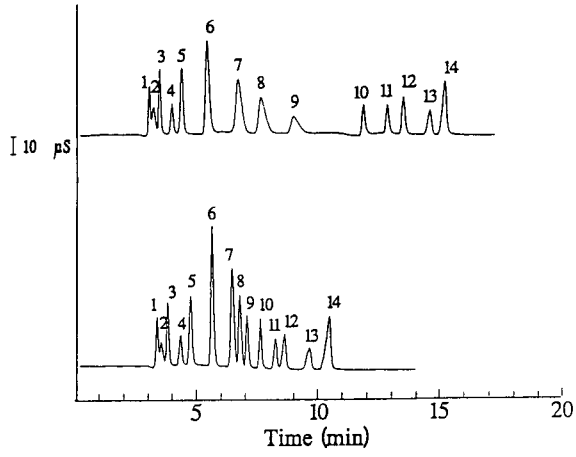

Fig. 5. Gradient separation of 14 anions on AS10 resin loaded with D222. Gradient conditions: top chromatogram: linear gradient from 30 m*M* NaOH to 30 m*M* LiOH from 0 to 10 min; bottom chromatogram: step gradient from 30 m*M* NaOH to 30 m*M* LiOH at time of injection. Peaks as in Fig. 2.

The difference between the two types of gradients can be explained by the rate at which the column capacity is changing. The rate of bleed of sodium from the column was measured by performing both linear and step gradients on the AS10 based column. The eluent was collected in 1-ml fractions before it entered the suppressor, where the eluent cations are removed from the eluent stream prior to detection. These samples were analyzed for the concentration of sodium present in the eluent as it left the column. The results are plotted in Fig. 6, with the concentration of sodium present in the eluent plotted against the time elapsed since the start of the gradient. Also included is the calculated gradient profile that should be observed if there were no macrocycle on the column. This plot shows that the sodium concentration in the eluent drops much more rapidly in the step gradient case than in the linear gradient case, resulting in a more rapid decrease in column capacity and faster elution of anions from the column. In both the linear and step gradient cases the concentration of sodium present in the column effluent is higher than predicted by the

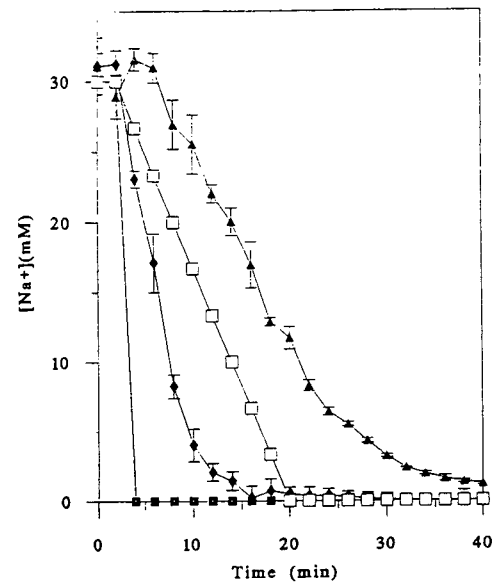

Fig. 6. Effect of gradient type on bleed of sodium from D222 column. Gradient conditions as in Fig. 3. ♦ = Step; ▲ = linear; ■ = theoretical step; □ = theoretical linear.

theoretical gradient profile due to the bleed of sodium bound to the macrocycle as the sodium in the eluent is replaced by lithium. The amount of sodium decreases rapidly in the early part of the gradient, but there is still some bleed of sodium from the column even after the sodium in the eluent has been completely replaced by lithium.

It should be noted that the baseline in both the linear and step gradient systems is unaffected by the gradient conditions; *i.e.* there is little change in the baseline during the course of the separation.

4. Conclusions

Gradient anion separations, in both linear and step mode, can be performed on macrocycle-based systems by changing only the identity of the eluent cation. Step gradients with these systems show resolving power similar to the linear gradients, with slightly reduced separation times. These step gradients simplify separations as compared to linear gradients, with less complex pumping equipment required. Such systems are highly dependent on the polymeric substrate. Specifically, the use of underivatized Dionex AS10 resin allows faster, more efficient separations than columns based on the chemically similar MPIC resin.

5. Acknowledgements

Funding for this research, as well as chromatographic substrates and column packing apparatus, were kindly provided by Dionex Corporation. The authors would also like to thank Max Mortensen and Tom Huxford, undergraduate research assistants, for their help in this work.

6. References

[1] R. Rocklin, C. Pohl and J. Schibler, *J. Chromatogr.*, 411 (1987) 107.
[2] R. Rocklin, M. Rey, J. Stillian and D. Campbell, *J. Chromatogr. Sci.*, 27 (1989) 474.
[3] W. Jones, P. Jandik and A. Heckenburg, *Anal. Chem.*, 60 (1988) 1977.
[4] J.D. Lamb and P.A. Drake, *J. Chromatogr.*, 482 (1989) 367.
[5] J.D. Lamb, P.A. Drake and K. Woolley, in P. Jandik and R.M. Cassidy (Editors), *Advances in Ion Chromatography*, Vol. 2, Century International, Medfield, MA, 1990, p. 197.
[6] R.G. Smith, P.A. Drake and J.D. Lamb, *J. Chromatogr.*, 546 (1991) 139.
[7] J.D. Lamb and R.G. Smith, *Talanta*, 39 (1992) 923.
[8] E. Blasius and K.P. Janzen, *Top. Curr. Chem.*, 98 (1981) 163.
[9] K. Kimura, H. Harino, E. Hayata and T. Shono, *Anal. Chem.*, 58 (1986) 2233.
[10] M. Lauth and P. Gramain, *J. Chromatogr.*, 395 (1987) 107.
[11] E. Blasius, K.P. Janzen, W. Klein, H. Klotz, V.B. Nguyen, T. Nguyen-Tien, R. Pfieffer, G. Scholten, H. Simon, H. Stockemer and A. Toussaint, *J. Chromatogr.*, 201 (1980) 147.
[12] M. Nakajima, K. Kimura and T. Shono, *Bull. Chem. Soc. Jpn.*, 56 (1983) 3052.
[13] M. Takagi and H. Nakamura, *J. Coord. Chem.*, 15 (1986) 53.
[14] T. Iwachido, H. Naito, F. Samukawa, K. Ishimaru and K. Toei, *Bull. Chem. Soc. Jpn.*, 59 (1986) 1475.
[15] H. Small, *Ion Chromatography*, Plenum Press, New York, 1990, p. 220.
[16] M. Betti, G. Giovanni, M. Onor and P. Papoff, *J. Chromatogr.*, 546 (1991) 259.

ELSEVIER

Journal of Chromatography A, 671 (1994) 95–99

JOURNAL OF CHROMATOGRAPHY A

Detection of transition metals during their separation in an isoconductive pH gradient

P.N. Nesterenko*, A.V. Ivanov

Department of Analytical Chemistry, Lomonosov State University, Leninskie Gory, 119899 Moscow, Russian Federation

Abstract

The possibility of the conductimetric detection of transition metals following separation with a linear pH gradient was demonstrated. Such detection is possible owing to the constant conductivity of the polyampholyte eluent over a wide pH range due to the use of a starting buffer with the same conductivity as the polyampholyte eluent. The separation of metals was performed on a column packed with tetraethylenepentamine-bonded silica.

1. Introduction

Chromatofocusing is a widely used ion-exchange chromatographic technique applied to the separation and purification of biological macromolecules owing to the difference in their isoelectric points [1]. The high resolving ability of the method is connected with the property of primary and secondary amino groups at the surface of a polybuffer ion exchanger (PBE) to form a linear pH gradient in the chromatographic column. Recently, it was shown that the principle of chromatofocusing can be modified and used for the concentration and high-performance separation of transition metals [2,3]. Such an ability is based on the property of functional amino groups at the surface of the PBE to form complexes of transition metals at a high pH of the eluent and their consequent destruction with a decrease in the pH gradient. Good separation was obtained with tetraethylenepentamino-bonded silica and a commercially available polysaccharide-based ion exchanger, PBE-94 [3].

A problem with the reliable detection of the separated metals arises in the separation of transition metals with an induced pH gradient. Spectrophotometric detection in a flow of effluent with postcolumn reaction with 4-(2-pyridylazo)resorcinol (PAR), as usually used, does not provide the reliable results, for the following reasons: (i) the difficulty of maintaining the optimum pH in the postcolumn reactor for quantitative complexation of metals with PAR during the pH gradient; the buffer capacity for polyampholyte eluents used in chromatofocusing is 75 μmol/pH unit/ml, which produces a significant decrease in the pH of the mixture by 1.0–1.5 after mixing the column effluent with the postcolumn reagent; (ii) the appearance of a

* Corresponding author.

0021-9673/94/$07.00
SSDI 0021-9673(94)00131-R

ghost peak at the end of the pH gradient due to the shift in the acid–base equilibrium of PAR (Fig. 1); and (iii) the significant complexing ability of the polyampholyte eluent used in chromatofocusing [4].

The determination of the separated metals in each fraction may solve the above problem, but it significantly complicates the detection procedure and affects the resulting profile of the chromatogram.

Another possible solution to the problem is to use conductivity detection. This is connected with the property of polyampholyte eluents to provide a constant conductivity in solutions with varying pH. The aim of this work was to show the potential of conductimetric detection for this chromatographic technique.

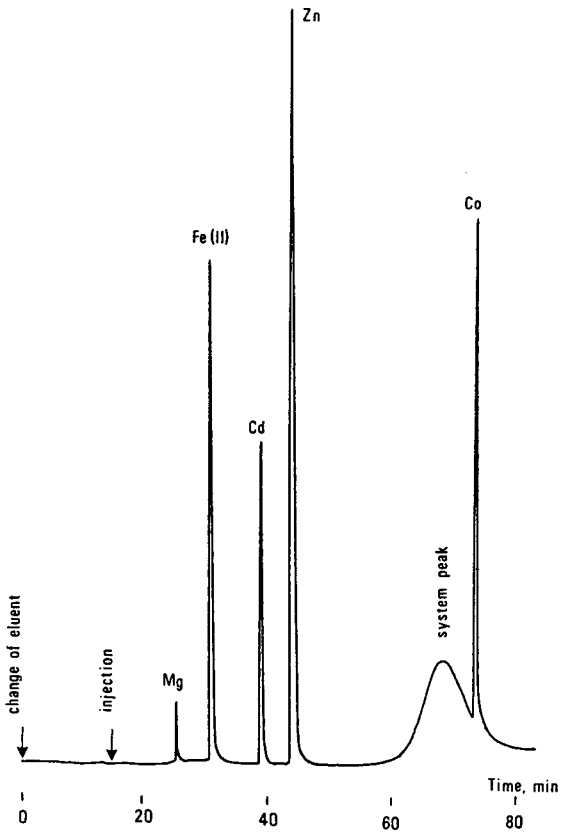

Fig. 1. Chromatogram of model mixture of metals. Column, 250 × 4.6 mm I.D. Tetren-SiO_2, particle size 10 μm; capacity, 0.28 mmol/g; starting buffer, 0.01 *M* Tris–HCl (pH 7.5); eluent, 1:20 Polybuffer 74 (pH 3.4); flow-rate, 1 ml/min; spectrophotometric detection at 540 nm with postcolumn reaction with PAR.

2. Experimental

2.1. Apparatus

An isocratic chromatographic system, consisting of a Beckman (Berkeley, CA, USA) Model 114M high-pressure pump, a Rheodyne (Cotati, CA, USA) Model 7125 injection valve, a Conductolyzer 5300B conductimeter (LKB, Bromma, Sweden), a Model 204 variable-wavelength spectrophotometric detector (Linear, Reno, NV, USA), a DP-700 integrator–recorder (Spectra-Physics, San Jose, CA, USA) and a RediRac 2112 fraction collector (LKB), was used. The stainless-steel chromatographic column was slurry packed with the silica-based polybuffer ion exchanger Tetren-SiO_2 from 2-propanol–water (1:3). The measurement of conductivity and conductimetric titration of the starting buffers and polyampholyte eluents were performed with a Model MM-34-04 conductimeter (Moscow, Russian Federation) equipped with smoothed platinum electrodes. The concentration of transition metals in the fractions was determined spectrophotometrically by reaction with PAR as described [5].

2.2. Reagents

The polybuffer ion exchanger Tetren-SiO_2 was prepared by modification of silica (Silasorb Si300, 10 μm; Lachema, Brno, Czech Republic) surface with 3-glycidoxypropyltriethoxysilane followed by treatment with tetraethylenepentamine (both reagents from Reachim, Moscow, Russian Federation) according to slightly modified procedure [6]. Aqueous solutions of Tris, glycylglycine and L-histidine (Serva, Heidelberg, Germany) were used as starting buffers. Dilute solutions of Polybuffer 74 (Pharmacia, Uppsala, Sweden) were used as polyampholyte eluents. The required pH of the eluents was adjusted with 0.1 *M* HCl. Stock solutions of transition

metals were prepared from the corresponding nitrates [sulphate for iron(II)].

3. Results and discussion

A number of papers have reported applications of different zwitterionic eluents such as N-substituted-aminoalkanesulphonic acids and aminocarboxylic acids for the determination of anions by ion chromatography [7–10]. The main advantage of these eluents in their low conductivity, providing sensitive detection in the "non-supressed" mode. Another advantage is the simplicity of suppression of the conductivity of zwitterionic eluents for their concentration gradient required for the elution of strongly retained solutes.

It is also known that carrier ampholytes used in isoelectrofocusing and the polyampholyte eluent Polybuffer 74 used in chromatofocusing are zwitterionic substances with higher molecular masses. They both have the following main properties [1,11,12]: background conductivity as low as 2–10 μS/cm; constant value of conductivity over a wide pH range; and good and constant buffer capacity in the same pH range.

The first step, conductimetric titration of Polybuffer 74 diluted 1:8 with 0.025 *M* histidine was performed to ensure the above-mentioned characteristics of Polybuffer 74. It was found that the conductivity of the 1:8 diluted solution of Polybuffer 74 and the buffer capacity are virtually constant over the pH range 3.9–7.1. The conductivity of the solution was 8–10 μS/cm. It should be noted that the same interval of pH covers the range of the pH gradient formed in the column.

The properties of Polybuffer 74 provide the possibility of forming an isoconductive linear pH gradient in the chromatographic column and consequently of performing conductimetric detection. Evidently, in this instance the Tetren-SiO_2 ion exchanger acts as a solid-phase suppressor with limited capacity. The initial chromatogram of a model mixture of transition metals obtained with a pH gradient is shown in Fig. 2. A good separation of manganese(II), cadmium(II), zinc(II) and cobalt(II) was obtained. The chromatographic peaks of the metals were detected by on-line measurement of the conductivity of the effluent and also by the spectrophotometric determination in the collected fractions by reaction with PAR. The sensitivity of detection in both instances is virtually identical. However, the background conductivity of the effluent during a chromatographic run is decreased corresponding to the pH profile. This is connected with the difference in the conductivity values of the starting buffer and the polyampholyte eluent. This difference can be minimized by optimization of the nature and concentration of the starting buffer and the polyampholyte

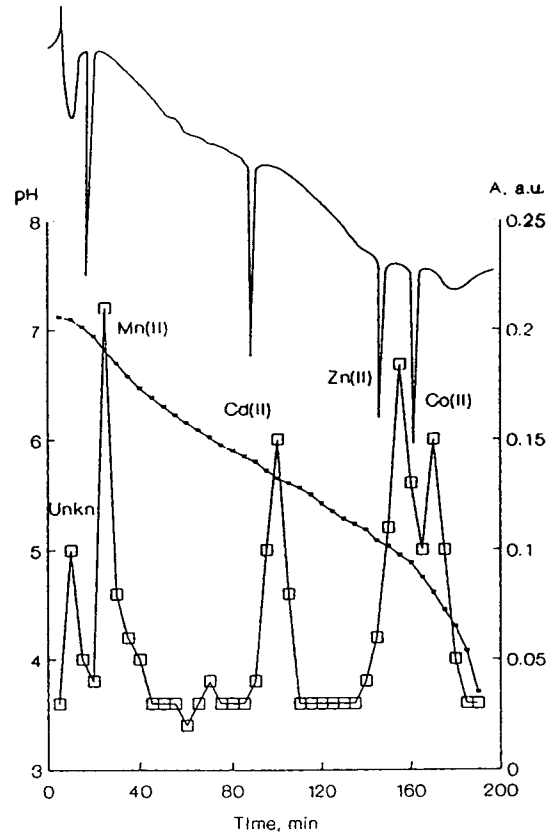

Fig. 2. Separation of standard mixture of metals. Column as in Fig. 1. Starting buffer, 0.025 *M* histidine–HCl (pH 7.5); eluent, 1:8 Polybuffer 74 (pH. 3.4); flow-rate, 1 ml/min; conductimetric and spectrophotometric detection at 540 nm with PAR in collected fractions ($V = 5$ ml).

eluent. The relationship between the conductivity of various starting buffers and the polyampholyte eluent and their concentration was investigated for this purpose (Fig. 3). The dilution of the starting buffer made on the basis of Tris, glycylglycine or histidine produces a greater decrease in conductivity in comparison with the dilution of Polybuffer 74. Hence during the optimum dilution good correspondence of the conductivities was achieved for the pair 0.004 *M* histidine–1:50 Polybuffer 74. As a result, no significant disturbance of the baseline was observed for this system of eluents during a blank chromatofocusing run.

The chromatogram of the model mixture of metals obtained under the optimum conditions (Fig. 4) demonstrates the straight baseline and the suitability of conductimetric detection of transition metals with the use of a pH gradient.

There are no data available on the chelating properties of Polybuffer 74. However, assuming

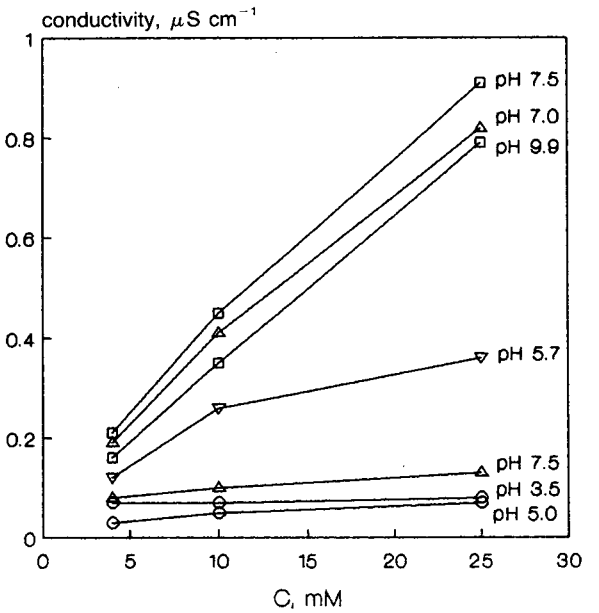

Fig. 3. Relationship between the conductivity of the starting buffers and of the polyampholyte eluent and the concentration and pH. □ = Tris; △ = histidine; ▽ = glycylglycine; ○ = Polybuffer 74.

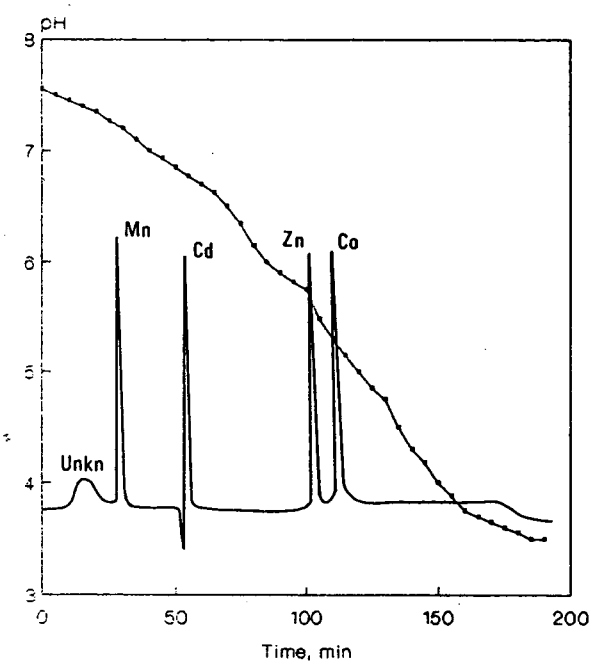

Fig. 4. Chromatogram of model mixture of metals using an isoconductive pH gradient. Column as in Fig. 1. Starting buffer, 0.004 *M* histidine (pH 7.6); eluent, 1:50 Polybuffer 74 (pH 3.4); flow-rate, 1 ml/min; conductimetric detection.

complexation for the polyampholyte eluent used and taking into account its low background conductivity, one can suggest a direct detection mode of the separated metals in the form of complexes with aminopolycarboxylic fragments of the zwitterionic molecules of polyampholyte eluent. In comparison with the results of the determination of the negatively charged complexes of transition metals with EDTA by "non-supressed" IC at a fixed pH of the eluent with conductivity detection [13,14], the sensitivity of detection was the same. The detection limits of metal ions with the isoconductive pH gradient system using 0.004 *M* histidine–1:50 Polybuffer 74 as the eluent were Fe(II) 10, Co(II) 10, Mn(II)15, Zn(II) 7 and Cd(II) 5 μg/l. Moreover, the sensitivity of the proposed chromatographic method can be simply improved by increasing the sample volume with preconcentration of transition metals on the same column.

4. Conclusions

The properties of different eluents used in chromatofocusing were investigated. An isoconductive pH gradient system consisting of 0.004 *M* histidine (pH 7.5) starting buffer and 1:50 Polybuffer 74 (pH 3.4) polyampholyte eluent is proposed for the separation of transition metals on a column of tetraethylenepentamine-bonded silica. The possibility of conductimetric detection of separated metals without "suppression" was demonstrated for a linear gradient from pH 7.5 to 3.5 formed during the separation.

5. References

[1] M.T. Hearn and D.J. Lyttle, *J. Chromatogr.*, 218 (1981) 483.
[2] P.N. Nesterenko and A.V. Ivanov, *Vestn. Mosk. Univ., Khim.*, 33 (1992) 574.
[3] P. Nesterenko and A.V. Ivanov, Presented at the *International Ion Chromatography Symposium, Linz, Austria, 1992*, N 10.
[4] P.G. Righetti, *Isoelectric Focusing: Theory, Methology and Applications*, Elsevier, Amsterdam, 1983.
[5] A.V. Ivanov, V.N. Figurovskaya and V.M. Ivanov, *Vestn. Mosk. Univ., Khim.*, 33 (1992) 570.
[6] A.J. Alpert and F.E. Regnier, *J. Chromatogr.*, 185 (1979) 375.
[7] K. Irgum, *Anal. Chem.*, 59 (1987) 358.
[8] K. Irgum, *Anal. Chem.*, 59 (1987) 363.
[9] O.A. Shpigun, I.N. Voloshchik and Yu.A. Zolotov, *Anal. Sci.*, 1 (1985) 335.
[10] O.A. Shpigun, I.N. Voloshchik and Yu.A. Zolotov, *Zh. Anal. Khim.*, 42 (1987) 1209.
[11] W.J. Gelsema, C.L. DeLigny and N.G. Van der Veen, *J. Chromatogr.*, 173 (1979) 33.
[12] W.J. Gelsema and C.L. DeLigny, *J. Chromatogr.*, 178 (1979) 550.
[13] B. Kondratjonok and G. Schwedt, *Fresenius' Z. Anal. Chem.*, 332 (1988) 333.
[14] D. Yan and G. Schwedt, *Fresenius' Z. Anal. Chem.*, 338 (1990) 149.

ELSEVIER

Journal of Chromatography A, 671 (1994) 101–108

JOURNAL OF CHROMATOGRAPHY A

Practical applications of element-specific detection by inductively coupled plasma atomic emission spectroscopy and inductively coupled plasma mass spectrometry to ion chromatography of foods

Douglas T. Heitkemper*, Lisa A. Kaine, David S. Jackson, Karen A. Wolnik

National Forensic Chemistry Center, Food and Drug Administration, 1141 Central Parkway, Cincinnati, OH 45202, USA

Abstract

Three practical examples are presented to demonstrate the utility of element-selective detection for ion chromatography (IC). The determination of As species in a liquid health food supplement by IC with inductively coupled plasma atomic emission spectroscopy (IC–ICP-AES) is shown to confirm results obtained for total As. IC–ICP-AES is also used to investigate the identity of an unknown peak in a sample of shrimp commercially treated with tripolyphosphate. Finally, results are presented for the determination of residual bromate in baked goods by IC with inductively coupled plasma mass spectrometry detection.

1. Introduction

The combination of ion chromatography (IC) with inductively coupled plasma atomic emission spectroscopy (ICP-AES) or inductively coupled plasma mass spectrometry (ICP-MS) provides a powerful analytical technique. In comparison to total element determinations by atomic spectrometric techniques, this hyphenated technique provides information regarding the chemical form of a particular element. The chemical form or nature of an element can greatly affect its function, bioavailability and toxicity. In addition, the ability to monitor a specific element(s) can eliminate chromatographic interferences associated with difficult matrices. This permits accurate, reliable analyses even when the separation of analyte from matrix is incomplete. ICP-AES and ICP-MS have high elemental sensitivity and are capable of monitoring more than one element simultaneously. The coupling of ICP-AES and ICP-MS with chromatography has been reviewed by several groups [1–4]. Arsenic, lead, mercury, selenium, tin and chromium have been the subject of the majority of studies involving element-specific detection for HPLC and IC [1–4]. In this paper, three applications of element-specific detection for food analysis will be discussed.

The Food and Drug Administration is responsible for ensuring that food products in the marketplace are safe; this includes health food supplements. The determination of toxic trace elements such as arsenic in mineral supplements is thus of interest. The use of IC–ICP-AES for the determination of As provides important

* Corresponding author.

SSDI 0021-9673(93)E0085-9

toxicity information since various species have widely differing toxicities. The technique can also be used to confirm the results obtained for total As.

Arsenic has been the element most studied by element-selective detection using both ICP-AES and ICP-MS. These studies have been reviewed elsewhere [2,3]. The advantage of element-specific detection in the IC determination of As(III) and As(V) has been demonstrated using a direct-current plasma [5,6]; however, no applications were reported.

Polyphosphates are added to seafood products to provide protection from moisture loss during processing [7]. However, the amount of polyphosphate used must be controlled in order to prevent the uptake of excess water by treated products. The potential for economic fraud through mislabeling or excessive use necessitates the development of analytical methodology for polyphosphates and their hydrolysis products. There are reports of both ICP-AES and ICP-MS detection for phosphates separated by HPLC [8,9]. In this work, ICP-AES detection is used in the investigation of an unknown peak found by IC with UV detection in samples of shrimp processed with sodium tripolyphosphate.

There is some concern regarding the health effects of residual bromate in bakery products. Potassium bromate is used in the baking industry as a dough conditioner. The majority of bromate is reduced to bromide during the baking process; however, residual bromate has been found in some baked goods. The determination of residual bromate using IC with conductivity detection is complicated because of inadequate sensitivity and the presence of interfering matrix species such as chloride [10]. The combination of gel-permeation liquid chromatography and ICP-MS has been used in the determination of several inorganic halogen species including bromate, but was not applied to bakery products [11]. IC–ICP-MS detection of bromate at m/z 79 and/or 81 provides excellent sensitivity and freedom from matrix interferences.

2. Experimental

2.1. Apparatus

The chromatographic system used consisted of a Dionex (Sunnyvale, CA, USA) system 4500i equipped with a gradient pump Module-2, liquid chromatography Module-3, variable-wavelength detector and an ASM autosampler. Analytical columns used in this work were the IonPac AS4A, IonPac AS7 and IonPac AS10 (250 × 4 mm, Dionex). Guard columns used were the IonPac AG4A, IonPac NG1 and IonPac AG10 (50 × 4 mm, Dionex).

A Thermo Jarrell Ash Model 1140 Plasma Atomcomp Polychromator ICP-AES system was used. The instrument was operated in an intensity *vs.* time data acquisition mode. The acquisition time was 3 s/point for the As detection work and 7.5 s/point for the P detection work. The acquisition time used depends on the length of the chromatographic run because the maximum number of time slices allowed in this operating mode is 100. The operating conditions were as follows: Ar coolant gas flow, 20 l/min; Ar auxiliary gas flow, 1.5 l/min; Ar nebulizer gas flow, 0.75 l/min; forward power, 950 W; P line monitored, 214.9 nm; As line monitored, 193.9 nm.

The ICP-MS system used was a VG/Fisons PlasmaQuad Model PQ2+ Turbo. The operating parameters used were as follows: Ar coolant gas flow, 14 l/min; Ar auxiliary gas flow, 1.1 l/min; Ar nebulizer gas flow, 0.82 l/min; forward power, 1350 W; resolution 0.8 u. For chromatographic sample introduction, the instrument was operated in the single ion monitoring mode with a 1-s integration time per data point. For the determination of bromate in baked goods, the ^{79}Br isotope was monitored.

The interface between the IC system and the ICP-AES or ICP-MS detector consisted of a *ca.* 48 in. (1 in. = 2.54 cm) length of 0.010 in. I.D. polyether ether ketone (PEEK) tubing. The tubing connected either the outlet of the UV cell or the conductivity detector cell to the inlet of a concentric nebulizer which is used for sample

introduction to both the ICP-AES and ICP-MS systems.

Chromatographic data obtained for both ICP-AES and ICP-MS were converted to ASCII files and imported into a spreadsheet program for evaluation of peak heights and retention times.

2.2. Reagents and standard solutions

The water used throughout this work was distilled and deionized (DDW). Sodium hydroxide used in preparing mobile phases was a 50% (w/w) solution (Fisher Scientific, Fair Lawn, NJ, USA). Nitric and perchloric acids used were double distilled (GFS Chemicals, Columbus, OH, USA). Sulfuric acid and ferric nitrate 9-hydrate were reagent grade.

Sodium arsenite and sodium arsenate standards were prepared from reagent-grade chemicals (Fisher) dissolved in DDW. Food-grade sodium tripolyphosphate was obtained from Monsanto (St. Louis, MO, USA). Sodium pyrophosphate decahydrate was obtained from Aldrich (Milwaukee, WI, USA) and sodium phosphate monobasic was obtained from EM Science (Gibbstown, NJ, USA). Stock standards of each (10 000 μg/ml) were prepared in DDW. Potassium bromide and sodium bromate stock standards (1000 μg/ml) were prepared from reagent-grade chemicals (Aldrich) dissolved in DDW.

3. Results and discussion

3.1. Determination of inorganic arsenic species in a liquid health food supplement

Element-specific detection has been used extensively in the analysis of arsenic because of large differences in the toxicity of various arsenic-containing species [2–4]. The use of conductivity detection for As(III) is difficult because of the low ionization constant of arsenous acid [6]. In this work, IC–ICP-AES is used to determine the oxidation state of inorganic As found in a liquid health food supplement.

Samples were simply diluted 1:10 with DDW and filtered through a 0.2-μm nylon syringe filter. Fig. 1 shows the separation of arsenite and arsenate spiked into a sample of the health food supplement at the 5 μg/ml level. A single standard addition was used to quantitate arsenate found in the samples. No arsenite was detected. The solution detection limits were 0.16 and 0.14 μg/ml for arsenite and arsenate, respectively. Ten background points were measured in a blank solution at the analyte retention time; and the detection limit was calculated as three times the standard deviation of these ten points divided by the sensitivity obtained for a 4 μg/l analyte standard.

Four samples were analyzed and good agreement was obtained with total As results determined directly by ICP-AES. The average and standard deviation for the total As measurements of four samples was 9.0 ± 0.1 μg/ml. In comparison, the IC–ICP-AES result was 9.1 ± 0.5 μg/ml of arsenate.

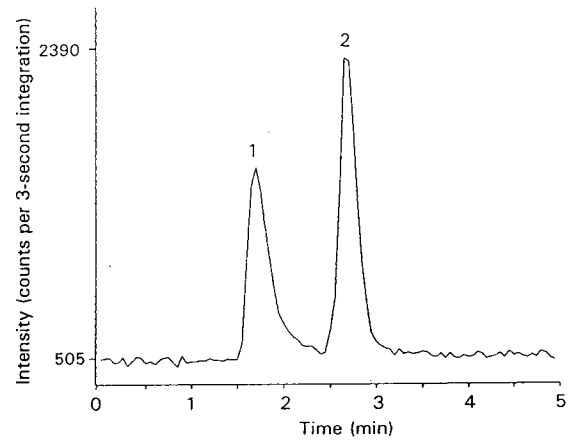

Fig. 1. As-specific detection in a liquid health food supplement. Peaks: 1 = 5 μg/ml As(III) spike; 2 = 5 μg/ml As(V) spike. Column, Dionex IonPac AS4A. Mobile phase, 40 m*M* sodium hydroxide. Flow-rate, 1.0 ml/min. Injection volume, 100 μl. Suppressor, Dionex AMMS-I. Regenerant, 12.5 m*M* sulfuric acid. Regenerant flow-rate, *ca.* 5 ml/min. Detection, ICP-AES 193.7 nm.

3.2. Investigation of polyphosphates in processed shrimp by IC–ICP-AES

A method for the determination of tripolyphosphate and its hydrolysis products in processed shrimp using IC with post-column reaction UV detection has been described elsewhere [12]. The presence of a peak of unknown identity when using UV detection was cause for some concern. The unknown peak eluted between peaks for tripolyphosphate and pyrophosphate and near the retention time for sulfate. However, a sulfate spike of the sample solution showed that the unknown was not sulfate. It was important to show that the peak was not a phosphate-containing species such as trimetaphosphate which is a known impurity in some commercially available sodium tripolyphosphates [13].

Shrimp samples were composited and prepared as described in ref. 12. Composited sample (0.5 g) was diluted 1:100 with DDW and shaken for 30 min. A portion of the extract was then filtered through a nylon syringe filter and a C_{18} sample preparation cartridge in series. Fig. 2 shows UV and ICP-AES chromatograms obtained for a sample of cooked processed shrimp which had been treated with tripolyphosphate. In this case, the outlet of the UV cell was connected directly to the ICP-AES instrument; thus the column effluent and the UV post-column reagent (0.1% ferric nitrate in 2% perchloric acid) were introduced to the plasma. The unknown peak (3) is only detected by the UV detector. Based on the strong ICP emission signal obtained for orthophosphate, pyrophosphate and tripolyphosphate peaks, it can be concluded that the unknown peak does not contain phosphorus and should not affect the analysis of tripolyphosphate and its hydrolysis products.

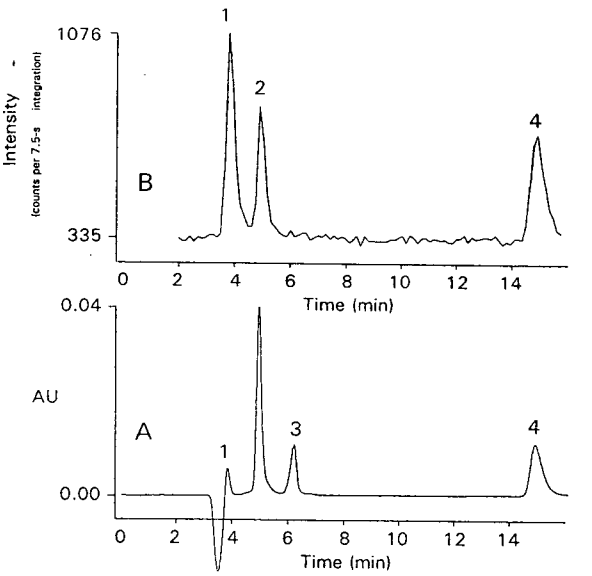

Fig. 2. Determination of polyphosphates in shrimp. (A) UV detection at 330 nm; (B) ICP-AES detection of P at 214.9 nm. Peaks: 1 = orthophosphate; 2 = pyrophosphate; 3 = unknown; 4 = tripolyphosphate. Column, Dionex IonPac AS7. Guard column, NG1. Mobile phase 70 m*M* nitric acid. Flow-rate, 0.5 ml/min. Injection volume, 100 μl. Post-column reagent for UV detection, 1 g/l ferric nitrate in 2% perchloric acid. Post-column reagent flow-rate, 0.5 ml/min.

3.3. Determination of bromate and bromide in baked goods by IC–ICP-MS

Investigations into the health risks associated with the use of potassium bromate in bread require the development of analytical methodology capable of quantitating bromate at the low ng/g level. Conductivity detection is hampered by insufficient sensitivity and interference from high chloride levels in baked goods [10]. IC–ICP-MS provides sufficient sensitivity and freedom from interferences to accurately quantitate bromate in a relatively straightforward manner.

Five slices of bread from different areas of the same loaf were cut (or torn) into small pieces approximately 1 cm^3, placed into a plastic ziplock bag, and mixed thoroughly. A 25-g sample of the composite was accurately weighed into a clean 250-ml Nalgene HDPE bottle and 200.0–225.0 g of DDW were added. The sample was then homogenized using a Kinematica Polytron homogenizer for approximately 2 min. A portion of the sample solution was then centrifuged at 2500 *g* for 5 min (in later work, the centrifuge step was omitted). Finally, a portion of the supernatant was passed through a 0.45-μm nylon

syringe filter and an activated Alltech Maxi-clean C_{18} sample preparation cartridge. This solution served as the sample solution. The C_{18} cartridge was activated by passing through 20 ml of methanol followed by 20 ml of DDW. The first 3 ml of sample through the syringe filter and C_{18} column were discarded.

A similar procedure was followed for bun and roll samples. One or two buns (or rolls) were sampled and treated in the same manner as the five slices of bread. In more recent studies, a single bun or roll has been cut into small pieces and the entire sample is diluted 1:10 with DDW, after which the sample is prepared as described above.

Samples should be stored frozen prior to preparation and analysis. Prepared samples should be analyzed as soon as possible after preparation.

A Dionex AS10 analytical IC column and AG10 guard column with a mobile phase of 150–180 m*M* NaOH at a flow-rate of 1 ml/min has been found to provide good separation of bromate, bromide and some unidentified interferences. A micromembrane suppressor, Dionex Model AMMS-II, has been utilized to reduce the amount of Na which reaches the ICP-MS system. Large amounts of Na introduced to the ICP-MS system can cause suppression of analyte signal and response drift. Bromate and bromide elute at retention times of approximately 6 and 17 min, respectively. In bread matrix, both the bromate and bromide peaks elute at slightly shorter retention times than found with standards presumably because of matrix effects. Peak height was used for quantitation due to difficulties associated with integrating peak areas using the present method of data collection and evaluation.

Peak height response was found to be linear over the range 1 to 1000 ng/ml for bromate and 2 to 500 ng/ml for bromide. The solution detection limit for bromate was 0.6 ng/ml. This corresponds to a method detection limit of approximately 6 ng/g in baked goods. For bromide the solution detection limit was 1.0 ng/ml. Detection limit was defined as the concentration of bromate which would result in a peak height equivalent to three times the standard deviation of 30 background points for a blank solution taken at the retention time of the analyte. For 10 consecutive injections of a 10 ng/ml bromate standard, a R.S.D. of 2.1% was obtained. Figures of merit obtained using the 150 m*M* sodium hydroxide eluent are summarized in Table 1.

Initially, an eluent of 180 m*M* sodium hydroxide was used. Four replicate injections of a fully prepared sample extract from hot dog buns resulted in an average of 80 ng/g bromate and 44 μg/g bromide with R.S.D.s of 7.9 and 5.0%, respectively. In a similar experiment with "brown and serve" bread sticks, five portions of extract were filtered through five syringe filters and C_{18} cartridges and analyzed. This resulted in an average of 8.2 μg/g bromate and 37 μg/g bromide with R.S.D.s of 8.2 and 7.0%, respectively. Thus in both cases the repeatability of sample injections was less than 10% R.S.D. for both bromate and bromide.

This chromatographic system (AS10 column with 180 m*M* NaOH eluent) was used to analyze several different sample types. Table 2 shows the results obtained for seven samples of buns and rolls. Bromate was found in six of the seven

Table 1
Figures of merit

	Bromate	Bromide
Solution detection limit (ng/ml)	0.6	1.0
Short-term precision (10 ng/ml)	2.1% ($n = 10$)	3.2% ($n = 4$)
Linear range (ng/ml)	1–1000	2–500
Correlation coefficient	0.9999	0.9998
Sensitivity (slope)	909 cps/ng/ml	483 cps/ng/ml
Log–log slope	0.98	0.99

Table 2
Results for buns and rolls, 180 m*M* NaOH eluent

Description	Bromate concentration (μg/g)	Bromide concentration (μg/g)
Steak rolls	1.6, 1.1	37, 33
Twist rolls	0.7, 0.3	39, 36
Hot dog buns	1.1, 0.08	45, 44
French rolls	<0.04	16, 14
Hot dog buns	0.08, 0.09	14, 14
Hot dog buns	0.8, 0.7	23, 23
Brown and serve bread sticks	10.5	35, 36

samples at concentrations ranging from 0.8 to 10.5 μg/g. Table 3 shows the results obtained for ten samples of sliced bread. The determination of bromate using this separation system is still somewhat hampered by the incomplete resolution of bromate and an interference. Based on the amount of interference seen in these ten bread samples, a conservative estimate of the bromate detection limit (0.04 μg/g) was made. None of the sliced bread samples analyzed was found to contain bromate at a concentration above the detection limit. Spike recoveries for a 0.1 μg/g bromate spike into three of the samples are also reported in Table 3. Recoveries for the three spiked samples were 78, 86 and 134%.

The use of 150 m*M* NaOH was found to provide adequate separation of the bromate peak and unidentified interference. Fig. 3 shows a spiked and unspiked chromatogram for a sample of white bread. The spike concentration was 1 ng/ml bromate (roughly 10 ng/g of sample). The bromate peak is well resolved from any interfering peaks. The same ten sliced bread samples as listed in Table 3 were analyzed using the 150 m*M* NaOH. In each case bromate was not detected.

The chromatogram shown in Fig. 4 was obtained from a sample of "brown and serve" Italian rolls. Ten separate rolls were prepared by homogenizing the entire rolls. Bromate was present at an average concentration of 3.5 μg/g of sample. The average bromide concentration

Table 3
Results for sliced bread, 180 m*M* NaOH eluent

Description	Bromate concentration (μg/g)	Bromide concentration (μg/g)
Buttermilk	<0.04	7.0, 6.6
Whole wheat	<0.04	6.6, 6.3
Multigrain	<0.04	5.8, 5.8
Whole grain	<0.04 (134%)	5.9, 5.9
White	<0.04	7.0, 6.0
Rye	<0.04 (86%)	6.4, 6.6
Light white	<0.04 (78%)	Not determined
White	<0.04	7.0, 6.8
Light white	<0.04	32, 32
White	<0.04	5.8, 5.3

Numbers in parentheses are recovery values for a 0.1 μg/g bromate spike (10 ng/ml in solution).

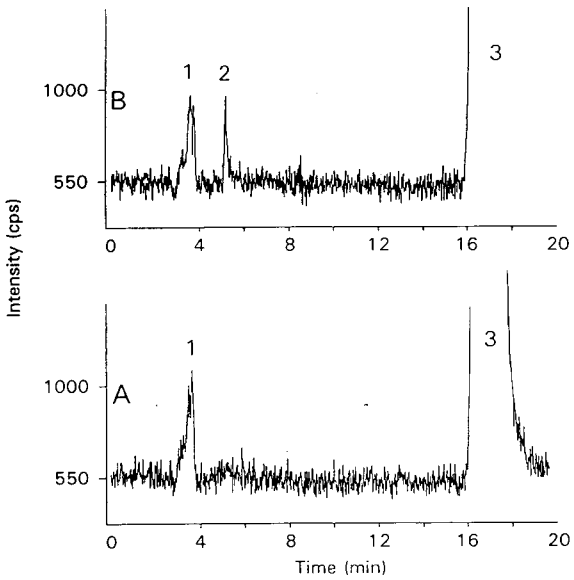

Fig. 3. Chromatograms of spiked and unspiked samples of white bread using ICP-MS detection. (A) Unspiked sample; (B) spiked sample, 1 ng/ml bromate spike. Peaks: 1 = unknown; 2 = bromate; 3 = bromide (off scale). Column, Dionex IonPac AS10. Guard column, AG10. Mobile phase, 150 m*M* sodium hydroxide. Flow-rate, 1.0 ml/min. Injection volume, 100 μl. Suppressor, Dionex AMMS-II. Regenerant, 25 m*M* sulfuric acid. Regenerant flow-rate, *ca.* 5 ml/min.

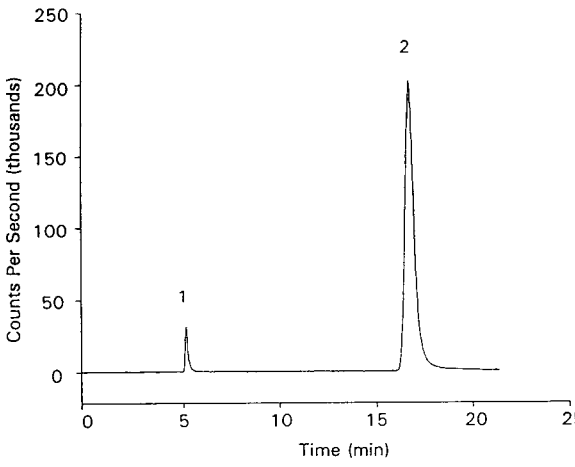

Fig. 4. Chromatogram of "brown and serve" Italian roll using ICP-MS detection. Peaks: 1 = bromate; 2 = bromide. Chromatographic conditions as for Fig. 2.

was 36 μg/g of sample. The R.S.D.s for the 10 samples were 8.1% and 8.9% for bromate and bromide concentrations, respectively.

4. Conclusions

Element specific detection for ion chromatography by ICP-AES or ICP-MS has been shown to resolve persistent separation problems in food analysis as well as provide additional confirmation of peak identity. The oxidation state of inorganic arsenic in a liquid health food supplement was determined by IC–ICP-AES. While ICP-AES is generally more tolerant of the eluents used in IC, ICP-MS provides enhanced sensitivity. The combination of IC and ICP-MS allows the requisite sensitivity and freedom from chromatographic interferences which are necessary to make an informed decision on the potential health risks associated with ingestion of bromate from baked goods.

5. Acknowledgement

The authors would like to thank the Division of Product Manufacture and Use, Center for Food Safety and Applied Nutrition, United States Food and Drug Administration for providing several of the bread samples.

6. References

[1] P.C. Uden, *Trends Anal. Chem.*, 6 (1987) 238–246.
[2] L. Ebdon, S. Hill and R.W. Ward, *Analyst*, 112 (1987) 1–16.
[3] S.J. Hill, M.J. Bloxham and P.J. Worsfold, *J. Anal. At. Spectrom.*, 8 (1993) 499–515.
[4] N.P. Vela, L.K. Olson and J.A. Caruso, *Anal. Chem.*, 65 (1993) 585A–597A.
[5] I.T. Urasa, S.H. Nam and V.D. Lewis, in P. Jandik and R.M. Cassidy (Editors) *Advances in Ion Chromatography*, Century International, Medfield, MA, 1990, pp. 93–110.
[6] I.T. Urasa and F. Ferede, *Anal. Chem.*, 59 (1987) 1563–1568.
[7] V. Tenhet, G. Finne, R. Nickelson and D. Toloday, *J. Food Sci.*, 46 (1981) 350–352.

[8] M. Morita and T. Uehiro, *Anal. Chem.*, 53 (1981) 1997–2000.
[9] S. Jiang and R.S. Houk, *Spectrochim. Acta*, 43B (1988) 405–411.
[10] K. Oikawa, H. Saito, S. Sakazume and M. Fujii, *Chemosphere*, 11 (1982) 953–61,
[11] V.V. Salov, J. Yoshinaga, Y. Shivata and M. Morita, *Anal. Chem.*, 64 (1992) 2425–2428.
[12] D.T. Heitkemper, L.A. Kaine, D.S. Jackson and K.A. Wolnik, in *Proceedings of the Third Joint Conference of the Atlantic Fisheries Technology Society and Tropical and Subtropical Fisheries Technology Society, Williamsburg, Oct. 1993*, in press.
[13] S. Greenfield and M. Clift, *Analytical Chemistry of Condensed Phosphates*, Pergamon Press, New York, 1975.

ELSEVIER

Journal of Chromatography A, 671 (1994) 109–114

JOURNAL OF CHROMATOGRAPHY A

Maximizing signal-to-noise ratio in direct current and pulsed amperometric detection

Roy D. Rocklin *, Tom R. Tullsen, Mark G. Marucco

Dionex Corporation, 1228 Titan Way, Sunnyvale, CA 94088-3603, USA

Abstract

The magnitude of signal obtained during d.c. and pulsed amperometric detection using a thin-layer type cell is dependent on several factors, two of which are controlled by the cell design. These two factors are the surface area of the working electrode and the mobile phase velocity over the surface of the working electrode. Mobile phase velocity is controlled by the thickness and width of the thin-layer channel gasket. In this report, the effect of varying working electrode size and gasket dimensions are studied. Using 1 mm diameter working electrodes and a 25 μm × 1.3 mm gasket, the minimum detection limit for dihydroxybenzylamine is about 6 femtomoles and for glucose, about 200 femtomoles.

1. Introduction

The most commonly used amperometric detector cell design is the thin-layer cell. In a typical construction, a thin gasket with a slot cut in the middle is sandwiched between two blocks: one a metal which forms the counterelectrode and the other a flat disk working electrode surrounded by insulating plastic. The block containing the working electrode is made by force-fitting a rod of working electrode material into the plastic block and polishing the surface to a flat finish. The slot cut in the gasket forms the thin-layer channel. The column effluent enters the thin-layer channel, rapidly develops laminar flow, and flows across the surface of the working electrode where the analytes are detected. The reference electrode is placed downstream from the working electrode.

Other amperometric detector designs include the use of tubular working electrodes and the "wall-jet" design, in which the column effluent impinges directly on (perpendicular to) the working electrode. Compared to these and other designs, the thin-layer cell has several advantages: (1) Construction is simple, requiring only a means of clamping the two blocks together without the gasket leaking. (2) The thin channel produces high mobile-phase linear velocity over the surface of the working electrode, which produces high signal magnitude. (3) The working electrode is easily cleaned by polishing. (4) The internal volume of the thin-layer channel can be made very low, thus minimizing peak dispersion contributed by the detector and efficiently sweeping out of the cell high-concentration components. (5) Cell resistance is very low due to the short distance between the working and counterelectrodes. This prevents voltage drop from lowering the actual potential on the working electrode and increases the linear calibration

* Corresponding author.

0021-9673/94/$07.00
SSDI 0021-9673(93)E1234-Q

range. (6) Any conductor available in rod form can be used as the working electrode.

Several studies have been published on the signal magnitude from thin-layer type amperometric detector cells using d.c. amperometry at a glassy carbon working electrode [1–9]. Equations are derived from fundamental principles of hydrodynamics and then compared to actual data. Eq. 1 has been derived and tested [6] and appears to be an accurate predictor of cell current (i). It is applicable to a thin-layer cell with a circular working electrode whose diameter is the same as the channel width, in which flow is laminar, and for analytes where the current is diffusion controlled; *i.e.* the reaction rate is limited by the rate of diffusion of analyte molecules to the surface of the working electrode and not by the rate of the electron transfer reaction.

$$i = 1.47nFU^{1/3}(DA/h)^{2/3}C \quad (1)$$

The number of electrons transferred in the redox reaction is n, F is the Faraday, U is the volume flow-rate, D is the analyte diffusion coefficient, A is the working electrode surface area, h is the height of the thin-layer channel; *i.e.* the thickness of the gasket, and C is analyte concentration. The equation parameters can be divided into two categories. Parameters n, U, D and C are determined by the analyte and mobile phase characteristics. Working electrode surface area A and thin-layer channel thickness h are the only cell parameters which control detector response. That signal is dependent on electrode surface area is obvious; the greater the surface area, the more analyte molecules can be detected. The dependence on channel height is actually a result of the effect of height on the linear velocity of flow over the surface of the working electrode. With a constant volume flow-rate, linear velocity is inversely proportional to h, so cell current is dependent on linear velocity to the 2/3 power. The effect of increasing linear velocity is to decrease the Nernst diffusion layer thickness. This increases the analyte concentration gradient at the working electrode surface, increasing cell current.

The true goal is maximizing signal-to-noise ratio and not just signal, so determining the effect of cell parameters on noise is just as important as determining their effect on signal. Several reports have dealt with the effect of cell parameters on both signal and noise [1,3,5,7,8]. In general, noise was found to be directly proportional to working electrode surface area. Signal-to-noise ratio should actually improve slightly as the working electrode surface area is decreased. However, for very small working electrodes, electronics noise is the limiting factor [5].

In this report, the effects of thin-layer channel thickness and working electrode size on signal-to-noise ratio are studied. In addition to theoretical considerations, practical limitations on these parameters are discussed. Two amperometric detection methods are used: d.c. amperometric detection of catecholamines using a glassy carbon working electrode and reversed-phase chromatography; and pulsed amperometric detection of carbohydrates using a gold working electrode and high-pH anion-exchange chromatography.

These two methods were selected for study because they are two of the most common applications of amperometric detection. In addition, the dependence of signal-to-noise ratio on cell design parameters for pulsed amperometry had not yet been addressed. Publications discussing the determination of catecholamines in urine and plasma appear frequently. Two recent articles deal with mobile phase selection [10] and sample preparation [11]. The principles of pulsed amperometric detection and how it is used to determine carbohydrates, alcohols, amines and sulfur species are discussed in two recent reviews [12,13].

2. Experimental section

Glassy carbon working electrodes with diameters of 1 and 3 mm were tested. Smaller or intermediate sizes were not available. Three gold working electrodes were tested; their diameters were 0.5, 1 and 3 mm. Thin-layer channel gaskets ranged from 25 to 125 μm thickness.

All chromatography was performed using Dionex liquid chromatography equipment. Both

Table 1
Potential *vs.* time waveform used to detect carbohydrates

Time (s)	Potential (V)	Integrate
0.00	0.10	
0.20	0.10	Begin
0.40	0.10	End
0.41	0.70	
0.60	0.70	
0.61	−0.10	
1.00	−0.10	

an Advanced Gradient Pump and a DX-500 GP40 gradient pump were used. Flow-rate was 1.0 ml/min and injection volume was 20 μl. The detector was a prototype version of the DX-500 ED40 electrochemical detector. Catecholamines were detected at 0.65 V *vs.* Ag/AgCl reference electrode. The mobile phase for catecholamines consisted of 57 m*M* citric acid, 43 m*M* sodium acetate, 0.1 m*M* disodium EDTA, 1 m*M* octanesulfonic acid (Dionex MPIC-CR2), and 20% methanol. The column was a Zorbax C-18 5 μm, 250 × 4.6 mm. Carbohydrates were detected using the potential *vs.* time waveform listed in Table 1. A CarboPac PA1 250 × 4 mm column was used with 100 m*M* sodium hydroxide mobile phase. All chemicals were reagent grade. Catecholamines were obtained from Aldrich (Milwaukee, WI, USA). Citric acid, sodium acetate, and disodium EDTA were obtained from Fluka (Buchs, Switzerland). Sodium hydroxide was made from 50% concentrate from Fisher (Pittsburgh, PA, USA).

Noise was measured peak-to-peak over a 2-min period of flat baseline. Each point for signal and noise in the tables is the average of six measurements.

3. Results and discussion

D.c. amperometry is routinely used to detect catecholamines [10,11]. A typical example is the chromatography of urinary catecholamines as shown in Fig. 1. Dihydroxybenzylamine (DHBA) is commonly used as an internal standard, and was chosen to be used as the standard compound for measuring signal-to-noise ratio in this study. Glucose was used as the standard compound for pulsed amperometric detection at a gold working electrode.

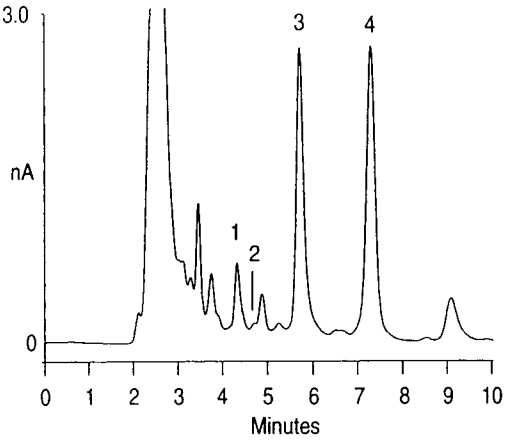

Fig. 1. Separation of catecholamines in alumina extract of urine. Catecholamines from 0.5 ml of urine diluted to 5 ml with 0.6 *M* Tris buffer at pH 8.5 plus 6.3 ng DHBA internal standard were adsorbed on 0.1 g activated alumina. Following a 10-min mixing period in an ice bath, the alumina was washed three times with 5 m*M* acetate buffer at pH 7.0. Catecholamines were released by rinsing the alumina with 0.2 ml of 0.3 *M* acetic acid. This solution was centrifuged and diluted to 1 ml for analysis. A 1 mm diameter glassy-carbon working electrode was used with a 25 μm thick by 1.3 mm wide gasket. Peaks: 1 = norepinephrine, 2 = epinephrine, 3 = DHBA, 4 = dopamine.

3.1. Channel thickness

Signal (peak height), baseline noise, and the resulting signal-to-noise ratios for DHBA as a function of thin-layer channel thickness are listed in Table 2. Detection is by d.c. amperometry at a glassy carbon working electrode. The same measurements using glucose with pulsed amperometric detection at a gold working electrode are also listed in Table 2. For both d.c. and pulsed amperometry, noise is independent of channel thickness while signal increases as the channel is made thinner. The obvious conclusion is that the thin-layer channel should be made as thin as possible. The limit on decreasing channel thickness is a result of practical and not theoretical considerations. First, the gasket must be

Table 2
Signal and noise for d.c. amperometric detection of 2 picomoles DHBA at a 1 mm diameter glassy carbon (G.C.) working electrode and pulsed amperometric detection of 2 picomoles glucose at a 1 mm diameter gold working electrode

Channel thickness (μm)	DHBA signal (pA)	G.C. noise (pA)	DHBA *S/N*	Glucose signal (pC)	Gold noise (pC)	Glucose *S/N*
25	376	0.38	1000	264	8.4	31
50	273	0.36	760	195	7.0	28
75	209	0.38	550	153	7.5	21
100	188	0.31	610	137	8.5	16
125	161	0.39	410	124	7.8	16

Thin-layer channel width and length were 1.6 mm × 12.7 mm.

strong enough to resist damage during normal use. Gaskets which are too thin stretch and tear too easily to be practical to use. Second, the two halves of the cell tend to deform slightly when squeezed together, and if the gasket is too thin, the working electrode may short against the counterelectrode. These two factors place a practical limit of 25 μm (0.001″) on thin-layer channel thickness with this type of cell design.

Using both d.c. and pulsed amperometry, cell current as a function of thin-layer channel thickness is proportional to $h^{-2/3}$, as predicted by eq. 1. A linear fit to a plot of peak height *vs.* $h^{-2/3}$ using the data in Table 2 produces a standard error of 9 pA for DHBA and 5 pC for glucose. Inspection of the plots shows similarity in residuals between the two plots, suggesting that part of the error is caused by small deviations in gasket thicknesses from nominal values.

3.2. Electrode diameter

Signal and noise measured using glassy carbon working electrodes with two diameters are listed in Table 3. The second and third entries list data obtained using the same thin-layer channel dimensions of 125 μm thickness by 3.5 mm width, referred to as the "large" gasket in the table. Both signal and noise decrease as the working electrode diameter is decreased. Signal-to-noise ratio is similar for the two working electrodes tested. The large gasket dimensions are appropriate for the 3 mm diameter working electrode but unnecessarily large for the 1 mm diameter electrode. Using a thinner and narrower thin-layer channel gasket (25 μm × 1.6 mm) with the 1 mm diameter working electrode increases the signal with no effect on noise, as shown in the first entry. In fact, the major advantage of the smaller diameter working electrode is that the cell gasket can be made narrower, thus increasing the linear velocity of mobile phase over the surface of the working electrode, which increases signal without affecting noise. Also, thinner gaskets can be used more easily with a smaller diameter working electrode without introducing mechanical difficulties such as deformation in the channel causing the working electrode to short against the counterelectrode.

Table 4 lists signal, noise, and signal-to-noise ratio for glucose using three gold working electrodes of 0.5, 1, and 3 mm diameter. Both peak height and baseline noise are proportional to working electrode area. Data in the last three rows in Table 4 were obtained using the "large" gasket. Using this common gasket, the 1 mm

Table 3
Signal and noise for d.c. amperometric detection of 2 picomoles DHBA at glassy carbon working electrodes

Electrode diameter (mm)	Gasket	Signal (pA)	Noise (pA)	*S/N*
1	Small	376	0.38	1000
1	Large	124	0.38	330
3	Large	674	2.02	334

The dimensions of the small and large gaskets were 25 μm × 1.6 mm × 12.7 mm and 125 μm × 3.5 mm × 12.7 mm.

Table 4
Signal, noise, and signal-to-noise ratio for 10 picomoles glucose at a gold working electrode

Electrode diameter (mm)	Gasket	Signal (pC)	Noise (pC)	*S/N*
1	Small	1742	11.7	149
0.5	Large	128	4.7	27
1	Large	459	9.2	50
3	Large	3079	70.8	43

The dimensions of the small and large gaskets were 25 μm × 1.3 mm × 6.35 mm and 125 μm × 3.5 mm × 12.7 mm.

diameter electrode produces the best signal-to-noise ratio, probably because a component of electronics noise is present in the 0.5-mm working electrode baseline. It is interesting that even though there is more than one order of magnitude difference in signal between the smallest and largest electrodes, the signal-to-noise ratios are less than a factor of two apart. The large gasket dimensions of 125 μm × 3.5 mm are appropriate for the 3 mm diameter working electrode but are unnecessarily large for the smaller electrodes. Using a 25 μm × 1.3 mm gasket with the 1 mm diameter working electrode, the signal-to-noise ratio is tripled. One might expect that a further increase in signal-to-noise ratio could be achieved using the 0.5-mm working electrode and an even narrower gasket. The difficulty with this approach is machining cell parts such that the working electrode is always placed in the center of the thin-layer channel. The cell must be designed to accommodate some tolerance in the placement of the gasket relative to the working electrode, and this tolerance places a lower limit on gasket width. As a result, it is difficult to gain the advantage of a narrower gasket from the use of a 0.5 mm diameter working electrode.

There are factors to consider other than signal-to-noise ratio when selecting cell design parameters. An example is the comparison of the 3 mm and 1 mm diameter gold working electrodes, as shown in Figs. 2 and 3. A large dip appears in the chromatogram from the 3-mm electrode at approximately 13 min and is barely noticeable using the 1-mm electrode. This dip is caused by

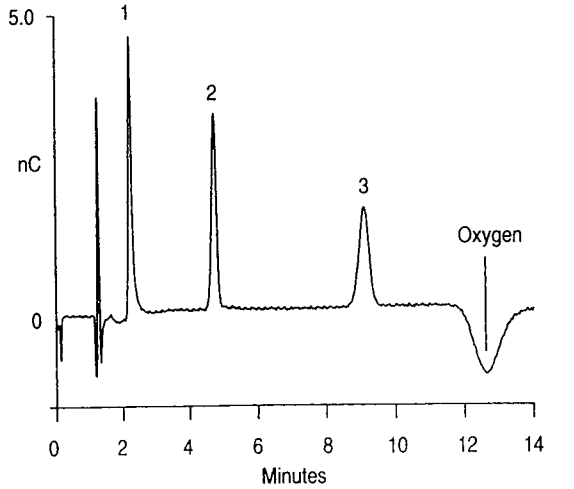

Fig. 2. Pulsed amperometric detection at a 3 mm diameter gold working electrode of 10 picomoles each of (1) sorbitol, (2) glucose and (3) sucrose. Gasket dimensions: 125 μm × 3.5 mm × 12.7 mm.

reduction of oxygen in the sample. Oxygen is reduced at negative potentials in base to hydrogen peroxide, which probably undergoes further reduction to water at the detection potential of 0.1 V. Detection occurs after a delay period of 0.2 s, which allows charging current to decay (see Table 1). It is possible that the 1 mm diameter

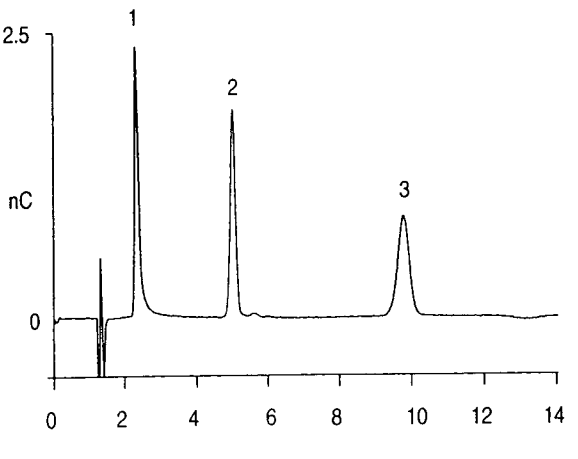

Fig. 3. Pulsed amperometric detection at a 1 mm diameter gold working electrode of 10 picomoles each of (1) sorbitol, (2) glucose and (3) sucrose. Gasket dimensions: 25 μm × 1.3 mm × 6.35 mm.

electrode is much less sensitive to oxygen because peroxide has been swept past the electrode by the time current is measured, while there is still detectable peroxide near the electrode surface with the larger 3-mm electrode. Reduced sensitivity to oxygen is further reason to select the 1 mm diameter gold electrode over the 3-mm electrode. In addition to the minimized oxygen dip, the 1 mm diameter gold electrode is much less sensitive to varying levels of oxygen in the mobile phase caused by incomplete degassing. Varying oxygen levels cause baseline wander if the electrode is sensitive to oxygen.

4. Conclusion

This study supports the conclusion that the cell should be designed with the narrowest and thinnest thin-layer channel gasket that is practical to use and with a working electrode slightly smaller than the gasket width. We have found the practical lower limit for these parameters to be a 25 μm × 1.3 mm thin-layer channel and a 1 mm diameter working electrode. Using a cell with these dimensions, extremely high sensitivities can be achieved, as demonstrated by the excellent signal-to-noise ratio for 10 picomoles each of carbohydrates shown in Fig. 3 and for 100 femtomoles each of four catecholamines shown in Fig. 4. Minimum detection limits can be calculated from the magnitudes of signal and noise in the chromatograms. Based on three times the noise levels of 12 pC using pulsed amperometry and 0.4 pA using d.c. amperometry, the minimum detection limit for glucose is about 200 femtomoles and for dihydroxybenzylamine, about 6 femtomoles.

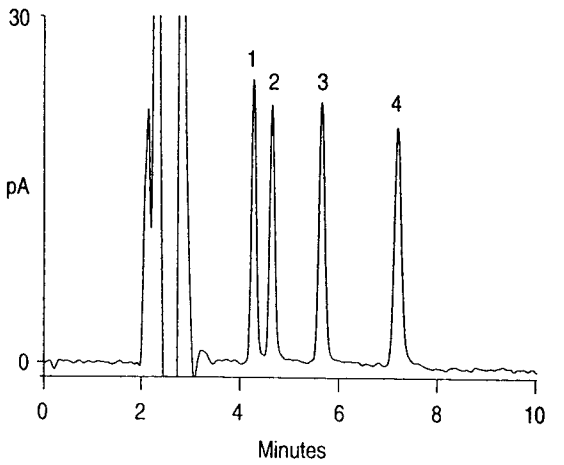

Fig. 4. Separation of 100 femtomoles each of (1) norepinephrine, (2) epinephrine, (3) DHBA and (4) dopamine. Detected using d.c. amperometry at a 1 mm diameter glassy carbon working electrode. Gasket dimensions: 25 μm × 1.3 mm × 6.35 mm.

5. References

[1] M. Righezza and A.M. Siouffi, *Analusis*, 20 (1992) 333.
[2] T.Y. Ou and J.L. Anderson, *J. Electroanal. Chem.*, 302 (1991) 1.
[3] S.G. Weber and J.T. Long, *Anal. Chem.*, 60 (1988) 903A.
[4] S. Prabhu and J. Anderson, *Anal. Chem.*, 59 (1987) 157.
[5] D.M. Morgan and S.G. Weber, *Anal. Chem.*, 56 (1984) 2560.
[6] J.M. Elbicki, D.M. Morgan and S.G. Weber, *Anal. Chem.*, 56 (1984) 978.
[7] H.W. van Rooijen and H. Poppe, *J. Liq. Chromatogr.*, 6 (1983) 2231.
[8] H.B. Hanekamp and H.J. van Nieuwkerk, *Anal. Chim. Acta*, 121 (1980) 13.
[9] S.G. Weber and W.C. Purdy, *Anal. Chim. Acta*, 100 (1978) 531.
[10] P.Y. Leung and C.S. Tsao, *J. Chromatogr.*, 576 (1992) 245.
[11] I.N. Papadoyannis, *HPLC in Clinical Chemistry.(Chromatographic Science Series*, No. 54), Marcel Dekker, New York and Basel, 1990, Ch. 15.
[12] D.C. Johnson, D. Dobberpuhl, R. Roberts and P. Vandeberg, *J. Chromatogr.*, 640 (1993) 79.
[13] D.C. Johnson and W.R. LaCourse, *Anal. Chem.*, 62 (1990) 589A.

ELSEVIER

Journal of Chromatography A, 671 (1994) 115–120

JOURNAL OF CHROMATOGRAPHY A

Analysis of aluminium in pharmaceutical products by post-column derivatization ion chromatography

J. Carnevale, P.E. Jackson*

Waters Chromatography Division of Millipore, Private Bag 18, Lane Cove, N.S.W. 2066, Australia

Abstract

Aluminium can be determined in pharmaceutical products using a chromatographic method with a cation-exchange separation and fluorescence detection after post-column derivatization with 8-hydroxyquinoline-5-sulphonic acid. The method had a detection limit of less than 0.5 ng/ml and the aluminium peak response was linear up to at least 1200 ng/ml. Chromatographic reproducibility was approximately 1–3% over the concentration range of 50–1200 ng/ml. Sample preparation involved boiling in 0.05 *M* sulphuric acid for 5 min. The average recovery for Al spikes in the range 10–1200 ng/ml, from a variety of pharmaceutical samples, was 99% with an R.S.D. of 5%. No interferences from either sample matrix effects or transition metals were found and the results of the chromatographic method agreed well with those obtained by inductively coupled plasma atomic emission spectroscopy.

1. Introduction

Chronic aluminium toxicity in animals and humans is well documented [1,2]. The clinical biochemistry of aluminium is mostly associated with its neurotoxicity (epilepsy, encephalopathy and Alzheimers disease) and renal failure in patients undergoing regular dialysis due to aluminium accumulation in kidneys [1]. Its toxicity in aquatic and soil systems has been shown to be dependent on its chemical speciation, while its mobility from soils into lakes and rivers is enhanced under conditions of increased acidity [3–5]. Hence, there is a continuing interest in the determination of trace levels of aluminium, and its various chemical species, in pharmaceutical products, soils and environmental samples.

Current analytical methods for the trace determination of aluminium in such samples mostly involves the use of spectroscopic techniques, such as graphite furnace atomic absorption spectroscopy (GFAAS) [6]. Such techniques suffer from a number of drawbacks, including high equipment costs, matrix interference effects and the ability to determine only total aluminium. Consequently, increasing attention has been focussed on the use of ion chromatography (IC) for the analysis of aluminium in a variety of sample matrices [7–12]. A number of reports have recently described the use of 8-hydroxyquinoline-5-sulphonic acid (8-HQS) as a post-column reagent for the fluorimetric detection of aluminium following chromatographic separation [7–10]. The use of micelle-forming surfactants in the post-column reagent, such as cetyltrimethylammonium bromide (CTAB), has been reported [9], whilst optimisation of the post-column reaction conditions has also been described [7]. The aim of this work was to investigate the applicability of IC for the quantitative determi-

* Corresponding author.

0021-9673/94/$07.00
SSDI 0021-9673(94)00011-W

nation of aluminium in injectable pharmaceutical preparations. As a concentration of 10 ng/ml was a regulatory requirement for the maximum allowable Al limit in water to be used for the preparation of such products, a principal objective of the chromatographic method was to be able to quantitate below this value and to achieve a detection limit in the order of 1 ng/ml Al.

2. Experimental

2.1. Instrumentation

The liquid chromatograph consisted of a Waters Chromatography Division of Millipore (Milford, MA, USA) Model 625 polyether ether ketone (PEEK) solvent-delivery system, 625 loop injector, 470 programmable fluorescence detector (excitation 395 nm, emission 500 nm) and a Millennium chromatography data manager. The post-column reagent was delivered with a Waters pneumatic reagent-delivery module (RDM) and mixed with the column effluent in a 1.0-ml knitted PTFE ninhydrin reaction coil. The column used was a Waters Protein-Pak SP-5PW (75 × 7.5 mm I.D.) cation-exchanger. Eluent and RDM flow-rates were both 1.0 ml/min and a volume of 50 μl was used for all injections.

2.2. Reagents

Water purified (18 MΩ) using a Millipore Milli-Q water-purification system (Bedford, MA, USA) was used for all solutions. The mobile phase consisted of 0.1 *M* potassium sulphate (Ajax, Sydney, Australia) adjusted to pH 3.0 with 5 *M* sulphuric acid. The post-column reagent (PCR) solution contained 0.004 *M* 8-HQS and 0.002 *M* CTAB in a 1.0 *M* sodium acetate–acetic acid buffer at pH 4.4. The PCR solution was prepared by dissolving 41.7 *g* sodium acetate trihydrate in Milli-Q water, adding 39.7 ml glacial acetic, 100 ml 0.04 *M* 8-HQS (Sigma, St. Louis, MO, USA) stock solution, 100 ml 0.02 *M* CTAB (Fluka, Buchs, Switzerland) stock solution and diluting the mixture to 1.0 l. A 1000-μg/ml stock aluminium solution in 0.1 *M* HNO_3 was prepared from $Al(NO_3)_3 \cdot 3H_2O$ (Ajax). A 10-μg/ml solution was prepared by dilution in 0.05 *M* sulphuric acid of the stock standard. All working standards, covering the concentration range of 2 to 1200 ng/ml, were freshly prepared daily from the 10-μg/ml solution by dilution in 0.05 *M* sulphuric acid. All eluents and post-column reagents were prepared daily, filtered and degassed with a Waters solvent-clarification kit.

2.3. Sample preparation procedures

All sample quantitation was performed using standards run at the same time as the unknowns. The general sample preparation procedure involved adding a sample aliquot (up to 5 ml) to an acid-washed 25-ml beaker, after which 100 μl of 5 *M* sulphuric acid were added and the solution boiled gently for 5 min. The solution was allowed to cool, quantitatively transferred to a 10-ml volumetric flask and the volume adjusted to the mark with Milli-Q water. Duplicate injections (50 μl) of these sample solutions were made. For samples such as 5% injectable glucose and injectable water, where dilution was undesirable, 100 μl 5 *M* sulphuric acid was added to 10 ml of sample in a 25-ml beaker and the solution boiled gently until the volume was reduced to approximately 7 ml. After cooling, this was quantitatively transferred to a 10-ml volumetric flask and the volume adjusted to the mark with Milli-Q water.

3. Results and discussion

3.1. Chromatographic method

This work describes the development of a procedure, based on that of Gibson and Willett [7], for the analysis of aluminium in pharmaceutical products, such as injectable glucose, saline solution and water. A higher-capacity cation-exchange column (Protein-Pak SP-5PW) was chosen for this work to allow for the direct injection of high ionic strength samples, such as

injectable saline. Mobile phase parameters, such as ionic strength and flow-rate, were initially optimised for the separation of aluminium on the Protein-Pak SP-5PW column. A 1.0-ml knitted PTFE reaction coil was added to the chromatographic system to allow sufficient time for the reaction of aluminium with the post-column reagent, which was delivered at an optimal flow-rate of 1.0 ml/min. A typical chromatogram of a 50-μl injection of a 2.0 ng/ml aluminium standard obtained using the Protein-Pak SP-5PW column and an eluent of 0.1 *M* potassium sulphate at pH 3.0 is shown in Fig. 1. The retention time of the Al peak was 6.1 min. The response was found to be linear over the range examined (2 to 1200 ng/ml) with a correlation coefficient >0.999. The chromatographic detection limit was calculated (at 3× baseline noise) to be less than 0.5 ng/ml for a 50-μl injection. Typical chromatographic reproducibilities for 50 and 100 ng/ml standards were 2–3% and <1%, respectively.

3.2. Sample preparation and interferences

A number of potential problems could arise during the quantitation of aluminium by IC. These include the presence of other aluminium complexes in solution which could interfere with the separation of the free Al^{3+} peak. The presence of other metal ions in the samples could interference either through the formation of fluorescent complexes that co-elute with the Al^{3+} peak or by quenching the aluminium peak fluorescence. Also, fluorescence quenching could occur as a result of co-elution with other components, such as glucose, active compounds and other matrix materials which are often present at high levels in pharmaceutical samples.

The problem of multiple Al complexes and their dissociation to form free Al has generally been addressed by preparing the sample in acidic conditions [7–9]. Figs. 2(1), and 3(1) show chromatograms obtained from the direct injection of saline and glucose solutions. Apart from the Al peak, two additional peaks (retention times 3.6 and 4.3 min) were detected in the saline and glucose samples. These additional peaks could be due to the elution of various Al complexes, to other metals, or both. Figs. 2(2) and 3(2) show the corresponding chromatograms obtained after the samples had been boiled in 0.05 *M* sulphuric acid, as detailed in the Experimental section. In both cases, there was a large increase in the size of the Al peak (and an increase in the total peak area) after sample treatment. In the case of the glucose sample, the two minor peaks almost disappeared, whilst in the case of the saline solution, the peak at retention time 4.3 min was still significant but markedly diminished.

These results indicated that Al was present in the samples as a number of complexed species, which could be broken down using acid treatment. The effect of increasing total peak area after sample acidification has also been reported

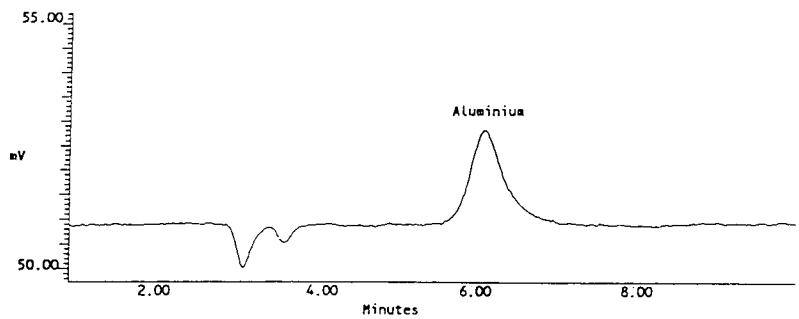

Fig. 1. Chromatogram of aluminium standard. Conditions: column: Waters Protein-Pak SP-5PW cation-exchanger; eluent: 0.1 *M* potassium sulphate at pH 3.0; flow-rate: 1.0 ml/min; injection volume: 50 μl; post-column reagent: 0.004 *M* 8-hydroxyquinoline-5-sulphonic acid, 0.002 *M* cetyltrimethylammonium bromide in 1.0 *M* sodium acetate–acetic acid buffer at pH 4.4, delivered at 1.0 ml/min; detection: fluorescence, excitation 395 nm, emission 500 nm. Solute: aluminium (2.0 ng/ml).

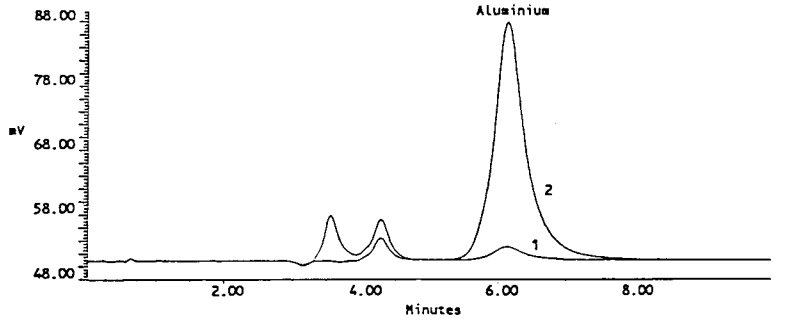

Fig. 2. Chromatogram of 0.9% NaCl saline solution obtained using (1) no acid treatment and (2) after boiling in 0.05 *M* sulphuric acid. Conditions as for Fig. 1 except sample dilution 10×. Solutes (concentration): 1 = aluminium (2.6 ng/ml); 2 = aluminium (30.6 ng/ml).

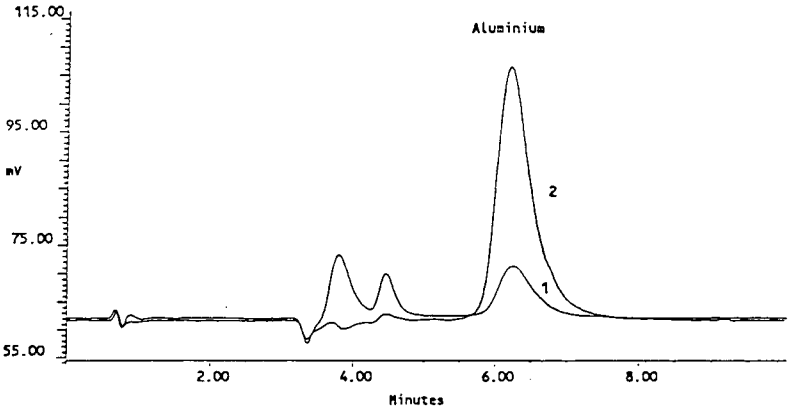

Fig. 3. Chromatogram of 50% glucose solution obtained using (1) no acid treatment and (2) after boiling in 0.05 *M* sulphuric acid. Conditions as for Fig. 1 except sample dilution 10×. Solutes (concentration); 1 = aluminium (14.5 ng/ml); 2 = aluminium (103.5 ng/ml).

previously and was shown to depend upon the specific nature of the Al complex [7]. Species, such as oxalate and fluoride, were shown to have no effect on the fluorescence response, indicating that Al complexes of these ions were fully decoupled by the 8-HQS. Alternatively, citrate reduced the fluorescence response, suggesting that these complexes were sufficiently stable to resist decomplexation and substitution by the 8-HQS [7]. In the case of both the glucose and saline samples, the significant increase in total peak area after acidification suggests that the complexing ions present in the samples must form relatively stable complexes with aluminium.

The effects of acid strength on the Al peak response were investigated for a representative matrix, a 50% glucose sample. The results of varying the sulphuric acid concentration from 0–0.05 *M* are summarised in Table 1. Increasing

Table 1
Effect of acid strength on Al quantitation for a 50% glucose sample

H_2SO_4 concentration (*M*)	Al found (ng/ml)
No acid	145
0.005	660
0.02	840
0.05	1035

Table 2
Al results obtained for duplicate sample injections

Sample	Al (ng/ml)	
	Inject 1	Inject 2
50% Glucose	1181	1201
5% Glucose	54.2	55.6
0.9% NaCl	305.8	303.6
Tap water	7.2	6.4
Production process water	1.6	1.3

the concentration beyond 0.05 *M* did not result in significantly higher Al peak responses and this acid concentration was used for all subsequent analyses. Other acids, such as hydrochloric and nitric acids, gave similar results to those obtained using sulphuric acid, however, the latter was chosen as it was more compatible with the mobile phase.

As previously discussed, the presence of other metals in the samples could potentially lead to chromatographic interferences or the possibility of Al fluorescence quenching. The injection of standard solutions (100 μg/ml) of cations which could potentially occur in pharmaceutical preparations, such as Ca^{2+}, Mg^{2+}, Zn^{2+}, Cd^{2+}, Fe^{3+} and Ni^{2+}, showed that only Zn^{2+} and Cd^{2+} gave a significant detection response. These cations, with retention times of 5.0 min for Zn^{2+} and 4.9 min for Cd^{2+}, however, were well resolved from the Al peak. Potential interferences due to matrix effects were investigated by analysing a 50% glucose sample at dilutions of 10, 20 and 40×. The Al results obtained of 1190, 1170 and 1140 ng/ml, respectively, indicated that there were no significant matrix effects.

3.3. Quantitation

The Al results and typical reproducibility obtained for duplicate injections of various pharmaceutical samples are shown in Table 2. The duplicate results showed good agreement at levels higher than 50 ng/ml, however, at levels of <10 ng/ml, the repeatability was not as good due to the fact that the Al peak was being quantitated closer to the detection limit. The accuracy of the chromatographic method was assessed by determining the recoveries of Al from standard addition spikes, with the results being shown in Table 3. The recoveries of spikes in the concentration range of 10 to 1200 ng/ml varied from 94 to 106%. The overall average recovery was 99%, which was excellent considering the potential problems of working these at trace levels. The results obtained by IC were also compared to those from inductively coupled plasma atomic emission spectroscopy (ICP-AES), as shown in Table 4. The chromatographic results showed reasonable agreement to those

Table 3
Recovery of Al from spiked samples

Sample	Al present (ng/ml)	Spiked Al (ng/ml)	Al found (ng/ml)	Recovery (%)
50% Glucose	1134	1000	2074	94
5% Glucose (S1)[a]	66.6	50	114.1	96
5% Glucose (S2)[b]	77.7	50	124.5	94
0.9% NaCl (S1)[a]	334	100	437	104
0.9% NaCl (S2)[b]	305	200	516	106
Milli-Q water	ND[c]	10	9.74	97

[a] Sample 1.
[b] Sample 2.
[c] Not detected.

Table 4
Comparison of Al results obtained using IC and ICP-AES

Sample	IC (ng/ml)	ICP-AES (ng/ml)
50% Glucose	1035, 1060, 1090	1030
5% Glucose	67, 78, 54, 56	85
0.9% NaCl	334, 305	306
BP water[a]	1.4	<0.3

The IC results represent single injections from different sample ampoules.
[a] BP water = Sterile water produced according to British Pharmacopeia.

obtained for the same sample types when using ICP-AES.

4. Conclusions

The feasibility of using IC for the trace analysis of aluminium in pharmaceutical products, based on a cation-exchange separation and fluorescence detection after post-column derivatization with 8-HQS, was successfully demonstrated. Sample preparation simply involved boiling in 0.05 *M* sulphuric acid for 5 mins. The chromatographic method had a detection limit of less than 0.5 ng/ml for a 50-μl injection and the aluminium peak response was linear up to at least 1200 ng/ml. The chromatographic reproducibility was approximately 1–3% over the concentration range of 50–1200 ng/ml. The average recovery of Al spikes in the range 10–1200 ng/ml, from a variety of pharmaceutical samples, was 99% with an R.S.D. of 5%, indicating satisfactory method accuracy. No interferences from either sample matrix effects or transition metals were found and the results of the chromatographic method agree well with those obtained by ICP-AES.

5. Acknowledgement

The authors wish to thank John Eames of CSIRO Minerals Exploration Division, North Ryde, N.S.W., Australia, for the ICP-AES results.

6. References

[1] P.W. Di Sciascio and G.F. Carter, *Clin. Biochem. Rev.*, 13 (1992) 60.
[2] S.W. King, J. Savory and M.R. Wills, *Crit. Rev. Clin. Lab. Sci.*, 14 (1981) 1.
[3] C.T. Driscoll, J.P. Baker, J.J. Bisogni and C.L. Schofield, *Nature*, 84 (1980) 161.
[4] M.G. Whitten and G.S.P Richie, *Commun. Soil Sci. Plant Anal.*, 22 (1991) 343.
[5] A. Tanaka, T. Tadano, K. Yamamoto and N. Kanamura, *Soil Sci. Plant Nutr.* (Tokyo), 33 (1987) 43.
[6] L.S. Clesceri, A.E. Greenberg and R.R. Trussell (Editors), *Standard Methods for the Examination of Water and Wastewater*, American Public Health Association, Washington, DC, 17th ed., 1989.
[7] J.A.E. Gibson and I.R. Willett, *Commun. Soil Sci. Plant Anal.*, 22 (1991) 1303.
[8] P. Jones, L. Ebdon and T. Williams, *Analyst*, 113 (1988) 641.
[9] J.I. Garcia Alonso, A. Lopez Gracia, A. Sanz-Medel, E.B. Gonzalez, L. Ebdon and P. Jones, *Anal. Chim. Acta*, 225 (1989) 339.
[10] K. Soroka, R.S. Vinthanage, D.A. Phillips, B. Walker and P.K. Dasgupta, *Anal. Chem.*, 59 (1987) 629.
[11] E. Kaneko, H. Hoshino, T. Yotsuyanagi, N. Gunji, M. Sato, T. Kikuta and M. Yuasa, *Anal. Chem.*, 63 (1991) 2219.
[12] A. Lopez, T. Rotunno, F. Palmisano, R. Passino, G. Tiravanti and P.G. Zambonin, *Environ. Sci. Technol.*, 25 (1991) 1262.

ELSEVIER

Journal of Chromatography A, 671 (1994) 121–129

JOURNAL OF CHROMATOGRAPHY A

Displacement post-column detection reagents based on the fluorescent magnesium 8-hydroxyquinoline-5-sulfonic acid complex

Charles A. Lucy*, Liwen Ye

Department of Chemistry, The University of Calgary, 2500 University Drive N.W., Calgary, Alberta, T2N 1N4 Canada

Abstract

This non-specific fluorescent reagent is based on the displacement mechanism, wherein a metal ion displaces Mg^{2+} from the $Mg(CDTA)^{2-}$ complex (CDTA = cyclohexylenedinitrilotetraacetic acid). The liberated Mg^{2+} then reacts with 8-hydroxyquinoline-5-sulfonic acid (HQS) to form an intensely fluorescent complex. For simultaneous addition of $Mg(CDTA)^{2-}$ and HQS^{2-}, the detector response is governed by the stabilities of both the CDTA and the HQS complexes of Mg^{2+} and the displacing metal. Under these conditions, alkaline earth metals respond positively, but no response is observed for transition metals such as Cu^{2+}, Ni^{2+} and Co^{2+}. For the sequential addition of $Mg(CDTA)^{2-}$ followed by HQS^{2-}, the detector response is governed by the relative stabilities of only the CDTA complexes of Mg^{2+} and displacing metal, and positive signals are observed for Mg^{2+}, Ca^{2+}, Sr^{2+}, Ba^{2+}, Mn^{2+}, Cu^{2+}, Ni^{2+} and Co^{2+}. The response for Mn^{2+} was linear from 25 to 2500 picomoles. The reagent pH affects the background intensity and the displacement kinetics, and to a lesser extent the fluorescence intensity.

1. Introduction

The ability to detect trace and ultra-trace concentrations of metal ions is an integral part of modern society. Ion chromatography has been used for applications as diverse as analyzing silicon wafer contamination [1], monitoring nuclear fission [2] and determining trace metals in the environment [3]. All of these applications used the non-specific 4-(2-pyridylazo) resorcinol (PAR) reagent for post-column detection of the metal ions by absorbance. Fluorescence is an intrinsically more sensitive technique than absorbance. The reagent 8-hydroxyquinoline-5-sulfonic acid (HQS) has achieved picomolar detection limits for Zn and Cd [4], Al [5] and Mg [6]. Unfortunately, most other metal–HQS complexes are either weakly fluorescent or non-fluorescent [7], thus inhibiting wider use of this sensitive reagent. No alternative metalloluminescent reagent exists which will react to form fluorescent compounds with a wide range of metals, as is desirable in ion chromatography.

Recently, Williams and Barnett [8] introduced a non-specific post-column reagent for fluorescent detection of trace metals in ion chromatography. This system used the displacement of Mg^{2+} from a Mg–EDTA (ethylenediaminetetraacetic acid) complex by other metal ions.

$$M^{n+} + Mg(EDTA)^{2-} \rightleftharpoons Mg^{2+} + M(EDTA)^{(4-n)-} \quad (1)$$

* Corresponding author.

0021-9673/94/$07.00
SSDI 0021-9673(93)E1194-5

The liberated Mg^{2+} reacts with HQS to form a strongly fluorescent complex. The intensity of the resultant fluorescent is proportional to the molar concentration of the metal ion.

$$Mg^{2+} + 2HQS^{2-} \rightleftharpoons \underset{\text{(fluorescent)}}{Mg(HQS)_2^{2-}} \quad (2)$$

Using this detection scheme, Williams and Barnett [8] achieved detection limits of 33 to 140 picomoles for a variety of metals. However, no discussion of the effect of experimental factors such as pH and order of reagent addition was given. Recent studies performed in our laboratory on the Zn–EDTA–PAR absorbance reagent have demonstrated that the kinetics and equilibrium of displacement reaction systems can be complex [9], and so are not easily optimized. This paper investigates the chemistry of HQS-based displacement post-column reagents so as to identify the key variables in the optimization of these reagents.

2. Experimental

2.1 Apparatus

The HPLC system consisted of a Waters metal-free solvent delivery system (Model 625, Waters Associates, Milford, MA, USA), a Rheodyne sampling valve (Model 9125, Rheodyne, Berkeley, CA, USA) fitted with a 50-μl loop and a fluorimetric detector (Model 470, Waters; excitation λ, 360 nm; emission λ, 500 nm). Chromatograms were digitized with a CHROM-1AT (Keithley MetraByte, Taunton, MA, USA) data acquisition board enhanced for faster data acquisition, and analyzed using LabCalc (Galactic, Salem NH, USA) on a 286-based microcomputer. In most experiments no column was present in the HPLC system, *i.e.*, the experiments were run in a flow injection analysis mode. When present the analytical column was a 150 mm × 3.9 mm I.D. Delta Pak C-18 (300 Å; 5 μm; Waters).

The post-column reagent was delivered by constant pressure pumping through application of nitrogen pressure (38 p.s.i.; 1 p.s.i. = 6894.76 Pa) to a multi-reagent cylinder [10,11] fitted with a six-port low-pressure switching valve (Model 5011, Rheodyne) to allow selection between up to six reagents and a three-way valve (Model 5031, Rheodyne) on an additional port on the cylinder to provide simultaneous flow of a second reagent. Low pressure tubing and fittings (Alltech) connected the post-column reagent delivery system to the effluent stream. Two configurations were used for addition of the post-column reagent. In configuration I, the carrier stream from the HPLC pump (0.5 ml/min) merged with the Mg–CDTA–HQS reagent (CDTA = cyclohexylenedinitrilotetraacetic acid) (0.4–0.5 ml/min, measured for each experiment) at the mixing tee (316 stainless steel, 90° ports), flowed through reaction coil 1, 510 cm of tightly spiraled 0.50 mm I.D. knitted PTFE (Teflon) tubing (RXN 1000 Coil, Waters; 1000 ml volume) and then directly to the detector. In configuration II, reaction coil 1 was as before and reaction coil 2 was either a 100 cm of 1.0 mm I.D. Teflon tubing or 48 cm of 0.25 mm I.D. polyether ether ketone (PEEK) tubing. Using this configuration, Mg–CDTA was added via the first mixing tee and HQS was added at the second tee.

Stopped-flow kinetic measurements were made using the instrument in configuration II. The HPLC pump provided a constant flow of $5 \cdot 10^{-5}$ *M* M^{2+} which was mixed sequentially with unbuffered 1 m*M* MgCDTA (pH ~ 6) and then 1 m*M* HQS in pH 8.0 bicine (0.6 *M*) buffer. The flow was stopped and the $Mg(HQS)_2^{2-}$ fluorescence was recorded *versus* time.

2.2 Reagents and standards

All reagent solutions were prepared using deionized water (Milli-Q Ultra Pure Water System, Millipore). Analytical grade reagents were used throughout. Post-column reagent solutions were prepared by dissolving HQS (Janssen Chimica) in the bicine (Sigma) buffer (0.3–0.6 *M*), adjusting the pH, purifying with a 3 cm × 1.5 cm I.D. column of Chelex 100 (149–297 μm sodium form, Bio-Rad), and adding an aliquot of $1.0 \cdot 10^{-3}$ *M* Mg–CDTA or Mg–EDTA stock

solution. The Mg–CDTA and Mg–EDTA stock solution were prepared by combining Mg^{2+} and the aminopolycarboxylate such that excess Mg^{2+} was present, and then passing the solution through a 3 cm × 1.5 cm I.D. column of Chelex 100 to remove the excess Mg^{2+}.

Stock metal solutions were prepared using analytical grade salts. Lower concentrations were then achieved by dilution in volumetric Nalgeneware.

3. Results and discussion

The reagent 8-hydroxyquinoline-5-sulfonic acid (HQS) and its parent compound (8-hydroxyquinoline; oxine) form stable complexes with a wide range of metals [12], but only a few of these complexes fluoresce significantly [7,13,14]. The differences in fluorescence observed for the various metals is due to the interaction of the ligand electrons involved in the fluorescence with the electron field of the metal [13]. Thus the HQS complexes that fluoresce most readily are those derived from cations with the most stable electron configurations, *i.e.*, either completely full or empty electron shells. Such metals include Cd^{2+}, Zn^{2+}, Mg^{2+} and La^{3+}. Magnesium is used in the displacement post-column reagent discussed herein, because it forms only a weak complex with aminopolycarboxylate ligands and will be displaced by the widest range of metals, thereby providing the most non-specific post-column detection.

3.1 Background signal from reagent

Only the 1:2 metal–HQS complex fluoresces [15]. The free reagent and the 1:1 complex do not contribute to the observed fluorescence. Thus the reagent background results solely from the residual $Mg(HQS)_2^{2-}$ present in the reagent solution. The background is then governed by the relative stability of the aminopolycarboxylate (L) and HQS complexes with Mg^{2+}:

$$Mg(HQS)_2^{2-} + L^{4-} \rightleftharpoons 2HQS^{2-} + MgL^{2-} \qquad (3)$$

The equilibrium constant governing the intensity of the background fluorescence, is thus:

$$K'_{background} = \frac{\alpha_{Mg^{2+}}\alpha_{L^{4-}}K_{MgL^{2-}}}{\alpha_{Mg^{2+}}(\alpha_{HQS^{2-}})^2\beta_{2,Mg(HQS)_2^{2-}}} = \frac{\alpha_{L^{4-}}K_{MgL^{2-}}}{(\alpha_{HQS^{2-}})^2\beta_{2,Mg(HQS)_2^{2-}}} \qquad (4)$$

That is, the intensity of the background will be a function of the stability constants of the magnesium–aminopolycarboxylate complex and the magnesium–HQS complex, the fractional composition of the ligands at the reagent pH, and the total concentration of HQS.

In their work, Williams and Barnett used EDTA as the complexing agent [8]. CDTA is an analog of EDTA, which, due to its greater structural rigidity, forms metal ion complexes that are ten to a thousand times more stable than those of EDTA [16]. Table 1 shows the relative background fluorescence observed for $Mg(EDTA)^{2-}$ and $Mg(CDTA)^{2-}$, and indicates that a lower background is achieved using CDTA, as expected based on literature stability constants [12,17] CDTA is therefore used in all further studies.

3.2 Signal from reagent

Table 2 shows that optimum sensitivity for $Mg(HQS)_2^{2-}$ is achieved at a pH from 8 to 11. This is in agreement with the results of Bishop [15], who observed that $Mg(HQS)_2^{2-}$ fluorescence efficiency increased to a maximum by pH 7 and decreased at higher pH values presumably due to the formation of either hydroxyl complexes or the hydroxide. Soroka *et al.* [7] also observed such behavior, although they reported a much narrower optimum pH range than evident in Table 2. A pH of 8.0 was used in all further experiments except those explicitly studying the effect of pH.

3.3 Simultaneous addition of Mg–CDTA and HQS

The maximum sensitivity that is achievable for any given metal with the Mg–CDTA–HQS re-

Table 1
Comparison of the background intensity for Mg–CDTA–HQS and Mg-EDTA-HQS post-column fluorescent reagents

pH	Background intensity[a]		Relative background Mg–CDTA/Mg–EDTA
	Mg–CDTA	Mg–EDTA	
8.0	0.201	0.530	0.38
9.1	0.127	0.352	0.36
10.0	0.070	0.196	0.36
10.75	0.043	0.149	0.29
12.1	0.025	0.178	0.14
12.8	0.024	0.246	0.098

Conditions: mode, flow injection analysis in configuration I; reaction coil 1, 510 cm of 0.5 mm I.D. tubing; carrier, 0.5 ml/min distilled water; reagent, 0.4 ml/min of 1 m*M* HQS with 0.3 *M* bicine adjusted to the appropriate pH; injection, 50 μl of 1 m*M* Mg–CDTA or Mg–EDTA.
[a] Background intensity is defined as the peak area observed for duplicate injections of Mg–CDTA and Mg–EDTA.

agent is that observed for Mg^{2+}. That is, maximum sensitivity is achieved when each metal ion displaces one Mg^{2+} from its CDTA complex. Calibration curves were determined for the injection of 500 to 5000 picomoles of a variety of metals. All of these plots were linear with correlation coefficients (r^2) greater than 0.99. Table 3 presents the results observed for a number of metal ions using simultaneous addition of $Mg(CDTA)^{2-}$ and HQS^{2-}. The sensitivity observed for magnesium differs from that in Table 2 due to variation in the reagent flow.

For the alkaline earth metals, the sensitivity of the Mg–CDTA–HQS reagent decreased with increasing atomic mass. Large alkaline earth metal ions do not form stable HQS complexes. As a result the overall equilibrium and associ-

Table 2
Effect of pH on the fluorescence intensity of the Mg-HQS complex

pH	Sensitivity [a]	Intercept
8.0	1.947 ± 0.001	−0.0042 ± 0.0005
9.1	2.00 ± 0.01	−0.0038 ± 0.0027
10.0	1.893 ± 0.001	−0.0056 ± 0.0001
10.75	1.851 ± 0.002	−0.007 ± 0.001
12.1	1.335 ± 0.004	−0.005 ± 0.001
12.8	0.59 ± 0.02	+0.002 ± 0.005
13.1	0.24 ± 0.03	+0.008 ± 0.009

Conditions: mode, flow injection analysis in configuration I; reaction coil 1, 510 cm of 0.5 mm I.D. tubing; carrier, 0.5 ml/min distilled water; reagent, 0.5 ml/min of 1 m*M* HQS in 0.3 *M* bicine adjusted to the indicated pH; injection, 50 μl of four Mg^{2+} standards ranging from 10–100 μM (500–5000 picomoles).
[a] Sensitivity is defined as the slope of the plot of peak area *versus* the picomoles of Mg^{2+} injected. The values have been multiplied by $1 \cdot 10^4$.

Table 3
Sensitivity of metal ions upon simultaneous addition of Mg-CDTA-HQS

Metal ion	Sensitivity[a]	Intercept	Relative sensitivity	$K'_{detection}$
Mg^{2+}	1.25	−0.0406	1.00	$10^{0.0}$
Ca^{2+}	0.75	+0.0124	0.60	$10^{8.6}$
Sr^{2+}	0.36	+0.0076	0.29	$10^{6.2}$
Ba^{2+}	0.02	+0.00048	0.01_9	$10^{4.0}$
Mn^{2+}	0.80	+0.00834	0.64	$10^{3.3}$
Hg^{2+}	0.15	+0.0059	0.12	–
Co^{2+}	nd [b]	–	–	$10^{1.1}$
Ni^{2+}	nd	–	–	$10^{-2.2}$
Cu^{2+}	nd	–	–	$10^{-3.4}$

Conditions: mode, flow injection analysis in configuration I; reaction coil 1, 510 cm of 0.5 mm I.D. tubing; carrier flow, 0.5 ml/min distilled water; reagent flow, 0.4 ml/min of 1 m*M* Mg–CDTA–HQS in 0.6 *M* bicine (pH 8.0).
[a] Sensitivity is defined as the slope of the plot of peak area versus the picomoles of Mg^{2+} injected. The values have been multiplied by 1×10^4.
[b] nd = Not detected.

ated constant for detection of alkaline earth metals are:

$$M^{2+} + 2HQS^{2-} + Mg(CDTA)^{2-} \rightleftharpoons Mg(HQS)_2^{2-} + M(CDTA)^{2-} \quad (5)$$

$$K'_{detection} = \frac{\beta'_{2,Mg(HQS)_2^{2-}} K'_{f,M(CDTA)^{2-}}}{K'_{f,Mg(CDTA)^{2-}}} = \alpha_M \alpha^2_{HQS^{2-}} \frac{\beta_{2,Mg(HQS)_2^{2-}} K_{f,M(CDTA)^{2-}}}{K_{f,Mg(CDTA)^{2-}}} \quad (6)$$

This situation is analogous to that observed for the determination of alkaline earth metals using the Zn–EDTA–PAR displacement reaction [9]. The overall detection efficiency for alkaline earth metals will be dependent on the fraction of the alkaline earth metal in the free form and on the fraction of HQS that is fully ionized. However, when these variables are maintained constant as in Table 3, $K'_{detection}$, and thus the detection sensitivity, decreases as the stability of the alkaline earth–CDTA complex decreases down the column of the periodic table.

For the divalent transition metals a different behavior was observed. Metals such as Mn^{2+} and Hg^{2+} responded to the Mg–CDTA–HQS reagent, whereas many other metals which form stronger CDTA complexes than Mg^{2+} showed no positive response. This difference in behavior results because the transition metals form stable complexes with HQS [12]. Under these conditions the free metal, M, is rapidly complexed by HQS, and thus the detection equilibrium is:

$$M(HQS)_2^{2-} + Mg(CDTA)^{2-} \rightleftharpoons Mg(HQS)_2^{2-} + M(CDTA)^{2-} \quad (7)$$

The equilibrium constant governing the detection of divalent transition metals is thus:

$$K'_{detection} = \frac{K_{f,M(CDTA)^{2-}} \beta_{2,Mg(HQS)_2^{2-}}}{K_{f,Mg(CDTA)^{2-}} \beta_{2,M(HQS)_2^{2-}}} \quad (8)$$

The fraction composition (α) of each ligand and metal appears in both the numerator and denominator, and so cancels out. Thus pH will not affect the degree to which a metal ion displaces Mg^{2+}, and so should have no thermodynamic effect on the observed detection sensitivities.

For divalent transition metals, the differing detection equilibrium (eqn. 7) results in a lower $K'_{detection}$ being required for detection than is the case for the alkaline earth metals. Mn^{2+} forms a HQS complex of greater stability than that of Mg^{2+}, but is nevertheless detected by the Mg–CDTA–HQS reagent as a result of the driving force provided by the stability of the $Mn(CDTA)^{2-}$ complex. Mercury responds weakly to the reagent. Unfortunately no stability constant data is available for comparison. Co^{2+} was predicted to respond weakly to the reagent ($K'_{detection} = 10^{1.1}$), whereas no signal was detectable. No response was observed for Ni^{2+} and Cu^{2+}, as was predicted (*i.e.*, $K'_{detection} < 1$) using the literature stability constants. Thus overall the agreement between the response predicted by eqn. 8 and that observed (Table 3) indicates that eqns. 7 and 8 govern detection for transition metal ions using simultaneous addition of $Mg(CDTA)^{2-}$ and HQS^{2-}.

The fluorescence intensity of the $Mg(HQS)_2^{2-}$ complex and the $K'_{detection}$ for divalent transition metals are independent of pH (Table 2 and eqn. 8, respectively). Therefore the sensitivity of the reagent for divalent transition metals should be independent of pH. Nevertheless, the sensitivity for Mn^{2+} was much greater at pH 8.0 [$(7.8 \pm 0.4) \cdot 10^{-5}$] than at pH 10.0 [$(1.27 \pm 0.04) \cdot 10^{-5}$]. This behavior results from the slow displacement of Mg^{2+} from its CDTA complex. The increased sensitivity upon lowering the pH results from acid catalyzed dissociation of the aminopolycarboxylate from the metal ion. This behavior is discussed further below. At pH 8.0, the response of the Mg–CDTA–HQS reagent to Mn^{2+} was linear from 25 to 2500 picomoles ($r^2 = 0.996$) with a slope of $(1.07 \pm 0.03) \cdot 10^{-4}$ and an intercept of 0.003 ± 0.007. Below 25 picomoles, standards were equivalent to the blank.

3.4 Sequential addition of Mg–CDTA and HQS

As discussed above, simultaneous addition of Mg–CDTA and HQS did not yield a positive

response for many of the metals that are of interest in ion chromatography. Williams and Barnett [8] added Mg–CDTA to the column eluent, allowed the mixture to react in a 50 cm × 0.8 mm I.D. reaction coil, and only then added the HQS. Using this order of reagent addition they observed a response for a much wider range of metals than was observed in Table 3.

Sequential addition of $Mg(CDTA)^{2-}$ and then HQS^{2-} performed herein also resulted in positive responses from a wide range of metals, as shown in Table 4. For the sequential addition of $Mg(CDTA)^{2-}$ and HQS^{2-}, the equilibrium established in the first reaction coil (Rxn Coil 1) is:

$$M^{2+} + Mg(CDTA)^{2-} \rightleftharpoons M(CDTA)^{2-} + Mg^{2+} \quad (9)$$

$$K'_{detection} = \frac{K_{f,M(CDTA)^{2-}}}{K_{f,Mg(CDTA)^{2-}}} \quad (10)$$

Metal ions displace Mg^{2+} based on the relative complex stability of the CDTA complexes. Thus as almost all metal ions form stronger CDTA complexes, Mg^{2+} is displaced by most metals. Upon the addition of HQS^{2-}, the Mg^{2+} is rapidly complexed to form the fluorescent $Mg(HQS)_2^{2-}$. Experiments performed herein indicate that even at the shortest reaction time studied (1.6 s) the reaction between Mg^{2+} and HQS^{2-} had proceeded to completion. Indeed, reaction half-lives on the order of a few milliseconds have been observed for the reaction between Mg^{2+} and 8-hydroxyquinoline (oxine) using relaxation kinetics techniques [18].

Thus, upon the addition of HQS^{2-} the operative equilibrium is that given by eqn. 7. For metals such as Cu^{2+}, Ni^{2+} and Co^{2+} this equilibrium lies far to the left [*i.e.*, $K'_{detection} < 1$ (eqn. 8)], and so thermodynamically no response would be expected, as had been observed above for the simultaneous addition of reagent. However, the $M(CDTA)^{2-}$ complex must dissociate in order for this equilibrium to be achieved. Given the high stability of this complex and the steric rigidity of CDTA, this process would be expected to be slow. Stopped-flow kinetic measurements of mixtures of $M(CDTA)^{2-}$ and $Mg(HQS)_2^{2-}$ revealed that the $Mg(HQS)_2^{2-}$ fluorescence decreases exponentially ($r > 0.99$) at a very slow rate; half-lives of 530, 16 000 and 24 000 s for Cu^{2+}, Co^{2+} and Ni^{2+}, respectively. Thus the use of a short reaction coil does not allow sufficient time for the mixed reagent to relax, and so the observed response will obey

Table 4
Response of metal ions upon sequential addition of Mg–CDTA and HQS

Metal ion	Sensitivity[a]	Intercept	Relative sensitivity	$K_{f,M\text{-}CDTA}/K_{f,Mg\text{-}CDTA}$
Mg^{2+}	0.95	−0.0167	1.00	$10^{0.0}$
Ca^{2+}	0.79	−0.0146	0.83	$10^{2.1}$
Sr^{2+}	0.55	+0.0117	0.58	$10^{-0.5}$
Ba^{2+}	0.089	+0.00056	0.09	$10^{-2.5}$
Mn^{2+}	1.06	−0.0196	0.64	$10^{6.4}$
Hg^{2+}	nd[b]	–	0.00	$10^{13.7}$
Cu^{2+}	0.70	−0.0172	0.73	$10^{10.8}$
Ni^{2+}	0.75	−0.0154	0.79	$10^{9.1}$
Co^{2+}	0.78	−0.0151	0.82	$10^{8.5}$

Conditions: mode, flow injection analysis in configuration II; reaction coil 1, 510 cm of 0.5 mm I.D. tubing; reaction coil 2, 50 cm of 0.25 mm I.D. tubing; carrier, 0.5 ml/min distilled water; Mg–CDTA, 0.4 ml/min of 1 m*M* unbuffered (pH ~ 6); HQS, 0.5 ml/min of 1 m*M* HQS in 0.3 *M* bicine (pH 8.0).

[a] Sensitivity is defined as the slope of the plot of peak area *versus* the picomoles of metal ion injected. The values have been multiplied by $1 \cdot 10^4$.

[b] nd = Not detected.

eqns. 9 and 10. Additional stopped-flow measurements of $M(EDTA)^{2-}$ complexes indicate that the dissociation rate of the $M(EDTA)^{2-}$ complex of most metals is sufficiently slow that similar behavior will be observed. A notable exception is Cu^{2+} for which we observed a dissociation half-life of 20 s for the EDTA complex. Therefore if EDTA were used rather than CDTA, it is important that reaction coil 2 be maintained short or else reduced sensitivities will be observed for kinetically labile metals such as Cu^{2+}.

In Table 4 the characteristics of calibration curves run using sequential addition of $Mg(CDTA)^{2-}$ and HQS^{2-} are reported for a number of metals. The sensitivity observed for the alkaline earth metals decreases with increasing atomic mass, as would be predicted by eqn. 10 based on the decreasing stability of the $M(CDTA)^{2-}$ complex down the group. Likewise a strong response is observed for Mn^{2+}, Cu^{2+}, Ni^{2+} and Co^{2+}, as predicted by eqn. 10. Only Hg^{2+}, which was predicted to respond strongly to the reagent, did not display the expected behavior. Further studies are being conducted to determine the cause of this anomaly. Nevertheless, the results shown in Table 4 indicate that the sensitivity of the Mg–CDTA–HQS reagent will depend on the relative stabilities of the CDTA complexes when the reagent components are added sequentially.

During the studies of simultaneous addition of $Mg(CDTA)^{2-}$ and HQS^{2-}, the kinetics of the displacement reaction, and thus the sensitivity, improved upon decreasing the pH of the reagent from 10 to 8. Unfortunately with simultaneous reagent addition, it was not possible to lower the pH further without decreasing the intensity of the Mg–HQS fluorescence [7,15]. With sequential addition, it is possible to adjust the pH of the Mg–CDTA reagent to optimize the displacement reaction kinetics and to adjust the pH of the HQS reagent to optimize the fluorescence response. Fig. 1 shows the detector response (relative to that for Mg^{2+}) at various $Mg(CDTA)^{2-}$ reagent pH values for a number of metals. The detection sensitivity of all of the metals passes through an optimum. Acid catalyzed decomplexation of the $Mg(CDTA)^{2-}$ complex results in enhancement of the sensitivity transition metals and calcium as the pH decreases from 10 to 6. However, further decreases in the pH result in reduced sensitivity, since not only is the $Mg(CDTA)^{2-}$ complex is weakened by the high H^+ concentration, but so is the stability of the metal CDTA complex. That is, while the Mg^{2+} is rapidly released by the CDTA, the other metals cannot form a stable complex with the CDTA. Thus for most metals the optimum pH is approximately 6.

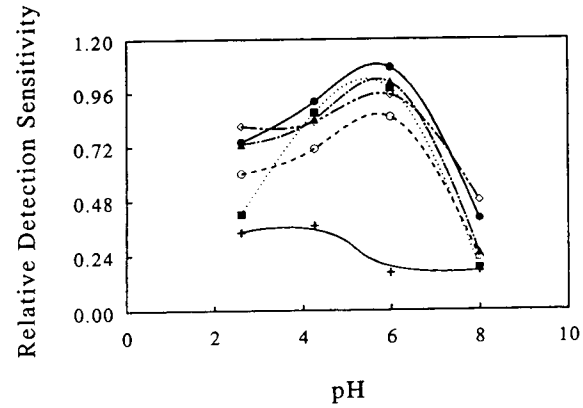

Fig. 1. Effect of the pH of the Mg–CDTA solution on the detection sensitivity for Cu^{2+}(◇), Mn^{2+} (●), Co^{2+} (▲), Ni^{2+} (■), Ca^{2+} (○) and Sr^{2+} (+). Experimental conditions: mode, flow injection analysis in configuration II; reaction coil 1, 510 cm of 0.5 mm I.D. tubing; reaction coil 2, 48 cm of 0.25 mm I.D. tubing; carrier flow, 0.5 ml min^{-1} of 0.01 *M* tartaric acid at various pH; Mg–CDTA reagent flow, 0.16 ml min^{-1} of 0.001 mol l^{-1} $Mg(CDTA)^{2-}$; HQS reagent, 0.22 ml min^{-1} of 0.001 mol l^{-1} HQS in 0.6 mol l^{-1} bicine buffer (pH 8.0); sensitivity, relative to that for Mg^{2+}.

Strontium is an exception to the above behavior. It displays optimal sensitivity between pH 2 and 4. Strontium forms a weaker complex with CDTA than Mg^{2+}, and so thermodynamically only a small portion of the Sr^{2+} would displace Mg^{2+}, as indicated by the low sensitivity observed in Table 3. Under acidic conditions, all of the Mg^{2+} and Sr^{2+} dissociates from the CDTA. When the pH is then increased by addition of the buffered HQS solution, CDTA will complex with the nearest metal ion. Thus the proportion of $Sr(CDTA)^{2-}$ formed depends primarily on the relative concentration of Sr^{2+} to

Mg^{2+}, although complexation kinetics can play a significant role as indicated by the low sensitivity for Ni^{2+} at pH 2.6. At higher pH values, the $Mg(CDTA)^{2-}$ is not fully dissociated, and so the sensitivity is dictated by the relative stabilities of the Mg^{2+} and Sr^{2+} complexes.

Fig. 2 shows the isocratic separation of transition metals and Fig. 3 shows a gradient separation of the lanthanide metals. Detection in both cases is by fluorescence after sequential addition of $Mg(CDTA)^{2-}$ and then HQS^{2-}. The sensitivity of the reagent is similar for most of the metals shown, and corresponds to a detection limit of approximately 5 ng injected (based on three times the baseline noise). These detection limits are comparable to those achievable with 4-(2-pyridylazo)resorcinol (PAR) using absorbance detection [19] and Mg–EDTA–HQS using fluorescence detection [8]. Decreasing the reagent concentration would further improve the detection limit by decreasing the intensity of the background. An enhanced sensitivity is expected for Zn^{2+} and Lu^{3+} as the HQS^{2-} complexes of these metals are strongly fluorescent, and so will contribute to the fluorescence from

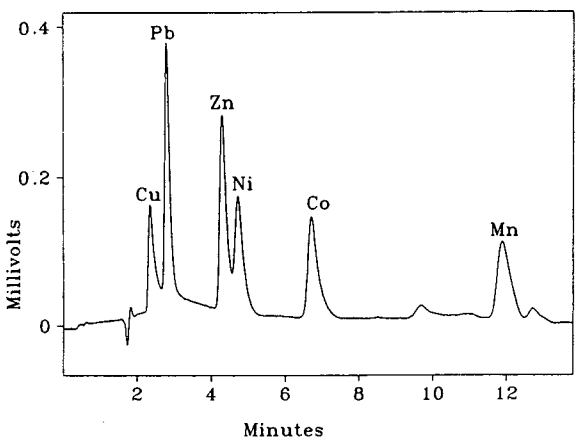

Fig. 2. Isocratic separation of transition metals. Column 5-μm Delta Pak C_{18}, 150 × 3.9 mm I.D.; eluent 0.05 mol l^{-1} tartarate (pH 3.4), 0.0024 mol l^{-1} $C_8SO_3^-$; flow-rate, 1.0 ml min^{-1}; injection, 50 μl of 3×10^{-5} mol l^{-1} each of Cu^{2+}, Pb^{2+}, Zn^{2+}, Ni^{2+}, Co^{2+} and Mn^{2+}; post-column reaction by sequential addition of 0.43 ml min^{-1} of 0.001 mol l^{-1} $Mg(CDTA)^{2-}$ followed by 0.43 ml min^{-1} of 0.001 mol l^{-1} HQS in 0.6 mol l^{-1} bicine (pH 12.17) (final solution pH 8.0); fluorescence excitation 360 nm, emission, 500 nm.

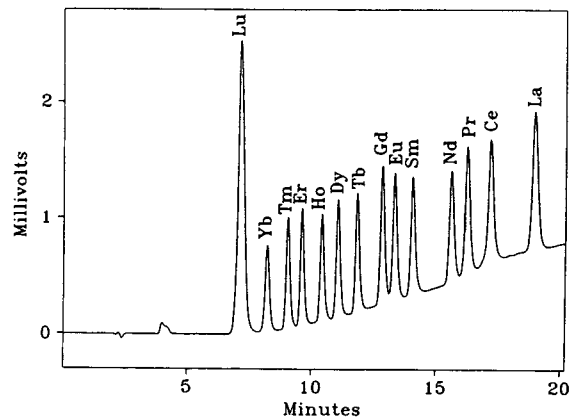

Fig. 3. Gradient separation of the lanthanide metals. Column 5-μm Delta Pak C_{18}, 150 × 3.9 mm I.D.; eluent 0.025 mol l^{-1} α-hydroxyisobutyric acid (HIBA) (pH 5.3) for 4 min then linearly increasing to 0.15 mol l^{-1} HIBA (pH 5.3) over 15 min, $[C_8SO_3^-]$ constant at 0.003 mol l^{-1}; flow-rate, 1.0 ml min^{-1}; injection, 50 μl of 7.5 mg l^{-1} each of Lu^{3+}, Yb^{3+}, Tm^{3+}, Er^{3+}, Ho^{3+}, Dy^{3+}, Tb^{3+}, Gd^{3+}, Eu^{3+}, Sm^{3+}, Nd^{3+}, Pr^{3+}, Ce^{3+} and La^{3+}; post-column reaction by sequential addition of 0.14 ml min^{-1} of 0.001 mol l^{-1} $Mg(CDTA)^{2-}$ in 0.25 mol l^{-1} MOPSO (pH 6.3) followed by 0.14 ml min^{-1} of 0.001 mol l^{-1} HQS in 0.6 mol l^{-1} 2-amino-2-methyl-1-propanol (AMP) (pH 12.17) (final solution pH 8.0); fluorescence excitation 360 nm, emission, 500 nm.

$Mg(HQS)_2^{2-}$. Such behavior has previously been observed in a similar detection system [8]. However, the Lu^{3+} sensitivity exceeds that predicted from the individual fluorescence contributions. The cause of this anomalous behavior is under further investigation.

4. Conclusions

A non-specific fluorescent reagent suitable for post-column reaction detection of metal ions is obtained from 8-hydroxyquinoline-5-sulfonic acid (HQS) by using the displacement mechanism. However, the system behavior is complex due to the presence of multiple interdependent equilibria, such as observed previously for the Zn–EDTA–PAR displacement reagent [9]. For the Mg–CDTA–HQS reagent, the governing equilibria are the complex formation of the Mg^{2+} and displacing metal ion with both $CDTA^{4-}$ and HQS^{2-}. Thus for simultaneous addition of

$Mg(CDTA)^{2-}$ and HQS^{2-}, the sensitivity is determined solely by the equilibrium between the various chelates.

In addition to the equilibrium effects, the displacement kinetics can also play an important role in the sensitivities observed for Mg–CDTA–HQS. Upon sequential addition of $Mg(CDTA)^{2-}$ and HQS^{2-} the slow decomplexation kinetics of the metal–CDTA complex precludes involvement of the HQS^{2-} complexes in the equilibrium governing detection, and thus the sensitivity is dependent solely upon the relative stabilities of the CDTA complexes with Mg^{2+} and displacing metal ion. Since Mg^{2+} forms a weaker CDTA complex than most other metal ions, sequential addition of reagent yields the desired non-specific fluorescent reagent.

Acknowledgement

This work was supported by the Natural Sciences and Engineering Research Council and by the University of Calgary through a University Research Grant. Presented at the *International Ion Chromatography Symposium* in Baltimore, MD, September 1993.

References

[1] K.A. Ruth and R.W. Shaw, *J. Chromatogr.*, 546 (1991) 243.
[2] R.M. Cassidy, S. Elchuk, N.L. Elliot, L.W. Green, C.H. Knight and B.M. Recoskie, *Anal. Chem.*, 58 (1986) 1181.
[3] A. Siriraks, H.M. Kingston and J.M. Riviello, *Anal. Chem.*, 62 (1990) 1185.
[4] P.K. Dasgupta, K. Soroka and R.S. Vithanage, *J. Liq. Chromatogr.*, 10 (1987) 3287.
[5] P. Jones, L. Ebdon and T. Williams, *Analyst*, 113 (1988) 641.
[6] T. Williams and N.W. Barnett, *Anal. Chim. Acta*, 259 (1992) 19.
[7] K. Soroka, R.S. Vithanange, D.A. Phillips, B. Walker and P.K. Dasgupta, *Anal. Chem.*, 59 (1987) 629.
[8] T. Williams and N.W. Barnett, *Anal. Chim. Acta*, 264 (1992) 297.
[9] C.A. Lucy and H.N. Dinh, *Anal. Chem.*, (1994) in press.
[10] L. Fossey and F.F. Cantwell, *Anal. Chem.*, 55 (1983) 1882.
[11] L. Fossey and F.F. Cantwell, *Anal. Chem.*, 57 (1985) 922.
[12] R.M. Smith and A.E. Martell, *Critical Stability Constants: Amines*, Vol. 2, Plenum Press, New York, 1975.
[13] H.M. Stevens, *Anal. Chim. Acta*, 20 (1959) 389.
[14] D.E. Ryan, A.E. Pitts and R.M. Cassidy, *Anal. Chim. Acta*, 34 (1966) 491.
[15] J.A. Bishop, *Anal. Chim. Acta*, 29 (1963) 172.
[16] R. Pribil, *Analytical Applications of EDTA and Related Compounds*, Pergamon Press, Braunschweig, Germany, 1972, p. 41.
[17] A.E. Martell and R.M. Smith, *Critical Stability Constants: Amino Acids*, Vol. 1, Plenum Press, New York, 1974.
[18] D.N. Hague and M. Eigen, *Trans. Faraday Soc.*, 62 (1966) 1236.
[19] R.M. Cassidy and S. Elchuk, *J. Chromatogr. Sci.*, 18 (1980) 217.

ELSEVIER

Journal of Chromatography A, 671 (1994) 131–139

JOURNAL OF CHROMATOGRAPHY A

On-line analysis of alkaline samples with a flow-through electrodialysis device coupled to an ion chromatograph

Paul R. Haddad*, Soehendra Laksana

Department of Chemistry, University of Tasmania, GPO Box 252C, Hobart, Tasmania 7001, Australia

Abstract

A flow-through device suitable for on-line neutralization of strongly alkaline samples using electrodialysis is described. This device comprises an anode compartment filled with a slurry (2:1, w/v) of 1 m*M* octane sulfonic acid and hydrogen-form cation-exchange resin, a 300 μl sample chamber bounded by two cation-exchange membranes, and a cathode compartment filled with dilute sodium hydroxide. An alkaline sample (up to 1 *M* sodium hydroxide) passed through the device at a rate of 0.1 ml/min is neutralized and with the aid of a switching valve, the treated sample can be routed directly to a suppressed ion chromatographic system for determination of inorganic anions. The design parameters for the electrodialysis devices have been studied, including the type of membrane used, the size of the electrodes, the shape of the sample compartment, and the applied power. Optimal performance was obtained with planar stainless-steel electrodes and with 2 W of power. Recoveries of inorganic anions from treated samples were close to quantitative with the exception of nitrite, for which losses were observed. The on-line electrodialysis is shown to be suitable for the treatment of sodium hydroxide solutions, but was less successful when applied to solutions of sodium carbonate and sodium tetraborate. The system has been used for the determination of fluoride in forage vegetation after preparation of the sample by fusion with sodium hydroxide. Good agreement was obtained with results from colorimetric determination of fluoride.

1. Introduction

Donnan dialysis, in which ions of a specified charge pass selectively through an ion-exchange membrane, has been used for matrix normalization [1], sample preconcentration [2] and sample clean-up [3] in ion chromatography (IC). Electrodialysis, wherein an electric field is applied to enhance the performance of a conventional Donnan dialysis experiment, has also recently found use in IC [4–7] and in high-performance liquid chromatography [8,9]. The IC applications of electrodialysis include the treatment of strongly acidic samples prior to the determination of magnesium(II) and calcium(II) using a dual anion-exchange membrane tube device [4], and the treatment of alkaline samples (up to 1 *M* sodium hydroxide) prior to the determination of trace levels of inorganic anions by suppressed IC [5]. In both cases, the electrodialysis was performed off-line. A flow-through electrolytic device has been reported [6] which has the primary function of suppression of IC eluents prior to conductivity detection. This device, called a "self regenerating suppressor (SRS)", uses a similar configuration of membranes to that employed in the micromembrane suppressor [10], but with the addition of two electrodes. The SRS employs

* Corresponding author.

0021-9673/94/$07.00
SSDI 0021-9673(94)00059-I

the electrolysis of deionized water as a source of hydronium ions which are then involved in a conventional suppression reaction [11] capable of neutralizing sodium hydroxide eluents as concentrated as 150 m*M*. Whilst the primary role of the applied power is to provide a source of hydronium ions for the suppression reaction, it is probable that electrodialysis also plays a significant role in the operation of this device. The SRS has also been shown to be applicable to the treatment of concentrated acids and bases prior to IC analysis [7]. Since the SRS does not have the necessary capacity to neutralize such samples during a single passage through the device, the sample is recycled a sufficient number of times until the pH reaches a level appropriate for the subsequent IC analysis. When a current of 500 mA was used, a 50% sodium hydroxide solution could be neutralized using three cycles through the SRS.

For some time we have been studying the use of dialytic methods for the treatment of alkaline samples, chiefly because of the importance of alkaline fusion as a sample dissolution method in IC [11]. An off-line electrodialysis cell was developed which achieved neutralization of a 1 *M* sodium hydroxide sample in 11 min without loss of solute anions, except for fluoride and nitrite [5]. Losses of these two ions were attributed to the formation of neutral, protonated species inside the membrane, with subsequent egress from the sample chamber by diffusion through the cation-exchange membrane used. Careful choice of the membrane enabled such losses to be minimized. In the present work, modifications to the off-line electrodialysis cell have been made to produce a flow-through electrodialysis cell which permits on-line treatment of the sample, followed by direct injection onto the IC. Variations to the shape of the sample chamber, the size of the electrodes and the nature of the cation-exchange membrane are examined in order to optimize the flow-through cell design and to minimize the heat generated inside the cell. In addition, the utility of the procedure for use with samples containing high levels of carbonate or borate is studied and the method is applied to the determination of fluoride in vegetation samples prepared by hydroxide fusion. The results are compared with those obtained by colorimetry.

2. Experimental

2.1. Instrumentation

The ion chromatograph consisted of a Millipore-Waters (Milford, MA, USA) Model 510 pump, Model U6K injector and Model 430 conductivity detector, operated in both the suppressed and non-suppressed modes. The column used for the suppressed mode was a Dionex HPIC AS-4A anion separator with AG-4A guard column, connected to an anion micromembrane suppressor. A Waters Reagent Delivery Module was used to pass the regenerant of 12.5 m*M* sulfuric acid through the suppressor. The column used for the non-suppressed mode was a Millipore-Waters IC Pak HR anion-exchange column (75 × 4.6 mm I.D.). Sodium ion was determined using a Millipore-Waters IC Pak C cation column, 50 × 4.6 mm I.D. All chromatographic separations were carried out at room temperature with an eluent flow-rate of 1.2 ml/min and chromatograms were recorded on a Millipore-Waters Maxima 820 data station.

2.2. Flow-through electrodialysis device

The flow-through electrodialysis cell was developed from the two-membrane static electrodialysis cell described previously [5] and was constructed as a series of perspex blocks held together with longitudinal screws to form a three-compartment cell separated by cation-exchange membranes, as depicted in Fig. 1.

The sample chamber was designed to allow the sample to flow during the electrodialysis process. Electrodes were constructed from stainless-steel plates (60 × 25 × 0.7 mm), inserted into the electrode compartments and connected to the power supply. The membranes were supported with a perspex sheet attached to each electrode solution compartment, through which had been drilled numerous closely spaced holes, 2 mm in diameter. The volume of both the anode and cathode compartments was 15 ml, whilst the

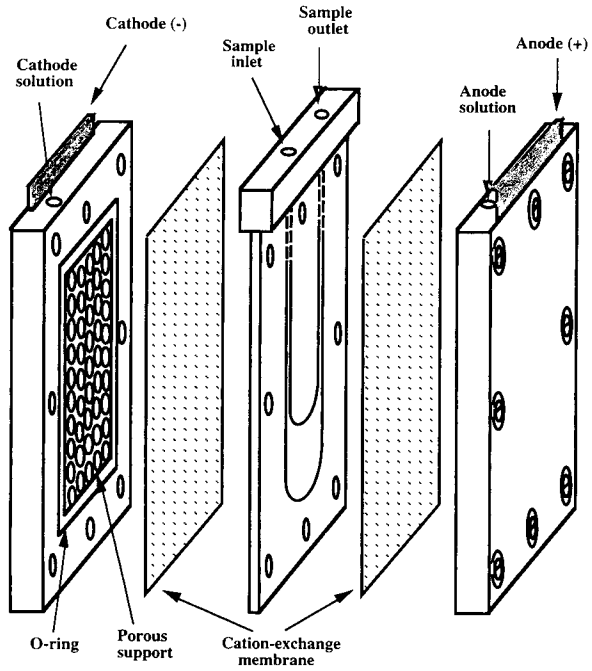

Fig. 1. Flow-through electrodialysis cell.

sample compartment contained 300 μl. A BioRad (Richmond, CA, USA) microprocessor-controlled electrophoresis power supply (Model 3000 Xi) was used in the fixed power and fixed current modes.

The sodium hydroxide sample solution was passed through the sample compartment of the cell at a constant flow-rate of 0.1 ml/min using a syringe pump (Razel Scientific Instruments, Stamford, CT, USA), whilst a d.c. potential was applied at constant power (2 W) to the electrodes at the two ends of the cell. The outlet of the sample compartment was connected to a six-port switching valve fitted with a standard 20-μl sample loop so that direct injection of the neutralized sample solution onto the IC system was possible.

2.3. Reagents

All chemicals used were of analytical reagent grade and the water employed for the preparation of standard solutions and eluents was purified on a Millipore (Bedford, MA, USA) Milli-Q water treatment system. Samples and eluents were filtered through a Millipore 0.45-μm membrane filter and degassed in an ultrasonic bath prior to use. The eluent used for the suppressed IC mode contained 2 m*M* sodium bicarbonate and 2 m*M* sodium carbonate. The eluent used for the non-suppressed IC system contained 0.1 *M* boric acid and 1.9 m*M* tartaric acid adjusted to pH 4.5 with the addition of sodium hydroxide solution. The eluent for sodium determination contained 0.5 *M* EDTA and 2 m*M* nitric acid.

Standard stock solutions of inorganic anions were prepared by dissolving appropriate amounts of the sodium salts in water. Working solutions of these ions were obtained by diluting the stock solutions with sodium hydroxide to give a final concentration of 1 *M* NaOH. The inorganic anion concentrations in the sample solution were fluoride (3 μg/ml), chloride (3 μg/ml), nitrite (6 μg/ml), bromide (6 μg/ml), nitrate (6 μg/ml), sulfate (8 μg/ml) and phosphate (10 μg/ml). A standard solution containing the same concentrations of anions was made up in water and was used to calibrate the instrument.

The hydrogen ion donating medium used in the anode compartment was a slurry of BioRad AG 50W-X8 hydrogen form cation-exchange resin, 200–400 mesh, in 1 m*M* octanesulfonic acid (2:1, w/v). The cathode compartment was filled with 0.1 *M* sodium hydroxide. Octanesulfonic acid solution was prepared by passing a solution of sodium octanesulfonate through a glass column packed with 100 g of BioRad AG 50W-X8 hydrogen form cation-exchange resin, 37–74 μm. The cation-exchange resin was washed thoroughly with Milli-Q water prior to use. The cation-exchange membranes used in this work were obtained from Tokuyama Soda Company (Tokyo, Japan) (Neosepta CM-2 and CMS) and Asahi Glass Company (Tokyo, Japan) (CMV).

2.4. Sample preparation procedures

Vegetation samples for this work were obtained from the vicinity of an aluminium smelter and were prepared as follows. Approximately 2.0 g of ground, dried sample was weighed into a nickel crucible and 10 ml of 5 g/l calcium oxide

was added to form a slurry. The crucible was placed on a hotplate, charred for 1 h and transferred to a muffle furnace at 600°C for 2 h. Sodium hydroxide pellets (3 g) were added and the fusion continued for 3 min at 600°C. The crucible was then removed from the furnace and swirled carefully to suspend the particulate matter until the melt solidified. After cooling, the fused sample was dissolved and diluted with water in a 100 ml volumetric flask to give a final hydroxide concentration of 0.75 *M*.

3. Results and discussion

3.1. Design of the flow-through electrodialysis device

The first goal of this work was the design and construction of a flow-through cell suitable for the neutralization of strongly alkaline solutions, while at the same time allowing the cell to be connected directly to an IC system. The cell requires compartments for housing the sample, the hydrogen ion donating medium (anode compartment) and the receiver solution (cathode compartment). This configuration was obtained by modifying our previous static electrodialysis cell design [5] to include a sample compartment made by cutting a flow-path into a perspex sheet, both sides of which were covered by planar cation-exchange membranes. The upper part of the perspex sheet was drilled and threaded to make an inlet and outlet so that the sample was able to flow during the electrodialysis process. Three types of sample compartments were made, as shown in Fig. 2. The electrode compartment was constructed by machining a chamber in the centre of a perspex block. Several holes were drilled from the upper section of the perspex block for introducing the electrode and the required solution into the compartment. Mechanical support for the membrane was required and was provided by perforated perspex sheets which formed one wall of each electrode chamber. The components of the cell were held together with longitudinal screws, to form the flow-through electrodialysis cell shown in Fig. 1.

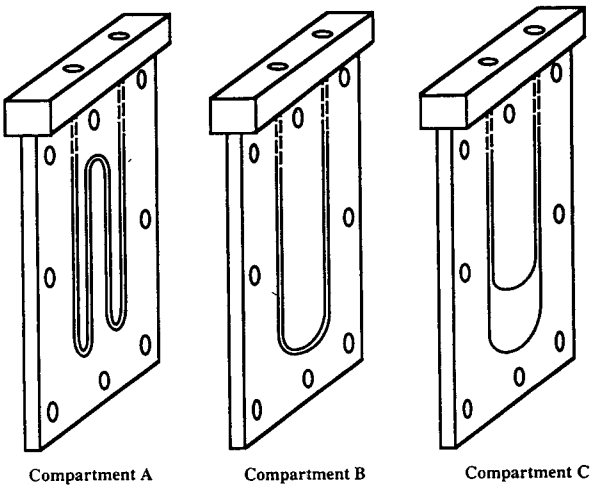

Fig. 2. Sample compartments constructed for the flow-through electrodialysis cell.

Previous work had demonstrated that the neutralization process could be achieved by applying either constant current or constant power. Preliminary tests on the flow-through cell using sample compartment A (shown in Fig. 2), a Neosepta CM-2 cation-exchange membrane and platinum wire electrodes (50×0.2 mm O.D.) showed that a constant current in the range of 110–130 mA or a constant power of at least 4 W was required to neutralize a solution of 1 *M* NaOH at a flow-rate of 0.1 ml/min. A higher sample flow-rate could be accommodated by applying a greater constant current or power, but this also caused the sample solution to heat up which ultimately distorted the membranes. Fig. 3 shows the current required for neutralization at different sample flow-rates. Recovery studies were undertaken to assess the loss of anions from the sample during dialysis at constant currents of 110, 120 and 130 mA. The recovery values were generally higher at lower applied current but the most consistent results were obtained when 120 mA was used as the applied current. Under the experimental conditions described above, a considerable amount of heat was generated inside the flow-through cell after several cycles of sample neutralization, resulting in pronounced buckling of the membranes. Increasing the total conductivity of the

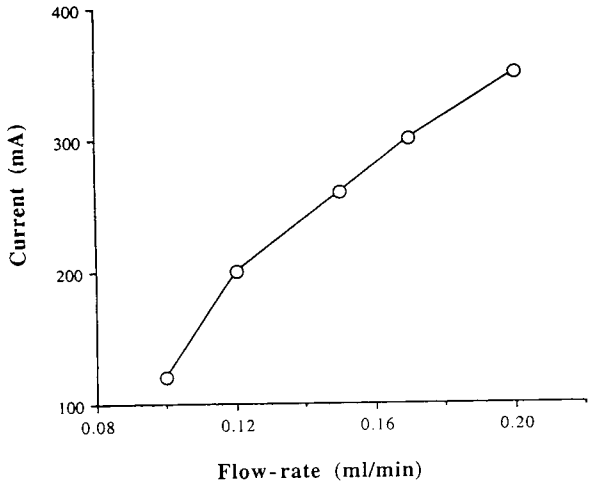

Fig. 3. Constant current required for the neutralization of 1 *M* NaOH using the flow-through electrodialysis cell at different flow-rates.

cell by addition of cation-exchange resin beads (AG 50W-X8, H^+ form, 37–74 μm) to the sample flow-chamber was attempted but this actually caused heat production to increase.

Two alternative sample compartments (B and C in Fig. 2) were evaluated as a means to reduce the heat generated inside the cell. Despite differences in the accommodated sample volume (290, 155 and 300 μl for compartments A, B and C, respectively, in Fig. 2), the thickness and the contact area of the flow gallery, all compartments required approximate currents of 120 mA for the neutralization of 1 *M* NaOH sample solution. However, the sample compartments showed varying resistance, as indicated by the differences in power and potential when a constant current of 120 mA was applied to each of the three sample compartments. Compartment C (300 μl), which had the greatest contact area to the sample solution, gave the best performance and was used for all further work.

The resistance of the cell, and hence the amount of heat generated, is influenced by the size of the electrodes. For this reason, two platinum wire electrodes (50 mm long with diameters of 0.2 and 0.3 mm) and a series of stainless-steel plate electrodes (thickness 0.7 mm, length 45 mm and widths in the range 3–15 mm) with different surface areas were evaluated in an effort to decrease the cell resistance. The results obtained showed that the plate electrodes gave superior performance to wire electrodes and that an electrode of 12 mm width generated the highest current at lowest potential when constant power was applied to the cell. Increasing the size of the electrode to 15 mm gave only a marginal change in performance. The final design of the flow-through cell incorporated stainless-steel plates ($0.7 \times 25 \times 60$ mm) as electrodes, with which a current of 120 mA was generated when a constant power of 2 W was applied to the cell. These conditions were shown to have no detrimental effects on the mechanical stability of the membrane, even after 8 h of continuous neutralization (to pH 7) of 1 *M* NaOH solution flowing at 0.1 ml/min through the cell.

3.2. Selection of the membrane

Previous work [5] has shown that the permselectivities of the membranes, assessed by determining the recoveries of a range of inorganic anions initially added to NaOH solution before the samples were subjected to electrodialysis, played an important role in ensuring the success of the process. Recovery experiments using three different types of membranes (Neosepta CM-2, Neosepta CMS and Asahi CMV) were undertaken using a constant power of 2 W (which correlated to a current of 120 mA). The results are given in Table 1, from which it can be seen that suitable recoveries were obtained for all ions except for nitrite, with the Neosepta CM-2 membrane giving the best overall performance. The ability to successfully treat samples containing fluoride with the CMS membrane is an improvement over the static electrodialysis cell described previously and is attributable to the fact that loss of fluoride by diffusion of hydrogen fluoride through the membrane does not occur to any significant extent since this species is formed only when the sample is about to exit the cell. Chromatograms showing a mixture of inorganic anions in Milli-Q water and in 1 *M* NaOH after electrodialytic treatment using the Neosepta

Table 1
Percentage recovery of anions (present in the range 3–10 μg/ml) from 1 *M* NaOH solution after electrodialysis at 2 W using various cation-exchange membranes in the flow-through cell

Anion	Membrane		
	Neosepta CM-2	Neosepta CMS	Asahi CMV
F^-	84.3 (3.5)	95.8 (3.0)	73.4 (5.2)
Cl^-	99.2 (2.1)	89.0 (4.8)	84.7 (4.2)
NO_2^-	53.0 (4.2)	53.3 (2.6)	48.4 (3.8)
Br^-	94.6 (2.5)	92.5 (3.5)	72.5 (2.7)
NO_3^-	98.4 (3.0)	88.5 (5.3)	74.5 (6.1)
HPO_4^{2-}	99.6 (1.0)	93.2 (4.5)	84.6 (3.4)
SO_4^{2-}	98.5 (2.4)	94.0 (5.2)	85.2 (5.0)

The range derived from 8 replicates is shown in parentheses.

CM-2 membrane are given in Fig. 4. The two chromatograms are virtually identical, except for the low recoveries of fluoride and nitrite in the treated sample.

3.3. Electrodialysis of carbonate and tetraborate solutions

Alkaline fusion techniques commonly involve alkalis other than sodium hydroxide, for example sodium carbonate and sodium tetraborate. These have been used for the dissolution of samples such as glass [12], insoluble waste-water precipitate [13] and rock materials [14] prior to IC determination. The electrodialysis method described in this paper has been applied successfully to the neutralization of sodium hydroxide solutions and we now consider its utility for the neutralization of sodium carbonate and sodium tetraborate solutions.

Electrodialysis of 1 *M*, 0.5 *M* and 0.2 *M* sodium carbonate solutions was carried out at varying values of constant applied power using the flow-through cell. The pH of these solutions after the electrodialytic treatment are shown in Table 2, from which it can be seen that relatively high values of applied power were required to bring the pH reached of the dialysate to approximately 7. This can be attributed to the fact that the electrodialysis results in the formation of

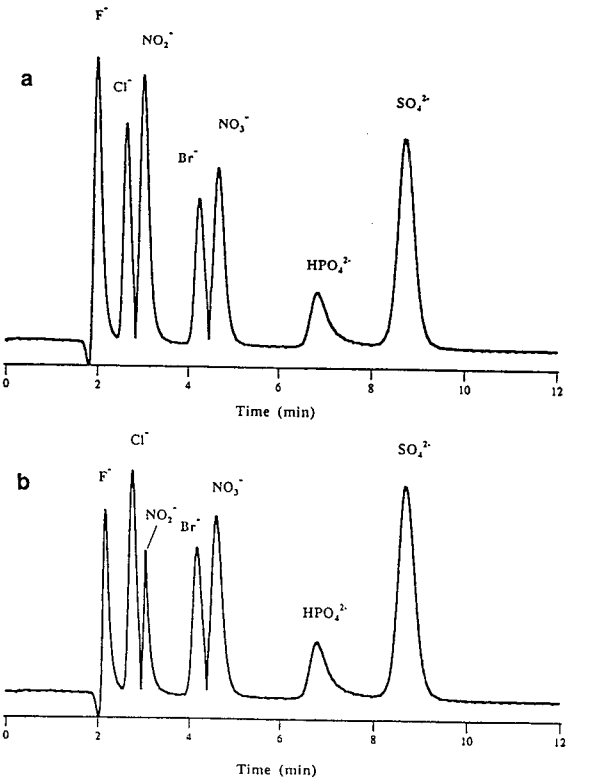

Fig. 4. Chromatograms of inorganic anions (3–10 μg/ml) in (a) Milli-Q water and (b) 1 *M* NaOH after electrodialytic treatment using Neosepta CM-2 membranes. Injection volume: 20 μl. Eluent: 2.0 m*M* Na_2CO_3–2.0 m*M* $NaHCO_3$. Column: Dionex HPIC-AS4A with AG4A Guard Column and AMMS Suppressor.

bicarbonate and carbonic acid, producing a buffered system. The high concentration of residual carbonate and bicarbonate in the final solution caused saturation of the suppressor system when

Table 2
pH of Na_2CO_3 solutions after electrodialysis using the flow-through cell at various values of applied power

Applied power (W)	pH		
	1.0 *M* Na_2CO_3	0.5 *M* Na_2CO_3	0.2 *M* Na_2CO_3
2.0	9.0	8.5	8.0
3.0	9.0	8.0	7.5
4.0	8.5	7.5	7.0
5.0	8.0	7.0	7.0

the dialysed sample was analyzed by suppressed IC, producing severe baseline distortions in the chromatogram. The electrodialysis of 0.1 *M* sodium tetraborate was also carried out using the flow-through electrodialysis cell and the pH of this sample was reduced from 9.5 to 6. However, the chromatogram obtained for the treated solution again showed severe distortion due to boric acid produced by the dialysis.

The displacement efficiency of the electrodialysis technique, which usually governs the capacity of the neutralization process, was examined by determining the concentration of residual sodium in the dialysate solutions after treatment of samples of sodium hydroxide, sodium carbonate and sodium tetraborate. The results are shown in Table 3. Displacement efficiencies close to 100% were obtained for 1 *M* sodium hydroxide and 0.1 *M* sodium borate, with much lower efficiencies being observed for sodium carbonate.

The above results suggest that the electrodialysis procedure has practical application only when sodium hydroxide is used as the flux for fusion procedures involving IC analyses.

3.4. Determination of fluoride in forage vegetation samples

Fluoride is a major environmental pollutant from an aluminium smelter and can be absorbed and accumulated in the tissues of plants which grow in the vicinity of the smelter. Whilst there is no standardised method yet for sample preparation prior to fluoride analysis, acid leaching and hydroxide fusion are the most commonly employed techniques. These processes are frequently followed by distillation and colorimetric determination after reaction with alizarin fluorine blue-lanthanum reagent [15]. Other determination procedures, such as potentiometry [16–18], have also been reported.

The determination of fluoride in a highly alkaline sample matrix has been approached using ion-exclusion chromatography [19], however problems associated with this method when applied to the determination of fluoride in vegetation samples after hydroxide fusion have been reported recently [20]. Elevated levels of silica present in the samples resulted in a build-up of silica on the column, reducing column performance. An ion-exchange separation approach combined with solid-phase reagent conductivity detection, following dilution and neutralization steps using hydrogen ion cartridges, was selected as being most appropriate.

In the present work, vegetation samples obtained from the vicinity of an aluminium smelter were prepared by hydroxide fusion and the sample solution then neutralized using the flow-through electrodialysis cell connected to a suppressed IC system. The flow-rate of the sample through the cell was 0.1 ml/min, a constant power of 2 W was applied for the neutralization process, and Neosepta CMS membranes were used. The results obtained by IC were compared with those obtained by colorimetry following sample preparation by hydroxide fusion, and the results are shown in Table 4. Two standard reference materials (powdered timothy grass) are

Table 3
Residual sodium present in various alkaline solutions after electrodialytic treatment

Solution	Na^+ in original solution (μg/ml)	Na^+ in dialysed solution (μg/ml)	Displacement efficiency (%)
1 *M* NaOH	23 000	108 (56)	99.5 (0.2)
1 *M* Na_2CO_3	46 000	20 500 (700)	55.4 (0.5)
0.5 *M* Na_2CO_3	23 000	2250 (65)	90.2 (0.3)
0.2 *M* Na_2CO_3	9200	216 (42)	97.7 (0.5)
0.1 *M* $Na_2B_4O_7 \cdot 10H_2O$	4600	28 (8)	99.4 (0.2)

The range derived from 5 replicates is shown in parentheses.

Table 4
Comparative results for fluoride in vegetation samples

Sample	Ion chromatography (μg/g)	Colorimetry (μg/g)
Vegetation 1	156 (3)	135
Vegetation 2	554 (12)	560
Vegetation 3	7.6 (1.0)	7
Vegetation 4	106 (4)	110
Standard timothy grass 1	68.1 (1.6)	64
Standard timothy grass 2	269 (9)	277

Results are expressed in terms of the dry mass of the sample. The range derived from 5 replicates is shown in parentheses.

included in Table 4 and the fluoride content of these has been determined using a number of methods, such as titration with thorium nitrate following fusion and distillation, colorimetry following fusion and microdistillation from sulfuric acid, and ion-selective electrode measurement after oxygen bomb decomposition [21]. It has been suggested that the colorimetric measurement with on-line distillation determines the "total" fluoride while IC determines only "free" fluoride in the hydroxide fused sample [20], hence some difference between the results might be anticipated. However, the data in Table 4 show good correlation between the two methods.

The chromatogram obtained for an electrodialysed sample solution using suppressed IC with a carbonate/bicarbonate eluent is shown in Fig. 5. The fluoride present in the sample is well resolved from other anions and can be quantified readily. It was also noticed that there was no interference from the elevated level of silica in the fused sample, either in the electrodialysis cell or on the chromatography column throughout the analyses. This represents an advantage in using the electrodialysis cell over hydrogen ion neutralization cartridges.

The feasibility of employing non-suppressed IC for the determination of fluoride in the electrodialysed sample solution was also investigated. The presence of carbonate (from CO_2) in the neutralized solution often causes interference with the determination of early eluted anions, such as fluoride and chloride, when non-suppressed IC is employed. Such interference has

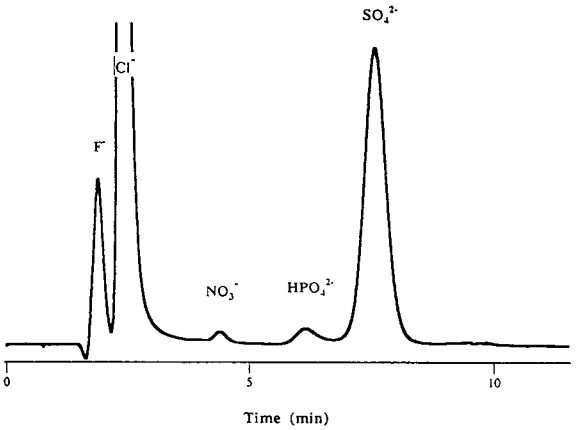

Fig. 5. Chromatogram of electrodialysed vegetation sample. Conditions as for Fig. 4, except that Neosepta CMS membranes were used.

been overcome by the use of tartrate/borate eluents operated in the pH range 3–5 [22,23], since at this pH the carbonate is completely protonated and is therefore eluted at the void volume. However, when the eluent strength was adjusted to 0.1 *M* boric acid and 1.9 m*M* tartaric acid (at pH 4.5) in order to give adequate retention of fluoride, poor detection sensitivity resulted and analysis of the electrodialysed samples by this method was not practicable.

4. Conclusions

This study has shown that clean-up of strongly alkaline solutions prior to ion chromatographic analysis can be achieved on-line with the aid of a flow-through electrodialysis device fitted to a six-port switching valve. Optimum performance of the flow-through electrodialysis device was achieved by employing a sample chamber which accommodated 300 μl of sample, using stainless-steel plate electrodes ($0.7 \times 25 \times 60$ mm), and by passing the sample at a constant flow-rate of 0.1 ml/min through the cell while applying a constant power of 2 W. Under these conditions, 1 *M* NaOH sample solution could be neutralized in approximately 3 min.

The electrodialytic treatment was found to be applicable to sodium hydroxide solutions only,

but this is considered to be a minor drawback of the technique since many insoluble solid samples can be dissolved by fusion with sodium hydroxide. The flow-through cell could be used to successfully treat samples containing fluoride without loss when Neosepta CMS membranes were used. This represents an advantage over the static electrodialysis cell reported earlier. The system was used successfully to determine fluoride in forage vegetation samples after sample preparation by hydroxide fusion.

5. Acknowledgements

We thank Mr. Peter Dove of the University of Tasmania for the design and construction of the electrodialysis device. Financial assistance for the project from Waters Chromatography Division of Millipore is also gratefully acknowledged.

6. References

[1] J.A. Cox and Z. Twardowski, *Anal. Chim. Acta*, 119 (1980) 39.
[2] J.A. Cox, E. Dabek-Zlotorzynska, R. Saari and N. Tanaka, *Analyst (London)*, 113 (1988) 1401.
[3] S. Laksana and P.R. Haddad, *J. Chromatogr.*, 602 (1992) 57.
[4] Y. Okamoto, N. Sakamoto, M. Yamamoto and T. Kumamaru, *J. Chromatogr.*, 539 (1991) 221.
[5] P.R. Haddad, S. Laksana and R.G. Simons, *J. Chromatogr.*, 640 (1993) 135.
[6] S. Rabin, J. Stillian, V. Barreto, K. Friedman and M. Toofan, *J. Chromatogr.*, 640 (1993) 97.
[7] A. Siriraks and J. Stillian, *J. Chromatogr.*, 640 (1993) 151.
[8] A.J.J. Debets, W.Th. Kok, K.-P. Hupe and U.A.Th. Brinkman, *Chromatographia*, 30 (1990) 361.
[9] A.J.J. Debets, K.-P. Hupe, W.Th. Kok and U.A.Th. Brinkman, *J. Chromatogr.*, 600 (1992) 163.
[10] J. Stillian, *Liq. Chromatogr.*, 3 (1985) 802.
[11] P.R. Haddad and P.E. Jackson, *Ion Chromatography: Principles and Applications*, Elsevier, Amsterdam, 1990.
[12] C. McCrory-Joy, *Anal. Chim. Acta.*, 181 (1986) 277.
[13] L.W. Green and J.R. Woods, *Anal. Chem.*, 53 (1981) 2187.
[14] G.W. Kramer and B.W. Haynes, *Report of Investigations 8661*, US Bureau of Mines, Pittsburgh, PA, 1982.
[15] L.S. Clesceri, A.E. Greenberg and R.R. Trussell (Editors), *Standard Methods for the Examination of Water and Wastewater*, American Public Health Association, Washington, DC, 17th ed., 1989.
[16] M. Oehme and H. Stray, *Fresenius Z. Anal. Chem.*, 306 (1981) 356.
[17] W.F. Pickering, *Talanta*, 33 (1986) 661.
[18] K. Nicholson and E.J. Duff, *Analyst (London)*, 106 (1981) 904.
[19] R.E. Hannah, *J. Chromatogr. Sci..*, 24 (1986) 336.
[20] S.C. Grocott, L.C. Jefferies, T. Bowser, J. Carnevale and P.E. Jackson, *J. Chromatogr.*, 602 (1992) 257.
[21] *Official Methods of Analysis*, Association of Official Analytical Chemists, Washington, DC, 15th ed., 1990, p. 52.
[22] T. Okada, *J. Chromatogr.*, 403 (1987) 27.
[23] T. Okada and T. Kuwamoto, *J. Chromatogr.*, 403 (1987) 35.

ELSEVIER

Journal of Chromatography A, 671 (1994) 141–149

JOURNAL OF CHROMATOGRAPHY A

Pre-concentration techniques for bromate analysis in ozonated waters

Howard Weinberg

Department of Environmental Sciences and Engineering, School of Public Health, University of North Carolina, CB 7400, Chapel Hill, NC 27599-7400, USA

Abstract

Ozonation of surface waters that contain bromide result in the formation of bromate which has been identified as a potential carcinogen. Regulation of bromate at the preferred concentration of less than 5 μg/l is being delayed due to lack of a validated analytical method for quantification at this level. This paper describes the integrated use of a silver cation resin to reduce closely eluting chloride from aqueous samples followed by a chelation column to remove leached silver prior to pre-concentration of 4-ml samples on an anion-exchange column. A borate eluent used under gradient conditions allows for bromate determination at 0.5 μg/l in treatment plant waters that, hitherto, were reported to be devoid of bromate.

1. Introduction

Although bromate has been used in the beverage and bread-making industry for some time, there are now new risk assessment data that indicate bromate as a potential carcinogen [1]. The drinking water industry, in its efforts to reduce the amount of halogenated by-products in finished water, is poised to encourage more use of ozone technology to achieve this goal. However, recent studies have revealed the formation of bromate at levels in excess of 10 μg/l in bromide-rich waters which have been ozonated [2]. The World Health Organization, taking a conservative view, recently recommended a limit of 25 μg/l bromate in drinking water [3], in part due to the inability to effectively quantify lower levels. The United States Environmental Protection Agency (U.S. EPA), on the other hand, has suggested restrictions on bromate in drinking water based on extrapolations of toxicological studies which use high bromate doses on animals to the levels associated with average drinking habits in humans [4]. With this standpoint and following negotiation with various interest groups from both the general public and industry, a regulatory level of 10 μg/l bromate has been settled for in the United States in the short term [5]. In fact, the life-time risks associated with bromate ingestion from drinking water require much more stringent regulations. In order to comply with lower level restrictions it is necessary to have available an analytical technique which can simply and rapidly analyze bromate at the low μg/l levels. Currently, the practical quantitation level (PQL) for bromate in drinking water is 10 μg/l [6] based on the ion chromatographic (IC) techniques commonly applied by the U.S. EPA in the determination of inorganic anions in water [7] and the modifications to this approach taken specifically for bromate analysis [8,9]. This technique involves the direct injection of up to 100 μl of aqueous sample onto an anion-exchange column with

0021-9673/94/$07.00
SSDI 0021-9673(93)E0068-6

subsequent elution using suppressed conductivity detection. Anion elution order is such that employing the commonly used carbonate eluent, levels of bromate at or near the detection limit were often swamped by the peak due to chloride which is always present in natural waters at a level of 3 orders of magnitude higher. In order to alleviate this problem, researchers have employed a cation resin in the Ag^+ form as a pre-treatment step to precipitate out a large proportion of the chloride in the aqueous sample prior to injection into the IC system [10,11].

In a gallant attempt to extend this methodology to the analysis of bromate at sub ppb levels, Hautman [12] devised a selective anion concentration technique in which 12 replicate "heart-cut" analyses of 1 ml samples were successively injected and the bromate selectively diverted to a concentration column. Although this method achieved a PQL of 0.25 μg/l in natural water samples, the analysis time for each individual sample was 4 hours and only the bromate constituent was quantified.

There are no reports in the literature on the use of direct pre-concentration for increased sensitivity in bromate detection in aquatic matrices. The major fear associated with this approach has been the non-selectivity of concentration of all the anions present in the aqueous sample and the consequent possibility of overloading the concentrator column. However, coupled with the use of pre-treatment to selectively reduce the quantity of certain anions in excess with respect to the trace quantities of bromate, the technique of pre-concentration is a viable solution to the challenge of lowering the detection limits for bromate in aquatic matrices.

2. Experimental

2.1. Aqueous samples

The development of an analytical approach was undertaken initially on synthetic aqueous samples with a controlled ionic strength which paralleled that expected in typical samples obtained in water treatment. Once developed, the analytical method was applied and validated on samples obtained from natural water sources which were subjected to controlled laboratory ozonation. The characteristics of these two groups of samples are summarized in Table 1. Once validated, the method was then used to determine the bromate levels in the effluent of various water treatment plants utilizing ozone and where ambient bromide levels were different.

2.2. Sample preparation

As the goal of this work was to quantify low μg/l levels of bromate in the presence of high mg/l levels of chloride, sample pre-treatment for chloride reduction was undertaken by syringe filtering all aqueous samples through an On-Guard Ag cation resin (Dionex, Sunnyvale, CA, USA) at a rate of about 2 ml/min. The resin functions by selectively removing the silver salts with low solubilities. While this value is low for silver chloride and bromide (0.89 and 3.7 mg/l, respectively), bromate is unaffected by the resin as its silver salt has a much higher solubility (13.3 g/l).

In order to prevent the leached silver from these resins reaching the concentrator or analytical columns, a chelator column (MetPac CC-1, Dionex) was introduced between the sample loop and the concentrator column.

Table 1
Characteristics of aqueous matrices analyzed

Characteristic	Synthetic water [a] (mg/l)	Natural water [b] (mg/l)
TOC [c]	<1 (C)	7.56 (C)
Chloride	50	7.0
Nitrate	44	0.25
Sulfate	60	24
Bromide	0.2	0.05

[a] Synthetic water made by dilution of concentrates of each anion in deionized, distilled water with minimum resistance of 18.2 MΩ · cm.
[b] Natural water source was University Lake, Carrboro, NC, USA.
[c] TOC = Total organic carbon.

2.3. Instrumentation

The ion chromatographic system used in this work was the Dionex Model 4500i which was employed with the following modifications in operation. A 4-ml pre-treated aqueous sample was loaded into a loop designed from 7 m of 0.1 cm internal diameter polypropylene tubing and placed in the loading position (port numbers 3 and 6) across a 6-port rotary injection valve (Rheodyne, Cotati, CA, USA). While in this position, deionized, distilled water held in a 4-l Nalgene bottle was pumped at 0.75 ml/min, using a pulse-dampened single-piston pump, across the chelator column and through a 4-way slider valve (at port number 4) and out to waste (at port number 8). Simultaneously, the eluent for the ion chromatography was flowing at 2 ml/min through the AG10-SC concentrator column placed across the loop position on the opposite side of the slider valve (port numbers 1 and 5). The borate eluent then flowed through the AS9SC analytical column, anion membrane suppressor (AMMSII) and conductivity detector (module CDM-2). The plumbing for the chromatographic system is shown in Fig. 1 and illustrates the positions of the two valves for sample loading and sample analysis. In the preconcentration step (valve positions shown in the insert), the deionized distilled water is used to flush the 4-ml aqueous sample at 0.75 ml/min through the MetPac CC-1 chelator column and on to the concentrator column in the same direction as eluent flow. After loading, the valves are switched back to their original positions and the concentrated sample is swept on to the analytical column. During this time, the next sample can be loaded into the loop. The analysis of bromate was performed using a 5 m*M* sodium tetraborate–boric acid eluent. Immediately after elution of the bromate peak, the eluent strength was raised to 50 m*M* to purge the remaining anions from the column. Conductivity suppression was achieved with 25 m*M* sulfuric acid regenerant at a flow rate of 10 ml/min. With a clean, equilibrated chromatographic system, a typical background conductivity at the start of the analytical run was 4 μS.

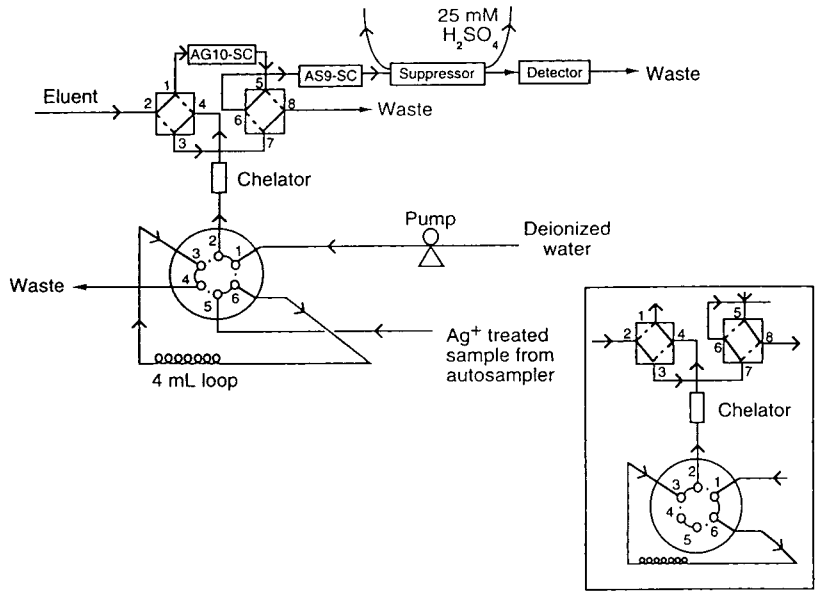

Fig. 1. Schematic of IC plumbing for loop loading or sample analysis (valve positions for sample pre-concentration shown in the insert).

2.4. Reagents

The reagent water used in the preparation of standards, eluents, and synthetic water matrix was prepared in the laboratory by a Corning 3-l mega-pure all-glass distillation system (Model LD-2a, Corning, NY, USA). The source water for the still was purified tap water which had passed through a cartridge-type deionizer (Corning Ultra High Purity) filtering and demineralizing the water. The cartridge is replaced once a month or when the conductivity of the effluent water rises above a pre-determined value.

Boric acid and sodium tetraborate decahydrate used in the preparation of a 100 m*M* concentrate for eluent use were both ACS grade materials assayed at >99.5% purity (Fisher Scientific, Pittsburgh, PA, USA). Dilutions of this stock to both 5 m*M* and 50 m*M* were made as required from the reagent water and were filtered through Whatman glass fiber filters (Whatman, Clifton, NJ, USA) in an all-glass Buchner filtration system prior to use. Sulfuric acid used as the suppressor regenerant was Ultrex purity grade (J.T. Baker, Phillipsburg, NJ, USA). Sodium bromate, chloride, nitrate, sulfate and bromide used in the preparation of the synthetic aqueous solutions were all assayed at 99% purity or higher (Aldrich, Milwaukee, WI, USA). Ethylene diamine in liquid form used in the residual disinfectant quenching experiments was also obtained from Aldrich and assayed at >99% purity.

2.5. Method

Synthetic aqueous solutions at an ionic strength of 2.74 mequiv./l were made up according to the description in Table 1. Repeated injections of 4 ml of these solutions, containing 5 μg/l bromate after passing through the silver resin and the chromatographic system described in Fig. 1, without the chelation column caused a gradual but very distinct deterioration in the resolution between bromate and the remaining chloride. This manifested itself in two ways; gradual reduction in retention time of the bromate peak and eventual coalescence of the bromate and chloride peaks. This is demonstrated in Fig. 2. The inclusion of the chelation column as shown in Fig. 1 allowed in excess of 100 injections of samples containing 10 μeq of anions before any significant deterioration in column performance could be discerned. At this time, the concentrator and analytical columns were restored to their full capacity by washing with acetonitrile for 20 min at 1 ml/min. Additional problems were identified if an anion trap placed in the eluent stream ahead of the slider valve was allowed to become overloaded or was removed. Anion impurities in the eluent will accumulate on the concentrator column and decrease its available capacity for sample anions if the anion trap does not function very effectively. Organic impurities can also affect the performance of the chromatography and may leach into aqueous samples which are stored for long periods in polymer-based autosampler vials. Preparation of these vials requires that after washing, they are filled with reagent water, capped and left to stand overnight. After this step, the vials are rinsed again several times with reagent water before being rinsed and then filled with aqueous sample to be analyzed.

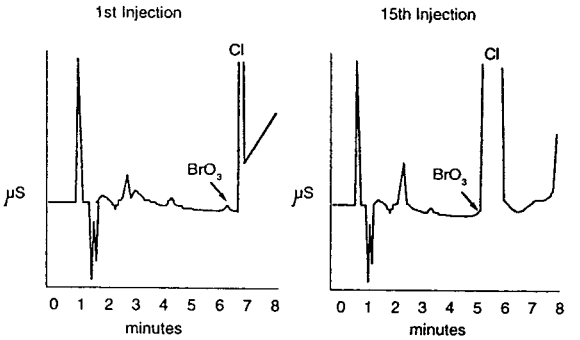

Fig. 2. Loss of bromate resolution from chloride. (Note: plumbing of Fig. 1 used without chelation column).

3. Results

3.1. Calibration

In view of the aim to optimize pre-concentration for the greatest sensitivity of bromate detection, no attempt was made in this method to quantify other anions. The chromatographic

conditions were determined from repeated injections of bromate in synthetic water and then the conditions were applied to water treatment samples for validation. Quality assurance of bromate calibration was undertaken by statistical analysis of the chromatographic response obtained from 7 injections at the 0.5 μg/l level. This concentration was selected as the lowest practical level at which a discernable response was obtained relative to the detector noise. The method detection limit (MDL) was determined according to the Code of Federal Regulations [13]:

$$MDL = tS + b$$

where $t = 3.143$ (Student's t value for 6 degrees of freedom and 99% confidence level), S = standard deviation of seven replicate analyses, and b = mean value of blank.

The blanks in these experiments were the reagent water in the synthetic matrix and raw University Lake water in the natural water matrix. In both cases, the background level of bromate was at the noise level. Applying the above definition for detection limits, a value below that selected for the determination was indicated in both matrices. An alternative approach was to study the signal-to-noise ratio and select the signal which is at 3 times the noise signal as a practical reporting level (PRL). Table 2 summarizes the statistics of both approaches and indicates that all detection limits are below the selected 0.5 μg/l level, although the actual values are slightly different for both matrices. Since quantification in field samples will normally be required in natural water matrices, it is more practical to apply the higher detection limit in sample analyses.

Calibration curves in both matrices were established from triplicate injections of bromate-spiked aqueous matrix in the range 0–5 μg/l. The regression coefficient (r^2) for both synthetic and natural water matrices was very acceptable (0.996–0.997). A typical chromatogram of one of the calibration points (1.28 μg/l) is shown for the synthetic water matrix in Fig. 3a.

Recovery studies of bromate spiked into both matrices at the 5 μg/l level indicated a slight loss of analyte in natural water compared to synthetic water and this was reflected in the slightly lower gradient of the natural water calibration curve. This is quite a common occurrence among environmental samples and has often been the source of controversy in deciding absolute concentrations in one matrix when calibration is undertaken in another. In this case, the difference is statistically insignificant although the analyst will have to assure a similar comparison when analyzing natural waters with different physical characteristics.

3.2. Laboratory controlled ozonation of surface water

The natural water characterized in Table 1 was collected at the entrance to the Orange County Water and Sewage Authority treatment plant, Carrboro, NC. 500-ml samples placed in a 1-l

Table 2
Method detection limits of bromate

	Synthetic water	Natural water
Mean concentration (μg/l) [a]	0.514	0.628
Standard deviation S (μg/l)	0.098	0.069
Statistical MDL (μg/l) [b]	0.31	0.22
Height at t_R = 5.97 min in blank (noise)	2148	3977
3 × noise	6444	11931
Noise detection limit (μg/l) [c]	0.13	0.35
Recovery of 5 μg/l spike (%)	107	95

[a] Mean value of 7 repeated injections of 0.5 μg/l bromate spiked into each matrix.
[b] Determined as 3.143s + blank.
[c] Bromate detection limit at signal-to-noise ratio of 3:1.

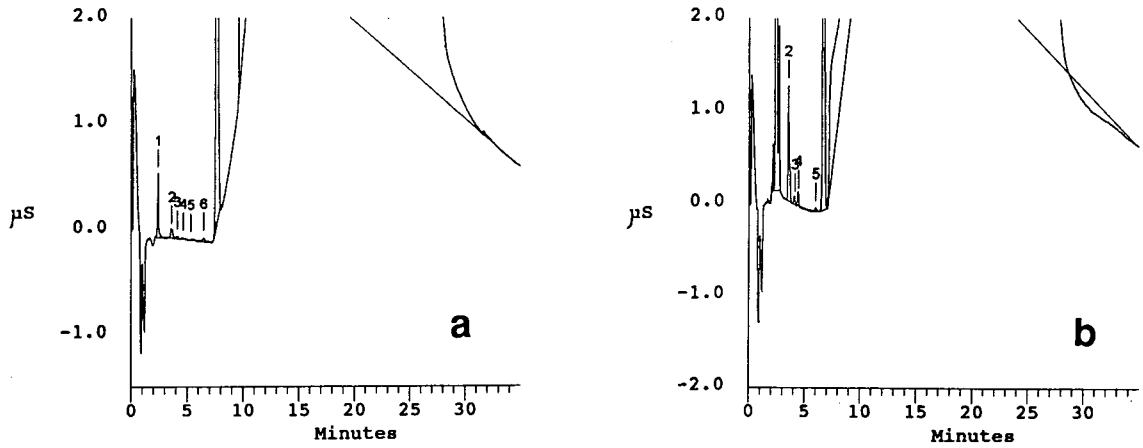

Fig. 3. Chromatogram of bromate; (a) at 1.28 μg/l in synthetic water: retention time of peak no. 6 = 6.45 min; peak area = 745 756; peak height = 35 625); (b) in ozonated University Lake water: retention time of peak no. 5 = 5.97 min; concentration of bromate found (peak no. 5) = 1.1 μg/l; peak area = 336 216 peak height = 36 708.

washing bottle were attached to a Model 200 Sander ozonizer (Erwin Sander, Vetze-Eltze, Germany) supplied by air. Ozone was supplied to the sample so that an approximate transfer of 1 mg ozone to 1 mg TOC was achieved. After ozonation, a sample was poured into a 100-ml Erlenmeyer flask and purged gently with pure nitrogen (99.9%) to remove any residual ozone from the solution. The sample was then filtered through an Ag^+ resin cartridge and into two clean autosampler vials for duplicate analysis.

For quality control purposes a sample of the raw surface water was similarly treated without ozonation. The resulting chromatogram using the stated analytical conditions and the plumbing of Fig. 1 is shown in Fig. 3b for the ozonated sample. Utilizing a calibration curve in the range of 0.5–5 μg/l bromate in synthetic water, bromate was quantified in the ozonated water at 1.1 μg/l. A 5 μg/l spiked sample of the ozonated water produced the chromatogram in Fig. 4 illustrating a recovery of 105%.

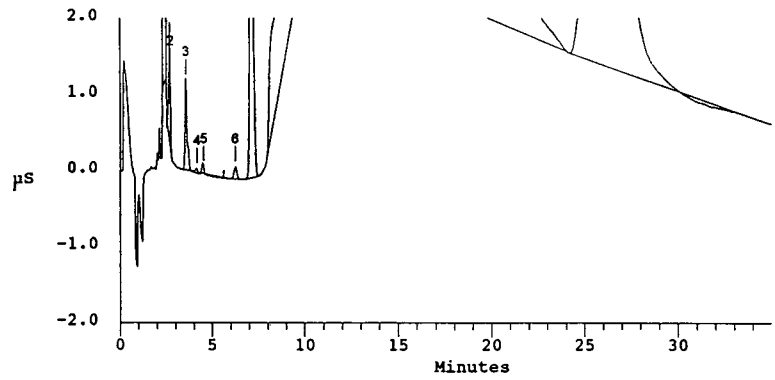

Fig. 4. Chromatogram of ozonated University Lake water with a 5 μg/l bromate spike; concentration of recovered bromate (peak no. 6) = 5.25 μg/l.

3.3. Quenching of residual disinfectant

Water treatment plants and consumers' drinking water will often contain residual disinfectants such as free chlorine, chloramines, or chlorine dioxide. Residual ozone could also be present in samples collected for bromate analysis drawn immediately after ozonation. If samples containing these oxidants were injected onto an ion exchange column, the oxidant would attack the active sites on the column causing irreversible damage. Similarly, if oxidants remain in the sample at the time of collection, bromate concentration might change as a result of continued reaction. It is therefore essential to quench such samples from residual disinfectant and such a procedure in ion chromatography should involve non-ionic reagents that will not interfere with the chromatography. In the case of ozone and chlorine dioxide, it is usually sufficient to purge the sample with nitrogen gas for 5 min. Experiment has shown that this does not cause any loss in bromate from the sample. Chlorinated samples cannot be quenched by purging and consequently require the addition of a quenching reagent. Moreover, when bromide is present in the sample, both chlorine and ozone can react with it to produce the hypobromite ion. It is this species that is directly responsible for the formation of bromate in aqueous solution [14] and thus it is essential that it be removed from the sample at the time of collection. The reagent of choice was ethylene diamine (EDA) and Fig. 5 illustrates the effectiveness of a 50 mg/l addition of EDA to natural water containing spiked bromide to 0.2 mg/l and ozonated at a 1:1 ozone:TOC level. In the absence of EDA, bromate continues to grow in concentration with time (Fig. 5a), whereas its presence appears to stabilize bromate concentration (Fig. 5b).

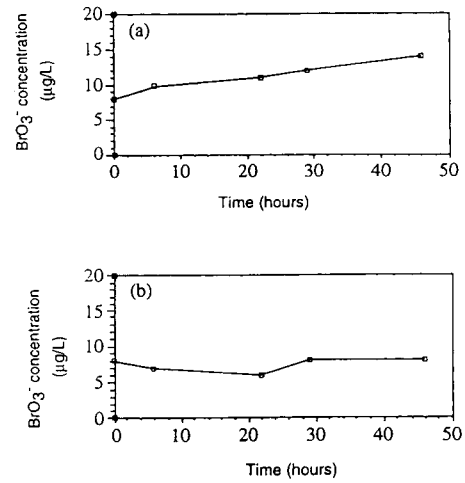

Fig. 5. Change in bromate concentration in ozonated spiked surface water; (a) without EDA quench (b) in the presence of 50 mg/l EDA.

3.4. Analysis of ozonated waters from treatment plants

Water samples were collected at various points in the treatment plants in 40-ml glass vials (Pierce, Rockford, IL, USA) equipped with polypropylene screw caps that had Teflon-faced silicone septa. Prior to dispatching these bottles to the plants, a few drops of an EDA solution (equivalent to 2 mg) were placed in the bottom of each. For the purpose of quality control, one vial was filled with reagent water and EDA solution and sent with the collection vials to each plant. This particular study focussed on analyzing samples taken prior to and following ozonation in order to quantify trace amounts of bromate. In order to characterize the sampled water, applied ozone dose and raw water TOC data were supplied by the plant and ambient bromide levels were measured with direct injection ion chromatography of a separate sample [6]. The bromate content was analyzed first using direct injection of a 100-μl sample using the same analytical conditions as previously described without chelation and pre-concentration. The purpose was to identify if bromate concentrations were in excess of 5 μg/l. If they were, the sample was diluted with synthetic water to bring the concentration in the range 0.5–5 μg/l and then the sample was reanalyzed using the pre-concentration technique. If no chromatographic response was detected by direct injection of the sample, pre-concentration was applied without dilution. The results of these

Table 3
Bromate formation in ozonated natural waters

Treatment plant	O_3:TOC (mg/mg)	Ambient Br^- (mg/l)	BrO_3^- formed (μg/l)
A	3:2.8	0.02	5
B [a]	9.2:11.6	0.18	10
C [a]	2.5:2.9	0.05	8
D_1 [a]	1.5:2.6	0.28	10
D_2 [a]	1.4:3.2	0.22	18
E	6:5.4	0.03	1.1
F	4:7.6	0.04	0.8

[a] Samples diluted 1:10 with synthetic water prior to analysis.

analyses are shown in Table 3 and in no case was bromate detected prior to ozonation. Fig. 6 illustrates the chromatogram obtained for plant F where bromate elutes at 3.47 min. This analysis was performed using the same analytical conditions as described earlier except that the run eluent was adjusted to a 10 m*M* borate mix and the regenerant flow adjusted upwards to maintain a background conductivity of 4–8 μS. Under these conditions, the analytical run time was reduced to 30 min.

4. Conclusions

Although the pre-concentration technique described here succeeded in most of the plants surveyed, highly colored surface waters analyzed prior to ozonation created some analytical problems. These raw waters contain high levels of dissolved humic materials which occupy active sites on the analytical column. This causes poor resolution of bromate from chloride in spite of pre-treatment to reduce chloride concentration and renders bromate detection impossible in highly colored raw waters. However, following ozonation of such waters, this interference is removed and resolution between the two anions is accomplished. If these colored waters are mistakenly injected onto the analytical or concentration columns, the columns are best regenerated by cleaning for about 1 h with a 4:1 mixture of acetonitrile and 1 *M* sodium chloride.

The method described in this paper has been validated for the analysis of bromate in ozonated waters at a detection limit of 0.5 μg/l which is about an order of magnitude less than currently available using traditional direct injections of samples. In practice, this method should be applicable to most aqueous samples containing bromate from as low as 0.5 μg/l to sub mg/l levels. It is important, however, to demonstrate the recovery of bromate from the matrix under investigation by analyzing samples spiked with bromate at concentration in the range expected to be found in the samples. Sample treatment and analysis using this analytical technique can be automated to an extent that total analysis

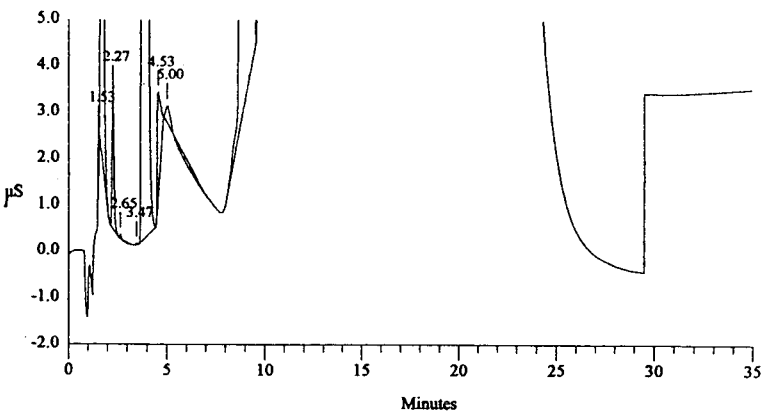

Fig. 6. Chromatogram of bromate formed in plant F at t_R = 3.47 min using a 10 m*M* borate eluent.

time is less than 45 min per sample making this method viable for laboratory monitoring of bromate in drinking water.

5. Acknowledgements

The author would like to express his appreciation to the Ville de Laval, Quebec, Canada for the use of their facilities during interlaboratory assessment of this method and Environment Quebec for supplying some of the natural water samples. Dionex Corporation supported this research through the loan of equipment and accessories and special thanks are extended to Robert Joyce for his support and technical assistance throughout this work. Some of the experimental procedures were developed during the author's research leave at Ecole Polytechnique, Montréal, Canada. Their financial assistance during this period is gratefully acknowledged. A special thanks is given to the dedicated editorial and graphical assistance given by Amanda Stang.

6. References

[1] Y. Kurokawa, S. Aoki, Y. Matsushima, N. Takamura, T. Imazawa and Y. Hayashi, *J. Natl. Cancer Inst.*, 77 (1986) 977.

[2] W.H. Glaze and H.S. Weinberg, *Identification and Occurrence of Ozonation By-Products in Drinking Water*, American Water Works Association Research Foundation, Denver, CO, 1993.

[3] WHO, *Revision of the WHO guidelines for drinking-water quality*, WHO, Geneva, 1991.

[4] Y. Patel, *Review of Ozone and By-Products Criteria Document*, U.S. EPA, Washington, DC, 1992.

[5] S. Regli, *Draft D/DBP Rule Language*, U.S. EPA Office of Groundwater and Drinking Water, Washington, DC, 1993.

[6] C.-Y. Kuo, S.W. Krasner, G.A. Stalker and H.S. Weinberg, *Proceedings of the American Water Works Association Water Quality Technology Conference, San Diego, CA, 1990*, American Water Works Association, Denver, CO, 1991.

[7] U.S. EPA, *The Determination of Inorganic Anions in Water by Ion Chromatography*, Method 300.0, U.S. EPA, Washington, DC, 1989.

[8] D.P. Hautman and M. Bolyard, *J. Chromatogr.*, 602 (1992) 65.

[9] D.P. Hautman and M. Bolyard, *J. AWWA*, 84 (1992) 78.

[10] R.J. Joyce and H.S. Weinberg, *Proceedings of the Pittcon, New Orleans, LA, March 1993*, 1993.

[11] G.L. Amy and M.S. Siddiqui, *Proceedings of the American Water Works Association Annual Confeerence, Philadelphia, PA, 1991*, American Water Works Association, Denver, CO, 1992.

[12] D. Hautman, *Proceedings of the American Water Works Association Water Quality Technology Conference, Toronto, Canada, 1992*, American Water Works Association, Denver, CO, 1993, p. 993.

[13] U.S. Office of the Federal Register, *Protection of Environment: Definition and Procedure for the Determination of the Method Detection Limit*, Code of Federal Regulations, 40 (136B) 510, 1987.

[14] W.R. Haag and J. Hoigné, *Vom Wasser*, 59 (1982) 237.

ELSEVIER

Journal of Chromatography A, 671 (1994) 151–157

JOURNAL OF CHROMATOGRAPHY A

On-line preconcentration and ion chromatography of triazine compounds

Giovanni Sacchero, Corrado Sarzanini*, Edoardo Mentasti

Department of Analytical Chemistry, University of Turin, Via P. Giuria 5, 1025 Turin, Italy

Abstract

An ion chromatographic method was developed for the determination of triazine herbicides in environmental samples. Considering the polar nature of triazines, a cation-exchange column with a multi-mode pellicular packing was used. Optimization of the eluent (organic modifier concentration and ionic strength) is described with reference to the separation, on-line clean-up and preconcentration procedure. Several enrichment materials were evaluated and detection limits below 100 ng/l were achieved with a reversed-phase silica. The determination of triazines in tap water and river water samples was performed with UV detection (220 or 263 nm).

1. Introduction

Triazine herbicides are widely used in agriculture and their determination is of great importance in environmental studies and water control. The residual amount of these compounds in rivers and ground waters is normally very low so that samples require preconcentration and clean-up procedures.

The first triazine preconcentration techniques were based on liquid–liquid extraction but owing to their high cost and long analysis times they were replaced by solid-phase extraction. The solid phases used for enrichment of triazines include cation-exchange resins, adsorbent copolymers, porous octadecylsilica and graphitized carbon black [1–4]. As natural samples usually require a matrix-removal step, double-trap systems have been developed [4]. They consist of two successive solid-phase extractions, which allow analytes to be retained and the concentration of interferents to be reduced as a final result. Such methods are usually off-line and only a few studies have integrated on-line preconcentration and determination in the same apparatus [5,6].

The methods actually used for the determination of trace amounts of triazines include gas chromatography [3,7] and high-performance liquid chromatography (HPLC) [8–13]. LC methods are to be preferred for polar or thermolabile analytes [8]. Liquid–liquid partition chromatography represents the most popular HPLC technique for triazine determinations with a variety of detection methods, including mass spectrometry [14]. A reversed-phase ion interaction study for the separation of triazines has recently been reported [15], but ion chromatographic (IC) separation is not usually considered in triazine determinations.

In this work, an IC separation method was developed and coupled with an on-line (single or

* Corresponding author.

0021-9673/94/$07.00
SSDI 0021-9673(93)E1197-8

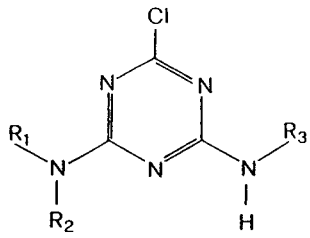

Names	R_1	R_2	R_3	pK_a
Simazine	H	Et	Et	1.7
Atrazine	H	Et	i-Pr	1.7
Propazine	H	i-Pr	i-Pr	1.7
Terbutylazine	H	Et	t-Bu	2.0
Cyanazine	H	Et	CH_3 C-C≡N CH_3	1.0

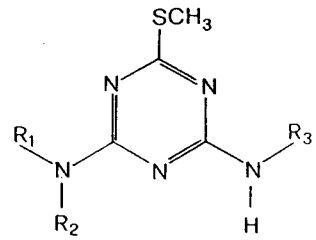

Names	R_1	R_2	R_3	pK_a
Ametryne	H	Et	i-Pr	4.1
Prometryne	H	i-Pr	i-Pr	4.1
Terbutryne	H	Et	t-Bu	4.3

Fig. 1. Structures and pK_a values of Cl- and S-triazines. Et = Ethyl; i-Pr = isopropyl; t-But = *tert.*-butyl.

double) trap system in order to determine trace amounts of triazine herbicides in natural waters. The analytes investigated included eight 1,3,5-triazines, containing either chlorine or sulphur (Fig. 1).

2. Experimental

2.1. Reagents

Acetonitrile (chromatographic grade), phosphoric acid, sodium hydroxide and sodium chloride were of analytical-reagent grade from Merck. All solutions were prepared with high-purity water obtained with a Milli-Q System (Millipore, Bedford, MA, USA).

Reference standards for triazines were obtained from Riedel-de Haën (Seelze, Germany) (98.0–99.9% purity).

Stock standard solutions of triazines (200 mg/l) were prepared in acetonitrile and stored in the dark at 4°C. Working standard solutions were obtained daily by successive dilutions with water of the stock standard solutions.

The eluents, filtered and degassed under vacuum, were acetonitrile–water mixtures containing sodium phosphate buffer (1.0 m*M* H_3PO_4 + NaOH up to pH 4.5).

2.2. Apparatus

An LC 5000 liquid chromatograph (Varian, Walnut Creek, CA, USA) equipped with a Rheodyne injector and a UV 100 spectrophotometric detector was used. A 100-μl loop was used throughout. Chromatograms and data were registered with a Vista 401 data system. A second Rheodyne injection valve was used as a switching valve in the double-trap preconcentration system. Samples were preconcentrated with a DQP-1 pump (Dionex, Sunnyvale, CA, USA).

2.3. Procedure

The separation column was a Dionex OmniPac PCX 500 (250 × 4 mm I.D.). The preconcentration columns investigated for on-line optimization were OmniPac PCX 500 Guard (50 × 4 mm I.D.) (Dionex) and silica-based microcolumns (4 × 4 mm I.D.) LiChrospher 100 RP-18 (5 μm), LiChrospher 100 RP-8 (5 μm), LiChrospher 100 Si 60 (5 μm), LiChrospher 100 CN (5 μm) and LiChrospher 100 DIOL (5 μm) (all from Merck). Other preconcentration columns were obtained by packing a Merck cartridge holder (20 × 3.5 mm I.D.) with 0.16 g of Supelclean Envi-18 (40–60 μm) or with Supelclean Envi-Carb (Supelco, Bellefonte, PA, USA).

Preconcentration flow-rates were 4.0 ml/min for the silica-based microcolumns and 2.0 ml/min for the polymer-based cation-exchange col-

umn. After the sample loading (100.0 ml), the preconcentration column was rinsed with 10.0 ml of high-purity water. The Supelclean Envi-18 stationary phase was activated before use by washing with 10 ml of hexane–diethyl ether (50:50, v/v) followed by 6 ml of methanol and rinsing with 6 ml of water.

After optimization, the eluent composition was acetonitrile–buffer (70:30, v/v), the buffer being 1.0 m*M* phosphate (pH 4.5) containing 30 m*M* NaCl; the flow-rate was 0.7 ml/min.

Unless stated otherwise, UV detection was performed at 220 nm.

3. Results and discussion

3.1. Ion chromatographic separation

The analytes, according to their pK_a values (Fig. 1), may be in cationic form at appropriate pHs. The cation-exchange column chosen for the determination of triazines utilizes a multi-mode pellicular packing to combine an ion-exchange and a reversed-phase mechanism. Several parameters, *i.e.*, pH, dielectric constant, ionic strength and organic modifier concentration, affect the separation of triazines and were considered in eluent optimization. An acidic pH was chosen in order to take advantage of the ion-exchange mechanism.

Chromatographic retention times (t_R) were the means of triplicate determinations and the dead time (t_0) was evaluated by injection of water (water dip), taken as an unretained peak.

As expected, the k' values decrease sharply with increase in acetonitrile concentration, indicating a substantial contribution of liquid–liquid partitioning to the retention mechanism. The additional contribution of an ion-exchange mechanism allows greater flexibility than that obtained with reversed-phase columns during the optimization of the separation procedure. In this instance, in comparison with previous HPLC results [15], the IC separation shows an inversion for the retention order of ametryne and terbutylazine which can be related to their pK_a values. Fig. 2 shows the variation of k' for

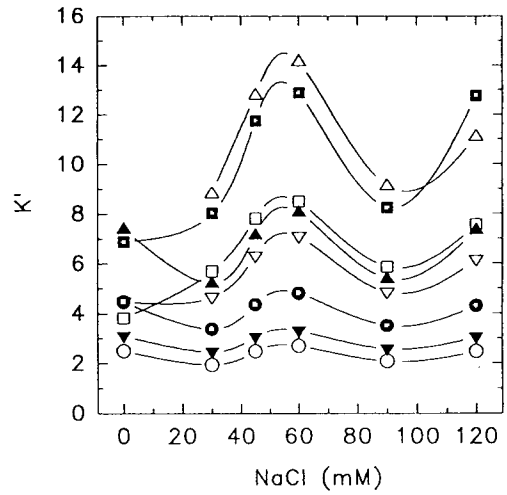

Fig. 2. Effect of ionic strength on capacity factors (k') of triazines. ○ = Cyanazine; ▼ = simazine; ● = atrazine; ▽ = propazine; □ = ametryne; ▲ = terbutylazine; ■ = prometryne; △ = terbutryne. Chromatographic conditions: mobile phase, acetonitrile–buffer (60:40, v/v) containing NaCl as shown (buffer composition: 1.0 m*M* H_3PO_4 and NaOH up to pH 4.50); flow-rate, 0.7 ml/min; samples 100 μl; each species 6.0 mg/l.

triazines as a function of ionic strength. Sodium chloride was chosen as an ionic strength modifier taking into account its low absorbance at the detection wavelength. The complex chromatographic trends that the triazines show, are due to the different effects of ionic strength on the various species. The capacity factors of the more polar S-triazines (ametryne, prometryne and terbutryne) are affected by both a stronger ion-exchange competition and liquid–liquid partition equilibria. The two effects, concomitant to the ionic strength improvements, are opposite and tend to give lower and higher k' values, respectively. The retention of Cl-triazines is less influenced by ionic strength than S-triazines and shows, for low ionic strength values, opposite behaviour with respect to the S-triazines. The optimized eluent composition allows, without preconcentration, detection limits below 80 μg/l to be achieved (Table 1) with UV detection (220 nm). The values were decreased (1000-fold) to the ng/l level after the optimization of the clean-up and preconcentration procedure (see below). The linear calibration ranges for the triazines

Table 1
Detection limits and linear ranges ($r > 0.995$), without preconcentration, for triazines

Analyte	Detection limit (μg/l)	Linear range (mg/l)
Cyanazine	10	0.5–10
Simazine	20	0.5–6
Atrazine	20	0.5–10
Propazine	30	0.3–6
Terbutylazine	20	0.5–6
Ametryne	20	0.5–10
Prometryne	30	1–10
Terbutryne	80	1–10

studied are summarized in Table 1. Fig. 3 shows a typical chromatogram for all the investigated triazines, obtained with the stated eluent composition.

3.2. On-line preconcentration with single trap

For lowering the detection limits of triazines through an enrichment step prior to the chromatographic separation, an on-line preconcentration procedure was developed. For this purpose the 100-μl injection loop was replaced with a microcolumn and the enrichment efficiency was evaluated for different stationary phases. The efficiency represents the ability of the column to retain and to release quantitatively the analytes in both the loading and release steps. Moreover, the microcolumn should allow adequate matrix removal. The preconcentration recovery for the eight triazines was evaluated by comparing the peak areas obtained by direct injection (100-μl loop) of samples (2.0 mg/l for Cl-triazines and 5.0 mg/l for S-triazines) with those obtained by loading the preconcentration column (100.0-ml mixtures, 2.0 μg/l for Cl-triazines and 5.0 μg/l for S-triazines).

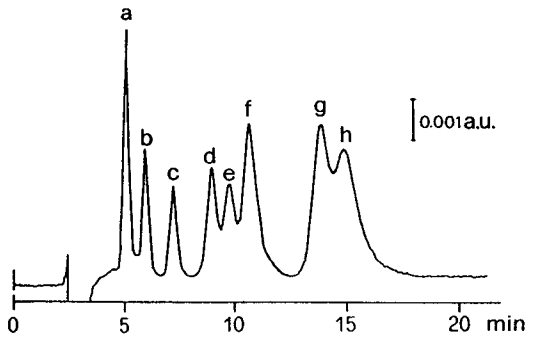

Fig. 3. Chromatogram of (a) cyanazine (100 μg/l), (b) simazine (100 μg/l), (c) atrazine (100 μg/l), (d) propazine (200 μg/l), (e) terbutylazine (100 μg/l), (f) ametryne (100 μg/l), (g) prometryne (200 μg/l) and (h) terbutryne (400 μg/l). Chromatographic conditions: mobile phase, acetonitrile–buffer (70:30, v/v) (buffer composition: 1.0 m*M* H_3PO_4 and NaOH up to pH 4.50, containing 30 m*M* NaCl); flow-rate, 0.7 ml/min; sample, 100 μl.

Several stationary phases and packings (listed under Experimental) were tested. Only Omnipac PCX 500 and Supelclean Envi-18 gave satisfactory results (see Table 2).

As the analytes show both a hydrophobic and an ionic retention mechanism, a multi-mode pellicular cation-exchange PCX guard column was used for preconcentration. The column packing is the same as in the separation column. It requires a low flow-rate in sample loading (2.0 ml/min) because of its high back-pressure due to the polymeric resin. Recoveries ranged between 25 and 86% and sub-μg/l detection limits (Table 2) were obtained. Acidified samples (pH 1.0) were also processed to enhance the ion-exchange contribution to the retention of cationic species but under these conditions hydrogen ion competition did not allow the yields to be improved.

Table 2
Recoveries and detection limits for triazines (three replicates)

Analyte	Recovery (%)		Detection limit (μg/l)	
	a	b	a	b
Cyanazine	30	93 ± 5	0.3	0.04
Simazine	56	97 ± 3	0.3	0.03
Atrazine	83	98 ± 1	0.4	0.04
Propazine	86	96 ± 2	0.8	0.08
Terbutylazine	25	99 ± 3	0.8	0.08
Ametryne	38	102 ± 7	1	0.07
Prometryne	80	104 ± 4	1	0.07
Terbutryne	34	104 ± 5	2	0.07

On-line preconcentration with (a) OmniPac PCX 500 Guard and (b) Supelclean Envi-18; samples, 100.0 ml.

The silica-based preconcentration columns may be used with a high sample flow-rate in the loading step and with a high back-pressure during elution. Therefore, in order to reduce the loading duration, a 4.0 ml/min loading flow-rate was maintained for such microcolumns without too high a back-pressure. Among the silica-based packings, only LiChrospher 100 RP-18 and Supelclean Envi-18 gave significant recoveries. LiChrospher 100 RP-18 gave a low recovery (10%) for all the analytes and this value did not change significantly on varying the sample pH. Supelclean Envi-18 gave quantitative recoveries for S-triazines and 93–99% for Cl-triazines (Table 2). The detection limits were 30–80 μg/l (signal-to-noise ratio = 3). The two hydrophobic silica materials differ with Supelclean Envi-18 having a higher surface area, and this explains the higher recoveries reached with this material.

Such an optimized on-line preconcentration method with a single trap was applied to a real sample (Turin tap water). A 100.0-ml sample was analysed but matrix interferences were too high at the maximum absorption wavelength of triazines (220 nm). The second absorbance maximum of triazines at 263 nm, which is characterized by lower intensity, was selected for detection, being free from interferences. Nevertheless, higher detection limits were obtained and all the triazines were detected at sub-μg/l levels. Fig. 4 shows the chromatogram obtained for a tap water sample analysed without or with addition of spikes (simazine, ametryne and terbutryne, 500 ng/l each).

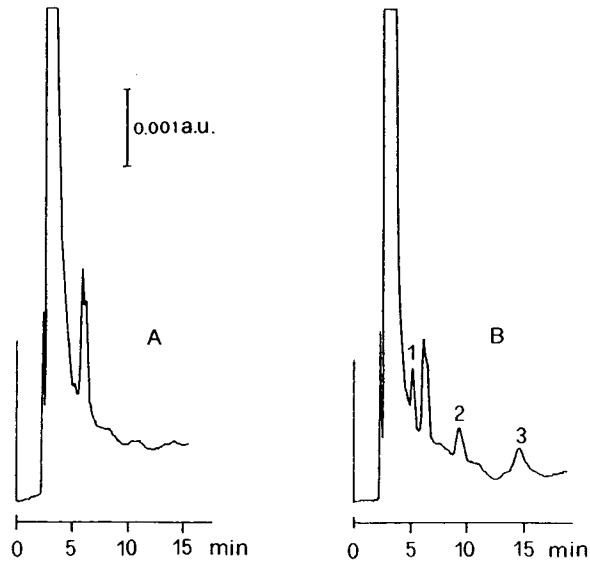

Fig. 4. Analysis of tap water with single-trap preconcentration and IC separation. (A) 100.0-ml samples as such and (B) spiked with (1) cyanazine, (2) propazine and (3) prometryne, 500 ng/l of each species. Chromatographic conditions: mobile phase, acetonitrile–buffer (70:30, v/v) (buffer composition: 1.0 m*M* H_3PO_4 and NaOH up to pH 4.50, containing 30 m*M* NaCl); eluent flow-rate, 0.7 ml/min; sample loading flow-rate, 4.0 ml/min; detection at 263 nm.

3.3. *On-line preconcentration with double trap*

In order to achieve good detection limits also in the presence of interferents usually found in natural waters, *e.g.*, river waters, a double-trap preconcentration system was developed. The system (Fig. 5) utilizes the previous column (Supelclean Envi-18) coupled with a LiChrospher 100 RP-18 microcolumn which is characterized by a high retention ability for lipophilic compounds and shows a very low (<10%) retention for triazines.

Other double-trap on-line enrichment procedures have been described [5,6]. Both methods use a combination of reversed-phase and ion-exchange traps, whereas in this work two reversed-phase adsorbents were used: the first retains all lipophilic compounds while the second is a specially treated reversed-phase material for trapping triazine derivatives.

Fig. 5 shows the loading and eluting procedures. When the two injection valves are in the load position (Fig. 5a) the sample passes through both columns. The LiChrospher 100 RP-18 microcolumn retains the organic liphophilic substances while allowing triazines to reach the second Supelclean Envi-18 microcolumn, where they are preconcentrated. The system is then rinsed with 10 ml of high-purity water, both Rheodyne values are switched to the injection position (Fig. 5b) and only the triazine analytes are injected towards the separation column by exclusion of the LiChrospher column. The latter

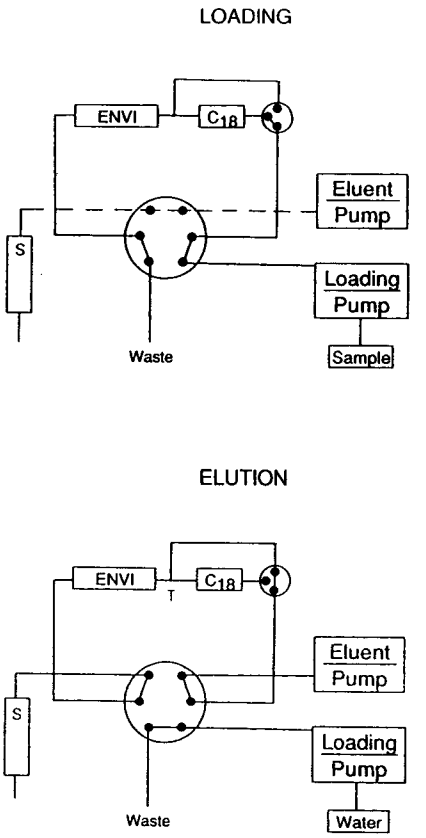

Fig. 5. Block diagram of the double-trap preconcentration apparatus in (a) the loading mode and (b) the elution mode.

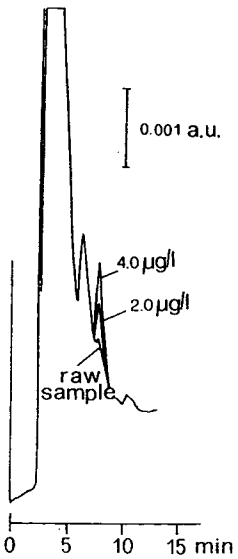

Fig. 6. Analysis of tap water with double-trap preconcentration and IC separation. 100.0-ml samples as such and spiked with atrazine (2.0 and 4.0 μg/l). Chromatographic conditions: mobile phase, acetonitrile–buffer (70:30, v/v) (buffer composition: 1.0 m*M* H_3PO_4 and NaOH up to pH 4.50, containing 30 m*M* NaCl); eluent flow-rate, 0.7 ml/min; sample loading flow-rate, 4.0 ml/min; detection at 263 nm.

microcolumn is cleaned by passing the eluent for 2 min before the next analysis.

The on-line double-trap system was applied to river water analysis (Po river, Turin). Fig. 6 shows the chromatogram obtained by loading 100.0-ml samples injected as such or after addition of spikes (2.0 and 4.0 μg/l of atrazine). Samples were filtered (0.45 μm) before the analysis.

4. Conclusions

The developed IC procedure is suitable for triazine detection and determination at levels down to 10 μg/l. By coupling on-line clean-up and preconcentration procedures the method permits the trace analysis of river water samples, also at a less sensitive wavelength for UV detection, as removal of spectral interferences from sample impurities can be achieved with the treatment. However, it should be noted that the occurrence of "matrix" peaks in real samples with a heavy matrix could affect the detection limits reported in Table 1. The use of gradient elution might improve the chromatographic resolution of the present procedure (shown in Fig. 3), especially for those samples with the concomitant presence of all triazines.

5. Acknowledgements

Financial support from the Ministero dell'Università e della Ricerca Scientifica e Tecnologica (MURST, Rome) and from the Italian National Research Council (CNR, Rome) is gratefully acknowledged.

6. References

[1] I. Liška, J. Krupcik and P.A. Leclercq, *J. High Resolut. Chromatogr.*, 12 (1989) 577.
[2] J. Sherma, *Anal. Chem.*, 59 (1987) 18.
[3] J.C. Moltó, Y. Picó, G. Font and J. Mañes, *J. Chromatogr.*, 555 (1991) 137.
[4] M. Battista, A. Di Corcia and M. Marchetti, *Anal. Chem.*, 61 (1989) 935.
[5] V. Coquart and M.C. Hennion, *J. Chromatogr.*, 585 (1991) 67.
[6] E.R. Brouwer, I. Liska, R.B. Geerdink, P.C.M. Frintrop, W.H. Mulder, H. Lingeman and U.A. Th. Brinkman, *Chromatographia*, 32 (1991) 445.
[7] H. Bagheri, J.J. Vreuls, R.T. Ghijsen and U.A. Th. Brinkman, *Chromatographia*, 34 (1992) 5.
[8] D. Barceló, *Chromatographia*, 25 (1988) 928.
[9] D.S. Owens and P.E. Sturrock, *Anal. Chim. Acta*, 188 (1986) 269.
[10] W.J. Günther and A. Kettrup, *Chromatographia*, 28 (1989) 209.
[11] G. Durand and D. Barcelò, *J. Chromatogr.*, 502 (1990) 275.
[12] W. Schüssler, *Chromatographia*, 27 (1989) 431.
[13] G. Karlaganis, R. Von Arx, H.U. Ammon and R. Camenzind, *J. Chromatogr.*, 549 (1991) 229.
[14] D. Barceló, *Org. Mass Spectrom.*, 24 (1989) 898.
[15] G. Sacchero, S. Apone, C. Sarzanini and E. Mentasti, *J. Chromatogr. A*, 668 (1994) 365.

ELSEVIER

Journal of Chromatography A, 671 (1994) 159–163

JOURNAL OF CHROMATOGRAPHY A

Elimination of matrix interferences in ion chromatography by the use of solid-phase extraction disks

Raaidah Saari-Nordhaus*, Lakshmy M. Nair, James M. Anderson, Jr.

Alltech Associates, Inc., 2051 Waukegan Road, Deerfield, IL 60015, USA

Abstract

The use of solid-phase extraction disks as a sample clean-up device is described. The disks contain a membrane composed of resin beads permanently enmeshed in a polytetrafluoroethylene membrane, housed in a medical-grade polypropylene housing. The resin within the membrane is functionalized to retain specific types of components from the sample. Several chemistries are developed to remove various interfering components. The recovery of the ions after sample treatment is examined.

1. Introduction

Ion chromatography (IC) has become a popular analytical method for the determination of anions and cations. The method is simple, fast, and requires minimum sample preparation. For most samples, only dilution and filtration are required before injection. In certain cases where the sample contains components that can damage the column, are too acidic or too basic, or one or more components are present in great excess, a more sophisticated technique is usually necessary to eliminate matrix interferences.

Solid-phase extraction (SPE) is one of the most common techniques for eliminating matrix interferences in chromatography [1]. It is easy to use, requires small sample volume, and a wide variety of stationary phases are available commercially in convenient disposable cartridges. In previous work, we discussed the use of SPE cartridges for eliminating matrix interferences in IC [2,3]. These cartridges are packed with IC-grade resin functionalized to retain or neutralize certain components in the sample matrix. Matrix inteferences such as acidic or basic solutions, high level of halides, or sulfates, or hydrophobic components are successfully eliminated using these cartridges. Two major drawbacks of the packed bed SPE cartridges are bed channeling and higher back pressure. Bed channeling results in non-uniform flow, reducing the full capacity of the cartridge. The narrow internal diameter of the cartridge sometimes causes high back pressure, complicating the sample clean-up process.

This paper examines the use of SPE disks as a sample clean-up device for ion chromatography. The disks contain a membrane composed of resin beads permanently enmeshed in a polytetrafluoroethylene (PTFE) membrane, housed in a medical grade polypropylene housing. The resin within the membrane is functionalized to retain specific types of components from the sample. Several chemistries are developed to remove various interfering components. The

* Corresponding author.

0021-9673/94/$07.00
SSDI 0021-9673(93)E1227-Q

recovery of the ions after sample treatment is examined.

2. Experimental

2.1. Instrumentation

Chromatography was performed on an Alltech (Deerfield, IL, USA) IC system that consists of a Model 325 high-performance liquid chromatography (HPLC) pump, a Model 330 column heater, a 335 suppressor module, and a Model 350 conductivity detector. Sample introduction was done with a Model 9125 Rheodyne (Cotati, CA, USA) injector. All data were recorded on a Spectra-Physics (Santa Clara, CA, USA) SP 4400 Chromjet integrator. The Alltech Universal Anion column (150 mm × 4.6 mm) and the Alltech Universal Anion 300 columns (150 mm × 4.6 mm and 100 mm × 4.6 mm) were used to separate the anions.

Fig. 1 shows the construction of the SPE disk. The 25-mm membrane impregnated with ion-exchange media is housed in a medical-grade polypropylene housing. The inlet and outlet of the housing accepts a luer-hub syringe and needle, respectively. The ion-exchange capacity of the 25 mm disk is 1.5 mequiv. The membrane is rigid, eliminating the need for additional frits.

2.2. Reagents

Standards and eluent buffers were made from reagent-grade chemicals obtained from Aldrich Chemical (Milwaukee, WI, USA). Distilled deionized water was used throughout.

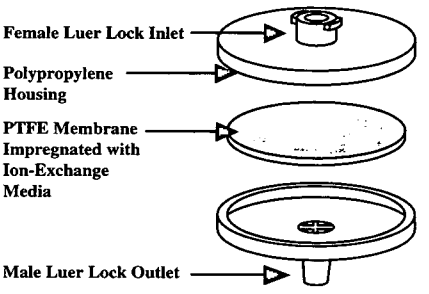

Fig. 1. The construction of the SPE disk.

2.3. Procedure

Before applying sample, the disk is pre-conditioned by passing 5–10 ml of IC-grade water through the device using a luer-hub syringe. The sample (approximately 3 ml) is then passed through the disk at a flow-rate of 1.0 ml/min or less. The first 1 ml of the eluate is discarded to avoid partial dilution of the analytes. The remaining eluate is collected for analysis. The amount of contaminants that need to be removed from the sample must not exceed the total capacity of the disk. More than one SPE disk can be used in series to increase its capacity.

3. Results and discussion

SPE disks are a new generation of solid-phase extraction device. They have been used widely for extracting environmental pollutants from aqueous matrices [4–6], and for the purification and separation of biological fluids [7]. This paper describes the first application of SPE disks for eliminating matrix interferences in ion chromatography.

The membrane disk used for the applications described here are composed of 60% cation-exchange resin and 40% PTFE. The resin is styrene–divinylbenzene with a sulfonic acid functional group. Three forms of SPE disks, cation exchange in the hydrogen, silver and barium form, are used for various applications. The ion exchange capacity for the 25-mm disk is 1.5 mequiv. Because of the styrene–divinylbenzene based resin, the membrane is stable from pH 1 to 14.

As sample is passed through the packing, specific chemical interactions take place which selectively retain certain components of the matrix while other components pass through unchanged. The chemical characteristics of the membrane determine which sample components are retained.

3.1. SPE disk in the H^+ form

The SPE disk in the H^+ form provides a reliable method to neutralize samples containing high concentration of hydroxide ions or to remove cations before anion analysis. The disk neutralizes hydroxide from the sample through an acid–base neutralization reaction:

$$\text{Disk-H}^+ + \text{M}^+\text{OH}^- \rightarrow \text{Disk-M}^+ + \text{H}_2\text{O}$$

where M^+ = cations. The cations from the sample exchanges with the hydrogen ion from the disk. The released hydrogen ion reacts with hydroxide to form water. Anions pass through the disk unchanged.

Fig. 2a and b show applications of the SPE disk in the H^+ form to neutralize hydroxide. The high hydroxide concentration in the process cleaning solution overloads the low-capacity column and masks the peaks of interest. It also causes a large system peak which requires almost 40 min to subside. After passing the sample through the disk, the hydroxide is neutralized to water and the fluoride, chloride, and sulfate can be quantitated easily. In Fig. 2b, a suppressor-based IC system was is used. The high hydroxide concentration causes a large negative water dip, which interferes with the peaks of interest. After treatment with the IC-H^+ disk, the ions of interest are easily quantified.

SPE disk in the H^+-form may also be used to remove excess cations from samples. Fig. 3 shows an application of SPE disk in the H^+ form to remove an amine. The high amine concentration interferes with the early eluting chloride peak and causes a large system peak. After treatment with the disk, the chloride and sulfate is easily quantified. The size of the system peak is also reduced.

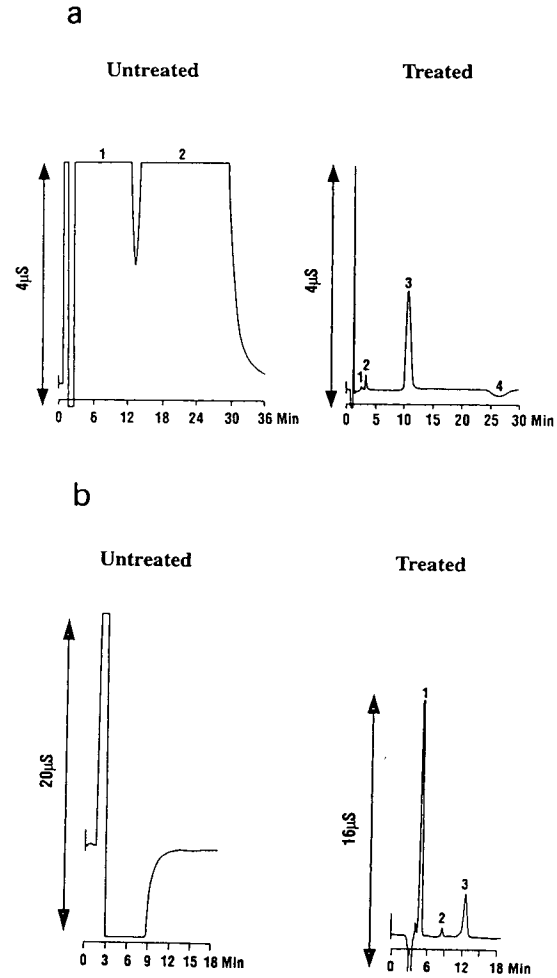

Fig. 2. (a) Process cleaning solution (ammonium hydroxide). Peaks: 1 = fluoride; 2 = chloride; 3 = sulfate; 4 = system peak. Column, Universal Anion (150 mm × 4.6 mm); eluent, 4 m*M* phthalic acid, pH 4.5 with LiOH; flow-rate, 1.0 ml/min; detector, conductivity; injection volume: 100 µl. (b) Battery electrolyte (potassium hydroxide). Peaks: 1 = chloride; 2 = nitrate; 3 = sulfate. Column, Universal Anion 300 (100 mm × 4.6 mm); eluent, 1.7 m*M* $NaHCO_3$–1.8 m*M* Na_2CO_3; flow-rate, 1.0 ml/min; detector, chemically suppressed conductivity; injection volume, 100 µl.

3.2. SPE disk in the Ag^+ form

The SPE disk in the Ag^+ form provides a reliable method to remove or reduce excess halides from the sample before analysis of other anions. The silver contained on the membrane functional group reacts with halides from the sample to form insoluble silver salts:

$$\text{Disk-Ag}^+ + \text{M}^+\text{X}^- \rightarrow \text{Disk-M}^+ + \text{AgX}$$

where X = Cl, Br, I. Anions that form insoluble or partially soluble silver salts such as chloride, bromide, iodide, and carbonate will be removed

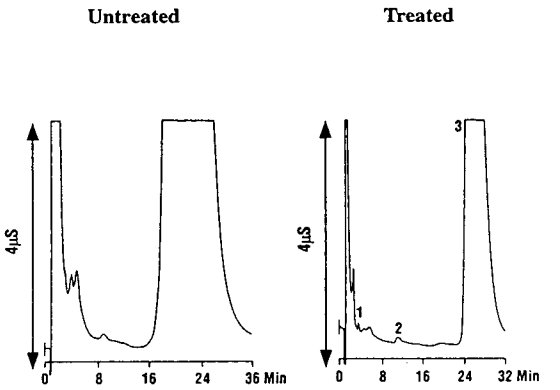

Fig. 3. Trace anions in technical grade hexamethylene tetramine. Peaks: 1 = chloride; 2 = sulfate; 3 = system peak. Column, Universal Anion (150 mm × 4.6 mm); eluent, 4 m*M* phthalic acid, pH 4.5 with LiOH; flow-rate, 1.0 ml/min; detector, conductivity; injection volume, 100 µl.

completely or partially from the sample. Other anions such as fluoride, nitrite, nitrate, phosphate, and sulfate will pass through unchanged.

Fig. 4 shows an application of the SPE disk in the Ag^+ form in removing axcess chloride. Chloride in the untreated sample masks the nitrate peak, making it impossible to quantitate. After the treatment, the nitrate and sulfate can be determined easily.

When carbonate–hydrogencarbonate eluent is used for the anion analysis using suppressor-based IC, the use of SPE devices in the Ag^+ form is not recommended. Since silver carbonate is sparingly soluble [8], the silver from the sample after the treatment process may form a precipitate in the analytical column. Since the amount of sample injected is very small, it will not block the column. However, when chloride or other halides are injected onto the column in subsequent analyses, the peak may dissappear or the sensitivity may decrease due to the formation of silver halides in the column. Excess silver in the analytical column can be removed by passing dilute nitric acid through the column. For applications that require the use of the SPE devices in the Ag^+ form, non-suppressed IC methods should be used. If a suppressor-based IC method must be used, eluants other than carbonate–hydrogencarbonate should be used.

3.3. SPE disk in the Ba^{2+} form

The SPE disk in the Ba^{2+} form is used to remove sulfate before analysis of other anions. The sulfate is removed from the sample through the formation of barium sulfate:

$$\text{Disk-Ba}^{2+} + \text{M}^{2+}\text{SO}_4^{2-} \rightarrow \text{Disk-M}^{2+} + \text{BaSO}_4$$

where M = cations. Since barium phosphate is sparingly soluble, this disk may also reduce phosphate concentration if it is present in high concentrations. The concentration of other an-

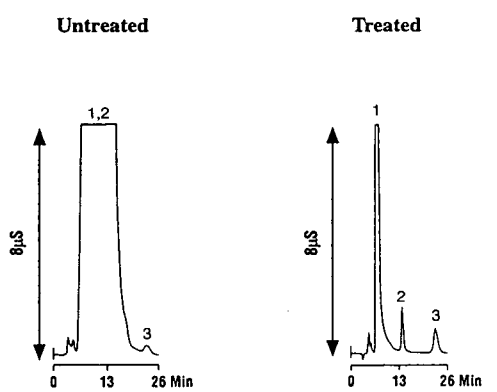

Fig. 4. Anions in HCl digest paper coating. Peaks: 1 = chloride; 2 = nitrate; 3 = sulfate. Column, Universal Anion 300 (150 mm × 4.6 mm); eluent, 1.7 m*M* $NaHCO_3$–1.8 m*M* Na_2CO_3; flow-rate, 1.0 ml/min; detector, chemically suppressed conductivity; injection volume, 100 µl.

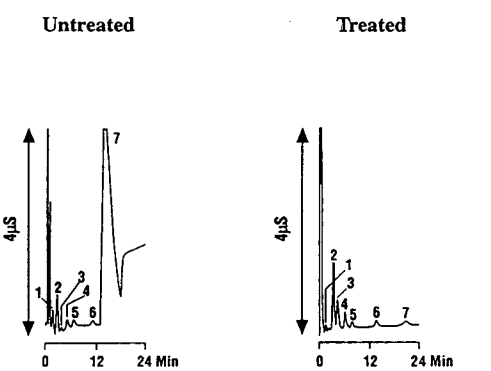

Fig. 5. Anions in battery acid. Peaks: 1 = fluoride; 2 = chloride; 3 = nitrite; 4 = bromide; 5 = nitrate; 6 = phosphate; 7 = sulfate. Column, Universal Anion (150 mm × 4.6 mm); eluent, 5 m*M* *p*-hydroxybenzoic acid, pH 7.9 with LiOH; flow-rate, 1.0 ml/min; detector, conductivity; injection volume, 100 µl.

Table 1
Recovery of anions with SPE disks

Anions (mg/l)	Average recovery (%) ($n = 3$)	R.S.D. (%)
SPE disk in the H^+ form		
Fluoride (10)	97	0.52
Chloride (20)	98	1.03
Nitrite (20)	40	3.78
Bromide (20)	102	0.91
Nitrate (20)	104	1.34
Phosphate (30)	86	1.21
Sulfate (30)	99	0.64
SPE disk in the Ag^+ form		
Fluoride (5)	106	0.83
Chloride (500)	–	–
Nitrite (10)	97	1.32
Bromide (10)	–	–
Nitrate (10)	105	0.35
Phosphate (15)	93	1.41
Sulfate (15)	110	1.56
SPE disk in the Ba^{2+} form		
Fluoride (10)	95	1.11
Chloride (20)	101	0.25
Nitrite (20)	92	1.15
Bromide (20)	95	0.89
Nitrate (20)	95	0.75
Phosphate (30)	104	1.72
Sulfate (30)	–	–

ions such as fluoride, chloride, nitrite, bromide, and nitrate will not be affected. Fig. 5 shows an application of the SPE disk in the Ba^{2+} form for removing excess sulfate before the analysis of trace anions in battery acid. The battery acid was diluted 50 times before passing through the disk. Sulfate in the untreated sample produces baseline disruption and reduces the retention time of other anions.

3.4. Recovery of anions with SPE disks

Table 1 shows the recovery data of the SPE disks. The data were obtained by comparing standard solutions analyzed before and after treatment with the SPE disks. With the exception of nitrite (with the SPE disk in the H^+ form), the recoveries of other anions are reasonably good. The poor recovery of nitrite with all sample pretreatment devices is well known [3,9]. In the presence of hydrogen ion, nitrite forms nitrous acid, which in water will quickly convert to nitric oxide (gas) and nitric acid (nitrate). As presented in Table 1, the recovery of nitrate is higher than 100%, due to the oxidation of nitrite.

The recovery data obtained using the SPE disks are comparable to the data obtained using the packed bed SPE cartridges studied earlier [3]. No recovery advantage is observed with the SPE disk. However, the highly uniform packing of the SPE disks eliminate bed channeling often encountered with packed bed SPE devices. Because of the thinner and wider bed, the back pressure is lower, making it easier to push the sample through the disks. Several samples may be processed simultaneously using a vacuum manifold.

4. Conclusions

SPE disks provide a reliable method for eliminating matrix interferences in ion chromatography. Matrix interferences such as basic solutions and high level of halides and sulfate are successfully eliminated using these SPE disks. With the exception of nitrite, the recovery of all anions are reasonable good.

5. References

[1] J. Horack and R.E. Majors, *LC·GC*, 11 (1993) 74.
[2] R. Saari-Nordhaus, J.M. Anderson, Jr. and I.K. Henderson, *Am. Lab.*, August (1990) 18.
[3] I.K. Henderson, R. Saari-Nordhaus and J.M. Anderson, Jr., *J. Chromatogr.*, 546 (1991) 61.
[4] D.F. Hagen, C.G. Markell, G.A. Schmitt and D.D. Blevins, *Anal. Chim. Acta*, 236 (1990) 157.
[5] C.G. Markell, D.F. Hagen and V.A. Bunnell, *LC·GC*, 9 (1991) 332.
[6] T. McDonnel, J. Rosenfeld and A. Rais-Firouz, *J. Chromatogr.*, 629 (1993) 41.
[7] G.M. Hearn and D.O. Hall, *Am. Lab.*, January (1993) 28H.
[8] R.C. Weast and M.J. Astle (Editors), *CRC Handbook of Chemistry and Physics*, CRC Press, Boca Raton, FL, 1980, pp. B81–B144.
[9] P.R. Haddad, S. Laksana and R.G. Simons, *J. Chromatogr.*, 640 (1993) 135.

ELSEVIER

Journal of Chromatography A, 671 (1994) 165–171

JOURNAL OF CHROMATOGRAPHY A

Trace level determination of bromate in ozonated drinking water using ion chromatography

Robert J. Joyce*, Harpreet S. Dhillon

Dionex Corporation, 1228 Titan Way, Sunnyvale, CA 94088, USA

Abstract

Bromate is one of the disinfection by-products produced by the ozonation of drinking water. The US Environmental Protection Agency is considering regulating bromate to the low μg/l level. A method using ion chromatography has been developed which will quantify bromate at this level, even in the presence of high (mg/l) levels of common anions such as chloride and sulfate. A borate eluent system was used to improve the separation of bromate from chloride. The level of chloride in the sample was reduced by pretreating the sample using a silver-form cation-exchange resin. The lower chloride level allowed a larger sample volume and preconcentration which reduced the bromate method detection limit to 1 μg/l.

1. Introduction

During the 1970s it was discovered that the chlorination of drinking water produced carcinogens, such as the trihalomethanes. Since then, environmental regulatory agencies, as well as drinking water treatment technologists worldwide, have been aggressively researching alternative disinfection methods which minimize the production of by-products of significant health risk. Ozonation has emerged as one of the most promising alternatives to chlorination. However, ozonation does tend to oxidize bromide, which is present naturally in source waters, to bromate. The following equations show the pathway by which bromide (Br^-) is oxidized by ozone to bromate (BrO_3^-) through the intermediate formation of hypobromite (OBr^-). These equations also show that ozone does not oxidize hypobromous acid (HOBr) to bromate. Since increased acid (H_3O^+) will favor the formation of hypobromous acid, this suggests that ozonation at a low pH will tend to minimize bromate formation. (Fig. 1)

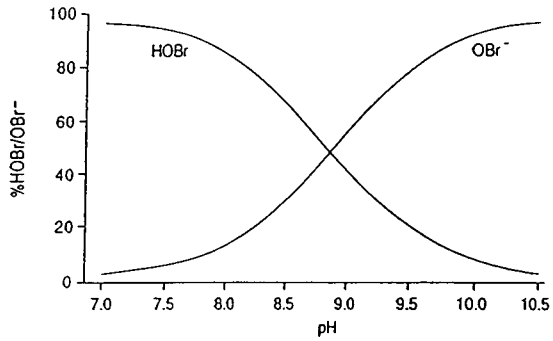

Fig. 1. Hypobromous acid equilibria in aqueous solution. Ozonating at pH 7 or lower minimizes the production of hypobromite, which in turn minimizes the formation of bromate. $pK_a = 8.8$ at 20°C.

* Corresponding author.

0021-9673/94/$07.00
SSDI 0021-9673(94)00171-5

Table 1
Bromate health risk

Risk level[a]	Trichloroethylene (μg/l)	Carbon tetrachloride (μg/l)	Bromate (μg/l)
10^{-4}	260	27	5
10^{-5}	26	2.7	0.5
10^{-6}	2.6	0.27	0.05

[a] Probable increase in deaths due to a cancer $10^{-5} = 1$ in 100 000 people.

$$Br^- + O_3 + H_2O \rightarrow HOBr + O_2 + OH^-$$

$$HOBr + H_2O \rightarrow H_3O^+ + OBr^-$$

$$OBr^- + 2O_3 \rightarrow BrO_3^- + 2O_2$$

$$HOBr + O_3 \rightarrow \text{No reaction}$$

The final concentration of bromate is dependent on the amount of bromide in the source water and applied ozone. Bromate has been judged by both the US Environmental Protection Agency (EPA) and the World Health Organization as a potential carcinogen, even at the low μg/l level. Table 1 shows a comparison of health risk levels for bromate and selected chlorinated organics which are currently regulated in drinking water. Many regulatory agencies, world-wide, prefer to regulate potential carcinogens to the 10^{-5} health risk level or lower. Current EPA plans are to regulate bromate in ozonated water to < 10 μg/l while further health risk studies are underway. Accordingly analytical methods must be found to quantify bromate at these levels, so as to aid in researching ozonation process design options to minimize this contaminant.

Currently, the separation of bromate in a drinking water matrix is accomplished by using direct-injection ion chromatography (IC) with conductivity detection. The detection limit for bromate using this methodology is 7.3 μg/l [2]. Table 2 shows the method detection limits (MDLs) that were achieved by EPA researchers when using a 200-μl injected sample on a Dionex IonPac AS9-SC column using a borate-based eluent. Injecting a larger sample erodes chromatographic efficiency and does not significantly improve MDLs. The drawback to this method is that the amount of bromate present in a typical ozonated water sample is near or below the current detection limit. This paper reports the development of a modified IC method which significantly improves the MDLs for bromate.

Table 2
Method detection limits using the AS9 column

Anion	Spiking concentration (μg/l)	Statistical MDL[a] (μg/l)	Noise MDL[b] (μg/l)	Conservative MDL (μg/l)
ClO_2^-	10.0	3.39	2.94	3.4
ClO_3^-	25.0	5.18	9.44	9.4
BrO_3^-	10.0	7.31	5.92	7.3
Br^-	10.0	3.92	8.34	8.3

Conditions: 9 m*M* NaOH–36 m*M* boric acid, 1 ml/min, 200-μl injection.
[a] Method detection limit, MDL = (S.D.)·(t_s) 99.5%, where $t_s = 3.71$ for a single sided Student's *t*-test distribution at a 99.5% confidence.
[b] MDL = 3 × noise.

2. Experimental

2.1. Chromatographic system

All chromatography was performed using a Dionex (Sunnyvale, CA, USA) DX-300 chromatograph equipped with an advanced gradient pump (AGP), a liquid chromatography module (LCM-3) and a conductivity detector (CDM-3). A Dionex automated sampler module (ASM) was utilized for sample loading. An additional inert double stack four-way slider valve was placed between the rotary injection valve and the analytical column. The rotary valve and the four-way slider valve were controlled by the AGP. A Dionex DQP single-piston pump was used to flush the sample from the sample loop onto the concentrator column. Eluents were vacuum degassed while sonicating for 15 min.

Four types of columns were used in the system. An IonPac AS9-SC was used for analyte separation. An IonPac AG9-SC and an IonPac AG10 served as concentrator columns. An IonPac AG9-SC column was utilized as a guard column. An IonPac MetPac CC-1 column was used as a metal scrubber column. Conductivity detection was carried out in the external water mode using an Anion Self Regenerating Suppressor. A chromatographic data system (AI-450; Dionex) was used for instrument control and for data collection and processing.

2.2. Chemicals

Boric acid, >99%, from Aldrich (Milwaukee, WI, USA), sodium hydroxide, 50% (w/w) from Fisher Scientific (Pittsburgh, PA, USA) and 17.8 MΩ cm deionized water were used for eluent preparation. Anion standards (1000 mg/l) were prepared from the corresponding sodium salts from Fisher Scientific. Dilute working standard solutions are prepared daily from 1000 mg/l stock standard solutions. All standard solutions were stored in polyethylene containers.

2.3. Sample pretreatment

With high levels of chloride in the sample matrix the exchange sites on the AG9/AS9-SC columns are overloaded and bromate cannot be detected as a separate peak. Chloride is removed by passing the sample through the Dionex OnGuard Ag cartridge. The cartridge packing is a silver-form high-capacity, strong-acid, cation-exchange resin, which is designed to remove chloride from the sample matrices. The cartridge capacity is 1.8–2.0 mequiv. per cartridge. Fig. 2A illustrates that, when attempting to determine bromate at the 10 μg/l level in the presence of a high chloride level (*i.e.* 64 mg/l), the resolution is not sufficient to separate bromate from chloride. Fig. 2B shows that by treating the sample with the OnGuard Ag cartridge the chloride level is reduced to approximately 0.4 mg/l which is sufficient to resolve bromate from chloride.

The lower chloride level allows a larger sample volume to be concentrated which improves the bromate response. A drawback for using the OnGuard Ag cartridges is the leaching of silver from the cartridge into the sample matrix. The accumulation of silver on the analytical and concentrator columns over time will affect column efficiency. To avoid this potential problem,

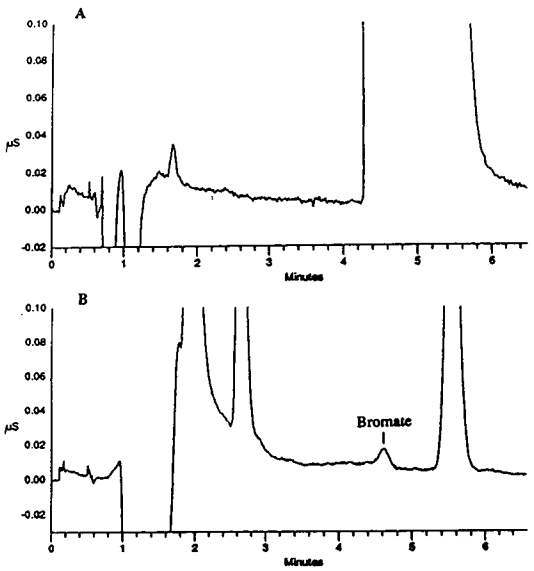

Fig. 2. Bromate determination. Direct injection (sample volume 200 μl) on a AS9-SC column, using borate eluent. (A) Sample not treated with OnGuard Ag; (B) OnGuard Ag-treated sample.

a Dionex MetPac CC-1 column is installed between the rotary injection valve and the four-way slider valve. The MetPac CC-1 column not only removes the silver but also removes any other cations which may foul the analytical column.

2.4. System operation

The chromatographic conditions are listed in Table 3. The determination of bromate utilizing this method is a three-step process as illustrated in Fig. 3: (1) loading the sample loop, (2) washing the sample onto the concentrator, (3) separating the anions of interest on the analytical column. Fig. 3A illustrates the sample being loaded into the sample loop using the auto-sampler. During this time, the AGP pumps eluent 1 to the AS9-SC column. After the loop is filled, the DQP is turned ON and it washes the sample from the sample loop onto the concentrator column using deionized water (Fig. 3B). The sample loop is rinsed two and one-half times its volume to ensure that all of the sample is transferred onto the concentrator. The concentrator column strongly retains anionic species such as bromate, chloride and sulfate. Fig. 3C shows the concentrator column being switched in line with the IonPac AS9-SC, at this point the retained anions are eluted to the analytical column. After the chloride elution the remaining anions are purged off the analytical column using eluent 2.

3. Results and discussion

3.1. Concentrator columns

The performance of concentrator columns is limited by column capacity and ion-exchange competition. The column resin can trap only a certain quantity of analyte. Once the column capacity is exceeded, the trapping will not be quantitative. The processes become more complicated when concentrating ions having widely different affinities for the resin. In this case an anion such as sulfate, which has a high affinity for the resin and which is present in much higher concentration, can act as an eluent, causing displacement of bromate.

Two concentrator columns were employed for this study, an IonPac AG9-SC and an IonPac AG10 column. The AG9-SC is a low-capacity anion-exchange column which exhibits the lower recovery for 1 μg/l bromate in the presence of other ions that are of much higher concentration. Table 4 shows a decrease in recovery for bromate as the sulfate concentration increases. The AG10 is a moderate-capacity column, and it can tolerate twice (15 *vs.* 30 μg/l) the sulfate concentration compared to the AG9-SC column. Fig. 4 illustrates the results of the IC analysis of bromate after preconcentrating 5 ml of an On-Guard-treated test sample containing 30 mg/l sulfate. The AG10 concentrator column retained a high percentage (*ca.* 90–100%) of the bromate,

Table 3
Chromatographic conditions

Guard column	AG9-SC
Analytical column	AS9-SC
Concentrator column	AG9-SC or AG10
Metal trap column	MetPac CC-1
Eluents	Eluent 1: 40 m*M* boric acid–20 m*M* NaOH, eluent 2: 250 m*M* boric acid–100 m*M* NaOH
Eluent flow-rate	2.0 ml/min
Rinsing reagent	Deionized water
Rinsing flow-rate	2.0 ml/min
Sample volume	5.0 ml
Detection	Suppressed conductivity, auto suppression, external water mode

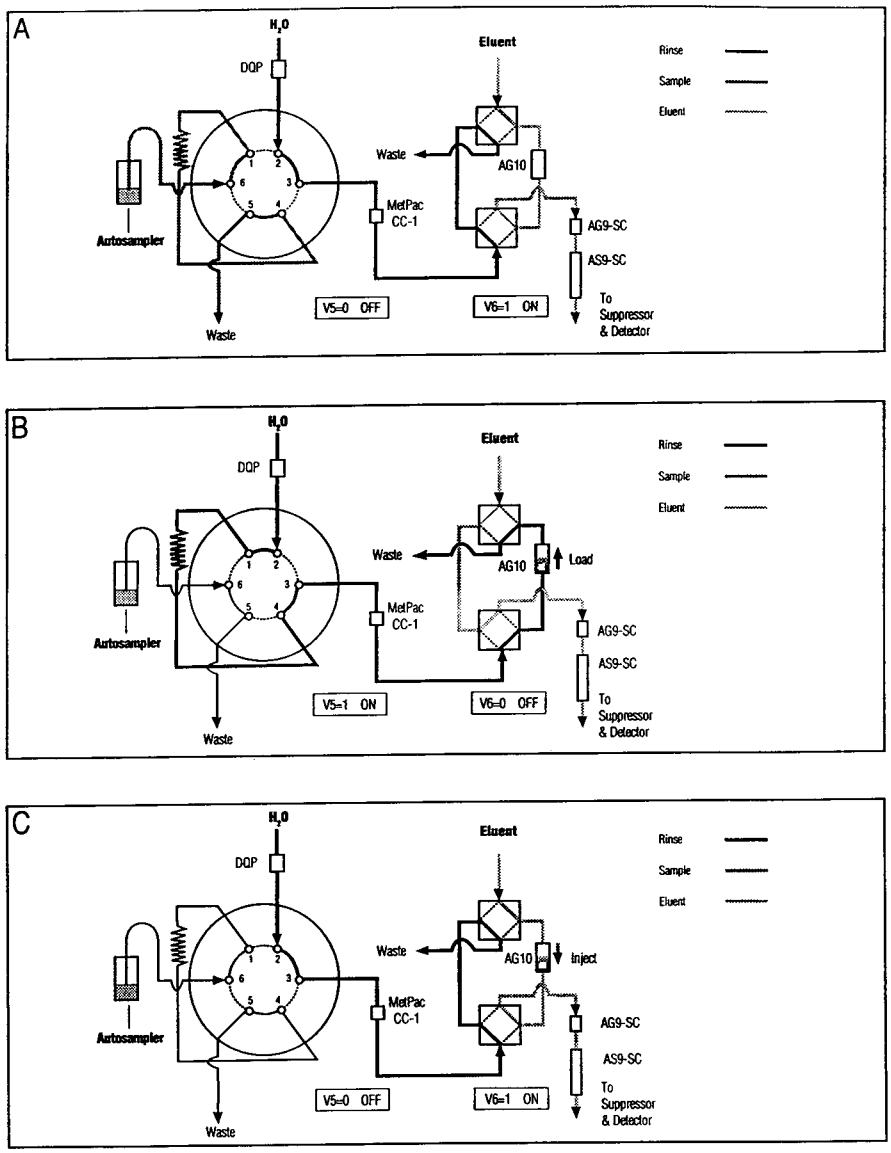

Fig. 3. Preconcentration suppressed IC system configuration. (A) Loading sample loop; (B) sample washed onto concentrator column; (C) retained anions eluted to AS9-SC analytical column.

while the bromate was eluted from the AG9-SC column by the sulfate.

Since the EPA plans to regulate bromate in ozonated water to <10 μg/l, 3–5 ml sample volume must be concentrated. Analyte anions such as bromate, chloride and sulfate are retained on the concentrator column as the sample loop is rinsed with deionized water. The anions are then eluted from the concentrator column and separated on the AS9-SC analytical column. Later-eluting anions such as sulfate are purged from the analytical column using 250 m*M* boric acid–100 m*M* sodium hydroxide eluent. After purging for 5 min, the AS9-SC column is equili-

Table 4
Effect of sulfate on recovery (%) of 1 μg/l bromate

Sulfate (mg/l)	Recovery (%)	
	AG9-SC (7 μequiv./column)	AG10 (34 μequiv./column)
5	98.5	99.7
10	96.2	99.3
15	94.5	99.3
20	0	98.7
25	0	96.5
30	0	92.3
35	0	0

Sample volume: 5 ml; test matrix: fluoride 2 mg/l, bromate 0.001 mg/l, chloride 64 mg/l (reduced to *ca.* 0.4 mg/l using OnGuard Ag), nitrate 20 mg/l, sulfate as listed.

brated with the chromatography eluent for 7–10 min. The equilibration time is placed at the beginning of the analysis as the sample loop is being filled and the sample is flushed onto the concentrator column. The total analysis time for this method is 25 min. Table 5 shows the bromate MDLs that have been achieved when preconcentrating a raw water sample both before and after ozonation. Using this method, a bromate MDL of 1 μg/l or less can be achieved.

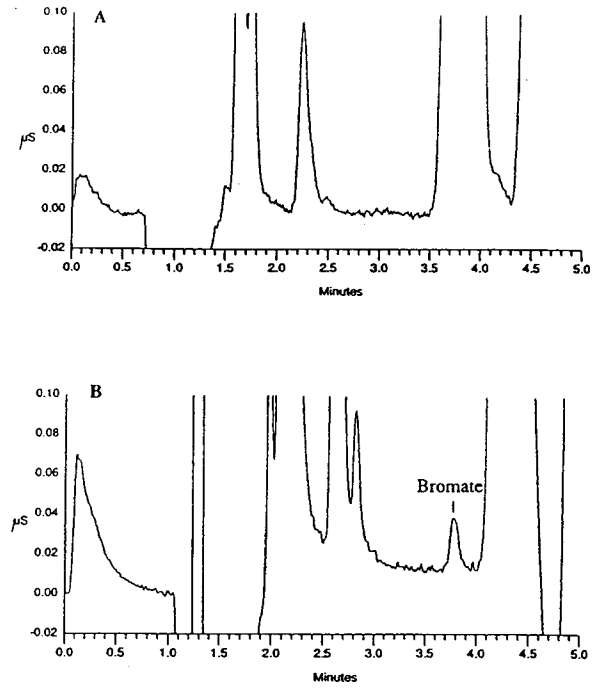

Fig. 4. Evaluation of concentrator columns for bromate analysis by preconcentrating 5 ml of sample. Sample concentration: bromate (0.001 mg/l); chloride [64 mg/l (reduced to *ca.* 0.4 mg/l using OnGuard Ag)]; bromide (2 mg/l); nitrate (20 mg/l); phosphate (10 mg/l); sulfate (30 mg/l). (A) AG9-SC column bromate shows no recovery of 1 μg/l bromate; (B) AG10 column shows 92.3% recovery.

Table 5
Determination of bromate in drinking water, 5 ml, preconcentrated

Sample	Bromate present (μg/l)	Bromate added (μg/l)	Bromate found (μg/l)[a]	*n*	S.D. (μg/l)	MDL (μg/l)[b]
Raw water	ND[c]	1	1.05	7	0.09	0.27
	ND	5	5.1	6	0.29	0.91
	ND	10	10.0	7	0.58	1.74
Raw water (ozonated)	1.1	0	1.1	7	0.04	0.12
	1.1	1	1.2	7	0.11	0.33
	1.1	5	4.7	7	0.70	2.10
	1.1	10	10.0	5	1.52	5.11

[a] Reference to 10 μg/l fortification of matrix.
[b] Method detection limit, MDL = (S.D.) · (t_s) 99.5%, where t_s = 3.71 for a single sided Student's *t*-test distribution at a 99.5% confidence.
[c] ND = Not detected (< 0.1 μg/l).

Table 6
Method detection limits for bromate analysis of ozonated drinking water using chemically suppressed IC

Sample volume injected	Inject mode	MDL (μg/l)
200 μl	Direct	5
5 ml	Preconcentrated	1

4. Conclusions

An improved method for the determination of trace level bromate has been developed. As summarized in Table 6 low-level, bromate MDLs can be achieved on the AS9-SC column using a borate eluent and chemically suppressed conductivity detection. Reduction of the chloride concentration in the sample matrix combined with preconcentration are the major modifications to the existing method.

5. Acknowledgements

The authors are grateful to Dr. Howard Weinberg, University of North Carolina and James N. Scott, Santa Clara Valley Water District for providing ozonated water samples. They would also like to thank Edward Kaiser, Dionex Corporation, for his assistance in preparing this manuscript.

6. References

[1] W.R. Haag and J. Hoigne, *Environ. Sci. Technol.*, 17 (1983) 261.
[2] D.P. Hautman and M. Bolyard, *J. Chromatogr.*, 602 (1992) 65.

ELSEVIER

Journal of Chromatography A, 671 (1994) 173–179

JOURNAL OF CHROMATOGRAPHY A

Determination of lanthanides in Kola nitrophosphate solution by cation-exchange ion chromatography

Abdulla W. Al-Shawi*, Roger Dahl

Norsk Hydro a.s, Research Centre, N-3901 Porsgrunn, Norway

Abstract

Lanthanides and yttrium are present in Kola phosphate rock. Digestion of this rock with concentrated nitric acid in the Odda process of fertilizer production leads to the dissolution of these metals in the resulting nitrophosphate solution. This nitrophosphate solution is considered as a complex analytical matrix. In this paper, we present an analytical method with a total analysis time of 18 min for the direct determination of lanthanides and yttrium in the above nitrophosphate solution, based on cation-exchange ion chromatography. The analytical columns involved in this method are silica-based cation exchanges. Elution was carried out with a concentration gradient of HIBA (α-hydroxyisobutyric acid) at a pH range between 3.8 and 4.2, coupled with post-column spectrophotometric detection with PAR or ARSENAZO III at 530 and 658 nm respectively. These silica columns can also offer the direct analysis of lanthanides in organic solutions taken from experimental research samples, investigating the extraction of these metals from the nitrophosphate solution by liquid–liquid extraction.

1. Introduction

Norsk Hydro has been involved in fertilizer production since 1905. The fertilizer production plant located at Hydro Porsgrunn, Norway, utilizes the Odda process of fertilizer production, which involves the digestion of phosphate rock with concentrated nitric acid to produce a nitrophosphate solution [1].

This nitrophosphate solution is cooled down to −5°C to crystallize calcium nitrate, which is removed by filtration. The mother liquor resulting from this crystallization will undergo further treatment in the fertilizer production process chain. Table 1 shows the complete analytical data of a mother liquor solution obtained from the digestion of Kola phosphate rock.

The digestion of Kola phosphate rock, which is relatively rich in lanthanides, produces a mother liquor solution containing these metals. In contrast to the wet process of fertilizer production, in which sulphuric acid is used to achieve the digestion, a large percentage of the lanthanide salts precipitate with the gypsum [2].

Several articles have been published investigating the recovery of lanthanides and yttrium from this nitrophosphate solution [3]. Some investigations were abandoned because of the lack of an analytical procedure for these metals [4]. Norsk Hydro Research Centre, Porsgrunn, has undertaken a feasibility study on the recovery of these metals from the mother liquor solution in the Odda process of fertilizer production. The success of this study depended, to a large extent, on the accuracy of the analytical data produced from a large number of samples.

Lanthanides play an important role in many current technological industries. These include

* Corresponding author.

0021-9673/94/$07.00
SSDI 0021-9673(93)E1136-N

Table 1
Typical composition of a Kola mother liquor solution

Ion	Range of concentration
P	10.17–9.27%
Ca	3.26–3.09%
F	0.31–0.28%
Total N	11.16–11.40%
$N\text{-}NO_3^-$	6.13–6.34%
$N\text{-}NH_4^+$	5.03–5.06%
Na	2105–1600 mg/l
Mg	510–430 mg/l
Al	3668–3400 mg/l
Ti	580–840 mg/l
V	83–79 mg/l
Mn	191–190 mg/l
Fe	2175–2000 mg/l
Cu	37–38 mg/l
Zn	26–28 mg/l
Sr	5133–5100 mg/l
Ba	151–130 mg/l
Y	212–240 mg/l
La	1238–1200 mg/l
Ce	2350–2375 mg/l
Pr	220–230 mg/l
Nd	950–965 mg/l
Sm	125–121 mg/l
Eu	35–36 mg/l
Gd	90–94 mg/l
Tb	9–11 mg/l
Dy	45–60 mg/l
Ho	8–9 mg/l
Er	16–24 mg/l
Tm	2–2.3 mg/l
Yb	8–11 mg/l
Lu	1–1.3 mg/l
Th	12–11 mg/l
U	4–4.2 mg/l

the nuclear, metallurgy, electronic, ceramic and laser industries. They are also important catalysts in the petroleum industry and as fluorescent labels for biological molecules. Determination of lanthanides in geological materials is also important, especially for petrogenetic studies [5].

The ideal method for the determination of lanthanides would combine the advantages of high specificity and sensitivity, high precision and accuracy, complete element cover and low cost. A variety of instrumental methods have been used, including neutron activation analysis [6], mass spectrometry [7], X-ray fluorescence spectrometry [8], atomic absorption spectrometry [9] and inductively coupled plasma (ICP) with atomic emission spectrometry [10] (ICP-AES) or with mass spectrometry [11] (ICP-MS). Absorption methods with spectrophotometric reagents, on the other hand, are simple, reliable and low-cost methods for routine analysis. A large number of spectrophotometric reagents have been proposed to increase the sensitivity for the determination of either individual lanthanide ions or total lanthanide content [12].

An ion chromatograph coupled with a post-column detection technique can take advantage of this enhanced sensitivity of the lanthanide ion with spectrophotometric reagents. Post-column detection of metal ions today represents an important analytical mechanism [13].

2. Experimental

2.1. Instrumentation

A Dionex 4000i (Dionex, Sunnyvale, CA, USA) eluent pump system with 50 μl injection volume, a Gilson Model 221 autosampler (Gilson, France) and a Spectra-Physics UV150 detector (Spectra-Physics, Santa Clara, CA, USA) were used. Data handling was performed with a multichrom system (VG Instruments, UK).

The analytical columns used were silica based with strong cation-exchange functionality: Nucleosil ET 250/8/4 SA10 (Macherey–Nagel, Düran, Germany) and Supelcosil LC-SCX (Supelco, USA).

The post-column reagent was introduced (0.7 ml/min) via a low-volume T-mixer with a helium-pressurized delivery system. The length of the reaction coil between the mixing tee and the detector was 10 cm.

2.2. Reagents

Eluent, standards and sample solutions were prepared with pretreated water via ion exchange and double distillation, then passed through a Milli-Q water purification system (Millipore,

Waters Chromatography Division, Oslo, Norway).

The pH of 0.4 *M* α-hydroxyisobutyric acid (HIBA) (Fluka) was adjusted with lithium hydroxide (Fluka). Elution was achieved with a concentration gradient of HIBA, 0.04 to 0.08 *M* in 5 min, then increasing to 0.3 *M* in 15 min at an eluent flow-rate of 1 ml/min.

The eluted metal ions were detected after post-column reaction with 4-(2-pyridylazo)resorcinol (PAR) (0.2 m*M*, 1 *M* glacial acetic acid 100% and 3 *M* NH_3) [14] at 530 nm or with Arsenazo III [2,2′-(1,8-dihydroxy-3,6-disulphonaphthylene-2,7-bisazo)bisbenzenearsonic acid] (0.1 m*M*, and 0.5 *M* glacial acetic acid 100%) [15] at 658 nm.

Standard solutions (1000 μg/ml) of the lanthanides were obtained from Teknolab (Drøbak, Norway).

2.3. Sample preparation

Aqueous samples were diluted with water or very dilute acid (0.05 *M* HNO_3) to prevent rare earth phosphates precipitation, and filtered through a 0.45-μm filter before injection. The mother liquor solution was diluted 1:100 and the extracted mother liquor raffinate was diluted 1:50.

Organic samples were diluted with methanol or acetonitrile and filtered through a 0.45-μm filter before injection. The organic samples were diluted 1:100.

3. Results and discussion

Several articles have been published dealing with the analysis of lanthanides in different analytical solutions. Although the chemistry of the chromatography can vary, the detection method is identical in all of them.

The analysis of lanthanides using an organic resin cation-exchange column and an organic anion-exchange column has been reported [14]. Elution was achieved by concentration gradient of α-hydroxyisobutyric acid or oxalic and diglycolic acids respectively.

A recent method for the separation and determination of the lanthanides, based on ion interaction chromatography, has been reported [15]. The most recent version of this approach uses gradient elution with sodium octanesulphonate as an ion interacting reagent. This provides virtual ion-exchange sites by adsorption on a non-polar (C_{18}) stationary phase with α-hydroxyisobutyric acid as the complexing eluting component.

The direct analysis of the nitrophosphate solution obtained from the Odda process of fertilizer production on an organic exchange column (Dionex IonPac CS3) produced unsatisfactory chromatograms, consisting of overlapping and tailing peaks. Dionex IonPac CS3 columns are packed with an agglomerated particles, which have a pellicular structure. The poor separation efficiency may be due to the relatively large particle size of the stationary phase and the degree of organic polymer cross-linking. A more likely hypothesis for the poor efficiency is that the column was overloaded, as can easily happen with low-capacity Dionex columns.

Application of the ion interaction technique to the analysis of lanthanides in this nitrophosphate matrix has also produced negative results. This was because of the low solubility of rare earths phosphate in the eluent, which contains 10% (v/v) organic modifier, either methanol or acetonitrile [15]. Ion interaction chromatographic separation of lanthanides which does not involves organic modifier was not attempted in this study [16,17].

The negative results obtained using the above techniques prompted the investigation into another stationary phase material or a more suitable mobile phase.

In this work, silica-based cation-exchange columns produced much sharper peaks with good peak separation and excellent calibration curves. Table 2 illustrates some examples of the calibration and coefficient values obtained with PAR detection.

These lanthanides examples are listed because they are representative of the heavy lanthanides (Lu), middle lanthanides (Eu) and light lanthanides (Pr and La). Other lanthanides produced

Table 2
Calibration and coefficient values

Metal	Linear range (μg/ml)	Area (μV s)	Coefficient
Lu	1.0	249040.640	0.99991
	2.0	512355.750	
	5.0	1290546.015	
Eu	2.0	895150.624	0.99894
	5.0	2358007.030	
	10.0	4470265.620	
Pr	5.0	1219345.465	0.99561
	10.0	2774559.370	
	20.0	5010205.620	
La	5.0	567226.875	0.99782
	10.0	1291062.340	
	20.0	2422444.200	

similarly good calibration and coefficient of determination values.

The detection limit of each lanthanide depended on the detection reagent and the nature of the particular lanthanide involved (Table 3).

Fig. 1 shows the difference in sensitivity for the lanthanides with two post-column reagents. Analysis of the mother liquor solution was performed with Arsenazo III detection, as this reagent is more selective for lanthanides. PAR detection was used in organic samples since the organic layer of the extraction system contains many fewer interfering ions because of the selectivity of the organic extractant mixed in an aliphatic hydrocarbon diluent.

Detection limits were calculated on a 50 μl injection loop volume.

The most important advantage gained of applying this method to a nitrophosphate fertilizer solution is that the analytical media can be applied directly for analysis. To demonstrate the reproducibility of this chromatographic method, the relative standard deviation of multiple (ten) injections was calculated and found to be ±0.7–3.0% for samples (organic and aqueous) detected with PAR and ±0.6–2.5% for samples (organic and aqueous) detected with Arsenazo III. These repeatability experiments were conducted on

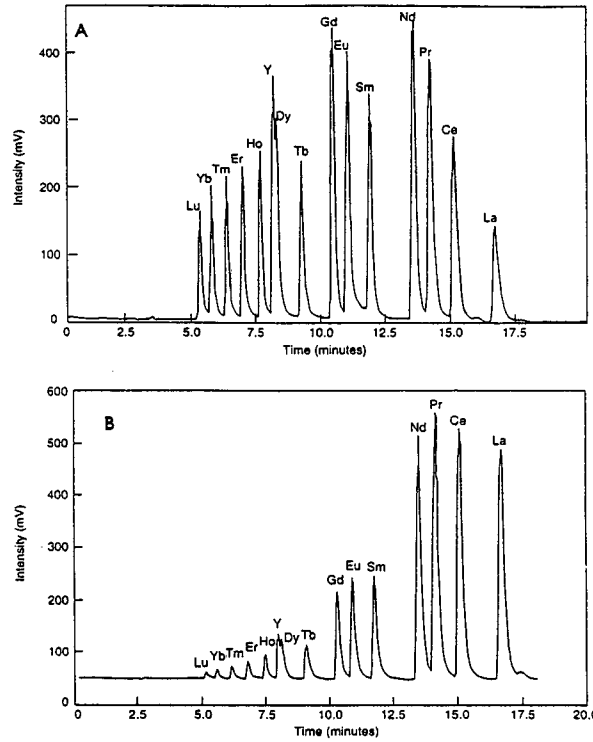

Fig. 1. Standard solution analysis: Lu, Yb, Tm, Er, Ho, Y, Dy, Tb 5 μg/ml; Gd, Eu, Sm, 10 μg/ml; Nd, Pr, Ce, La, 20 μg/ml. Injection loop: 50 μl. Supelcosil LC-SCX column 250/4.6 mm. Elution with HIBA pH 4.2 (0.04 *M* to 0.08 *M* in 5 min, then to 0.3 *M* in 15 min). Eluent flow-rate: 1 ml/min. Post-column reagent flow-rate: 0.7 ml/min. (A) PAR detection; (B) Arsenazo III detection.

samples whose concentration was more than ten times the detection limit.

To demonstrate the accuracy of this method in an aqueous medium a comparison was made

Table 3
Detection limits of lanthanides

Metal	Detection limit PAR (μg/l)	Detection limit Arsenazo III (μg/l)
Lu, Yb, Tm, Er, Ho, Dy, Tb and Y	100	1000
Gd, Eu, Sm	500	500
Nd, Pr, Ce, La	1000	100

between the analytical data obtained by this method and data taken from the ICP-MS technique analysis [18] of an identical mother liquor sample. Table 4 demonstrates the comparison.

The accuracy of this method in an organic matrix has not been evaluated because of the limited availability of independent analytical instrumentation to perform such an analysis. However, calculation of the distribution coefficient of each lanthanide, which can be obtained from the ratio of each lanthanide concentration (g/l) in the organic phase to the same lanthanide concentration in the aqueous phase (g/l), produced values similar to those reported in literature [19].

Increasing the eluent HIBA concentration or pH resulted in decreased retention times. In aqueous solution, lanthanides are present as trivalent cations. Since the ionic properties of the lanthanides are similar, they cannot be separated easily by cation exchange as trivalent cations. However, the selectivity of the ions can be increased with the use of appropriate chelating agents such as HIBA. Because the chelating agents are negatively charged, the result is a net decrease in the charge of the metal as the complex, with the largest decrease for the strongest complex.

Table 4
Lanthanides analytical data of a typical mother liquor solution

Lanthanide	ICP-MS (μg/ml)	IC (μg/ml)
Lu	0.64	0.50
Yb	6.90	7.10
Tm	1.50	1.40
Er	16.00	16.50
Ho	6.70	6.50
Y	190.00	185.00
Dy	43.00	45.00
Tb	11.00	10.00
Gd	110.00	110.00
Eu	31.00	34.00
Sm	110.00	109.00
Nd	850.00	856.00
Pr	220.00	219.00
Ce	2100.00	2150.00
La	1400.00	1385.00

The smallest ions, the last lanthanides in the series, form the strongest complexes and are least positively charged. Therefore, when the lanthanides are separated by cation exchange with HIBA in the eluent, the elution order is Lu → La [14].

An example of the application of this method directly to a mother liquor solution (see Table I for composition) taken from a fertilizer production line is shown in Fig. 2. The sample was diluted with water (1:100) and injected directly. Fig. 2 shows some interference near the samarium peak and an unknown peak near the lanthanum peak with PAR detection. Fig. 2 also shows overlapping between yttrium and dysprosium peaks.

This unknown peak near lanthanum and the overlapping peak with samarium can be eliminated from the analytical chromatograms by applying post-column detection with Arsenazo III. The resolution of the yttrium–dysprosium peak can be performed by reducing the eluent pH from 4.2 to 3.9. Fig. 3 demonstrates the resulting chromatogram by the application of these two conditions. It is important to emphasize here that the yttrium–dysprosium peak can be also resolved by PAR detection, provided that eluent pH is maintained at 3.9.

Fig. 4 shows the analysis of an organic sample diluted with methanol (1:100), with PAR detection, which was taken from experimental re-

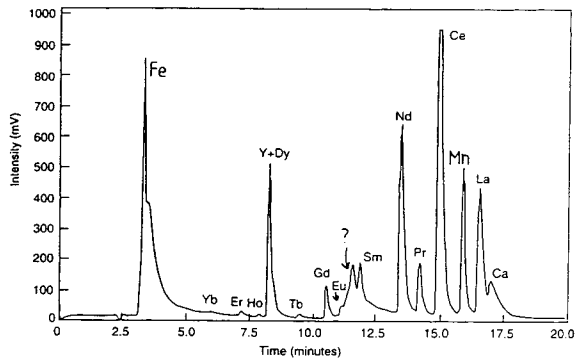

Fig. 2. Analysis of a nitrophosphate mother liquor solution by PAR detection. Sample dilution 1:100 with 0.05 *M* HNO_3. Similar chromatographic conditions to Fig. 1.

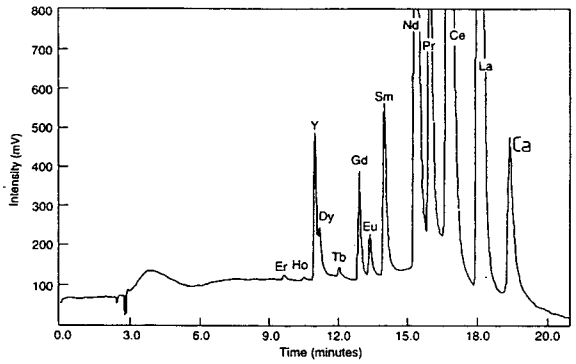

Fig. 3. Analysis of a nitrophosphate mother liquor solution by Arsenazo III detection. Sample dilution 1:100 with 0.05 *M* HNO_3. Similar chromatographic condition to Fig. 1, but eluent pH 3.9.

search tests, investigating the feasibility of lanthanides extraction from this nitrophosphate solution. A variety of organic extractants in various diluents were involved in this study. Arsenazo III can also be utilized to detect lanthanides in organic matrix.

These organic analyses were important in determining the extraction coefficient of each lanthanide under a particular set of conditions. This ability of a silica-based cation-exchange column to directly analyse organic solution is essential, since an organic-based cation exchange column is sensitive to non-polar organic solvents.

The stability of these silica-based cation-exchange columns was monitored. The analysis of over 250 samples both organic and aqueous on one column did not affect the peak efficiency of the column (identical peak retention time, height and half-length width). The most important factor affecting the lifetime of these columns is the eluent pH. The eluent pH would have to be between 3 and 7 to ensure maximum lifetime [20].

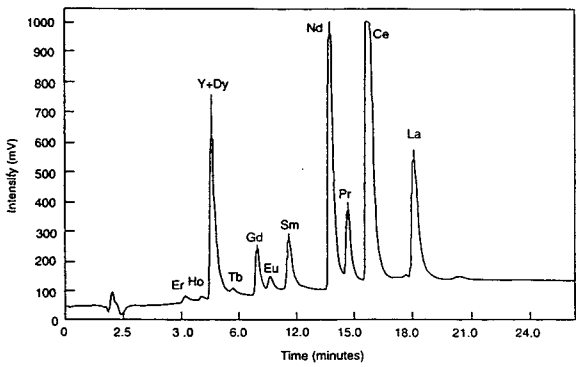

Fig. 4. Direct analysis of an organic solution by PAR detection. Sample dilution 1:50 with methanol. Injection loop 50 μl. Nucleosil SA10, 250/4.6 mm. Elution with HIBA pH 4.2 (0.04 *M* to 0.3 *M* in 15 min). Eluent flow-rate: 1 ml/min. Post-column reagent flow-rate: 0.7 ml/min.

4. Summary

The nitrophosphate solution obtained from the digestion of phosphate rock with concentrated nitric acid in the Odda process of fertilizer production is a complex analytical matrix. The direct analysis of this solution by cation-exchange chromatography or ion interaction chromatography utilizing organic modifiers reported in the chemical literature has produced unsatisfactory results.

We used a silica-based cation-exchange column to perform the analytical separation. Elution was achieved by a concentration gradient of HIBA (0.04 *M* to 0.08 *M* in 5 min, then to 0.3 *M* in 15 min) at pH 3.8–4.2, and post-column detection with PAR or Arsenazo III, followed by spectrophotometric visible detection at 530 nm and 658 nm, respectively.

Mother liquor solutions and extraction raffinate solutions were analysed using Arsenazo III detection, since it is more selective for the lanthanides than PAR. Analysis of organic solution was performed by PAR, since organic phase matrix has fewer metal impurities because of the selectivity of the organic extractant employed.

5. References

[1] G. Kongshaug, *Ullmann's Encyclopedia of Industrial Chemistry*, Vol. A19, VCH, Weinheim, 1991, pp. 421–463.
[2] R. Kijkowska, *Phosphorus Potassium*, 164 (1989) 24.
[3] V.P. Judin and H.E. Sund, *Hydrometallurgy*, (1981) F4/1.
[4] B.G. Russell, *Bulletin No. 1*, Minerals Bureau, Department of Mines, Johansberg, South Africa, 1977.

[5] B.T. Kilbourn, in R.G. Bautista and N. Jackson (Editors), *Proceedings of an International Symposium held jointly by TMS and AusIMM during the TMS Annual Meeting, San Diego, CA, March 1992*, TMS (Minerals, Metals, Materials), Warrendale, PA, 1991, p. 209.
[6] P. Vukotic, *J. Radioanal. Chem.*, 78 (1993) 105.
[7] F.W.E. Strelow and P.F.S. Jackson, *Anal. Chem.* 46 (1974) 1481.
[8] I. Roelandts, *Anal. Chem.*, 53 (1981) 676.
[9] L.H.J. Lajunen and G.R. Choppin, *Rev. Anal. Chem.*, 9 (1989) 91.
[10] M.S. Rathi, P.P. Khanna and P.K. Mukherjee, *Talanta*, 38 (1991) 329.
[11] N. Shibata, N. Fudagawa and M. Kubota, *Anal. Chem.*, 63 (1991) 636.
[12] H. Onishi and C.V. Banks, *Talanta*, 10 (1963) 399.
[13] P.R. Haddad and P.E. Jackson, *Ion Chromatography* (*Journal of Chromatography Library*, Vol. 46), Elsevier, Amsterdam, 1990, p. 387.
[14] *Technical Note 23*, Dionex, Sunnyvale, CA, 1987; *Technical Note 27*, Dionex, Sunnyvale, CA, 1992.
[15] R.M. Cassidy, *Chem. Geol.*, 67 (1988) 185.
[16] C.H. Knight, R.M. Cassidy, B.M. Recoskie and L.W. Green, *Anal. Chem.* 56 (1984) 474.
[17] S. Elchuk, C.A. Lucy and K.I. Burns, *Anal. Chem.* 64 (1992) 2339.
[18] M. Vadset, *0-91067, Pr1-21172.01*, Norwegian Institute For Air Research, Oslo, 1992.
[19] H. Seto and T. Mori, *Metall. Rev. MMIJ*, 6 (1989).
[20] A. Klingenberg and A. Seubert, *J. Chromatogr.*, 640 (1993) 167.

ELSEVIER

Journal of Chromatography A, 671 (1994) 181–191

JOURNAL OF CHROMATOGRAPHY A

Determination of thorium and uranium in mineral sands by ion chromatography

P.E. Jackson*,[a], J. Carnevale[a], H. Fuping[b], P.R. Haddad[b]

[a]*Waters Chromatography Division of Millipore, Private Bag 18, Lane Cove, N.S.W. 2066, Australia*

[b]*Department of Chemistry, University of Tasmania, G.P.O. Box 252C, Hobart, Tasmania 7001, Australia*

Abstract

Thorium and uranium can be determined by ion chromatography using a C_{18} reversed-phase column and a complexing eluent of hydroxyisobutyric acid followed by post-column derivatization with Arsenazo III and detection at 658 nm. A number of sample dissolution and clean-up procedures were evaluated in order to permit the application of the chromatographic method to the analysis of mineral sands. Dissolution procedures investigated included a variety of acid digestions and alkali fusion with peroxide, borate, carbonate, hydroxide and pyrosulphate fluxes. Sample clean-up protocols were then studied in order to overcome matrix interference effects. The optimal sample preparation procedure involved a tetraborate fusion/nitric acid leach followed by either cation-exchange pretreatment, or simply dilution in concentrated hydroxyisobutyric acid, depending upon the sample type. The results obtained using the chromatographic method showed good agreement with X-ray fluorescence and inductively coupled plasma mass spectrometry for ilmenite, synthetic rutile, zircon and rutile mineral sands with detection limits (in the original mineral sand) in the order of 1.0 μg/ml for the two analytes.

1. Introduction

The determination of thorium and uranium at trace levels in environmental samples is typically carried out using techniques such as radiochemistry [1], atomic absorption spectroscopy [1], neutron activation analysis [2], inductively coupled plasma mass spectrometry (ICP-MS) [3], isotope dilution mass spectrometry [4] and X-ray fluorescence (XRF) [5]. However, these techniques are often not suited to routine analysis, due to interferences from other metals present in the matrix, cost of operation or poor detection limits [6,7]. Ion chromatography (IC) has been widely applied to the separation of lanthanides and also thorium and uranium [6–10]. These species are typically separated on a C_{18} reversed-phase column using a mobile phase containing an ion interaction reagent (*e.g. n*-octanesulphonate) and a complexing agent (*e.g.* hydroxyisobutyric acid, HIBA) followed by post-column derivatization using either Arsenazo III {3,6-bis[(*o*-arsenophenyl)azo]-4,5-dihydroxy-2,7-naphthalene disulfonic acid} or PAR [4-(2-pyridylazo) resorcinol] with visible detection.

Thorium(IV) and uranium(IV), as the uranyl ion, exhibit somewhat different retention behaviour to the lanthanides and it has been shown that their HIBA complexes can be retained on a C_{18} column without the need for an ion interaction reagent (IIR) in the mobile phase [11,12]. Also, when mandelic acid was used as the complexing ligand, thorium(IV) and the uranyl

* Corresponding author.

0021-9673/94/$07.00
SSDI 0021-9673(93)E0036-T

ion could again be retained on a C_{18} column without the need for an anionic IIR in the mobile phase [13], and it has recently been proposed that such complexes are retained by a mechanism of hydrophobic adsorption rather than dynamic cation-exchange [14]. Alternatively, thorium and uranium have also recently been separated by cation-exchange chromatography using a gradient of hydrochloric acid and sodium sulphate prior to post-column reaction detection [6].

Many of the above IC separations have been applied to the determination of thorium and uranium in samples including natural waters [6,11], uranium ore [11], irradiated fuel materials [9,10,12] and geological matrices such as bassalt, phosphate rock and river sediments [6,7]. The IC determination of thorium and uranium in mineral sands is a complex problem due to the fact that the sample matrix is very difficult to get into solution. Indeed, IC appears to have been used only once previously for the analysis of metal cations in mineral sands [15].

In this paper, a number of sample preparation procedures were evaluated to enable the determination of thorium and uranium in mineral sands by IC. Dissolution procedures investigated included acid leaching and alkali fusion with peroxide, borate, carbonate, hydroxide and pyrosulphate fluxes. Sample clean-up protocols, including solvent extraction, cation-exchange and selective complexation, were then studied in order to overcome the interference effects of the dissolution matrix upon the chromatographic process. The results obtained using the IC method were compared to those from XRF and ICP-MS for ilmenite, synthetic rutile, zircon and rutile mineral sands.

2. Experimental

2.1. Instrumentation

The liquid chromatograph consisted of a Waters Chromatography Division of Millipore (Milford, MA, USA) Model 590 solvent-delivery system, either a U6K injector or a WISP 712 autoinjector, Model 441 fixed-wavelength UV–Vis detector operated at 658 nm and an 820 Maxima data station. The post-column reagent was delivered (at *ca.* 30 p.s.i.; 1 p.s.i. = 6894.76 Pa) with a Waters pneumatic reagent delivery module (RMD). The analytical column used was a Waters μBondapak C_{18} (300 × 3.9 mm I.D.) reversed-phase column, operated at ambient temperature. Sample digest solutions were loaded through the cation-exchange pretreatment cartridges using a Waters Model 501 solvent-delivery system.

2.2. Reagents

Water purified using a Millipore Milli-Q Water purification system (Bedford, MA, USA) (18 MΩ) was used for all solutions. The mobile phase consisted of 400 m*M* α-hydroxyisobutyric acid (Sigma, St. Louis, MO, USA) and 10% methanol (HPLC grade obtained from Waters) adjusted to pH 4.0 with sodium hydroxide. The analytical mobile phase was operated at a flow-rate of 1.0 ml/min. The post-column reagent solution contained 0.13 m*M* Arsenazo III (BDH, Poole, UK), 10.0 m*M* urea (May & Baker, Dagenham, UK) and 62 m*M* acetic acid and was delivered through a stainless steel "T" piece at a flow-rate of 1.0 ml/min. All eluents and post-column reagents were prepared daily, filtered and degassed with a Waters solvent-clarification kit. Thorium and uranium standards were prepared from thorium(IV) nitrate and uranyl nitrate (Ajax Chemicals, Sydney, Australia), respectively. Sample pretreatment was carried out using either Alltech (Deerfield, IL, USA) IC H^+ Maxiclean cartridges (sulphonic acid functionalized, *ca.* 1 g of 5 mequiv./g resin), Waters Accell CM Sep-Pak cartridges (carboxylic acid functionalized, *ca.* 0.4 g of 350 μequiv./g silica) or Waters ion-exclusion Guard-Pak insert cartridges (sulphonic acid functionalized, *ca.* 0.2 g of 5 mequiv./g resin).

2.3. Sample dissolution procedures

Ilmenite, synthetic rutile, zircon and rutile mineral sand samples were prepared using a

variety of acid leach and fusion procedures, which are detailed below:

Acid leach

Samples (0.5 g) were weighed into 250 ml flasks and 20 ml of concentrated perchloric and nitric acids added. The samples were refluxed for 1 h and boiled to near dryness, cooled and 2.0 g of HIBA were added. The samples were adjusted to pH 4.0 with sodium hydroxide and made up to 100 ml.

Peroxide fusion

Samples (0.5 g) were weighed into a platinum crucible with 4.0 g of sodium peroxide and fused at 1100°C for 15 min. The melt was dissolved with 15 ml of 50% sulphuric acid and 15 ml of 30% hydrogen peroxide; then cooled, diluted, filtered and made up to 100 ml.

Carbonate–tetraborate fusion

Samples (0.5 g) were weighed into a platinum crucible with 1.0 g sodium carbonate and 1.0 g sodium tetraborate and fused at 1100°C for 15 min. The melt was poured into a solution of 20 ml concentrated nitric acid, 5 ml 30% hydrogen peroxide and 25 ml water. The crucible was placed into the above solution and warmed on a hotplate to dissolve the melt. The crucible was then removed, washed with water, the solution cooled and made up to 100 ml.

Tetraborate fusion

Samples (0.5 g) were weighed into a platinum crucible with 2.0 g sodium tetraborate and fused at 1100°C for 15 mins. The melt was poured into a solution of 5 ml concentrated nitric acid and 50 ml water. The crucible was placed into the above solution and warmed on a hotplate to dissolve the melt. The crucible was then removed, washed with water, the solution cooled, filtered and made up to 100 ml.

Pyrosulphate fusion

Samples (0.5 g) were weighed into a vicor quartz 250-ml conical flask with 5.0 g potassium pyrosulphate and fused over a meaker burner at 800–900°C to obtain a clear melt. The melt was cooled and 10 ml of concentrated sulphuric acid was added. The solution was warmed to dissolve the melt then 5 ml of concentrated hydrochloric acid and 50 ml water were added. The solution was cooled and made up to 100 ml.

Tetraborate–carbonate fusion

Samples (0.5 g) were weighed into a platinum crucible with 2.5 g sodium tetraborate and 1.0 g sodium carbonate and fused at 1100°C. The melt was poured into a solution of 10 ml concentrated sulphuric acid and 40 ml water. The crucible was placed into the above solution and warmed on a hotplate to dissolve the melt. The crucible was removed, washed with water, the solution cooled and made up to 100 ml.

Hydroxide fusion

Samples (0.5 g) were weighed into a zirconium crucible with 4.0 g sodium hydroxide and fused at 1100°C for 15 min. Concentrated nitric acid (15 ml) was added to the crucible and the slurry heated to near dryness on a hotplate. The solution was cooled, filtered and made up to 100 ml.

2.4. Cation-exchange pretreatment procedure

The final cation-exchange sample pretreatment procedure used to evaluate the various fusion/digest approaches consisted of firstly conditioning the ion-exclusion cartridge with 5.0 ml of 7.5 *M* nitric acid followed by 5.0 ml of water. The sample digest was then loaded onto the cartridge at 2.0 ml/min with an HPLC pump after diluting the sample to ensure that the acid concentration did not exceed 0.2 *M* in order to allow quantitative binding of thorium and uranium ions. The cartridge was then washed with 1.0 ml water to remove the interstitial sample and flushed with air to remove the water. Finally, the bound thorium and uranium were eluted from the cartridge with 2.0 ml of 2.0 *M* HIBA into a pre-rinsed 4.0 ml autosampler vial and the cartridge flushed with air to ensure complete collection of the entire 2.0-ml volume.

3. Results and discussion

3.1. Preliminary investigations

In a previous paper, we investigated the retention behaviour of thorium(IV) and uranium (as the uranyl ion) complexes of HIBA on a C_{18} reversed-phase column and proposed that such complexes are retained by a mechanism of hydrophobic adsorption [14]. Optimal conditions were established for the determination of thorium and uranium which utilized a mobile phase of 400 m*M* HIBA and 10% methanol at pH 4.0 with a μBondapak C_{18} column, a post-column reagent of Arsenazo III and detection at 658 nm. In this paper, we investigate the possibility of applying the above chromatographic method to the determination of thorium and uranium in ilmenite, synthetic rutile, zircon and rutile mineral sands. Fig. 1 shows a chromatogram obtained from a 100-μl injection of a 10 μg/ml standard of thorium and uranium using the conditions described above. Thorium and uranium exhibit appreciably different retention behaviour to the rare earth elements and are completely resolved from these potentially interfering species using this chromatographic approach. Another advantage of this technique was

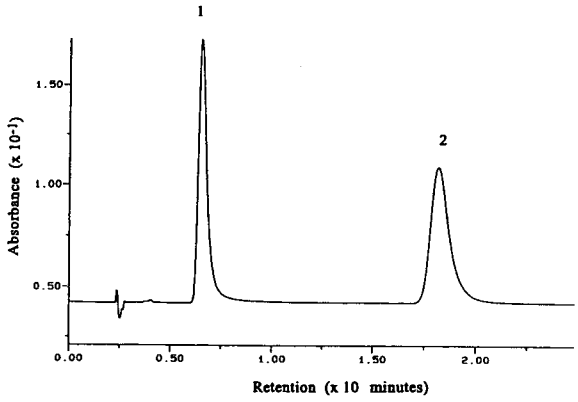

Fig. 1. Separation of thorium and uranium standard. Conditions: column, Waters μBondapak C_{18}; eluent, 400 m*M* HIBA, 10% methanol at pH 4.0; flow-rate, 1.0 ml/min; injection volume, 100 μl; post-column reagent, 0.13 m*M* Arsenazo III, 10.0 m*M* urea, 62 m*M* acetic acid delivered at 1.0 ml/min; detection, visible at 658 nm. Solutes: 1 = thorium (10 μg/ml); 2 = uranium (10 μg/ml).

that it allowed the injection of large sample volumes before significant peak broadening occured, resulting in detection limits (at 3× signal-to-noise) of 3.0 and 5.0 ng/ml (using a 1000-μl injection) for thorium and uranium, respectively. The calibration curves were linear (correlation coefficients > 0.9999) from detection limit to approximately 5.0 μg/ml for the same injection volume. Beyond this sample loading, the analyte response overranged the detector. As thorium was typically found in mineral sands at higher concentrations than uranium, calibration curves were routinely prepared for the two analytes using different solute concentrations and injection volumes.

However, despite the excellent linearity and detection limits of the chromatographic method, initial results obtained using direct injection of samples prepared using a peroxide fusion (described in the Experimental) gave very low results (*ca.* 10% recovery) when compared to those obtained with XRF, as detailed in Table 1. The mineral sand samples were then prepared using an alternative dissolution method, a perchloric and nitric acid leach procedure and the results obtained by direct injection of the samples are also shown in Table 1. These results indicated one of two possibilities; that either the sample dissolution procedures did not quantitatively release thorium and uranium from the matrix, or that the dissolution matrix was somehow interfering with the subsequent chromatographic analysis. It has been reported previously [16], for the determination of lanthanides by liquid chromatography, that sulphuric acid levels in the injected solution of >0.09 *M* reduced the peak heights and retention times of rare earth elements (REEs) when using oxalate as the complexing agent in the mobile phase. The acidity of the sample altered the formation constants of REEs complexes and therefore influenced the degree of complexation of the REEs. In the case of thorium– and uranium–HIBA complexes, it appeared that other (complexing) ions in the sample digest solution were competing with HIBA in the coordination sphere of both thorium and uranium. Consequently, these species were chromatographed as other

Table 1
Thorium and uranium concentrations in original mineral sand samples obtained using direct injection and peroxide fusion or acid leach sample dissolution

Sample	IC		XRF[a]	
	Thorium (μg/g)	Uranium (μg/g)	Thorium (μg/g)	Uranium (μg/g)
Ilmenite				
Peroxide fusion	86.4	ND	490	10
Acid leach	426	8.9		
Synthetic rutile				
Peroxide fusion	69.9	ND	430	15
Acid leach	56.2	ND		
Zircon				
Peroxide fusion	ND	48.6	179	217
Acid leach	21.1	ND		
Natural rutile				
Peroxide fusion	8.0	8.0	53	54
Acid leach	29.2	ND		

ND = Not detected.
[a] XRF = Results obtained on solid samples.

complexed forms, most of which appeared to elute at the column void volume.

The effect of sample acidity on the chromatographic behaviour of thorium was confirmed by preparing 10 μg/ml thorium standard solutions made up in either 1.0 *M* sulphuric, nitric or hydrochloric acids. The recoveries for the thorium peak were 23, 71 and 87% in sulphuric, nitric and hydrochloric acids, respectively, when compared to a standard prepared in Milli-Q water. Sulphate, nitrate and chloride all from stable complexes with thorium [17] and effectively compete with HIBA in the coordination sphere of the thorium. In fact, the recovery results reflect the degree of stability of the relative complexes, *i.e.* sulphate forms more stable anionic complexes with thorium than does nitric acid, than does hydrochloric acid [17]. Hence, the poor recoveries were obtained as a result of the other (more polar) complexes of thorium eluting at the column void volume. When the 10 μg/ml thorium standard solution was made up in 0.1 *M* sulphuric acid, the recovery for the thorium peak was precisely 100%; however, such an acid concentration was much too low to effect dissolution of the mineral sand fusion melt. Additionally, when a 10 μg/ml thorium standard solution was made up in 1.0 *M* sulphuric acid and neutralized with sodium hydroxide before injection, the recovery for the thorium peak was only 8%. This result indicated that either the hydroxyl anion could also compete with HIBA in the coordination sphere of thorium, or that the sulphate complex of thorium was more stable under alkaline conditions. The effect of other anions on the uranium recovery was similar to that for thorium, although not as dramatic as uranium formed more stable HIBA complexes than thorium.

Evidently, some form of further sample treatment prior to the chromatographic determination was necessary in order to determine if the sample fusion/acid dissolution procedures were successfully releasing thorium and uranium from the mineral sand matrix. Options would include a very large dilution of the sample digest; the use of an alternative chromatographic approach where the thorium and uranium response were not affected by the presence of other ions in solution; or the removal of thorium and uranium

from the dissolution matrix prior to injection. Unfortunately, thorium and uranium are present in the samples at such low concentrations that a large dilution is impractical and other chromatographic approaches, whether using an ion-exchange, reversed-phase or ion interaction separations, are also likely to be affected by the presence of elevated levels of ions in the sample digest as they all rely on some degree of complexation with the mobile phase to elute the thorium and uranium ions.

3.2. Sample pretreatment

It appeared then that the most appropriate solution to the interference problems was to remove the thorium and uranium from the dissolution matrix prior to the chromatographic step. Two approaches were investigated; solvent extraction and solid-phase (cation-exchange) extraction. It has long been established that thorium and uranium can be extracted from aqueous solutions containing high concentrations of certain metal nitrates using oxygen-containing organic solvents [18]. However, extraction of a 10 μg/ml thorium and uranium standard solution (containing 1.0 g/ml aluminium nitrate) with ethyl acetate resulted in recoveries of only 30 and 80% for thorium and uranium, respectively. This approach was abandoned after attempts to extract a fusion/digestion sample with ethyl acetate were unsuccessful due to the formation of stable emulsions.

Cassidy [7] has previously used solid-phase (cation-exchange) extraction to concentrate RREs from rock digest matrices prior to chromatographic determination. Alternatively, an iminodiacetate functionalized chelating resin has also been shown to allow preconcentration of uranium and thorium from rock digests prior to gradient cation-exchange separation [6]. Investigation of the binding affinities of thorium and uranium in nitric acid indicated that both thorium and uranium would bind quantitatively to strong cation-exchange resin, provided that the nitric acid concentration of the solution was no greater than 0.1 *M* [17]. At higher nitric acid concentrations, uranium shows significantly decreasing affinity for the cation-exchanger due formation of anionic nitrate complexes. The recoveries of thorium and uranium on several different cation-exchange cartridges were then evaluated using a cation-exchange "pretreatment" protocol based on that of Cassidy [7]. This involved loading an appropriate volume of sample onto a cartridge which had been previously conditioned with 5 ml of 0.1 *M* nitric acid followed by 1.0 ml of Milli-Q water. The cartridge with the retained sample was washed with 1.0 ml of Milli-Q water, eluted with varying volumes of 7.5 *M* nitric acid and the effluent collected in a 20-ml beaker. This solution was evaporated to just dryness on a hotplate in the beaker and the sample reconstituted with 2 ml of 400 m*M* HIBA.

The use of cation-exchange cartridges to quantitatively recover thorium and uranium was initially investigated using a high-capacity IC H^+ Maxiclean cartridge and standard solutions. A 10 μg/ml thorium and uranium standard solution was loaded onto the Maxiclean cartridge and the effluent collected. Chromatographic analysis of the effluent indicated that both Th and U were quantitatively binding to the cartridge. Eluting the bound metals with 10 ml of 7.5 *M* nitric acid resulted in recoveries of only 40 and 55% for thorium and uranium, respectively. Evidently, the sample was quantitatively binding to the cartridge and 10 ml of 7.5 *M* nitric acid was insufficient to quantitatively remove the thorium and uranium from the cartridge. The use of a larger elution volume (30 ml) of 7.5 *M* nitric acid resulted in improved recoveries of 55 and 90% for thorium and uranium, respectively; however, it appeared that the cartridge capacity was too high to permit quantitative elution within a reasonable volume of nitric acid.

Two lower-capacity cation-exchangers were then investigated for their ability to be used with the cation-exchange pretreatment procedure; an Accell weak acid functionalized cartridge and an ion-exclusion Guard-Pak strong acid functionalized cartridge. Both these cartridges gave quantitative (100%) recoveries for a 10 μg/ml thorium and uranium standard solution using an elution volume of only 10 ml of 7.5 *M* nitric acid.

Having established that the two lower-capacity cation cartridges allowed quantitative recoveries for standard solutions, mineral sand samples prepared using an hydroxide fusion were then "pretreated" using the cation-exchange procedure prior to injection. The fusion/digest solutions were diluted a further 10× to reduce the acid concentration to *ca.* 0.1 *M* in order to ensure quantitative binding of thorium and uranium and 20 ml was loaded using an HPLC pump. The samples were then eluted with 10 ml of 7.5 *M* nitric acid, evaporated to just dryness and reconstituted in 2.0 ml 400 m*M* HIBA. The results obtained for illmenite, synthetic rutile and zircon mineral sands using both the cation-exchange cartridge pretreatment are shown in Table 2.

The use of the ion-exclusion cartridge pretreatment allowed good results to be obtained for the illmenite sample, however, lower recoveries were obtained using the Accell cartridge. While appropriate for standard solutions, it appeared that the weak acid functionalized Accell cartridge did not have sufficient capacity to quantitatively retain thorium and uranium from dilute acid solutions and no further work was carried out using these cartridges. Fig. 2a shows a chromatogram of a 100-μl injection of illmenite prepared by hydroxide fusion directly injected with no pretreatment, while Fig. 2b shows a chromatogram of a 100 μl of the same sample after cation-exchange pretreatment. The chromatograms clearly show that the recovery and peak shape for thorium were significantly improved using the cation-exchange pretreatment for illmenite samples. However, the results obtained for the synthetic rutile and zircon samples were still poor, perhaps indicating that the hydroxide sample fusion/digestion procedure was inappropriate for these mineral sand types.

Having established the feasibility of using cation-exchange pretreatment to eliminate the dissolution matrix inference problems prior to the chromatographic step, a number of fusion/

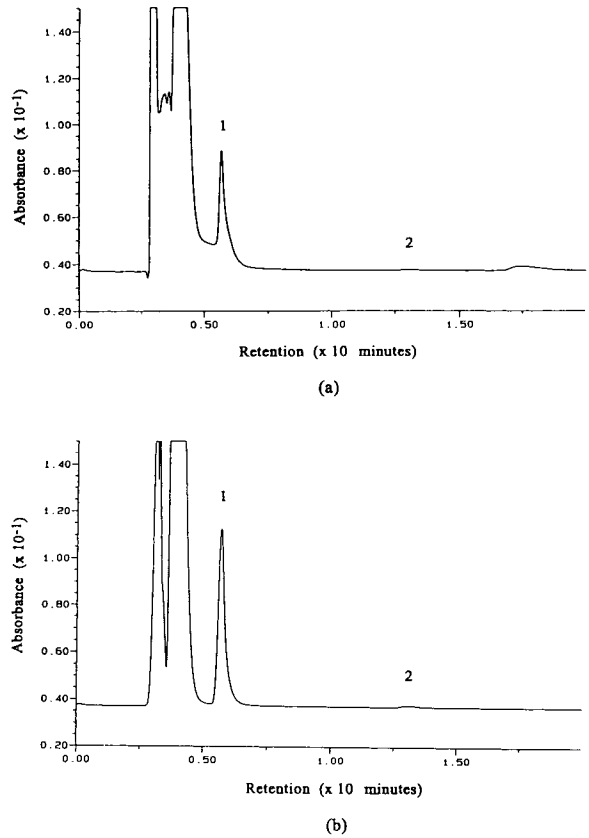

Fig. 2. Chromatogram of ilmenite prepared by hydroxide fusion obtained using (a) direct injection and (b) cation-exchange pretreatment. Conditions as for Fig. 1, except solutes (original concentration): (a) 1 = thorium (465.6 μg/ml), 2 = uranium (13.4 μg/ml) and (b) 1 = thorium (238.7 μg/ml), 2 = uranium (7.4 μg/ml).

Table 2
Thorium and uranium concentrations in original mineral sand samples obtained using hydroxide fusion and cation exchange pretreatment

Sample	Thorium (μg/g)	Uranium (μg/g)
Ilmenite		
No pretreatment	195	9.8
Ion-exclusion cartridge	466	13.4
Accell cartridge	438	3.9
Synthetic rutile		
Ion-exclusion cartridge	332	27.3
Zircon		
Ion-exclusion cartridge	21	ND

ND = Not detected.

digest procedures were then evaluated for use in conjunction with the pretreatment procedure. The cation-exchange pretreatment procedure was modified slightly with 2.0 *M* HIBA being used to elute the bound thorium and uranium from the ion-exclusion cartridge, instead of 7.5 *M* nitric acid. This approach gave similar recoveries to the nitric acid elution; however, it avoided the time consuming nitric acid evaporation step and also allowed the possibility for the pretreatment procedure to be automated. The final cation-exchange pretreatment procedure used is detailed under Experimental. The results obtained using a variety of fusion/digestion approaches for ilmenite, synthetic rutile and natural rutile samples prior to cation-exchange pretreatment and chromatographic analysis are detailed in Table 3.

The results indicated that an hydroxide fusion appeared to be appropriate for ilmenite samples, although it was not appropriate for other sample types. A tetraborate fusion procedure appeared to be appropriate for natural rutile, while carbonate–tetraborate, pyrosulphate and tetraborate–carbonate procedures all gave poor recoveries for this sample, particularly for uranium. The most significant differences between the first two procedures and the latter three was that TiO_2 was insoluble and precipitated from the acid solution to be filtered off with either of the first two approaches; however, it remained in solution when using the other fusion/digestion approaches. It appeared highly probable that the Ti(IV) cation in the digest solution was eluting the more weakly retained uranyl cation from the ion-exclusion cartridge during the sample loading step, resulting in low uranium recoveries. This was confirmed by the fact that ICP-MS analysis of the four natural rutile digests shown in Table 3 all yielded similar results for thorium and uranium, indicating that the solutes were being released into the fusion/digestion solutions, but that the chromatographic recoveries obtained after the pretreatment procedure depended upon the dissolution method used.

Table 3
Thorium and uranium concentrations in the original samples obtained using various fusion/digest procedures and cation-exchange pretreatment prior to chromatographic analysis

Sample	Thorium (μg/g)	Uranium (μg/g)
Ilmemite		
Hydroxide fusion	466	13.4
Tetraborate–carbonate fusion	314	ND
Synthetic rutile		
Tetraborate–carbonate fusion	332	ND
Natural rutile		
Tetraborate–carbonate fusion	56.4	25.3
Tetraborate fusion	62.0	53.1
Pyrosulphate fusion	63.4	11.1
Carbonate–tetraborate fusion	47.7	4.9

ND = Not detected.

The tetraborate fusion/nitric acid digestion procedure appeared to be the most appropriate for all the sample types and was further evaluated for use in conjunction with the cation-exchange procedure. All the mineral sand types were prepared using the tetraborate fusion/nitric acid digestion procedure after which the samples were treated using the cation-exchange pretreatment procedure described under Experimental. The results of the chromatographic analysis, together with the XRF results, are shown in Table 4. The ilmenite sample was fused/digested twice and the natural rutile sample was fused/digested five times, hence the multiple entries in the table for these samples. Fig. 3a–d show chromatograms obtained of the four mineral sand types prepared using the tetraborate fusion/nitric acid digestion and cation exchange pretreatment. The ilmenite and synthetic rutile chromatograms are shown at an injection volume of 200 μl in order to clearly highlight the uranium peak, although the thorium in these two sample types was typically quantitated using a 25–50-μl injection. Considering the differences between the two methods of analysis, the results showed remarkably good agreement. Analysis of the natural rutile digest by ICP-MS gave results for thorium and uranium of 69 and 48 μg/ml respectively, which compared very well to the average results obtained by IC of 60.6 μg/ml

Table 4
Thorium and uranium concentrations in the original samples obtained using tetraborate fusion/nitric acid leach and cation exchange pretreatment prior to chromatographic analysis

Sample	IC		XRF[a]	
	Thorium (μg/g)	Uranium (μg/g)	Thorium (μg/g)	Uranium (μg/g)
Ilmenite	487	15.0	490	10
	462	12.9		
Synthetic rutile	382	12.8	430	15
Zircon	167	184	179	217
Natural rutile	63.0	47.4	53	54
	59.4	48.9		
	59.1	49.6		
	59.5	49.9		
	62.0	53.1		

thorium (2.9% R.S.D.) and 49.8 μg/ml uranium (4.2% R.S.D.).

3.3. Direct sample injection

The cation-exchange pretreatment described above effectively isolated the thorium and uranium from the fusion/digest matrix in a HIBA solution before injection into the liquid chromatograph. The procedure could no doubt have been automated by addition of a sample enrichment pump and six-port column switching valve to the system, in a similar fashion to the preconcentration of thorium and uranium on a HIBA-enriched C_{18} cartridge [14]. The analysis of samples using a direct injection approach would be preferable to the cation-exchange pretreatment; however, as discussed previously, this would require a very large dilution which was impractical at the thorium and (particularly) uranium concentrations present in the original mineral sands. The success of the cation-exchange pretreatment nevertheless indicated that if the thorium and uranium could be fully coordinated with HIBA in the digest solution, then direct injection of the sample would be possible. As the chromatographic detection limits for the thorium and uranium were 3.0 and 5.0 ng/ml, respectively, using a 1000-μl injection, it was decided to attempt quantitation of the tetraborate fusion/nitric acid digest solutions by direct injection after dilution in HIBA.

The digestion solutions were diluted a further 1:10 and HIBA added to contain a final concentration of 400 m*M* before injection into the liquid chromatograph. Injection volumes of 1000 μl were required for uranium quantitation in ilmenite and synthetic rutile, while a 250-μl injection was used to quantitate thorium in these samples. Both thorium and uranium could be quantitated in zircon and natural rutile samples after a 500-μl injection. Table 5 summarizes the results and precision obtained by IC using the direct injection/HIBA dilution method and Fig. 4 shows a typical chromatogram obtained for a zircon sample (*i.e.* compare to Fig. 3c obtained using the cation-exchange pretreatment). The results showed excellent agreement to those obtained using the cation-exchange pretreatment, although the precision was generally not as high, particularly for the two cations in the natural rutile sample and also uranium in the ilmenite and synthetic rutile, as these solutes were being detected at concentrations approaching the method detection limits. Also, the direct injection approach was not as robust as the cation-exchange procedure as significant increases in the acid concentration of the fusion/

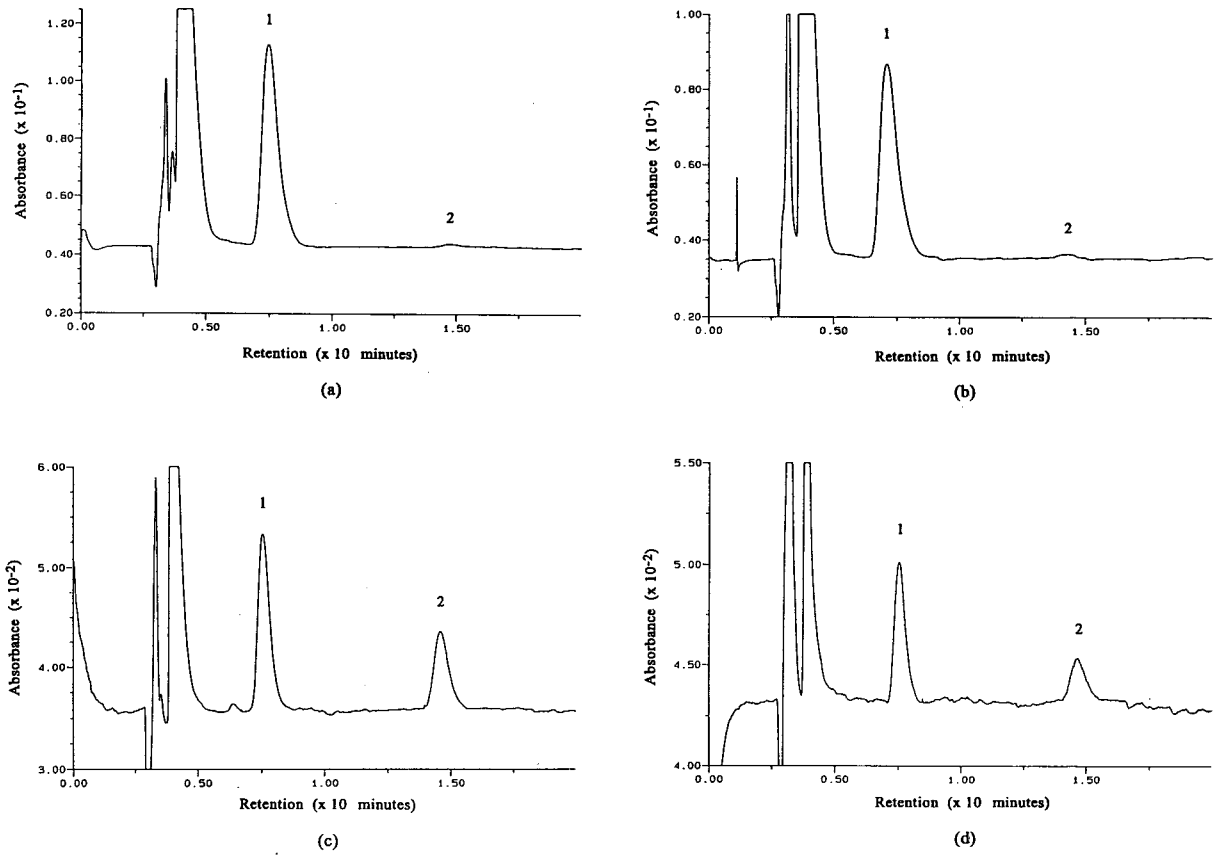

Fig. 3. Chromatograms of ilmenite (a), synthetic rutile (b), zircon (c) and natural rutile (d) prepared by tetraborate fusion/nitric acid digestion and cation-exchange pretreatment. Conditions as for Fig. 1, except injection volume: 200 μl for (a), 200 μl for (b), 100 μl for (c) and 100 μl for (d); solutes (original concentration): (a) 1 = thorium (462.4 μg/ml), 2 = uranium (12.9 μg/ml), (b) 1 = thorium (381.6 μg/ml), 2 = uranium (12.8 μg/ml), (c) 1 = thorium (167.2 μg/ml), 2 = uranium (184.2 μg/ml) and (d) 1 = thorium (59.4 μg/ml), 2 = uranium (48.9 μg/ml).

Table 5
Thorium and uranium concentrations in the original samples obtained using tetraborate fusion/nitric acid leach and direct injection after dilution in HIBA

Sample	Thorium (μg/g)	Uranium (μg/g)
Ilmenite	493 (0.4% R.S.D.)	18.3 (8.1% R.S.D.)
Synthetic rutile	382 (0.5% R.S.D.)	8.4 (10.0% R.S.D.)
Zircon	171 (2.13% R.S.D.)	199 (1.6% R.S.D.)
Natural rutile	68.6 (7.4% R.S.D.)	46.9 (9.2% R.S.D.)

R.S.D. obtained from five replicate injections.

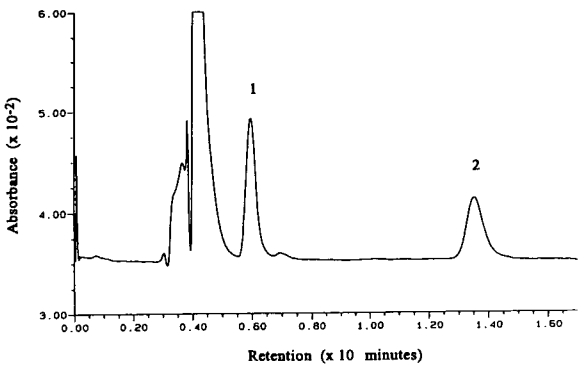

Fig. 4. Chromatogram of zircon prepared by tetraborate fusion/nitric acid digestion and direct injection/HIBA dilution method. Conditions as for Fig. 1, except injection volume: 500 μl; solutes (original concentration): 1 = thorium (167.2), 2 = uranium (195.8 μg/ml).

digestion solution resulted in low recoveries for both thorium and uranium.

4. Conclusions

Thorium and uranium can be analyzed in mineral sands by IC using a C_{18} reversed-phase column and an eluent of hydroxyisobutyric acid followed by post-column derivatization with Arsenazo III and visible detection at 658 nm. Sample preparation involved a tetraborate fusion/nitric acid leach followed by either cation-exchange pretreatment or direct injection after dilution in concentrated hydroxyisobutyric acid. The cation-exchange pretreatment resulted in higher precision and could be applied to more acidic sample digests; however, the direct injection approach gave comparable results when using the recommended dissolution procedure and offered significant time savings. The results obtained using the chromatographic method showed excellent agreement with those generated using the significantly more costly techniques of XRF and ICP-MS for ilmenite, synthetic rutile, zircon and rutile mineral sands.

5. Acknowledgements

The authors wish to thank Ian Gough for supplying the mineral sand samples, digestion procedures and the XRF and ICP-MS results; also Tony Cliffe, Tim Bowser, Mike Dowling, Roy Day and Gillian Whitney for helpful discussions.

6. References

[1] L.S. Clesceri, A.E. Greenberg and R.R. Trussell (Editors), *Standard Methods for the Examination of Water and Wastewater*, American Public Health Association, Washington, DC, 17th ed., 1989.
[2] T. Honda, T. Oi, T. Ossaka, T. Nozaki and H. Kakihana, *J. Radioanal. Nucl. Chem.*, 139 (1990) 65.
[3] Y. Igarashi, C.K. Kim, Y. Takatu, K. Shiraishi, M. Yamamoto and N. Ikeda, *Anal. Sci.*, 6 (1990) 157.
[4] A.G. Adriaens, J.D. Fassett, W.R. Kelly, D.S. Simons and F.C. Adams, *Anal. Chem.*, 64 (1992) 2945.
[5] P. Robinson, N.C. Higgins and G.A. Jenner, *Chem. Geol.*, 55 (1986) 121.
[6] M.P. Harrold, A. Siriraks and J. Riviello, *J. Chromatogr.*, 602 (1992) 119.
[7] R.M. Cassidy, *Chem. Geol.*, 67 (1988) 185.
[8] A. Mazzucotelli, A. Dadone, R. Frache and F. Baffi, *J. Chromatogr.*, 349 (1985) 137.
[9] R.M. Cassidy, S. Elchuk, N.L. Elliot, L.W. Green and B.M. Recoskie, *Anal. Chem.*, 58 (1986) 1181.
[10] C.H. Knight, R.M. Cassidy, B.M. Recoskie and L.W. Green, *Anal. Chem.*, 56 (1984) 474.
[11] A. Kerr, W. Kupferschmidt and M. Attas, *Anal. Chem.*, 60 (1988) 2729.
[12] R.M. Cassidy, S. Elchuk, L.W. Green, C.H. Knight, F.C. Miller and B.M. Recoskie, *J. Radioanal. Nucl. Chem.*, 139 (1990) 55.
[13] S. Elchuk, K.I. Burns, R.M. Cassidy and C.A. Lucy, *J. Chromatogr.*, 558 (1991) 197.
[14] H. Fuping, P.R. Haddad, P.E. Jackson and J. Carnevale, *J. Chromatogr.*, 640 (1993) 187.
[15] J.-M. Hwang, J.-S. Shih, Y.-C. Yeh and S.-C. Wu, *Analyst*, 106 (1981) 869.
[16] E.A. Jones, H.S. Bezuidenhout and J.F. van Staden, *J. Chromatogr.*, 537 (1991) 227.
[17] F.W.E. Strehlow, R. Rethemeyer and C.J.C. Bothma, *Anal. Chem.*, 37 (1965) 107.
[18] L. Imrie, *Z. Anorg. Chem.*, 164 (1927) 214.

ELSEVIER

Journal of Chromatography A, 671 (1994) 193–196

JOURNAL OF CHROMATOGRAPHY A

Determination of organic acids by ion chromatography in rain water in the State of Zulia, Venezuela

José A. Morales*[,a], Hilda L. de Medina[a], Marlene G. de Nava[a], Harvi Velásquez[a], Magaly Santana[b]

[a]*Laboratorio de Química Ambiental, Departamento de Química, Facultad Experimental de Ciencias, Universidad del Zulia, Maracaibo 4011, Venezuela*

[b]*IVIC, Atmospheric Chemistry Laboratory, Apartado 21827, Caracas 1020-A, Venezuela*

Ion-exchange chromatography with a Dionex Model QIC system was used to identify and determine formic and acetic acid in event rains collected at the La Esperanza site (Zulia, Venezuela). Pyruvic acid was observed infrequently and always at very low concentrations. The method can be adapted for the routine determination of these acids, giving results in less than 12 min (only the chromatogram without column clean-up). A set of calibration graphs for mixed standards with different concentration ranges (0.5–80 μM) with a good linear regression ($R^2 = 0.9992$–1.0000) were used. The estimated limit of quantification was <0.2 μM for both acids. Replicate analyses of four different fractions of a certain sample taken and preserved with chloroform showed relatively good reproducibility (R.S.D. *ca.* 7%) for both acids, and the results were well within acceptable data quality limits. Both the absolute organic acid concentrations and the ratio of organic acid concentrations to inorganic acid concentrations were significantly lower in La Esperanza than those reported at other rural Venezuelan sites. Organic and inorganic anion balances revealed a low potential contribution (*ca.* 7%) of formic and acetic acid to the acidity of the rain (volume-weighted average pH = 4.1). In other rural Venezuelan sites these acids contributed over 60% to the free acidity.

1. Introduction

Organic acids have been observed in precipitation from both polluted and remote regions of the world. These acids may be emitted by stationary and/or mobile sources and are also formed in polluted air by chemical reactions including the reaction of ozone with olefins [1]. Biogenic emissions from vegetative sources have been suggested as important natural sources for formic and acetic acid [2].

Ion chromatography (IC) has been applied in the analysis of environmental samples [3] and, because of its high accuracy and reliability, chemically suppressed IC has recently been specified by the US Environmental Protection Agency (EPA) as the method of choice for the determination of ion composition in rainfall samples. There are numerous organic and inorganic acids present in precipitation samples and both acid types need to be determined accurately for proper accounting of atmospheric chemistry processes and precipitation ionic balances. The natural tendency is to develop a single method that can determine all the acids. However, to cover adequately all the common acids, the best

* Corresponding author.

0021-9673/94/$07.00
SSDI 0021-9673(94)00231-W

solution is to use a combination of gradient, isocratic and ion-exclusion methods [4] or with the use of capillary ion chromatographic analysis.

This paper describes an ion chromatographic method for the determination of organic acids in event rains, and reports the contribution of formic and acetic acid to the acidity of rain in a rural site of Zulia State, Venezuela.

2. Experimental

2.1. Sampling

Event rains ($n = 41$) were collected from November 1988 to November 1989 in a rural site (La Esperanza) located at the Lake Maracaibo Basin (Zulia State), *ca.* 100 km south and downwind of the El Tablazo Petrochemical complex and the city of Maracaibo.

The sample collector unit consisted of a large, square Plexiglas funnel, with a collecting area of 0.25 m^2, mounted 2 m away from the surface, and a 20-l polythylene bottle. The system was kept completely closed (free from contamination) and was opened only at the beginning of a rainfall event. A fraction of the rain samples was preserved with HPLC-grade $CHCl_3$ (3:500, v/v) in polythylene bottles and cooled to 4°C immediately after the rainfall to avoid biological degradation of organic acids. After each sampling, the container and funnel were thoroughly rinsed with distilled, deionized water. The conductivity of the final rinse was checked to ensure that all the sample was removed.

2.2. Reagents

High-purity reagents were used throughout together with Milli-Q-purified Water, deionized and then filtered through a 0.2-μm Whatman membrane. Standard solutions of the organic acids (formic, acetic and pyruvic) were prepared from their sodium salts (analytical-reagent grade; Fisher Scientific). A mixed 100 m*M* stock standard solution was prepared for each organic anion and preserved with $CHCl_3$. Calibration standards were prepared from a 1 m*M* mixed standard solution using a series of dilutions, and always with preservation with $CHCl_3$.

2.3. Equipment and operating conditions

The IC equipment used was a Dionex Model QIC equipped with an APM analytical pump, HPIC-AS4A separator and AMMS suppressor columns, a conductivity detector and a data processing system using a double-channel recorder to measure peak height. The APM continuously pumps the eluent through the whole system. High-performance ion chromatographic (HPIC) guard columns are used primarily to protect analytical columns. These columns filter particulate matter from the eluent and sample aliquots. The fibre suppressor contains a tubular cation-exchange membrane. Eluent passes through the inside of the membrane and dilute acid (5.0 m*M* H_2SO_4) regenerant solution flows counter-current to the eluent on the outside of the membrane. This type of suppressor can be operated continuously and does not require periodic regeneration. The suppressor column chemically converts the highly conductive species of the eluent (1.5 m*M* $Na_2B_4O_7$) into the significantly less conductive, weakly ionized species $H_2B_4O_7$ (the background conductivity of the eluent can be reduced to a negligible level), resulting in increased detection sensitivity for the analytes.

After the system reaches equilibrium, a test sample is loaded and injected into the path of the eluent, which carries the sample into the highest efficiency separator column (S_4); here the anions are separated according to factors such as pK_a, eluent pH and resin type. The resin based consists of poly(styrene–divinylbenzene) copolymer and involves the use of low-capacity pellicular ion exchange on the bead surface.

The eluent anion ($B_4O_7^{2-}$) competes with the sample anions for the exchange sites of the resin. This causes the sample anions to move down the column at different rates and leave the column as separated peaks, and be detected by a conductivity detector. The detection signal is registered as peak height.

3. Results and discussion

3.1. Qualitative and quantitative analysis

The IC technique does not distinguish between undissociated and dissociated forms of organic acids and the values obtained correspond to the total undissociated and dissociated compounds ($AH + A^-$):

$$AH \rightleftharpoons A^- + H^+$$

$$[A]_{total} = [AH] + [A^-]$$

If the total concentrations of organic acids, their pK values and the pH of the sample are known, the levels of concentration of dissociated and undissociated acids can be calculated.

The organic acids commonly found in precipitation-related samples as reported in the literature are formic, acetic, propionic, lactic, pyruvic, etc. [4,5]. The resolution of analytes and the analysis time for a mixed standard solution and a sample of rainfall are shown in Fig. 1. As can be seen, the standard and unknown sample exhibit well defined resolution and symmetrical peaks (not broadened), giving results in less than 12 min. Peak identification was based on retention times.

Formic and acetic acid were the major organic acids found in the rainfall. Pyruvic acid was always observed at very low concentrations, and therefore the conditions were optimized for the determination of formic and acetic acid. A set of calibration graphs for mixed standards with different concentration ranges (0.5–80 μM) with a good linear regression ($R^2 = 0.9992$–1.0000) were used (Table 1). When, in an 8-h period, the standards were injected at 30-min intervals, no significant changes in gain (R.S.D. $< 2\%$) were observed, and therefore it was not necessary to run standards at frequent intervals.

In order to calculate the experimental error in the determination of the organic acids, in the rain event E_{41} four fractions were taken and preserved with chloroform. The analysis of these fractions showed relatively good reproducibility (R.S.D. $\approx 7\%$) for both organic acids, and therefore the results were well within acceptable data quality limits. The calculated limit of quantification was <0.2 μM for both acids.

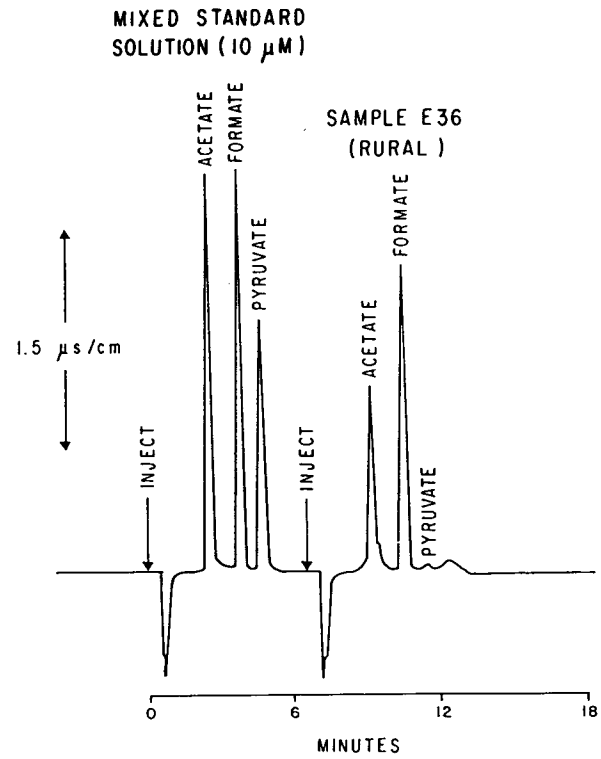

Fig. 1. Chromatogram of organic acids for a sample of precipitation from La Esperanza, Venezuela, and for a standard solution.

Table 1
Calibration graphs (formate + acetate)

Standard solution (μM)	Formate	Acetate
0.5; 1; 3; 5; 10 (scale: 1 μs)	$y = 23.2x - 2.8$ ($R^2 = 1.0000$)	$y = 22.3x + 5.9$ ($R^2 = 0.9998$)
10; 15; 20; 30 (scale: 3 μs)	$y = 7.1x + 0.8$ ($R^2 = 1.0000$)	$y = 6.6x + 8.5$ ($R^2 = 0.9997$)
30; 40; 60; 80 (scale: 10 μs)	$y = 1.8x + 8.0$ ($R^2 = 0.9994$)	$y = 1.2x + 14.5$ ($R^2 = 0.9992$)

y = Peak height (mm); x = concentration (μM).

3.2. Organic acid concentrations

In general, the ionic concentration in rainfall is inversely proportional to the volume. The volume-weighted average concentration (VWAC) homogenizes the low-precipitation events with high ionic concentrations and the high-precipitation events with dilute concentrations. The equation used for calculating the VWAC is

$$\text{VWAC (x)}_i = \frac{\sum_{i=1}^{n} P_i[\text{x}]_i}{\sum_{i=1}^{n} P_i}$$

where $[\text{x}]_i$ = ionic concentration of the event rain i (μM) and P_i = amount of rainfall i (mm).

The VWACs of formic and acetic acid in rain water at the La Esperanza site were lower than those reported at other Venezuelan rural sites (Table 2). The highest levels (up to 34.4 μM for acetic and 24.4 μM for formic acid) were obtained at the beginning of the rainy season (April and May) when the vegetation is beginning to grow and flower. This may indicate a possible biological source of these acids in the atmosphere. Organic and inorganic anion balances revealed a low contribution (*ca.* 7%) of these acids to the acidity of the rain (93% is due to inorganic acids [6], and the volume-weighted average pH is 4.1). In other rural sites these organic acids contributed over 60% to the free acidity [7].

It seems clear that, in La Esperanza, the higher contributions of inorganic acids, mainly H_2SO_4 [6], can be attributed in part to anthropogenic activities. The monitoring site is downwind of potentially important SO_2 and NO_x sources: the Cardon–Amuay and probably Aruba–Curacao refineries, the El Tablazo Petrochemical complex and the city of Maracaibo (*ca.* $2 \cdot 10^6$ inhabitants). In contrast, the eastern Venezuelan savannah region is virtually unaffected by anthropogenic emissions, natural sources being responsible for the acidity of its rains. Comparisons between precipitation in impacted and remote regions indicate that, although possibly important near large population and industrial centres, anthropogenic emissions are probably not major sources for organic acids in precipitation over broad geographic regions [2].

Table 2
Volume-weighted average concentrations of formic and acetic acid in Venezuela rural rains

Location	Formic acid (μM)	Acetic acid (μM)
La Esperanza[a]	4.4	5.5
Guri [7]	6.6	4.3
Chaguaramas [7]	8.5	7.8
La Paragua [7]	9.3	9.5

[a] This work ($n = 41$).

4. Acknowledgements

The Council for Human and Scientific Development (CONDES) of the University of Zulia is thanked for its financial support. John Jennings is acknowledged for revision of the English manuscript.

5. References

[1] D. Grosjean, *Environ. Sci. Technol.*, 23 (1989) 1506.
[2] W.C. Keene and J.N. Galloway, *J. Geophys. Res.*, 91 (1986) 14466.
[3] W.T. Frankenberger, Jr., *J. Chromatogr.*, 504 (1990) 211.
[4] V. Cheam, *Analyst*, 117 (1992) 1137.
[5] W.C. Keene, J.N. Galloway and J.D. Holden, Jr., *J. Geophys. Res.*, 88 (1983) 5122.
[6] J.A. Morales and C. Bifano, in S.E. Schwartz and W.G.N. Slinn (Editors), *Proceedings of the 5th International Conference on Precipitation Scavenging and Atmosphere–Surface Exchange Processes, Richland, WA, July 15–19, 1991*, Hemisphere, 1992, p. 1449.
[7] E. Sanhueza, M.C. Arias, L. Donoso, N. Graterol, M. Hermoso, I. Marti, J. Romero, A. Rondón and M. Santana, *Tellus*, 44B (1992) 54.

ELSEVIER

Journal of Chromatography A, 671 (1994) 197–203

JOURNAL OF CHROMATOGRAPHY A

Ion chromatography with UV detection for the determination of thiosulfate and polythionates in saline waters

S.I. Weir*[,a], E.C.V. Butler[b], P.R. Haddad[c]

[a]*Institute of Antarctic and Southern Ocean Studies, University of Tasmania, Hobart, Tasmania, Australia*
[b]*CSIRO Division of Oceanography, Marine Laboratories, GPO Box 1538, Hobart, Tasmania 7001, Australia*
[c]*Department of Chemistry, University of Tasmania, Hobart, Australia*

Abstract

A high-performance liquid chromatographic method was developed for the determination of the sulfur oxy-anions, thiosulfate and polythionates, in natural saline waters. This method utilises preconcentration techniques to effectively enrich the analytes whilst discriminating against the high chloride concentrations present, and is based on the novel combination of an ion-exchange pre-column in succession with a reversed phase analytical column and an eluent based on a water–acetonitrile mixture containing tetrabutylammonium ions and carbonate buffer. The limit of detection is 1 n*M* for trithionate and 0.3 n*M* for tetrathionate and pentathionate when concentrating 6 ml of 1:50 diluted seawater. The method has a precision of 0.25% for concentrations of 1 μM. Analysis time is approximately 30 mins.

1. Introduction

The analysis of mixtures of sulfur oxyanions in aqueous solution is a valuable and necessary tool for investigating the chemistry of sulfur-rich waste water effluents such as mining and milling wastes, oil-shale retort wastes, paper and pulp wastes, and acid-mine drainage. Hydrochemical processes also involve mixtures of dissolved sulfur species in various oxidation states, *e.g.*, redox processes in sulfur-rich ground waters and geothermal waters, pyrite oxidation in alkaline waters and sulfur oxidation in soils [1].

The sulfur oxy-anions thiosulfate ($S_2O_3^{2-}$) and the polythionates ($S_nO_6^{2-}$) are important intermediates in aquatic biogeochemical processes such as the oxidation of elemental sulfur and reduced sulfur species. Thiosulfate is also a common product of the inorganic oxidation of sulfide ions and iron sulfides, as well as the disproportionation of bisulfite and sulfite ions. Both thiosulfate and polythionates are oxidised or reduced by several groups of bacteria [2].

The study and quantitation of these compounds can provide clues to determine the rates and pathways of chemically and biologically mediated sulfur transformations in aquatic systems. A convenient technique for the determination of these compounds is ion chromatography, in particular the use of reversed phase columns with ion-interaction reagents [3–6]. Of the procedures developed, however, none are

* Corresponding author. Present address: CSIRO Division of Oceanography, Marine Laboratories, GPO Box 1538, Hobart, Tasmania 7001, Australia.

0021-9673/94/$07.00
SSDI 0021-9673(93)E1132-J

directly applicable to the analysis of these compounds in saline waters. Interference from the high concentrations of chloride in the sample is the problem. This paper describes a method of analysis for thiosulfate and polythionates in saline waters.

2. Materials and methods

2.1. Instrumentation

The ion chromatographic system was composed of an ETP Kortec K35D HPLC pump, a Rheodyne 7125 injector with a 200-μl sampling loop and a SPD-10AV Shimadzu UV–Vis spectrophotometric detector. Samples for preconcentration were loaded onto the precolumn by way of a Rheodyne 7000 six-port switching valve which was operated manually. The analytical column was a Hamilton PRP-1 reversed-phase column, 10 μm particle size (150 × 4.1 mm) and was protected by a Brownlee PRP-1 guard cartridge (PRP-GU, 30 × 4.6 mm) in a Brownlee 30 mm MPLC cartridge holder. The precolumn used for sample preconcentration was a Waters IC-PAK, 10 μm particle size (5.0 × 6.0 mm) housed in Waters Guard-Pak precolumn module. Chromatograms were displayed on a Yew type 3056 dual-pen recorder; the detector output was also fed, via an analog-to-digital interface, to an IBM-style personal computer for processing with integration and data analysis software (DAPA SCIENTIFIC PTY LTD, Kalamunda, Australia).

2.2. Reagents

The mobile phases used for ion-interaction separations comprised water treated with three-cartridge Milli-Q water purification system, acetonitrile (ACN), Waters low-UV PIC-A ion-interaction reagent, sodium carbonate, sodium hydrogencarbonate and sodium chloride. Eluents were prepared by diluting the acetonitrile (expressed as a percentage of total volume[a]), ion-interaction reagent, buffers and sodium chloride with Milli-Q water to volume. Eluent was filtered through a 0.45-μm membrane filter and degassed by ultra-sonicating under vacuum. Stock solutions of thiosulfate and polythionates were prepared by dissolution of an accurately weighed amount of salt in Milli-Q water. Analytical-grade sodium thiosulfate was obtained from Ajax Chemicals, sodium tetrathionate dihydrate was obtained from Fluka. Potassium trithionate and potassium pentathionate were synthesised [7].

2.3. Chromatographic procedures

General procedure: All chromatographic separations were carried out at room temperature (20 ± 2°C) using an eluent flow-rate of 0.5 ml/min. Dilute standard solutions prepared in eluent were injected directly onto the column. Analytical and concentrator columns were equilibrated with eluent. Equilibration was established when a steady baseline was observed and retention of a standard solution was reproducible. Detector wavelength was set at 205 nm.

2.4. Sample pre-concentration

Pre-concentration of samples was carried out using a six-port switching valve (Fig. 1) with flow paths varied according to the following sequence.

(A) Equilibration of the columns. With both the concentrator column and the analytical column in the eluent flow path (INJECT position), eluent was pumped through the system at 0.5 ml/min.

(B) Loading sample onto concentrator column. The switching valve was rotated to place the concentrator column off line while the analytical column remained in the eluent flow path (LOAD position). The sample volume was then loaded, followed by a wash step.

(C) Elution of sample from concentrator column. The switching valve was rotated to the position used in A above and solutes were eluted

[a] Reference to % modifier as ACN–water (20:80) indicates 200 ml of ACN made up to 1000 ml with Milli-Q water.

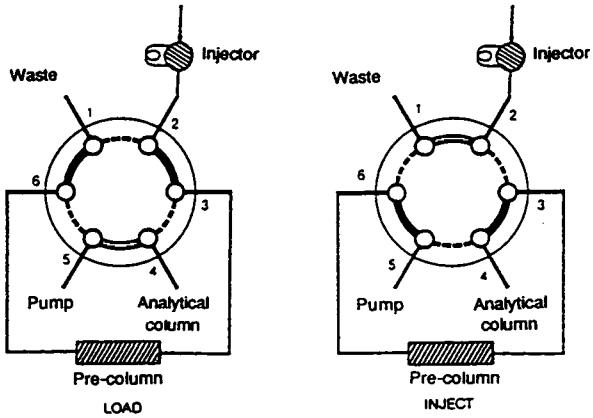

Fig. 1. Switching valve showing the load and inject positions.

from the concentrator column and carried to the analytical column for subsequent separation.

3. Results and discussion

3.1. Initial experiments

The chromatographic conditions selected to achieve the resolution of thiosulfate and polythionates ($n = 3$–5) were based on those used by Steudel and Holdt, [4] and were as follows; acetonitrile–water (25:75), 1.5 m*M* low-UV PIC-A, 0.3 m*M* sodium carbonate and 0.3 m*M* sodium hydrogencarbonate. Before proceeding with the sample preconcentration approach, the existing direct injection ion-interaction method was modified to maximise sensitivity for the separation of thiosulfate and polythionates (Fig. 2).

3.2. Choice of ion-pair reagent

One of the key eluent parameters that governs retention is the length of the carbon chains on the ion-interaction reagent (IIR). In general, as the carbon chain number increases, retention of the R_4N^+ salt increases [8]. Three alkyl chain lengths were tested, tetrapropylammonium (TPrA), tetrabutylammonium (TBA) and tetrapentylammonium (TPeA) all with the phosphate counter anion. Initial experiments using 1.5 m*M* $TPeA \cdot PO_4$ exhibited a capacity factor at least twice that observed with $TBA \cdot PO_4$, thus making $TPeA \cdot PO_4$ undesirable as an ion-pair reagent for the polythionates under the conditions used. Further experiments using $TPrA \cdot PO_4$

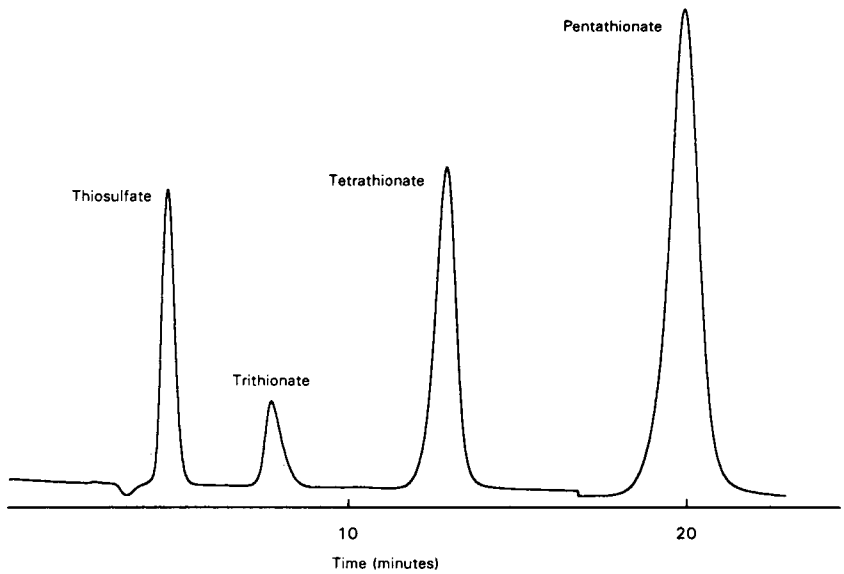

Fig. 2. Injection of 200 μl of a mixed standard of 10 μM of thiosulfate, trithionate, tetrathionate and pentathionate. Column: Hamilton PRP-1, reversed phase 5 μm particles, 150 × 4.1 mm. Eluent: ACN–water (25:75), 1.5 m*M* low-UV PIC-A, 0.6 m*M* carbonates. Detection: 205 nm, 0.04 AUFS.

were also unsuccessful, an eluent of 1.5 m*M* TPrA · PO_4 in ACN–water (28:72) gave little retention, with the early species eluting with the solvent front. Thus the TBA · PO_4 proved to be the most effective IIR for the separation of thiosulfate and the polythionates under the conditions used.

Effects of the counter ion have been described by Iskandarani and Pietrzyk [8]. Comparison of the TBA · OH, TBA · Ac and Waters low-UV PIC-A (incorporating TBA–HSO_4) found all to be suitable for separation with slight alteration of conditions. However, low-UV PIC-A was the most suitable because of the lower background absorption of this reagent at 205 nm.

Although PIC-A was determined to be the most suitable IIR for this study, previous studies using the IIR tetrabutylammonium acetate found it to satisfactorily separate the analyte species in the presence of chloride within a shorter retention time. The hygroscopic nature of this reagent however limited its use for precise eluent preparation.

3.3. On-column matrix elimination

In contrast to the specific methods of matrix elimination whereby matrix ions are reduced or removed prior to analysis using pre-columns or membranes, a more general approach described as on-column elimination [9,10] involves the use of the major matrix ion as the eluent. When this is done the column is effectively in the form of the matrix ion and therefore shows little or no retention of this anion when it is directly injected. Since the purpose of these studies was to find chromatographic conditions which tolerated high levels of chloride, it was necessary to employ a detection method which shows little response to this species. UV absorbance detection was well suited for this purpose.

Optimal eluent conditions were sought for the separation of the thiosulfate and polythionate anions using chloride as the matrix anion. On-column matrix elimination was shown to be effective in reducing the effects of direct injections of up to 0.1 *M* sodium chloride. A plot of log retention time *versus* log sodium chloride concentration included in the eluent, revealed

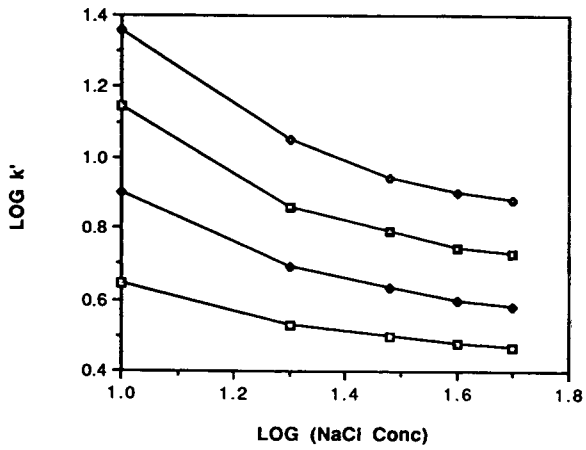

Fig. 3. Variation of solute retention with the concentration of chloride in the eluent. □ = S_2O_3; ◆ = S_3O_6; ■ = S_4O_6; ◇ = S_5O_6.

the optimal eluent to contain sodium chloride in the concentration range of 30–45 m*M* (Fig. 3).

The higher level of chloride included in the eluent (45 m*M*) would be expected to result in satisfactory separation of analytes in saline standard solution. However, a lower value was adopted to ensure solutes did not elute too close to the solvent front. The optimal eluent was therefore determined to be ACN–water (25:75), 1.5 m*M* low-UV PIC-A, 0.6 m*M* carbonates (3 m*M* sodium carbonate, 0.3 m*M* sodium hydrogencarbonate) and 35 m*M* NaCl. The chromatogram obtained with this eluent is shown in Fig. 4.

3.4. Pre-concentration

Eluent composition and concentrator column characteristics were selected to discriminate against the retention of chloride on the preconcentration column. The eluent is required to remove the analyte species from the pre-concentration column in minimum time, and as quantitatively as possible (*i.e.* 90% removal in 200 μl). In addition, analyte anions should elute late from the analytical column to facilitate ease of preconcentration.

Prior to preconcentration procedures, the eluent composition for optimum separation of analyte anions, thiosulfate and polythionates

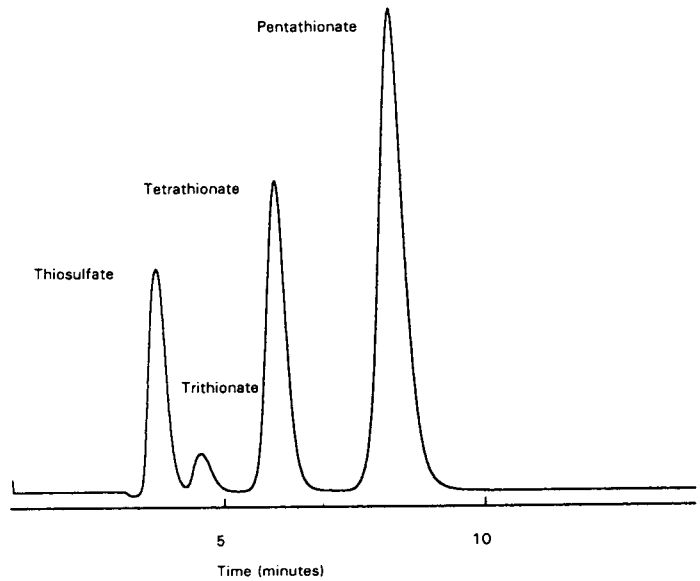

Fig. 4. Separation of a 200-μl injection of 10 μM of thiosulfate and the lower polythionates trithionate, tetrathionate and pentathionate. Column: Hamilton PRP-1, reversed phase 10 μm particles, 150 × 4.1 mm. Eluent: ACN–water (25:75), 1.5 mM low-UV PIC-A, 0.6 mM carbonates and 35 mM sodium chloride. Detection: 205 nm, 0.04 AUFS.

($n = 3$–5), was determined to be ACN–water (25:75), 1.5 mM low-UV PIC-A, 0.6 mM carbonates and 35 mM NaCl. Preliminary experiments showed the polythionate anions to be tightly bound to the ion exchange resin in the concentrator column when in the presence of chloride, with thiosulfate being less well retained. The eluent was therefore required to have a high eluting capacity in order to transfer the solute anions from the concentrator column, yet still retain the properties which enable effective separation and determination of the analyte anions on the analytical column. These eluent requirements were met by the addition of the UV transparent anion, perchlorate (ClO_4^-), the most effective counter ion at reducing retention times [11]. Reoptimisation of the eluent was therefore required and is summarised below:

(1) Addition of ClO_4^- was required to strip analytes from the pre-column; this change decreased the retention time for all species on the analytical column.

(2) In order to counteract the decreased retention times observed after the addition of the perchlorate anion, both the carbonate and the IIR concentrations were increased. This resulted in increased retention times for all species.

(3) The concentration of sodium chloride was decreased marginally to improve separation between trithionate and an early eluting broad peak. This modification also resulted in increased retention times for all species.

The optimised eluent which effectively stripped the analyte from the pre-column prior to successful separation on the analytical column was determined to be: ACN–water (25:75), 2 mM carbonates (1 mM Na_2CO_3, 1 mM $NaHCO_3$), 30 mM NaCl, 10 mM low-UV PIC-A and 3 mM $NaClO_4$. A typical chromatogram obtained for the preconcentration of 6 ml of a 1 μM mixed polythionate standard solution is given in Fig. 5.

Breakthrough experiments were performed in order to determine the length of time the solute ions, thiosulfate and trithionate, were held on the concentrator column, which in turn was influenced by the concentration of chloride ion present. There was no need to test the higher polythionates as they would be more effectively retained on the column than trithionate. Thiosul-

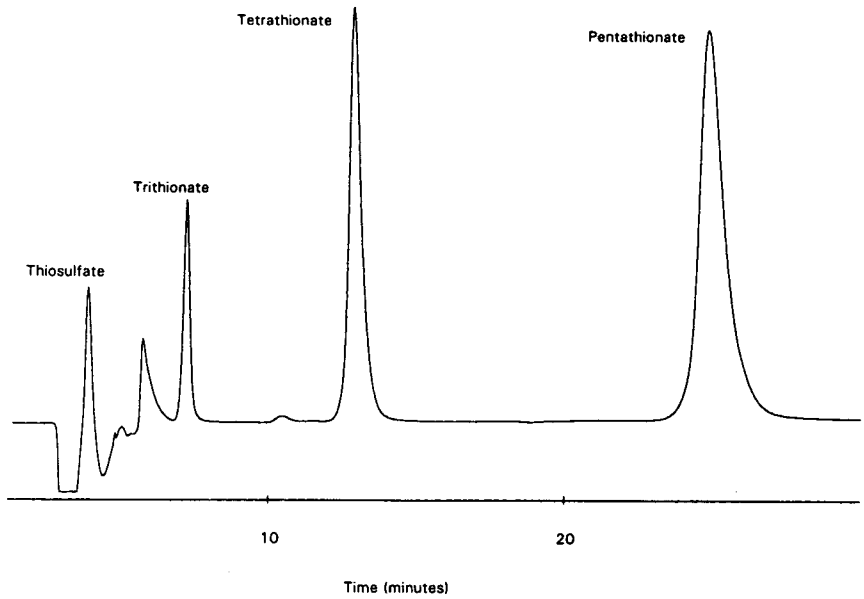

Fig. 5. Separation of a 6-ml sample of 1 μM of thiosulfate and the lower polythionates trithionate, tetrathionate and pentathionate. Column: Hamilton PRP-1, reversed phase 10 μm particles, 150 × 4.1 mm. Eluent: ACN–water (25:75), 10 mM low-UV PIC-A, 3 mM ClO_4^-, 30 mM NaCl, 2 mM carbonates. Detection: 205 nm, 0.05 AUFS.

fate showed significantly smaller breakthrough times than trithionate for the same concentration of sodium chloride. The optimum sodium chloride concentration for preconcentration, at which analytes could still be effectively retained on the concentrator column, was determined to be 0.01 M. Therefore sodium chloride solutions higher than this concentration would be required to be diluted to this level. Approximately 9.0 ml of sample can be injected before 2 mM trithionate breaks through the concentrator column. However, a considerably smaller volume can be injected if thiosulfate is still to be retained by the concentrator column due to the low affinity this species has for the resin packing.

Empirical trials were set up to investigate the following: (a) the volume of sample loaded onto the pre-column and (b) the type and volume of solution used in the wash step during sample loading, with the following results.

(a) The sample volume load employed for trial studies was 6.0 ml. This volume resulted in the successful determination of the polythionates ($n = 3$–5), however, the thiosulfate peak definition was lost in a large system peak, evident in Fig. 5.

(b) Trials utilising the following: no wash step, wash step using diluted sodium chloride solution, and wash step using Milli-Q water, found the latter to provide the best separation. The sodium chloride solutions served to mask the trithionate peak in the separation, while no wash step resulted in a peak approximately half the area of that peak obtained using the Milli-Q wash solution. The volume adopted for trial studies was 3.0 ml.

3.5. Performance characteristics

Precision was assessed by repeatedly injecting samples of the mixed standard solution, with each component at a concentration of 1 μM. For 20-μl injections, the relative standard deviation ($n = 6$) for the polythionates was 0.25%. The detection limit for trithionate was calculated to be 1 nM for a 6-ml sample volume of 0.01 M NaCl mixed standard loaded onto the precolumn (Detection limits were defined as two times baseline noise). Detection limits for tetrathionate and pentathionate were approximately three times more sensitive. While lower detection limits would be achievable with larger injection

volumes, this would be at the expense of thiosulfate which would be lost in the separation. Analytes were pre-concentrated by a factor of 10 (relative to direct injection) when a 6-ml volume sample was loaded.

4. Conclusions

An ion chromatography method was developed for the determination of the sulfur oxyanions, thiosulfate and polythionates, in saline waters. This method utilises preconcentration techniques to effectively enrich the analyte sample whilst discriminating against the high chloride concentrations present, and is based on the novel combination of an ion-exchange pre-column in succession with a reversed-phase analytical column and an eluent based on a water–acetonitrile mixture containing tetrabutylammonium ions and carbonate buffers. Baseline resolution of the polythionates ($n = 3$–5) was achieved in the elution order trithionate, tetrathionate and pentathionate in the presence of 0.01 *M* sodium chloride.

5. References

[1] C.O. Moses, D.K. Nordstrom and A.L. Mills, *Talanta*, 31 (1984) 331–339.
[2] J.O. Nriagu, R.D. Cocker and A.L.W. Kemp, *Limnol. Oceanogr.*, 24 (1979) 383–389.
[3] S.B. Rabin and D.M. Stanbury, *Anal. Chem.*, 57 (1985) 1130–1132.
[4] R. Steudel and G. Holdt, *J. Chromatogr.*, 361 (1986) 379–384.
[5] B. Takano and K. Watanuki, *Talanta*, 35 (1988) 847–854.
[6] B. Takano, M.A. McKibben and H.L. Barnes, *Anal. Chem.*, 56 (1984) 1594–1600.
[7] F. Feher, *Handbook of Preparative Inorganic Chemistry*, Vol. 1, Academic Press, New York, 2nd ed., 1975, pp. 397–402.
[8] Z. Iskandarani and D.J. Pietrzyk, *Anal. Chem.*, 54 (1988) 2427–2431.
[9] K. Ito and H. Sunahara, *J. Chromatogr.*, 502 (1990) 121.
[10] Marheni, P.R. Haddad and A.R. McTaggart, *J. Chromatogr.*, 546 (1991) 221–228.
[11] P.R. Haddad and P.E. Jackson, *Ion Chromatography: Principles and Applications*, Elsevier, Amsterdam, 1990, p. 177.

ELSEVIER

Journal of Chromatography A, 671 (1994) 205–209

JOURNAL OF CHROMATOGRAPHY A

Application of multi-dimensional liquid chromatography to the separation of some transition and heavy metals

I.N. Voloschik*, M.L. Litvina, B.A. Rudenko

V.I. Vernadsky Institute of Geochemistry and Analytical Chemistry, Russian Academy of Science, 19 Kosygin Street, 117975 Moscow, Russian Federation

Abstract

Multi-dimensional liquid chromatography was applied to the separation of the toxic metals Cd^{2+} and Pd^{2+} and other transition and heavy metals in sea, natural and waste waters to enhance the selectivity and determination sensitivity. The separation and determination of Cu^{2+}, Ni^{2+}, Co^{2+}, Mg^{2+}, Ca^{2+}, Sr^{2+} and Fe^{2+} were achieved on a dynamically coated sorbent column with conductimetric detection. After passing through the conductimetric cell, the eluate zones containing insufficiently separated components were withdrawn from the eluate flow and injected into a second ion chromatographic system. Complete separation of Pb^{2+}, Zn^{2+}, Mn^{2+} and Cd^{2+} was achieved on this second column filled with a chelate sorbent containing iminodiacetate groups. UV detection with postcolumn reaction with 4-(2-pyridylazo)resorcinol was used in the second system.

1. Introduction

The development of new ion chromatographic (IC) techniques for the separation and determination of metals in natural, waste and industrial waste waters is an important task. Transition and heavy metals are toxic when their concentrations in water exceed certain values. The most toxic heavy and transition metals are Hg^{2+}, Cu^{2+}, Pb^{2+}, Cd^{2+}, Cr^{3+}, Zn^{2+} and Ni^{2+} and the most toxic alkaline earth metals are Be^{2+}, Ba^{2+} and Sr^{2+}.

In some instances, isocratic IC separation is not achieved for multi-component mixtures of these metals. In order to increase the selectivity of separation of metals with a similar sorption properties and to eliminate interferences by macro-components (*e.g.*, Mg^{2+} and Ca^{2+} in sea water), we used the method of multi-dimensional chromatography.

2. Experimental

A Hewlett-Packard Model 1084A liquid chromatograph with two high-pressure pumps and a spectrophotometric detector was used. A Rheodyne (Berkeley, CA, USA) sample injector, a high-pressure switching valve equipped with a 100-μl loop, combined with iminodiacetate (IDA)-containing sorbent-packed cartridge (3×3 mm I.D.); and a conductimetric detector were included in the multi-dimensional chromatographic scheme. Postcolumn reaction with 4-(2-pyridylazo)resorcinol (PAR) [1] was performed with an additional low-pressure pump. The analytical columns used were 100×3 mm I.D. filled with 7.5-μm Silasorb C_{18} (Tessek,

* Corresponding author.

0021-9673/94/$07.00
SSDI 0021-9673(94)00203-L

Prague, Czech Republic), 150 × 3 mm I.D. filled with a chelating sorbent with IDA groups (Elsiko, Russian Federation) and 50 × 3 mm I.D. packed with chelating Amidoxim sorbent containing amidoxime groups (Elsiko). All chemicals were of analytical-reagent grade and purified water obtained using a Milli-Q apparatus (Millipore) was used throughout.

3. Basis of multi-dimensional chromatography

This method was applied previously in IC for the determination of organic and inorganic anions [2–5]. Multi-dimensional chromatography is named by analogy with planar chromatography, where the components of the mixture are separated in consecutive order by two different eluents in different dimensions to increase the selectivity.

Fig. 1 shows a scheme of the multi-dimensional IC device and Fig. 2 shows an example of its application. As can be seen from Fig. 2, neither

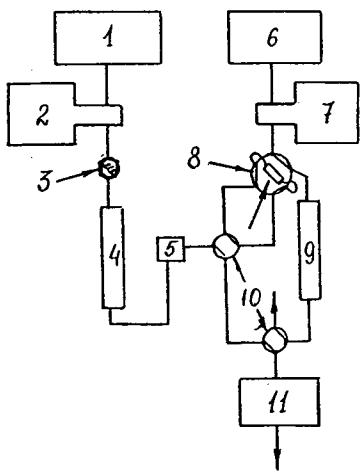

Fig. 1. Schematic diagram of multi-dimensional ion chromatographic system. 1 = Eluent 1; 2 = pump 1; 3 = injector 1; 4 = separation column 1; 5 = conductimetric detector; 6 = eluent 2; 7 = pump 2; 8 = injector 2 with precolumn; 9 = separation column 2; 10 = switching valves; 11 = UV–Vis detection system including postcolumn reaction with PAR.

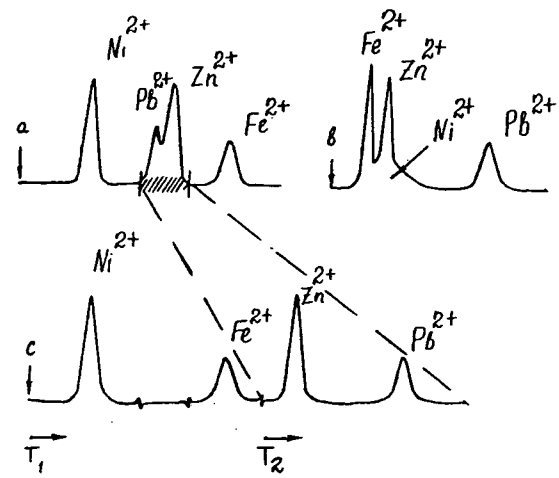

Fig. 2. Example of application of the multi-dimensional IC scheme. (a) Metal separation on column 1 in isocratic regime; (b) metal separation on column 2 in isocratic regime; (c) metal separation according to the multi-dimensional IC scheme. T_1 = Time of separation on column 1; T_2 = time of separation on column 2.

of the two IC systems separates selectively all four components of a mixture of metals with isocratic elution. Pb^{2+} and Zn^{2+} ions are not selectively separated by the first system and Fe^{2+} and Zn^{2+} ions are not selectively separated from Ni^{2+} by the second system. However, the combination of these two chromatographic systems in the multi-dimensional method permits this problem to be solved. After separation on the first column and detection of the sufficiently separated components, the eluate zone containing poorly separated Pb^{2+} and Zn^{2+} is withdrawn from the eluate flow by the additional switching valve (Fig. 1). The withdrawn zone of the eluate passes to the preconcentration column via the injector of the second separation system. The second system selectively separates Pb^{2+} and Zn^{2+} ions. Thus all the components are selectively separated and determined by the combination of two chromatographic systems.

Our preliminary task was to devise isocratic IC systems for the selective separation of metals. The combination of such systems in the multi-

dimensional scheme was then applied to the analysis of metal mixtures

4. Results and discussion

There are two main approaches to IC separation of transition and heavy metals: in the form of their anionic complexes and in their cationic form. We performed the determination of heavy and transition metal anionic complexes with oxalate ion. The separation was carried out on the complexing sorbent Amidoxim, which has a silica gel-based matrix with amidoxime functional groups [6].

The metal–oxalate complexes were separated by ion-exchange and complexing mechanisms on this sorbent. The factors that influence the selectivity of metal separation were studied and the optimum conditions for the determination of transition and heavy metals were established. Fig. 3 illustrates the separation of metal mixtures under different conditions and shows that the Amidoxim sorbent can be used successfully for the determination of Cd^{2+}, Pb^{2+}, Zn^{2+}, Ni^{2+}, Co^{2+} and Cu^{2+}. The very strong retention of Fe^{2+} on this sorbent should be mentioned, as this eliminates the interference of iron on the determination of other metals.

The determination of metals in their cationic form on dynamically coated and chelating sorbents was studied. We used Silasorb C_{18} sorbent treated with dodecylbenzenesulphonic acid under static conditions as the dynamically coated sorbent, and chelating silica gel-based sorbent with IDA groups. For each sorbent the optimum conditions for the separation of the metals were found.

Fig. 4 shows the most rapid and selective separation of metals using the dynamically coated sorbent and ethylenediamine–citric acid–tartaric acid solution (pH 3.2) as the eluent. A high separation selectivity was achieved for most of the metals with the exception of the Pb^{2+}–Zn^{2+} and Mn^{2+}–Cd^{2+} pairs (for these pairs the cations have the same retention time).

The separation of metal cations using the

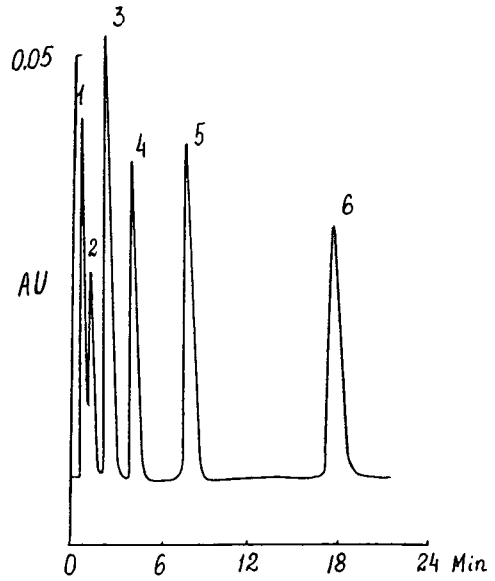

Fig. 3. Separation of transition metals on Amidoxim column. Column, 50 × 3 mm I.D., packed with Amidoxim sorbent; eluent, 5 m*M* oxalic acid; flow-rate, 1 ml/min (pH 2.2); detection, UV–Vis at 540 nm; postcolumn PAR reaction. Peaks: 1 = Cd^{2+}; 2 = Pb^{2+}; 3 = Co^{2+}; 4 = Zn^{2+}; 5 = Ni^{2+}; 6 = Cu^{2+}.

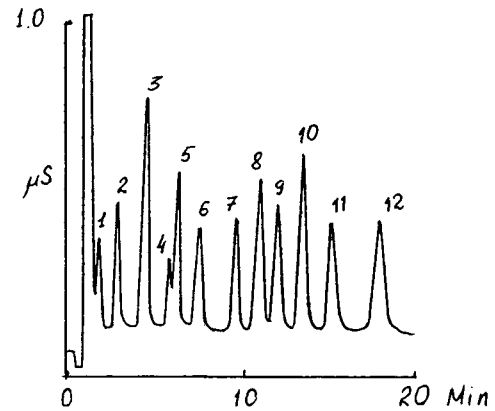

Fig. 4. Separation of transition and alkaline earth metals on dynamically coated column. Column, 100 × 3 mm I.D., packed with Silasorb C_{18}, coated with dodecylbenzenesulphonic acid; eluent, 2.5 m*M* ethylenediamine–2.5 m*M* citric acid–2.5 m*M* tartaric acid (pH 3.2); flow-rate, 1 ml/min; detection, conductimetric. Peaks: 1 = Fe^{3+}; 2 = Cu^{2+}; 3 = Ni^{2+}; 4 = Pb^{2+}; 5 = Zn^{2+}; 6 = Co^{2+}; 7 = Fe^{2+}; 8 = Mg^{2+}; 9 = Cd^{2+}; 10 = Ca^{2+}; 11 = Sr^{2+}; 12 = Ba^{2+}. Metal concentrations, 1–10 mg/l.

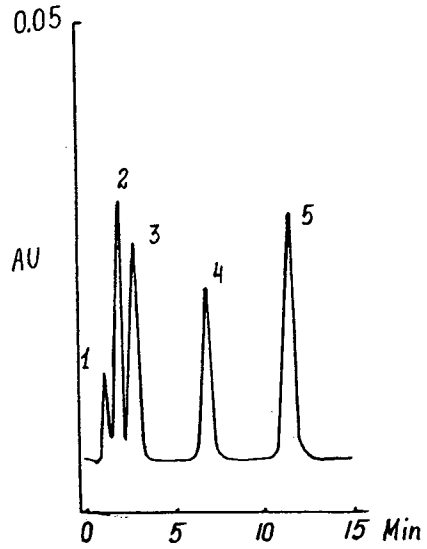

Fig. 5. Separation of transition metals on IDA-containing sorbent. Column, 150 × 3 mm I.D., packed with IDA sorbent; eluent, 15 m*M* oxalic acid–3 m*M* ethylenediamine (pH 2.8); flow-rate, 1 ml/min. Peaks: 1 = Fe^{2+}; 2 = Co^{2+}; 3 = Zn^{2+}; 4 = Cd^{2+}; 5 = Pb^{2+}.

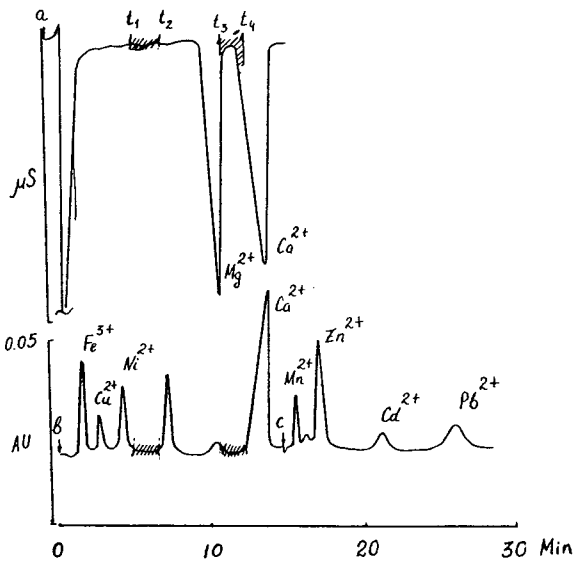

Fig. 6. Separation of metal mixtures using the multi-dimensional IC scheme. (a) Separation of metals on dynamically coated column. Conditions as in Fig. 4. t_1, t_2, t_3, t_4 = Times of valve switching; withdrawn zones of insufficiently separated metals are stained. (b) Separation of metals on dynamically coated column. Conditions as in Fig. 4. (c) Separation of metals on IDA column. Conditions as in Fig. 5.

IDA-based chelating sorbent [7] is shown in Fig. 5. This sorbent is well known for its high selectivity for the separation of heavy and transition metal cations. As Fig. 5 shows, the selective separation of Co^{2+}, Zn^{2+}, Cd^{2+} and Pb^{2+} was achieved, and macro amounts of Mg^{2+}, Ca^{2+} and Fe^{3+} did not interfere. Cu^{2+} and Fe^{3+} cations are very strongly retained on this sorbent.

The selectivity of the metal separations was evaluated for each chromatographic system studied. It was found that metals with similar sorption properties are present in each system, but for each system these metals are different. For this reason it was possible to arrange the multi-dimensional IC system for the simultaneous determination of heavy and transition metals according to the scheme is Fig. 1. The switching mechanism is interactive with the conductimetric detector (5 in Fig. 1) and the switching is done manually by the analyst.

Separations of multi-component metal mixtures are shown in Fig. 6. In this instance the separation selectivity was increased by combining the sample separation on the dynamically coated sorbent using an eluent consisting of ethylenediamine–citric acid–tartaric acid with a second separation of the selected eluate zone on the chelating IDA sorbent with an oxalic acid-containing eluent.

The analysis of an Azov sea water sample taken near a metallurgical plant using the multi-

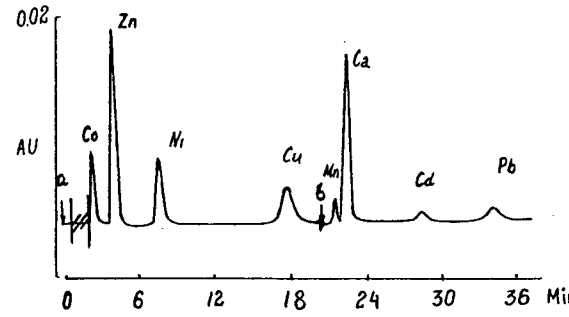

Fig. 7. Determination of transition metals in Azov sea water using multi-dimensional IC. (a) Separation on Amidoxim column, Conditions as in Fig. 3. (b) Separation on IDA column. Conditions as in Fig. 5. Withdrawn zones of insufficiently separated metals are shaded.

dimensional scheme is shown in Fig. 7. The metal concentrations in the sample were 0.005–0.05 mg/l.

The technique described has been demonstrated to be suitable for the determination of heavy, transition and some alkaline earth metals, and for the investigation of unknown samples by isocratic and multi-dimensional ion chromatography.

References

[1] N. Cardellicchio, S. Cavalli and J.M. Riviello, *J. Chromatogr.*, 640 (1993) 207.
[2] Th.B. Hoover and G.D. Yager, *Anal. Chem.*, 56 (1984) 221.
[3] A.A. Ivanov, I.N. Voloschik and O.A. Shpigun, *Zn. Anal. Khim.*, 44 (1989) 699.
[4] M. Muragama, M. Suzuki and S. Takitani, *J. Chromatogr.*, 466 (1989) 355.
[5] C. Umile and J.F.K. Huber, *J. Chromatogr.*, 640 (1993) 27.
[6] P.N. Nesterenko, T.I. Tihomirova, V.N. Fadeeva, I.B. Yuferova and G.V. Kudriavtsev, *Zh. Anal. Khim.*, 46 (1991) 1108.
[7] G. Bonn, S. Reiffenstuhl and P. Jandik, *J. Chromatogr.*, 499 (1990) 669.

ELSEVIER

Journal of Chromatography A, 671 (1994) 211–215

JOURNAL OF CHROMATOGRAPHY A

Short Communication

Automatic monitoring system for acid rain and snow based on ion chromatography

K. Oikawa*[,a], K. Murano[b], Y. Enomoto[c], K. Wada[d], T. Inomata[e]

[a]*Niigata College of Pharmacy, 5-3-12 Kamisinei-cho, Niigata 950-21, Japan*
[b]*National Institute for Environmental Studies, 16-2 Onogawa, Tukuba 305, Japan*
[c]*Sibata Scientific Technology Ltd., 3-1-25, Ikenohata Taito-ku, Tokyo 110, Japan*
[d]*Nippon Dionex Co., Ltd., 1-2-3 Iriya Taito-ku, Tokyo 110, Japan*
[e]*Yokogawa Analytical Systems Inc., 1-16-10 Nakamachi, Musasino, Tokyo 160, Japan*

Abstract

In order to investigate the mechanism of acid precipitation formation, its relationship with meteorological conditions and the source of pollutants contained in it, it was found to be much more important to know the distribution of the concentrations of various ions such as Cl^-, NO_3^-, SO_4^{2-}, Na^+, K^+, NH_4^+, Ca^{2+} and Mg^{2+} than its pH and electrical conductivity that used to be chiefly monitored. A reliable monitoring system for acid precipitation was developed by combining an improved pH electrical conductivity monitor and an ion chromatograph. Chemical data obtained by continuous precipitation monitoring were correlated with meteorological data.

1. Introduction

In the past decade, acid precipitation, which exerts an increasing influence on life on and in soil and water, has become the object of major social concern on a worldwide scale. Countermeasures to prevent its further propagation are required in order to preserve the equilibrium of ecological systems. Topics of interest concerning acid precipitation include sources of pollutants (anthropogenic, sea water, etc.), atmospheric chemistry, long-range transport of polluted air masses, scavenging and deposition of pollutants and the influence of weather on these processes. In particular, measurements of the concentrations of ions such as Cl^-, NO_3^-, SO_4^{2-}, Na^+, K^+, NH_4^+, Ca^{2+} and Mg^{2+} are indispensable when studying the influence of acid precipitation on life on earth and in water [1–5].

In compliance with the above requirements, we have developed an automatic monitoring system for acid precipitation by combining an instrument to measure pH and electrical conductivity (EC) and an ion chromatograph. The system permits continuous unattended operation for 2 weeks even at sites with heavy snowfall, and allows ion chromatographic (IC) measurements even for precipitation of very low ionic content (EC below 20 μS/cm) [6–8].

2. Experimental

2.1. Apparatus and sampling

The system (Fig. 1) consists of two units, namely, a sampling system that measures pH,

* Corresponding author.

0021-9673/94/$07.00
SSDI 0021-9673(93)E1242-R

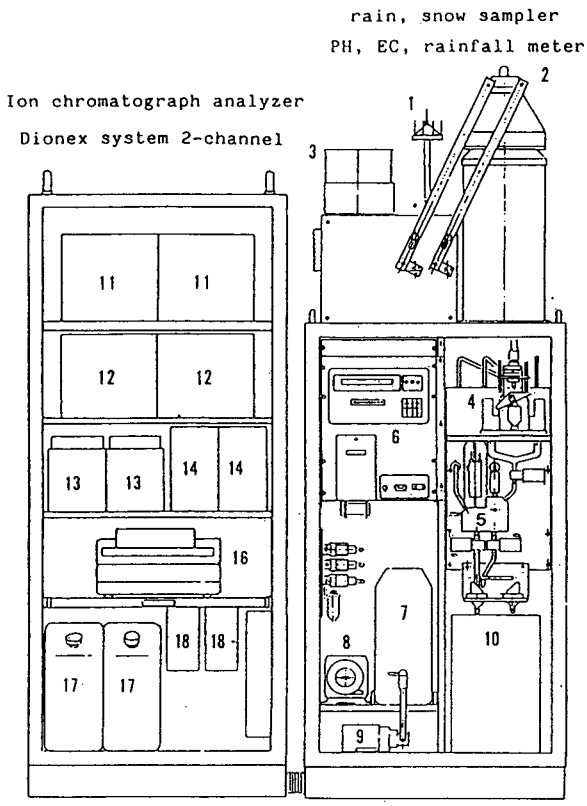

Fig. 1. Schematic diagram of acid precipitation monitor. 1 = Rain sensor; 2 = lid; 3 = dust jar; 4 = rain gauge; 5 = cell and sensors; 6 = display printer; 7 = tank for clean water; 8 = air pump; 9 = injector pump; 10 = sampling tank; 11 = CDM-3 IC detector; 12 = eluent solution tank; 13 = DX IC pump; 14 = anion, cation column injection port; 16 = data processing unit; 17 = waste liquid tank; 18 = suppressor (ASRS, CSRS).

EC and the amount of precipitation at intervals of 0.5 mm and an ion chromatograph capable of measuring concentrations of ions such as Cl^-, NO_3^-, SO_4^{2-}, Na^+, K^+, NH_4^+, Ca^{2+} and Mg^{2+} per 1 mm of precipitation.

By adoption of a glass electrode of the flow-through type for purified water, shown in Fig. 2, this system permits pH measurements even at EC lower than 20 μS/cm.

The ion chromatograph used was either from Dionex or from Yokogawa Analytical Systems, both of which have two-channel systems allowing the simultaneous determination of cations and anions. They are equipped with a suppressor to decrease the background conductivity of the

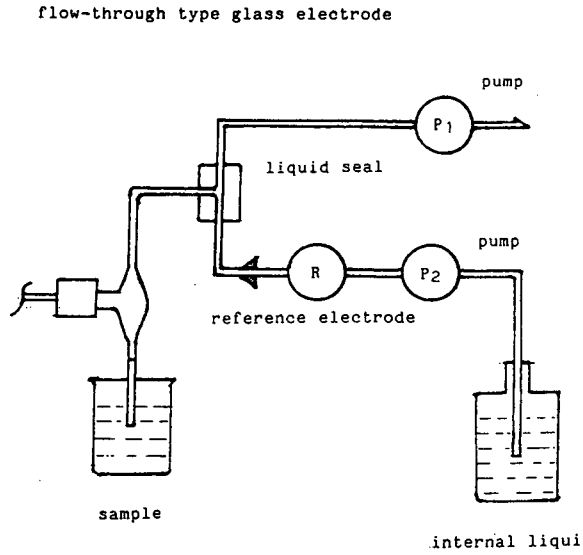

Fig. 2. pH meter for purified water.

eluent solution, ensuring measurements of high sensitivity and accuracy for low ionic concentrations.

The Dionex unit, having a membrane suppressor assembled with an electrode, does not need additional liquid as it has a regenerating system for eluent solution discharged form the detector. The Yokogawa unit contains a micromembrane suppressor. As soon as the detector of this monitoring system detects precipitation, its pump starts and, after 35 min, standard liquid (a mixture of several kinds of ions) is automatically fed into the system and analysed to produce calibration diagram. Subsequently, automatic analysis of rainfall sampled by the pump is conducted in real time as shown in the time chart in Fig. 3.

When precipitation is detected by the rain sensor (1), the cover of the precipitation collector (2) is opened and moves to the dust jar (3). The amount of precipitation is measured by a rain gauge (4) and pH, EC and temperature are measured (5). Part of the precipitated water is injected into the ion chromatograph through a filter.

In the Dionex system, a pump (DX100), detector (CDM-3), column, self-regenerating suppressors for anions (ASRS) and for cations (CSRS) in two channels are installed for the

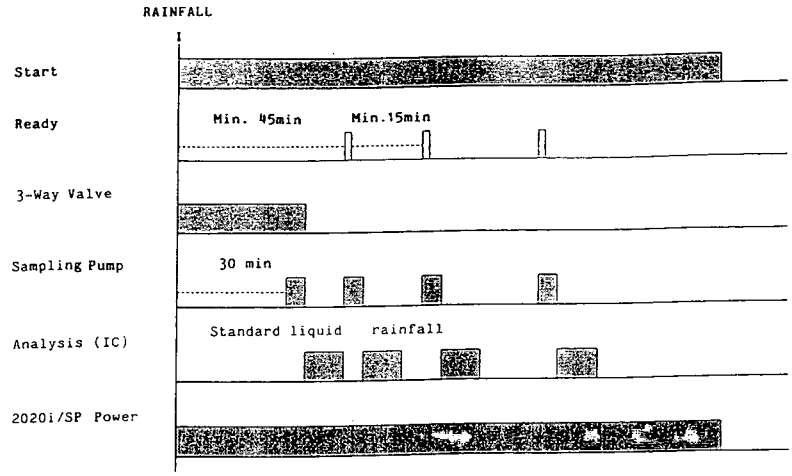

Fig. 3. Automatic ion analyser for acid rain (time chart).

simultaneous measurement of anions and cations.

Data on precipitation analysis processed by the chromatogram processor are printed and then stored on floppy disk via a recording unit (6).

2.2. Reagents

The eluent was prepared from of high-purity grade Na_2CO_3, $NaHCO_3$ and methanesulphonic acid (Waco Junyaku) and distilled water.

Stock standard solutions of the various ions (each 1000 mg/l) were prepared from NaCl, $NaNO_3$, Na_2SO_4, $(NH_4)_2SO_4$, KCl, $Mg(NO_3)_2 \cdot 6H_2O$ and $CaCl_2 \cdot 2H_2O$ of high-purity grade (Waco Junyaku) and distilled water. From these stock standard solutions, mixed working standard solutions including all of the above ions were prepared.

3. Results and discussion

3.1. Analytical conditions

Conditions for the determination of anions and cations using the ion chromatograph are given in Table 1.

Examples of anion and cation separations of snow conducted by means of the Dionex system are shown in Fig. 4a and b, respectively.

3.2. Preparation of artificial rainwater

Artificial rainwater with ion concentrations equal to the annual mean concentrations found in Japan was prepared [9]: chloride 1.60, nitrate 1.10, sulphate 4.80, sodium 1.00, ammonium 0.55, potassium 0.10, magnesium 0.20 and calcium 0.80 μg/ml (pH 4.7).

3.3. Reproducibility test by using artificial rainwater

Tests of the system on a 24-h basis making use of artificial rainfall of 1 mm/h were repeatedly carried out for 20 days to evaluate the reproducibility of the measurement and performance of the system on a long-term basis. During that period, stable measurement was verified without any malfunction of the system. Owing to the adoption of the Dionex ion chromatograph equipped with both ASRS and CSRS, which does not require the supply of regenerated solution, the system was operated free from maintenance throughout that period.

The results are given in Table 2. The relative standard deviations (R.S.D.) for ions such as chloride, nitrate, sulphate, sodium, magnesium and calcium appear very reasonable (2–3%), but

Table 1
Analytical conditions for Dionex ion chromatograph for the measurement of anions and cations

	Anions	Cations
Model	Dionex DX100	Dionex DX100
Detector	Dionex CDM-3	Dionex CDM-3
Guard column	50 × 4 mm I.D. Ion Pac AG4A-SC	50 × 4 mm I.D. Ion Pac CG12
Separation column	250 × 4 mm I.D. Ion Pac AS4A-SC	250 × 4 mm I.D. Ion Pac CS12
Eluent	1.8 m*M* Na_2CO_3–1.7 m*M* $NaHCO_3$	20 m*M* CH_3SO_3H
Flow-rate of eluent	1.7 ml/min	1.1 ml/min
Sample volume	50 μl	50 μl
Suppressor	ASRS[a]	CSRS[b]

[a] ASRS = anion self-regenerating suppressor for recycling eluent solution after flowing through the detector.
[b] CSRS = cation self-regenerating suppressor for recycling eluent solution after flowing through the detector.

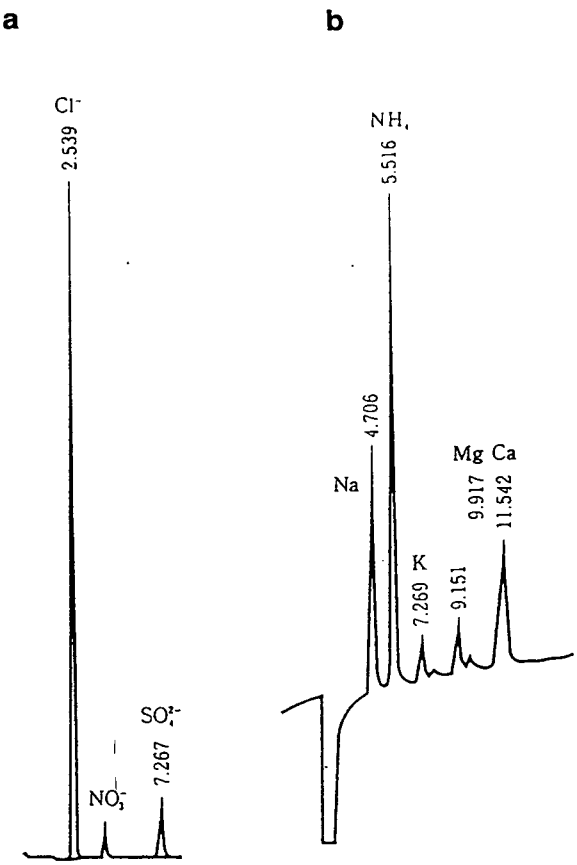

Fig. 4. Examples of (a) anion and (b) cation separations in snow. Numbers at peaks are retention times in min.

those for ammonium (4.6%) and potassium (8.7%) are poor, probably because of the difficulty in separating the two adjacent peaks of these components in the chromatogram. In the context of field measurements, this degree of variation for ammonium and potassium can be accepted.

3.4. Limit of sensitivity

As shown in Table 3, reasonable detection limits at a signal-to-noise ratio of 3 are obtained.

The data suggest direct field measurements of these chemicals at low concentrations can be feasible without any preliminary treatment of the sample or the use of a condensation column.

4. Conclusions

Until recently, monitoring of acid precipitation has been limited to measurements of pH, EC and quantity of rainfall. Therefore, there were insufficient data available to investigate quickly the mechanism of its generation or to locate the origin of its components, although time-consuming analysis by sending rainwater accumulated in storage tanks for 1–2 weeks to a remote laboratory having ion chromatographs has been possible.

Table 2
Results of reproducibility of a running test using an artificially prepared rainwater sample (24 h) $n = 31$

Ion	Content (mg/l)	Minimum (mg/l)	Maximum (mg/l)	Mean (mg/l)	R.S.D. (%)
Chloride	1.6	1.44	1.65	1.58	2.5
Nitrate	1.10	1.05	1.18	1.10	3.4
Sulphate	4.80	4.31	5.10	4.85	3.0
Sodium	1.00	0.99	1.09	1.07	2.2
Ammonium	0.55	0.54	0.06	0.57	4.6
Potassium	0.10	0.09	0.12	0.10	8.7
Magnesium	0.20	0.19	0.22	0.20	2.5
Calcium	0.80	0.76	0.86	0.82	2.7

With the present system, combining an automatic sampling unit and an ion chromatograph, enabling real-time measurement of various ions in addition to pH, EC, etc., reliable monitoring of variations in ion concentrations with time or changes in barometric pressure and wind direction is feasible, thus ensuring very accurate analysis of the generation of acid precipitation and correlations with its source and weather conditions in the future.

Table 3
Detection limits for ions in rainwater (signal-to-noise ratio = 3)

Ion	Detection limit (μg/l)	Ion	Detection limit (μg/l)
Chloride	5	Sodium	5
Nitrate	10	Ammonium	10
Bromide	15	Potassium	10
Sulphate	25	Magnesium	5
		Calcium	10

5. Acknowledgements

The authors are grateful to Mr. K. Wakui, town office of Tsunami-cho, Mr. S. Takahashi, president of the Niigata Highland Agricultural Experiment Station, and Miss. N. Imaizumi and Mr. T. Goto, Niigata College of Pharmacy, for their cooperation.

6. References

[1] E.J. Forland and Y.T. Gjessing, *Atmos. Environ.*, 9 (1975) 339.
[2] J.D. Thornton and S.J. Eisenreich, *Atmos. Environ.*, 16 (1982) 1945.
[3] B. Reynolds. *Atmos. Environ.*, 17 (1983) 2849.
[4] Y. Gjessing, *Atmos. Environ.*, 18 (1984) 825.
[5] L.A. Barrie, *Atmos. Environ.*, 18 (1984) 1459.
[6] G.S. Raynor and J.P. McNeil, *Atmos. Environ.*, 13 (1978) 149.
[7] W.H. Asman, *Water Air Soil Pollut.*, 13 (1980) 235.
[8] M.D. Seymour and T. Stout, *Atmos Environ.*, 17 (1983) 1483.
[9] *Annual Report on the Environment, 1991*, Environment Agency, Government of Japan.

ELSEVIER

Journal of Chromatography A, 671 (1994) 217–223

JOURNAL OF CHROMATOGRAPHY A

Determination of aromatic sulphonates in surface waters by high-performance liquid chromatography with coupled fluorescence and UV detection

Orfeo Zerbinati*, Giorgio Ostacoli

Dipartimento di Chimica Analitica, Università di Torino, v. Giuria 5, I-10125 Turin, Italy

Abstract

An HPLC procedure for determining anthraquinonesulphonates in the presence of both benzene- and naphthalensulphonates in river water was developed. Enrichment of analytes was accomplished by means of solid-phase extraction, based on an RP-18 reversed-phase silica cartridge coated with an aliphatic amine. The analytes were separated by ion-pair chromatography with coupled fluorescence and UV detection, which resulted in a convenient way to discriminate derivatives of benzene and of naphthalene from those of anthraquinone. The peaks of anthraquinonesulphonates were identified by measuring the ratio of their absorbances at two different wavelengths. Four of the target analytes were found in water from the river Bormida (Italy).

1. Introduction

Aromatic sulphonates have been found in some European rivers (Rhine [1,2], Elba [1], Chriesbach [3] and Bormida [4]) and even in the tap water of Amsterdam [5]. These compounds are of anthropic origin, and therefore their presence in environmental and drinking water should be avoided. They are hydrophilic, stable and not readily biodegradable. Biological water purification plants have low efficiency in removing them from wastes [3]. Moreover, aromatic sulphonates can persist in the environment and can propagate easily owing to their hydrophilic characteristics. They have a wide application range in the dye, detergent and cement industries. Benzene-, naphthalene- and anthraquinonesulphonates (BZS, NS and AQS, respectively), together with their amino and hydroxy derivatives, are byproducts of the synthesis and application of dyes. Complex mixtures of these substances can pollute rivers which receive wastes from dye industries.

Analytical methods based on TLC [6], ion-exchange electrokinetic chromatography [7], ion-pair chromatography (IPC) on RP-8 or RP-18 silica [8–14], on-line enrichment on PLRP-S sorbent followed by either ion chromatography or IPC with diode-array detection [2,5], on-line enrichment on Carbopack B and subsequent IPC [3] and enrichment on a modified RP-18 silica and IPC with fluorescence detection [4] have been proposed. Preconcentration on a Dowex WGR weak anion exchanger [15] or ion-pair extraction [16] followed by derivatization and GC–MS analysis, high-performance capillary electrophoresis–MS [17] and ion chromatography–MS [18] have also been proposed. None of these studies combined a pretreatment capable of a good extraction yield for AQS

* Corresponding author.

0021-9673/94/$07.00
SSDI 0021-9673(93)E1224-N

together with a chromatographic analysis suitable for the identification of singly- and doubly-charged AQS in the presence of NS and BZS in environmental water samples.

In this work, a procedure for the preconcentration of aromatic sulphonates and an IPC method for the separation and identification by serial UV–fluorimetric detection of BZS and singly- and doubly-charged NS and AQS are described.

2. Experimental

2.1. Reagents

All aqueous solutions were prepared with ultra-high-quality (UHQ) water obtained by passing deionized water through an Elga-Stat water purification apparatus (Elga, High Wycombe, UK). Methanol and acetonitrile, both of HPLC grade with low UV absorption, and cetyltrimethylammonium bromide (CTAB) were obtained from Aldrich (Milan, Italy). The compounds listed in Table 1 were obtained from Aldrich or Kodak (Prodotti Gianni, Milan, Italy). Inorganic reagents were obtained from Carlo Erba (Milan, Italy). Solid-phase extraction (SPE) columns were obtained from Merck (Bracco, Milan, Italy).

Stock standard solutions of the investigated sulphonates were prepared with UHQ water, kept in dark-glass flasks, stored in a refrigerator (4°C) and were used within 1 week.

2.2. Apparatus

The HPLC system consisted of a Pye Unicam (Cambridge, UK) PU 4015 pump, a Rheodyne (Cotati, CA, USA) valve fitted with a 20-μl loop and a 250 × 4.6 mm I.D. Adsorbosphere C_8, (5 μm) column (Alltech, Deerfield, IL, USA). The

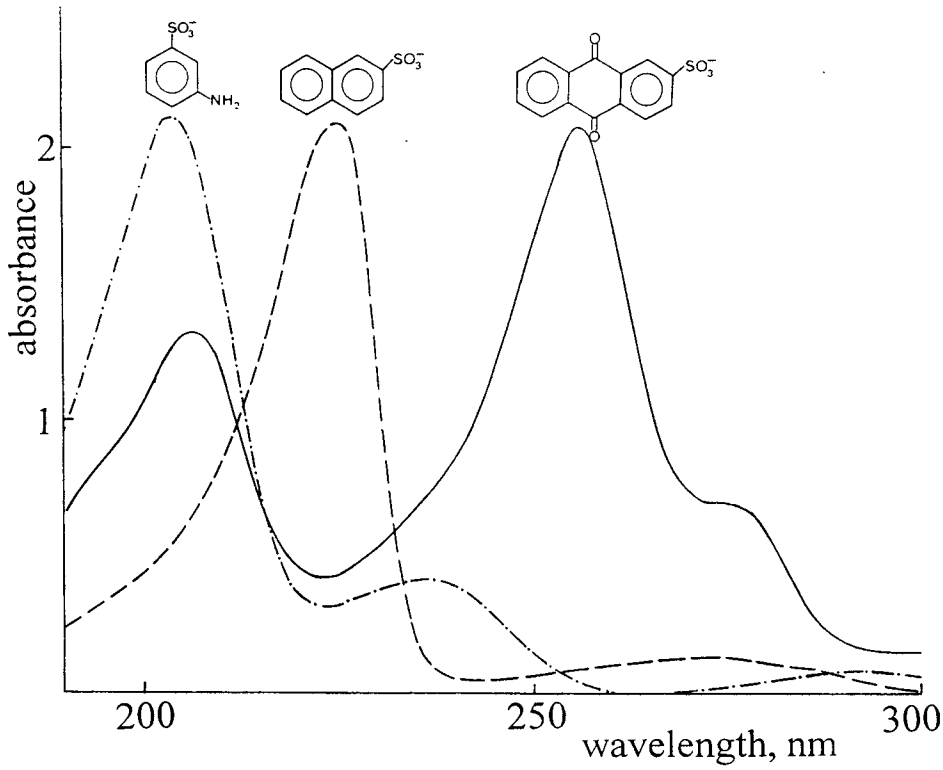

Fig. 1. UV spectra of sulphanilate, 2-naphthalenesulphonate and 2-anthraquinonesulphonate.

eluent was degassed by means of a stream of helium.

The fluorimetric detector was a Hitachi (Tokyo, Japan) F-400 computerized spectrofluorimeter, equipped with an 18-μl flow cell and an analogue output. The UV chromatograms were obtained with a Kontron Instruments (Milan, Italy) Model 430 dual-wavelength detector. A Softron (Gräfeling, Germany) PC Integration Pack was adopted for data acquisition and analysis.

3. Results

3.1. Chromatography

Detector conditions

AQS strongly absorbs UV radiation at longer wavelengths than NS and BZS. Typical UV spectra of AQS, NS and BZS are shown in Fig. 1. It can be seen that they are well differentiated; a wavelength of 258 nm can be chosen for the UV detection of AQS, because at this wavelength the intensity of the signals produced by NS and BZS is much smaller than that produced by AQS. The fluorescence detection of BZS and NS and the collection of their fluorescence spectra were performed as reported previously [10].

Optimization of chromatographic conditions

As chromatographic conditions suitable for the separation of both mono- and disulphonate anions of benzene, naphthalene and anthraquinone were needed, the four compounds mentioned in Fig. 2 were chosen to test the influence on capacity factors of pH, organic content of mobile phase and ion-pair reagent concentration. The results are shown in Fig. 2. The hold-up time was determined from the deflection of the baseline that followed injection. Unless specified other-

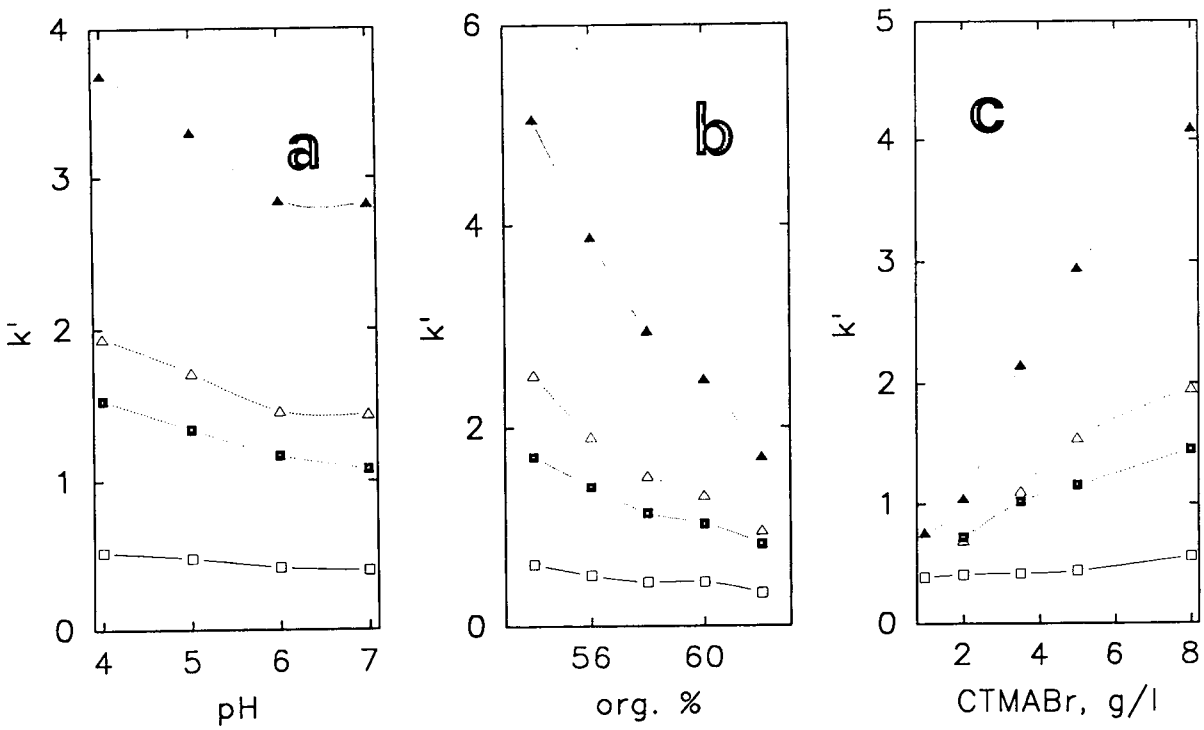

Fig. 2. Effects on k' of (a) pH, (b) organic content and (c) ion-pair reagent concentration. □ = Sulphanilate; ■ = 1-anthraquinonesulphonate; △ = 1,5-anthraquinonesulphonate; ▲ = 2-hydroxy-3,6-naphthalenesulphonate.

wise, the composition of the mobile phase was 1 g l^{-1} of ammonium phosphate (pH 7.0), acetonitrile–water (58:42) and 5 g l^{-1} of CTAB.

The same eluent composition (with a flow-rate of 1 ml min^{-1}) was adopted for the analysis of real samples, as an acidic pH produced poor peak shapes for most of the investigated compounds and both the organic solvent content and the ion-pair reagent concentration adopted gave an acceptable resolution with a short analysis time. Gradient elution was also tried, but longer times were required, as column conditioning was needed after each analysis. Isocratic conditions were preferred, with the additional advantage of obtaining more reproducible retention times.

Chromatograms

The chromatograms of standard mixtures of fluorescent and non-fluorescent aromatic sulphonates are shown in Fig. 3. The absorbance of NS and BZS at 258 nm is much lower than that of AQS, and consequently it was observed that the UV peaks of NS and BZS became comparable in height to those of AQS only if the concentrations of the substances belonging to the former two groups were from one to two orders of magnitude larger than those of AQS. The fluorescent analytes contained in the standard solution employed for running the chromatogram showed in Fig. 3c gave a UV signal that was not distinguishable from the baseline. This was due both to the higher sensitivity of fluorimetric compared with UV detection (which allowed the use of more dilute standards) and to the lower molar absorptivity (at 258 nm) of NS and BZS compared with that of AQS.

Table 1 gives the retention times of the investigated substances, together with the ratio between the absorbances measured at 258 and 275 nm. Those ratios, together with retention times, were used for the identification of non-fluorescent UV absorbers.

Quantitative analysis was based on peak-height measurements. For real samples, standard additions of the identified substances were necessary in order to determine their concentrations.

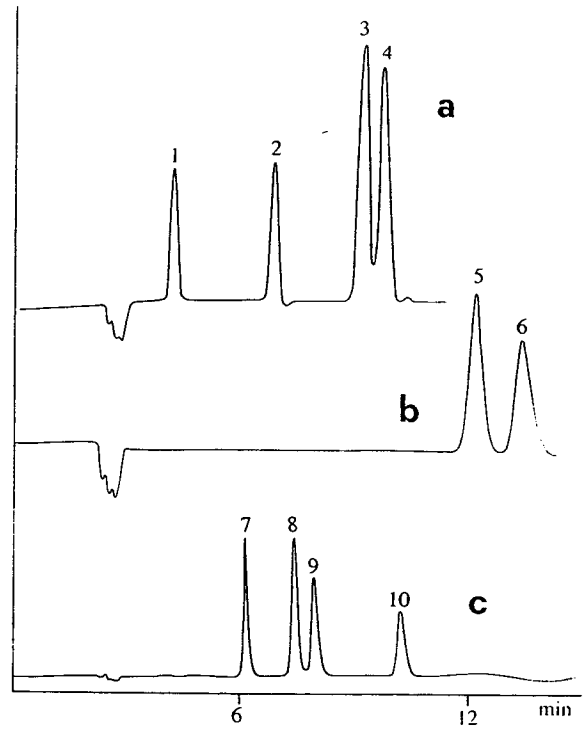

Fig. 3. Chromatograms of a standard mixture. NS = naphthalenesulphonate; NDS = naphthalenedisulphonate; AQS = anthraquinonesulphonate; AQDS = anthraquinonedisulphonate. (a) Fluorescence detection $\lambda_{ex} = 240$ nm, $\lambda_{em} = 660$ nm; (b) fluorescence detection, $\lambda_{ex} = 250$ nm, $\lambda_{em} = 455$ nm; (c) UV detection (258 nm). Peaks: 1 = sulphanilate, 0.25 mg l^{-1}; 2 = 2-NS, 0.25 mg l^{-2}; 3 = 2,7-NS, 0.5 mg l^{-1}; 4 = 1,5-NS, 1 mg l^{-1}; 5 = 2-hydroxy-6,8-NDS, 0.1 mg l^{-1}; 6 = 2-hydroxy-3,6-NDS, 0.1 mg l^{-1}; 7 = 1-AQS, 10 mg l^{-1}; 8 = 1,5-AQDS, 30 mg l^{-1}; 9 = 2-AQS, 10 mg l^{-1}; 10 = 2,6-AQDS, 10 mg l^{-1}.

3.2. Sample pretreatment

As the real samples contained non-ionic interferents, a clean-up procedure capable of removing them was required. Therefore, the real samples were eluted through an RP-18 SPE cartridge; no effect on the concentrations of standard solutions of sulphonates was observed.

Preconcentration of the analytes was also needed. An SPE procedure based on RP-18 silica coated with CTAB by absorbing it from a 0.4% aqueous solution [4], already employed for

Table 1
Chromatography of aromatic sulphonates

Substance[a]	Retention time (min)	Detection[b]	Absorbance ratio[c]
1-AQS	6.20	3	3.7 ± 0.1
2-AQS	7.56	3	3.7 ± 0.1
1,5-AQDS	8.05	3	6.7 ± 0.1
2,6-AQDS	10.31	3	3.1 ± 0.1
2-NS	6.73	1	1.0 ± 0.5[d]
2,7-NDS	9.10	1	1.0 ± 0.5[d]
1,5-NDS	9.60	1	0.3 ± 0.2[d]
2-OH-6,8-NDS	12.10	2	1.0 ± 0.7[d]
2-OH-3,6-NDS	13.30	2	1.0 ± 0.8[d]
Sulphanilate	4.08	1	1.2 ± 1[d]

[a] AQS = anthraquinonesulphonate; AQDS = anthraquinonedisulphonate; NS = naphthalenesulphonate; NDS = naphthalenedisulphonate.
[b] 1 = fluorescence detection, $\lambda_{ex} = 240$, $\lambda_{em} = 660$ nm; 2 = fluorescence detection, $\lambda_{ex} = 250$, $\lambda_{em} = 455$ nm; 3 = UV detection (258 nm).
[c] Absorbance at 258 nm/absorbance at 275 nm ± absolute error.
[d] Molar absorptivity <500.

the analysis of BZS and NS, was tried also for AQS, but poor recoveries were obtained. Standard solutions of AQS were analysed after eluting them through the treated SPE cartridges, and the amount of eluted AQS was found to be undetectable, showing that the stationary phase effectively retained these compounds. Nevertheless, elution with methanol did not recover significant amounts of adsorbed AQS, although BZS and NS were almost quantitatively recovered under the same conditions. On the other hand, the chromatographic order of elution of AQSs and NSs indicated that some NSs were retained on an apparently similar stationary phase even longer than were AQSs, but nevertheless the SPE recoveries of NSs were higher. It must be noted that CTAB and AQS were adsorbed on the solid phase for SPE under different conditions to the chromatographic ones, and that SPE cartridges were dried with an air flow after adsorption of analytes; these reasons can probably explain the different behaviour of AQS in chromatography and SPE. Therefore, a different anion exchanger, consisting of an RP-18 SPE silica cartridge coated with an aliphatic amine, was tried. A 400-mg RP-18 SPE cartridge was loaded by eluting 2 ml of an aqueous solution of 0.01 *M* octyldimethylammonium acetate adjusted to pH 4. The analytes were desorbed by 2 ml of methanol. High recoveries were obtained for all the investigated substances, except sulphanilate, which was only partially retained. The extraction yields, together with the detection limits resulting after tenfold preconcentration of the samples, are reported in Table 2.

The influences of pH and inorganic salt concentrations on the recoveries from standard solutions were investigated. A 30 g l^{-1} concentration of NaCl did not significantly influence the recoveries of AQS, whereas it halved the recoveries of NS; in contrast, 2 g l^{-1} of Na_2SO_4 did not significantly alter the recoveries of NS, whereas it reduced slightly (by 5–10%) those of AQS. A slight increase in hydrogen ion concentration (pH 4) had no observable effect.

A disadvantage of this stationary phase was the limited ion-exchange capacity, (*ca.* 1 μequiv. g^{-1}). A 400-mg cartridge was saturated with an equimolar mixture of 50 μg of the four AQSs listed in Table 2. The breakthrough volume (10 mg l^{-1} solutions) ranged from 5 to 11 ml for

Table 2
SPE of aromatic sulphonates

Substance[a]	Mean recovery ± S.D. ($n = 3$) (%)	Detection limit ($\mu g\ l^{-1}$)[b]
1-AQS	80 ± 5	20
2-AQS	80 ± 7	60
1,5-AQDS	81 ± 3	20
2,6-AQDS	81 ± 6	40
2-NS	113 ± 13	1
2,7-NDS	118 ± 16	2
1,5-NDS	111 ± 20	20
2-OH-6,8-NDS	86 ± 6	1
2-OH-3,6-NDS	89 ± 11	2
Sulphanilate	10 ± 10	200

[a] Abbreviations as in Table 1.
[b] Detection limit as measured after preconcentration (signal-to-noise ratio = 3, preconcentration factor = 10).

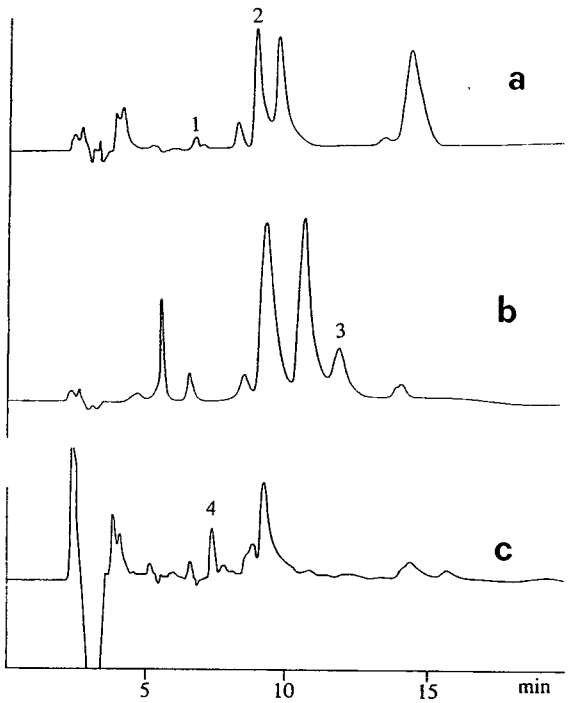

Fig. 4. Chromatograms of a water sample. (a) Fluorescence detection, $\lambda_{ex} = 240$ nm, $\lambda_{em} = 660$ nm; (b) fluorescence detection, $\lambda_{ex} = 250$ nm, $\lambda_{em} = 455$ nm; (c) UV detection (258 nm). Peaks: 1 = 2-NS, 0.32 mg l^{-1}; 2 = 2,7-NS, 3.46 mg l^{-1}; 3 = 2-hydroxy-6,8-NDS, 0.65 ml l^{-1}; 4 = 1,5-AQDS, 1.1 mg l^{-1}.

AQSs and NSs, whereas it was 0.5 ml for sulphanilate.

3.3. Analysis of river water

The river water, after being used by a factory in the production of dyes, is returned to the river. Four samples of that returned water were treated as described and then analysed. The chromatogram obtained for one of those samples is shown in Fig. 4. Four of the target analytes were found to be present. Their concentrations in the four samples ranged between 0.32 and 3.52 mg l^{-1}.

The identity of the naphthalenesulphonates was ascertained by comparing their fluorescence spectra with those of standards stored in a library, as reported previously [4]. The identity of the 1,5-anthraquinonesulphonate was confirmed by its absorbance ratio: a volume of 6.7 ± 0.1 was found, in good agreement with the expected value. The retention times of the remaining UV peaks did not coincide with any of the examined AQSs.

4. Conclusions

An HPLC procedure for the analysis of anthraquinonesulphonates in the presence of naphthalene- and benzenesulphonates in river water has been described. Sample clean-up and SPE preconcentration of the analytes were optimized. This method was successfully applied to the analysis of samples of polluted river water.

5. References

[1] F.T. Lange and H.J. Brauch, presented at the *Symposium on Polar Organic Pollutants in the Environment Basle, 1993.*
[2] E.R. Brouwer, J. Słobodnik, H. Lingeman and U.A.Th. Brinkman, *Analusis*, 20 (1992) 121.
[3] B. Altenbach and W. Giger, presented at the *Symposium on Polar Organic Pollutants in the Environment, Basle, 1993.*
[4] O. Zerbinati, G. Ostacoli, D. Gastaldi and V. Zelano, *J. Chromatogr.*, 640 (1993) 231.

[5] E.R. Brower, T.M. Tol, H. Lingeman and U.A.Th. Brinkman, *Quím. Anal.*, 12 (1993) 88.
[6] H.S. Freeman, Z. Hao and W.-N. Hsu, *J. Liq. Chromatogr.*, 12 (1989) 919.
[7] S. Terabe and T. Isemura, *Anal. Chem.*, 62 (1990) 652.
[8] H. Miyoshi, T. Nagai and M. Ishikawa, *Bull. Shizuoka Pref. Inst. Publ. Health Environ. Sci.*, 27 (1984) 45.
[9] C. Pettersson and G. Schill, *Chromatographia*, 28 (1989).
[10] E. Arviddson, L. Hackzell, G. Schill and D. Westerlund, *Chromatographia*, 25 (1988) 430.
[11] P. Jandera, J. Churáček and B. Taraba, *J. Chromatogr.*, 262 (1983) 121.
[12] P. Jandera, J. Churáček and J. Bartosova, *Chromatographia*, 13 (1980) 485.
[13] H. Grossenbacher, T. Thurnheer, D. Zürrer and A.D. Cook, *J. Chromatogr.*, 360 (1986) 219.
[14] H. Zou, Y. Zhang, X. Wen and P. Lu, *J. Chromatogr.*, 523 (1990) 247.
[15] T. Tsukioka, H. Ozawa and T. Murakami, *Anal. Sci.*, 7 (1991) 897.
[16] H. Kataoka, T. Okazaki and M. Makita, *J. Chromatogr.*, 473 (1989) 276.
[17] W.C. Brumley, *J. Chromatogr.*, 603 (1992) 267.
[18] I.S. Kim, F.I. Sasinos, D.K. Rishi, R.D. Stephens and M.A. Brown, *J. Chromatogr.*, 589 (1991) 177.

ELSEVIER

Journal of Chromatography A, 671 (1994) 225–229

JOURNAL OF CHROMATOGRAPHY A

Ion chromatographic determination of anions and cations at ultra-low concentrations in Alpine snow

Ulrike Nickus *, Michael Kuhn

Institute of Meteorology and Geophysics, University of Innsbruck, Innrain 52, A-6020 Innsbruck, Austria

Abstract

As part of the international project ALPTRAC the acid deposition at high Alpine sites was investigated. This paper reports on experiences with ion chromatography in the μg/kg range that was characteristic for the samples, and on the sample contamination and its sources. Particular emphasis is given to a drop of ionic concentration from the first to the second injection drawn from the vials of the automated sampler. This drop was observed at detection ranges of 3 μS/cm and less and amounted to 17 μg/kg for sodium, 14 μg/kg for chloride and 1 to 4 μg/kg for magnesium, calcium and sulphate.

1. Introduction

Various studies have shown ecosystems in the Alpine region to be very sensitive to the impact of pollutants. The amount of pollutants accumulated in the Alpine snowpack during the winter half year is of special importance for the acidification of mountain lakes and runoff. The rapid release of pollutants occurring with the onset of snowmelt —up to 80% of the bulk solute is released with the first third of the meltwater— can be very harmful to such ecosystems.

To investigate, among other topics, the amount of substances deposited in wet and dry form at heights of 3000 m above sea level and more, an international project (ALPTRAC) was started in 1990. Measurements performed on glaciers in the Tyrolean Alps show that ionic loads there are as high as or even exceed the amounts measured at valley stations in Tyrol (due to the general increase of precipitation with height). Mean concentrations of ions dissolved in the snowpack, on the contrary, amount to only 25 to 50% of the ionic concentrations found in precipitation of low lying stations [1,2] indicating background conditions in the μg/kg range, comparable to those in polar regions [3–5]. These low concentrations are mainly observed in snow layers of December to February precipitation, when glaciers lie well above the height of the atmospheric mixing layer and again after the onset of snowmelt in May or June (see Table 3).

While the meteorological and glaciological implications of the investigation will be reported elsewhere, this paper will focus on the methods of detection of ultra-low ionic concentrations. We report on the precautions taken to keep sample contamination from collecting to analysis as small as possible, on experiences with ion chromatography in the ppb range and on one

* Corresponding author.

0021-9673/94/$07.00
SSDI 0021-9673(93)E0074-5

aspect we did not find mentioned in the literature before, that is the difference in ionic concentration between two subsequent injections made from one vial using the automated sampler.

2. Experimental

2.1. Sampling and sample preparation

Samples are taken from snow pits dug on glaciers at heights of 3000 m above sea level. In vertical profiles snow layers of 10 cm thick is cut off with a plexiglas tube and filled into air-tight screw bottles made of polyethylene.

Bottles and anything that may come into contact with the samples, are mechanically cleaned in the laboratory, rinsed with diluted HCl, and then carefully soaked and rinsed several times with ultrapure water, so that no residues can be detected. For the transport between laboratory and sampling site all material is packed into clean plastic bags. As additional precaution against contamination overall clothing of polyamide cleaned rubber gloves, and breathing masks are worn during sampling procedure. Samples are transported in frozen state into the laboratory. Until analysis they are kept in the deep freezer at a temperature of −18°C. Just before analysis with the ion chromatograph they are thawed at room temperature. Vials used for the automated sampler are well rinsed with the sample before being filled and closed with a filter cap.

2.2. Ion chromatography

All ions of interest are analysed with a Dionex DX-100 instrument. We use a two-column set system with suppressed conductivity detection. The conductivity cell is at constant temperature, so that no noise or baseline drift is normally observed down to the 0.3 μS/cm range.

System control as well as data collection and processing is done by the Dionex AI-450 chromatography software (version 3.32).

Mono- and divalent anions and cations are separated in single, isocratic runs, respectively. Further details of the analysis are summarised in Table 1.

A Dionex automated sampler with 5-ml vials is used to deliver the sample to the sample loop. A volume of 200 μl for the sample loop has proved to be very practicable for this application.

Eluents, anion regenerant and all standard solutions are prepared with ultrapure water of resistivity > 18 MΩ cm at 25°C. Individual stock solutions of 1000 mg/kg (ppm) are diluted to mixed standard solutions of concentrations varying from the mg/kg to the μg/kg (ppb) range. Standard solutions are always prepared just before calibration.

Table 1
Experimental conditions for ion chromatographic analysis

Parameter	Anions	Cations
Ions determined	Cl^-, NO_3^-, SO_4^{2-}	Na^+, NH_4^+, K^+, Mg^{2+}, Ca^{2+}
Analytical column	Ion Pac-AS4A	Ion Pac-CS12 (4 mm)
Guard column	Ion Pac-AG4A	Ion Pac-CG12 (4 mm)
Suppression	AMMS II (using a pressurized delivery system)	CSRS-I (4 mm)
Eluent	4 m*M* Na_2CO_3 1.5 m*M* $NaHCO_3$	21 m*M* Methanesulfonic acid
Regenerant	12.5 m*M* H_2SO_4	
Eluent flow-rate	2 ml/min	1 ml/min
Run time	3.0 min	8.5 min
Background conductivity	20 μS/cm	1 μS/cm

A three-level quadratic calibration is used, standards are external.

2.3. Contamination problems

Contamination of the sample

In the laboratory sample contamination occurs from the moment the sample bottle is opened until the sample is injected into the chromatographic system. To estimate the amount of sample contamination by the laboratory air we analysed ultrapure water of 18.1 MΩ cm resistivity.

No anions and no ammonium and potassium were detected in the ultrapure water. For magnesium we measured a mean concentration of 0.8 μg/kg, for calcium of 1.1 μg/kg. Standard deviation amounted to 0.3 μg/kg for magnesium, respectively 0.6 μg/kg for calcium. Sodium concentrations showed the highest variations. We found samples without sodium as well as samples with sodium concentrations up to 3 μg/kg.

This ion content represents a mean, but generally varying contamination of any sample, that cannot be avoided in our laboratory. The concentrations of magnesium, calcium and sodium are considered as "blank" values. They increase the real ionic concentrations and should thus be subtracted from measured values of any sample.

Contamination of the instrument

From every vial used with the Dionex autosampler up to three injections can be made.

We found that there are differences in ionic concentrations between the first and the second injection at the 3 μS/cm and lower detection ranges. Concentration values of most ionic species analysed diminish from the first to the second injection. No further decrease, however, was observed between the second and the third injection.

This effect was most pronounced for chloride and sodium, while no changes could be seen for nitrate, ammonium and potassium. The difference between the first and the second injection appeared to be independent of the measured concentration. It varied from 17 μg/kg for sodium and 13 μg/kg for chloride to 4 μg/kg for sulphate down to 2–3 μg/kg for calcium and about 1 μg/kg for magnesium.

In view of this reproducible value of the difference we concluded that the effect was introduced in the process of extracting the sample from the vial into the analytical system. The first injection has higher concentrations since it contains not only the ions of the sample but also rinses away ions that have been deposited before on surfaces coming into contact with the sample during the injection process, *e.g.* the filter or the end of the tubing connecting the sampler to the injection valve.

This contamination effect can put a limit to analysis at the lower detection ranges, as it was observed especially with sodium. No reproducible results could be achieved in ranges of less than 0.1 μS/cm. For both calibration and analysis of samples that require detection ranges of 0.3 to 3 μS/cm, only values of the second injection were used. Detection ranges of 10 μS/cm are not sensitive enough to resolve this contamination effect.

2.4. Detection limits

Measurements to determine detection limits were performed with artificial samples of low ionic content. From a series of 8 injections for both anions and cations method detection limits (MDL) were established according the US Environmental Protection Agency (EPA) definition [6]:

$$\mathrm{MDL} = t(n-1, 1-a\mathrm{R}=0.99)\sigma \quad (1)$$

σ is the standard deviation for the particular ion, t is the Student factor amounting to 3.499 for $n-1$ degrees of freedom and a significance at the 1% level ($1-a=0.99$).

Results for anions and cations are summarised in Table 2. Apart from sodium and chloride method detection limits of about 1 μg/kg were found for all ions. The comparatively high MDL of almost 4 μg/kg for sodium was attributed to contamination effects, which were most pro-

Table 2
Method detection limits for anions and cations (MDL), mean concentrations ($\bar{x}$) and standard deviations (σ) in μg/kg

	Cl^-	NO_3^-	SO_4^{2-}	Na^+	NH_4^+	K^+	Mg^{2+}	Ca^{2+}
MDL	1.7	0.9	1.2	3.7	1.1	1.4	1.0	1.2
x	12.2	17.3	18.2	12.8	2.9	1.9	3.4	5.4
σ	0.49	0.26	0.33	1.06	0.32	0.40	0.30	0.33

nounced and showed the highest variation for this ion.

MDL for chloride amounted to almost 2 μg/kg. The wider scattering compared to nitrate or sulphate was due to the overlapping of the chloride peak with the negative water peak in the detection ranges of 3 μS/cm and less. Using a lower concentrated eluent this effect may be diminished.

The detection limits we determined for our application lie in the range reported in literature (*e.g.* refs. 3, 7 and 8). The variety in experimental conditions of ion chromatographic analysis and the different definitions used to establish detection limits, however, restrict a direct comparison.

2.5. Ionic balance

A common method for evaluating analytical results of water samples is to calculate the ionic balance:

$$C = [H^+] + [Na^+] + [NH_4^+] + [K^+] + [Mg^{2+}] + [Ca^{2+}] - [Cl^-] - [NO_3^-] - [SO_4^{2-}] \quad (2)$$

We found a general anion deficit in agreement with other studies of snow (*e.g.* refs. 1, 9 and 10). The mean ratio Σ anions/Σ cations amounted to 0.43, ranging from 0.3 to 0.6.

The anion deficit may be due to any not measured anion (we did not measure hydrogencarbonate and organic compounds like formic and acetic acid), or to analytical errors, whose relative importance increases with decreasing ionic loads, especially near the detection limit.

3. Results

The ionic concentrations we measured in the high Alpine snowpack cover a range of three orders of magnitude, from about 3 mg/kg for nitrate in spring down to some μg/kg for alkali and alkaline earth metals (Table 3). During our investigations ion chromatography has proved to be a very practicable and sensitive method for the detection of major ions in Alpine snow.

Even in snow of low ion content concentrations of anions and ammonium lie a ten to hundred times higher than the corresponding detection limits (Fig. 1a). For metals, however, concentration values in the range of the corresponding detection limit are frequent. In a few cases concentrations below the detection limit are found, especially for magnesium (Fig. 1b).

Table 3
Ionic concentrations (μg/kg) found in distinct snow layers at about 3000 m above sea level; April 17, 1993 and June 25, 1993

	Cl^-	NO_3^-	SO_4^{2-}	Na^+	NH_4^+	K^+	Mg^{2+}	Ca^{2+}
April	50	2600	980	35	693	10	11	70
June	21	79	43	9	18	1	1	9

The concentration difference between June and April is caused by the release of pollutants from the snowpack during melting.

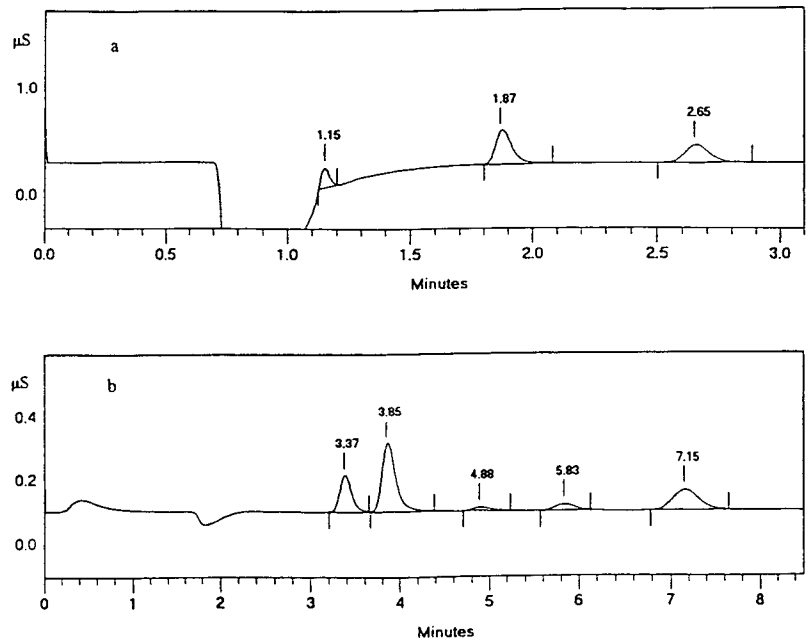

Fig. 1. Typical chromatogram of Alpine snow of low ionic concentrations. (a) Anions (chloride 16.5 µg/kg, nitrate 65.1 µg/kg, sulphate 36.7 µg/kg). (b) Cations (sodium 4.9 µg/kg, ammonium 16.5 µg/kg, potassium 2.3 µg/kg, magnesium 0.1 µg/kg, calcium 4.2 µg/kg).

4. Acknowledgement

This paper is a contribution of the Institute of Meteorology and Geophysics, University of Innsbruck, to the ALPTRAC program and has been sponsored by the Austrian Research Foundation (P7810 Geo).

5. References

[1] H. Puxbaum, A. Kovar and M. Kalina, *NATO ASI Ser.*, G28 (1991) 273–297.
[2] U. Nickus, *Ph.D. Thesis*, Institute of Meteorology, University of Innsbruck, Innsbruck, 1991.
[3] M. Legrand, M. De Angelis and F. Maupetit, *J. Chromatogr.*, 640 (1993) 251–258.
[4] P.A. Mayewsky, W.B. Lyons, M.J. Spencer, M.S. Twickler, C.F. Buck and S. Whitlow, *Nature*, 346 (1990) 554–556.
[5] G. Piccardi, R. Udisti and E. Barbolani, *Ann. Chim. Ital.*, 79 (1989) 701–712.
[6] *Test Methods, EPA-600/4-82-057*, United States Environmental Protection Agency, Cincinnati, OH, 1982.
[7] C.F. Buck, P.A. Mayewsky, M.J. Spencer, S. Whitlow and D. Barrett, *J. Chromatogr.*, 594 (1992) 225–228.
[8] W. Shotyk, *J. Chromatogr.*, 640 (1993) 309–316, 317–332.
[9] D.W. Gunz and M. Hoffmann, *Atmos. Environ.*, 24 A (1990) 1661–1671.
[10] F. Maupetit and T.D. Davies, *NATO ASI Series*, G28 (1991) 299–301.

ELSEVIER

Journal of Chromatography A, 671 (1994) 231–237

JOURNAL OF CHROMATOGRAPHY A

Ion chromatographic separation and quantitative analysis of fluoroacetic acid and formic acid in soil

Andrew F. Kingery, Herbert E. Allen*

University of Delaware, Department of Civil Engineering, Newark, DE 19716, USA

Abstract

An analytical method has been developed for the determination of fluoroacetic acid (FC2A) and formic acid (FA) which previously co-eluted in ion chromatographic analysis. The separation is based upon a solvent compatible, ion-exchange column. The analytes are retained by ion exchange, but selectivity is provided by a mechanism that has reversed-phase characteristics. Low detection limits (0.1 μg FC2A/g soil) are achieved through the use of a preconcentrator column. The method is designed to detect small amounts of FC2A in the presence of high concentrations of FA, a major interference found in some western soils. Sample preparation is minimal. The method has been applied to Rocky Mountain Arsenal (RMA) Standard Soil and to samples collected at RMA.

1. Introduction

Fluoroacetic acid (FC2A) is an extremely potent rodenticide first reported shortly after the end of the Second World War [1]. The compound is still commonly referred to under the laboratory serial number "1080" (sodium fluoroacetate) assigned by the Economic Investigations Laboratory, US Fish and Wildlife Service, at Patuxet, MD, USA. LD50s for FC2A are extremely low, ranging from 66 μg/kg (dog, oral) to 714 μg/kg (man, oral) [2]. It is currently used as a rodenticide in New Zealand and Australia [3]. FC2A has been historically used in the western US for the control of coyotes and wolves. The US Environmental Protection Agency (USEPA, Washington, DC, USA) has recently denied Federal Insecticide, Rodenticide, and Fungicide Act (FIFRA) registration of FC2A [4].

The Rocky Mountain Arsenal (RMA) is a military installation located near Denver, CO, USA, contaminated with waste from chemical warfare agent, pesticide, and other chemical manufacturing processes. The site is presently being remediated under the set of statues known collectively as "Superfund". F2CA is a suspected chemical of concern at the site. FC2A has been suggested as a possible byproduct from chemical warfare agent manufacture [5]. Historical information indicates that FC2A was used at RMA for the control of small mammals during the 1960s and 1970s. Application of FC2A for small mammal control was usually accomplished through the hand (or mechanical) broadcast of treated grain baits. Previous investigations have found quantities of suspected FC2A in RMA soils. However, the analytical method used did not separate FC2A from formic acid (FA), a

* Corresponding author.

0021-9673/94/$07.00
SSDI 0021-9673(94)00123-Q

naturally occurring compound at RMA [6]. Additionally, the existing detection limit of 2 μg/g for FC2A exceeded the desired, risk-based, detection limit of 0.2 μg/g [7]. Formic acid concentrations may be as high as 40 μg/g in RMA soil.

Most of the existing methods for the analysis of FC2A utilized derivatization followed by quantification by GC [8–19] or HPLC [20–22]. Derivatization methods have, in general, long preparation times and variable recoveries. Ion-pair methods [23] or ion chromatographic methods [24] designed for the analysis of formulations lack sensitivity. The US Army Toxic and Hazardous Materials Agency (USATHAMA) method previously in use at RMA does not discriminate against the formic acid interference. ^{19}F NMR has been used for investigations into FC2A metabolism [25–27]. NMR is highly specific, but suffers from low sensitivity. Fluoride ion-specific electrodes are sensitive, but non-specific to FC2A [28,29].

The method presented in this paper is based upon the use of new solvent compatible anion chromatographic columns that can utilize multiple retention mechanisms for the separation of organic acids that have similar ion-exchange characteristics. We have recently applied the same approach to the separation of five chemical warfare agent related compounds, pinacolyl methylphosphonic acid, isopropyl methylphosphonic acid, ethyl methylphosphonic acid, methyl methylphosphonic acid, and methylphosphonic acid [30]. The method uses high concentrations of organic modifier (acetonitrile) to separate FC2A and FA while the compounds are retained by ion exchange on the solvent compatible column.

2. Experimental

2.1. Materials

Type I deionized water was obtained from a Barnstead (Dubuque, IA, USA) NANOpure reagent water system fed by a Corning still. Optima grade acetonitrile (ACN) was obtained from Fisher Scientific (Pittsburgh, PA, USA). NaOH solutions were prepared using 50% (w/w) Fisher certified reagent. Regenerant solution was prepared from trace metal grade H_2SO_4 (Fisher). Fluoroacetic acid (>96%) was obtained from Aldrich (Milwaukee, WI, USA). Formic acid (>95%) was purchased from Fisher. Ag^+-form strong cation-exchange solid-phase extraction cartridges (Ag^+-SPE) were obtained from Alltech Chromatography. All other chemicals used were ACS grade or reagent grade.

2.2. Apparatus

The basic chromatographic system was a 4500i ion chromatograph with GPM pump, AMMS-II micromembrane suppressor, and a PED (conductivity mode) detector, all from Dionex (Sunnyvale, CA, USA). Samples were injected by a Dionex ASM autosampler, set either in loop or concentrator mode (<1 ml/min). The system was controlled, and data collected, by a Dionex AI-450 interface and software (Version 3.21) from an IBM PS/2 Model 35 PC. Dionex OmniPac PAX-100 column and OmniPac PAX-100G guard column were used as the stationary phase. Either a 250-μl loop or an OmniPac PAX-500G guard column (as a preconcentrator) were used for injection. The preconcentrator column was loaded in reverse flow by the ASM prior to injection, and had a minimum of tubing [<2 cm of 0.010 in. (0.0254 cm) I.D.] on the down-flow (towards the stationary phase) side to minimize carry over.

2.3. Procedure

The following four eluents were used: (1) deionized water, (2) 1 m*M* NaOH, (3) 100% ACN, and (4) 200 m*M* NaOH. Regenerant (50 m*M* H_2SO_4) was stored under helium in 4-l plastic reservoirs, pressurized to provide a flow-rate through the suppressor of 7–8 ml/min. When using the autosampler for extended and untended operations, regenerant is the limiting reagent in the system. Two 4-l reservoirs were

linked in series to provide in excess of 16 h operating time.

Soil (2 g) was extracted with 20 ml deionized water in 50-ml glass centrifuge tubes by shaking for 1 h on a reciprocal shaker (100 rpm). Equilibrated suspensions were centrifuged, and the supernatant filtered through a 0.45-μm membrane filter. Free metals in the extract were complexed by the addition of 10 μl of 0.1 *M* EDTA to prevent precipitation inside the chromatograph. Excess chloride, a major interferant which can cause unacceptable peak broadening, was removed by solid-phase extraction with Ag^+ strong cation-exchange resin (Ag^+-SPE).

Eluent flow-rate was 1 ml/min. The gradient program used 0.2 m*M* NaOH–70% (v/v) ACN from 0–15 min (after a 20 min equilibration) with a ramp to 60 m*M* NaOH–70% ACN from 15–20 min and held for 5 min. The ramp is required to elute strongly retained analytes prior to the next run. Detection was by suppressed conductivity.

3. Results and discussion

3.1. Aqueous method development

The initial experiments were performed using a 200 μg/l combined standard (CS) of FC2A and FA. A 250-μl loop was used. FA elutes just prior to FC2A using ion exchange as the sole retention mechanism (Fig. 1). The elution order of FC2A and FA reverses with increasing concentration of organic modifier. However, an analysis of the capacity factors indicates that reversed-phase behavior occurs only at organic modifier concentrations exceeding 40% (Fig. 2). This is in contrast to the alkyl methylphosphonates which exhibited the classical reversed-phase response at all concentrations of organic modifier. We speculate that the effect may be due to column swelling effects [31] exceeding the reversed-phase effect at low organic modifier concentrations because of the small size of FC2A and FA.

An optimization experiment was completed using a two-factor, four-by-six level, fractional

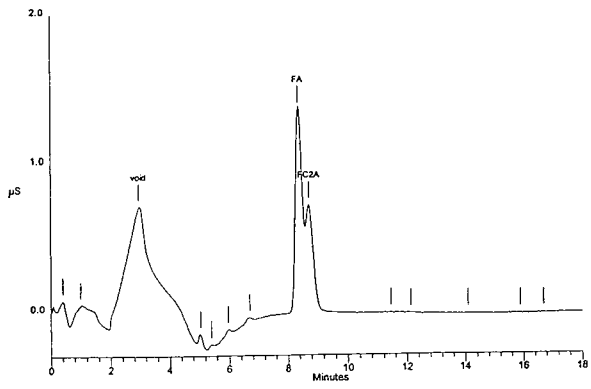

Fig. 1. Separation of FC2A and FA under conventional ion-exchange conditions. Experimental: 0.8 m*M* NaOH–10% (v/v) ACN; 1 ml/min; 250-μl loop; 250 μg/l each analyte.

factorial design [32]. NaOH was varied at 1.2, 0.8, 0.4, and 0.2 m*M*. ACN was varied at 10, 25, 40, 55, 70 and 85% (v/v). All samples used a isocratic mobile phase from 0–15 min, ramping to 60 m*M* NaOH from 15–25 min with the same concentration of organic modifier, and flow-rate of 1 ml/min.

Response was measured as the resolution between FC2A and FA. The resolution response was fitted to a quadratic function with a linear interaction term as the simplest function that would significantly fit ($p = 0.05$) the results (Fig. 3).

Acceptable resolution between FC2A and FA was chosen to be 1.5, but due to the expected

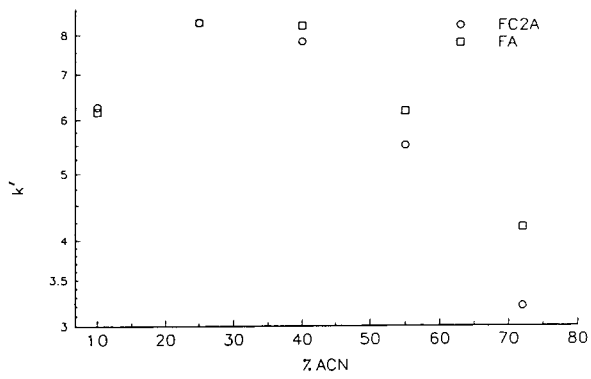

Fig. 2. Effect of organic modifier on the capacity factors of (○) FC2A and (□) FA. Experimental: 0.2 m*M* NaOH; 1 ml/min; 250-μl loop; 200 μg/l each analyte.

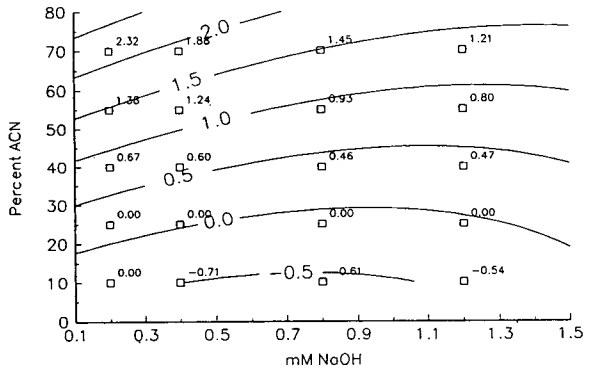

Fig. 3. Resolution between FC2A and FA as a function of mobile phase composition.

high levels of FA in the samples, an eluent composition was chosen [0.2 m*M* NaOH–70% (v/v) ACN] that produced the highest resolution compatible with our experience with soil matrices. Self-elution of soil extracts at the head of the column can be a problem when using eluent concentrations less than 0.2 m*M* NaOH.

The gradient program was designed to provide a long enough initial elution to separate the compounds, particularly when using the preconcentrator column, and to insure that late eluting compounds would be removed from the column. When using the preconcentrator column, retention times increase as the column is overloaded with FA and other interferences because of self-elution.

Initial calibration of the aqueous method using the preconcentrator column was accomplished using a concentration range from 0.5–20 μg/l FC2A. The results were linear, but with a non-zero intercept due to a minor interference.

3.2. Soils method development

The aqueous method was extended to soils using the techniques we have developed for the analysis of alkyl methylphosphonates. Lakewood Sand, a standard, well characterized, New Jersey soil was used as a test soil. Spiked soil samples were shaken on a reciprocal shaker for 24 h at 125 rpm to insure equilibration. Calibration experiments using Lakewood Sand demonstrated that the method produced a linear response from 0.05 to 2.5 μg/g FC2A, and with a zero intercept. Calculation of the mass balance indicated that sorption by the soil is not significant in the concentration range tested.

The calibration was repeated with the addition of 5 μg/g of FA. The response factors were compared by Student's *t*-test and found to be statistically similar ($p < 0.05$) [32]. A test using 2 μg/g FC2A and 50 μg/g FA on Lakewood Sand showed good resolution ($R_s = 1.88$) between the compounds (Fig. 4).

3.3. RMA Standard Soil

RMA Standard Soil was obtained during a site visit to RMA. The soil is a reddish-brown, sandy, well-mixed material with a very small percentage of particles exceeding 2 mm (0.6%). The soil had been previously air dried in storage.

A fractional matrix calibration was performed using RMA Standard Soil spiked with 0.02–2.00 μg/g of FC2A with a cross calibration of 0–10 μg/g of FA. The results were linear ($r = 0.994$), had a zero intercept, and showed insignificant differences between the samples spiked with FC2A only, and those spiked with added FA (Fig. 5).

Retention time of FC2A did vary from sample to sample because of variances in the ionic strength of the sample. Fluoride was used as a

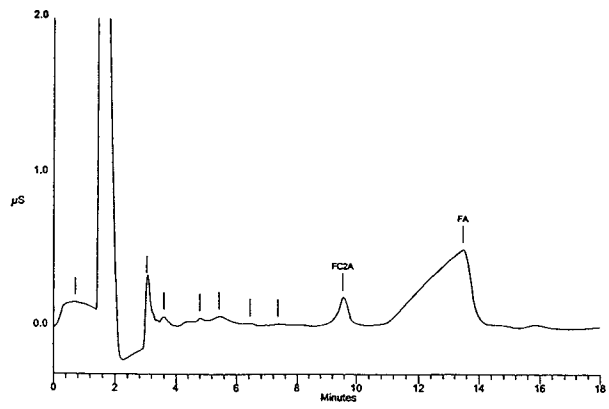

Fig. 4. Lakewood Sand soil spiked with FC2A and FA. 2 g soil/20 ml deionized water; 250-μl loop; 2 μg/g FC2A and 50 μg/g FA.

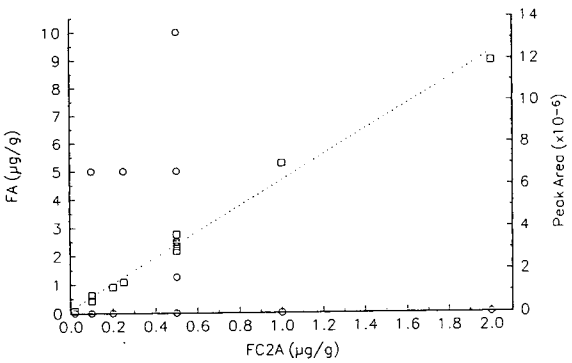

Fig. 5. Experimental design (○) and results (□) of RMA Standard Soil calibration.

reference peak. Retention time variance is much less of a problem when using a loop injector. The sample size is smaller, and sample movement in the preconcentrator column is wholly controlled by the elution strength of the sample.

RMA Standard Soil did sorb significant amounts of FC2A, in contrast to the Lakewood Sand soil. However, recovery was constant (60 ± 4%, $n = 12$) across the range tested. A Langmuir sorption isotherm was insignificantly different from a linear sorption isotherm.

The amount of FA present was estimated by the method of standard additions. The range of this method, using the preconcentrator column, is 0.1–2 µg/g of FC2A. The chromatographic peaks representing FA had generally poor peak shape due to column overloading, with a resultant increase in the variability of the integrated peak areas.

3.4. RMA field samples

Fifteen field samples suspected of containing FC2A were collected by Woodward-Clyde Federal Services (Denver, CO, USA) from three borings on RMA. The core samples were field-packed in plexiglass cylinders and immediately refrigerated. The samples were express shipped to the University of Delaware in coolers packed with "blue ice". Upon receipt, the samples were transferred to a refrigerator and maintained at 4°C. Samples were not removed from the original sample containers until just prior to analysis.

Each sample was transferred to new plastic bags and homogenized by hand. A subsample (about 20 g) was removed, weighed, and placed in a vacuum desiccator for drying. Another subsample (2.00 g) was processed and chromatographed according to the soils method described above.

No fluoroacetic acid was detected in any of the samples (Fig. 6). Formic acid was detected in every sample. Estimated FA concentrations ranged from 1–45 µg/g (Table 1). The FA concentration data was verified by replacing the preconcentrator with a 250-µl loop, and repeating the analysis with a new calibration. All of the three samples checked resulted in sightly lower concentrations, with deviations of −7 to −23%.

The absence of FC2A in the RMA samples

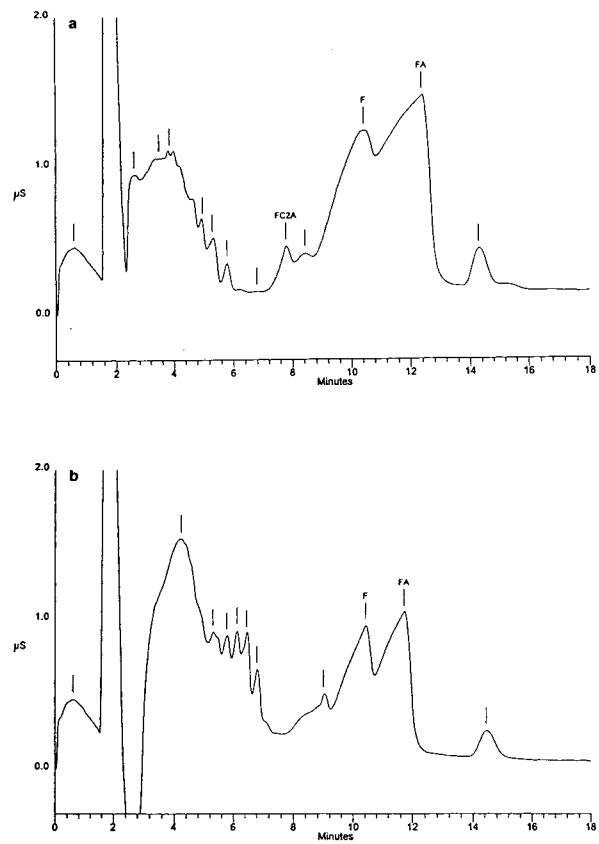

Fig. 6. (a) RMA Standard Soil spiked with 0.5 µg/g FC2A and 10 µg/g FA. (b) RMA sample 3003S011.

Table 1
RMA field sample results

Boring and sample ID	Sample depth (m)	Moisture (%)	Est. FA (μg/g)
Boring 3003			
3003S011	0–0.3	8.90	6.4
3003S031	0.61–0.91	18.51	9.1
3003S051	1.22–1.52	30.63	44.6
3003S101	2.74–3.05	29.97	11.9
3003S151	4.27–4.57	30.41	10.3
Boring 2635			
2635S011	0–0.3	5.26	8.2
2635S031	0.61–0.91	7.00	1.9
2635S051	1.22–1.52	10.94	1.5
2635S101	2.74–3.05	15.71	2.8
2635S151	4.27–4.57	17.51	1.6
Boring 2636			
2636S011	0–0.3	5.89	1.7
2636S031	0.61–0.91	11.78	1.2
2636S051	1.22–1.52	11.68	3.8
2636S101	2.74–3.05	11.74	1.5
2636S151	4.27–4.57	2.72	1.3

was not surprising. Ample evidence exists for the biodegradation of FC2A in soil matrices [33–39]. The degradation products have been shown to be glycolate and fluoride [40–42]. Half-times for FC2A degradation are on the order of days for acclimated soils [38] or weeks for freshly exposed soils [34]. The time since application of FC2A to RMA soils is at least 20 years.

4. Conclusions

The method presented here can quantitatively analyze water and soil samples suspected of containing FC2A in the presence of several major interferences, including relatively high concentrations of formic acid. The method is sensitive, quantitative, requires minimal sample preparation, and is suitable for the routine analysis of environmental samples in site investigations and fate studies. A confirmatory detector, such as a mass spectrometer, would improve the method. The method is also suitable for application studies and could be easily modified to accept other sample matrices, such as food and animal tissue.

5. Acknowledgement

This work was supported in part by the US Army, Program Manager for Rocky Mountain Arsenal (Denver, CO, USA), under Contract No. DAAA05-92-R-0014.

6. References

[1] E.R. Kalmbach, *Science*, 102 (1945) 232–233.
[2] N.I. Sax and R.J. Lewis, *Dangerous Properties of Industrial Materials*, Vol. III, Van Nostrand Reinhold, New York, 7th Ed., 1989, pp. 1747, 3066.
[3] C.R. Worthing (Editor), *The Pesticide Manual*, British Crop Protection Council, Farnham, 1991.
[4] USEPA, *Federal Register*, Vol. 55, No. 154, Notices, 1990, 32574–32579.
[5] D.H. Rosenblatt, T.A. Miller, J.C. Dacre, I. Mual and D.R. Cogley, *Problem Definition Studies on Problem Environmental Pollutants, II*, US Army Medical Bioengineering Research and Development Laboratory, Fort Detrick, MD, 1975, TR 7509.
[6] US Army Toxic and Hazardous Materials Agency, *USATHAMA Method AAA9, Isopropyl Methylphosphonic Acid, Methylphosphonic Acid and Fluoroacetic Acid in Soil*, Aberdeen Proving Ground, MD, 1987.
[7] Program Manager for Rocky Mountain Arsenal, *Integrated Endangerment Assessment/Risk Characterization for RMA*, Denver, CO, 1992.

[8] H.M. Stahr, W.B. Buck and P.F. Ross, *J. Assoc. Off. Anal. Chem.*, 57 (1974) 405–407.
[9] J.E. Peterson, *Bull. Environ. Contam. Toxicol.*, 13 (1975) 751–757.
[10] W. Hyde, J. Kiesey, P.F. Ross and H.M. Stahr, *Analytical Toxicology Methods Manual*, Iowa State University Press, Ames, IO, 1977.
[11] I. Okuno and D.L. Meeker, *J. Assoc. Off. Anal. Chem.*, 63 (1980) 49–55.
[12] I. Okuno, D.L. Meeker and R.R. Felton, *J. Assoc. Off. Anal. Chem.*, 65 (1982) 1102–1105.
[13] I. Okuno, G.E. Connolly, P.J. Savarie and C.P. Breidenstein, *J. Assoc. Off. Anal. Chem.*, 67 (1984) 549–553.
[14] E.J. Huggins, H.H. Casper and C.D. Ward, *J. Assoc. Off. Anal. Chem.*, 71 (1988) 579–581.
[15] H.H. Casper, T.L. McMahon and G.D. Paulson, *J. Assoc. Off. Anal. Chem.*, 68 (1985) 722–725.
[16] D.G. Burke, D.K.T. Lew and X. Cominos, *J. Assoc. Off. Anal. Chem.*, 72 (1989) 503–507.
[17] B.A. Kimble, *Analytical Method for the Determination of Compound 1080 in Sheepskin and Wool*, US Department of Agriculture, Denver Wildlife Research Center, Denver, CO, 1990.
[18] H. Ozawa and T. Tsukioka, *Anal. Chem.*, 59 (1987) 2914–2917.
[19] H. Ozawa and T. Tsukioka, *J. Chromatogr.*, 473 (1989) 251–259.
[20] D.M. Collins, J.P. Fawcett and C.G. Rammell, *Bull. Environ. Contam. Toxicol.*, 26 (1981) 669–673.
[21] A.C. Ray, L.O. Post and J.C. Reagor, *J. Assoc. Off. Anal. Chem.*, 64 (1981) 19–24.
[22] H.L. Kramer, *J. Assoc. Off. Anal. Chem.*, 67 (1984) 1058–1061.
[23] W.J. Allender, *J. Liq. Chromatogr.*, 13 (1990) 3465–3471.
[24] B.A. Kimble, *Compound 1080 Grain Bait Assay*, US Department of Agriculture, Denver Wildlife Research Center, Denver, CO, 1989.
[25] M.L. Baron, C.M. Bothroyd, G.I. Rogers, A. Staffa and I.D. Rae, *Phytochemistry*, 26 (1987) 2293–2295.
[26] R.L. Frost, R.W. Parker and J.V. Hanna, *Analyst*, 114 (1989) 1245–1248.
[27] B. Tecle and J.E. Casida, *Chem. Res. Toxicol.*, 2 (1989) 429–435.
[28] G. Livanos and P.J. Milham, *J. Assoc. Off. Anal. Chem.*, 67 (1984) 10–12.
[29] *Official Methods of Analysis of the Association of Official Analytical Chemists*, Association of Official Analytical Chemists, Arlington, VA, 15th ed., 1990.
[30] A.F. Kingery and H.E. Allen, *Anal. Chem.*, 66 (1994) 155–159.
[31] J.R. Stillian and C.A. Pohl, *J. Chromatogr.*, 499 (1990) 249–266.
[32] G.E.P. Box, W.G. Hunter and J.S. Hunter, *Statistics for Experimenters: An Introduction to Design, Data Analysis and Model Building*, Wiley, New York, 1978.
[33] M. Kelly, *Nature*, 208 (1965) 809–810.
[34] W.A.L. David and B.O.C. Gardiner, *Nature*, 209 (1966) 1367–1368.
[35] C.L. Bong, A.L.J. Cole and J.R.L. Walker, *Soil Biol. Biochem.*, 11 (1979) 13–18.
[36] J.R.L. Walker and C.L. Bong, *Soil Biol. Biochem.*, 13 (1981) 231–235.
[37] J.J.M. Meyer, N. Grobbelaar and P.L. Steyn, *Appl. Environ. Microbiol.*, 56 (1990) 2152–2155.
[38] D.H. Wong, W.E. Kirkpatrick, D.R. King and J.E. Kinnear, *Soil Biol. Biochem.*, 24 (1992) 833–838.
[39] D.H. Wong, W.E. Kirkpatrick, D.R. King and J.E. Kinnear, *Soil Biol. Biochem.*, 24 (1992) 839–843.
[40] P. Goldman, *J. Biol. Chem.*, 240 (1965) 3434–3438.
[41] P. Goldman and G.W.A. Milne, *J. Biol. Chem.*, 241 (1966) 5557–5559.
[42] P. Goldman, G.W.A. Milne and D.B. Keister, *J. Biol. Chem.*, 243 (1968) 428–434.

ELSEVIER

Journal of Chromatography A, 671 (1994) 239–248

JOURNAL OF CHROMATOGRAPHY A

Simultaneous ion-exclusion chromatography–cation-exchange chromatography with conductimetric detection of anions and cations in acid rain waters

Kazuhiko Tanaka*,[a], Kazutoku Ohta[a], James S. Fritz[b], Susumu Matsushita[c], Akiyoshi Miyanaga[c]

[a]*National Industrial Research Institute of Nagoya*[☆], *1-1, Hirate-cho, Kita-ku, Nagoya-shi, Aichi 462, Japan*
[b]*Ames Laboratory and Chemistry Department, Iowa State University, Ames, IA 50011-3020, USA*
[c]*Tokyo Research Centre, Tosoh Corporation, 2743-1, Hayakawa, Ayase-shi, Kanagawa 252, Japan*

Abstract

A simple, selective and sensitive method was investigated for simultaneously determining anions (Cl^-, NO_3^-, SO_4^{2-}) and cations (Na^+, NH_4^+, K^+, Mg^{2+}, Ca^{2+}) in acid rain and related environmental waters in central Japan. The method involves simultaneous ion-exclusion–cation-exchange chromatography with conductimetric detection on a polyacrylate weakly acidic cation-exchange resin column with a weak-acid eluent. With the weak-acid eluent (tartaric acid) both anions and cations were separated simultaneously, based on ion-exclusion and cation-exchange mechanism. Owing to the presence of H^+ ions in the tartaric acid eluent, the detector response was positive for the anions and negative for the cations. Using a 5 m*M* tartaric acid–7.5% methanol–water eluent, good simultaneous separation and detection were achieved in about 30 min. The results indicated an ionic balance of about 100% between the anions (including HCO_3^-) and the cations (including H^+).

1. Introduction

The acid rain caused by SO_2 and NO_x in air is a major environmental pollution problem, not only in Europe and North America but also in Japan. Frequent analyses of acid rain waters is essential to establish the effect of acidification of the aquatic environment caused by air pollution. Therefore, it is very important to develop effective methods for automatically monitoring acid rain and related environmental waters.

The major ionic components of acid rain are H^+, Na^+, NH_4^+, K^+, Mg^{2+} and Ca^{2+} as cationic components and Cl^-, NO_3^- and SO_4^{2-} as anionic components [1]. The ionic balance between these nine ionic components is almost 100%, and their simultaneous determination is therefore very important.

There are several different ion chromatographic (IC) strategies for the simultaneous determination of anions and cations. The cations can be converted into anions by using a complexing agent such as EDTA and then all species are separated and detected as anions [2]. In another approach, a mixed-bed ion-exchange column containing both cation and anion exchangers was

* Corresponding author.
☆ Former name: Government Industrial Research Institute, Nagoya.

0021-9673/94/$07.00
SSDI 0021-9673(93)E1276-6

used for the simultaneous separation of mono- and divalent anions and cations using a single sample injection [3]. IC using anion- and cation-exchange columns in series, followed by UV or conductivity detection, has also been reported [4,5].

The purpose of this study was to develop a simple, selective, efficient and highly sensitive IC method for the simultaneous determination of anions and cations, and to apply simultaneous ion-exclusion–cation-exchange chromatography (CEC) with conductimetric detection to acid rain and related environmental waters. A polyacrylate-based weakly acidic cation-exchange resin column and a weak-acid eluent were used for the simultaneous separation of anions by ion exclusion and cations by cation exchange. Based on selectivity, sensitivity, stability and utility, a conductometric detector was chosen for the simultaneous detection of both anions and cations.

2. Experimental

2.1. Chromatographic system

The IC system used was a Tosoh CCPD non-suppressor ion chromatograph with a non-metallic eluent delivery pump operating at 1–1.2 ml/min. A Tosoh CM-8000 conductimetric detector was used. A Tosoh SC-8010 chromatographic data system was used for instrument control and for data collection and processing.

2.2. Eluents

Eluents consisting of water, strong acid–water, weak acid–water and methanol–water were compared for the simultaneous separation of both anions and cations. All eluents were continuously degassed with a Tosoh SD-8022 on-line degasser.

2.3. Columns

The ion-exclusion–CEC separation of both anions and cations was carried out on a Tosoh TSKgel OA-PAK weakly acidic cation-exchange resin column (H^+ form) with polyacrylate copolymer (particle size 5 μm) (300 mm × 7.8 mm I.D.). The ion-exclusion chromatographic separation of HCO_3^- with ion-exchange enhancement of conductivity detection [6] was carried out on a Tosoh TSKgel-SCX strongly acidic cation-exchange resin columns (H^+ form and Na^+ form, in series) with polystyrene–divinylbenzene copolymer (particle size 5 μm) (each 100 mm × 7.8 mm I.D.).

2.4. pH measurement

The pH values of samples were measured with a Toa Denpa IM-40S ion meter with a glass electrode.

2.5. Chemicals

All chemicals were of analytical-reagent grade. Deionized, distilled water was used for the preparation of standard solutions and eluents.

Stock standard solutions of anions and cations were prepared by dissolving appropriate amounts of acids, alkalis and alkaline earth metal salts in water.

2.6. Sample pretreatment

Samples were collected in or near the city of Nagoya, which is located in central Japan. For the forest soil extraction water samples, the samples were subjected to IC analysis after extraction by ultrasonication with acid rain water for 15 min. The soil, which is a typical brown forest soil in Japan, was collected in Kumamoto, located in western Japan. All samples were subjected to IC analysis after filtration with a 0.45-μm membrane filter.

3. Results and discussion

3.1. Selection of eluent

The cation-exchange resin column used is commercially available under trade-name

TSKgel OA-PAK. The column is packed with a weakly acidic cation-exchange resin and is usually used for the ion-exclusion chromatographic separation of weakly ionized organic acids by using strong-acid (sulphuric acid) or weak-acid (phosphoric acid) eluents. The effectiveness of weak-acid eluents such as succinic and benzoic acid with $pK \approx 4$ in the ion-exclusion chromatography of various organic weak acids on a strongly acidic cation-exchange resin has been reported by Tanaka and Fritz [7].

On the other hand, it is well known that such weakly acidic cation-exchange resins are capable of separating rapidly and efficiently mono- and divalent cations under isocratic conditions by elution with a strong-acid eluent. Accordingly, it was expected that such acidic eluents would be applicable as the common eluent for the simultaneous separation of anions and cations by ion exclusion and cation exchange. In order to accomplish the simultaneous separation of anions by the ion-exclusion mechanism and cations by the cation-exchange mechanism, several kinds of eluents with different acidity were tested.

Fig. 1 shows the separation of strong acid anions (Cl^-, NO_3^-, SO_4^{2-}), weak-acid anions (PO_4^{3-}, $HCOO^-$, CH_3COO^-, HCO_3^-) and mono- and divalent cations (Na^+, NH_4^+, K^+, Mg^{2+}, Ca^{2+}) by elution with water, a strong acid and weak acids.

When water was used as the eluent, it was possible to separate the weak acid anions alone, except for PO_4^{3-}, from the strong acids by ion exclusion, as shown in Fig. 1A. The separation of the cations is impossible because all of them are fixed on the resin. When a strong acid (sulphuric acid) was used as the eluent, it was possible to separate the cations alone by cation exchange, as shown in Fig. 1B. The separation of the anions is impossible because all of the anions are incompletely ion excluded from the resin. When weak acids (tartaric and citric acid and EDTA) with $pK_1 \approx 2$–3 were used as the eluent, it was possible to separate simultaneously the anions and cations by ion exclusion and cation exchange, respectively, as shown in Fig. 1C–E.

As can be seen from Fig. 1C–E, although all of anions except HCO_3^- were detected conductimetrically, the detector responses were much lower with weak-acid anions such as $HCOO^-$ and CH_3COO^- than with strong-acid anions such as SO_4^{2-}, Cl^-, and NO_3^-. HCO_3^-, which is a very weakly acidic anion, was not detected. This means that the ionization of the weak-acid anions is suppressed, depending on the acidity and concentration of the acidic eluent.

The detector response was positive for the anions and negative for the cations. The detector response for the cations is negative because this method is based on indirect conductimetric detection.

Considering the resolution of both anions and cations, separation time, detection sensitivity, and eluent background conductivity, it was concluded that the best choice for the eluent is tartaric acid.

3.2. Effect of tartaric acid concentration

In order to optimize the simultaneous separation and detection of cations and anions, the effect of tartaric acid concentration in the eluent on the retention volumes (V_R) of the anions and cations was investigated.

In the ion-exclusion chromatographic separation of the anions, the V_R values of the anions increased with increasing concentration of tartaric acid in the eluent. The peak resolution also increased, as shown in Fig. 2A. In the CEC separation of the cations, the V_R values of the cations decreased drastically on increasing the concentration of tartaric acid in the eluent. The peak resolution was also increased, as shown in Fig. 2B.

The eluent background conductivity increased on increasing the tartaric acid concentration in the eluent (694 $\mu S\ cm^{-1}$ at 6 m*M*). Because an increase in the eluent conductivity caused a decrease in the sensitivity of conductivity detection, it was concluded that a much lower eluent concentration of tartaric acid should be used to obtain a reasonable peak resolution and separation speed. From the above results, it was concluded that the optimum concentration of tartaric acid for the simultaneous ion-exclusion–CEC separation of the cations and anions is *ca.* 3–5 m*M*.

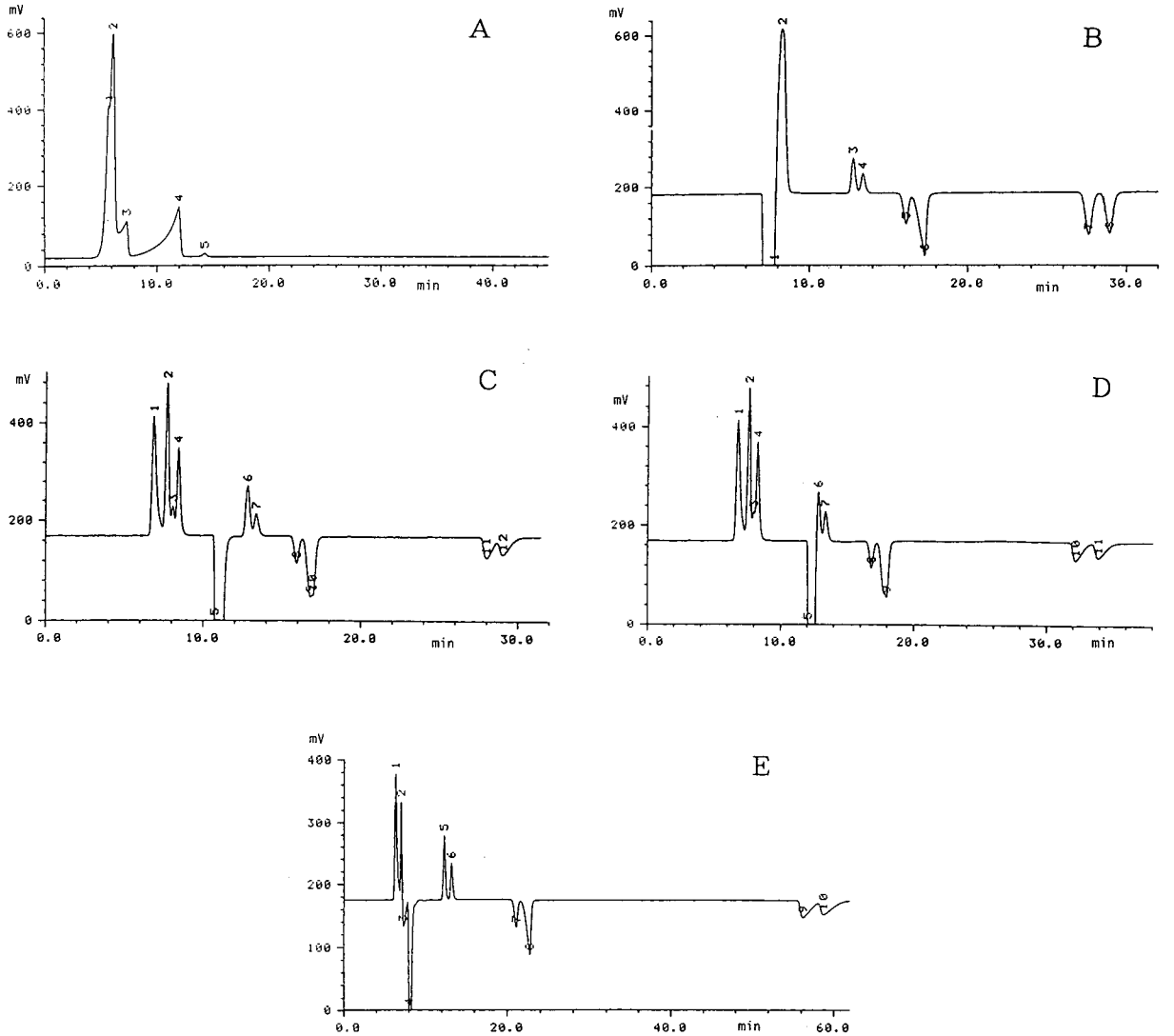

Fig. 1. Typical simultaneous ion-exclusion–CEC of anions and cations obtained by elution with (A) water, (B) strong acid and (C–E) weak acids. Column, Tosoh TSKgel OA-PAK polyacrylate-based weakly acidic cation-exchange resin; column temperature, room temperature (26°C); detector sensitivity, 1000 mV = 100 μS cm^{-1}; eluent flow-rate, 1 ml/min; injection volume, 0.1 ml; sample, mixture of 0.1 m*M* HNO_3, KCl, NH_4NO_3, $(NH_4)_2SO_4$, $NaHCO_3$, $CaCl_2$, $MgCl_2$, KH_2PO_4, 1 m*M* HCOOH and 5 m*M* CH_3COOH. Eluents (conductivity): (A) water (0 μS cm^{-1}); (B) 1 m*M* sulphuric acid (693 μS cm^{-1}); (C) 6 m*M* tartaric acid (694 μS cm^{-1}); (D) 6 m*M* citric acid (636 μS cm^{-1}); (E) 1 m*M* EDTA (409 μS cm^{-1}). Peaks: (A) 1 = SO_4^{2-}; 2 = Cl^-; NO_3^-; PO_4^{3-}; 3 = $HCOO^-$; 4 = CH_3COO^-; 5 = HCO_3^-; (B) 1 = eluent dip; 2 = SO_4^{2-}, Cl^-, NO_3^-, PO_4^{3-}; 3 = $HCOO^-$; 4 = CH_3COO^-; 5 = Na^+; 6 = NH_4^+, K^+; 7 = Mg^{2+}; 8 = Ca^{2+}; (C) 1 = SO_4^{2-}; 2 = Cl^-; 3 = PO_4^{3-}; 4 = NO_3^-; 5 = eluent dip; 6 = $HCOO^-$; 7 = CH_3COO^-; 8 = Na^+; 9 = NH_4^+; 10 = K^+; 11 = Mg^{2+}; 12 = Ca^{2+}; (D) 1 = SO_4^{2-}; 2 = Cl^-; 3 = PO_4^{3-}; 4 = NO_3^-; 5 = eluent dip; 6 = $HCOO^-$; 7 = CH_3COO^-; 8 = Na^+; 9 = NH_4^+, K^+; 10 = Mg^{2+}; 11 = Ca^{2+}; (E) 1 = SO_4^{2-}; 2 = Cl^-; 3 = PO_4^{3-}, NO_3^-; 4 = eluent dip; 5 = $HCOO^-$; 6 = CH_3COO^-; 7 = Na^+; 8 = NH_4^+, K^+; 9 = Mg^{2+}; 10 = Ca^{2+}.

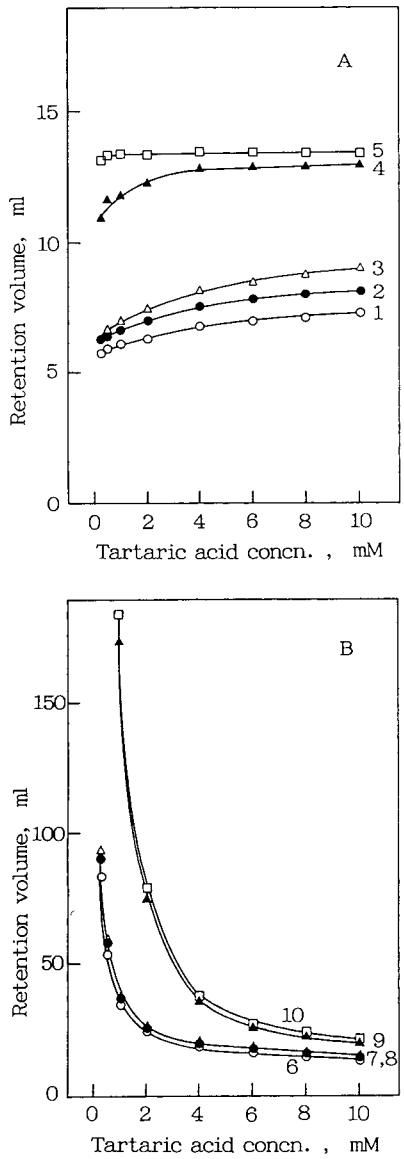

Fig. 2. Effect of tartaric acid concentration in the eluent on retention volumes (V_R) of (A) anions and (B) cations. Lines: 1 = SO_4^{2-}; 2 = Cl^-; 3 = NO_3^-; 4 = $HCOO^-$; 5 = CH_3COO^-; 6 = Na^+; 7 = NH_4^+; 8 = K^+; 9 = Mg^{2+}; 10 = Ca^{2+}. Chromatographic conditions as in Fig. 1.

3.3. Effect of methanol concentration

In order to accomplish a reasonable resolution of both anions and cations, the effect of methanol concentration in 4 m*M* tartaric acid eluent on the V_R values of the anions and cations was investigated.

The V_R values of the anions were almost unchanged, except that of acetate ion, as shown in Fig. 3A. Those of the cations increased gradually for monovalent cations and decreased gradually for divalent cations, as shown in Fig. 3B. From these results, the best concentration of

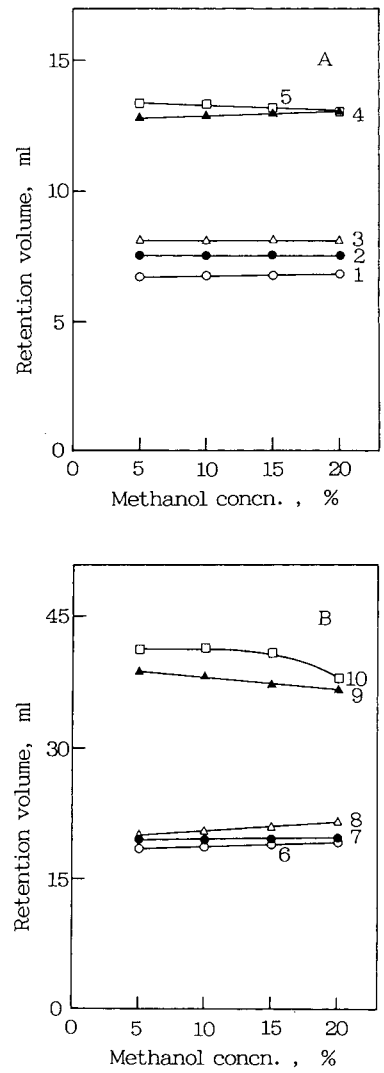

Fig. 3. Effect of methanol concentration in 4 m*M* tartaric acid eluent on retention volumes (V_R) of (A) anions and (B) cations. Lines: 1 = SO_4^{2-}; 2 = Cl^-; 3 = NO_3^-; 4 = $HCOO^-$; 5 = CH_3COO^-; 6 = Na^+; 7 = NH_4^+; 8 = K^+; 9 = Mg^{2+}; 10 = Ca^{2+}. Chromatographic conditions as in Fig. 1.

methanol in the eluent was concluded to be *ca.* 7.5%.

Although the simultaneous separation of the anions and cations was accomplished by ion-exclusion–CEC with elution with 3 m*M* tartaric acid–7.5% methanol–water (Fig. 4A), the separation time was long. Therefore, the tartaric acid concentration in the eluent was increased from 3 to 5 m*M* and the flow-rate was increased from 1.0 to 1.2 ml/min. Fig. 4B shows the ion-exclusion–CEC of the anions and cations with elution with 5 m*M* tartaric acid–7.5% methanol–water. A high-resolution chromatogram was obtained under these elution conditions.

As the conductimetric detector response was positive for anions and negative for cations, the polarity of the signal from the detector was changed automatically from negative to positive, in order to measure easily the CEC peak areas of the cations, after the ion-exclusion chromatographic separation of the anions.

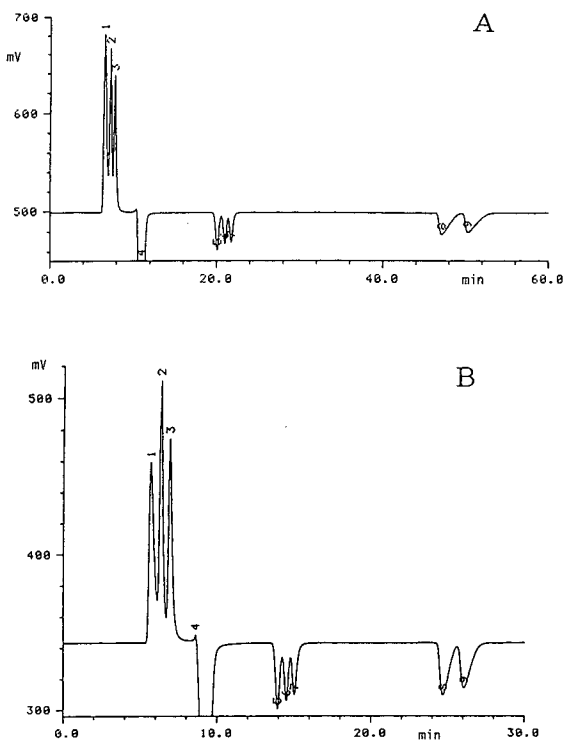

Fig. 4. Simultaneous ion-exclusion–CEC separation of anions and cations by elution with (A) 3 m*M* tartaric acid–7.5% methanol–water at 1 ml/min and (B) 5 m*M* tartaric acid–7.5% methanol–water at 1.2 ml/min. Eluent conductivity: (A) = 389 μS cm^{-1}; (B) = 536 μS cm^{-1}. Peaks: 1 = SO_4^{2-}; 2 = Cl^-; 3 = NO_3^-; 4 = eluent dip; 5 = Na^+; 6 = NH_4^+; 7 = K^+; 8 = Mg^{2+}; 9 = Ca^{2+}. Other chromatographic conditions as in Fig. 1.

3.4. Retention volumes of common anions and cations

Table 1 gives the V_R values of common anions and cations obtained by elution with 3 m*M* tartaric acid–7.5% methanol–water.

For the retention of monovalent weak-acid anions such as NO_2^-, F^-, $HCOO^-$ and CH_3COO^-, the V_R values depended on their pK_1 ($NO_2^- < F^- < HCOO^- < CH_3COO^-$). The V_R of PO_4^{3-}, which is a weak-acid anion (pK_1 = 2.1), was smaller than that of NO_3^- (strong-acid anion), because the charge of PO_4^{3-} is −2 (HPO_4^{2-}) and that of NO_3^- is −1 in the acidic eluent.

For the retention of mono- and divalent strong-acid anions such as SO_4^{2-}, $S_2O_3^{2-}$ and Cl^-, the V_R values depended on their charge ($Cl^- < SO_4^{2-} = S_2O_3^{2-}$) rather than their p$K_1$ values (complete dissociation).

For the retention of monovalent strong-acid halide anions such as Cl^-, Br^- and I^-, which are ionized completely, the V_R values appear to be

Table 1
Retention volumes of common anions and cations on elution with 3 m*M* tartaric acid–7.5% methanol–water

Ion[a]	V_R (ml)	Ion	V_R (ml)
SO_4^{2-} (S)	6.77	Li^+	20.76
$S_2O_3^{2-}$ (S)	6.80	Na^+	21.12
Cl^- (S)	7.43	NH_4^+	22.07
PO_4^{3-} (W)	7.62	K^+	22.43
Br^- (S)	7.75	Rb^+	22.23
NO_3^- (S)	7.98	Cs^+	22.37
I^- (W)	9.12	Mg^{2+}	44.40
NO_2^- (W)	11.02	Ca^{2+}	47.47
F^- (W)	11.26	Sr^{2+}	48.20
$HCOO^-$ (W)	12.67	Ba^{2+}	67.80
CH_3COO^- (W)	13.26		

[a] S = Strong-acid anion; W = weak-acid anion.

dependent on their ionic radii rather than their pK_1 values (complete dissociation). Although the reason is not clear, another effect such as the hydrophobic adsorption effect based on the difference in their ionic radii might be predominant in this separation. The hydrophobic adsorption effect is well known as a side-effect in the separation of common inorganic anions by ion-exchange chromatography with a polymeric resin.

Therefore, in ion-exclusion chromatography using a weakly acidic cation-exchange resin and a weak-acid eluent, it was found that the V_R values of the anions were strongly related to their pK_1 values and the charge as the main effect in the ion-exclusion chromatography and their hydrophobicity as a side-effect. As has been reported by Tanaka *et al.* [8], the V_R values of common strong- and weak-acid anions on a strongly acidic cation-exchange resin column by elution with water are increased in proportion to the increase in their pK_1 values and the hydrophobicities.

For the CEC separation of cations by the cation-exchange mechanism, the V_R values of the cations were strongly related to their cation-exchange affinities (their ionic radii and charge). The elution order of mono- and divalent cations was almost identical with that in conventional CEC.

3.5. Calibration

Calibration graphs were obtained by plotting peak areas against the concentrations of anions and cations. Linear calibration graphs were obtained in at least the concentration ranges 0–0.8 m*M* for the anions and 0–0.4 m*M* for the cations.

3.6. Detection limits

The detection limits of the anions and cations at a signal-to-noise ratio of 3 are given in Table 2. Although the eluent background conductivity is relatively high (536 $\mu S\ cm^{-1}$) because of the use of tartaric acid as the eluent, these values were reasonable for application to various acid rains and related environmental waters.

Table 2
Detection limits of major anions and cations related to acid rain water determined by elution with 3 m*M* tartaric acid–7.5% methanol–water

Ion	Detection limit[a]	
	μM	ppb
SO_4^{2-}	0.16	15
Cl^-	0.10	3.6
NO_3^-	0.14	9
Na^+	0.20	4.6
NH_4^+	0.30	5.4
K^+	0.32	12.5
Mg^{2+}	0.28	6.8
Ca^{2+}	0.28	11.2

[a] Signal-to-noise ratio = 3.

3.7. Reproducibility

The reproducibility of the ion-exclusion–CEC chromatographic peak areas of anions and cations with elution with 3 m*M* tartaric acid–7.5% methanol–water was 0.02–0.2% ($n = 6$). Reproducible chromatograms were obtained during repeated chromatographic runs.

3.8. Application of ion-exclusion–CEC to acid rain waters

In order to evaluate the effect of acid rain on the aquatic environment, it is essential to demonstrate the effectiveness of the present method when applied to various environmental waters including acid rain waters and forest soil waters of different pH.

First, the ion-exclusion–CEC method was applied to the simultaneous determination of anions and cations in several rain waters of different pH. Fig. 5 shows the ion-exclusion–CEC of anions and cations in a typical acid rain water at pH 4.81 taken near Nagoya. A good simultaneous separation of the anions and the cations was obtained and it was found that this acid rain water sample contains SO_4^{2-}, NO_3^-, Cl^-, Na^+, NH_4^+, K^+, Mg^{2+} and Ca^{2+}.

Table 3 gives the results for the anions and the cations, including H^+, in the above rain water

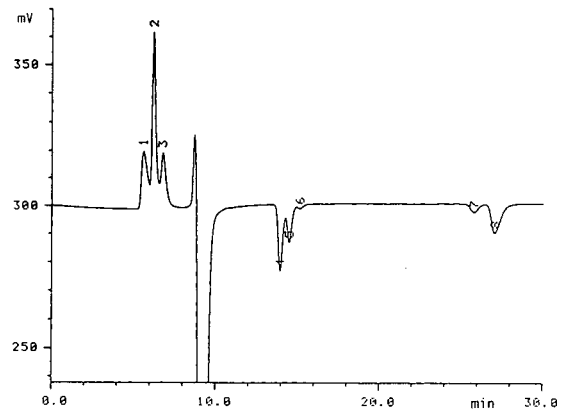

Fig. 5. Simultaneous ion-exclusion–CEC of anions and cations in rain water of pH 4.81 taken near Nagoya. Peaks: 1 = SO_4^{2-}; 2 = Cl^-; 3 = NO_3^-; 4 = Na^+; 5 = NH_4^+; 6 = K^+; 7 = Mg^{2+}; 8 = Ca^{2+}. Chromatographic conditions as in Fig. 4.

samples. The pH values of these samples were in the range 4.21–5.49. The results showed that this method is very useful for the simultaneous determination of the anions and cations in acid rain water because the ion balance (anions/cations) ranged from 0.98 to 1.07, except for the rain water sample at pH 5.49, which had an ion balance of 0.80. This might be due to the presence of HCO_3^- and the lack of detection of HCO_3^- by ion-exclusion–CEC. Therefore, the ion-exclusion chromatography of HCO_3^- with conductimetric detection using a conductivity enhancement column [6] was carried out to determine the ion balance of environmental waters of neutral pH.

3.9. Application of ion-exclusion–CEC and ion-exclusion chromatography to environmental waters related to acid rain

Figs. 6 and 7 show (A) a typical ion-exclusion–CEC of anions and cations and (B) ion-exclusion chromatogram of HCO_3^- in forest soil water (pH 7.20) and in brown forest soil extraction water (pH 4.95), sonicated with acid rain water (pH 4.72), respectively, taken in or near Nagoya.

Good ion-exclusion–CEC separation of the anions and the cations and ion-exclusion chromatographic separation of HCO_3^- were accomplished for the forest soil water of neutral pH. The results obtained showed that this environmental water contains SO_4^{2-}, NO_3^-, Cl^-, Na^+, NH_4^+, K^+, Mg^{2+} and Ca^{2+}, in addition to HCO_3^-, as shown in Fig. 6A and B.

On the other hand, ion-exclusion–CEC of the brown forest soil extraction water showed the presence of the cations and anions and ion-exclusion chromatography showed the presence of unidentified weak acids and no HCO_3^-, as shown in Fig. 7A and B. This unidentified peak might be due to organic weak acids because the sample was taken from the surface layer of the forest brown soil containing humic substances from biodegraded plants and bacteria. The peak identification of this organic weak acid will be the subject of future research.

Table 4 gives the results for anions including HCO_3^- and cations including H^+, together with the ion balance (anions/cations), for various acid rains and related environmental waters obtained

Table 3
Determination of major anions and cations in rain waters by ion-exclusion–CEC

Rain water	Concentration (mequiv./l)									Ion balance (anions/cations)
	SO_4^{2-}	Cl^-	NO_3^-	Na^+	NH_4^+	K^+	Mg^{2+}	Ca^{2+}	H^+ (pH)	
A	0.051	0.034	0.035	0.018	0.054	0.005	0.004	0.018	4.34	1.03
B	0.035	0.015	0.034	0.005	0.044	0.002	0.001	0.002	4.21	1.00
C	0.007	0.008	0.007	0.005	0.009	0.0005	0.0005	0.0005	4.87	0.98
D	0.016	0.006	0.010	0.001	0.024	0.001	ND[a]	0.001	4.80	1.07
E	0.006	0.016	0.003	0.016	0.005	0.001	0.003	0.003	5.49	0.80

[a] Not detected.

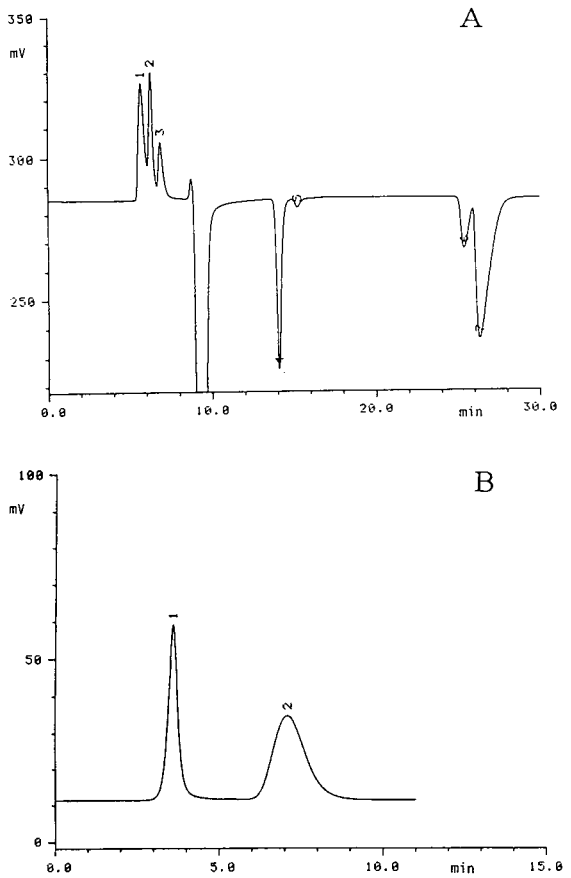

Fig. 6. (A) Simultaneous ion-exclusion–CEC chromatogram of anions and cations and (B) ion-exclusion chromatogram of HCO_3^- in forest soil water of pH 7.20. Chromatographic conditions [6]: (B) eluent, water; columns, Tosoh TSKgel-SCX strongly acidic cation-exchange resin in the H^+ form and Na^+ form in series (each 100 mm × 7.8 mm I.D.). Peaks: (A) $1 = SO_4^{2-}$; $2 = Cl^-$; $3 = NO_3^-$; $4 = Na^+$; $5 = K^+$; $6 = Mg^{2+}$; $7 = Ca^{2+}$; (B) 1 = strong-acid anions; $2 = HCO_3^-$. Other chromatographic conditions as in Fig. 4.

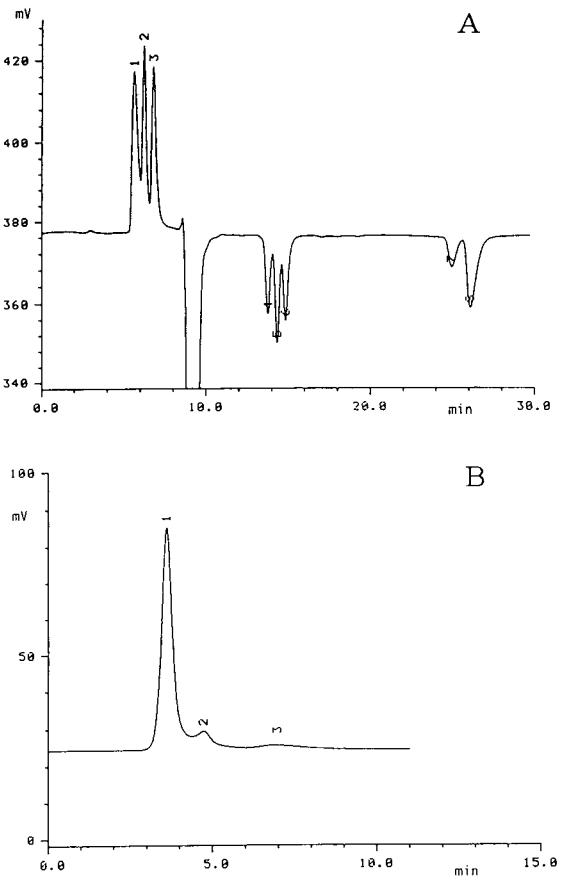

Fig. 7. (A) Simultaneous ion-exclusion–CEC chromatogram of anions and cations and (B) ion-exclusion chromatogram of HCO_3^- and weak acids in brown forest soil extraction water (pH 4.57) sonicated with rain water at pH 4.72. Peaks: (A) $1 = SO_4^{2-}$; $2 = Cl^-$; $3 = NO_3^-$; $4 = Na^+$; $5 = NH_4^+$; $6 = K^+$; $7 = Mg^{2+}$; $8 = Ca^{2+}$; (B) 1 = strong-acid anions; 2 = unidentified weak acid, $3 = HCO_3^-$. Chromatographic conditions as in Fig. 4.

by ion-exclusion–CEC and ion-exclusion chromatography. The results show that the ion balances for all the environmental water samples except the forest soil extraction water samples are reasonable. For the forest soil extraction water, despite the absence of HCO_3^-, the ion balance was below 1.0 (0.65 and 0.85). This might be due to the presence of other organic weak acids in the forest soil.

4. Conclusions

A method for the simultaneous determination of anions and cations, based on the simultaneous separation of the anions and cations by both ion-exclusion and cation-exchange mechanisms, with conductimetric detection has been developed. The separation and detection are selective for the anions and cations. The method was

Table 4
Determination of major anions and cations in acid rain and related environmental waters by ion-exclusion–CEC and ion-exclusion chromatography

Sample	Concentration (mequiv./l)										Ion balance (anions/cations)
	HCO_3^-	SO_4^{2-}	Cl^-	NO_3^-	Na^+	NH_4^+	K^+	Mg^{2+}	Ca^{2+}	H^+ (pH)	
Rain water (A)	ND[a]	0.061	0.077	0.039	0.057	0.037	0.002	0.013	0.065	4.81	0.94
Rain water (B)	ND	0.042	0.014	0.036	0.005	0.037	ND	0.002	0.012	4.45	1.01
Forest soil water (A)	0.490	0.120	0.057	0.038	0.170	ND	0.015	0.087	0.459	7.20	0.98
Forest soil water (B)	0.270	0.160	0.100	0.020	0.190	ND	0.027	0.170	0.210	6.97	0.92
Forest soil extraction water (A)[b]	ND	0.110	0.058	0.071	0.061	0.080	0.070	0.038	0.110	4.95	0.65
Forest soil extraction water (B)[b]	ND	0.080	0.045	0.053	0.030	0.046	0.019	0.022	0.062	4.57	0.86
Snow water	ND	0.013	0.029	0.008	0.024	0.003	0.001	0.004	0.013	5.09	0.94
River water (A)	0.350	0.240	0.170	0.036	0.350	ND	0.026	0.072	0.390	7.03	0.95
River water (B)	0.960	0.930	0.540	0.150	1.500	ND	0.130	0.150	0.680	7.19	1.05
Lake water (A)	0.170	0.290	0.190	0.019	0.180	ND	0.040	0.130	0.370	6.78	0.93
Lake water (B)	0.550	0.290	0.180	0.063	0.220	ND	0.065	0.10	0.660	6.97	1.04

[a] ND = Not detected.
[b] Sonicated with acid rain water at pH 4.72.

successfully applied to the simultaneous determination of anions and cations in several acid rains and related environmental waters, which is very important for evaluating the effect of acid rain on the aquatic environment.

5. Acknowledgements

We thank Mr. T. Yamada and Mr. Y. Ohashi of Aichi Institute of Technology for technical assistance and Dr. H. Harada of Kumamoto University for the gift of forest soil samples. This work was supported by the Agency of Industrial Science and Technology of the Ministry of International Trade and Industry in Japan, based on a Cooperative Agreement of Science and Technology for acid rain monitoring research between the National Industrial Research Institute of Nagoya and Ames Laboratory and Iowa State University.

6. References

[1] W. Stumm and J.J. Morgan, *Aquatic Chemistry. An Introduction Emphasizing Chemical Equilibria in Natural Water*, Wiley, New York, 2nd ed., 1981.
[2] M. Yamamoto, H. Yamamoto, Y. Yamamoto, S. Matsushita, S. Baba and T. Ikushige, *Anal. Chem.*, 56 (1984) 832.
[3] D.M. Brown and D.J. Pietrzyk, *J. Chromatogr.*, 466 (1989) 300.
[4] H. Small and T.E. Miller, *Anal. Chem.*, 54 (1982) 462.
[5] V.K. Jones and J.D. Tartar, *J. Chromatogr.*, 312 (1984) 456.
[6] K. Tanaka and J.S. Fritz, *Anal. Chem.*, 59 (1987) 708.
[7] K. Tanaka and J.S. Fritz, *J. Chromatogr.*, 361 (1986) 151.
[8] K. Tanaka, T. Ishizuka and H. Sunahara, *J. Chromatogr.*, 174 (1979) 153.

ELSEVIER

Journal of Chromatography A, 671 (1994) 249–252

JOURNAL OF CHROMATOGRAPHY A

Determination of carbonate, inorganic anions and anionic metal complexes by single-column ion chromatography with conductimetric and UV detection

I.N. Voloschik*, M.L. Litvina, B.A. Rudenko

V.I. Vernadsky Institute of Geochemistry and Analytical Chemistry, Russian Academy of Science, 19 Kosygin Street, 117975 Moscow, Russian Federation

Abstract

The determination of carbonate ion and some transition metals in the form of their EDTA anionic complexes by single-column ion chromatography (IC) is reported. Determinations were carried out on a column packed with a silica-based sorbent with a tetraalkylammonium base, linked by long hydrocarbon radicals. The simultaneous separation and determination of the anions F^-, Cl^-, NO_2^-, Br^-, NO_3^-, HPO_4^{2-} and SO_4^{2-} and anionic EDTA complexes of Al^{3+}, Cu^{2+}, Zn^{2+}, Cd^{2+} and Pd^{2+} were achieved. Sodium citrate solution (pH 3.9) was used as the eluent for the determination of carbonate ion and potassium hydrogenphthalate solution (pH 6.5) for the determination of anionic metal–EDTA complexes.

1. Introduction

We used ion chromatography (IC) to determine ionic components in natural, waste and technological waters and some geological materials. However, it is not possible to determine all relevant ions using the traditional IC conditions [1–4]. We have established conditions for the determination of anions that make it possible to determine both inorganic anions and carbonate ion and also anionic complexes of some transition metals simultaneously. The determination was performed by single-column IC with conductimetric and UV detection. The ionic separation was carried out using columns filled with silica-based sorbents with a tetraalkylammonium base linked to their matrix.

2. Experimental

Analyses were carried out with a Hewlett-Packard Model 1084A liquid chromatograph with a UV detector (fixed wavelength of 254 nm) and a conductimetric detector. The separation columns used were 50 × 3 mm I.D. and 100 × 3 mm I.D. Dianion-1 and 150 × 4 mm I.D. Dianion-2 (Elsiko, Russian Federation). Potassium hydrogenphthalate and sodium citrate solutions were used as eluents. The anionic metal–EDTA complexes were obtained by adding equivalent amounts of EDTA disodium salt to metal salt solutions. The loop size was 175 μl.

3. Results and discussion

Carbonate ion was determined by single-column IC because it is a weak acid anion. Un-

* Corresponding author.

0021-9673/94/$07.00
SSDI 0021-9673(94)00204-M

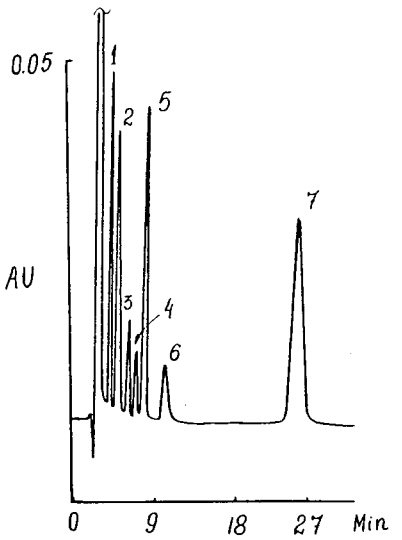

Fig. 1. Chromatogram of inorganic anions. Column: 100 × 3 mm I.D. Dianion-1; eluent 1 m*M* potassium hydrogenphthalate (pH 6.6); flow-rate, 1 ml/min; detection, UV at 254 nm. Peaks: 1 = HCO_3^-; 2 = Cl^-; 3 = NO_2^-; 4 = Br^-; 5 = NO_3^-; 6 = HPO_4^{2-}; 7 = SO_4^{2-}.

fortunately, the determination cannot always be carried out with acceptable sensitivity and selectivity. Fig. 1 shows the chromatogram of an inorganic anion mixture including carbonate ion. This separation was performed with the Dianion-1 column with potassium hydrogenphthalate as eluent. It can be seen that the carbonate ion has a short retention time. The carbonate peak can interfere with the peaks of weakly retained macrocomponents of the sample. Particular difficulties arise in the use of this method for the determination of carbonate in brines.

In order to increase the separation selectivity and determination sensitivity, we suggest the use of sodium citrate solution as the eluent. Detection can then be carried out with a conductimetric detector. The advantages of this eluent are that citric acid is hardly adsorbed on the hydrophobic sorbent surface and that the system peak is eliminated. In addition, the retention of carbonate under these conditions is much stronger than that with the phthalate eluent.

We studied the influence of the eluent pH on the carbonate signal and retention time. It was found that the maximum separation selectivity and sensitivity of determination for carbonate were achieved at pH 4.6.

Figs. 2 and 3 show chromatograms for Moscow drinking water and Lake Baikal water obtained on the Dianion-2 column with sodium citrate (pH 4.6) as eluent. A small amount of sodium hydrogenphthalate was added to the eluent to eliminate the non-linear sorption of nitrate ion. These chromatograms demonstrate the good results achieved. In spite of the low eluent pH, carbonate ion is detected as a positive peak, resulting from the high pressure used: the carbonic acid dissociates under high pressure in the first step to a greater extent than without pressure.

The retention time of carbonate is increased by the use of the citrate eluent and by the possible presence of non-ionic sorption of the carbonic acid on the sorbent. After passing through the column, the pressure of the chromatographic system falls and the degree of

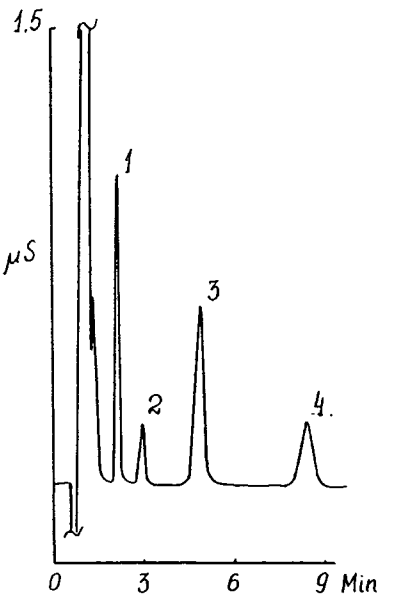

Fig. 2. Determination of carbonate ion and other inorganic anions in Moscow drinking water. Column, 150 × 4 mm I.D. Dianion-2; eluent, 2 m*M* citric acid–0.1 m*M* phthalic acid (pH 4.6); flow-rate, 1 ml/min; detection, conductimetric. Peaks: 1 = Cl^- (4.8 mg/l); 2 = NO_3^- (2.5 mg/l); 3 = HCO_3^- (10 mg/l); 4 = SO_4^{2-} (6.0 mg/l). Sample dilution 1:4.

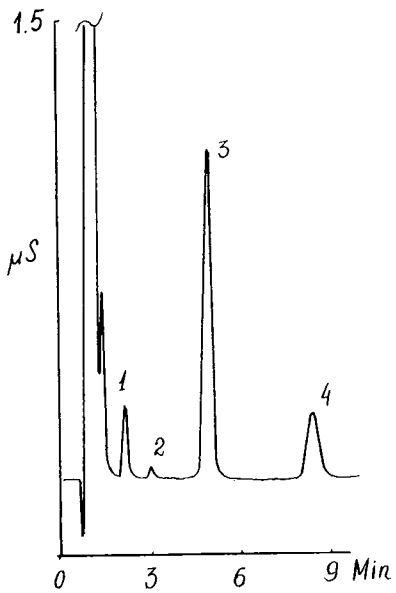

Fig. 3. Determination of carbonate ion and other inorganic anions in the Lake Baikal water. Conditions as in Fig. 2. Peaks: 1 = Cl^- (1.1 mg/l); 2 = NO_3^- (0.4 mg/l); 3 = HCO_3^- (18.5 mg/l); 4 = SO_4^{2-} (6.6 mg/l).

dissociation of the carbonic acid decreases. The conductivity increases because of the ion-exchange equilibrium shift. There is a linear dependence of this signal shift on carbonate concentration in the sample, *i.e.*, the calibration graph is linear over a wide range of injected concentrations (0.05–100 ppm).

The limit of determination of carbonate is 0.005 mg/l. Doubly distilled and degased water was used to obtain the calibration graph. Doubly distilled water is not applicable without vacuum treatment for the preparation of standard low-carbonate solutions as it contains dissolved CO_2.

The optimized chromatographic conditions were successfully used in analyses of natural and waste waters, brines and fluid inclusions for their anionic constituents.

The choice of the Dianion-1 separation column for the separation of anions and anionic transition metal complexes was determined by its high separation selectivity of singly and doubly charged inorganic anions (Fig. 1). The phthalate eluent and UV detection are used. As Fig. 1 shows, the most frequently found anions, *viz.*, Cl^-, NO_2^-, NO_3^- and HPO_4^{2-}, are sufficiently separated by this column and are eluted faster than the sulphate ion. The retention time of the EDTA anion is much longer than that of sulphate and nearly twice as long as that of phosphate. Hence the EDTA anion does not hinder the determination of other inorganic anions, *i.e.*, SO_4^{2-} and the earlier eluted HPO_4^{2-}, NO_2^-, NO_3^- and Cl^-.

The choice of the eluent pH value was determined by the following factors: (1) the stability of the silica-based sorbent (pH 2–8), (2) the absence of a system peak in the chromatogram (pH 6) and (3) stability of the anionic metal–EDTA complexes. These conditions are fulfilled in a very restricted pH range (6–8). The selectivity of the separation of anions decreases and the time of analysis increases with increase in pH because of the stronger retention of the EDTA anion. This is why an eluent of pH 6.6 was chosen.

The charge of the above metal anionic complexes is −1 or −2 in the pH range 6–8. The ratio between singly and doubly charged anions may change according to the pH value, *i.e.*, the effective charge of the complex anion can appear fractional. Hence such anionic metal complexes must be eluted between singly and doubly charged anions. In addition, the retention times of the complexes may be affected by other factors that change the sorption properties of these complexes. The presumed retention times of the metal–EDTA anionic complexes were confirmed experimentally. A small change in the pH of the phthalate eluent noticeably influenced the separation selectivity of some anionic complexes and inorganic anions.

The optimum conditions providing the best separation selectivity of both the metal complexes and inorganic anions studied are 1 m*M* potassium phthalate as eluent at pH 6.35. Fig. 4 shows the chromatogram of a mixture of the inorganic anions and the anionic complexes of some transition metals obtained under these conditions. The absorption characteristics of the metal complexes in the UV range varies, which is why Al^{3+}, Cd^{2+} and Zn^{2+} detection is performed indirectly [5].

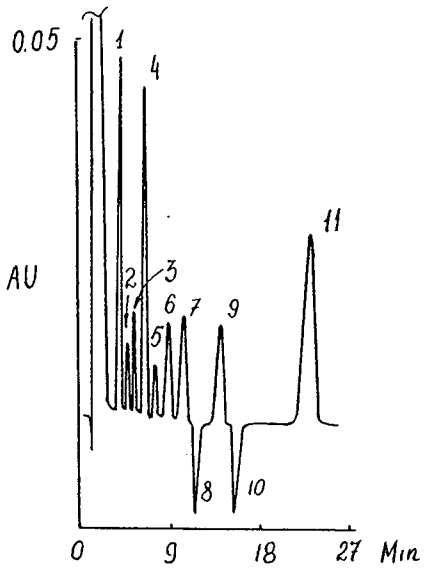

Fig. 4. Chromatogram of a mixture of inorganic anions and some metal EDTA anionic complexes. Column: 100 × 3 mm I.D. Dianion-1; eluent, 1 m*M* potassium hydrogenphthalate (pH 6.35); flow-rate, 1.5 ml/min; detection, UV at 254 nm. Peaks: 1 = Cl^-; 2 = NO_2^-; 3 = Br^-; 4 = NO_3^-; 5 = HPO_4^{2-}; 6 = Al^{3+}; 7 = Cd^{2+}; 8 = Pb^{2+}; 9 = Zn^{2+}; 10 = Cu^{2+}; 11 = SO_4^{2-}.

Cu^{2+} and Pb^{2+} are detected directly as the absorbance of their EDTA complexes at 254 nm is greater than that of for phthalate ion. The difference in the absorption characteristics of the metal complexes can produce interferences in detection in the determination of combined metals.

The limit of determination of the metals provided by the described technique is 0.01–0.05 ppm. The calibration graphs are linear over a wide range of concentrations (up to 0.05–100 ppm, $n = 5$, $r = 0.999$).

The described technique for the determination of metals was applied to waste and technological waters and proved highly sensitive for the determination of ions in multi-component mixtures.

References

[1] J.S. Fritz, D.L. Du Val and R.E. Barron, *Anal. Chem.*, 56 (1984) 1177.
[2] J.G. Tarter, *J. Chromatogr.*, 363 (1986) 191.
[3] K. Hayakawa, T. Sawada, K. Shimbo and M. Miyazaki, *Anal. Chem.*, 59 (1987) 2241.
[4] S. Matsushita, *J. Chromatogr.*, 312 (1984) 327.
[5] G. Schwedt and B. Kondratjonok, *Fresenius' Z. Anal. Chem.*, 332 (1989) 855.

ELSEVIER

Journal of Chromatography A, 671 (1994) 253–258

JOURNAL OF CHROMATOGRAPHY A

Determination of trace anions in isopropanol

Edward Kaiser *, Mary Jo Wojtusik

Dionex Corporation, 1228 Titan Way, Sunnyvale, CA 94088, USA

Abstract

Ion chromatography along with matrix elimination reliably determines low μg/l levels of anionic contaminants in isopropanol. The use of ion-exchange columns that are solvent compatible makes elimination of the isopropanol sample matrix possible and allows calibration standards to be prepared in deionized water. By concentrating a large amount of sample, detection limits for chloride, sulfate, phosphate and nitrate between 0.2 and 1.0 μg/l are achieved. The sample can be injected without sample pretreatment. The procedure is automated and yields a complete analysis in less than 1 h.

1. Introduction

In the manufacture of semiconductor materials, much attention is directed toward minimizing sources of contamination. Production yield and product reliability can be significantly compromised by contamination [1]. Of particular interest are those chemicals that contact the microelectronic circuitry. One such chemical is isopropanol (IPA), which is used to clean semiconductor surfaces [2,3].

Analysis of trace anions in IPA by wet chemical methods is laborious and time consuming. Procedures involve evaporation of a large volume of sample for several hours on a hot plate. Anions are determined by either colorimetric or turbidimetric methods, and each anion must be determined separately [4]. These techniques lack the sensitivity to detect trace concentrations (μg/l) as required by the semiconductor industry.

In the present study, ion chromatography (IC) is employed as an alternative approach for this analytical challenge. The Dionex IonPac ion-exchange columns used in this study are packed with highly cross-linked substrate resin. These columns can withstand up to 100% concentrations of organic solvents without damage to the resin [5]. This paper reports the results of evaluating IC as an analytical tool for detecting trace anions in IPA using matrix elimination on the IonPac AC10 ion-exchange column.

The determination of trace anions in IPA by IC must meet the following requirements; (1) the method must be sufficiently sensitive to detect low μg/l levels of chloride, sulfate, phosphate and nitrate; (2) direct injection of IPA without sample pretreatment is required to minimize sample contamination; (3) an automated analysis is necessary to provide cost effective sample turnaround time; and (4) a concentrator column must pre-concentrate anionic impurities while allowing uninhibited passage of IPA.

* Corresponding author. Address for correspondence: Dionex Corporation, 500 Mercury Drive, Sunnyvale, CA 94088-3603, USA.

0021-9673/94/$07.00
SSDI 0021-9673(94)00003-R

2. Experimental

2.1. Chromatographic system

All chromatography is performed on a Dionex (Sunnyvale, CA, USA) DX-300 ion chromatograph. The system consists of an advanced gradient pump (AGP), a liquid chromatography module (LCM-3) and a conductivity detector (CDM-3). For sample loading a Rheodyne 9126-038 valve is fitted with a 5-ml loop made from 0.037 in I.D. (0.94 mm) I.D. Tefzel tubing supplied by Dionex. To deliver the sample to the concentrator column an inert double stack four-way slider valve (Dionex) is used. Two Dionex Quic Pump (DQP) single-piston pumps are utilized, one for pumping the deionized water rinse solution (rinse-DQP) and the other for drawing sample from the sample container into the sample loop (sample-DQP). A pressurizable reservoir chamber (Dionex) large enough to accommodate the sample container is maintained at 8 p.s.i. (55 kPa) with helium.

All columns used in this study are manufactured by Dionex. The separations are performed on an IonPac AS10 analytical column (250 × 4 mm) and a IonPac AG10 guard column (50 × 4 mm). To concentrate the anions and eliminate the sample matrix, an IonPac AC10 concentrator column (50 × 4 mm) is used. The packing material for AC10, AG10 and AS10 is anion-exchange macroporous resin with 2000-Å pores. The resin consists of polyethylvinylbenzene cross-linked with 55% divinylbenzene. To this substrate, a layer of latex particle beads are permanently bonded. This latex layer consists of 65-nm particles fully functionalized with alkanol quaternary ammonium groups. Sodium hydroxide (100 m*M*) is used to elute the analyte anions from the AC10, AG10 and AS10 columns. An anion self regenerating suppressor (ASRS) from Dionex is used [6]. To prevent contamination of the sample with anionic impurities in the rinse solution, an anion trap column (ATC-1) is used. This column contains a high-capacity anion-exchange resin in the hydroxide form. The ATC-1 is initially prepared for use by flushing (2 ml/min) with 200 ml of 200 m*M* sodium hydroxide followed by 100 ml of deionized water at the same flow-rate. The ATC is periodically regenerated using this procedure. Table 1 summarizes the chromatographic conditions.

2.2. Chemicals

Reagent-grade chemicals are used for standard and eluent preparation. Semiconductor-grade IPA is from Olin Hunt Specialty Products (West Patterson, NJ, USA). Sodium hydroxide, 50% (w/w) is from Fisher Scientific (Pittsburgh, PA, USA). Deionized water with a specific resistance of 17.8 MΩ cm or greater from a Millipore (Bedford, MA, USA) Milli-Q water purification system is used to prepare all reagents and standards.

Anion standards (1000 mg/l) for chloride, sulfate, phosphate and nitrate are prepared from the sodium and potassium salts obtained from Fisher Scientific. The salts are dried for 30 min at 105°C in an oven and then cooled in a desiccator prior to weighing. Working standards are prepared by further diluting the 1000-mg/l standards to the range expected for the anions of interest. Dilute working standards are prepared weekly. Polyethylene containers presoaked with deionized water that has a specific resistance of 17.8 MΩ cm or greater are used to store samples and standards.

2.3. System operation

The trace anion analysis of IPA is accomplished in four steps: (1) filling the sample loop, (2) loading the concentrator, (3) eliminating the IPA matrix and (4) chromatographing the retained ions. Fig. 1 illustrates how the system performs these tasks. In step 1 (Fig. 1A), the sample-DQP pump draws the sample from the pressurized reservoir into the 5-ml sample loop on the Rheodyne valve (valve 5). Use of the pressurized reservoir chamber ensures that the sample loop is consistently filled without bubbles. A 7-min loading time at 1.5 ml/min flushes the loop with approximately two and one-half times its volume with each sample, minimizing carryover from previous samples. After the sample loop has been filled, deionized water from

Table 1
Chromatographic conditions

Guard column	IonPac AG10 (50 × 4 mm)			
Analytical column	IonPac AS10 (250 × 4 mm)			
Concentrator column	IonPac AC10 (50 × 4 mm)			
Trap column	ATC-1			
Eluent	100 m*M* NaOH			
Eluent flow-rate	1.0 ml/min			
Rinsing reagent	Deionized water			
Rinsing flow-rate	1.7 ml/min			
Sample volume	5.0 ml			
Sample fill rate	1.5 ml/min			
Detection	Suppressed conductivity, AutoSuppression, recycle mode			
AGP Program				
Time (min)	Eluent (%)	Valve 5	Valve 6	Remarks
0.0	100	0	1	Fill sample loop
7.0	100	1	0	Sample to AC10
17.0	100	0	1	Begin sampling[a]

[a] Begin sampling refers to data collection.

the rinse-DQP transfers the sample from the loop and to the AC10 concentrator column on the four-way slider valve (valve 6). Anions are retained on the concentrator column while the IPA passes through unretained assisted by washing the AC10 with deionized water from the rinse-DQP at 1.7 ml/min for 10 min (Fig. 1B). Activating valve 6 switches the AC10 in line with the eluent stream and the analytical columns. The anions are then eluted from the AC10 in the reverse direction of the concentration step and separated on the AS10 (Fig. 1C).

Special care is taken to minimize contamination. The deionized water used for preparing rinse solution, eluent and standards is free of measurable levels of ionic impurities, organics, microorganisms and particulate matter (larger than 0.2 μm). Polyethylene containers are soaked for at least 24 h with deionized water and rinsed several times prior to use. Polyethylene is used as a sample container because the use of glass results in a low recovery of phosphate. Disposable gloves (for cleanroom electronics applications) are worn at all times when handling apparatus that come into contact with standards or samples.

3. Results and discussion

3.1. Method performance

To achieve the low detection limits required by the Semiconductor Equipment and Materials International (SEMI) guidelines, a 5-ml sample volume is concentrated on a solvent-compatible AC10 concentrator column. Analyte anions are retained as the IPA matrix is eliminated by rinsing the column with deionized water. The analyte anions are then eluted from the concentrator column and separated on the AS10. The use of an isocratic method results in lower baseline noise in comparison to gradient methods. With lower baseline noise, signal-to-noise ratios are improved and sensitivity enhanced.

An advantage of this matrix elimination method is that standards can be prepared in deionized water and external calibration is performed rather than standard addition to each sample. Calibration curves are prepared for the four anions of interest based on standards prepared in deionized water and 99% IPA. The coefficients of determination (r^2) are calculated for chloride at concentrations of 1–300 μg/l, and for sulfate,

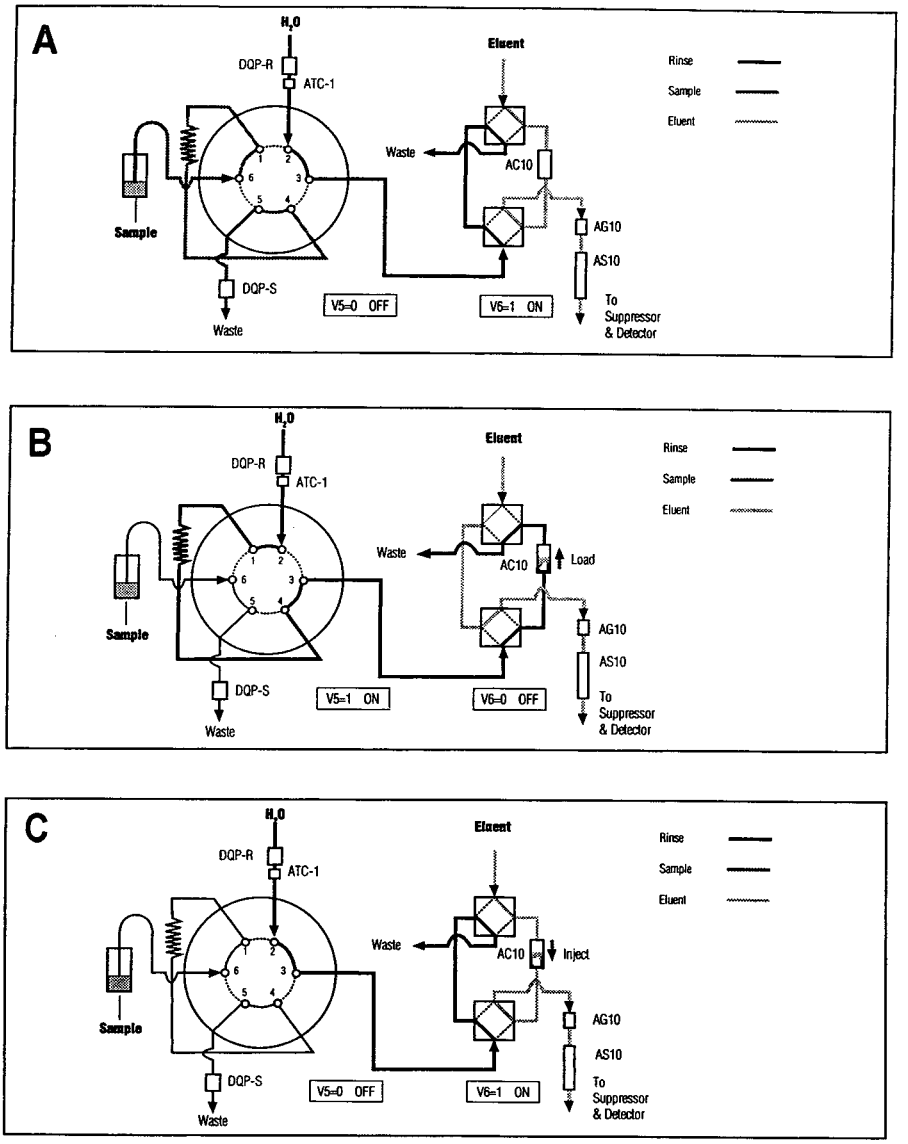

Fig. 1. IC matrix elimination instrument configuration. (A) Loading the sample loop, (B) loading the concentrator column and eliminating the matrix and (C) chromatographing the retained ions. V = Valve.

phosphate and nitrate at 5–500 μg/l. Results for both cases yield a linear response for the four anions with r^2 values greater than 0.9999.

Method detection limit (MDL) values are determined using the standard deviation for seven replicate analyses of IPA samples spiked with 10 μg/l of chloride, sulfate, phosphate and nitrate. A one-tailed Student's t test at the 99.5% confidence level for seven replicates is used for the statistical calculation. By concentrating a large sample volume and eliminating the IPA matrix, excellent retention time precision and low μg/l detection limits are achieved (Table 2). The stated detection limits are lower than the maximum limit of impurity specified by SEMI for ultra-high-purity IPA [7].

Table 2
Method performance of trace anions[a] in isopropanol

Anion	Retention time (min)	R.S.D. ($n = 7$) (%)		Method detection limit (μg/l)[b]	SEMI maximum limit of impurity (μg/l)[c]
		Retention time	Peak area		
Chloride	8.8	0.2	0.4	0.2	50
Sulfate	11.4	0.6	2.0	0.7	50
Phosphate	16.9	0.9	3.6	1.0	50
Nitrate	29.1	0.5	2.7	1.0	50

[a] For IPA spiked with 10 μg/l of each anion and number of samples analyzed, $n = 7$.
[b] Method detection limit = (S.D.) $\times$ $(t_S)_{99.5\%}$, where $(t_s) = 3.71$ for a single-sided Student's t test distribution at a 99.5% confidence.
[c] SEMI Guidelines for Isopropanol, Tier B [4].

A representative chromatogram of trace anions in semiconductor-grade IPA is shown in Fig. 2. Levels detected in this sample are well below the maximum limit of impurity: chloride 0.7 μg/l, sulfate 1.1 μg/l and nitrate 1.3 μg/l. The concentrations of these anions are calculated based on the calibration curve prepared in deionized water. An IPA sample spiked with 10 μg/l of the four anions of interest is shown in Fig. 3.

A system blank is determined by using 17.8 MΩ cm or greater deionized water as the sample. This blank consists of 22 ml of deionized water; 17 ml from the rinsing step and 5 ml from the sample loop The blank establishes baseline anion concentrations from such sources as the polyethylene sample container, the deionized water and the chromatograph. Any ionic contamination present in the deionized rinse water is magnified in proportion to the volume needed for the rinsing step. The importance of high-quality deionized water cannot be over-emphasized.

A chromatogram of a representative system blank is shown in Fig. 4. Sulfate is the only species of interest that is detected at 1.0 μg/l.

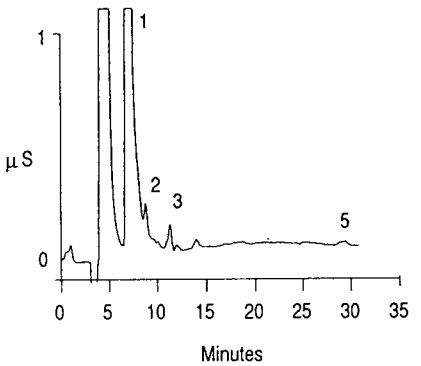

Fig. 2. Analysis of semiconductor-grade isopropanol by IC with matrix elimination. Sample: 100% isopropanol. Peaks: 1 = carbonate; 2 = chloride (0.7 μg/l); 3 = sulfate (1.1 μg/l); 5 = nitrate (1.3 μg/l). Sample volume: 5 ml; analytical column IonPac AS10 (250 × 4 mm); guard column IonPac AG10 (50 × 4 mm); concentrator column AC10 (50 × 4 mm); detection: suppressed conductivity, ASRS in recycle mode; eluent: 100 mM sodium hydroxide, isocratic; eluent flow-rate: 1.0 ml/min; rinsing reagent: deionized water; rinsing flow-rate: 1.7 ml/min.

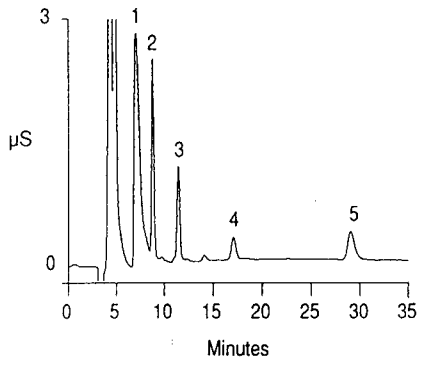

Fig. 3. Analysis of spiked isopropanol by IC with matrix elimination. Sample: 99% isopropanol and 1% aqueous standard; Peaks: 1 = carbonate; 2 = chloride; 3 = sulfate; 4 = phosphate; 5 = nitrate. IPA spiked with 10 μg/l of each of the analytes of interest. Chromatographic conditions as in Fig. 2.

Table 3
Spike/recovery of trace anions in 99% isopropanol

Anion	IPA blank (μg/l ± S.D., $n = 4$)	Spike in IPA (μg/l)	Found − blank (μg/l ± S.D., $n = 7$)	Recovery (%)
Chloride	0.7 ± 0.1	25	21.9 ± 0.2	88
Sulfate	Tr < 0.7	25	25.5 ± 3.2	102
Phosphate	ND < 1.0	25	25.1 ± 1.8	100
Nitrate	1.3 ± 0.2	25	26.3 ± 0.7	105

Tr = Trace; ND = not detected.

This is based on a one point calibration with a 5 μg/l sulfate standard which is corrected for the amount detected in the blank. The sample loop contributes 0.2 μg/l sulfate and the rinsing step contributes 0.7 μg/l sulfate to the total system blank. These values are meant to be approximations, since they are both below the detection limit. The contribution from the rinsing blank is common to all analyses. The peaks eluting before 5 min are fluoride and organic acids.

3.2. Method validation

Recovery of the four anions of interest is determined using a sample of IPA that was spiked with 25 μg/l of each anion. All concentrations are calculated using the aqueous calibration curve described earlier. After correction for the rinsing blank and the IPA blank, recovery values range from 88 to 105% for seven replicates are obtained. These results are summarized in Table 3. To meet the SEMI guidelines for method validation, a recovery of 75–125% must be demonstrated at 50% of the specified maximum limit of impurity [7].

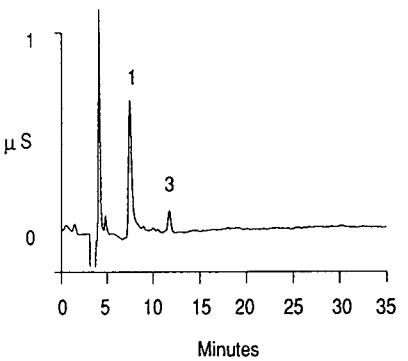

Fig. 4. System blank for IC with matrix elimination. Peaks: 1 = carbonate; 3 = sulfate (1.0 μg/l ≈ 0.7 μg/l for rinse step + 0.2 μg/l for loop volume). Chromatographic conditions as in Fig. 2.

4. Conclusions

Combined use of the IonPac AC10 concentrator column and matrix elimination provide an improved analysis of high-purity IPA for trace anionic contaminants. The success of this method is ensured by using high-purity deionized water for preparation of the rinse solution and standards. Chloride, sulfate, phosphate and nitrate are determined at low μg/l levels with excellent recovery. This technique can be useful as a quality control test in many high-purity applications.

5. References

[1] W. Kern, *J. Electrochem Soc.*, 137 (1990) 1887.
[2] R. Poliak, R. Matthews, P. Gupta, M. Frost and B. Triplett, *Microcontamination*, 10, No. 6 (1992) 45.
[3] W. Runyan and K. Bean, *Semiconductor Integrated Circuit Processing Technology*, Addison-Wesley, Redding, MA, 1990, p. 34.
[4] *Book of SEMI Standards 1993 Chemicals/Reagents Volume*, Semiconductor Equipment and Materials International, Mountain View, CA, 1993, p. 74.
[5] J.R. Stillian and C.A. Pohl, *J. Chromatogr.*, 499 (1990) 257.
[6] S. Rabin, J. Stillian, V. Barreto, K. Friedman and M. Toofan, *J. Chromatogr.*, 640 (1990) 105.
[7] *Book of SEMI Standards 1993 Chemicals/Reagents Volume*, Semiconductor Equipment and Materials International, Mountain View, CA, 1993, p. 145.

ELSEVIER

Journal of Chromatography A, 671 (1994) 259–264

JOURNAL OF CHROMATOGRAPHY A

Determination of catecholamines by ion chromatography and electrochemical detection

Corrado Sarzanini*[,a], Edoardo Mentasti[a], Mario Nerva[b]

[a]Department of Analytical Chemistry, University of Torino, Via P. Giuria 5, 10125 Turin, Italy
[b]Analytical Laboratory, Children's Hospital, Regina Margherita, P.zza Polonia 94, Turin, Italy

Abstract

An ion chromatographic method was developed for the fully automated routine clinical determination of urinary free catecholamines noradrenaline, adrenaline and dopamine with an internal standard (3,4-dihydroxybenzylamine). Simultaneous clean-up and separation of the analytes are achieved by an on-line purification step and a column-switching technique. The whole procedure requires 45 min. Both the prepurification microcolumn and the analytical column contain cation exchangers. Electrochemical detection was optimized with two working electrodes set at +500 mV for the cleaning step, and +700 mV for detection. Analytical recoveries for all three catecholamines were 90–95% and the detection limits (signal-to-noise ratio = 3) were 5.0, 10.0 and 10.0 pg for noradrenaline, adrenaline and dopamine, respectively.

1. Introduction

Catecholamines play an important role as neurotransmitters, having a marked influence on the vascular system and metabolic processes; disorders such as hypertension, neural crest tumours and Parkinsonism are indicated by excesses of these compounds [1]. Simple and selective methods are required for the routine determination of catecholamines in biological samples. Their determination is usually based on chromatographic separations using reversed-phase [2–5], cation-exchange [6] and supercritical fluid chromatography [7] coupled with electrochemical or fluorimetric detection. In most instances a preconcentration step is required owing to the lack of sensitivity and in order to purify samples before the analysis. Extraction procedures, either solid–liquid (namely alumina microcolumn [8], metal-loaded silica [4,9,10], immobilized boronates [11] or shielded hydrophobic phase columns [12]) or liquid–liquid (namely catecholamine–borate complexes [4,13]) have been developed in addition to a fully automated HPLC procedure [14], and the recoveries of analytes ranged between 63% and 100%. In cation-exchange chromatography [6] 3,4-dihydroxybenzylamine could not be used as an internal standard because it was co-eluted with adrenaline and more recently this method has been combined with a purification step based on an ion-exclusion procedure [15]. A highly sensitive determination of biogenic amines has been obtained by coulometric detection with multiple electrodes [16].

The aim of this work was to develop a routine method for the determination of catecholamines in urine samples based on cation-exchange sepa-

* Corresponding author.

0021-9673/94/$07.00
SSDI 0021-9673(93)E0035-S

ration with an on-line purification step and electrochemical detection.

2. Experimental

2.1. Apparatus and materials

The HPLC instrumentation was composed by a Gilson (Villiers-le-Bel, France) Model 305 and Model 307 double-pump system, a Model 401 diluter, a Model 232 autosampler equipped with a Rheodyne (Cotati, CA, USA) Model 7010 liquid chromatographic injector (100-μl sample loop) and a Model 7000 six-port switching valve. A Model Coulochem II electrochemical detector (ESA, Bedford, MA, USA) equipped with a Model 5011 dual coulometric–amperometric detector cell and a Hewlett-Packard (Palo Alto, CA, USA) Model 3393A reporter–integrator were used.

Ionpac CG-5 (13 μm) and Ionpac CG-10 (8.5 μm) polymeric cation-exchange microcolumns (Dionex, Sunnyvale, CA, USA) (50 × 4 mm I.D.) were used for sample prepurification and as a guard column, respectively. The analytical column was a Dionex Ionpac CS-10 (8.5 μm) (250 × 4 mm I.D.). Standard solutions were introduced into a 100-μl injection loop or loaded on to the Ionpac CG-5 for the prepurification procedure. After optimization (see below), the washing solution, for on-line sample purification, was water–methanol (90:10, v/v) containing 1.5 m*M* sodium formate at a flow-rate of 1.0 ml/min. The mobile phase was water–methanol (88:12, v/v) containing 120 m*M* sodium hydroxide and 260 m*M* formic acid and isocratic elutions were performed at a flow-rate of 0.9 ml/min. Prior to use, the eluent was filtered through a 0.2-μm membrane filter. Fig. 1 shows the on-line system and steps for the sample prepurification and chromatographic separation.

High-purity water obtained with a Milli-Q system (Millipore, Bedford, MA, USA) was used for preparing all solutions. Sodium hydroxide, formic acid, phosphoric acid and hydrochloric acid were purchased from Carlo Erba (Milan, Italy) and methanol from Riedel-de Haën (Schering, Selze, Germany). All reagents were of HPLC grade.

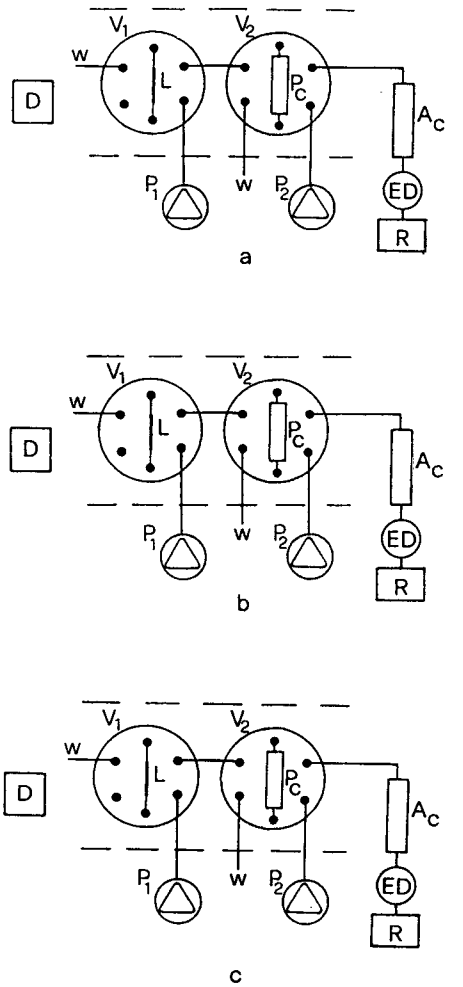

Fig. 1. Scheme and steps for sample purification and chromatographic elution. D = diluter–injector; L = loop (100 μl); P_1 and P_2 = pumps; V_1 and V_2 = six-port switching valves; P_c = column for sample purification (CG-5); A_c = analytical precolumn and column (CG-10, CS-10); ED = electrochemical detector; R = recorder. (a) V_1 and V_2 are switched, the sample is loaded into the loop (30 s), the purification column (CG-5) is washed and equilibrated, separation is run (20 min); (b) V_1 is switched, sample is transferred and purified into CG-5 (20 min), the analytical column is reconditioned; (c) V_2 is switched for 3 min and the sample is eluted into the analytical column.

Adrenaline (A), dopamine (DA), noradrenaline (NA) and 3,4-dihydroxybenzylamine (DHBA) were purchased from Sigma (St. Louis,

MO, USA). Stock standard solutions of A, DA and NA were prepared by dissolving 500 mg/l of each compound in 0.05 *M* H_3PO_4 and stored at −20°C. Working standard solutions (50 ng/ml A, 200 ng/ml DA and 50 ng/ml NA) were prepared daily by dilution with 0.05 *M* H_3PO_4 and finally diluted 1:1 (v/v) with 0.05 *M* H_3PO_4 solution containing 0.9 m*M* DHBA as an internal standard.

2.2. Urine samples

Urine samples (24 h collection) with 6 *M* HCl added (10 ml/l) were frozen at −20°C. Aliquots of urine were filtered through a Millex-GS 0.22-μm filter (Millipore, Saint-Quentin Yvelines, France), diluted 1:1 (v/v) with 0.9 m*M* DHBA and processed. Samples kept at 4°C or frozen at −20°C could be processed after 1 week and 6 months, respectively, without loss of analytes.

3. Results and discussion

3.1. Detection

A dual coulometric–amperometric detector cell (ESA Model 5011) was used for the detection of catecholamines. Different potentials were checked in order to optimize the sensitivity by total oxidation of the interfering compounds (first electrode) and to detect catecholamines (second electrode). Hydrodynamic voltammograms for the catecholamines (Fig. 2) show that their oxidation begins at 400 mV and a good sensitivity is reached at 700 mV. At lower values of the potential (200 mV) at the first electrode, with a constant value of 700 mV for the second electrode, all the interferents were not oxidized. The peak of DA was tailed and it became free from interferences at 400 mV or higher values. Low baseline noise and removal of interferents were obtained by working at potentials of 500 and 700 mV for the first and the second electrodes, respectively. Higher potentials at the second electrode showed an enhanced sensitivity, which is not required for this kind of sample.

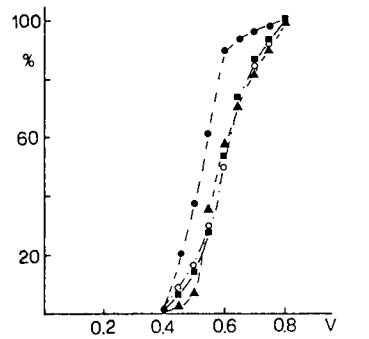

Fig. 2. Hydrodynamic voltammograms, applied voltage *vs.* detector response (as a percentage of maximum signal obtained). □ = Noradrenaline; ○ = adrenaline; ● = dopamine; ▲ = 3,4-dihydroxybenzylamine.

3.2. Chromatographic conditions

In order to develop the separation procedure, the pH, ionic strength and organic modifier content in the eluent were optimized in the following way: 100 μl of standard solutions were injected and run without the prepurification column using water–methanol (90:10, v/v). The eluent was 260 m*M* formic acid with NaOH concentrations ranging from 72 to 144 m*M* and pH values between 3.03 and 3.55. The pH values of the aqueous solution were chosen according to the pK_a of the catecholamines (9.7, 10.3 and 9.9 for NA, A and DA, respectively [17]) so as to have the analytes in cationic form. In addition, low pH values prevented the oxidation of catecholamines that occurs in basic medium. Fig. 3

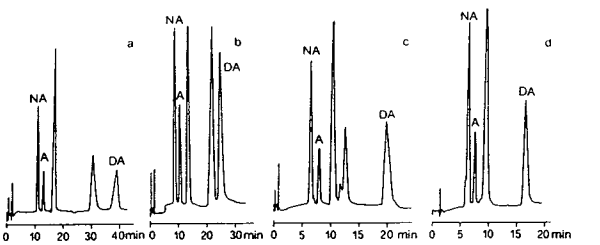

Fig. 3. Effect of sodium hydroxide concentration on retention times of noradrenaline (NA), adrenaline (A) and dopamine (DA). Chromatographic conditions: mobile phase, water–methanol (90:10, v/v) containing 260 m*M* formic acid and (a) 72 m*M* NaOH (pH 3.03), (b) 96 m*M* NaOH (pH 3.21), (c) 120 m*M* NaOH (pH 3.39) and (d) 144 m*M* NaOH (pH 3.55); flow-rate, 1.0 ml/min; injection volume, 100 μl.

shows that the retention times of the analytes decrease with increasing NaOH concentration, *i.e.*, Na^+ competes for cation sites, according to the ion-exchange mechanism. Experiments were also performed to evaluate the behaviour of the chromatogram as a function methanol concentration. Fig. 4 shows the chromatograms obtained for water–methanol mixtures containing 0, 10 and 20% methanol. The results indicate that the separation cannot be considered as a pure ion-exchange mechanism and a partition effect is also active. The best compromise between good resolution and acceptable retention times was obtained with water–methanol (90:10, v/v). For the analysis of urine samples a precolumn (CG-10) of the same kind as the separator was added to the system. This configuration caused an increase in the retention times of the analytes, and additional experiments showed that water–methanol (88:12, v/v) was the optimum composition of the eluent (Fig. 5).

3.3. Purification procedure

Owing to the complex matrix of urine, a clean-up step is required before the analysis. The loop was connected with a CG-5 cation-exchange microcolumn (see Section 2.1), which is characterized by a low hydrophobicity and the presence of some residual anion sites. This kind of column was selected in order to avoid strong retention of

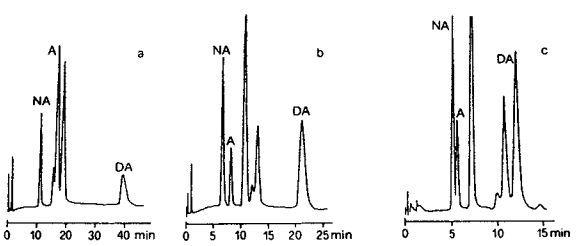

Fig. 4. Effect of methanol concentration on noradrenaline (NA), adrenaline (A) and dopamine (DA) retention times. Chromatographic conditions: mobile phase, water–methanol: (a) (100:0, v/v), (b) (90:10, v/v), (c) (80:20, v/v) containing 96 m*M* NaOH and 260 m*M* HCOOH (pH 3.21). Injection volume, 100 μl.

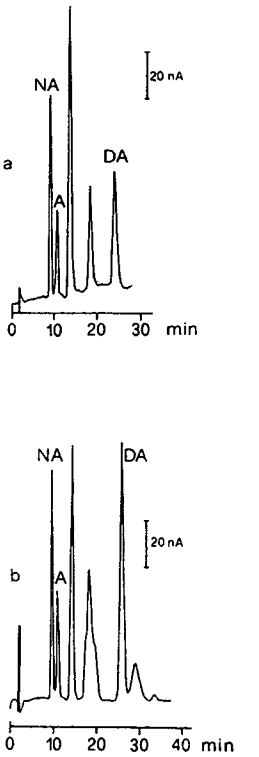

Fig. 5. Chromatograms obtained from: (a) standard (NA 50 ng/ml, A 25 ng/ml and DA 50 ng/ml); (b) urine sample (NA 34 ng/ml, A 21 ng/ml and DA 132 ng/ml). Chromatographic conditions: mobile phase, water–methanol (88:12, v/v) containing 120 m*M* NaOH and 260 m*M* HCOOH (pH 3.39); flow-rate 0.9 ml/min. Injection volume, 100 μl.

amines and oxidizable impurities present in urine that interfere in the determination of catecholamines. The following sequence was used: 100 μl (standard solution or sample with DHBA added as mentioned above) were loaded on to the loop, which was connected with the CG-5 column, where the sample was washed with water–methanol (90:10) containing 1.5 m*M* sodium formate at a flow-rate of 1 ml/min (actual pH 6.30). A detailed study was made to optimize the washing time in order to maximize the removal of interferences without decreasing the recovery of catecholamines. A washing time of 18 min was sufficient to remove the matrix and good reproducibility for the recovery of catecholamines

resulted up to 23 min. A washing time of 20 min was selected.

3.4. Recovery

The recovery was determined by comparing the peak areas obtained by direct injection of the standard solutions with those obtained by following the column-switching purification procedure with the same amount of catecholamines (n = 10). Volumes of 100 μl (50, 25, 100 and 100 ng/ml for NA, A, DA and DHBA, respectively) were injected and purified as indicated above. The recoveries found were NA 96%, A 90%, DA 94% and DHBA 95% with R.S.D.s of 2.6, 3.8, 2.9 and 2.0%, respectively. Urine samples analysed as such or spiked gave the same recoveries. During the optimization and validation of the method, 1000 samples were processed without a decrease in the column efficiency.

3.5. Linearity, detection limits and precision

Under the optimized chromatographic conditions, linear relationships between catecholamine (CAT) concentration and peak-area ratio (CAT/DHBA) (concentrations 0.20–1600 ng/ml NA, 0.20–800 ng/ml A and 0.78–3200 ng/ml DA) gave correlation coefficients of 0.9999, 0.9999 and 0.9998 for NA, A and DA, respectively. The detection limits were 5.0 pg (NA), 10.0 pg (A) and 10.0 pg (DA) at a signal-to-noise ratio of 3 (Table 1).

Table 2
Reproducibility for the whole procedure in the analysis of pooled urine (n = 10)

Catecholamines	Concentration (ng/ml)	S.D. (ng/ml)	R.S.D. (%)
Noradrenaline	23.65	0.45	1.89
Adrenaline	12.67	0.29	2.30
Dopamine	345.54	9.57	2.77

The reproducibility was evaluated by performing ten replicate analyses of an urine sample. Table 2 summarizes the results obtained.

3.6. Time optimization

The whole procedure of purification, separation and determination was improved by evaluating also the time required to transfer all the sample from clean-up column to the analytical column and the time to wash the prepurification column. Experiments with standard solutions and samples showed that after 3 min catecholamines are totally removed from the prepurification column and 20 min are required to wash it with the same solution as used to purify samples. Taking into account the time required for sample clean-up (20 min), by coupling the autosampler for sample injection, analysis and prepurification simultaneously performed required about 45 min.

Table 1
Linear response range and detection limit for catecholamines (n = 14)

Catecholamine	Linear range (ng/ml)	Correlation coefficient	Regression equation[a]	Detection limit (pg)
Noradrenaline	0.20–1600	0.9999	$y = 0.0019 + 0.0544x$	5.0
Adrenaline	0.20–800	0.9999	$y = 0.0178 + 0.0328x$	10.0
Dopamine	0.78–3200	0.9998	$y = 0.3797 + 0.0288x$	10.0

[a] y = Peak area ratio (CAT/DHBA); x = catecholamine concentration (ng/ml).

4. Conclusions

The ion chromatographic procedure developed for the simultaneous purification and determination of noradrenaline, adrenaline and dopamine gave the possibility of routine application to the analysis of urine samples with high sensitivity, good precision and a short time of analysis.

5. Acknowledgements

Financial support from the Ministero dell' Università e della Ricerca Scientifica e Tecnologia (MURST, Rome) and from the Italian National Research Council (CNR, Rome) is gratefully acknowledged.

6. References

[1] B. Kagedal and D.S. Goldstein, *J. Chromatogr.*, 429 (1988) 177.
[2] I. Molnar and C. Horvath, *Clin. Chem.*, 23 (1977) 473.
[3] T.P. Moyer and N.-S. Jiang, *J. Chromatogr.*, 153 (1978) 365.
[4] F. Smedes, J.C. Kraak and H. Poppe, *J. Chromatogr.*, 231 (1982) 25.
[5] A.A. Descombes and W. Haerdi, *Chromatographia*, 33 (1992) 83.
[6] P.T. Kissinger, C. Refshauge, R. Dreiling and R.N. Adams, *Anal. Lett.*, 6 (1973) 465.
[7] A.A. Descombes, J.-L. Veuthey and W. Haerdi, *Fresenius' Z. Anal. Chem.*, 339 (1991) 480.
[8] H. Tsuchiya, T. Koike and T. Hayashi, *Anal. Chim. Acta*, 218 (1989) 119.
[9] A.A. Descombes and W. Haerdi, *Chromatographia*, 28 (1989) 459.
[10] A. Coquet, A.A. Descombes, J.-L. Veuthey and W. Haerdi, *Fresenius' Z. Anal. Chem.*, 339 (1991) 475.
[11] K. Kemper, E. Hagemeier, D. Aherns, K.S. Boos and E. Schlimme, *Chromatogrophia*, 19 (1984) 288.
[12] D.J. Wang, Y. Qu, P. Hu and P.L. Zhu, *Chromatographia*, 31 (1991) 137.
[13] H. Tsuchiya and T. Hayashi, *J. Pharmacol. Methods*, 23 (1990) 21.
[14] R. Said, D. Robinet, C. Barbier, J. Sartre and C. Huguet, *J. Chromatogr.*, 530 (1990) 11.
[15] T. Seki, Y. Yanagihara and K. Noguchi, *J. Chromatogr.*, 515 (1990) 435.
[16] H. Takeda, T. Matsumiya and T. Shibuya, *J. Chromatogr.*, 515 (1990) 265.
[17] R.M. Smith and A.E. Martell, *Critical Stability Constants, Vol. 2 Amines*, Plenum Press, New York, 1975.

ELSEVIER

Journal of Chromatography A, 671 (1994) 265–271

JOURNAL OF CHROMATOGRAPHY A

Utilization of ion chromatography and statistics to determine important acids in chromium plating and electropolishing solutions

Samuel Sopok

U.S. Army Benet Laboratories, Watervliet, NY 12189, USA

Abstract

Inadequate monitoring of sulfuric and chromic acids in chromium plating solutions and phosphoric and sulfuric acids in electropolishing solutions is a serious problem for the industry resulting in poor quality products and wasted resources. This is especially true for the narrow tolerances required to chromium plate cannon systems. Current online and offline instrumental analysis methods either do not result in acceptable precision or are time consuming. Two similar methods, which are improvements on existing ion chromatographic methods, are presented here that provides acceptable analysis and monitoring of these acids in this chromium plating process coupled with an extensive statistical evaluation of the experimental data. For chromium plating solutions, the resultant means and precisions are 2.50 ± 0.11 g/l sulfuric acid and 250 ± 5 g/l chromic acid. For electropolishing solutions, these values are 685 ± 4 g/l phosphoric acid and 845 ± 5 g/l sulfuric acid.

1. Introduction

Inadequate monitoring of sulfuric and chromic acids in chromium plating solutions and phosphoric and sulfuric acids in electropolishing solutions is a serious problem for the industry resulting in poor quality products and wasted resources. This is especially true for the narrow tolerances required to chromium plate cannon systems. For chromium plating solutions, the optimum operating ranges are 2.40–3.10 g/l sulfuric acid and 230–270 g/l chromic acid. For electropolishing solutions, the optimum operating ranges are 640–730 g/l phosphoric acid and 795–895 g/l sulfuric acid. Current online and offline instrumental analysis methods, either do not result in acceptable precision or are time consuming [1–5]. Two similar methods, which are improvements on existing ion chromatographic methods, are presented here that provides acceptable analysis and monitoring of these acids in this chromium plating process coupled with an extensive statistical evaluation of the experimental data.

2. Experimental

The following gives the details of the experimental procedures, materials, and apparatus used. Strict analytical chemistry methods and procedures are followed throughout this experimental section [6].

A Model 2020i Dionex ion chromatograph (Dionex Corporation, Sunnyvale, CA, USA) was used which includes an autosampler, computer/controller, computer/integrator, and suppressed conductivity detector [7].

0021-9673/94/$07.00
SSDI 0021-9673(94)00004-S

The initial conditions for the autosampler module are: local/remote is local, run/hold is hold then run, status is search, size is 5 ml, type is sample, inj is 1, tray is in/empty, type is loop, mode is prop, bleed is on, and inj/vial is 1.

The initial conditions for the analytical pump module are: local/remote is remote, start/stop is stop, flow is 2.3 ml/min, pressure limit select low alarm is 100 p.s.i. (1 p.s.i. = 6894.76 Pa), pressure limit select high alarm is 1000 p.s.i., and argon valve pressure is 100 p.s.i..

The initial conditions for the conductivity detector module are: local/remote is remote, cell is on, auto offset is off, temp. comp. is 0, and output range is 30 μS.

The initial conditions for the advanced chromatography module are: load/inject is inject, valve A is off, valve B is off, local/remote is remote, separator column is HPIC-AG4 (Dionex), suppressor column is AMMS (Dionex), argon valve pressure is 100 p.s.i., regenerate flow is 5 ml/min, argon regenerate pressure is 6 p.s.i., and the injection loop is 10 μl.

Fill the system reservoirs with the appropriate method eluent and regenerate. The analytical pump used for the eluent must be completely purged of air every time the eluent reservoir is filled. A properly functioning analytical pump is necessary for acceptable precision.

The conductivity detector should be periodically calibrated to 147 μS using 0.00100 *M* potassium chloride.

The initial programming conditions for the system computer/controller module's equilibration program are: time is 0.0 min, load/inj is inject, valve B is on, offset is off, relays are off, and endrun is off. Conditions are the same at time is 30.0 min except endrun is on.

The initial programming conditions for the system computer/controller module's analysis program are: time is 0.0 min, load/inj is load, valve B is on, offset is off, relays are off, and endrun is off. Conditions are the same at time is 0.1 min except relays is £2. Conditions are the same at time is 0.2 min except relays are off. Conditions are the same at time is 2.2 min except offset is on. Conditions are the same at time is 2.3 min except load/inj is inject and relays is £1. Conditions are the same at time is 10.0 min except relays are off and endrun is on. Eluent flow rate is 2.3 ml/min., eluent port £3 is used, temp. select is zero, valve A is continually off, temp. comp. is 1.7, cond. setting full scale is 30 μS, and AC outlets are all continually off.

The initial programming conditions for the system computer/controller module's halt program are: time is 0.0 min, load/inj is inject, valve B is off, offset is off, relays are off, and endrun is on. Eluent flow rate is 0.0 ml/min., no eluent port is selected, temp. select is zero, valve A is continually off, temp. comp. is zero, cond. setting full scale is 30 μS, and AC outlets are all off.

The initial scheduling conditions for the system computer/controller module's equilibration, analysis, and halt programs are one, eighteen, and one iterations, respectively.

The initial programming conditions for the system computer/integrator are: AT = 1024, PH = 1, PT = 5000, and MN = 0.

The next three paragraphs outline the special conditions for the determination of chromic or sulfuric acid in chromium plating solutions.

Two analytical reagent grade standard solutions are required. The first is a 2.95 ± 0.01 g/l sulfuric acid solution that meets American Chemical Society (ACS) and American Society For Testing Materials (ASTM) Standards [8,9]. The second is a 250 ± 1 g/l chromic acid solution that meets ACS and Federal Standards [10,11]. E. M. Science reagent grade chromium trioxide is the only material found in our experience that meets ACS standards allowing a maximum of 0.005% sulfate. Two other reagent grade solutions are also required: a 0.00360 *M* (0.38 ± 0.02 g/l) sodium carbonate eluent solution and a 0.0141 *M* (1.38 ± 0.04 g/l) sulfuric acid regenerate solution.

Preparation of a chromium plating solution standard for ion chromatographic analysis requires that one ml of each of the analytical reagent grade standard solutions (sulfuric and chromic acids) prepared above are diluted to the mark with deionized water in a 250 ml volumetric flask. Split sample solutions are prepared

the same. This 1:250 dilution coupled with the use of a 10 μl injection loop results in mean injection concentrations of 10 ppm sulfuric acid and 1000 mg/l chromic acid.

Only chromium plating solution sample 8 is run and is split into solutions 8-1 and 8-2. The chromium plating solution standard S and split samples 8-1 and 8-2 are placed in the autosampler in eighteen sealed 5 ml vials as follows: four S's, three S/8-1 pairs, three S/8-2 pairs, an S, and a deionized water.

The next three paragraphs outline the special conditions for the determination of sulfuric or phosphoric acid in electropolishing solutions.

One analytical reagent grade standard solution is required. It contains 685 ± 1 g/l phosphoric acid and 845 ± 1 g/l sulfuric acid. This standard solution is prepared and standardized using a previous method by this author [12]. Two other reagent grade solutions are required: a 0.00095 M (0.100 ± 0.005 g/l) sodium carbonate eluent solution and a 0.0141 M (1.38 ± 0.04 g/l) sulfuric acid regenerate solution.

Preparation of a electropolishing solution standard for ion chromatographic analysis requires that 0.400 ml of the analytical reagent grade standard solution (phosphoric and sulfuric acid mixture) prepared above is diluted to the mark with deionized water in a 2000 ml volumetric flask. Split sample solutions are prepared the same. This 1:5000 dilution coupled with the use of a 10 μl injection loop results in mean injection concentrations of 137 ppm phosphoric acid and 169 ppm sulfuric acid.

Only electropolishing solution sample 8P is run and is split into solutions 8P-1 and 8P-2. The electropolishing solution standard S and samples 8P-1 and 8P-2 are placed in the autosampler in eighteen sealed 5 ml vials as follows: four S's, three S/8P-1 pairs, three S/8P-2 pairs, an S, and a deionized water.

A chromatogram is generated for each chromium plating and electropolishing standard and sample solution, peak heights are determined, standard concentrations are known, sample concentrations and precisions are calculated using an extensive statistical method for reliability determinations.

3. Results and discussion

A statistical analysis is necessary to determine the reliability of the experimental ion chromatographic sample data in order to adequately monitor a given acid in the chromium plating process. The statistical evaluation has two parts.

In the first part of the statistical evaluation, samples are split, each split solution is analyzed in triplicate, and data from these split solutions are statistically compared.

Tables 1– 4 give the experimental peak height data for the acid standard and split sample solutions. For these Tables, raw peak height data

Table 1
Ion chromatographic peak height data for sulfuric acid in chromium plating solutions

	Std S H_2SO_4	Samp 8-1 H_2SO_4	Std S H_2SO_4	Samp 8-2 H_2SO_4
Rep 1	170 185	163 899	173 776	163 668
Rep 2	176 065	165 987	169 989	163 303
Rep 3	173 267	159 973	170 932	161 416
X_{avg}	173 172	163 286	171 566	162 796
S_{n-1}	2941	3053	1971	1209
S_p	–	2998	–	1635
$C_{95\%}$ (g/l)	–	0.115	–	0.063
t_R (min)	0.9	0.9	0.9	0.9

Peak heights expressed in IU.

Table 2
Ion chromatographic peak height data for chromic acid in chromium plating solutions

	Std S CrO_3	Samp 8-1 CrO_3	Std S CrO_3	Samp 8-2 CrO_3
Rep 1	667 793	678 899	678 874	675 566
Rep 2	671 066	682 189	688 216	693 419
Rep 3	672 645	687 026	652 000	686 209
X_{avg}	670 501	682 704	673 030	685 064
S_{n-1}	2474	4087	18 801	8981
S_p	–	3378	–	14 733
$C_{95\%}$ (g/l)	–	2.9	–	12.4
t_R (min)	1.9	1.9	1.9	1.9

Peak heights expressed in IU.

Table 3
Ion chromatographic peak height data for phosphoric acid in electropolishing solutions

	Std S H_3PO_4	Samp 8P-1 H_3PO_4	Std S H_3PO_4	Samp 8P-2 H_3PO_4
Rep 1	562 500	509 200	573 900	512 700
Rep 2	572 000	507 700	575 800	516 100
Rep 3	573 300	509 100	578 700	517 100
X_{avg}	569 267	508 667	576 133	515 300
S_{n-1}	5896	839	2417	2307
S_p	–	4211	–	2363
$C_{95\%}$ (g/l)	–	11.5	–	6.4
t_R (min)	1.8	1.8	1.8	1.8

Peak heights expressed in IU.

Table 4
Ion chromatographic peak height data for sulfuric acid in electropolishing solutions

	Std S H_2SO_4	Samp 8P-1 H_2SO_4	Std S H_2SO_4	Samp 8P-2 H_2SO_4
Rep 1	813 800	770 200	815 700	762 300
Rep 2	821 400	764 600	813 600	763 200
Rep 3	819 500	763 000	810 400	760 500
X_{avg}	818 233	765 933	813 233	762 000
S_{n-1}	3955	3781	2669	1375
S_p	–	3869	–	2123
$C_{95\%}$ (g/l)	–	9.1	–	5.0
t_R (min)	3.0	3.0	3.0	3.0

Peak heights expressed in IU.

is in integrator units (IC) and initially four equilibration standards are run before standard one. For Tables 1 and 2, standard solutions S and split sample solutions 8-1 and 8-2 are used after a 1:250 dilution. For Table 3 and 4, standard solutions S and split sample solutions 8P-1 and 8P-2 are used after a 1:5000 dilution.

For Tables 1–4, the mean X_{avg} and sample standard deviation S_{n-1} are calculated for each of these samples and its associated standard. The pooled sample standard deviation S_p is calculated from the standard deviation of each sample and its associated standard as follows:

$$S_p = [(S_1^2 + S_2^2)/2]^{0.5} \quad (1)$$

In addition, the ninety-five percent confidence level $C_{95\%}$ in grams per liter is calculated from the above quantities for each sample and its associated standard:

$$C_{95\%} = 2.266 \cdot S_p \cdot [\text{acid std conc/std } X_{avg}] \quad (2)$$

Finally, the mean retention time (t_R) in minutes is given for each standard and split sample solution.

The concentration data of the split sample solutions are given in Tables 5 and 6. As above, the mean X_{avg}, sample standard deviation S_{n-1}, and pooled sample standard deviation S_p are calculated. In addition, another quantity is calculated called the T-test value (T) for each sample solution from the following:

$$T = 1.225 \cdot [(X_{1,avg} - X_{2,avg})/S_p] \quad (3)$$

The experimental data of the split solutions of

Table 5
Concentration data for sulfuric and chromic acids in chromium plating solutions

	Samp 8-1 H_2SO_4	Samp 8-2 H_2SO_4	Samp 8-1 CrO_3	Samp 8-2 CrO_3
Rep 1	2.83	2.76	254	249
Rep 2	2.77	2.82	254	252
Rep 3	2.71	2.77	255	263
X_{avg}	2.77	2.78	254	255
S_{n-1}	0.060	0.032	0.577	7.37
S_p	–	0.048	–	5.22
T	–	0.254	–	0.234

Concentrations expressed in g/l.

Table 6
Concentration data for phosphoric and sulfuric acids in electropolishing solutions

	Samp 8P-1 H_3PO_4	Samp 8P-2 H_3PO_4	Samp 8P-1 H_2SO_4	Samp 8P-2 H_2SO_4
Rep 1	620	612	800	790
Rep 2	608	614	787	793
Rep 3	608	612	787	793
X_{avg}	612	613	791	792
S_{n-1}	6.9	1.1	7.5	1.8
S_p	–	4.9	–	5.5
T	–	0.13	–	0.17

Concentrations expressed in g/l.

a sample solution are compared to a 2.776 value using the T-test to see if they are statistically from the same original sample solution to a 95% confidence level. A sample solution passes this T-test if its resultant absolute value is less than the 2.776 value. This T-test addresses the reliability dilemma mentioned above since it either accepts or rejects a sample solution analysis; samples solutions that fail the T-test are statistically dissimilar and are re-sampled and re-analyzed.

In the second part of the statistical evaluation, the mean X_{avg} and normal population standard deviation (S_n) are calculated for the six respective replicates of the sample solutions that have passed the T-test. Since this was the case, the concentration data for the unsplit and original sample solutions are given in Table 7.

It is useful to evaluate the variations in precision for the materials and methods used. Volumes are calculated from the weight–volume relationship of the contained deionized water solution corrected for temperature. For ion chromatographic data, peak height is in integrator units (IU) and four equilibration replicates are run prior to data acquisition.

For chromium plating solutions, the six replicate experimental mean and precision of a Class A 1 ml micropipette is 1.0102 ± 0.0029 ml [6]. The six replicate experimental mean and precision of a Class A 250 ml volumetric flask is 249.49 ± 0.03 ml [6]. The six replicate experimental mean and precision of the titration of a 250 g/l chromic acid standard solution is 250.2 ± 0.2 g/l [11]. The six replicate experimental mean and precision of the titration of a 2.95 g/l sulfuric acid standard solution is 2.942 ± 0.004 g/l [9]. The six replicate peak height means and precisions of the ion chromatographic system determination of 2.95 g/l sulfuric acid and 250 g/l chromic acid standard solutions are given in Table 8. Six replicates by ion chromatography is equivalent to determining a split sample solution of 8.

For electropolishing solutions, the six replicate experimental mean and precision of a Class A 0.400 ml micropipette is 0.400 ± 0.002 ml [6]. The six replicate experimental mean and precision of a Class A 2000 ml volumetric flask is 2000 ± 2 ml [6]. The six replicate experimental mean and precision of the titration of a 685 g/l phosphoric acid standard solution is 685 ± 1 g/l [12]. The six replicate experimental mean and precision of the titration of a 845 g/l sulfuric acid standard solution is 845 ± 1 g/l [12]. The six replicate peak height means and precisions of the ion chromatographic system determination of 685 g/l phosphoric acid and 845 g/l sulfuric acid standard solutions are also given in Table 8. Six replicates by ion chromatography is equivalent to determining a split sample solution of 8P.

Clearly, the ion chromatographic system con-

Table 7
Reported concentration data for chromium plating and electropolishing solutions

	Samp 8 H_2SO_4	Samp 8 CrO_3	Samp 8P H_3PO_4	Samp 8P H_2SO_4
Rep 1	2.83	254	620	800
Rep 2	2.77	254	608	787
Rep 3	2.71	255	608	787
Rep 4	2.76	249	612	790
Rep 5	2.82	252	614	793
Rep 6	2.77	263	612	793
X_{avg}	2.77	254	612	792
S_n	0.04	4	4.0	4.5

Concentrations expressed in g/l.

Table 8
Ion chromatographic peak height precisions of chromium plating process standard acid solutions

	Samp 8 H_2SO_4	Samp 8 CrO_3	Samp 8P H_3PO_4	Samp 8P H_2SO_4
Rep 1	189 500	699 600	562 500	813 800
Rep 2	185 300	697 000	572 000	821 400
Rep 3	186 900	677 700	573 300	819 500
Rep 4	182 000	663 800	573 900	815 700
Rep 5	187 800	705 000	575 800	813 600
Rep 6	183 900	680 800	578 700	810 400
X_{avg}	185 900	687 317	572 700	815 700
S_n	2725	15 782	5032	3720

Peak heights expressed in IU.

tributes the greatest amount of variation in precision compared to all other sources given for both of the above methods.

For chromium plating solutions, the resulting precisions are in the range of 0.03–0.20 g/l sulfuric acid and 1–9 g/l chromic acid. For electropolishing solutions, the resulting precision are in the range of 2–7 g/l phosphoric acid and 2–8 g/l sulfuric acid. The data shows that these improved methods are sufficient to monitor these acids in the chromium plating process.

4. References

[1] K. Langford and J. Parker, *Analysis of Electroplating and Related Solutions*, Metals and Plastics Publication, Inc., Hackensack, NJ, 1986.

[2] *Chromium Plating Solution Analysis, Metal Finishing Guidebook*, Metal and Plastics Publication, Inc., Hackensack, NJ (1984).

[3] S. Sopok, *The Analysis of Metal Finishing Solutions by Ion Chromatography*, U.S. Army Benet Laboratories Technical Report, Watervliet Arsenal, Watervliet, NY, 1987.

[4] S. Sopok, *Determination of Phosphoric Acid, Sulfuric Acid, Chromic Acid, and Their Matrix Effects in Chromium Plating and Associated Polishing Solutions by Ion Chromatography*, U.S. Army Benet Laboratories Technical Report, Watervliet Arsenal, Watervliet, NY, 1988.

[5] S. Sopok, *Plat. Surf. Finish.*, in press.

[6] J. Fritz and G. Schenk, *Quantitative Analytical Chemistry*, 5th ed., Allyn and Bacon, Boston, MA, 1987.

[7] *Dionex Ion Chromatograph System Model 2020i Operating and Maintenance Manual*, Dionex Corp., Sunnyvale, CA, 1984.

[8] *Sulfuric Acid Specification*, American Chemical Society, Washington, DC, 1982.

[9] *Analysis of Sulfuric Acid*, ASTM Standard E233, American Society for Testing Materials, Philadelphia, PA, 1983.

[10] *Chromium Trioxide Specification*, American Chemical Society, Washington, DC, 1982.

[11] *Chromium Trioxide*, Federal Specification O-C-303D, General Services Administration, Washington, DC, 1986.

[12] S. Sopok, *Determination of Phosphoric and Sulfuric Acids in Polishing Solutions By Acid/Base Titration Using a pH Meter*, U.S. Army Benet Laboratories Technical Report, Watervliet Arsenal, Watervliet, NY, 1989.

ELSEVIER

Journal of Chromatography A, 671 (1994) 273–279

JOURNAL OF CHROMATOGRAPHY A

Analysis of pamidronate disodium in pharmaceutical dosage forms by ion chromatography

J. Quitasol*, L. Krastins

Physical and Analytical Chemistry, Pharmaceutical Division, Ciba-Geigy Corporation, Suffern, NY 10901, USA

Abstract

Pamidronate disodium, an amino bisphosphonate, is a potent new inhibitor of osteoclastic bone resorption. A simple assay method using ion chromatography has been developed for this compound and its dosage forms. The chromatographic system consists of an hydroxyethyl methacrylate polymer column with quaternary amine functionalities, nitrate anion eluent and a refractive index detector. The active ingredient was separated from possible impurities such as phosphate and phosphite ions, and β-alanine. The different dosage forms analyzed include ampul solutions, lyophilized powders, tablets and capsules. Analytical and chromatographic criteria were met exceedingly well for the analysis of the active ingredient and the different dosage forms.

1. Introduction

Pamidronate disodium pentahydrate or disodium-3-amino-1-hydroxy-propylidene-1,1-bisphosphonate pentahydrate (APD, Aredia™, Ciba-Geigy, Suffern, NY, USA) (Fig. 1), belonging to a group of chemical compounds known as bisphosphonates, is a potent inhibitor of osteoclastic bone resorption [1]. It has been used clinically for the treatment of tumor-related hypercalcemia [2,3] and Paget's disease [4].

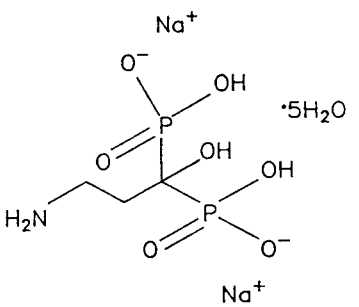

Fig. 1. Structure of APD.

APD has pK_a values ranging from 1.7 to 11.5 [5], thus it exists as an ionic specie over a broad pH range. The molecule has no detectable chromophore, making development of a chromatographic method a challenging task. The current methods that have been used in our laboratory are reversed-phase HPLC with pre-column derivatization with fluorescamine and isotachophoresis (ITP) for dosage and stability controls. The HPLC method requires a derivatization step to introduce a chromophore for analytical detection and the ITP technique needs specialized equipment. Both methods are slow and are sensitive to indefinite number of variables. Published analytical methods for bisphosphonates have similar requirements of derivatization pro-

* Corresponding author.

0021-9673/94/$07.00
SSDI 0021-9673(94)00175-9

cedure and/or specialized instrumentation [6–10].

A simple method using ion chromatography to assay APD active ingredient and its pharmaceutical dosage forms which include injectables, capsules and tablets, has been developed. It is carried out with commercially available and conventional HPLC equipment. Samples are dissolved in water, filtered and appropriate amounts are injected onto the column. Analytical and chromatographic criteria are met well for both the active ingredient and its dosage forms.

2. Experimental

2.1. Instrumentation, reagents and samples

Instrumentation and reagents

Waters (USA) HPLC equipment included a Model 510 pump, a 710B automatic sampler, a 720 system controller, a 410 differential refractometer and a column heating chamber. An Alltech (USA) Universal Anion column was used, packed with polyhydroxyethyl methacrylate-based macroporous polymer with quaternary amine functionalities (270001) and phthalate counterion. An Alltech guard cartridge (38106) with a prefilter was connected before the column. The mobile phase was 5 m*M* potassium nitrate adjusted to pH 3.5 with nitric acid. It was filtered through a 0.45-μm membrane filter and degassed before use. The flow-rate used was 1.2 ml/min. The column and the detector temperatures were maintained at 35°C throughout the run. The detector was set at a sensitivity of 256 and adjusted accordingly depending on the amount of sample injected.

Sample and standard preparation

The samples analyzed were the APD active ingredient and the different dosage forms of APD consisting of lyophilized powders, enteric coated pellets, enteric coated tablets and ampul solutions.

For the assay, solid samples were accurately weighed, dissolved and diluted with water to obtain test solutions with APD concentration of 3.0 mg/ml (anhydrous basis). Ampul solutions, 1 mg/ml (anhydrous basis), were used as is.

For the chromatographic evaluation and method validation, samples tested include the active ingredient and the different dosage forms, the active ingredient spiked with theoretical impurities and the active ingredient spiked into placebos of the different dosage forms.

Standard test solutions were prepared from the APD active ingredient reference standard. Required amounts were accurately weighed into a volumetric flask, dissolved and diluted to volume with water to contain either 3.0 mg/ml or 1.0 mg/ml APD (anhydrous basis) depending upon the sample being analyzed.

2.2. Procedure

The column was equilibrated with the mobile phase and replicate 20-μl injections of APD standard solution were made onto the column. The peak responses were recorded using an on-line computer (HP9153C). When the relative standard deviation of five injections of the standard solution was not more than 2.0%, and the tailing factor [11] of the APD peak was not more than 2.0, analysis was started.

A 20-μl volume of sample or standard test solutions was injected onto the column and the chromatograms were recorded and analyzed using an on-line computer.

3. Results and discussion

The primary goal was to develop a simple and reliable chromatographic assay method which can analyze APD in the different pharmaceutical dosage forms, free from placebo interference, and completely resolved from the synthetic impurities/degradation products such as β-alanine, phosphate and phosphite ions.

Initial work involved evaluation of several reversed-phase and ion-exchange columns in different modes of separations such as ion pairing, ion exchange and ion exclusion. Shown in Fig. 2a was the most promising result from these

initial experiments. Separation of APD, phosphate and phosphite was obtained using a system which consists of a polymethacrylate strong-anion exchange column, a 2 m*M* nitric acid eluent and a post-column detection set-up with ferric nitrate as the reactant. With this chromatographic system however, APD was not baseline resolved from the phosphate ion. Optimization of the system to completely resolve APD from the phosphate ion ($R_s \geq 1.5$) by varying the pH, ionic concentration and addition of organic modifier, was unsuccessful. Finally, replacement of the polymethacrylate column with a polyhydroxymethacrylate column (also with quaternary amine functionalities), and using 5 m*M* nitrate eluent at pH 3.5 with a refractive index detector, complete separation of APD, phosphate and phosphite was achieved as shown in Fig. 2b. The resolution of APD and phosphate was significantly better with $R_s \simeq 1.9$ and the other chromatographic figures of merit are all reasonably good (see Table 1). The improvement in selectivity with this system has been attributed to an interaction occurring between the analytes and the hydroxyethyl moiety of the polymer packing.

3.1. Nitrate eluent concentration

Anion eluents such as acetate, chloride and citrate were evaluated along with the nitrate anion. The best separation of APD, phosphate and phosphite was obtained with the nitrate anion as eluent. A linear response of the capacity factor of APD, phosphate and phosphite was obtained as the nitrate eluent was increased from *ca.* 1 to 10 m*M* (Fig. 3).

For the assay method, 5 m*M* nitrate eluent concentration was selected for speed, excellent separation and peak profiles, and free from interference.

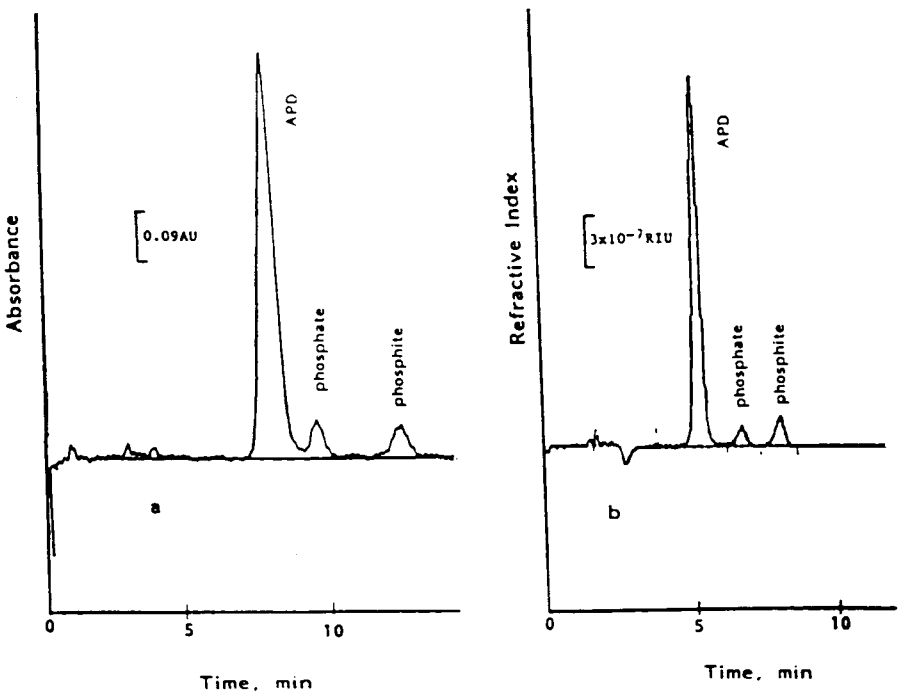

Fig. 2. Separation of APD, phosphate and phosphite on (a) methacrylate strong anion-exchange column (Super-sep Anion) with 2 m*M* HNO_3 eluent and UV detection at 300 nm after post-column reaction with $Fe(NO_3)_3$ and (b) hydroxyethyl methacrylate strong anion-exchange column (Universal Anion) with 5 m*M* KNO_3 eluent adjusted to pH 3.5 with nitric acid and refractive index detection.

Table 1
Chromatographic figures of merit

	APD	Phosphate	Phosphite
System precision			
R.S.D., %	0.25	2.20	1.58
Capacity factor, k'	1.94	2.75	3.50
S.D.	0.01	0.01	0.01
Tailing factor, T	1.0	0.98	0.95
S.D.	0.08	0.06	0.06
Resolution, R_s	1.9(a)	1.9(b)	–
S.D.	0.08	0.11	–

The system precision, as R.S.D. (%), was obtained from peak area response of six injections of standard solution containing APD, phosphate and phosphite. The capacity factor, k' (using water as the unretained peak), the tailing factor, T and the resolution, R_s between APD and phosphate (a), and between phosphate and phosphite (b), were determined according to ref. 11. Standard deviation (S.D.) was calculated for each figure of merit, with $n = 6$.

3.2. Eluent pH

The effect of eluent pH on the capacity factors, k', of APD, phosphate and phosphite at fixed eluent concentration of 5 mM nitrate, are shown in Fig. 4. Between pH 3 and 6, the k' of phosphate and phosphite remain essentially constant. A decrease below pH 3 was observed for phosphate and an increase above pH 6 was observed for both phosphate and phosphite. For APD k' increased with increasing pH with apparent changes in slopes of k' at several pH regions.

Since both the nitrate eluent and the quaternary ammonium groups (of the column) should be essentially ionized within the pH range studied (between 2.5 and 9.0), the retention behavior of APD, phosphate and phosphite at a specified pH, must be influenced primarily by their ionization constants. APD has pK values of 1.7, 2.7, 6.3, 10.8 and 11.5, with a zwitterion noted between pH 2 to 3 [5]. Orthophosphoric acid has pK values of 2.12, 7.21 and 12.67, and phophorous acid has values of 2.00 and 6.59 [12]. Between pH 3 and 6, the k' values of phosphate and phosphite were virtually unchanged indicating the predominance of one solute species, most likely the singly charged anion. Below pH 3, the

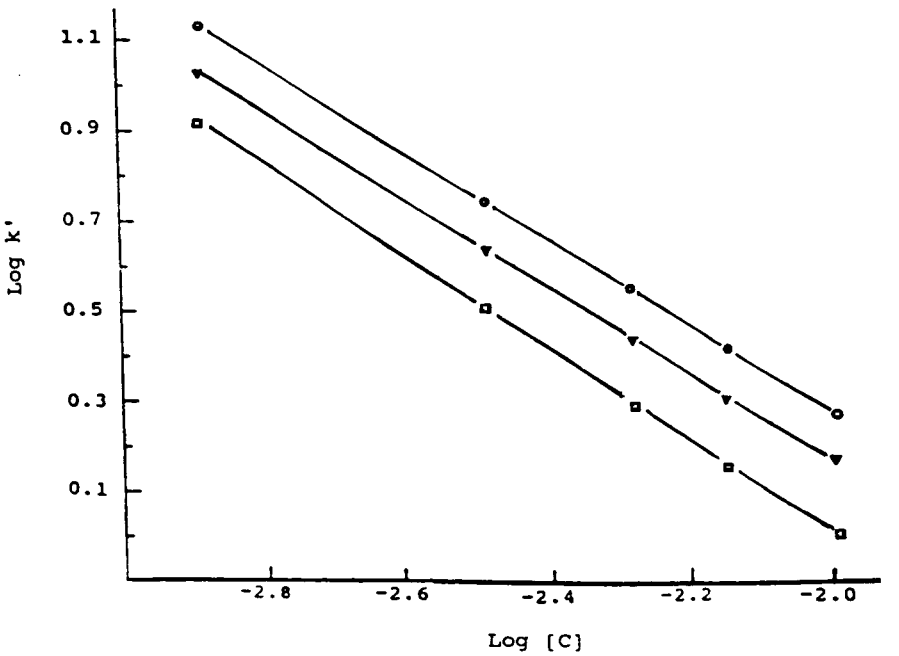

Fig. 3. Effect of eluent concentration, C: log k' *versus* log [C] for APD (□), phosphate (▼) and phosphite (●).

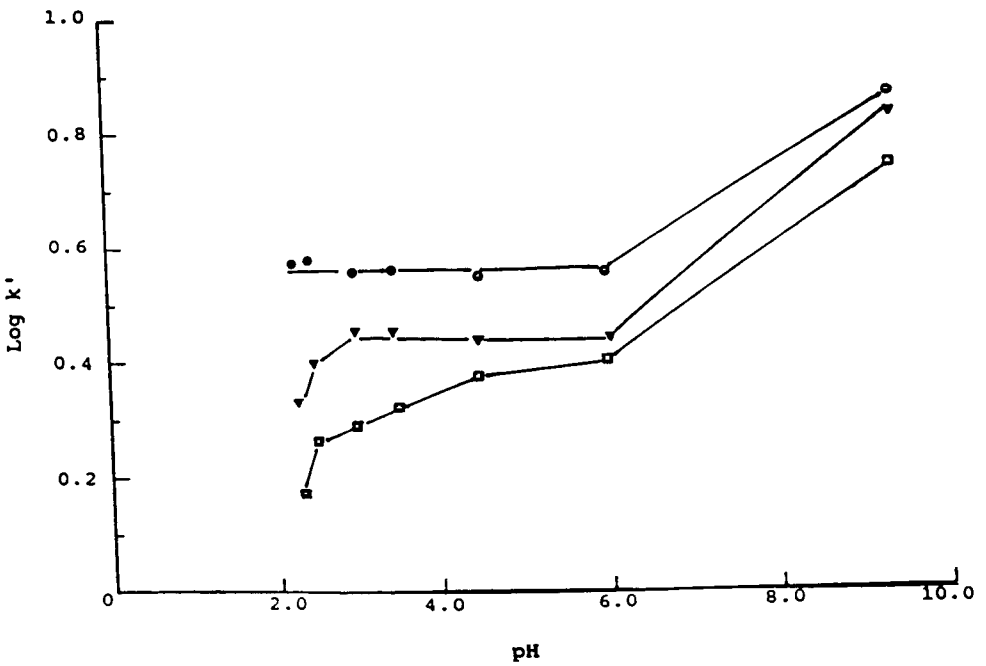

Fig. 4. Effect of pH: log k' *versus* pH for APD (□), phosphate (▼) and phosphite (○).

influence of the neutral species was apparent from a decrease in k', specifically for the phosphate. Above pH 6, the influence of the doubly charged species was similarly apparent from a drastic increase of k' for both phosphate and phosphite. For APD, k' increased with increasing pH and the slope of k' appeared to change at several pH regions. The different ionic species seem to exert influence on the retention behavior of APD, with one species predominating within certain pH range. At pH 3.5, which was the pH selected for the assay method, APD behaved as

Table 2
Analysis of APD in pharmaceutical products

Product (lot No.)	*n*	Claim potency	Found ± S.D.
Active ingredient (800388)	6	100.0%	99.6% ± 0.4
Ampul solutions (12/322/1)	6	5 mg/5 ml	4.9 mg/5 ml ± 0.04
Lyophilized powder (14/012/1)	6	30 mg	30.0 mg ± 0.2
Enteric-coated pellets in capsule (14/628/1)	6[a]	75 mg	75.8 mg ± 0.6
Enteric-coated tablets (PR 375-94)	10	150 mg	150.2 mg ± 0.9

[a] Two sets of samples of the enteric-coated pellets in capsule (3 and 3) were run on different days.

a singly charged anion. Presumably, at pH 3.5 the different ionic species including the zwitterion produced an effective net charge approaching minus one.

The choice of pH 3.5 for the assay method was made for the same reason as the choice of eluent concentration, *i.e.*, for speed, excellent separation and peak profiles and free from interference. Furthermore at pH 3.5, buffer was not necessary since a half unit change in pH from 3.5 did not significantly affect the chromatography nor the analytical results of APD, phosphate and phosphite.

3.3. Analytical application

The assay values obtained for the active ingredient and the different dosage formulations of APD are shown in Table 2, with typical chromatograms displayed in Fig. 5. A minimum of six samples of the different dosage forms were analyzed. The precision of the data and the

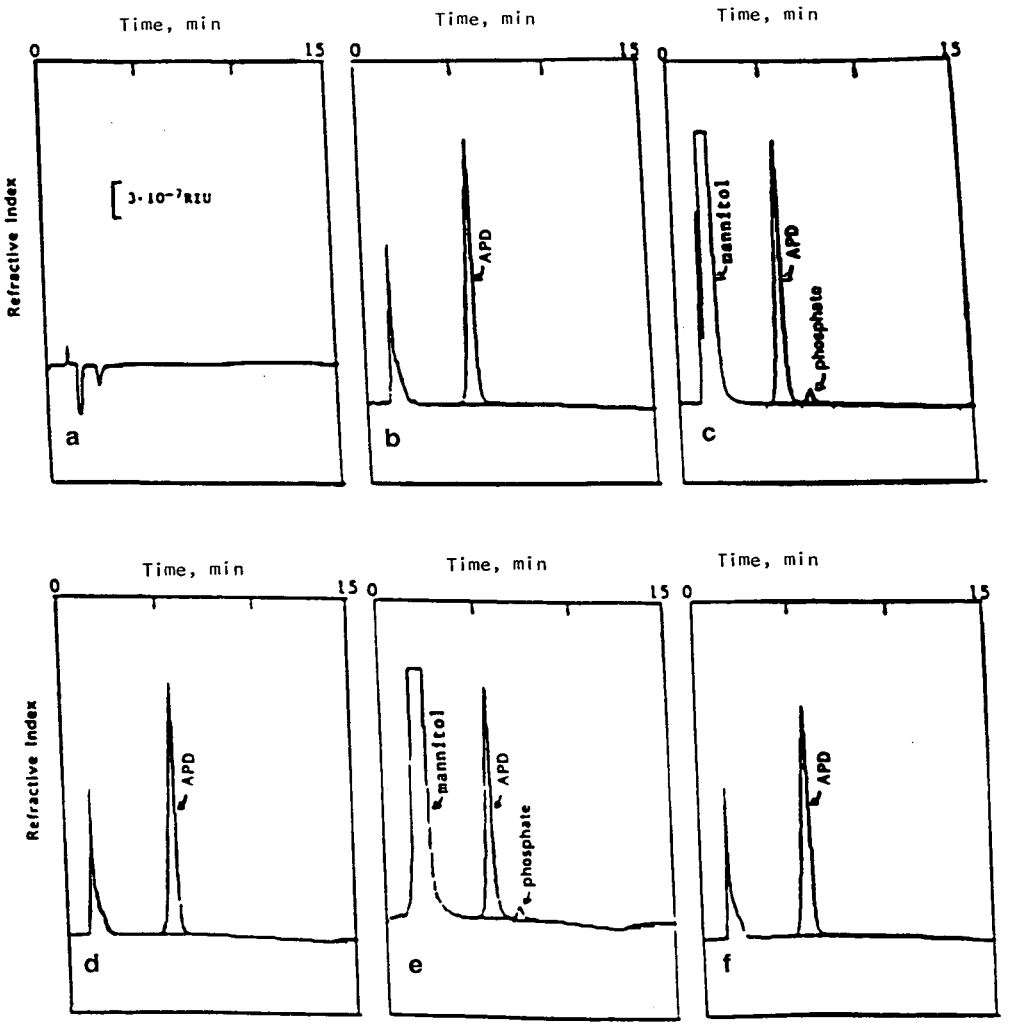

Fig. 5. Typical chromatogram of (a) water blank, (b) active ingredient, (c) lyophilized powder, (d) enteric coated tablet, (e) ampul solution and (f) enteric coated pellets in capsule. RIU = Refractive index units

agreement between the claim potency and the amount found were excellent.

The method was validated for the APD active ingredient and its dosage forms, using the analytical criteria of precision, accuracy and linearity.

Potential by-products and the formulation components of the different dosage forms which include isotonic and pH adjustors, binders, antifoaming and film-forming agents, anti-adherents and opacifiers did not interfere with the assay procedure for APD.

At least six columns from the same manufacturer have been tested so far and all have shown comparable results. On-line filter and a pre-column were always used to prolong column life.

4. Conclusions

A simple analytical method for APD, an amino bisphosphonate, has been developed using anion-exchange HPLC. It is carried out with commercially available and conventional HPLC equipment. The chromatographic system consists of a macroporous polymer column with quaternary amine functionalities, nitrate anion eluent and refractive index detector. APD active ingredient and the different dosage forms have been analyzed with excellent analytical and chromatographic results.

5. Acknowledgements

We wish to acknowledge and thank Dr. M. Bloch and Mr. E. Felber, Ciba-Geigy, Basel, Switzerland for supporting this work, Dr. H. Stober for technical discussion, and Mrs. S. Haggerty for all the secretarial support.

6. References

[1] H. Fleisch, R.G.G. Russel and M.D. Francis, *Science*, 165 (1969) 1262.
[2] F.J.M. van Breukelen, O.L.M. Bijvoet and A.T. van Oosterom, *Lancet*, i (1979) 803.
[3] H.P. Sleeboom, O.L.M. Bijvoet, A.T. van Oosterom, J.H. Gleed and J.L.H. O'Riordan, *Lancet*, ii (1983) 239.
[4] W.B. Frijlink, O.L.M. Bijvoet, J. te Velde and G. Heynen, *Lancet*, i (1979) 799.
[5] J. Quitasol and L. Krastins, unpublished results.
[6] G. Flesch and S.A. Hauffe, *J. Chromatogr.*, 489 (1989) 446.
[7] E. Kwong, A.M.Y. Chiu, S.A. McClintock and M.L. Cotton, *J. Chromatogr. Sci.*, 28 (1990) 563.
[8] T.L. Chester, E.C. Lewis, J.J. Benedict, R.J. Sunberg and W.C. Tettenhorst, *J. Chromatogr.*, 225 (1981) 17.
[9] P.T. Daley-Yates, L.A. Gifford and C.R. Hoggarth, *J. Chromatogr.*, 490 (1989) 329.
[10] J. Fels, J. Guyonnet, Y. Buger and W. Cautreels, *J. Chromatogr.*, 430 (1988) 73.
[11] *USP XXII, NF XVII*, United States Pharmacopeial Convention, Rockville, MD, 1990, p. 1567.
[12] R.C. Weast (Editor), *CRC Handbook of Chemistry and Physics*, CRC Press, West Palm Beach, FL, 59th ed., 1978–1979, p. D-203.

ELSEVIER

Journal of Chromatography A, 671 (1994) 281–285

JOURNAL OF CHROMATOGRAPHY A

Analysis of chiral carboxylic acids in wine by high-performance liquid chromatography with coupled UV and circular dichroism detection

Orfeo Zerbinati*, Riccardo Aigotti, Pier Giuseppe Daniele

Dipartimento di Chimica Analitica, Università di Torino, v. Giuria 5, I-10125 Turin, Italy

Abstract

A circular dichroism (CD) spectrophotometer, equipped with a flow cell, and a UV detector were connected in series and were used for coupled UV–CD detection of optically active carboxylic acids. The limits of detection and the linear range for the enantiomers of tartaric, malic, lactic and ascorbic acids are reported. Several wines were analysed and CD detection proved to be sensitive enough for accurate determinations. The combined UV–CD detection was helpful for identifying the peaks and allowed the calculation of enantiomeric ratios.

1. Introduction

The study of specific detectors for HPLC and ion chromatography (IC) is currently attracting a great deal of attention [1]. HPLC detectors based on optical activity are potentially advantageous because of their inherent selectivity; in fact, compounds that are not chiral (*e.g.*, solvents, buffers, impurities) will not interfere with analysis even if they co-elute with the analytes. Compared with polarimetric detection, circular dichroism (CD) detection is more sensitive and gives more stable baselines, as it is intrinsically insensitive to refractive index fluctuations [2], but it is necessary to operate in the linear range of the response [3].

Most of the applications developed to date have involved laboratory preparations; the number of real samples investigated is comparatively very small. UV and CD detectors in series have been employed for the determination of the enantiomeric excess of nicotine in leaf extracts [4]; the use of LC with combined UV and either polarimetric or CD detection allowed the identification of enantiomers of the pyrethroid insecticides [5]; the enantiomeric purity of scopolamine isolated from plant extract was determined using achiral–chiral coupled column chromatography with CD confirmation of the individual peaks [6]; a micro-flow cell device was adapted to a CD spectrometer for HPLC separation and structural analysis of proteins [7]; continuous acquisition of circular dichroism spectra during liquid chromatography was successfully performed and it was applied to the resolution of a racemic mixture of 2,2′-spirobi[2*H*-chromene] [8]; and racemic mixtures of alkylarylcarbinols were resolved and the absolute configurations of the fractions eluted were determined by means of CD detection [9].

* Corresponding author.

0021-9673/94/$07.00
SSDI 0021-9673(93)E0076-7

Analyses of the organic acid content of wines are routinely conducted; tartaric, malic, lactic and ascorbic acids are among the most important constituents of wines. Different stereoisomers of those acids can be present at a time; in wines, L-forms usually predominate over the D-forms (the concentration of the *meso* form of tartrate is normally negligible in comparison with those of its two optically active forms). D-Tartrate can originate from racemization, or may be added to achieve precipitation of the racemic calcium salt in order to avoid unwanted turbidity. D-Lactate derives from alcoholic fermentation of sugars, whereas its L-enantiomer comes from the conversion of the L-malate (malolactic fermentation), a bacterial process that is very important for the quality of wine; usually, the amount of the D-form is about one fifth of the total lactate [10].

In this paper, we demonstrate that an HPLC–UV–CD system is applicable to the analysis of wines for chiral organic acids, and that this system is also convenient for measuring their enantiomeric excess (e.e.) with adequate precision.

2. Experimental

2.1. Reagents

All aqueous solutions were prepared with ultra-high-quality (UHQ) water produced by an Elga-Stat water-purification apparatus (Elga, High Wycombe, UK). D-(−)-Lithium lactate (97%), L-(+)-lactic acid (>98%), D-(−)- and L-(+)-tartaric acid (>99%), L-(−)- and D-(+)-malic acid (>99%) and L-(+)-ascorbic acid (99.7%), together with C_{18} solid-phase extraction cartridges, were obtained from Merck (Bracco, Milan, Italy). Acetonitrile (HPLC grade) was obtained from Lab Scan (Delchimica, Naples, Italy). The solutions of the investigated substances were prepared with UHQ water immediately before use.

2.2. Apparatus

The HPLC system consisted of a Pye Unicam (Cambridge, UK) PU 4015 pump, a Rheodyne (Cotati, CA, USA) valve fitted with a 20-μl loop and a 250×4.6 mm I.D. Adsorbosphere C_{18} 5-μm column (Alltech, Deerfield, IL, USA). The eluent was degassed by means of a stream of helium. The UV detector was obtained from Perkin-Elmer (Norwalk, CT, USA).

CD detection was performed by means of a Jasco (Tokyo, Japan) J-600 computerized spectropolarimeter, which was equipped with a cylindrical, laboratory-made flow cell of 8 mm I.D. and 0.7 mm optical path length. The cell was constructed with two 10×10 mm quartz windows, spaced by a PTFE ring and mounted on a PTFE bearing. No light condenser [3] was employed, in order to avoid reduction of the light-flux energy caused by the system of lenses. The efficiency of the light-flux energy was estimated by comparing the high-tension voltage of the photomultiplier detector, measured with an ordinary 1-mm cell, with that measured with the flow cell; the measurements were corrected for the differences in light paths; both cells were filled with the chromatographic eluent. No decrease in the efficiency of the light-flux energy or an increase in the noise was observed.

2.3. Chromatographic conditions

An isocratic eluent, consisting of 0.1 *M* sodium dihydrogenphosphate adjusted to pH 2.5 by addition of 85% phosphoric acid solution, was used at a flow-rate of 1 ml min^{-1}. The column temperature was 23 ± 1°C.

A 4-s time constant and a 2-s step resolution (corresponding to a 4000-s maximum duration of the chromatographic run) were chosen for the CD spectrophotometer, in order to minimize the noise without sacrificing the definition of the chromatographic peaks.

After being collected, the CD chromatograms were smoothed; quantification of the analytes was performed on the basis of peak height.

2.4. Sample clean-up

A pretreatment of the wine samples was performed in order to decrease the content of

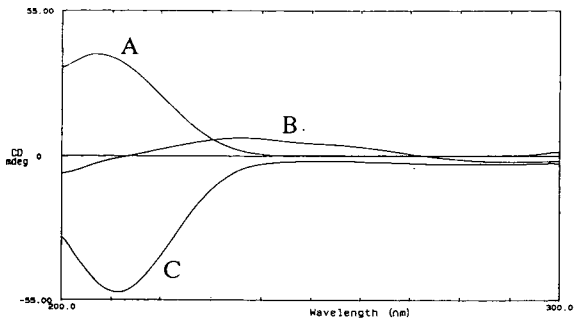

Fig. 1. CD spectra of pure enantiomers of chiral acids. Peaks: A = L-(−)-malic; B = L-(+)-ascorbic; C = L-(+)-tartaric acid. mdeg = 10^{-3} degrees.

non-polar substances potentially dangerous for the chromatographic stationary phase. The pretreatment consisted in a single elution of 1 ml of wine on a 400-mg C_{18} SPE cartridge. Preliminary tests were conducted on standard solutions of the investigated acids, the pH of which was adjusted at 3.5; they showed no evident interference of the pretreatment with the concentrations of the investigated analytes, as the recovery was 100 ± 4% ($n = 3$).

3. Discussion

Some typical CD spectra of the investigated acids are reported in Fig. 1. Tartaric, malic and lactic acid show their CD and UV maxima around 210 nm. Ascorbic acid has its CD maximum around 235 nm, whereas it shows its largest UV absorptivity at 260 nm. Both CD and UV detection of tartaric, malic and lactic acid were performed at 210 nm, whereas CD and UV detection of ascorbic acid were conducted at 235 and 210 nm, respectively. The CD spectrum of D-(+)-glucose was also examined; it was observed that no interference on the CD chromatograms of the acids could have derived from glucose, as it exhibits its CD activity at wavelengths shorter than 200 nm.

Fig. 2 shows the UV and CD chromatograms of a mixture of the L-enantiomers of tartaric, malic and lactic acid. As can be seen, there is no direct relationship between the sign of the optical rotatory power of the enantiomers and the sign of their CD peaks.

A linear correlation between CD signal and concentration was observed in the range 5–100 mM. The parameters of the calibration equa-

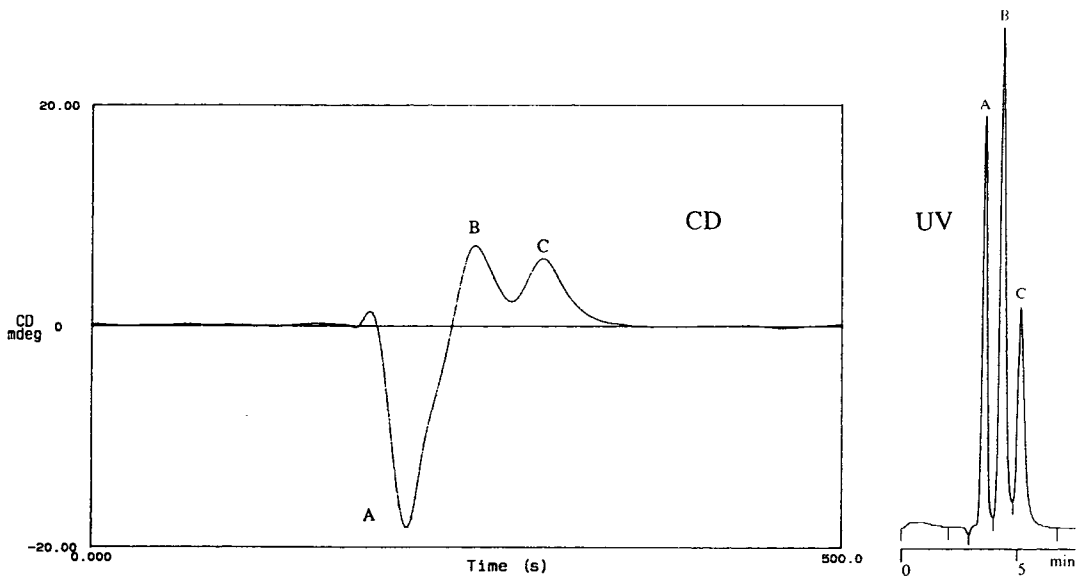

Fig. 2. CD and UV chromatograms of a mixture of three acids. Peaks: A = L-(+)-tartaric; B = L-(−)-malic; C = L-(+)-lactic acid. mdeg = 10^{-3} degrees.

Table 1
CD calibration equations and detection limits

Substance	*A*	*B*	*C*	*D*	*E*
Ascorbic acid	0.3 ± 0.2	87 ± 4	0.3	5	2.5
Tartaric acid	0.6 ± 0.4	700 ± 42	0.6	4	0.4
Malic acid	0.2 ± 0.2	137 ± 9	0.2	4	2
Lactic acid	0.2 ± 0.2	129 ± 5	0.1	4	2

Calibration equation: $y = A + Bx$; A = intercept ± S.D. [mdeg (10^{-3} degrees)]; B = slope ± S.D. (mdeg l mol^{-1}); x = concentration (mmol l^{-1}); C = standard error ($n = 3$); D = number of data points; E = detection limits (mmol l^{-1}) (signal-to-noise ratio = 2, injection volume = 20 μl).

tions, together with the observed detection limits, are reported in Table 1.

As an example of the results obtained, CD and UV chromatograms of an Italian red wine (Lambrusco from Emilia, "amabile" variety) are reported in Fig. 3. Only three of the UV-absorbing compounds were also detected by CD, thus helping in the validation of the peaks; ascorbic acid gave no CD signal, as detection was conducted at 210 nm. The concentrations of the L-enantiomers of tartaric, malic and lactic acid exceeded those of the remaining stereoisomers.

Table 2 reports the results obtained for different wines. The uncertainties in the concentrations of the L-enantiomers (or e.e., for tartaric acid), as given in Table 2, were calculated by considering the uncertainties in the coefficients of the CD calibration equations and those in the concentrations obtained by UV detection. The values of the experimental uncertainties, coupled with the enantiomer concentrations or e.e. in Table 2, allow a significant comparison of different wines. One of the samples was analysed twice, 9 and 11 months after the vintage. In this wine, the persistence of a relevant concentration of malic acid indicated that malolactic fermentation did not occur completely; the concentration of the D-(−)-lactate, due to the alcoholic fermentation, increased with time. Malic acid was not found in the remaining samples, whereas lactic acid was found in all the analysed wines except one.

4. Conclusions

Combined UV and CD detection was applied to analyses for chiral organic acids in wines. For this purpose, a CD spectrophotometer was equipped with a suitable flow cell. The CD

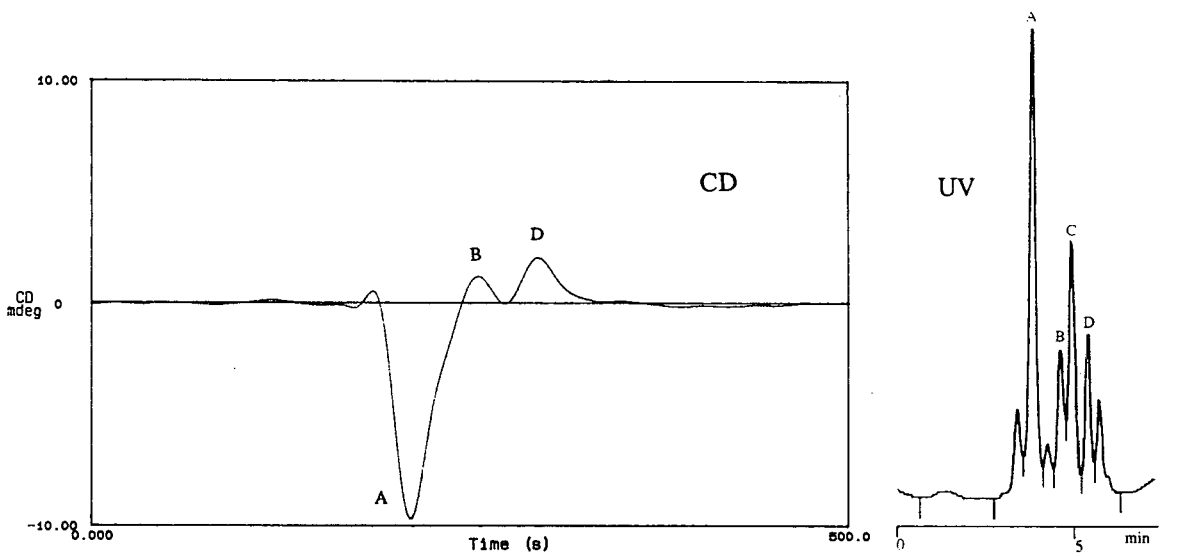

Fig. 3. CD and UV chromatograms of Lambrusco "amabile" wine. A = L-(+)-tartaric; B = L-(−)-malic; C = L-(+)-ascorbic; D = L-(+)-lactic acid. mdeg = 10^{-3} degrees.

Table 2
Analyses of wines

Wine and year	*A*	*B*	*C*	*D*	*E*	*F*	*G*
Lambrusco "amabile", 1992[a]	18.2 ± 0.7	7.5 ± 0.6	14.9 ± 0.6	10 ± 2	35 ± 1	30 ± 5	0.5 ± 0.05
Lambrusco "amabile", 1992[b]	17.4 ± 0.7	12.6 ± 1	17.6 ± 0.9	14 ± 3	46 ± 2	30 ± 4	0.55 ± 0.05
Moscato d'Asti, 1992	16.4 ± 0.7	6.8 ± 0.6	–	–	–	–	–
Barbera d'Alba, 1992	19.7 ± 0.8	10.8 ± 0.9	–	–	55 ± 2	37 ± 5	0.75 ± 0.08
Lambrusco "secco", 1992	22 ± 0.9	16 ± 1.3	–	–	58 ± 2	42 ± 6	1.8 ± 0.1
Limnio, 1989	14.3 ± 0.6	7.1 ± 0.7	–	–	37 ± 2	22 ± 3	2.1 ± 0.1
Côtes du Rhône, 1992	9.3 ± 0.4	3 ± 0.6	–	–	38 ± 2	22 ± 3	2.3 ± 0.1

All concentrations are expressed as mmol l^{-1} ± experimental uncertainty ($n = 3$). *A* = tartaric acid, total; *B* = L-(+)-tartaric, enantiomer excess; *C* = malic acid, total; *D* = L-(−)-malic acid; *E* = lactic acid, total; *F* = L-(+)-lactic; *G* = ascorbic acid, total. Note: the enantiomer concentration of ascorbic acid is not given, as its CD signal was lower than the detection limit.
[a] Analysed 9 months after vintage.
[b] Analysed 11 months after vintage.

detector was helpful in validating the UV peaks. It proved to be sensitive enough to allow the determination of the principal chiral organic acids contained in wine. The comparison of UV and CD quantitative results allowed the calculation of the enantiomer concentrations, or e.e., of tartaric, malic and lactic acid with experimental uncertainties that allowed a significant comparison of different wines.

5. References

[1] P.R. Fielden, *J. Chromatogr. Sci.*, 30 (1992) 45.
[2] J.K. Swadesh, *Am. Lab.*, February (1990) 5.
[3] J. Zukowski, Y. Tang, A. Berthod and D.W. Armstrong, *Anal. Chim. Acta*, 258 (1992) 83.
[4] N. Purdie and K.A. Swallows, *Anal. Chem.*, 61 (1989) 77A.
[5] C. Meinard, P. Bruneau and J. Perronnett, *J. Chromatogr.*, 349 (1985) 109.
[6] A.M. Stalcup, J.R. Faulkner, Y. Tang, D. Armstrong, L.W. Lewy and E. Regalado, *Biomed. Chromatogr.*, 5 (1991) 3.
[7] T. Takakuwa, Y. Kurosu, N. Sakayanagi, F. Kaneuchi, N. Takeuchi, A. Wada and M. Senda, *J. Liq. Chromatogr.*, 10 (1987) 2759.
[8] G. Brandl, F. Kastner, A. Mannschreck, B. Nölting, K. Andert and R. Wetzel, *J. Chromatogr.*, 586 (1991) 249.
[9] P. Salvadori, C. Rosini and C. Bertucci, *J. Org. Chem.*, 49 (1984) 5050.
[10] G. Sicheri, *Industrie Agrarie*, Hoepli, Milan, 1983.

ELSEVIER

Journal of Chromatography A, 671 (1994) 287–293

JOURNAL OF CHROMATOGRAPHY A

Determination of total nitrogen in water samples by means of high-pressure bombs and ion chromatography

Hilda Ledo de Medina*, Marinela Colina de Vargas, Julio Marin, Dannis Pirela

Universidad del Zulia, Facultad Experimental de Ciencias, Laboratorio de Quimica Ambiental, Maracaibo 4011, Zulia, Venezuela

Abstract

The standard method for the determination of organic nitrogen in water samples in the past has been based on the Kjeldahl digestion technique that converts organic nitrogen into ammonia, which can then be determined along with any ammonia originally present. However, this method is time consuming and the accuracy is variable because the effect of interferences causes unreliable results, especially in complex matrices. An alternative method for the determination of organic nitrogen is the alkaline peroxodisulphate digestion technique. This oxidizes all nitrogen in the sample using potassium peroxodisulphate in a strongly alkaline environment under high pressure and temperature. Nitrate is the sole product and can easily be determined by ion chromatography or by other methods (*e.g.*, cadmium reduction method). A method for total nitrogen determination was developed using 23-ml high-pressure bombs with potassium peroxodisulphate and sodium hydroxide to oxidize the organic nitrogen to nitrate. Urea and ammonium chloride were used as nitrogen compounds for calibration. The method was checked with the Kjeldahl method, showing good agreement (R.S.D. = 4.62%). Studies of digestion time were carried out to determine the optimum time in the pressure vessel. The results were checked with the cadmium reduction method (R.S.D. = 3.62%) for natural water samples. The recoveries with urea and ammonium chloride reagents were higher than 90%.

1. Introduction

The determination of total nitrogen (TN = inorganic plus organic fixed nitrogen) has largely been based on acid Kjeldahl digestion of nitrogenous organic compounds [1]. This procedure is tedious to perform and yields a total Kjeldahl nitrogen (TKN) value that includes only organic N and NH_4^+-N (not NO_2^-- and NO_3^--N) [2]. This method involves the determination of the total concentration of ammonia nitrogen and organic bound nitrogen according to the Kjeldahl method. The organic bound nitrogen is digested with a mixture of concentrated sulphuric acid and potassium sulphate with selenium or mercury as catalyst [3].

Manual distillation is still the primary method for the determination of nitrogen as ammonia from Kjeldahl digests of soils, plants, cereals, food and fertilizer products. It is also the standard procedure for the determination of protein in meat and meat products and for alcohol and other volatiles in the wine and beverage industry [4].

One of the limiting factors of the Kjeldahl nitrogen determination is that it normally re-

* Corresponding author.

0021-9673/94/$07.00
SSDI 0021-9673(94)00018-5

quires more than 2 h, or about 1 h using a heating block, whereas the measurement itself takes only a few minutes with an automated distillation apparatus [5].

An alternative method for the determination of organic nitrogen modified by D'Elia *et al.* [2] is the alkaline peroxodisulphate digestion technique. This oxidizes all nitrogen in the sample using potassium peroxodisulphate in a strongly alkaline environment under high temperature and pressure.

A modified peroxodisulphate digestion technique for TN determination has also been developed [6]. The oxidation, under alkaline conditions, reduces nitrogenous compounds to NO_3^- for measurement as the sole product under high temperature using a microwave digestion unit in place of an autoclave system. Nitrate can be determined by reduction to nitrite using a cadmium reduction column. Separate, rather than combined, nitrate–nitrite values are readily obtained by carrying out the procedure first with, and then without, the Cu–Cd reduction step [7].

However, this procedure leads to many problems with the measurement. The copperized cadmium column needs washing and preconditioning with buffer and/or EDTA solutions to sustain a high reduction activity for nitrate. Also, the presence of air in the solution removes the activity from the column [8].

In the digestion–chromatographic method proposed here, we used the peroxodisulphate digestion solution of Johnes and Heathwaite [6] and developed a modified technique for digestion and determination of TN. The method utilizes a high-pressure bomb in the peroxodisulphate digestion step. This technique converts all nitrogen in the sample into nitrate, which is determined using ion chromatography, giving a convenient and more accurate and rapid method of TN determination. By comparison, the chromatographic approach is simple, versatile and has the added advantage of being applicable over a wide range of concentrations.

A comparison was made between the proposed digestion–chromatographic method and the conventional Kjeldahl and nitrate–nitrite methods as prescribed in a standard text [7]. Known nitrogen-containing substances such as urea and ammonium chloride and a large number of samples of natural waters were investigated.

2. Experimental

Samples were taken from the rivers Motatán, Carache and Boconó, which are inflows of Lake Maracaibo. Water samples from Lake Maracaibo were also taken. The samples were preserved with concentrated sulphuric acid (2 ml/l) and refrigerated.

The reagents urea and ammonium chloride were used to confirm the validity of the method.

2.1. Determination of nitrate and nitrite

Apparatus

A Milton Roy 21D spectrophotometer was used.

Reagents

Cadmium powder (150 μm) was obtained from Merck. To prepare copper–cadmium, the cadmium particles (new or used) were cleaned with dilute HCl (1.2 *M*) and copperized with a 2% solution of copper sulphate in the following manner. Cadmium was washed with 1.2 *M* HCl and rinsed with distilled water, then 2 g of the cadmium were swirled in 100 ml of 2% copper sulphate solution until the blue colour partially faded. The copper sulphate solution was decanted and the procedure was repeated with fresh copper sulphate until a brown colloidal precipitated was formed. The cadmium–copper was washed with distilled water (approximately ten times) to remove all the precipitated copper.

To prepare the colour reagent 100 ml of concentrated phosphoric acid, 40 g of sulphanilamide and 2 g of N-1-naphthylethylenediamine dihydrochloride were added to approximately 800 ml of deionized water while stirring. Stirring was continued until dissolution was complete, then the solution was diluted to 1 l with water. The solution was stored in a brown bottle and kept in the dark when not in use.

Ammonium chloride–EDTA solution was prepared by dissolving 85 g of analytical-reagent grade ammonium chloride and 0.1 g of disodium ethylenediaminetetracetate in 900 ml of distilled water. The pH was adjusted to 8.5 with concentrated ammonia solution and the mixture was diluted to 1 l with water.

Stock standard nitrate and nitrite solutions (1000 mg/l NO_3-N and NO_2-N, respectively) were prepared in 100-ml volumetric flasks.

Procedure

To construct calibration graphs, working standard solutions were freshly prepared from the stock standard nitrate and nitrite solutions.

The efficiency of the reduction column was verified with a standard nitrite solution and comparison with a standard nitrate solution at the same concentration.

A calibration graph was prepared with standards of KNO_3 in the range 0.05–1.00 mg/l NO_3^--N by dilution of the stock standard nitrate solution. The concentrations were measured spectrophotometrically at 543 nm. After the digestion procedure, the absorbance was related to the total amount of nitrogen in the sample.

2.2. Determination of total Kjeldahl nitrogen

Apparatus

A Milton Roy 21D spectrophotometer, micro-Kjeldahl digestion and distillation units and a Metrohm E678 Titroprocessor were used.

Reagents

All the reagents were prepared following the procedure described in a standard text [7].

Procedure

A 100-ml volume of sample was mixed carefully with 50 ml of digestion reagent (10 ml of concentrated H_2SO_4, 6.7 g of K_2SO_4 and 1.25 ml of $HgSO_4$ solution) and added to a distillation flask. A few glass beads was added and, after mixing, the mixture was heated under a hood to remove acid fumes. The mixture boiled briskly until the volume was greatly reduced and copious white fumes were observed. Digestion was continued for an additional 30 min. As digestion continued, the sample turned clear. After digestion, the contents (cooled) were diluted to 300 ml with water and mixed. The flask was tilted and 50 ml of hydroxide–thiosulphate reagent were carefully added to form an alkaline layer at the bottom of the flask. The flask was connected to a steam distillation apparatus and shaken to ensure complete mixing. The mixture was distilled and 200 ml of the distillate were collected below the surface of 50 ml of absorbent solution. Boric acid was added as an indicator. Ammonia in the distillate was titrated with standard 0.02 *M* H_2SO_4 until the indicator turned a pale lavender.

2.3. Determination of total nitrogen by proposed digestion and ion chromatographic methods

Oxidizing reagent

A 15-ml volume of 3.75 *M* NaOH solution was added to 500 ml of deionized water, 50 g of $K_2S_2O_8$ were dissolved in the solution and the mixture was diluted to 1 l with water. This oxidizing reagent must be prepared freshly as required.

Digestion procedure

A 6-ml volume of oxidizing reagent was added to 4 ml of sample and placed in a PTFE crucible and capped. The crucible was placed in the stainless-steel body of a Parr-type bomb and closed by tightening the stainless-steel screw-cap. The system was placed in a preheated 105°C oven and kept at this temperature for 4 h. The bomb was opened after cooling to ambient temperature. Under the influence of pressure, temperature and pH, the organic and inorganic nitrogen compounds were converted into nitrate. The nitrate formed was measured by ion chromatography.

2.4. Determination of nitrate by ion chromatography

Samples and reagents

Samples were diluted tenfold before injection into the chromatograph because the SO_4^{2-} peak, derived from potassium peroxodisulphate, after the digestion procedure interferes in the detection of nitrate. A blank of the oxidizing reagent, after the digestion procedure, was injected into the chromatograph.

All reagents were of the highest purity and deionized water was used for dilutions. Calibration standards were prepared by diluting mixed stock standard solutions containing 1000 mg/l of NO_3^--N using a series of dilutions.

Apparatus

Samples were analyzed using a Dionex Model 2000i/SP ion chromatograph equipped with an anion precolumn (Dionex AG4A), an anion separation column (Dionex AS4A), a suppressor column (Dionex AMMS-II) and a conductivity detector. The mobile phase (flow-rate 2 ml/min) was 1.7 m*M* $NaHCO_3$–1.8 m*M* Na_2CO_3 and the regenerant solution was 12.5 m*M* H_2SO_4. The injection volume, conductivity sensitivity and chart speed were 100 μl, 30 μS and 0.5 cm/s, respectively.

Procedure

Standards and samples were injected into the ion chromatograph with an analysis time of 10 min, which permitted the elution of the sulphate peak, which was the last to elute. External standardization was used with recalibration after every ten samples during a run. A calibration graph was plotted of peak area against concentration and used to interpolate unknown concentrations.

3. Results and discussion

3.1. Ion chromagraphy

Digested and diluted samples were injected into the ion chromatograph to detect total nitrogen concentrations as nitrate. After injection, nitrate ion was eluted from the column, and detected with a conductivity detector and recorder and quantified with an integrator (Fig. 1).

The response for NO_3^- was linear in the working range 1.00–100 mg/l. An important feature of conductivity detection in ion chromatography is linearity of the response over a wide concentration range. Linearity of the response is guaranteed by the dependence of conductivity on concentration, provided that other effects or matrix effects do not intervene. The correlation coefficient for a linear least-squares fit was $r = 0.9996$. This showed that the conductivity detector gave a linear response over the whole calibration range used in this work. The relative standard deviation (R.S.D.) was 1.62% ($n = 8$).

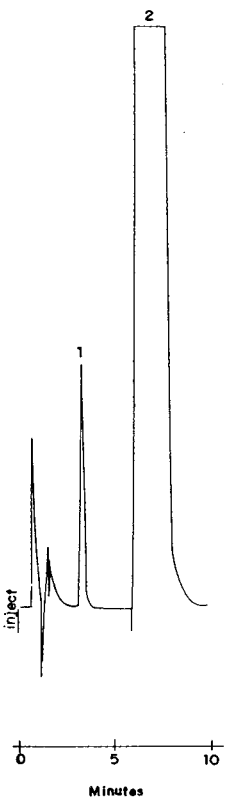

Fig. 1. Separation of nitrate in digested sample. Peaks: 1 = NO_3^- (0.88 mg/l); 2 = SO_4^{2-}.

3.2. Comparison of TKN spectrophotometric and chromatographic methods

Samples of water were analyzed for TN (TKN plus inorganic N) by standard methods and the results were compared with those obtained by the proposed digestion–ion chromatographic (IC) method. The recovery of TN was determined using analytical-reagent grade 99% urea and ammonium chloride. Table 1 gives results for TN obtained by the IC and Kjeldahl methods. The results obtained by the IC method show good recovery.

In Table 2, columns 1 and 2, the concentrations of nitrate measured in river waters and the urea and ammonia reagents, after the digestion step, by ion chromatography are compared with those obtained by the conventional spectrophotometric method using a copperized cadmium column. It is clear that the results obtained by the proposed method agree with those obtained using the standard method which involves the reduction of nitrate to nitrite. The R.S.D. using ion chromatography was 1.20% and that using a copperized cadmium column was 4.55% ($n = 5$). The mean difference between the values obtained was 3.67%.

Water samples with total nitrogen concentrations between 0.040 and 5.400 mg/l were analyzed using the proposed method and the Kjeldahl–nitrate–nitrite method (columns 1 and 3, Table 2). To decide if the difference between the methods is significant, a paired t-test was used because the samples contained substantially different amounts of analyte. As the calculated value of t is less than the tabulated value, the methods did not give significantly different values for the mean nitrogen concentration. By comparing squared standard deviations, the F-test shows whether the two methods show similar precision. The conclusion is that the proposed method does not differ from the Kjeldahl plus nitrate–nitrite method because no significant differences in the results were found. The proposed method generally reports more precise results (lower standard deviation). The mean difference between the values obtained by the methods used were 3.67% and 4.12%, as can be seen in Table 2.

Standard additions of different concentrations of nitrate were made to the water samples from Lake Maracaibo and the results are given in Table 3. The mean recovery of nitrate by the proposed method was 99.08%. This result indicates than suspected interferences are not significant.

A general comparison of the proposed method with the Kjeldahl and nitrate–nitrite methods to determine total nitrogen shows several advantages of the former. The tedious processes to determine TN using the Kjeldahl procedure plus the nitrate–nitrite method are not required in the proposed method. Moreover, the reduction of nitrate to nitrite is not necessary in the determination of nitrate, because it can be determined directly using ion chromatography. The proposed method eliminates the slow standard procedure which requires distillation of the whole digested sample. The Kjeldahl method produces substantial amounts of chemical waste

Table 1
Recoveries of nitrogen compounds using the Kjeldahl and IC methods

Compound	Nitrogen added (mg/l)	Mean recovery (%)[a]	
		Kjeldahl method	IC method
Urea	0.039	94.87	101.56
Ammonium chloride	2.800	105.71	102.86

[a] $n = 5$.

Table 2
Comparison of TN obtained by IC and TKN and inorganic N data obtained on water samples

Sample	Total nitrogen (N) (mg/l)							
	Ion chromatography[a]		Cadmium reduction[a]		TKN plus inorganic N (standard methods [7])		F-test	
	(1)	S.D.	(2)	S.D.	(3)	S.D.	(1) − (2)	(1)−(3)
Urea reagent	0.040	0.000	0.039	0.001	0.037	0.002	0.000	0.000
Ammonia reagent	2.880	0.001	–	–	2.960	0.002	–	4.000
Carache river	0.480	0.007	0.458	0.015	0.471	0.015	4.592	4.592
Motatán river	5.335	0.172	5.084	0.320	4.800	0.322	3.461	3.505
Boconó river	0.713	0.009	0.674	0.041	0.671	0.053	20.750	34.679

Mean difference:
(1) − (2) 3.67%.
(1) − (3) 4.12%.
Mean R.S.D., IC: 1.20% ($n = 5$).
Mean R.S.D., cadmium reduction: 4.55% ($n = 5$).
Mean R.S.D., TKN plus inorganic N: 4.57% ($n = 5$).
F (theoretical): 6.39 ($P = 0.05$).
t-Test (95%):
(1) − (2) Theoretical: 3.18
Calculated: 1.35.
(1) − (3) Theoretical: 2.78
Calculated: 1.50.
[a] After digestion procedure.

Table 3
Results of standard additions to Lake Maracaibo water for the determination of total nitrogen by ion chromatography

Sample No.	Total nitrogen concentration (mg/l)			
	Taken	Added as NO_3-N	Found	Recovery (%)
1	1.400	1.680	2.940	95.5
2	1.120	0.840	1.960	100.0
3	2.800	1.400	4.480	106.7
4	15.400	14.000	29.820	101.4
5	35.000	28.000	62.440	99.1
6	1.400	0.420	1.778	97.7
7	0.700	0.140	0.812	96.7
8	2.100	0.140	2.142	95.6

Mean recovery: 99.08%.
Mean R.S.D. 3.75% ($n = 3$).

with high concentrations of sodium hydroxide and low concentrations of the catalyst (selenium or mercury).

4. Conclusions

The TKN and spectrophotometric nitrate–nitrite results showed no significant difference from those obtained by the ion chromatographic method. The determination of nitrate ion by anion-exchange ion chromatography is reliable and gives reproducible results. The technique involves minimum handling and sample preparation. An additional benefit of the technique is the possibility of the determination of total nitrogen. The peroxodisulphate digestion–ion chromatographic method for determining total nitrogen is simple, sensitive, rapid, precise and suitable for the analysis of large numbers of samples. The analysis has the advantage of achieving high precision for samples while utilizing only small amounts of sample.

5. Acknowledgement

The authors thank the CONDES-LUZ for providing support for this work.

6. References

[1] S. McLeod, *Anal. Chim. Acta*, 266 (1992) 113.
[2] C. D'Elia, P. Steudler and N. Corvin, *Limnol. Oceanogr.*, 22 (1977) 761.
[3] H. Kroon, *Anal. Chim. Acta*, 276 (1993) 287.
[4] S. McLeod, *Anal. Chim. Acta*, 266 (1992) 107.
[5] M.H. Feinberg, J. Ireland-Ripert and R.M. Mourel, *Anal. Chim. Acta*, 272 (1993) 83.
[6] P. Johnes and L. Heathwaite, *Water Res.*, 26 (1992) 1281.
[7] American Public Health Association, American Waterworks Association and Water Pollution Control Federation, *Standard Methods for the Examination of Water and Wastewater*, American Public Health Association, New York, 17th ed., 1989, Ch. 4, p. 111.
[8] K. Takeda and K. Fujiwara, *Anal. Chim. Acta*, 276 (1993) 25.

ELSEVIER

Journal of Chromatography A, 671 (1994) 295–302

JOURNAL OF CHROMATOGRAPHY A

Progress and problems in organic microanalysis by ion chromatography

J.R. Kreling, J.S. Cowan, F. Block, J. DeZwaan*

Physical and Analytical Chemistry Research, 7255-209-008, The Upjohn Company, Kalamazoo, MI 49001, USA

Abstract

Results generated on a set of known samples, which were submitted as routine samples to the analysts, over a period of many years, are used as a basis for comparing microanalytical results. These comparisons are made for sulfur and chlorine determinations conducted with both the more common titrimetric methods and ion chromatographic methods. The variations observed in the chromatographic methods are studied in greater detail and a means of eliminating nearly all systematic variation is identified. These improved microanalytical procedures result in chromatographic determinations which are not only interference free, but also of significantly greater precision than was obtained using titration based methods. Although a method, similar to that used for sulfur and chlorine, could be developed for bromine, problems in generalizing them to fluorine and phosphorus determinations were encountered.

1. Introduction

Before the routine availability of accurate mass determinations and modern NMR techniques, the determination of elemental composition played a central role in structure elucidation procedures. For this reason a great deal of effort was directed toward developing analytical methods for determining hetero-atom composition (such as sulfur, phosphorous and the halogens) in organic materials [1–3]. These methods generally rely on sample combustion to convert the element of interest to an inorganic form, followed by chemical treatment to convert all of the element of interest to a single species which can then be quantitated by titration. Because most of these titrations are conducted directly on the mixtures produced in a combustion flask, they are subject to both physical and chemical interferences which may be difficult to control [4,5]. Despite being subject to numerous possible interferences, many of these methods remain in common use.

Microanalytical determinations of hetero-atom content continue to be frequently requested by synthetic and medicinal chemists since they provide an initial indication of sample quality and they are ultimately necessary for a structure proof. The continued need for the rapid and reliable determination of these elements on an expanding number of samples provides the motivation for the development of more efficient analytical methods that are free of interference. It was recognized early [6–9] that ion chromatographic (IC) analysis might provide an advantage over some of the titration procedures in these determinations because the inorganic forms of the hetero-atomic species produced in Schöniger combustions were ionic and could thus be separated and analyzed by IC. Initial indications

* Corresponding author.

SSDI 0021-9673(93)E1294-A

were that the IC procedures would be comparable in both accuracy and precision to the classical titrimetric procedures, but would offer the advantage of being subject to fewer interferences than the titrimetric procedures [10].

After several years of routine use for sulfur and chlorine determinations and after improvements to the initial procedures, IC analyses have been shown to not only completely eliminate all interferences but to also be superior to the titration methods in precision for these elements. The chromatographic procedures can also be readily automated and are easier to implement since operators are required to make no subjective judgements regarding either colorimetric endpoints or the possibility of interferences. The direct comparison of precision between assay types, as well as the exact effect of assay modifications on precision can only be made after studying a wide range of well characterized materials over a long time period. Because samples, extracted from the same set of known standard materials, have been consistently and systematically submitted, blindly, as routine samples to the analysts for many years and the deviations from the expected values which were reported, have been collected and recorded, various procedures and variations of these procedures can be directly compared for the determinations of chlorine and sulfur.

Based on the success of IC for the microanalysis of sulfur and chlorine, extending this same general procedure to the analysis of bromine, fluorine and phosphorus could result in similar improvements in assay performance while simultaneously diminishing the types of procedures run and the equipment required. The extension of these procedures was readily accomplished for bromine but significant obstacles were encountered in the cases of fluorine and phosphorus. Results on these elements will be presented and discussed.

2. Experimental

IC results were generated using Dionex Models 2010i and 2000i chromatographs using the Dionex columns (Dionex, Sunnyvale, CA, USA) indicated in Table 1. All determinations were made at ambient laboratory temperature. All detection was done using the conductivity

Table 1
Chromatographic conditions

	Assay		
	Sulfur/chlorine	Bromine	Fluorine
Column	Dionex AS3 separator column and AG3 guard column	Dionex AS9-SC separator column and AG9-SC guard column	Dionex HPICE AS1 separator column
Mobile phase	30 m*M* $NaHCO_3$ and 2.4 m*M* Na_2CO_3 in water	0.75 m*M* $NaHCO_3$ and 2.0 m*M* Na_2CO_3 in water	0.5 m*M* HCl in water
Flow-rate	2 ml/min	1 ml/min	1 ml/min
Temperature	Ambient	Ambient	Ambient
Injection volume	50 μl	50 μl	50 μl
Combustion solution	0.6% H_2O_2	0.6% H_2O_2	H_2O
Detection	Suppressed conductivity at 100 μS range using a Dionex Anion Micro-Membrane Suppressor (AMMS) with 0.0125 *M* H_2SO_4 as regenerant (regenerant flow-rate = 3 to 4 ml/min)	Suppressed conductivity at 100 μS range using a Dionex Anion Micro-Membrane Suppressor (AMMS) with 0.0125 *M* H_2SO_4 as regenerant (regenerant flow-rate = 3 to 4 ml/min)	Suppressed conductivity at 30 μS range using a Dionex AFS-2 Fiber Suppressor with 5 m*M* tetrabutyl-ammonium hydroxide as regenerant (regenerant flow-rate = 2 ml/min)

detectors incorporated into the Dionex systems. The suppression techniques and the chromatographic conditions used are given in Table 1.

All samples were prepared for chromatographic analysis using Schöniger oxygen flask combustion [11,12]. Sample sizes for combustion were established by targeting for 0.6 mg of sulfur, chlorine or fluorine and 1 mg of bromine and phosphorus, based on the estimated percentage by mass of these particular elements in the sample. The accurately weighed samples were wrapped in ashless combustion paper (A.H. Thomas). Combustion flasks of 1 l (A.H. Thomas, No. 66970-G20) were charged with oxygen and exactly 20 ml of an absorbent solution (see Table 1). These relatively large sample sizes were targeted to minimize the effects of low levels of the analyte elements which can be present in the combustion papers themselves (by far the largest blank, *ca* 5 μg, is observed for chlorine). Following combustion the samples were mechanically shaken for at least 20 min before transfer and analysis.

The instrument response was calibrated using standard solutions. These were prepared from chemically stable non-hygroscopic organic salts. Specifically, a standard solution was prepared by dissolving 936 mg of ephedrine sulfate and 909 mg of lincomycin hydrochloride in two liters of deionized (18 MΩ filtered) water. This solution and a 7:10 dilution of this solution were used as calibration standards. The measured area response was found to be linear over this range and well beyond (both lower and higher concentrations) for both sulfate and chloride.

The instrumental responses obtained were digitized and stored on a Harris computer. All integrations, standard curves, and calculations were completed on the computer using standard software.

The classical sulfur determinations reported were done by quantitatively transferring the contents of the combustion flask to a beaker and titrating with a 0.005 *M* $Ba(ClO_4)_2$ solution. The endpoint was determined by observing the color change produced in a mixture of thorin and methylene blue indicators. The classical results of chlorine reported were obtained by a coulometric titration [13] with Ag^+ after acidifying the contents of the combustion flask with nitric acid. A generating current of 20 mA was used and the endpoint was established by observing the change in potential between a silver indicating electrode and a saturated calomel electrode. Schöniger combustions for these assays were conducted as described above except that a 6% H_2O_2 absorbing solution was used for the sulfur determination and a 0.1 *M* KOH absorbing solution was used for the chlorine determination.

3. Discussion

One means of assessing the performance of a microanalytical procedure is to submit stable, non-hygroscopic samples which are indistinguishable from routine samples and to then tabulate the differences between the reported values and the known values. If the average of these differences is calculated a result of zero should be obtained if the assay is unbiased, while the standard deviation of these differences will give a measure of the precision of the assay. A program of this type has been in place for the evaluation of these assays at Upjohn for many years and the results obtained for sulfur and chlorine are presented for certain time periods. Since the same basic set of reference materials have been used over this entire time frame, it is possible to compare the various assay performances directly with between 30 and 40 blind knowns being submitted for each assay each year.

Reported in Table 2 are the standard deviations, calculated for the differences between the measured and expected values of the sulfur and chlorine blind knowns, as determined by the procedures which were in routine use for various time periods. It should be noted that the average difference from theory was well under 0.1% for all assays in all periods which demonstrates the overall accuracy of each of the methods. The data in Table 2 demonstrate that the precision of the sulfur and chlorine assays during 1961 and over the 1981–1985 period were basically identical. During these time periods, the same titrimetric procedures were being used, with the only significant difference being the person conduct-

Table 2
Standard deviations (wih the number of submissions, n, in parentheses) observed for the differences between the expected and measured values for sulfur and chlorine using a set of knowns which were systematically submitted blindly over different time periods

Time period	Standard deviations (μg)	
	Sulfur	Chlorine
1961	12.9 (43)	10.4 (46)
1981–1985	12.4 (245)	9.2 (260)
1986–1987	9.9 (81)	10.0 (78)
1987–1992	6.4 (237)	5.6 (234)

Sample sizes targeted the presence of 600 μg of the element of interest.

ing the assay. When the routine method of determination was changed to IC in 1986 for both sulfur and chlorine, the assay precision observed was very similar to the classical assays. Although there were no significant improvements in either accuracy or precision, as estimated by results on selected (interference free) materials of known composition, substantial practical benefits were realized from the change in procedure. The most important of these benefits was the complete elimination of chemical or physical interferences which had adversely affected up to 20% of these determinations using the titrimetric procedures.

Although the precision obtained using the chromatographic analysis was at least as good as had been obtained using the titrimetric procedures, the relative deviations on the order of 1.5%, which were observed for the blind knowns, was significantly greater than the 0.6% relative standard deviation obtained for peak areas upon reanalysis of samples. This difference in variability indicates that the assays are not performing at the limit of the chromatographic capabilities of the equipment and that improvements in sample preparation or assay calibration might result in improved results.

Unlike the titrimetric procedures, which relied on quantitative transfers, the chromatographic analysis determines concentration and thus relies on absolute volumetric accuracy. Of particular importance is the ratio of the volume of adsorbent solution delivered to the combustion flask and the volume of the glassware used to prepare the standard solutions which are used daily for calibration. Any actual difference in the ratio of these two volumes would produce a systematic bias in the results, while any variability in this ratio (temperature effects, etc.) would appear as assay variability. In an effort to reduce uncertainty related to volumetric variability, an automatic burette (Metrohm Herisau Model E 415), instead of a pipette, is used to deliver the adsorbent solution to the Schöniger flask.

The incorporation of standards, combusted using the same procedure as the samples, among the routine, service samples, provides an additional means of evaluating assay performance. It should be noted that these standards are not the materials which are systematically submitted to the analyst blindly but are in fact knowingly prepared by the analyst. Monitoring assay behavior, both within day (a single series of determinations) and between days, using these combusted standards, could be useful in characterizing the nature of assay variability observed and thus improving overall assay performance. An assay monitoring program of this type was implemented for sulfur–chlorine determinations by routinely inserting combusted samples of lincomycin hydrochloride (S = 6.95%; Cl = 7.69%) every fifth sample during the determinations of sulfur and chlorine (sulfur and chlorine determinations are always made during a single chromatographic series). Dividing the theoretical value of sulfur or chlorine by the corresponding experimental result for the standard sample, using the calibration obtained from stock solutions of dissolved standards, yields a ratio (R) whose magnitude is related to assay accuracy and precision. The variation observed in R is directly influenced by sources of variation in the assays and therefore related to assay performance.

In an effort to separate sample preparation (handling) variations from chromatographic (in-

strumental) variations, variations in R were determined both within and between standard samples during a single chromatographic analysis period by preparing multiple combusted standard samples and running them more than once during the period (usually once early and once late in the run). The results obtained for the within day variations in R for the January through June (1993) time period are given in Table 3, and indicate essentially the same variability for the within-sample and between-sample variation over this time period. Because these variations are essentially the same, the sample weighing and combustion process do not appear to add significant variability to the assay.

The between-day variability of the assays is established by determining the standard deviations of the daily mean values of $R(R^*)$. R^* values were calculated by averaging all values of R determined during the course of running a single sample set, including both the determinations on separate combusted standards (typically 5 per day) and repeats of these standards (typically 3 per day). The variations found in these values are given in Table 3 for both sulfur and chlorine. The magnitude of these deviations correspond to relative standard deviations of 0.44% for sulfur and 0.54% for chlorine. The average values of the R^* values over the January through June time period was 0.96 for sulfur and 0.97 for chlorine. Both the within-day variability (R) and the between-day variability (R^*) will contribute to the overall variability of the assay as reflected by the data in Table 2.

Since both sulfate and chloride were present in both the stock standard solutions used and in the material (lincomycin hydrochloride) used as a combusted standard, it is possible to directly compare the variations observed in R^* values determined for each element. One means of making this comparison would be to plot the difference between the R^* of sulfur on a given day with the value of R^* on the preceding day *versus* the corresponding differences observed in the chlorine R^* values. This comparison is made in Fig. 1. Based on the manner in which these data scatter around a line of unit slope, passing through the origin, a correlation between changes in the sulfur ratio and chlorine ratios must exist. A systematic bias is, therefore, present and the variability reflected in R^* is not completely random. Although the exact nature of this systematic bias has not been explicitly defined, and may be complex, it is clear that, if the (daily) assay bias which is represented by the correlation of the variations in Fig. 1 could be eliminated, overall assay performance should be significantly improved.

A simple means of approximating this correction would be to use the daily average, R^*, as a correction factor for the elemental composition, $\%X$, determined using the standard solution calibrations as shown in Eq. 1.

$$\%X_{\text{corrected}} = R^* \cdot \%X_{\text{measured}} \quad (1)$$

When the effects of daily biases are removed from the experimental values of elemental composition, using Eq. 1, a substantial improvement in assay performance can be demonstrated as shown in Table 2 for the 1987–1992 time period. The variability of the assay results,

Table 3
Standard deviations determined based on a sample size of 600 μg with n, the number of determinations, in parentheses

Element	Standard deviation (μg)		
	R value within-day		Between-day R^*
	Within sample	Between samples	
Sulfur	5.4 (111)	4.9 (213)	2.8 (37)
Chlorine	3.1 (111)	4.4 (213)	3.1 (37)
Bromine	5.5 (42)	5.6 (86)	

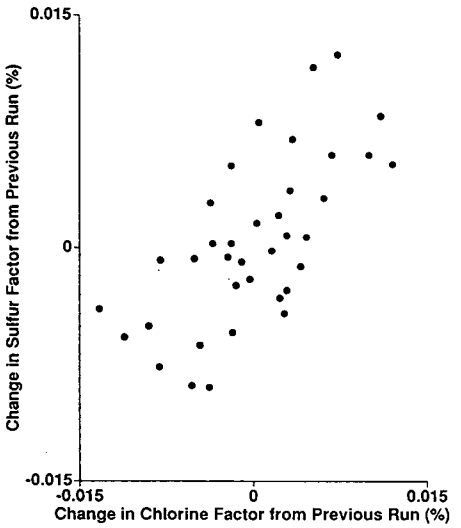

Fig. 1. Change from the previous value observed in R^* determined for sulfur plotted *versus* the corresponding change observed for chlorine.

determined using a wide range of sample types and over a long time period, are now more nearly comparable to the chromatographic precision available from our instrumentation.

Because of the excellent microanalytical results produced by the IC technique for sulfur and chlorine, extending this procedure to other hetero-atomic species such as bromine, fluorine and phosphorus would be desirable. This could potentially lead to improvements in the accuracy and precision of these determinations, as well as require the maintenance and support of only one overall assay procedure for all of these elements. This generalization of the procedure was first attempted for bromine determinations. The chromatographic conditions used for the bromine assay are given in Table 1. An example of the chromatogram obtained for a sample containing chlorine, nitrogen, bromine and sulfur is shown in Fig. 2. Unlike the more common titration assays, it is clear from Fig. 2 that no significant inferences from chlorine in the sample should be expected. The major problem encountered with this assay, after several years of routine use, is degradation in column performance leading to incomplete resolution of the bromide and nitrate peaks. This is a significant

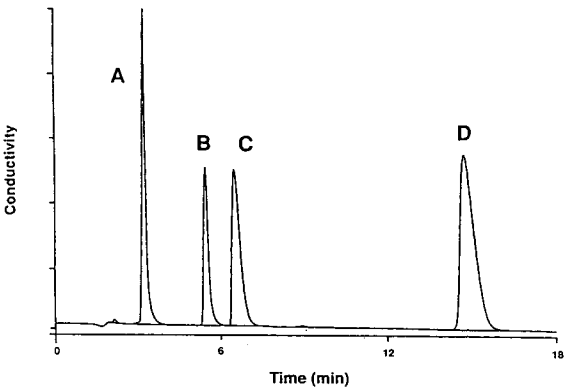

Fig. 2. Chromatogram of a combustion solution containing chloride (A), bromide (B), nitrate (C) and sulfate (D) ions which was obtained using the chromatographic system developed for bromine analysis.

problem because nitrate will be present in all samples analyzed and, at the level of accuracy and precision expected from this determination, anything less than complete baseline resolution of these peaks degrades assay performance. Column lifetimes are limited to around a thousand samples because of this problem.

The performance of the chromatographic assay, on a set of standard materials is presented in Table 4. Also presented in Table 4 are the results reported on these samples by well known external laboratories. In the case of the chlorine containing samples, only one lab indicated the ability to analyze bromine in the presence of chlorine. The sample sent to the laboratory, which indicated the ability to determine bromine in the presence of chlorine, was clearly marked as containing chlorine when submitted. Although the results reported in Table 4 represent a one time event to compare laboratories, they are representative of our experience with outside determinations of bromine.

Fluorine is another example of an element for which microanalytical results from outside sources are often less than satisfactory. The IC analysis of fluoride ion was also found to give good precision for both dissolved standards (R.S.D. = 0.95%) and combusted standards (R.S.D. = 1.5%). The chromatographic system used for fluoride determination is given in Table 1 and is based on an ion-exclusion column for

Table 4
Results obtained by various labs on bromine standards

Expected result (%)	IC result (%)	Result (%)		
		Laboratory 1	Laboratory 2	Laboratory 3
37.33	37.36	37.79	34.38	37.99
21.39[a]	21.01	43.49	NR[b]	NR
18.11	18.05	18.33	17.58	17.67
20.06	20.04	NR	20.52	20.44
20.56[a]	20.48	39.65	NR	NR

[a] Sample contained chlorine and was labelled as such.
[b] NR = Not run.

weak acids, since insufficient retention of fluoride ion is obtained on typical anion columns.

Although the assay precision obtained for fluoride ion appeared good, the data obtained on combusted materials indicated the presence of a significant bias in the assay. The results in Table 5 were generated by using dissolved fluorine standards for calibration. The negative bias was always observed when samples were combusted and indicates that there is a significant recovery problem associated with the Schöniger combustion. The recovery problem for fluoride following sample combustion in a Schöniger flask has been reported earlier [14]. The elimination of borosilicate glass in the combustion flask through the use of plastic combustion flasks did not eliminate the recovery problems as was indicated in some publications [15,16]. Because the source and nature of this assay bias remains unexplained, the chromatographic determination of fluorine has not been implemented as a routine assay.

Another element for which sample combustion problems complicate the analysis is phosphorus. In this case it is well known that many different phosphorus species are formed. For the purpose of analysis by IC, the most desirable form would be orthophosphate since this species could be analyzed using the same chromatographic system used for bromine. In addition to orthophosphate, however, substantial levels of pyrophosphate, tripolyphosphate and, sometimes, tetrapolyphosphate are formed. Fig. 3 illustrates the

Table 5
Results obtained on combusted fluorine standards using dissolved standards to quantify the ion chromatographic response

Sample	F (μg)		
	Expected	Found	Difference
1	596	549	−47
2	621	584	−57
3	583	538	−45
4	662	615	−47
5	614	581	−33
1	596	555	−41
2	621	576	−45
3	583	537	−46

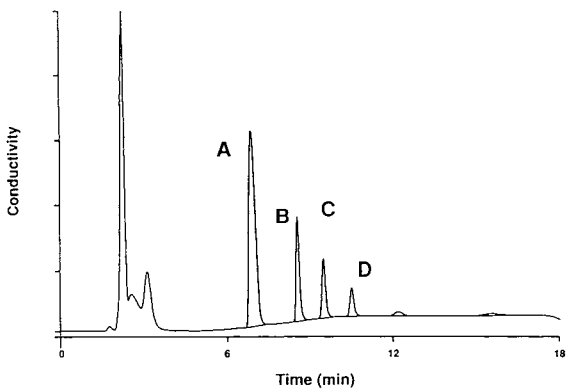

Fig. 3. Gradient chromatogram showing the presence of orthophosphate (A), pyrophosphate (B), tripolyphosphate (C), tetrapolyphosphate (D), etc. in the absorbent solution from a Schöniger combustion of a phosphorus-containing sample.

various phosphorus-containing species produced during the combustion of a phosphorous containing sample. The gradient conditions described in ref. 17 were used to produce the chromatogram in Fig. 3. Although chemical procedures for converting all forms of phosphorus to orthophosphate have been developed and widely applied, they involve refluxing the sample after addition of strong acid. In addition to adding a major interference to the anion chromatogram, procedures of this type are labor intensive and are not ideal for concentration determinations. Recently enzymatic procedures, that require no refluxing, have been developed in our laboratory which will completely convert all phosphorus species, generated in a Schöniger combustion, to orthophosphate. Since the cost of the enzymes is negligible (cents per sample) and since they can be readily obtained, this procedure appears to form the basis for a future IC micro-determination for phosphorous.

4. References

[1] J.F. Alicino, A.I. Cohen and M.E. Everhard, in I.M. Kolthoff and P.J. Elving (Editors), *Treatise on Analytical Chemistry*, Part II, Section B-1, Vol. 12, Wiley, New York, 1965, p. 57.
[2] J.S. Fritz and M.Q. Freeland, *Anal. Chem.*, 26 (1954) 1593.
[3] E.C. Olson, in I.M. Kolthoff and P.J. Elving (Editors), *Treatise on Analytical Chemistry*, Part II, Section B-1, Vol. 14, Wiley, New York, 1971, p. 1.
[4] J.S. Fritz and S.S. Yamamura, *Anal. Chem.*, 27 (1955) 1461.
[5] J.S. Fritz, S.S. Yamamura and M.J. Richard, *Anal. Chem.*, 29 (1957) 158.
[6] H. Small, T.S. Stevens and W.C. Bauman, *Anal. Chem.*, 47 (1975) 1801.
[7] J.F. Colaruotolo and R.S. Eddy, *Anal. Chem.*, 49 (1977) 824.
[8] F. Smith, Jr., A. McMurtrie and H. Galbraith, *Microchem. J.*, 22 (1977) 45.
[9] C. Wang and J.G. Tarter, *Anal. Chem.*, 55 (1983) 1775.
[10] J.R. Kreling, F. Block, G.T. Louthan and J. DeZwaan, *Microchem. J.*, 34 (1986) 158.
[11] W. Schöniger, *Microchim. Acta*, (1955) 123.
[12] W. Schöniger, *Microchim. Acta*, (1956) 869.
[13] E.C. Olson and A.F. Krivis, *Microchem. J.*, 4 (1960) 181.
[14] A. Steyermark, *Microchem. J.*, 3 (1959) 399.
[15] R.N. Rogers and S.K. Yasuda, *Anal. Chem.*, 31 (1959) 616.
[16] E.C. Olson and S.R. Shaw, *Microchem. J.*, 5 (1961) 101.
[17] *Ion Chromatography Cookbook*, Dionex Corporation, Sunnyvale, CA, 1987, Ch. II, p. 5.

ELSEVIER

Journal of Chromatography A, 671 (1994) 303–308

JOURNAL OF CHROMATOGRAPHY A

Use of ion chromatography for the verification of drug authenticity

Lisa A. Kaine*, Douglas T. Heitkemper, David S. Jackson, Karen A. Wolnik

National Forensic Chemistry Center, US Food and Drug Administration, 1141 Central Parkway, Cincinnati, OH 45202, USA

Abstract

Investigations of drug authenticity focus on both bulk drugs and finished products. Excipients and contaminants from manufacturing processes may be used as "chemical fingerprints" to track drug sources. This paper describes the ion chromatographic determination of sodium lauryl sulfate, chloride, phosphate and citrate in drug formulations as applied to drug authenticity cases.

1. Introduction

In recent years, the quality and authenticity of drugs, especially generics, have come under intense public scrutiny. The Food and Drug Administration (FDA) has legal and scientific processes, such as the New Drug Application (NDA) and Abbreviated New Drug Application (ANDA), by which it approves new and generic drugs. However, the agency must ensure that drugs are produced only by approved manufacturers, and that the formulations and processes which have been approved are followed.

Methodology to detect contaminants in drugs is necessary for investigations of authenticity. Analysis of contaminants in bulk drugs may be used as a "chemical fingerprint" to track bulk drugs since various manufacturing processes may contribute characteristic residual chemicals to the fingerprint. Several investigators have used analysis of contaminants to distinguish between samples: Neumann and Gloger [1] utilized capillary gas chromatography for the analysis of impurities in heroin, and Wolnik *et al.* [2] used inductively coupled plasma–optical emission spectroscopy to distinguish between manufacturers of cyanide in Tylenol tamperings.

Investigations of authenticity may also focus on finished products. Manufacturing processes use distinct excipients: buffers such as phosphate and citrate in injectables, fillers such as mannitol, sorbitol, dibasic calcium phosphate, calcium sulfate and lactose, and lubricating agents such as sodium lauryl sulfate in tablets [3]. The absence or presence of various excipients may indicate deviations from approved formulations and/or processes, or counterfeit products.

Ion chromatography is an important analytical technique in forensic investigations of drug authenticity. In this paper, two cases in which ion chromatography was used to discrimin-

* Corresponding author.

SSDI 0021-9673(94)00012-X

ate between investigative samples will be discussed.

2. Experimental

2.1. Apparatus

The instrumentation used included a Dionex (Dionex, Sunnyvale, CA, USA) 4500 ion chromatograph with gradient pump, Rheodyne Model 9126 injector (10-μl loop), pulsed electrochemical detector in the conductivity mode, automated sampler module, and AI-450 software program for data collection and calculation. The column used was a Dionex Omnipac PAX-500, 250 × 4 mm and the suppressor was an Anion Micromembrane Suppressor (AMMS) II, also from Dionex.

2.2. Reagents, standards and samples

Water used in these studies was purified using a Millipore (Bedford, MA, USA) Milli-Q system. Eluents were prepared from 50% (w/w) aqueous sodium hydroxide, Optima-grade methanol and acetonitrile (Fisher Scientific, Fair Lawn, NJ, USA). Standards were prepared with sodium lauryl sulfate and citric acid monohydrate (Sigma, St. Louis, MO, USA) and certified ion chromatography anion standard mixture (Dionex).

Sodium lauryl sulfate (SLS) stock standard was prepared from SLS dissolved in methanol. Working standards were prepared by appropriate dilutions of the stock with methanol. All other standards were prepared in distilled deionized water (DDW).

Tablet coatings were physically removed by scraping or peeling. The remainder of each tablet was reduced to powder and three tablets composited together. Three portions of each composite were accurately weighed and extracted with methanol, then filtered through 0.2-μm nylon 66 syringe filters. All other samples were diluted with DDW and filtered through 0.2-μm nylon 66 syringe filters.

3. Results and discussion

3.1. Sodium lauryl sulfate in generic human drug case

Before new drug formulations are marketed, extensive testing is required to prove both efficacy and safety. Generics, however, require less testing since the innovator has already characterized the active drug. Manufacturers must document manufacturing processes, and manufacturers of generics must also submit finished product from pilot batches for bioequivalence testing. Any formulation differences which exist between the innovator and generic product must not affect the bioavailability and safety of the drug.

Excipients include all of the ingredients in a finished product other than the active ingredient. Many types of excipients are used including binders, fillers, disintegrating agents, lubricants, flavors and sweetening agents [3]. Excipients can affect the disintegration rates of tablets and the bioavailability of water-soluble drugs. As such, changes in the manufacturing process are not allowed after a drug has been approved unless an amendment to the manufacturer's application is approved.

Suspicions arose from investigative information that a manufacturer's lot submitted for bioequivalence testing (the biolot) was not produced by the same formulation as the marketed product. Tablets can be prepared by three different methods: wet granulation in which ingredients are mixed in a slurry, dry granulation which involves the compaction of powders at high pressure, and direct compression [3]. Each of the methods has both advantages and disadvantages. It was suspected that SLS, a lubricant, was used in the formulation of the marketed product, but not in the biolot formulation. Tablets were analyzed for SLS to determine if the biolot and production lots were the same.

An existing method for the analysis of linear alkyl sulfates in surfactants by ion chromatography was used to quantitatively determine SLS [4]. Gradient conditions are listed with Fig. 1. The tablets in question were also analyzed concurrently at FDA Division of Drug Analysis

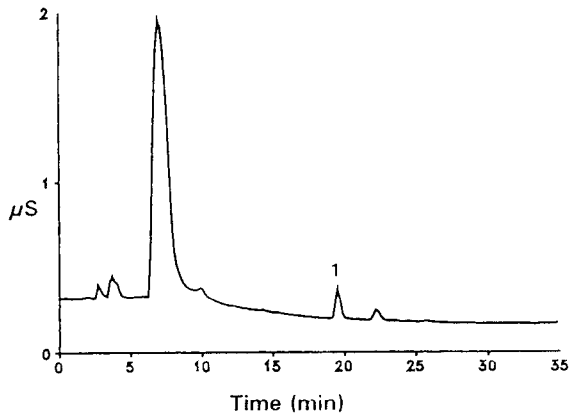

Fig. 1. Determination of sodium lauryl sulfate in a tablet. Peak 1 = SLS. Column: Omnipac PAX-500; flow-rate: 1.0 ml/min. Gradient program: eluent 1: 18 MΩ water; eluent 2: acetonitrile–water (90:10); eluent 3: 200 m*M* NaOH; eluent 4: methanol–water (45:55). Suppressor: AMMS-II; regenerant: 12.5 m*M* sulfuric acid at 10 ml/min.

Time (min)	Eluent 1 (%)	Eluent 2 (%)	Eluent 3 (%)	Eluent 4 (%)
0.0	80	0	10	10
20.0	30	50	10	10
40.0	10	70	10	10
50.0	10	70	10	10
50.1	80	0	10	10
60.0	80	0	10	10

using a modification of a US Pharmacopeia method [5]. SLS was converted to lauryl alcohol and determined in that form by GC–MS. SLS was positively identified by GC–MS in all samples except for the biolot, but was not quantitated.

Calibration curves of SLS prepared in methanol were linear in the range studied (20–200 μg/ml) with a slope of 27 527 area response counts per μg/ml, *y*-intercept −189 428 area response counts, and correlation coefficient equal to 0.9995. Repeatability of response and retention time were 3.1 and 0.8% relative standard deviation, respectively. A limit of detection (LOD) was not calculated statistically due to the slope of the baseline but was defined as the lowest concentration of standard for which a definitive peak was observed. Solution LOD was 2 μg/ml, equivalent to a LOD in the tablets studied of 40 μg SLS per gram tablet.

The SLS determined in several lots of the tablet in question from the same manufacturer are presented in Table 1. Three samples were weighed and extracted from each lot (four from lot C). The amount of active drug in the tablets (5 mg *versus* 10 mg) did not affect the analysis of SLS. Spike recoveries were performed to determine the effectiveness of the methanol extraction. Although SLS is soluble in water [6], no SLS was detected in the aqueous extracts of the tablets. The SLS concentration was 0.3 m*M* in the aqueous extracts, which is below the critical concentration for micellar formation. Perhaps the interaction of SLS with the other ingredients in the tablet prevented extraction with water. The percent recovery from methanol was very dependent upon the method of spike preparation. The first method consisted of adding 2.2 mg SLS to 0.4 g of composited tablet. A 0.05-g portion of the spiked sample was extracted with 2 ml of methanol. The sample was then filtered and injected onto the Omnipac column. Recovery of SLS through this procedure was only an average of 60%. The second method, however, had an average spike recovery of 92%. In this method, 1.1 mg SLS was added to a smaller portion of composited tablet (0.2 g), but the entire spiked sample was extracted with 5 ml of

Table 1
Concentration of sodium lauryl sulfate in drug tablets

Lot[a]	10 mg active μg SLS/g tablet	Lot	5 mg active μg SLS/g tablet
A	2396	D	2960
	2229		3092
	2352		2923
B	3093		
	3374		
	2864		
C	2984		
	3008		
	2831		
	2911		

[a] Three to four samples prepared per lot.

methanol. This extract was then diluted 1:1 with methanol and filtered through a nylon 66 filter. It is suspected that the poor recovery of the first spike method was due to incomplete mixing of the SLS with the sample. Since the entire sample was extracted in the second method, there were no homogeneity problems. The distribution of SLS in the finished tablets from the manufacturer was homogeneous since the percent relative standard deviation between multiple samplings of each lot range from 2.7 to 8.2% R.S.D.

No SLS was detected, either by ion chromatography or GC–MS, in the lot submitted for bioequivalency testing. However, SLS was determined by ion chromatography at an average level of 2584 μg/g tablet in the finished product. The limit of detection for SLS in the tablet was 65 times greater than the level of SLS declared. It was concluded from this information, in conjunction with other chemical analyses and investigative information, that the biolot was not produced by the same formulation as the marketed product. Although the presence or absence of SLS, an approved excipient in drugs, may not seem to be a major issue, it is very important that manufacturers follow the master formulations which have been approved by FDA and tested for bioequivalency.

3.2. Anions in veterinary drug case

It was evident from the very first analysis in the following case, that fraud was involved. The sample, a liquid veterinary drug, did not contain the active drug which was declared on the label. However, the details of the operation were not as evident and ion chromatography proved to be a valuable technique in piecing together the details.

The suspect samples contained a different active ingredient which is used to treat the same medical condition as the falsely declared drug. The substitute drug, however, is less expensive, and not as potent as the labeled drug. The motive for fraud became clear. Package the cheaper drug as the more expensive labeled drug and a greater profit will be made. If the counterfeiter had not put any active ingredient in his product, the scam would have quickly failed. In order to make a stronger legal case, it was important to find the source of material in the counterfeit containers.

The substitute drug is available as either the hydrochloride or the phosphate salt. Using this information, three sets of samples were analyzed on an Omnipac Pax-500 column. The solvent resistance of this column was necessary in order to minimize sample preparation and possible damage the organic drug might do to an ion chromatography column. Samples were diluted sufficiently that filtration was the only sample pretreatment necessary. The column was cleaned with 90% aqueous acetonitrile. The three sets of samples consisted of: legitimate substitute drug from a manufacturer who had sold product to the suspect distributors, samples confiscated from warehouses, and suspect samples confiscated from dealers.

Fig. 2 illustrates the separation of chloride, sulfate, phosphate and citrate in a suspect sample. Calibration curves were linear (correlation coefficients >0.9990) in the ranges studied (Cl^- 0.7–30 μg/ml; PO_4^{3-} 3–155 μg/ml; citrate 5–50 μg/ml). Plots were constructed comparing chloride concentration *versus* the concentration (expressed in molarity) of substitute drug (refer to Fig. 3); phosphate concentration *versus* the con-

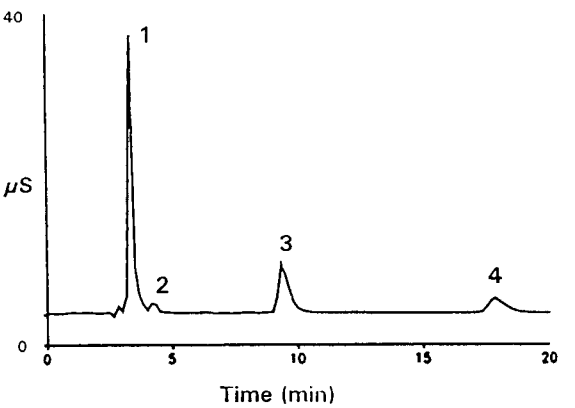

Fig. 2. Separation of anions in a veterinary drug on the Omnipac PAX-500 column. Eluent: 40 m*M* NaOH–5% methanol; flow-rate: 1.0 ml/min; suppressor: AMMS-II; regenerant: 12.5 m*M* sulfuric acid at 5 ml/min. Peaks: 1 = chloride; 2 = sulfate; 3 = phosphate; 4 = citrate.

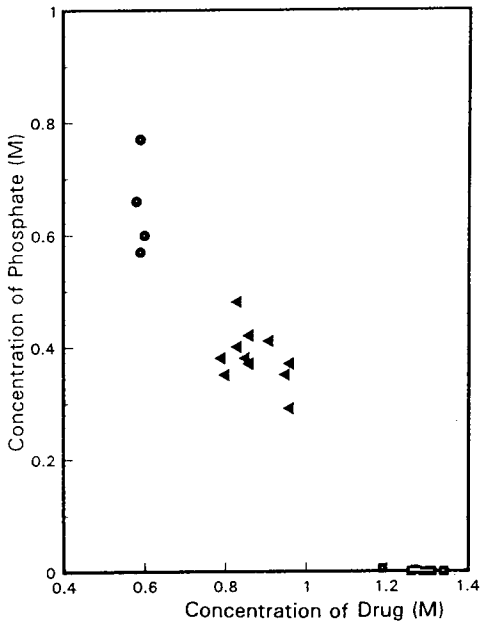

Fig. 3. Veterinary drug: molarity of phosphate plotted against molarity of substitute drug for three sets of samples. ● = Legitimate; ◀ = suspect; ■ = warehouse.

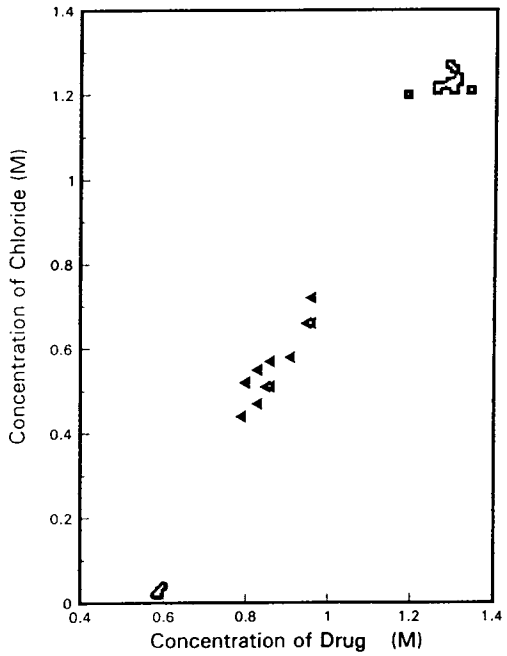

Fig. 4. Veterinary drug: molarity of chloride plotted against molarity of substitute drug for three sets of samples. Symbols as in Fig. 3.

centration of substitute drug (refer to Fig. 4); and citrate concentration *versus* the concentration of substitute drug (refer to Fig. 5). Citrate is a commonly used buffer in certain veterinary drugs. In each of the plots a trend was noted: the data divided into three distinct groups well separated from each other. The legitimate product had equimolar phosphate and active (of substitute drug) concentration, no chloride and the highest level of citrate. Samples seized from warehouses, however, all had low phosphate and citrate, but had equimolar substitute drug and chloride levels. Suspect samples packaged as the more expensive drug all had levels of phosphate, citrate, chloride and substitute drug which were in between the legitimate substitute drug and warehouse samples. The suspect samples were mislabeled, since they contained none of that active ingredient, however, they also contained counterfeit substitute product.

Legitimate product contained approximately 0.6 *M* substitute drug in the phosphate form and 0.2 *M* citrate, while the warehouse samples

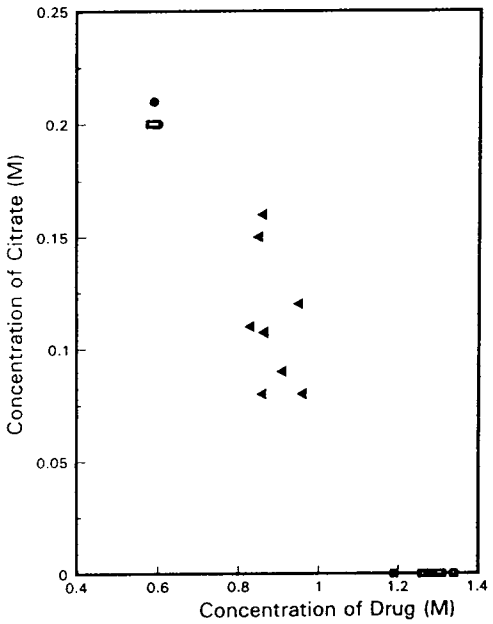

Fig. 5. Veterinary drug: molarity of citrate plotted against molarity of substitute drug for three sets of samples. Symbols as in Fig. 3.

Table 2
Comparison of chloride, phosphate, citrate and substitute drug concentrations in veterinary drug samples

Sample	Cl^- (*M*)	PO_4^{3-} (*M*)	Substitute drug (*M*)	Citrate (*M*)
Legitimate[a]	ND[b]	0.6	0.6	0.2
Warehouse[c]	1.2	ND	1.2	ND
Legitimate/2[d]	ND	0.3	0.3	0.1
Warehouse/2[d]	0.6	ND	0.6	ND
Legitimate + warehouse 1:1	0.6	0.3	0.9	0.1
Suspects[e]	0.6	0.4	0.9	0.1

[a] Average of four samples
[b] ND = Not detected.
[c] Average of fifteen samples.
[d] For purposes of explanation, concentrations of legitimate or warehouse were divided by two.
[e] Average of eleven samples.

contained the drug in the hydrochloride form (1.2 *M*) only. On average, the suspects contained 0.9 *M* substitute drug, 0.4 *M* phosphate, 0.6 *M* chloride and 0.1 *M* citrate. The suspect samples had the same concentrations as if the legitimate material and warehouse samples had been mixed one to one (refer to Table 2). Based upon the described plots, as well as packaging, investigative information, and results of other chemical analyses, the following conclusion was made. Suspects were adding warehouse material to legitimate substitute drug to increase its potency, then packaging it as the more expensive drug.

4. Conclusions

Most drug manufacturers adhere to the law and follow good manufacturing practices. However, counterfeit and unscrupulous manufacturers do exist. In order to ensure that drugs are produced only by approved manufacturers and with approved formulations, our analyses must become more and more sophisticated. The utility of ion chromatography was demonstrated in two cases by the analysis of sodium lauryl sulfate, chloride, phosphate and citrate.

5. Acknowledgements

Thanks to Lorrie Lin, National Forensic Chemistry Center (NFCC), for the HPLC analyses of active ingredients, Thomas Bruggemeyer, NFCC, for statistical analysis, and B.J. Westenberger of Division of Drug Analysis, FDA, St. Louis, MO, USA for the GC–MS analysis of SLS.

References

[1] H. Neumann and M. Gloger, *Chromatographia*, 16 (1982) 261–264.
[2] K.A. Wolnik, F.L. Fricke, E. Bonnin, C.M. Gaston and R.D. Satzger, *Anal. Chem.*, 56 (1984) 466A–470A.
[3] *United States Pharmocopeia XXII, The National Formulary NF XVII*, United States Pharmocopeia Convention, Rockville, MD, 1989, pp. 1696–1697.
[4] R.W. Slingsby and M.A. Rey, *Omnipac Guidebook: Methods Development and Troubleshooting*, Dionex, Sunnyvale, CA, 1991, p. 64.
[5] *United States Pharmocopeia XXII, The National Formulary NF XVII*, United States Pharmocopeia Convention, Rockville, MD, 1989, pp. 1980–1981.
[6] *Handbook of Pharmaceutical Excipients*, American Pharmaceutical Association, Washington, DC, 1986, pp. 271–272.

ELSEVIER

Journal of Chromatography A, 671 (1994) 309–313

JOURNAL OF CHROMATOGRAPHY A

Determination of haloacetic acids by ion chromatography

Lakshmy M. Nair*, Raaidah Saari-Nordhaus, James M. Anderson, Jr.

Alltech Associates, Inc., 2051 Waukegan Road, Deerfield, IL 60015, USA

Abstract

Two ion chromatography methods for the determination of haloacetic acids are described in this paper. The first method is based on anion-exchange separation with suppressed electrical conductivity detection. The second method is based on anion-exclusion separation with UV detection. Both methods are simple and fast. The detection limits for the haloacetic acids are in the μg/l range. Applications of these methods for the determination of haloacetic acids in some real world samples are shown.

1. Introduction

Haloacetic acids are present in many samples due to their use in various industrial applications. Trace amounts of these acids are found in drinking water as chlorination by-products. Mono-, di- and trichloroacetic acids are used as base materials for colorant manufacturing, pharmaceutical synthesis and antiseptics, respectively. Trichloroacetic acid is also used as a herbicide and as an important intermediate in chemical industry. Trifluoroacetic acid is used to cleave peptides from solid-phase resins in peptide synthesis. Many haloacetic acids are toxic and having reliable methods for their determination is very important.

The standard method for determining halogenated acetic acids is by liquid–liquid extraction and gas chromatography (GC) with electron-capture detection. This method is described in US EPA method 552 [1] and is applicable to the determination of six halogenated acetic acids in drinking water, ground water and raw water. Even though the detection limits for the acids are in the low μg/l range, this method is complicated and time consuming. Determination of acetic, dichloroacetic and trichloroacetic acids by high-performance liquid chromatography (HPLC) has also been reported [2]. The method is based on ion-interaction separation with UV detection at 210 nm. Separation of mono-, di- and trichloroacetic acid by ion-exchange chromatography was reported by Houdeau *et al.* [3]. A silica-based anion exchanger was used for the separation, combined with refractive index detection.

Two ion chromatography (IC) methods are described in this paper for the determination of haloacetic acids. The first method is based on anion exchange separation with suppressed electrical conductivity detection. The second method is based on anion exclusion separation with UV detection. IC is one of the fastest growing analytical techniques for the determination of ionic species. It offers simple, reliable and inexpensive means for the simultaneous separation and determination of inorganic and organic ions in complex mixtures. Both IC methods described

* Corresponding author.

0021-9673/94/$07.00
SSDI 0021-9673(93)E1138-P

here are fast and simple. The detection limits are in the μg/l range. Sample preparation for IC analysis is less time consuming than the GC technique and the instrumentation is simple. However, the detection limits for haloacetic acids by GC method are much lower than the methods described here.

2. Experimental

Anion chromatography was performed on an Alltech (Deerfield, IL, USA) ion chromatography system that consists of a Model 325 HPLC pump, a Model 335 suppressor module, and a Model 320 conductivity detector. A Rheodyne (Cotati, CA, USA) Model 9125 injection valve was used to introduce the sample. For anion-exclusion chromatography, the same HPLC pump and injector were used along with an Alltech Model 330 column heater and a Linear (Linear Instruments, Reno, NV, USA) Model 204 UV–VIS detector. The temperature of the column heater was maintained at 35°C. All data were recorded on a Spectra-Physics (Santa Clara, CA, USA) SP 4400 Chromjet integrator.

The Alltech Universal Anion 300 Column (150 mm × 4.6 mm) was used to separate the halo-acids by anion-exchange chromatography. For the ion-exclusion method, a Wescan (Alltech) Anion Exclusion Column (300 mm × 7.8 mm) was used. All reagents and standards were prepared from reagent-grade chemicals (Aldrich, Milwaukee, WI, USA) and distilled deionized water.

3. Results and discussion

3.1. Ion-exchange method

A suppressor-based IC method [4] is used for the separation of haloacetic acids by ion exchange. The haloacetic acids are separated on an anion-exchange column with a basic sodium carbonate–hydrogencarbonate eluent. The column effluent flows to a suppressor device before entering the conductivity detector. The suppressor exchanges the cations from the eluent and sample for hydronium ions forming carbonic acid (low conductivity) and fully protonated haloacetic acids (high conductivity). This results in a decrease in conductivity for the eluent and an increase in conductivity for the sample ions. Over all detection sensitivity for the anions is improved considerably [4]. Various suppressor devices are available. The method described here uses an Alltech Solid Phase Chemical Suppressor (SPCS) [5]. The SPCS consists of a suppressor module which houses a 10-port switching valve and two disposable cartridges. The cartridges are packed with specially treated sulfonated polystyrene–divinylbenzene cation-exchange resin in the hydrogen form. The SPCS is connected between the analytical column and the conductivity detector. The flow diagram of the SPCS is shown in Fig. 1. The eluent from the analytical column flows through one cartridge at a time. While one cartridge is being used, the effluent from the detector flows through the other cartridge to pre-equilibrate the cartridge. This reduces the baseline shift due to conductance change when the valve is switched.

Fig. 2 shows the anion-exchange separation of acetic, monochloroacetic (MCA), dichloroacetic (DCA) and trichloroacetic (TCA) acids. The acids are separated on a hydroxyethyl methacrylate based anion-exchange stationary phase with sodium carbonate–hydrogencarbonate eluent. Carbonate–hydrogencarbonate eluent seems to be the best counter ion for the separation since TCA has high affinity toward the stationary phase. When sodium tetraborate or

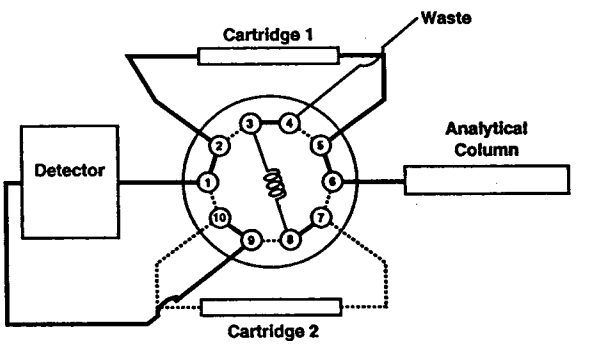

Fig. 1. Flow diagram of the SPCS system.

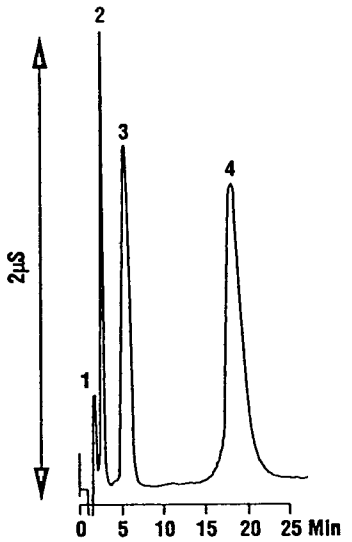

Fig. 2. Separation of chloroacetic acids by anion exchange. Peaks: 1 = acetate (10 mg/l); 2 = monochloroacetate (10 mg/l); 3 = dichloroacetate (20 mg/l); 4 = trichloroacetate (20 mg/l). Column: Universal Anion 300 (150 mm × 4.6 mm). Eluent: 2.2 m*M* sodium carbonate–2.8 m*M* sodium hydrogencarbonate. Flow-rate: 2 ml/min. Detector: conductivity. Injection volume: 100 μl.

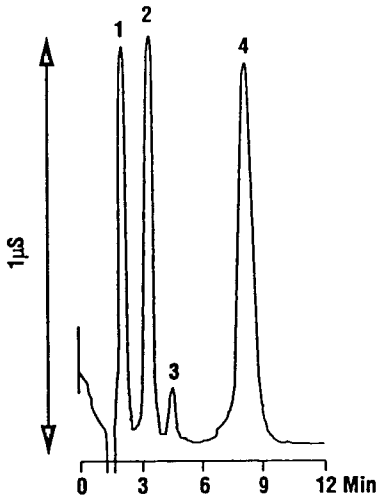

Fig. 3. Separation of bromoacetic acids by anion exchange. Peaks: 1 = acetate (10 mg/l); 2 = bromoacetate (10 mg/l); 3 = chloride; 4 = dibromoacetate (10 mg/l). Column: Universal Anion 300 (150 mm × 4.6 mm). Eluent: 2.2 m*M* sodium carbonate–2.8 m*M* sodium hydrogencarbonate. Flow-rate: 2 ml/min. Detector: conductivity. Injection volume: 100 μl.

sodium hydroxide eluent (common eluents used with suppressor-based IC) were used for this separation, DCA and TCA were retained on the column too long. Three chloroacetic acids along with acetic acid are separated within 18 min with excellent resolution and sensitivity by carbonate–hydrogencarbonate eluent. The same method can be used for the separation of acetic, monobromoacetic (MBA), dibromoacetic (DBA) acid and trifluoroacetic (TFA) acids. Fig. 3 shows the separation of monobromoacetic acid and dibromoacetic acid. If both chloro and bromo acids are present in the same sample, bromoacetic acid may co-elute with monochloroacetic acid. Other anions are well resolved from each other. The resolution can be modified easily by either changing the concentration of the eluent or the length of the column.

3.2. Ion-exclusion method

Ion exclusion is commonly used to separate weakly ionized anions such as carboxylic acids, organic acids and weak acid anions. Ion-exclusion mechanisms are based on the separation of molecular compounds by differences in partitioning between the interstitial mobile phase (usually water) and the stagnant mobile phase within the pores of the resin [6]. A strong inorganic acid eluent combined with a sulfonated cation-exchange column is normally used for the separation. Both conductivity and UV detection have been used. The method developed here uses phosphoric acid eluent with UV detection at 210 nm. UV detection was chosen due to high conductivity of the phosphoric acid eluent. The sample acids are detected with lower sensitivity with conductivity detection. Other eluents such as dilute sulfuric acid or nitric acid were also tried for the separation. These eluents are found to be inappropriate for haloacetic acid separation because of the poor sensitivity and bad resolution.

Fig. 4 shows a separation of TCA, DCA, acetic acid and MCA by the anion-exclusion method. TCA is more ionized than the other anions, and elutes rapidly from the column, followed by DCA, acetic acid and MCA. Other haloacids such as bromo, dibromo and trifluoro acetic acids can be separated by the same meth-

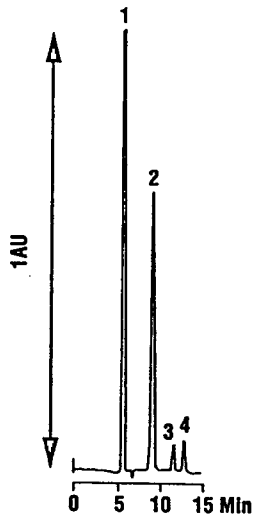

Fig. 4. Separation of chloroacetic acids by anion exclusion. Peaks: 1 = trichloroacetic acid (10 mg/l); 2 = dichloroacetic acid (10 mg/l); 3 = acetic acid (10 mg/l); 4 = monochloroacetic acid (10 mg/l). Column: Anion exclusion (300 mm × 7.8 mm). Eluent: 1% phosphoric acid. Flow-rate: 0.8 ml/min. Detector: UV, 210 nm. Injection volume: 100 μl.

ods, but may co-elute with other haloacids if they are present in the sample.

The anion-exchange separation is suitable for MCA, TFA and bromoacetic acid separation because sensitivity for these acids is better than with the ion-exclusion method. The ion-exclusion method is more advantageous to trichloro, dichloro and dibromo acetic acids separation because of higher sensitivity. Both methods have some co-elution problems, but depending on the nature of the analytes, either method can be used for the analysis.

3.3. Method detection limits

The detection limits calculated as 3× signal-to-noise ratio based on 100 μl injection volume using both methods are summarized in Table 1. The detection limits vary from 5 to 130 μg/l. These values are higher than the values reported in US EPA method 552 as shown in Table 1, however IC methods are simpler and require less sample preparation. The GC method requires liquid–liquid or micro-extraction which can be time consuming. Sample preparation for IC analyses requires simple dilution and filtration. The GC method is more sensitive than IC, hence the method described here are not suitable for monitoring haloacetic acids in drinking water, raw water and ground water. The detection limits by IC may be improved by pre-concentration of the sample.

3.4. Applications

The application of these methods for real samples are shown in Fig. 5. Fig. 5a, b and c show separations of peptide, antiseptic and drinking water samples using the ion-exchange method. The peptide sample was dissolved in deionized water and filtered through a 0.2-μm

Table 1
Method detection limits for haloacetic acids

Haloacetic acid	Method detection limit (μg/l)[a]		
	Ion exchange	Ion exclusion	Method 552[b]
Acetic acid	12.0	130.0	–
Monochloroacetic acid	8.0	70.0	0.10
Dichloroacetic acid	16.0	8.0	0.09
Trichloroacetic acid	80.0	5.1	0.06
Trifluoroacetic acid	12.0	65.0	–
Bromoacetic acid	21.0	85.0	0.08
Dibromoacetic acid	30.0	90.0	0.05

[a] 100 μl Injection volume, calculated as 3× signal-to-noise ratio.
[b] Method detection limits in reagent water reported in US EPA method 552.

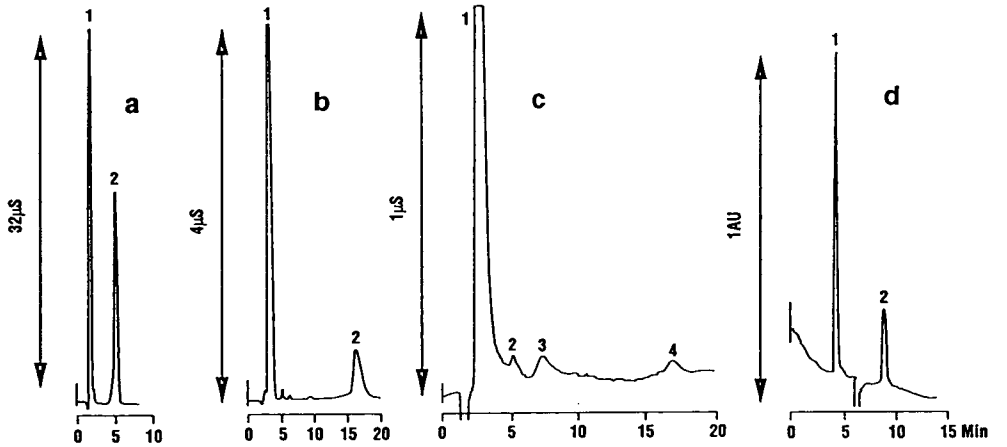

Fig. 5. Separations using ion-exchange (a, b, c) and ion exclusion methods (d). Columns: (a, b, c) Universal Anion 300 (150 mm × 4.6 mm). Eluent: 2.2 m*M* sodium carbonate–2.8 m*M* sodium bicarbonate. Flow-rate 2 ml/min. Detector: Conductivity. Injection volume: 100 µl: (d) Anion exclusion (300 mm × 7.8 mm). Eluent: 1% Phosporic acid. Flow-rate 0.8 ml/min. Detection: UV at 210 nm. Injection volume: 100 µl. Samples: (a) Peptide sample. Peaks: 1 = acetate; 2 = trifluoroacetate. (b) Antiseptic solution. Peaks: 1 = chloride; 2 = trichloroacetate. (c) Water spiked with haloacetic acids. Peaks: 1 = chloride; 2 = dichloroacetate (30 µg/l); 3 = dibromoacetate (60 µg/l); 4 = trichloroacetate (160 µg/l). (d) Herbicide. Peaks: 1 = trichloroacetic acid; 2 = dichloroacetic acid.

syringe filter before injection. The antiseptic solution was diluted 20-fold in deionized water and injected. The water sample was spiked with 30 µg/l DCA, 60 µg/l DBA and 160 µg/l TCA, respectively. Fig. 5d shows the analysis of herbicide using the ion-exclusion method. The sample was diluted in deionized water before injection.

4. Conclusions

IC provides a simple and sensitive method for the analysis of haloacetic acids. Either ion exchange with suppressed conductivity detection or ion exclusion with UV detection methods may be used for the determination. Compared to the GC method, IC is easier for routine analyses of haloacetic acids. The detection limits by both IC methods are in the ppb range. Because GC method is more sensitive, the IC methods described here are not suitable for US EPA work. Studies to improve the detection limits are under investigation. Some co-elution problems may occur depending on the analytes of interest, but can be avoided by choosing either one of the methods.

5. References

[1] *Method 552, The Determination of haloacetic acids in Drinking Water by Liquid/Liquid Extraction and Gas Chromatography with Electron Capture Detection*, US Environmental Protection Agency, Cincinnati, OH, 1989.
[2] S. Husain, R. Narsimha, S.N. Alvi and R.N. Rao, *J. Chromatogr.*, 600 (1992) 316–319.
[3] M. Houdeau, M. Thibert and M. Caude, *Analusis*, 5 (1977) 286–290.
[4] D.T. Gjerde and J.S. Fritz, *Ion Chromatography*, Hüthig, New York, 2nd ed., 1987, Ch. 6.
[5] R. Saari-Nordhaus and J.M. Anderson, Jr., *Am. Lab*, (1994) in press.
[6] J. Morris and J.S. Fritz, *LC · GC*, 11 (1993) 513.

ELSEVIER

Journal of Chromatography A, 671 (1994) 315–322

JOURNAL OF CHROMATOGRAPHY A

Analysis of substrates and metabolites in fermentation broth by ion chromatography

R.S. Robin Robinett*, Wayne K. Herber

Virus and Cell Biology, Merck Research Laboratories, Sumneytown Pike, WP26B-1116 West Point, PA 19486, USA

Abstract

Reliable methods to quantitate microbial fermentation nutrients and metabolites are essential for improved process monitoring and control. Analysis of culture media components by ion chromatography was completed for several recombinant and pathogenic microorganisms. Specific applications include monitoring of carbohydrates, alcohols, and inorganic cations. Isocratic methods were used with pulsed amperometric detection for carbohydrates and alcohols, and conductivity detection for inorganic cations. Sample preparation was a simple dilution of filtered broth with water. All isocratic analysis times were 20 min. An additional gradient method was utilized for certain carbohydrate mixtures. These analyses accurately monitor over fifty nutrients and metabolites present in fermentation media.

1. Introduction

Reliable methods to quantitate common microbial nutrients and metabolites are essential for improved fermentation process monitoring and control. Measurement of carbohydrates, alcohols, and inorganic cations are very important when investigating and understanding microbial physiology and for many aspects of fermentation process development. Improvements in process performance may be achieved by supplementation with organic [1] or inorganic [2] nutrients, by developing defined media to replace complex media formulations [3], and by defining fermentation endpoints. Process consistency can also be documented. Methods reported for carbohydrate monitoring include enzymatic [4], colorimetric [5], HPLC–refractive index detection [6,7], and HPLC–UV [8] assays. Alcohols have been measured using enzymatic [9], near-infrared spectroscopy [10], and gas chromatography [4] assays. Atomic absorption [4] and colorimetric [11] assays have been used for inorganic cation monitoring.

This paper describes four ion chromatography methods which quantitate nutrients and metabolites present in common fermentation media including carbohydrates (galactose, glucose, ribose, fructose), sugar alcohols (glycerol, inositol, mannitol, sorbitol), ethanol, and inorganic cations (calcium, magnesium, ammonium, potassium, sodium). Sample preparation for all analyses is a simple dilution of filtered broth with water before injection. All isocratic assays have analysis times of 20 min or less. These methods have been successfully used to analyze chemical-

* Corresponding author.

0021-9673/94/$07.00
SSDI 0021-9673(93)E1275-5

ly defined and complex culture media for various recombinant and pathogenic microorganisms fermentations.

2. Experimental

2.1. Chemicals

Sodium hydroxide (50% w/w) and hydrochloric acid (11.6 *M*) were obtained from Fisher Scientific (Malvern, PA, USA). Glacial acetic acid (HPLC grade, CH_3COOH), and perchloric acid (70%, Ultrex ultrapure reagent, $HClO_4$) were obtained from Baker (Phillipsburg, NJ, USA). Tetrabutylammonium hydroxide (55% aqueous solution, TBAOH), was obtained from Sachem (Austin, TX, USA). D,L-2,3-Diaminopropionic acid (DAP) was obtained from Sigma (St. Louis, MO, USA). All stock carbohydrate and alcohol standards were prepared from analytical reagent grade material obtained from either Pfanstiehl (Waukegan, IL, USA) or Fluka (Ronkonkoma, NY, USA). All inorganic cation standards were prepared from chloride salts (purity >97%) obtained from Sigma. All solutions were prepared with double distilled, chemically purified water (Millipore, Bedford, MA, USA).

2.2. Carbohydrate chromatographic system and eluents

Carbohydrate analysis was performed using a Dionex Ion Chromatography (Sunnyvale, CA, USA) system which consisted of a gradient pump, pulsed amperometric detector with gold electrode, autosampler, and a data handling system. The separation was accomplished using a CarboPac PA1 analytical column (Dionex, 250 × 4 mm, P/N 35391) and a CarboPac PA1 guard column (Dionex, 50 × 4 mm, P/N 43096) with a 50-μl filled loop injection.

The isocratic carbohydrate analysis used 150 m*M* NaOH mobile phase at a flow-rate of 1 ml/min. Settings for pulsed amperometric detection (PAD) were potentials E1 = 0.05, E2 = 0.65, E3 = −0.95, times T1 = 2, T2 = 2, T3 = 5 and range = 2. Total run time was 20 min.

The gradient carbohydrate analysis used water (A) and 50 m*M* NaOH–3 m*M* CH_3COOH (B) for mobile phases with an eluent flow-rate of 1 ml/min. The mobile phase composition was held constant for 13.8 min at a composition of 94%A–6%B, was varied linearly to 0%A–100%B over the next 11.2 min, and then returned to the original composition by the end of the run (40 min). The settings for the PAD detector were E1 = 0.05, E2 = 0.60, E3 = −0.65, T1 = 5, T2 = 2, T3 = 1 and range = 2.

2.3. Alcohol chromatographic system and eluents

Isocratic alcohol analysis was performed using a Dionex DX-100 chromatography system along with a PAD apparatus (platinum electrode), autosampler, and a data handling system. The separation was performed using an IonPac ICE-AS1 analytical column (Dionex, 250 × 4 mm, P/N 35330) with a 100 m*M* $HClO_4$ mobile phase, a flow-rate of 0.8 ml/min, and a 750-μl reaction coil. The PAD settings were: E1 = 0.2, E2 = 1.25, E3 = −0.1, T1 = 4, T2 = 1, T3 = 4, and range = 1. A 10-μl sample was injected using a filled loop injection. The total run time was 20 min.

2.4. Inorganic cation chromatographic system and eluents

Isocratic inorganic cation analysis was performed using a Dionex DX-100 chromatography system, conductivity detector, autosampler, and data handling system. The separation was achieved using an IonPac CS10 analytical column (Dionex, 250 × 4 mm, P/N 43118) and an IonPac CG10 guard column (Dionex, 50 × 4 mm, P/N 43119) with a 20 m*M* HCl–4 m*M* DAP mobile phase at a flow-rate of 1 ml/min. The regenerant system used a Dionex AutoRegen cation cartridge with 0.1 *M* TBAOH. A range setting of 30 was used with the conductivity detector. The injection method was a 10-μl filled loop. Total run time for the analysis was 20 min.

2.5. Data system

A Dionex Advanced Computer Interface (ACI), Model III was used to transfer data to an AST Premium 486/33TE computer. Data reduction and processing was accomplished using Dionex AI-450 software, version 3.3.

2.6. Preparation of standards and samples

Stock carbohydrate and alcohol standards were prepared at a concentration of 10 mg/ml in water. Stock inorganic cation standards were prepared at a concentration of 1 mg/ml for NaCl and KCl and 2 mg/ml for NH_4Cl, $MgCl_2$, and $CaCl_2$ in water. All standards were stored in 1.8 ml aliquots at −70°C in 2-ml Wheaton vials (Wheaton, Millville, NJ, USA) with screw caps. Standards were not sensitive to these storage conditions (data not shown). Dilutions of stock standards were made daily to prepare 10, 25, 50, 100, 250 and 500 μg/ml carbohydrate standards. Alcohol stock standards were diluted to prepare 10, 25, 50, 100, and 250 μg/ml. Inorganic cation stock standard were diluted daily to prepare either 0.5, 1.25, 2.5, 5, 12.5 and 25 μg/ml standards for NaCl and KCl or 1, 2.5, 5, 10, 25, and 50 μg/ml standards for NH_4Cl, $MgCl_2$, and $CaCl_2$. Diluted stock standards were used to generate standard curves.

Fermentation samples were prepared by making dilutions of filtered fermentation broth in water. A dilution of at least 1:25 was used for all samples.

3. Results and discussion

The isocratic carbohydrate analysis allowed quantitation of important microbial substrates and metabolites including pentoses (ribose, arabinose), hexoses (galactose, glucose, and fructose), disaccharides (lactose, sucrose, maltose), and sugar alcohols (mannitol and sorbitol). Separation of these compounds can be achieved in 20 min with the general elution order being alcohols, pentoses, hexoses and then disaccharides. The order of elution of monosaccharides largely corresponds to their bulk pK_a values [12]. Ethanol and glycerol can be detected with the carbohydrate method, but since their retention times are very similar, accurate quantitation may not be possible in cases where both components are present as metabolites. When monosaccharides are the primary carbon source, the run time may be shortened when chemically defined media are used which do not contain the later eluting disaccharides. When di- or trisaccharides are used as the primary carbon sources, higher molarity mobile phase may be used to shorten run times.

Example chromatograms depicting standards analyzed using isocratic and gradient methods have been described previously [13]. Typical standard curves for a pentose, hexose, disaccharide and sugar alcohol can be found in Fig. 1. Standard curve ranges are typically 10–500 μg/ml for carbohydrates and 10–250 μg/ml for alcohols. The large dynamic range of the standard curves minimizes the number of repeats due to inappropriate dilutions. Because of the large dynamic range, a cubic fit is used to better describe the standard curve.

Table 1 shows intraday and interday validation data for galactose, a common fermentation nutrient. Similar data (not shown) were obtained for five other carbohydrates. All validation data

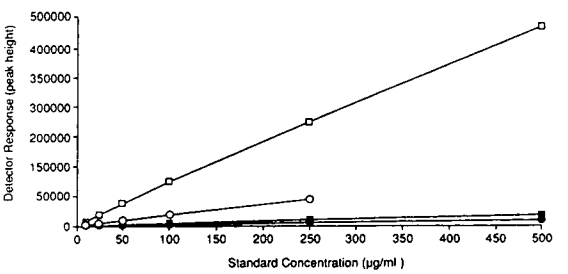

Fig. 1. Typical calibration curves for ribose, galactose, lactose, and glycerol generated using the isocratic carbohydrate analysis. Standard curve range 10 to 500 μg/ml. Ribose (■): amount = $1.40 \cdot 10^{-15}y^3 + 2.42 \cdot 10^{-10}y^2 + 1.03 \cdot 10^{-3}y + 4.87$, $R^2 = 0.999988$; galactose (□): amount = $-2.77 \cdot 10^{-19}y^3 + 3.76 \cdot 10^{-12}y^2 + 6.22 \cdot 10^{-5}y + 0.32$, $R^2 = 0.999999$; lactose (●): amount = $6.31 \cdot 10^{-15}y^3 - 6.11 \cdot 10^{-10}y^2 + 2.18 \cdot 10^{-3}y + 0.004$, $R^2 = 0.999989$; glycerol (○): amount = $4.20 \cdot 10^{-17}y^3 - 9.93 \cdot 10^{-12}y^2 + 2.53 \cdot 10^{-4}y + 0.25$, $R^2 = 0.999999$.

Table 1
Intraday and interday validation data for the isocratic carbohydrate analysis

Standard concentration (μg/ml)	Validation type	n	Galactose R.S.D. (%)
10	Intraday	6	1.8
25	Intraday	6	0.8
50	Intraday	6	1.0
100	Intraday	6	0.4
250	Intraday	6	1.1
500	Intraday	6	0.2
10	Interday	67	5.8
25	Interday	67	2.1
50	Interday	67	1.8
100	Interday	67	0.9
250	Interday	67	0.2
500	Interday	67	0.05

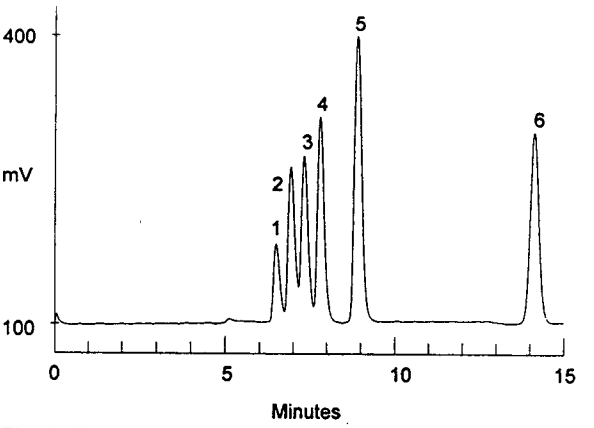

Fig. 2. Chromatogram of a mixture of alcohol standards (100 μg/ml) separated using an isocratic method. Injection volume 10 μl. Peaks: 1 = inositol, 2 = arabinitol, 3 = erythritol, 4 = galactitol, 5 = glycerol, and 6 = ethanol.

were generated using standards spiked into water. Data for spike recovery into fermentation medium is reported elsewhere [13]. The interday validation occurred over a two and one half year period and was generated using six different chromatography columns. Several thousand injections of standards and fermentation samples were run during this time without compromising assay accuracy, indicating that this is a rugged and reliable assay.

An ion-exclusion method was implemented to accurately quantitate glycerol and ethanol. This method was also isocratic with an analysis time of 20 min. The general order of elution correlated with molecular mass; retention of low-molecular-mass alcohols (*e.g.* ethanol) is based mainly on inclusion whereas higher-molecular-mass alcohols are retained by adsorptive interactions with the resin [14]. A chromatogram depicting elution of five alcohol standards is shown in Fig. 2. Fig. 3 shows typical standard curves for glycerol and ethanol over a range of 10 to 250 μg/ml. As with the carbohydrate analysis, this large dynamic range minimizes sample repeats.

Intraday and interday validation data for ethanol and glycerol analyses are shown in Table 2. The interday validation occurred over a ten-month period and was generated using one chromatography column. Over 2200 injections of standards and fermentation samples were run during this time with retention time changes of <1% for glycerol and <2% for ethanol.

Five common inorganic cations important in certain microbial fermentations were analyzed using a cation-exchange method. The isocratic cation analysis allowed quantitation of monovalent (sodium, ammonium, and potassium) and divalent (magnesium and calcium) inorganic cations. Separation of these compounds was performed in 20 min with monovalent cations eluting first. Retention time increased as the size of

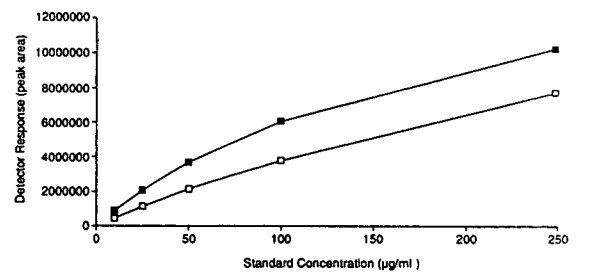

Fig. 3. Typical calibration curves for ethanol and glycerol generated using the isocratic alcohol analysis. Standard curve range 10 to 250 μg/ml. Glycerol (●): amount = $9.54 \cdot 10^{-20}y^3 + 2.72 \cdot 10^{-13}y^2 + 1.14 \cdot 10^{-5}y - 0.49$, $R^2 = 1.000000$; ethanol (□): amount = $-4.89 \cdot 10^{-20}y^3 + 2.10 \cdot 10^{-12}y^2 + 1.88 \cdot 10^{-5}y + 0.93$, $R^2 = 0.999995$.

Table 2
Intraday and interday validation data for the isocratic alcohol analysis

Standard concentration (μg/ml)	Validation type	n	R.S.D. (%)	
			Ethanol	Glycerol
10	Intraday	6	3.1	5.3
25	Intraday	6	4.0	5.2
50	Intraday	6	2.4	2.6
100	Intraday	6	6.1	1.9
250	Intraday	6	0.7	0.6
10	Interday	40	2.6	3.3
25	Interday	40	2.4	2.5
50	Interday	40	0.8	1.1
100	Interday	40	1.1	0.2
250	Interday	40	0.1	0.1

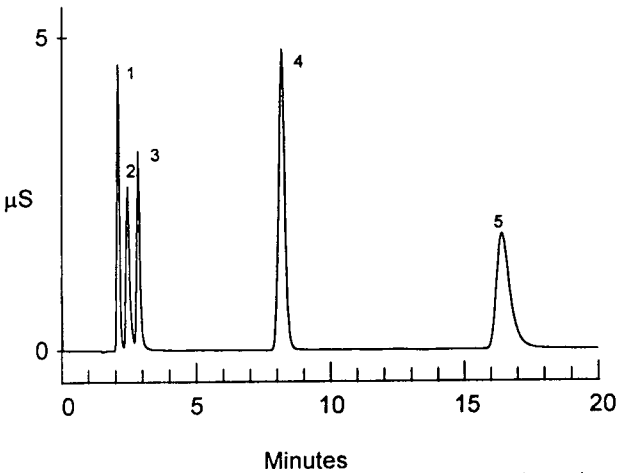

Fig. 4. Chromatogram of a mixture of inorganic cation standards (5 μg/ml or 10 μg/ml concentration for sodium and potassium or ammonium, magnesium and calcium, respectively) separated using an isocratic method. Injection volume 10 μl. Peaks: 1 = sodium, 2 = ammonium, 3 = potassium, 4 = magnesium, and 5 = calcium.

the ion in the hydrated state increased [15]. An example chromatogram showing the elution of these five inorganic cation standards is found in Fig. 4 and typical standard curves are found in Fig. 5. Again, a large dynamic range for analysis was used (0.5 to 25 μg/ml for sodium and potassium or 1 to 50 μg/ml for ammonium, magnesium and calcium).

Intraday and interday validation data for cation analysis (Table 3) shows R.S.D.(%) $\leq$ 5% for all components. The interday validation occurred over seventeen months and was generated using two different chromatography col-

Table 3
Intraday and interday validation data for the isocratic cation analysis

Standard concentration (μg/ml)	Validation type	n	R.S.D. (%)				
			Ammonium	Magnesium	Calcium	Sodium	Potassium
0.5	Intraday	6				0.02	5.0
1	Intraday	6	3.0	0.6	2.3	4.2	1.8
2.5	Intraday	6	2.5	0.7	1.3	2.0	2.1
5	Intraday	6	4.4	1.3	1.2	0.8	1.8
10	Intraday	6	2.0	0.4	0.5		
12.5	Intraday	6				2.8	1.2
25	Intraday	6	5.0	1.1	0.8	3.3	0.9
50	Intraday	6	3.2	1.3	1.3		
0.5	Interday	23				6	5.1
1	Interday	23	7.4	4.7	3.9	2.9	2.2
2.5	interday	23	3.2	2.3	4	2.6	2.2
5	Interday	23	2.9	1.3	1.6	0.7	0.6
10	Interday	23	1.6	0.4	0.5		
12.5	Interday	23				0.4	0.06
25	Interday	23	0.5	0.2	0.13	0.4	0.05
50	Interday	23	0.6	0.07	0.14		

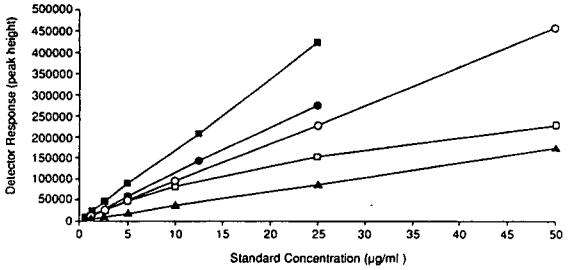

Fig. 5. Typical calibration curves for sodium chloride, ammonium chloride, potassium chloride, magnesium chloride, and calcium chloride using the isocratic cation analysis. Standard curve range 0.5 to 25 μg/ml for sodium and potassium and 1 to 50 μg/ml for ammonium, magnesium and calcium. Sodium (■): amount = $-6.03 \cdot 10^{-17}y^3 + 3.38 \cdot 10^{-11}y^2 + 5.54 \cdot 10^{-5}y - 0.01$, $R^2 = 0.999995$; ammonium (□): amount = $8.53 \cdot 10^{-16}y^3 + 3.58 \cdot 10^{-10}y^2 + 8.90 \cdot 10^{-5}y - 0.11$, $R^2 = 0.999998$; potassium (●): amount = $1.02 \cdot 10^{-16}y^3 - 1.75 \cdot 10^{-11}y^2 + 8.68 \cdot 10^{-5}y + 0.14$, $R^2 = 0.999973$; magnesium (○): amount = $-5.63 \cdot 10^{-17}y^3 + 3.78 \cdot 10^{-11}y^2 + 1.04 \cdot 10^{-4}y - 0.12$, $R^2 = 0.999992$; calcium (▲): amount = $-1.06 \cdot 10^{-15}y^3 + 2.37 \cdot 10^{-10}y^2 + 2.74 \cdot 10^{-4}y - 0.18$, $R^2 = 0.999972$.

umns. Sample analysis was routinely performed using dilutions of 1:1000 or 1:2000 to lower analyte concentrations to within the standard curve range. Sample matrix effects were negligible because of the large dilutions used for analyses. Over 2000 injections of standards and fermentation samples were analyzed during this time.

The isocratic carbohydrate analysis was used to generate a time course profile for a *Haemophilus influenzae* fermentation in a complex medium containing glucose (Fig. 6). Preferential utilization of some minor carbohydrates supplied by complex medium components, which are not easily measured by other methods, can be monitored using this analysis [13]. This information may be helpful when trying to elucidate biochemical pathways, improving process performance by nutritional supplementation, or formulating a chemically defined medium.

In instances where both glucose and galactose are used as carbon sources by the microorganism, a gradient carbohydrate method was required to quantitate the individual hexoses because of their similar retention times in the

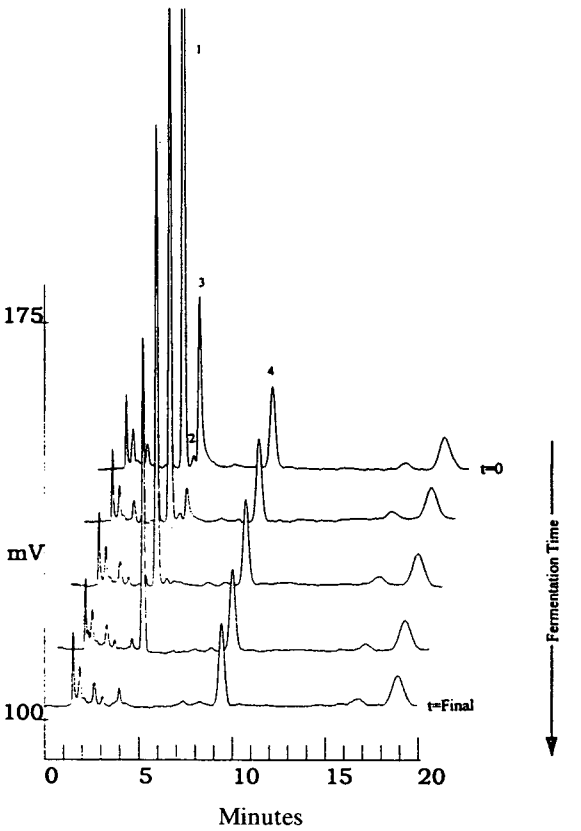

Fig. 6. A time course of representative chromatograms show isocratic carbohydrate analyses of fermentation broth samples for *Haemophilus influenzae* grown in complex media [16]. Peaks: 1 = glucose, 2 = fructose, 3 = ribose, 4 = sucrose.

isocratic analysis [13]. Fig. 7 shows a time course from a *Saccharomyces cerevisiae* fermentation where both glucose and galactose were present at the beginning of the fermentation. These chromatograms show the utilization of galactose after the depletion of glucose which is consistent with the known repression of galactose metabolism by glucose in yeast.

Another important component of investigating and understanding certain physiological events is the generation and subsequent utilization of alcohols, especially glycerol and ethanol. A time course showing glycerol and ethanol levels in a *S. cerevisiae* fermentation is found in Fig. 8. The glycerol peak can be seen to increase throughout

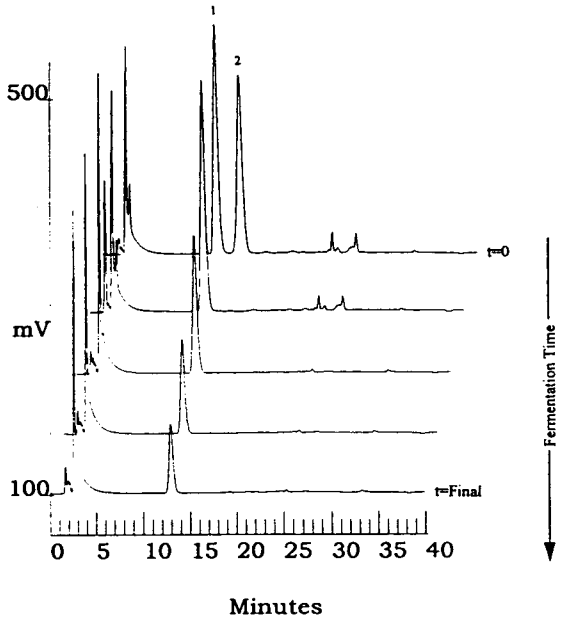

Fig. 7. A time course of representative chromatograms show gradient carbohydrate analyses of fermentation broth samples for *Saccharomyces cerevisiae* grown in complex media containing yeast extract and soy peptone. Peaks: 1 = galactose, 2 = glucose.

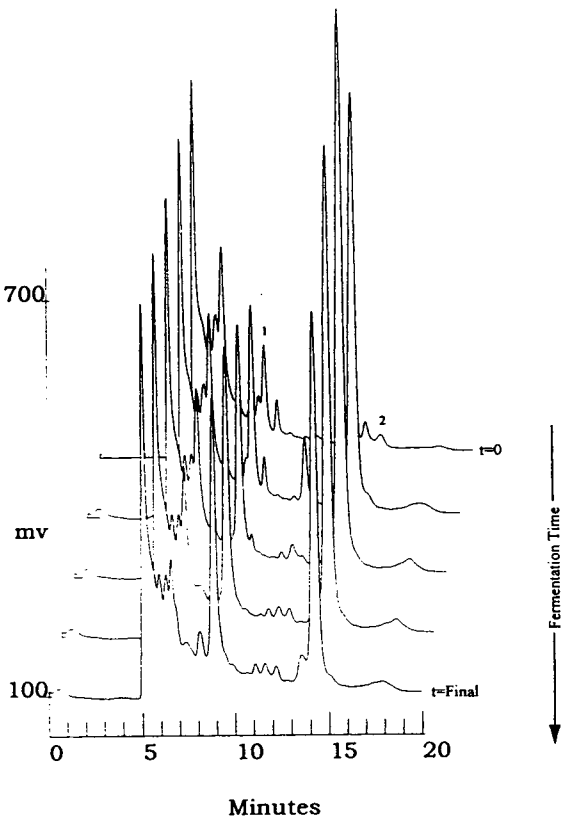

Fig. 8. A time course of representative chromatograms show isocratic alcohol analyses of fermentation broth samples for *Saccharomyces cerevisiae* grown in complex media containing yeast extract and soy peptone. Peaks: 1 = glycerol, 2 = ethanol.

the fermentation while the ethanol peak is absent in the $t = 0$ sample, increases in concentration, and then decreases. This information is useful for documenting process consistency since aerobic utilization of ethanol is dependent upon adequate aeration and other nutritional influences. Other alcohols can also be identified using this method and data could be obtained for these alcohols if their levels changed significantly over the time course of a fermentation.

While often overlooked, inorganic cations are essential for microbial growth and fulfill specific metabolic and structural roles. For example, potassium is used for active transport by yeast and ammonia can be generated or consumed in many microbial processes. Fig. 9 shows a series of chromatograms from a time course of fermentation where five inorganic cation levels were measured. The time course shows that some cation concentrations change dramatically; potassium becomes undetectable and then reappears at the end of the fermentation, while others, such as magnesium, retain a constant concentration throughout the fermentation. This information can be used to design improved medium formulations.

The four ion chromatography methods described here are very versatile for monitoring many common microbial fermentation substrates and metabolites in complex or chemically defined media for various recombinant and pathogenic microorganisms. The methods described are reliable, rugged, and demonstrate very good intraday, interday, and inter-column reproducibility. Because of the ease of sample preparation and the short analyses times, these

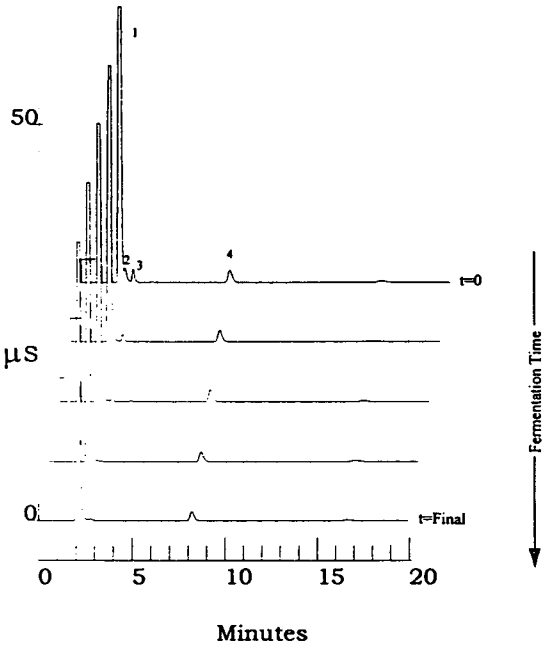

Fig. 9. A time course of representative chromatograms show isocratic cation analyses of fermentation broth samples for *Saccharomyces cerevisiae* grown in chemically defined media [17]. Peaks: 1 = sodium, 2 = ammonium, 3 = potassium, 4 = magnesium.

methods are potentially useful for on-line monitoring or process control.

4. Acknowledgements

The authors would like to thank Dr. Hugh George, Dr. Jeffrey Fu, James Bailey and Charles Parker for fermentation samples that were analyzed. Also, Dr. Hugh George and Dr. Randy Greasham for editorial comments.

5. References

[1] K. Sato, S. Goto, S. Yonemure, K. Sekine, E. Okuma, Y. Takagi, K. Hon-Nami and T. Saiki, *Appl. Environ. Microbiol.*, 58 (1992) 734.
[2] B.K. Robertson and M. Alexander, *Appl. Environ. Microbiol.*, 58 (1992) 38.
[3] L. Yee and H.W. Blanch, *Biotechnol. Bioeng.*, 41 (1993) 221.
[4] R.P. Jones, *Process Biochem.*, 21 (1986) 183.
[5] S. Chung, X. Wen, K. Vilholm, M. De Bang, G. Christian and J. Ruzicka, *Anal. Chim. Acta*, 249 (1992) 77.
[6] U. Rinas, H.-A. Kracke-Helm and K. Shügert, *Appl. Microbiol. Biotechnol.*, 31 (1989) 163.
[7] A. Plaga, J. Stümpfel and H.-P. Fiedler, *Appl. Microbiol. Biotechnol.*, 32 (1989) 45.
[8] F. Weigang, M. Reiter, A. Jungbauer and H. Katinger, *J. Chromatogr.*, 497 (1989) 59.
[9] K.D. Reda and D.R. Omstead, *Computer Control of Fermentation Processes*, CRC Press, Boca Raton, FL, 1990, p. 73.
[10] A.G. Cavinato, D.M. Mayes, Z.H. Ge and J.B. Callis, *Anal. Chem.*, 62 (1990) 1977.
[11] J. Huth, S. Werner and H.G. Müller, *J. Basic Microbiol.*, 30 (1990) 8.
[12] Y.C. Lee, *Anal. Biochem.*, 189 (1990) 151.
[13] W.K. Herber and R.S.R. Robinett, *J. Chromatogr.*, submitted for publication.
[14] W.R. LaCourse, D.C. Johnson, M.A. Rey and R.W. Slingsby, *Anal. Chem.*, 63 (1991) 134.
[15] J. Weiss, *Handbook of Ion Chromatography*, Dionex, Sunnyvale, CA, 1986, p. 36.
[16] C.E. Carty, R. Mancinelli, A. Hagopian, F.X. Kovach, E. Rodriguez, P. Burke, N.R. Dunn, W.J. McAleer, R.Z. Maigetter and P.J. Kniskern, *Dev. Ind. Microbiol.*, 26 (1985) 763–767.
[17] G.M. O'Connor and F. Sanchez-Riera, *Biotechnol. Bioeng.*, 39 (1992) 293.

ELSEVIER

Journal of Chromatography A, 671 (1994) 323–329

JOURNAL OF CHROMATOGRAPHY A

Determination of saccharin in shrimp by ion chromatography and capillary gas chromatography–mass spectrometry

Douglas T. Heitkemper*, David S. Jackson, Lisa A. Kaine, Kevin A. Mulligan, Karen A. Wolnik

US Food and Drug Administration, National Forensic Chemistry Center, Cincinnati, OH 45202, USA

Abstract

A procedure is described for the detection, identification and determination of saccharin in shrimp. Undeclared use of this regulated substance has been noted. Shrimp is extracted with water, and the extract is treated with a C_{18} solid-phase extraction cartridge and a chloride removal cartridge. The method detection limit is 2 μg/g saccharin in shrimp. Recovery of a 16 μg/g saccharin spike averaged 91 ± 6%. The identity of saccharin is confirmed by gas chromatography–mass spectrometry of the methyl derivative which is prepared using an on-column methylating agent.

1. Introduction

The non-nutritive sweetener, saccharin, is subject to regulation and labeling constraints because of questions concerning possible adverse health effects. This additive is commonly used in beverages and prepared foods such as desserts, canned fruit and sauces. Analysis typically involves reversed-phase high-performance liquid chromatography [1–7]. Development of a method for the determination of saccharin in processed shrimp products was necessary because of the possibility of undeclared use of saccharin by some shrimp processors. Yip and Doucette [8] developed a method for saccharin, sodium benzoate, and potassium sorbate in preserved fish products because existing HPLC procedures for other food products were found to form troublesome emulsions. However, their method requires a relatively lengthy column chromatography sample preparation procedure.

Ion chromatography (IC) has been used to determine saccharin in gums, mints, candies, mouthwashes, cough syrups, and soft drinks [9,10]. Generally, minimal sample preparation has been necessary, often consisting of no more than filtration of an aqueous extract. In light of this, it was anticipated that IC might serve as the basis for a simpler analytical method than HPLC [8].

In circumstances where the illicit use of saccharin is suspected, gas chromatography with mass spectrometric detection (GC–MS) can provide confirmation of the presence of saccharin because of its increased power of identification. Saccharin has been determined in biological fluids by GC–MS after paired ion extraction and formation of the methyl derivative using a reaction with methyl iodide [11].

This paper describes a rapid, direct IC method for the quantitative determination of saccharin in

* Corresponding author.

SSDI 0021-9673(93)E1246-V

shrimp. The separation used was adapted from a method for the determination of saccharin in soft drinks [10]. Confirmation for the presence of saccharin is provided via a GC–MS method which utilizes on-column derivatization.

2. Experimental

2.1. Apparatus

The IC instrument used consisted of a Waters Action analyzer (Millipore, Milford, MA, USA) with a Waters 700 Satellite WISP, 600E gradient module, 431 conductivity detector, and Maxima 820 software on a 386/25 microcomputer for data collection and calculation. The column used was a Dionex IonPac AS5, 250 × 4 mm with an IonPac AG5 guard column, 50 × 4 mm (Dionex, Sunnyvale, CA, USA). A Dionex Anion Micromembrane Suppressor II was also used.

The GC–MS instrument used consisted of a Hewlett-Packard (HP) (Palo Alto, CA, USA) 5917A mass-selective detector interfaced to an HP 5890 Series II gas chromatograph. The system is controlled and the data are collected and analyzed by HP G1034B software running on a HP Vectra 386/25 microcomputer. The analysis was performed on a narrow-bore methyl silicon capillary column (DB-1; 10 m × 0.18 mm I.D., 400 nm film thickness; J&W Scientific, Folsom, CA, USA).

2.2. IC Operating conditions

The IC method utilizes an isocratic eluent consisting of 33 m*M* sodium hydroxide, 7.7 m*M* sodium carbonate, 8 m*M* 4-cyanophenol and 2% (v/v) acetonitrile. The eluent flow-rate was 1.0 ml/min. The regenerant was 12.5 m*M* sulfuric acid at a flow-rate of 5 ml/min. The volume of sample extract injected onto the column was 100 μl. The base range of the conductivity detector was 50 μS.

2.3. GC–MS Operating conditions

The column head pressure was set to 5 kPa for a column flow-rate of 0.7 ml/min. A sample injection of 0.002 ml in the splitless mode was used with a split vent interval of 1.5 min and a split vent flow of about 30 ml/min.

The initial temperature of the oven was 50°C. After injection, this temperature was held for 2 min, and then increased to 100°C at a rate of 70°C/min followed by an increase to 250°C at a rate of 10°C/min.

The following detector conditions were used with the Hewlett-Packard 5971A. The instrument was autotuned for general scanning. A solvent delay of 5.00 min was set. The mass spectrum scan range was 30 to 330 a.m.u. with the threshold set at 500.

After each run, the column temperature was maintained at 250°C while two injections of MethElute reagent were made to clean the injection liner and to prevent carryover between runs. A 10-min interval was allowed for the material to exit from the column before starting the next run.

2.4. Reagents and standards

Distilled deionized water (DDW) was used in these studies (Milli-Q system, Millipore, Bedford, MA, USA). Saccharin reagent was obtained from Aldrich (98+%; Milwaukee, WI, USA). All other IC reagents were of the highest available purity. A 100 μg/ml IC stock standard of saccharin was prepared by dilution with DDW. Working IC standards were prepared at the 0.1, 0.5, 5.0 and 25 μg/ml levels.

A solution of 0.2 *M* trimethylanilinium hydroxide (TMAH) in methanol (MethElute Reagent; Pierce, Rockford, IL, USA) was used for the GC–MS on-column methylation reaction. All other GC–MS reagents were of the highest available purity.

2.5. IC Sample preparation

Frozen shrimp were thawed and the shells and tails removed. Approximately 15–30 shrimp were composited using a food processor. An accurately weighed 1-g portion of the composite was diluted with 80 ml of DDW in a 125-ml high-density polyethylene bottle. The solution was mixed for 30 min using a mechanical shaker

and centrifuged to remove heavier particulate from the solution. Approximately 8–10 ml of the extract were filtered through a 0.2-μm filter, an activated 300 mg C_{18} sample preparation cartridge (Maxiclean, Alltech) and a silver sample pretreatment cartridge (OnGuard Ag, Dionex) in series at a rate of approximately 1 ml/min. The filtrate served as the analytical sample.

2.6. GC–MS Sample preparation

A 2-g portion of thawed, composited shrimp was placed in a 20-ml glass vial and shaken with 10 ml of DDW. This mixture was centrifuged for 5 min at 2000 *g*. The aqueous supernatant was transferred to another vial and washed with 10 ml of diethyl ether. The ether wash should be discarded. Centrifugation was sometimes required to separate the organic and aqueous layers.

To the aqueous layer, 1.5 g of sodium chloride and 0.2 ml of hydrochloric acid were added and then thoroughly mixed by shaking. A 10-ml volume of diethyl ether was used to extract the saccharin from the acidified aqueous solution. The mixture was centrifuged (5 min, 2000 *g*) to provide two clear layers with a thin white band of solid material at the interface. The extraction was repeated and the ether extracts combined and dried over 1.5 g of sodium sulfate. The ether was evaporated just to dryness and the extract was reconstituted in 0.25 ml of TMAH for analysis by GC–MS.

3. Results and discussion

3.1. Determination of saccharin using IC

Fig. 1 shows a typical chromatogram of a 0.1 μg/ml saccharin standard. The saccharin peak elutes at a retention time of approximately 5.0 min. Peak area responses were used to quantitate saccharin throughout this work. A relative standard deviation (R.S.D.) of 1.2% was obtained for ten replicate injections of a 1 μg/ml saccharin standard. Peak area response was found to be linear with saccharin concentration over the range 0.1 to 25 μg/ml with a correlation

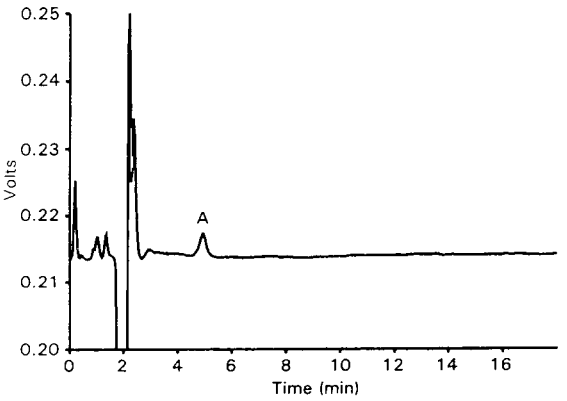

Fig. 1. Ion chromatogram obtained for a 0.1 μg/ml saccharin standard. Peak A = saccharin.

coefficient of 0.9996. The slope of the calibration curve was 297208 area counts/ppm and the *y*-intercept was −21022 area counts. The instrumental detection limit (IDL) for saccharin was found to be 0.02 μg/ml. IDL was defined as three times the standard deviation of blank baseline signal divided by the slope of the calibration curve.

The determination of saccharin in shrimp was complicated by a high level of chloride in the samples. The samples of interest had also been processed with sodium chloride. Excessive tailing of the chloride peak often obscured the saccharin peak. This problem was minimized by passing the samples through Ag sample pretreatment cartridges. These cartridges contain an Ag cation-exchange resin which will remove much of the chloride from the sample. Experimentally it was found that Ag cartridges with a capacity of at least 1.8 mequiv./cartridge provided more consistent removal of chloride and thus better reproducibility of the saccharin peak than cartridges with smaller capacities.

After reduction of chloride in the samples through the use of the Ag cartridges, an orthophosphate peak is resolved from the chloride peak. The orthophosphate peak is easily lost in the large chloride signal in samples which have not been treated with the Ag cartridge. The orthophosphate peak tails significantly, and the saccharin peak elutes in the tail. Fig. 2 shows the chromatogram obtained from a processed shrimp sample after treatment with the Ag cartridge.

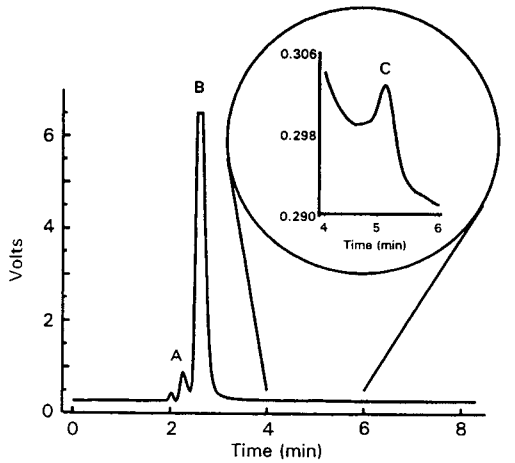

Fig. 2. Ion chromatogram obtained for a sample of shrimp containing saccharin. Peaks: A = chloride; B = orthophosphate; C = saccharin at a concentration of 0.31 μg/ml which corresponds to 25 μg/g in shrimp.

A C_{18} sample preparation cartridge was used to help remove organic materials prior to injection onto the IC column. Proteins and other organics can be retained on the IC column causing irreversible damage. Saccharin standards which were passed through both silver and C_{18} cartridges were not retained on the cartridges. Saccharin was spiked into an aliquot of unprocessed shrimp matrix at the level of 16 μg/g and taken through the extraction procedure. The percent recovery through the method averaged 91 ± 6% (n = 5). The reproducibility of saccharin peak area response for ten replicate injections of a processed shrimp sample with an average concentration of 25 μg/g was 3.2% R.S.D.

A method detection limit (MDL) was estimated at 2 μg/g in shrimp. An unprocessed shrimp sample was prepared as discussed previously and orthophosphate was added to the sample solution at approximately the same level (50 μg/ml) as found in the sample chromatogram shown in Fig. 2. The method detection limit was defined as three times the standard deviation of ten replicate analyses of an 8 μg/g saccharin spike to this sample.

Saccharin was detected in both cooked and uncooked processed shrimp samples. Uncooked shrimp samples were boiled for 5 min to imitate the cooking process. Saccharin concentrations did not significantly change after boiling whole shrimp in water for up to 5 min. Therefore, any saccharin added to raw shrimp prior to cooking should still be detected in the analysis of cooked product.

A single sample of processed shrimp was analyzed on three occasions over a six-week period. Concentrations of 26 (n = 2), 20 (n = 5) and 23 (n = 3) μg/g saccharin were obtained on the 1st, 35th and 43rd days, respectively. The average and 95% confidence limit of all values was determined to be 22 ± 2.1 μg/g saccharin. Clearly, the method provides consistent results over the 6-week period.

Earlier IC work utilized a 1:40 dilution of the shrimp matrix. Recoveries were somewhat lower in the less dilute solution, usually averaging approximately 75%. Lower recoveries were presumably the result of the larger amount of processed shrimp matrix (which includes added salt) involved. Several sample types have been analyzed using the 1:40 dilution. No saccharin was detected in three samples of raw unprocessed shrimp. Five samples of "in-process" shrimp and their associated brines were found to contain concentrations of saccharin ranging from 12–35 μg/g. Saccharin was also detected in five of six finished products at concentrations ranging from 8 to 40 μg/g. The presence of saccharin in the five finished products was confirmed qualitatively using GC–MS as discussed in the next section.

3.2. *Identification of saccharin in shrimp using GC–MS*

The extraction of saccharin from an acidified food matrix with diethyl ether has been described elsewhere [12]. In this work, shrimp samples were deproteinized by acidification with hydrochloric acid and saccharin was extracted with diethyl ether. The extract was taken to dryness and reconstituted in 0.2 M TMAH, a flash (or on-column) methylation reagent which has been used to derivatize a variety of drugs [13].

Fig. 3 shows a chromatogram obtained for a sample of shrimp which did not contain sac-

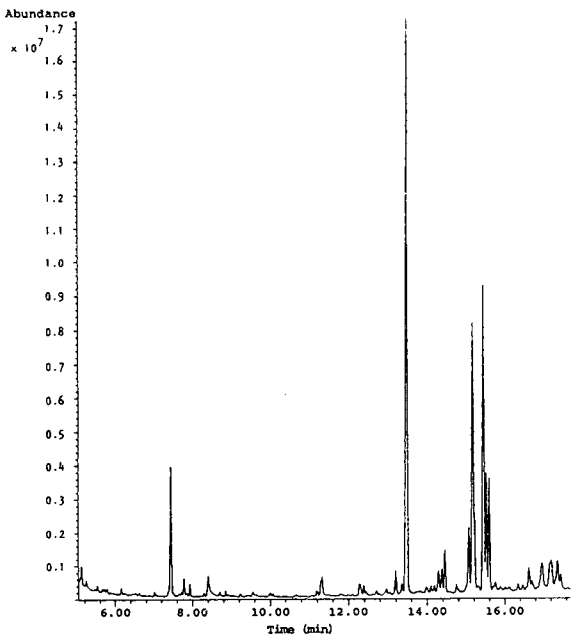

Fig. 3. GC–MS total ion current chromatogram of an untreated shrimp extract.

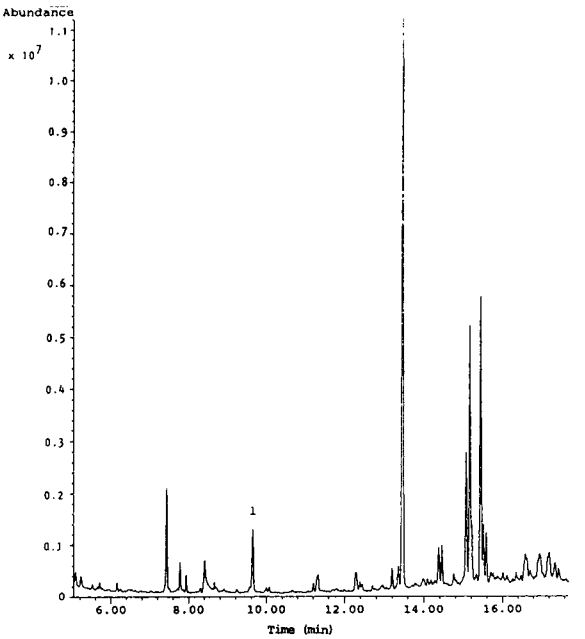

Fig. 4. GC–MS total ion current chromatogram of shrimp sample spiked with saccharin at 23 μg/g and taken through the method. Peak 1 = N-methylsaccharin.

charin. A number of prominent peaks are present with retention times as follows; 13.50, 15.07, 15.18, 15.46 and 15.60 min. Based upon a search of a commercially available database of mass spectra [14], these appear to be methyl esters of hexadecanoic acid, octadecanoic acid and octadecadienoic acids.

When saccharin was spiked into the shrimp matrix at a level of 23 μg/g, the chromatogram shown in Fig. 4 was obtained. A peak with the mass spectrum of the N-methyl derivative of saccharin [11] occurs at 9.65 min. This peak is cleanly resolved from the components of the matrix. The mass spectrum was matched [probability based matching (PBM)-reverse] against a commercially available database of mass spectra [14] and returned N-methylsaccharin with a match quality of 97 (Fig. 5).

Saccharin was spiked into an aliquot of shrimp matrix at the level of 23 μg/g and taken through the extraction procedure. The average percent recovery for two determinations was 36% (range = 8).

Although the recovery is somewhat disappointing, the method is useful for detecting and identifying saccharin at the 20 μg/g level. The mass spectrum of the methyl derivative shows a strong molecular ion ($m/z = 197$) and a number of other high mass ions which bodes well for the selectivity and robustness of the procedure across different matrices.

The recovery can probably be improved by enhancements to the extraction procedure such as the use of solid phase extraction to collect saccharin from the deproteinized extract and subsequent elution with isopropanol which forms a useful binary azeotrope with water. Moreover, use of selected-ion monitoring coupled with an internal standard of suitable retention and fragmentation would improve the signal stability. Based upon a reference spectrum, such a standard may be 2,4-dinitromethylbenzoate.

On a practical note, one important aspect to the use of on-column methylation is that incompletely reacted material may deposit in the injection port liner or on the column. This could produce a significant blank in subsequent runs. It

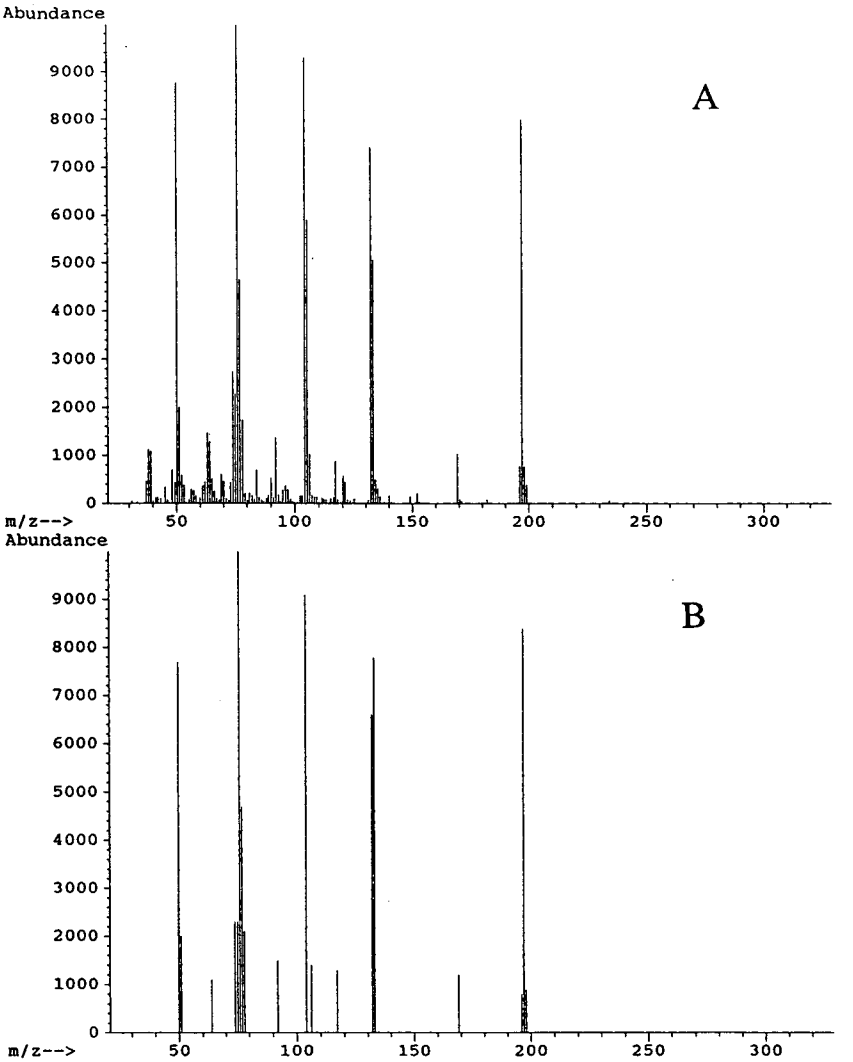

Fig. 5. Comparison of (A) the mass spectrum for the peak assigned to N-methylsaccharin in Fig. 4 and (B) a reference spectrum for N-methylsaccharin [14].

is important to flush the system as described earlier with blank injections of the methylating reagent to control this feature.

4. Conclusions

A rapid IC procedure for the determination of saccharin in shrimp has been developed. This approach is simpler than existing HPLC methodology. The method is capable of detecting saccharin in shrimp at the 2 μg/g level and has demonstrated recoveries of 91 ± 6% at 16 μg/g. Confirmation of the presence of saccharin can be effectively accomplished by capillary GC of the N-methyl derivative which is prepared "on-line" using a flash methylation reagent.

5. References

[1] Y. Ikai, H. Oka, N. Kamamura and N. Yamada, *J. Chromatogr.*, 457 (1988) 333.

[2] H. Terada and Y. Sakabe, *J. Chromatogr.*, 346 (1985) 333.
[3] A.M.K. Sjoberg, *J. Assoc. Off. Anal. Chem.*, 71 (1988) 1210.
[4] A.M.K. Sjoberg and T.A. Alanko, *J. Assoc. Off. Anal. Chem.*, 70 (1987) 58.
[5] A.M. Di Pietra, V. Cavrini, D. Bonazzi and L. Benfenati, *Chromatographia*, 30 (1990) 215.
[6] J.T. Hann and I.S. Gilkison, *J. Chromatogr.*, 395 (1987) 317.
[7] T.S. Tibbels, R.A. Smith and S.M. Cohen, *J. Chromatogr.*, 441 (1988) 448.
[8] W. Yip and Y. Doucette, *FDA Internal Communication, LIB 3106*, US Food and Drug Administration, Washington, DC, 1986.
[9] T.A. Biemer, *J. Chromatogr.*, 463 (1989) 463.
[10] *Application Note 47*, Dionex Corporation, Sunnyvale, CA, 1985.
[11] C. Pantarotto, M. Salmona, R. Fanelli, M. Bianchi and K. Szczawinska, *J. Pharm. Sci.*, 70 (1981) 871.
[12] K. Helrich (Editor), *Official Methods of Analysis of the Association of Official Analytical Chemists*, Association of Official Analytical Chemists, Arlington, VA, 15th ed., 1990, p. 1172.
[13] E. Brochmann-Hansen and T.O. Oke, *J. Pharm. Sci.*, 58 (1969) 370.
[14] *Wiley Database, part No. HP59943B*, Hewlett-Packard, Palo Alto, CA, 1986.

ELSEVIER

Journal of Chromatography A, 671 (1994) 331–337

JOURNAL OF CHROMATOGRAPHY A

Use of on-line ion chromatography in controlling water quality in nuclear power plants

Thomas O. Passell

Electric Power Research Institute, P.O. Box 10412, Palo Alto, CA 94303, USA

Abstract

Electric utilities that operate nuclear power plants must adhere to a tighter range of water coolant specifications that are commonly required in steam systems powered by other means such as coal, oil or natural gas. The reason for this situation is the higher negative impact of a failure in the coolant and steam piping relative to non-nuclear heat sources. This negative impact arises from the unique need of a nuclear reactor core to require cooling after shutdown of the chain reaction —due to the heat from undecayed radioactive fission products in the uranium fuel rods. Also, the cost of down time for repairs of corrosion damage in such stations is greater than for fossil fired plants because these nuclear plants are base loaded (running at *ca.* 100% power for several hundreds of days) and the replacement power required during their shutdown time must be provided by sources more costly by factors up to *ca.* 2. Since corrosion damage in nuclear plants usually occurs under crevice conditions in components such as steam generators where boiling occurs, even very small (parts per billion, ppb) initial feedwater concentrations of corrosive impurity salts such as sodium, chloride and sulfate may concentrate to corrosive brines —leading to breaches of the pressure boundaries from localized cracking or intergranular attack. This attack penetrates even the more corrosion-resistant alloys such as Inconel 600, Incoloy 800 and the stainless steels. Ion chromatography is the only technology able to readily measure ppb concentrations of such corrosive ions on a near real time basis, and to differentiate among different oxidation states of ions such as nitrate, nitrite, sulfate, thiosulfate, etc. These oxidation states respond to the general oxidizing tendency of the coolant —another variable that controls localized corrosion. A number of examples of the use of on-line ion chromatography in troubleshooting corrosion problems in light-water reactors will be given.

1. Introduction

Why would nuclear power stations need on-line ion chromatography (IC)? The answer: "to signal the onset of transient corrosive conditions from intrusions of ionic or ion-producing species into the water coolants". In the mid-1970s, it became apparent that expensive components in nuclear power stations were undergoing corrosion damage of a localized nature from concentrations of only a few parts per billion (ppb, w/w) of ions such as sulfate, sodium and chloride into the steam-producing water cycle. These ions were often associated with transient events which seldom coincided with the customary times for the "once a shift" or less frequent grabbing of a water sample for laboratory analysis. The on-line instruments in place such as conductivity meters did respond to such intrusions, but they seldom contained the information desired for fixing the trouble in a timely fashion. Significant damage sometimes occurred because the operators' de-

0021-9673/94/$07.00
SSDI 0021-9673(94)00095-Q

layed action until the instrument's readings were corroborated by laboratory analyses delivered hours to days later.

Into this situation in the late 1970s entered the laboratory ion chromatograph, able to reliably measure almost any positive or negative ionic species in water at ppb levels. But could a laboratory instrument be configured for the rugged conditions of on-line use at several different sample locations around the steam loop? It appeared likely, since large beds of ion-exchange resins had been widely used in a plant environment for many years for water treatment. After all, were not these devices just miniaturized versions of the reliable ion-exchange beds?

An Electric Power Research Institute (EPRI) research project was approved with the objective of three plant demonstrations of on-line IC [1,2]. Those three demonstrations have since led to installations at almost half of all USA nuclear stations. Further penetration of the power industry market for on-line IC can be expected as designs become less demanding of operator attention.

Applications of the on-line IC in the USA nuclear power industry are organized below based upon the separate coolant loops to emphasize the unique nature of the water impurities and additives commonly found in each.

2. Pressurized water reactors (PWRs)

2.1. Secondary side coolant

The secondary side coolant in PWRs was the first to be considered for application of on-line IC for two main reasons: (1) Corrosion damage of the steam generator was a very expensive problem that needed solution, and (2) the coolant impurities were suspected as possible causes of some of the damage mechanisms. Analysis of the sulfate ion, one of the most significant of these impurities, was the key to convincing many PWR operators to install an on-line IC. Why sulfate? Sodium and chloride already had a number of procedures capable of ppb sensitivity, sodium more than chloride. Sulfate was a far more difficult problem analytically. Furthermore, sulfate was in many steam systems far more abundant than chloride. Not only did it enter from cooling water in-leakage at the turbine condenser from both brackish and non-brackish waters, but internal sources such as the sulfonated cation resin of condensate polishers and sulfuric acid cation resin regenerant leachate were often dominant. Worse yet, as the anion resin of a mixed bed condensate polishing system gradually degraded its kinetics due to fouling by organics and other species, the first ion to show reduced kinetics for removal was the sulfate ion —due to its slower diffusivity arising from its two negative charges. It almost became, in many stations, a sulfate ion-dominated world!

Some of the early on-line data obtained in PWRs were dominated by sulfate ion spikes, more from resin intrusions than from condenser in-leakage. Figs. 1 and 2 show the first sulfate spikes seen by on-line IC in the EPRI program, observed at the Rancho Seco PWR right after a turbine trip (a sudden drop to near zero power) at points upstream and downstream of the deep bed condensate polisher beds. All the three ions, chloride, sodium and sulfate were observed in the upstream (hot well) sample, but sulfate was dominant in both up and down stream samples. Notice that the polisher was removing both the singly ionized sodium and chloride ions, but less than 25% of the doubly charged sulfate ion. All

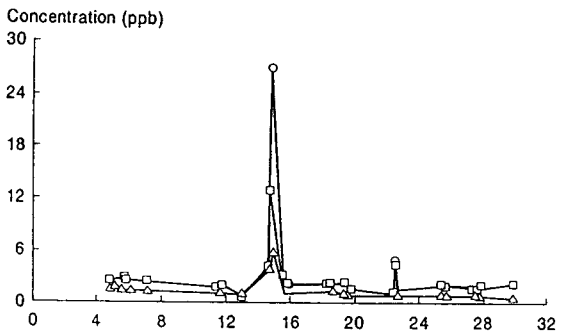

Fig. 1. Sulfate (○), chloride (□) and sodium (△) ion concentrations measured with on-line IC in the condenser hotwell of a PWR during a 22-day period in January 1982 within which a turbine trip occurred (x-axis: days).

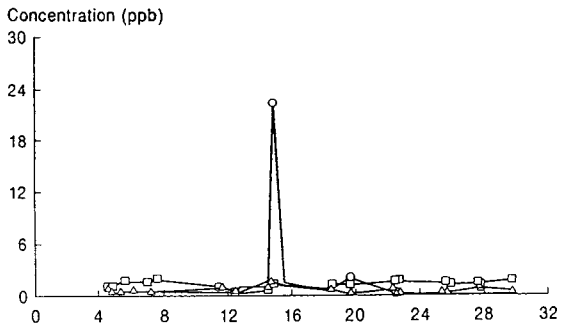

Fig. 2. Sulfate (○), chloride (□) and sodium (△) ion concentrations measured with on-line IC downstream of the condensate polisher ion-exchange bed during the same period as in Fig. 1 (x-axis: days).

three undoubtedly were entering the system water from deposits on dry, turbine cycle surfaces wetted during the sudden reduction of power. Conventional wisdom of that time would have expected all three to be removed by the polisher. It is probable that the polisher resin was kinetically fouled so it became a virtual separator for two negative ions! The point not to be missed in this story is the value of on-line data to see this transient and to learn from it the probable remedy —in this case to replace or refurbish the fouled anion resin.

It quickly became apparent that the on-line IC was proving an effective tool for quality assurance of the effluent from condensate polishers installed in many plants, and for troubleshooting their operation. Other ions, mostly anions, were found to be present but none of them were as significant corrosive agents as sulfate. However, the second most interesting anion class found were the weak carboxylic acids acetate, glycolate and formate, chief of which was acetate.

Acetate is even more ubiquitous than sulfate in PWR steam cycles. Eventually its source was discovered —tramp organics enter the cycle through the makeup water system or as lubricants left from maintenance on internal surfaces. All are thermally degraded partially to acetate. Before the time of the on-line IC, it was widely believed that all organics degraded all the way to carbonates (carbon dioxide) in the steam cycle. Apparently, acetate is an extremely stable species in these nuclear steam cycles with peak temperatures of generally less than 320°C.

Acetate could be quantified for the first time at ppb levels with the on-line IC and its fractional contribution to the cation conductivity (CC) determined. (CC is actually the conductivity of water measured downstream of a hydrogen form cation-exchange column —thus making acids of all anions present— and hence is a measure of the totality of anions present in the water. It is used to remove the conductivity effect of ammonium or amine cations, the pH control additives present at levels far higher than all the anions other than hydroxide). High levels of acetate (tens of ppb), while essentially benign from a corrosion standpoint, would often increase operator concerns because of their effect on increasing CC. The on-line IC was able to distinguish when the CC was due to really corrosive anions and when it was merely reflecting the acetate from an organic intrusion. Fig. 3 shows the acetate (and formate) ion concentration measured during the morpholine ON–OFF–ON test at Beaver Valley Unit 1 [3].

The morpholine story brings out another chapter in the on-line ion chromatograph's contribution to improvement of PWR secondary water chemistry. Morpholine is an organic amine base

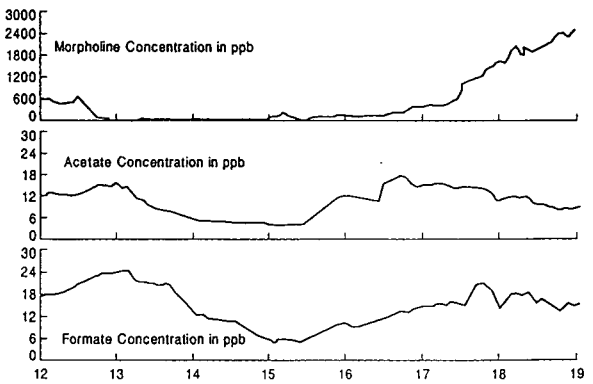

Fig. 3. Acetate and formate concentrations measured by on-line IC for water from the heater drain receiver tank of the Beaver Valley Unit 1 PWR during the 7-day ON–OFF–ON morpholine test (x-axis: days; y-axis: ppb).

less volatile than the commonly used ammonia under all volatile treatment (AVT). Its lower volatility allowed the pH of condensate in the wet steam region of the turbine cycle to be raised by amounts that significantly reduced the flow-assisted corrosion of carbon steel surfaces in that part of the loop. While that effect reduced the frequency of piping replacements, it had a much more significant effect. The iron oxide corrosion product particulate input to the steam generator was correspondingly reduced. This reduction in iron oxide deposits in the steam generator had a beneficial effect in reducing the rate of localized corrosion in that component, because the sludge deposits had enhanced the concentration of corrosive ions produced when boiling occurs within their porous structure.

How is all this related to the role of the on-line IC? In at least two ways: (1) acetate was always produced as a thermal degradation byproduct of morpholine addition and therefore the increase in CC had to be shown to be due to the benign acetate and not to the aggressive sulfate or chloride ions and (2) morpholine itself needed to be monitored in the presence of ammonia (ammonia is still present under morpholine-based AVT from morpholine thermal decomposition as well as from decomposition of the hydrazine added for oxygen control). The anion IC column measured the acetate ion and the cation IC column quantified morpholine.

Later other amines such as ethanolamine less volatile and with a higher base strength were found as improved replacements for morpholine. The on-line IC was up to the challenge —the new amine was just another peak on the cation chromatogram! Fig. 4 is a chromatogram showing separation of the ammonium and ethanolammonium ions from the work of Shenberger *et al.* [4]. Again, the on-line IC provided the assurance needed to overcome objections to a new PWR secondary side water chemistry, without which the changeover might have been significantly delayed.

Another area where the on-line IC has proven essential is in measuring the ions present in so-called "hideout return" (HR). Many ionic substances in water precipitate or adsorb on heat

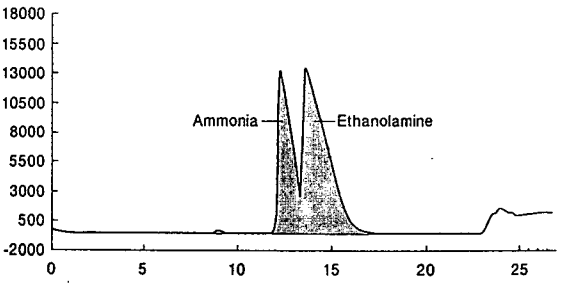

Fig. 4. On-line IC cation column chromatogram for ammonium and ethanolammonium ions, two species which had required significant adjustment in eluent conditions for adequate separation. Ammonia 500 ppb, ethanolamine 3 ppm (x-axis: time in min; y-axis: μS/cm).

transfer surfaces such as steam generator tubes and in the crevices between those tubes and their support plates. The HR studies occur during a cooldown in preparation for a refueling outage of some 40 to 80 days, so they must be conducted with little impact on the shutdown schedule. By noting the time of return, the puzzle of what solids constitute the chief storage mechanisms for both corrosive and benign ions can be better understood. Figs. 5 and 6 illustrate the pattern of HR reported by Bostic and Burns [5] using on-line IC. In this case the manganous ion dominates the positive ions returning from hideout, a discovery made possible by on-line IC. The full significance of manganese ions to crevice corrosion remains to be understood.

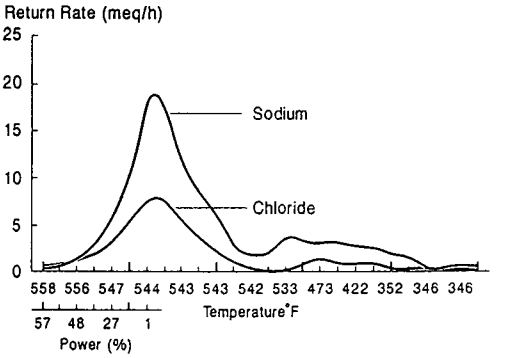

Fig. 5. Hideout return of sodium and chloride ions as a function of temperature and power level in a PWR steam generator measured by on-line IC during a gradual shutdown prior to refueling.

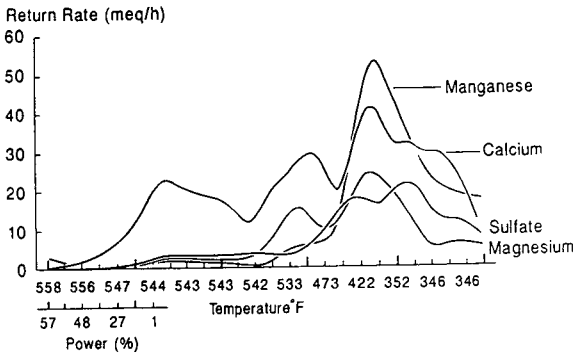

Fig. 6. Hideout return of calcium, magnesium, manganese and sulfate ions in steam generator water measured by on-line IC during the same shutdown of a PWR shown in Fig. 5.

The frequently more abundant ions such as silicate and borate can also now be quantified by on-line IC in spite of their being extremely weak acids [6]. The object is to find the likely pH of the crevices from which much of the HR comes, and plan water chemistry strategies to bring crevice pH into the more benign neutral range. The semi-volatile weak organic acids that are stable in these steam loops have a potential to neutralize the current predominantly caustic crevices. Again, on-line IC will be needed to keep such additives under constant control, should they be found useful in the future.

Finally, on-line IC has been used in at least one case for early warning of PWR primary–secondary leakage [7]. In this case, the extreme sensitivity of the IC cation column for lithium ions (low ppt levels) allowed detection of this leak before even the radiation monitors sensitive to radioactive species could detect it, as they did two weeks later when the leak had grown in size. Lithium-7 ions are present on the primary side at levels in the ppm range as natural products of the boron-10 (n,α) reaction, boron being present at the hundreds of ppm level as boric acid for reactivity control.

2.2. PWR primary side coolant

While, to my knowledge, on-line IC has not been applied to surveillance of PWR primary coolant, specific problems have been addressed by various short-term campaigns on the primary water. These usually have revolved around sulfate intrusions, suspected to arise from the ion exchange resins in the chemical and volume control system (CVCS). The generally reducing chemistry of the primary PWR coolant arising from the use of dissolved hydrogen gas, has led to speculation that sulfate could be reduced to more aggressive reduced sulfur species such as sulfite, sulfide and thiosulfate. Some of these anionic species could be readily observed by on-line IC to either confirm or refute this conjecture, which is still unresolved.

2.3. Makeup water systems

Since makeup occurs at about 1% of total system flow in many power system coolant loops, it represents an opportunity for intrusions of corrosive impurities if the makeup output quality should degrade. On-line ion chromatographs for secondary water often have one sample line from the makeup system output as a check on this source of impurity intrusion. Such upsets usually occur during periods when the resin beds or membrane systems near the end of their use cycle due to exhaustion or fouling.

3. Boiling water reactors (BWRs)

Coolants in BWRs are less complex than PWRs because no ionic additives are used. This simplifies the analytical problem for IC. However, the fluids are measurably radioactive, making IC applications deal with the nuisance of small volumes of socalled mixed wastes —mildly toxic eluent chemicals combined with mildly radioactive waters. Water quality has traditionally been followed with on-line conductivity and pH meters plus measures of oxidizing tendency such as electrochemical potential (ECP) or measures of the main species that influence ECP, namely dissolved oxygen and hydrogen gases.

Recently, the reactor water (water that circulates through the reactor core), was found to have higher conductivity than the sum of known impurities commonly seen such as sodium, sul-

fate, nitrate and chloride. A major effort using both on-line and off-line IC resulted in the discovery of the culprit: the chromate ion. This ion arose from corrosion of the stainless-steel feedwater heater system piping during normal operation with spikes occurring whenever an abrupt increase in ECP occurred. Such abrupt changes were observed in many stations when a transition from hydrogen (reducing) water chemistry (HWC) to normal (oxidizing) water chemistry (NWC) was experienced. This phenomena has been interpreted as the release of chromate by sudden oxidation of a piping surface layer of solid chromium oxide in the +3 Cr oxidation state to dissolved chromate ion in the +6 Cr oxidation state. Fig. 7 shows one such chromate spike observed by on-line IC at the Nine Mile Point unit 1 BWR, while Fig. 8 gives the correponding hydrogen gas concentration [2]. Note the timing of the chromate spike occuring just after hydrogen is shut off.

Other interesting ionic changes occurring during changes from NWC to HWC and *vice versa* have been observed by on-line IC. The changes observed involved known species present at a concentration of a few ppb and they followed known and expected chemical changes. For example, nitrate ion [nitrogen (N) in the +5 state] present at 4 ppb under NWC was observed to be transformed successively to nitrite ion (N in +3 state) and ammonium ion (N in −3 state) on going from NWC to HWC at one plant. The

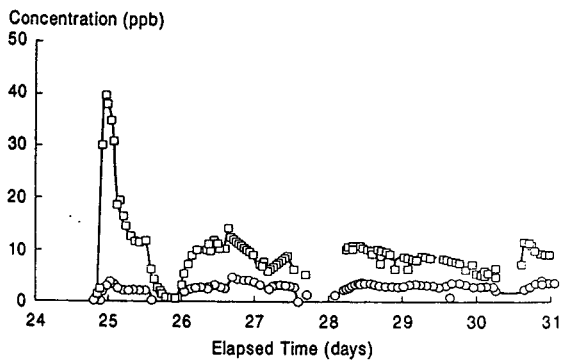

Fig. 7. Chromate (□) and nitrate (○) ion concentrations measured by on-line IC in the reactor water of a BWR following the transition from hydrogen (reducing) water chemistry to normal (oxidizing) water chemistry.

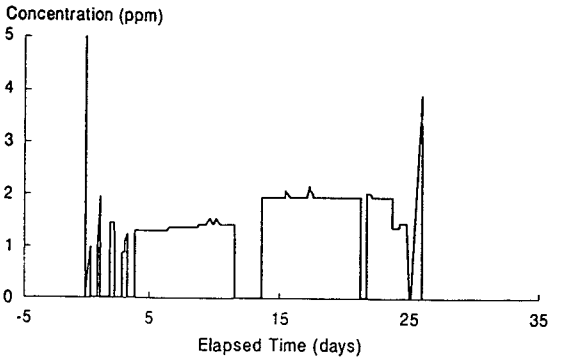

Fig. 8. Dissolved hydrogen gas concentration in the feedwater of a BWR prior to and during the chromate and nitrate ion measurements shown in Fig. 7.

nitrogen species were also detectable on a radiation detector using the 10-min radionuclide nitrogen-13 produced by the N-14(n,2n)N-13 reaction on a small fraction of the nitrogen atoms passing through the reactor core. Since the ratio of two species of differing oxidation state varies with ECP some indication of the latter can be acquired by on line IC.

Another area of concern to BWR operators is the quality of the water downstream of the condensate polishers and the reactor water cleanup system resin beds. Here again the on-pine IC was equal to the task. Copper ion removal has been the focus of several campaigns in this arena. For as yet undetermined reasons, copper is an unusually aggressive species inducing several forms of localized corrosion on the zirconium alloy fuel rod cladding in the core. The on-line IC has been used to check polisher outlet concentrations of copper down to the 0.1 to 1 ppb levels commonly observed [8].

4. The future

I see no end in sight for the uses of on-line IC in the power industry. Particularly when extrapolating from the history of the past 15 years, one could with some confidence predict many more exciting discoveries to be made in the chemistry and transport of both corrosive and benign ionic substances in high-temperature

water and steam. Here are a few of my predictions: (1) using on-line IC for control, the role of the acetate and glycolate ions will be found to be significant in both crevice corrosion and in iron oxide deposit transport in PWR secondary side coolant and may eventually lead to the use of these ions as additives during frequent on-line episodes of chemical control of deposits; (2) on-line IC will be increasingly used in waste water processing within the power station with the objective of recycling an increasingly greater fraction of such water into makeup; (3) analogous to the discovery of the manganous ion as an indicator of erosion–corrosion of carbon steel piping, other trace element ions will be found which signal corrosion of other metals and alloys used in steam power systems. For example, the oxygenated anions molybdate, tungstate, niobate produced by oxidative corrosion of ferrous alloys containing molybdenum, tungsten and niobium are observable by an on-line IC anion column with modified eluent.

5. Acknowledgements

Many researchers among EPRI contractors, EPRI member utilities, and several of my EPRI colleagues have made possible the developments mentioned in this paper. EPRI's efforts beginning in 1979 were effectively implemented by James Simpson, Michel Robles, Dragomir Dutina, Costas Spalaris, Steven Nagy, Beth McAllister and Douglas Rodgers and others of the General Electric Company. Utility personnel involved actively in on-line IC implementation were Arshad Alvi, Roger Miller, Jack Bills, Kevin Nietmann, Peter Crinigan, Frances Cutler, David Auerswald, Jon Noyes, Lewis Crone, Richard Eaker, Michael Funderburk, Mark Bridges, Richard Michael, John Wiley, Duane Mowry, Martin Prystupa, William Terrasi, Tracy Vannoy, Paul Nottingham, David Rhoades, Scott Wilkinson, Willow Junlowjiraya, Dennis Bostic, Samuel Harvey, Raymond Doebler, Andrew O'Dell, Dennis Oltmanns, Chris Diehl, Randall Lewis, Sue Blacklock, Norman Davis, Susan Miller, Chris Buck, Vic Linnenbom and Andy Dulick. I appreciate the support given by my colleagues at EPRI including Edwin Zebroski, Louis Martel, Robert Shaw, Chris Wood, Don Rubio, John Taylor, Stan Green, Chuck Welty, Sue Hobart and Robin Jones. In England Michael Sadler and Roy Weeden were active early users of on-line IC. Particularly helpful employees of Dionex Corporation have been Greg Franklin, Dan Campbell, Karen Haak, Debra Berg, Denise Eubanks, Bob Joyce, Steve Carson, Adrienne Meuter and Jean Berthold. I apologize in advance for omitting mention of many other significant contributors to the effective use of on-line IC in the nuclear power industry.

6. References

[1] M.N. Robles and J.L. Simpson, *On Line Ion Chromatography at Three PWR's; EPRI Report NP-4121, Research Project 1447-01*, Electric Power Research Institute, Palo Alto, CA, September 1985.

[2] M.N. Robles, J.L. Simpson, D. Dutina and T.O. Passell, *In-Plant Measurement of Corrosive Ions in Water; EPRI Report NP-6308, Research Project 1447-01*, Electric Power Research Institute, Palo Alto, CA, September 1989.

[3] J.M. Riddle, T.O. Passell and V.J. Linnenbom, *Proc. Int. Water Conf., Eng. Soc. West. Pa.*, 47th (1986) 244–254.

[4] D.M. Shenberger, J.D. Zupanovich, J.L. Walker and N.W. Nolan, *Loop Testing of Alternative Amines for All-Volatile Treatment Control in PWR's; EPRI Report TR-100756, Research Project S409-11*, Electric Power Research Institute, Palo Alto, CA, June 1992.

[5] D.W. Bostic and G.D. Burns, *Proceedings of the EPRI Condensate Polishing Workshop, Scottsdale, AZ, June 18–21, 1991*; available upon request to T.O. Passell.

[6] M.N. Robles, personal communication, 1992.

[7] L.E. Crone, personal communication, 1992.

[8] R.G. Hahnemann and R.E. Lewis, *Proceedings of the 1993 Dionex Ion Chromatography Symposium for the Power Industry, Denver, CO, May 19–21, 1993*, Dionex, Sunnyvale, CA, 1993.

ELSEVIER

Journal of Chromatography A, 671 (1994) 339–350

JOURNAL OF CHROMATOGRAPHY A

Determination of carbohydrates in wood, pulp and process liquor samples by high-performance anion-exchange chromatography with pulsed amperometric detection

Joseph Sullivan*, Maurice Douek

Pulp and Paper Research Institute of Canada, 570 St. John's Boulevard, Pointe Claire, Quebec H9R 3J9, Canada

Abstract

A rapid and sensitive method has been developed for the determination of monosaccharides present in the sulphuric acid hydrolyzates of wood, pulp, magnesium-based spent sulphite liquor, kraft weak black liquor and newsprint papermachine white water. Hydrolyzates were purified using an off-line, solid-phase extraction technique, employing cross-linked N-polyvinylpyrrolidone and strong anion-exchange resin. High-performance anion-exchange chromatography with pulsed amperometric detection was used to separate and quantify wood monosaccharides present in the purified hydrolyzates. Monosaccharide results obtained by ion and gas chromatographic methods were in good agreement for all samples examined. The effect of acid concentration on monosaccharide yields from the hydrolysis of process liquors was also investigated.

1. Introduction

The determination of carbohydrates in wood, pulp and process liquors and effluents is of particular significance to paper makers and researchers in the pulp and paper industry. One of the prime objectives of any pulping process is to minimize the degradation of polysaccharides. Consequently, it is important to have an accurate and sensitive method for quantifying wood carbohydrates in a wide variety of complex matrices, in order to determine the effect of various pulping and bleaching processes. In addition, sensitive methods capable of analyzing relatively low levels of carbohydrates in samples such as white water may be required in order to assess the impact of closure as mills move to reduce the use of fresh water. Over the years, a number of chromatographic methods have been developed to meet these needs. Older techniques, such as the classic paper chromatographic method of Saeman *et al.* [1] are no longer widely used, and have largely been replaced by gas chromatographic (GC) and high-performance liquid chromatographic (HPLC) methods. However, many of the GC and HPLC methods suffer from some serious limitations in terms of sensitivity, selectivity, ease of use and applicability.

GC methods require that the monosaccharides be converted to volatile derivatives such as alditol acetates [2–4] and trimethylsilyl (TMS) ethers [5–7] prior to analysis. Many of the derivatization procedures are complex and time consuming.

A number of HPLC methods utilizing low-efficiency anion-exchange [8–10], borate-complex ion-exchange [11,12], ligand-exchange and amino [13–22] columns to separate mono- and

* Corresponding author.

0021-9673/94/$07.00
SSDI 0021-9673(94)00127-U

oligosaccharides, followed by refractive index (RI), ultraviolet (UV), colorimetric, fluorescence, enzymatic and fixed potential electrochemical detection have been reported. However, these methods often utilize columns which afford poor resolution, have narrow operating pH ranges, exhibit poor stability, require high operating temperatures and are easily fouled by sample matrix contaminants. Moreover, RI and UV detectors exhibit low sensitivity and specificity of response toward carbohydrates.

High-performance anion-exchange chromatography coupled with pulsed amperometric detection (HPAEC–PAD) is a relatively new technique and offers a powerful alternative to traditional HPLC methods. Ion-exchange columns used in HPAEC are polymer-based, can tolerate eluents ranging in pH from 0 to 14, and can therefore be cleaned with strong acids and bases. In addition, the PAD response is reported to be linear over four orders of sugar concentration [23] with monosaccharide levels in the 10–100 pmol range routinely detectable [24]. Moreover, PAD is about two orders of magnitude more sensitive for these analytes than UV or RI detectors [25], and is to a great extent free from interferences.

The application of HPAEC–PAD for the determination of carbohydrates was first reported by Rocklin and Pohl [26]. Over the last decade, a number of additional publications describing the use of HPAEC–PAD for the determination of mono- and polysaccharides in the acid and enzymatic hydrolyzates of wood and/or pulp [27,28]; lignocellulose [29]; soil, manure and biomass [25,30–33]; marine and aquatic plants [34]; complex biological samples [35–37]; food products [38–41]; and fibrous substrates [42,43] have appeared. In addition, comprehensive reviews of recent developments in the chromatographic analysis of carbohydrates by HPLC [44] and HPAEC–PAD [45,46] have been published.

One of the major problems associated with analyzing carbohydrates in pulp and paper samples using any LC technique is severe column fouling and degradation that can occur as a result of the high concentration of sample contaminants co-injected onto HPLC or HPAEC columns. The acid hydrolyzates of wood and pulp are relatively free from contaminants and pose little threat to the LC column. However, process liquors (such as kraft weak black and spent sulphite liquors) contain high concentrations of lignin, carboxylic/sulphonic acids, humic substances and lower levels of other wood extractives that can adsorb irreversibly on the stationary phase of a HPLC column [16]. Since these samples are so difficult to analyze, it is not surprising to find that no publication to date has described the application of HPAEC–PAD for the determination of carbohydrates in pulp and paper process liquors. This report describes the development of a simple and relatively inexpensive off-line, mixed-mode solid-phase extraction (SPE) procedure which effectively removes contaminants from wood and pulp acid hydrolyzates, and both unhydrolyzed and acid hydrolyzed process liquors, prior to carbohydrate analysis using HPAEC–PAD. A comparison of carbohydrate results obtained for a number of samples using HPAEC–PAD and GC methods is presented. The effect of sulphuric acid concentration on the yield of monosaccharides from the hydrolysis of polysaccharides present in various process liquors has also been investigated.

2. Experimental

2.1. Wood and pulp samples

The following solid samples were studied: wood samples of aspen (*Populus deltoides*) and pine (*Pinus radiata*); unbleached kraft pulp and a chlorite-delignified thermomechanical pulp (TMP). Wood samples were extracted with ethanol to remove extractives and then ground in a Wiley mill to pass a 0.4-mm screen. Air-dried samples were subjected to a two-step (primary and secondary) hydrolysis procedure similar to that used by Borchardt and Piper [2] (in the current work, primary hydrolysis time was 30 rather than 60 min as described [2]). Sample moisture content was determined by thoroughly drying a small portion of each sample at 105°C in a hot-air oven. At the end of the hydrolysis period, the samples were cooled to room temperature and neutralized to either pH 5–6 with

concentrated NH_4OH (GC analysis) or pH 6–7 with NaOH (HPAEC–PAD analysis). The neutralized samples were then transferred to 100-ml volumetric flasks and diluted to volume with water. All samples were refrigerated until sample clean-up and analysis were performed.

2.2. Process liquors

Magnesium-based spent sulphite liquor (Mg-SSL), kraft weak black liquor (WBL) and newsprint papermachine white water (PMWW) samples were obtained either from Paprican's pilot plant or from various Canadian pulp and paper mills. Liquors were subjected to secondary hydrolysis only. Typically, 10 ml of spent pulping liquor and 20 ml of white water were mixed with 1 ml and 2 ml of 72% (w/w) H_2SO_4, respectively, and sufficient water was added to give a total volume of 29 ml. Liquors were then hydrolyzed, neutralized and diluted to volume (50 ml) as described in Section 2.1 for solid sample hydrolyzates.

2.3. Reagents

All monosaccharides were obtained from Sigma (St. Louis, MO, USA) or Aldrich (Milwaukee, WI, USA). Aqueous stock monosaccharide standards (1000 mg/l) were prepared weekly and stored at 4°C. Dilute standards (0.5–150 mg/l) were prepared daily. NaOH solution (50%, w/w) was purchased from ACP (Montreal, Canada) and was used to prepare eluents (3, 100 and 350 m*M* NaOH) and post-column reagent (350 m*M* NaOH). Deionized water was sparged for 30 min with nitrogen to remove dissolved carbon dioxide prior to use in chromatography and/or preparation of dilute NaOH solutions. Sulphuric acid (96%, w/w) and ammonium hydroxide (28%, w/w) were purchased from Anachemia (Montreal, Canada).

2.4. Solid-phase extraction

The following SPE sorbents were evaluated (approximately 300 mg of each sorbent were contained in a 3-ml polypropylene tube equipped with 20-μm polyethylene frits, unless specified otherwise): Supelclean LC-SAX, strong anion-exchange resin (3-quaternary aminopropyl, chloride form); LC-SCX, strong cation-exchange resin (3-propylsulphonic acid, hydrogen form), were purchased from Supelco (Bellefonte, PA, USA). In addition, SAX resin, SPE tubes and frits were purchased as separate items from the same supplier to allow for the preparation of custom-packed SPE tubes. Cross-linked N-polyvinylpyrrolidone (PVP), was obtained from Aldrich. Chromsep, octadecylsilane (ODS) cartridges containing 200 mg of packing in 4-ml polypropylene tubes were obtained from Chromatographic Specialties (Brockville, Canada).

Custom-packed SPE tubes containing PVP/SAX were prepared by first placing a polyethylene frit in an empty SPE tube followed by about 300 mg of SAX, 150–200 mg of PVP, and finally another frit to retain the sorbents. Each SPE tube was then conditioned with 5 ml of water (pH 7) in order to remove any contaminants from the resin which might interfere with the subsequent carbohydrate analysis. This washing step also serves to wet the resin and adjust its pH, prior to sample application.

Prior to analysis of samples using HPAEC–PAD, a 1-ml aliquot of the neutralized and diluted hydrolyzate or process liquor was transferred to either a 10-ml (white water samples) or 25-ml (spent pulping liquors) volumetric flask containing sufficient internal standard (I.S., 2-deoxy-D-glucose) to give a final I.S. concentration of 5 mg/l. A portion of the diluted sample (*ca.* 5 ml) was then transferred to a 10-ml syringe which was attached to a conditioned SPE tube. The sample was forced through the SPE tube packing at a rate of 1–2 ml/min, and the last 3 ml of eluate were retained for carbohydrate analysis.

2.5. High-performance anion-exchange chromatography

The HPAEC–PAD analyses were performed on a Dionex (Sunnyvale, CA, USA) 4000i ion chromatograph equipped with a quaternary gradient pump module (GPM). Samples were injected via a Dionex high-pressure injection valve equipped with a 100-μl sample loop. Monosac-

charides were separated on Dionex CarboPac PA guard (25 × 4 mm) and PA-1 analytical (250 × 4 mm) columns at a flow-rate of 1.0 ml/min, at ambient temperature (*ca.* 25°C). A 5-μm filter was attached to the inlet of the guard column to prevent particulate plugging of the columns. The eluents used in this work and their relative proportions are shown in Table 1. Eluent 1 was nitrogen sparged, deionized water, eluent 2 was 100 m*M* NaOH, eluent 3 was 350 m*M* NaOH.

After post-run flushing for 10 min with eluent 3, the column was equilibrated with the initial mobile phase for 10 min prior to the next sample injection. All mobile phases were stored under nitrogen to prevent absorption of atmospheric CO_2. Carbonate will act as a displacing ion and shorten retention times. Sodium hydroxide (350 m*M*) was added to the eluent stream, post-column at a rate of 0.8 ml/min via a low-dead-volume plastic mixing tee. Carbohydrates were detected using a Dionex Model PAD-1 detector equipped with gold working and silver reference electrodes (Ag electrode was filled with 350 m*M* NaOH), operating with the following working electrode pulse potentials and durations: $E_1 = +0.05$ V ($t_1 = 300$ ms), $E_2 = +0.60$ V ($t_2 = 120$ ms), $E_3 = -0.80$ V ($t_3 = 300$ ms). The PAD response time was set to 1 s and the range was 10 μA full scale. Chromatographic data were collected and plotted using a Hewlett-Packard (Avondale, PA, USA) Model 3390A integrator.

2.6. Gas chromatography

For GC analysis, a 200-μl aliquot of the neutralized secondary hydrolyzate (pH 5–6) was reduced, acetylated and extracted into CH_2Cl_2 according to the method of Harris *et al.* [4]. The monosaccharides derivatives (alditol acetates) were stored at 4°C until GC analysis was performed. Monosaccharide derivatives were chromatographed on a Hewlett-Packard 5890A gas chromatograph equipped with a DB-225 capillary column (30 m × 0.25 mm I.D., 0.25 μm film thickness, J & W Scientific, Folsom, CA, USA) and a flame ionization detector under the following conditions: high-purity helium was used as carrier and detector make-up gas; carrier gas flow-rate was 1.5 ml/min; injector and detector temperatures were 250°C; oven temperature program, 220 to 235°C at 1°C/min, hold 2 min; injection mode, split injection (20:1). Total run time was 17 min and chromatographic data were collected and plotted using a Hewlett-Packard Model 3396A integrator.

Table 1
Eluents used to separate wood monosaccharides using HPAEC

Eluent	Eluent proportions (%, v/v)		
	0–40 min	40.1–50 min	50.1 min
1	97	0	97
2	3	0	3
3	0	100	0

3. Results and discussion

3.1. Optimization of HPAEC–PAD conditions

In the initial phase of our investigation, we were concerned with optimizing eluent composition, flow-rate and column flushing conditions in order to achieve maximum separation of the five main wood monosaccharides and internal standard, while minimizing analysis time and variations in retention time. Very good separation of all monosaccharides was obtained using 3 m*M* NaOH delivered at 1 ml/min, as indicated in Fig. 1. In previous work carried out in our laboratory [47], it was found that monosaccharide retention time decreased and peak area increased with each consecutive injection of standards. The variation in retention time was attributed to carbonate build-up during the run, but no explanation was offered for the peak area variability. Carbonate, along with acetate, nitrate and sulphate have been shown to have a high affinity for the anion-exchange column, easily displacing hydroxide ion. A high level of sulphate is present in the sulphuric acid hydrolyzates studied, moreover acetate is present in wood, pulp and process liquor hydrolyzates in

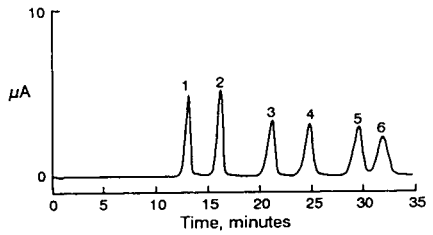

Fig. 1. Typical HPAEC–PAD chromatogram obtained for a standard mixture of wood monosaccharides. Each component present at 5 mg/l. Peaks: 1 = 2-deoxyglucose; 2 = arabinose; 3 = galactose; 4 = glucose; 5 = xylose; 6 = mannose. For analytical conditions, see Experimental section.

significant amounts. In order to obtain reproducible retention times, it is therefore essential that a post-run flush of the column with a strong NaOH solution be performed to wash strongly retained species. A 10-min post-run flush of the column with 350 m*M* NaOH, followed by a 10-min equilibration with the initial mobile phase was found to give satisfactory results. An insufficient column equilibration period could result in shorter or variable retention time because of elevated levels of OH^- remaining on the column.

The stability of the column and detector under the optimized chromatographic conditions was assessed by carrying out replicate analyses of a standard wood monosaccharide solution. As indicated in Table 2, highly reproducible retention times and relative peak areas were obtained for each monosaccharide studied.

Table 3
Linear regression data for peak area *versus* wood monosaccharide plot

Monosaccharide	Intercept	Slope	Correlation coefficient (R)
Arabinose	−0.29	1.87	0.999
Galactose	0.041	1.56	0.999
Glucose	0.11	1.75	0.999
Xylose	−0.021	1.79	0.999
Mannose	−0.078	1.60	0.999

3.2. Linearity of detector response

The detector response (peak area) for a given monosaccharide must be linear over a large concentration range in order to analyze samples containing disparate levels of monosaccharides in one chromatographic run. An example of such a sample is kraft pulp hydrolyzate, which may contain up to 150 mg/l of glucose and only 1–2 mg/l of arabinose or galactose. As shown in Table 3, the PAD response for each monosaccharide was linear over the concentration range (0.5–150 mg/l) studied, with correlation coefficients of 0.999 or better for each analyte.

In this work, 2-deoxy-D-glucose is added to hydrolyzates and used to quantify monosaccharides. Consequently, it is also essential that the relative response factor (RRF) of each monosaccharide with respect to the internal standard be linear over a wide concentration

Table 2
Repeatability ($n = 7$) of retention time and peak area, obtained for a standard wood monosaccharide solution containing 10 mg/l of each wood monosaccharide and 5 mg/l of internal standard

Monosaccharide	Retention time (min)		Relative peak area	
	Mean	R.S.D. (%)[a]	Mean	R.S.D. (%)
2-Deoxy-D-glucose	12.8	1.4	7.1	1.9
Arabinose	15.7	1.5	18.7	1.5
Galactose	20.8	1.5	15.8	1.5
Glucose	24.6	1.5	17.3	1.5
Xylose	29.2	1.5	17.8	0.9
Mannose	31.6	1.6	15.4	0.9

[a] R.S.D. = Relative standard deviation.

range, since accurately known RRFs are integral to the accurate determination of monosaccharide levels. The RRF of a given monosaccharide is given by Eq. 1.

$$RRF_S = \frac{A_{I.S.}}{A_S} \cdot \frac{C_S}{C_{I.S.}} \quad (1)$$

where $A_{I.S.}$ and A_S are the areas of the internal standard and monosaccharide peaks, respectively; $C_{I.S.}$ and C_S are the concentrations of the internal standard and monosaccharides, respectively. Eq. 1 is easily rearranged to give Eq. 2, a convenient form for determining RRF linearity.

$$\frac{A_{I.S.}}{A_S} = RRF_S \cdot \frac{C_{I.S.}}{C_S} \quad (2)$$

A plot of $A_{I.S.}/A_S$ *versus* $C_{I.S.}/C_S$ was prepared for each monosaccharide, over the concentration range 0.5–150 mg/l, with internal standard present at 5 mg/l in each case. Linear regression analysis of the data showed that the RRF of each wood monosaccharide was linear over the concentration range, with a correlation coefficient of at least 0.999 in each case. The RRFs for the five wood monosaccharides, obtained from the plot of Eq. 2 were: arabinose 0.78, galactose 0.93, glucose 0.82, xylose 0.80, mannose 0.92.

3.3. Evaluation of solid-phase extraction sorbents

Several publications describing the use of commercially available SPE sorbents, such as SAX, SCX, diol, cyano and amino-functionalized silica, for off-line sample clean-up of unhydrolyzed and acid and enzymatic hydrolyzates of various substrates, prior to carbohydrate analysis, have recently appeared [25,30,31,32,41]. In addition, an on-line sample clean-up scheme has recently been described by Marko-Varga and co-workers [13,16], in which three small columns containing SAX, amino-functionalized silica along with a non-silica-based hydrophobic polymer are used to purify fermentation broths. However, the effectiveness of these sorbents for sample cleanup have been quantified by only a few of these workers. Both Marko-Varga and co-workers [13,16], and Martens and Frankenberger [25,30,31], have demonstrated that SAX is very effective at removing coloured compounds from various sample hydrolyzates. In addition, Bio-Gel P-2 (Bio-Rad), a polyacrylamide gel with a low exclusion limit, also has been reported to be effective for this purpose [25]. Consequently, we assessed the potential of various SPE sorbents by determining the extent to which the five principal wood monosaccharides and internal standard could be recovered from aqueous solutions. Two standard monosaccharide solutions containing low (2–10 mg/l) and high (15–150 mg/l) levels of each component were used for this purpose. The eluates from the sorbents were analyzed for carbohydrate content and the results compared to those obtained with samples not passed through sorbents. All of the sorbents examined retained less than 5% of each monosaccharide, indicating that they were all potentially useful for sample clean-up.

The relative effectiveness of sorbents in removing sample contaminants from spent sulphite and weak black liquors were then determined. Wood and pulp hydrolyzates generally contain significantly lower levels of contaminants and were not included in this evaluation.

Magnesium-based spent sulphite liquor

Lignosulphonic acids comprise about half of the total dissolved organic matter present in spent sulphite liquor [48]. The non-carbohydrate matrix components present in this type of sample cause major problems in saccharide determination, as demonstrated in a previous study [47], and illustrated in Fig. 2. It is evident from this chromatogram that non-carbohydrate components have adsorbed onto the stationary phase of the column, severely reducing its efficiency, and resulting in co-elution of these contaminants with the monosaccharides. Extensive column flushing with strong NaOH eluent was required to restore column performance.

The relative effectiveness of various sorbents was assessed by recording the UV–Vis absorption spectrum (200–500 nm) of a neutralized (pH

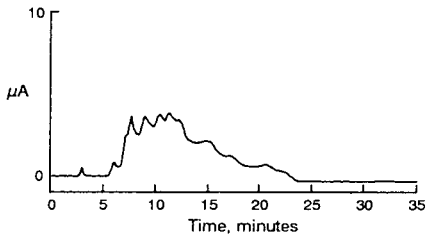

Fig. 2. HPAEC–PAD chromatogram of an acid hydrolyzate of Mg-SSL (sample from Paprican's pulping pilot plant) without sample clean-up [47].

6.5) and diluted (1:100, v/v) sample of Mg-SSL, before and after SPE. The absorption spectra of the original Mg-SSL and of samples after treatment with SPE sorbents are shown in Fig. 3A. The original Mg-SSL sample absorbs strongly from about 400 nm and below. The same liquor treated with ODS and SCX showed only a small

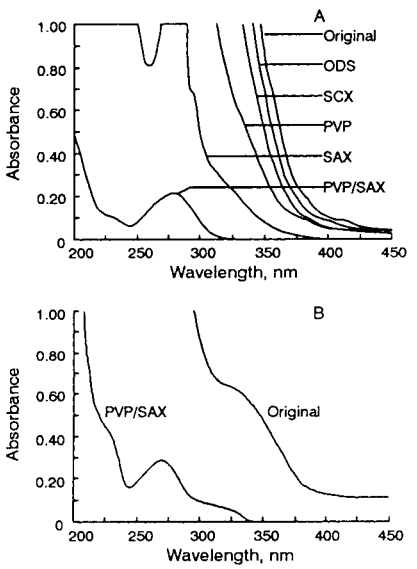

Fig. 3. The absorption spectra (200–500 nm) of an unhydrolyzed Mg-SSL (A) and an acid hydrolyzate of WBL (B), before and after SPE treatments with various sorbents (ODS = octadecylsilane; SCX = strong cation-exchange resin; PVP = cross-linked N-polyvinylpyrrolidone; SAX = strong anion-exchange resin). The pH of the Mg-SSL and WBL hydrolyzate was adjusted to 6.5 with NaOH, and diluted 1:100 and 1:125, respectively, prior to SPE. Spectra for the Mg-SSL and WBL samples were recorded with a Perkin-Elmer Model lambda 3B and a HP Model 8452A UV–Vis spectrophotometers, respectively. Water was used as reference in both cases.

decrease in absorption, and the eluate was still highly colored, indicating that these sorbents were only marginally effective at removing humic substances, and therefore, are not useful sorbents for this application. Samples treated with PVP and SAX showed a marked reduction in absorbance in the UV region, and both were significantly less colored. The final SPE sorbent tested was a hybrid sorbent, consisting of PVP–SAX [*ca.* 1:2 (w/w)]. This sorbent combination effectively removed a large proportion of the unwanted compounds from the sample, which absorb in the UV–Vis region. A small peak, with a maximum at about 278 nm in the spectrum of the PVP–SAX-treated sample is probably due to the absorption of low levels of lignosulphonic acids still remaining after sample clean-up. The order of effectiveness of the SPE sorbents is ODS < SCX ≪ PVP < SAX ≪ PVP–SAX.

Sanderson and Perera [49] have demonstrated that cross-linked PVP is extremely effective at removing polyphenolic and catechin type compounds from plant extracts, without affecting the saccharides present in the sample. More recently, reports of its use as a chromatographic sorbent for the fractionation of humic material [50] and the separation of aromatic acids, aldehydes and phenols [51] have appeared. The sorbent forms hydrogen bonds with phenolic hydroxyl and carboxyl groups, with the strength of the sorbent–phenol binding depending primarily on the number of these groups present in the molecule [51].

The mechanism by which SAX removes contaminants such as lignosulphonic acids from samples involves ion exchange. Lignosulphonic acids ($R-SO_3H$) are strong acids, and are therefore completely dissociated at pH 6–7, existing as anions (*e.g.*, lignosulphonates, $R-SO_3^-$) in solution. The SAX silica-based support has a quaternary amino-functionalized surface with Cl^- as a counter ion, which can be represented as silica–C_3H_6–$NR_3^+Cl^-$. As the sample passes through the SAX sorbent, the $R-SO_3^-$ displaces the Cl^- from the resin and therefore is likely removed from solution as follows:

$$\text{silica}-C_3H_6-NR_3^+Cl^- + R-SO_3^- \rightarrow \text{silica}-C_3H_6-NR_3^+\ ^-O_3S-R + Cl^-$$

Although carboxylic acids are weak acids, they are also completely dissociated at or near neutral pH, and interact with the SAX resin in the same fashion.

Weak black liquor

WBL contains higher levels and a broader range of organic and inorganic compounds than does spent sulphite liquor, and therefore represents the most difficult matrix one is ever likely to encounter. The effectiveness of PVP–SAX sorbents in purifying a hydrolyzed weak black liquor sample (neutralized to pH 6.5 with NaOH and diluted 1:125 with water) was assessed by measuring the UV–Vis absorption spectra before and after SPE, using the conditions described for Mg-SSL. The absorption spectra of the untreated, and PVP–SAX-treated WBL hydrolyzates are shown in Fig. 3B. The absorption spectrum of the untreated sample shows a number of strong absorption bands from 200–400 nm, primarily arising from the numerous aromatic compounds (such as lignin and phenols) present in the hydrolyzate. The spectra of the PVP–SAX-treated sample shows fewer and much less intense absorptions over the same wavelength range, indicating significant removal of aromatic compounds. In addition, the eluate from the sorbents was observed to be nearly colourless. The general scheme for purifying hydrolyzates is described in the Experimental section.

3.4. Effect of acid concentration on monosaccharide yield from process liquors

Suitable conditions for carrying out the hydrolysis of wood and various fibrous substances with sulphuric acid have been documented [1–4,12,20], and usually include primary and secondary hydrolysis steps. Hydrolysis of process liquors are generally carried out under the same secondary hydrolysis conditions (time and temperature) used for wood and pulp [12,20]. However, to our knowledge, the effect of sulphuric acid concentration on the yield of monosaccharides from the hydrolysis of process liquors and effluents has not been reported and was therefore examined for the three types of liquors used in this work, using secondary hydrolysis conditions only. This experiment was conducted on different samples from those referred to earlier in this paper. Aliquots of 10 ml of Mg-SSL and WBL were treated with 0.5, 1.0, 1.5 and 2.0 ml of 72% H_2SO_4, while 20-ml aliquots of PMWW were hydrolyzed with 0.25, 0.5, 1.0, 2.0 and 3.0 ml of 72% H_2SO_4. In each case the final volume was adjusted to 29 ml with water prior to hydrolysis at 121°C for 60 min. The monosaccharides in each hydrolyzate were quantified using SPE–HPAEC–PAD and the results for each sample were plotted against acid/sample (v/v) ratios. As indicated in Fig. 4, the concentration of each monosaccharide generally increases with increasing acid/sample ratio, reaches a maximum, and then decreases or levels off. In spite of the wide differences in chemistry (*e.g.*, alkalinity and dissolved solids content) and saccharide concentrations between the three samples, the optimum yield of monosaccharides appears to be reached at about the same acid/

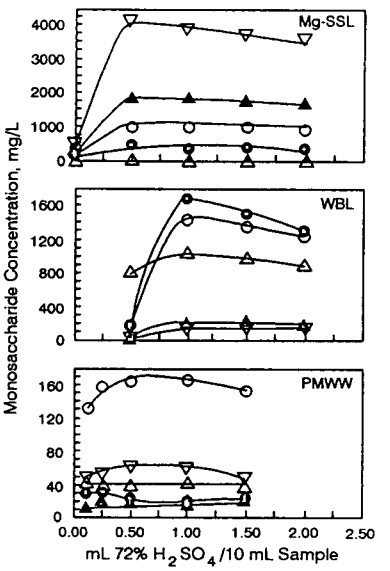

Fig. 4. Variation in the yield of wood monosaccharides from Mg-SSL, WBL and PMWW samples with varying amounts of 72% (w/w) H_2SO_4. All samples hydrolyzed for 60 min at 121°C. △ = Arabinose; ○ = galactose; ▲ = glucose; ● = xylose; ▽ = mannose. For HPAEC–PAD conditions, see Experimental section.

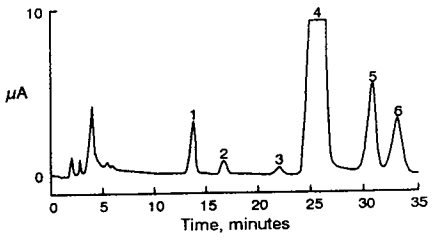

Fig. 5. SPE–HPAEC–PAD chromatogram of an unbleached kraft pulp hydrolyzate. Internal standard present at 5 mg/l. See Fig. 1 for peak identities and the Experimental section for analytical conditions.

sample ratio (1:10) for each sample. Accordingly, this ratio was used for the hydrolysis of the three types of liquors. Other liquors, particularly those with high solids content, may require higher ratios to achieve the same result.

3.5. Analysis of carbohydrates in wood, pulp and process liquors

Wood and pulp

A typical chromatogram of an unbleached kraft pulp hydrolyzate which serves to illustrate the selectivity of HPAEC is shown in Fig. 5. In spite of the high level of glucose present in the sample, the adjacent galactose peak is well resolved. Carbohydrate results obtained by HPAEC–PAD and GC methods for samples of aspen and pine wood, TMP (chlorite delignified) and unbleached kraft pulp are summarized in Table 4. As indicated in the Table, very good agreement between both methods was observed in all cases. The precision of both methods was determined by carrying out replicate analysis of the unbleached kraft pulp hydrolyzate. The relative standard deviation for the HPAEC–PAD and GC methods ranged between 3 to 7% and 2 to 12%, respectively.

Process liquors

Samples of unhydrolyzed and hydrolyzed Mg-SSL and WBL were subjected to PVP–SAX clean-up and then analyzed by HPAEC–PAD. Typical chromatograms of the hydrolyzed liquors are shown in Fig. 6A and B, respectively. Excellent resolution of all peaks was observed in both cases. For example, even though the Mg-SSL sample contained a relatively high level of xylose, no significant overlap with the adjacent mannose peak was observed. Unhydrolyzed Mg-SSL contained very low levels of each monosaccharide, while the unhydrolyzed WBL sample contained no monosaccharides, as expected.

The recovery of monosaccharides from Mg-SSL and WBL (pilot plant sample) was assessed by spiking dilute solutions of each hydrolyzed liquor with known amounts of each wood monosaccharide. Original and spiked hydrolyzates

Table 4
Comparison of HPAEC–PAD and GC carbohydrate results for aspen, pine, TMP and unbleached kraft pulp hydrolyzates

Monosaccharide	Monosaccharide concentration (%, w/w)							
	Aspen		Pine		TMP		Kraft	
	HPAEC ($n=2$)	GC ($n=2$)	HPAEC ($n=2$)	GC ($n=2$)	HPAEC ($n=4$)	GC ($n=2$)	HPAEC ($n=6$)	GC ($n=5$)
Arabinose	0.7	0.6	2.2	2.3	0.7	0.6	0.8	0.7
Galactose	1.1	ND[a]	2.7	2.3	0.4	0.4	0.6	0.6
Glucose	46.7	45.1	44.2	43.7	84.9	87.4	73.8	73.3
Xylose	14.7	15.8	6.0	6.9	8.7	8.0	7.3	7.4
Mannose	2.8	2.5	12.2	11.4	6.8	6.1	6.0	5.8
Total	66.0	64.0	67.3	66.6	101.5	102.5	88.5	87.8

[a] ND = Not detected.

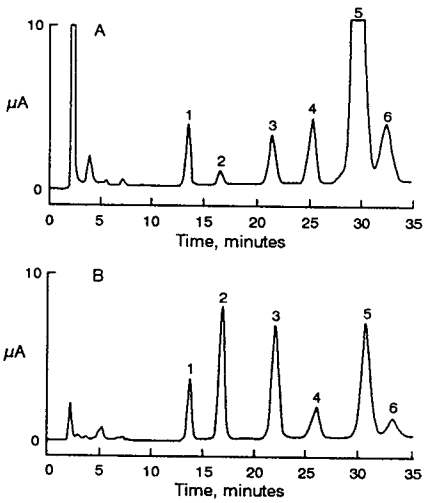

Fig. 6. SPE–HPAEC–PAD chromatograms of hydrolyzed Mg-SSL (A) and WBL (B). Internal standard present at 5 mg/l in both samples. See Fig. 1 for peak identities and the Experimental section for analytical conditions.

were then subjected to SPE using PVP–SAX, and analyzed for carbohydrate content. All of the wood monosaccharides were quantitatively recovered from both types of hydrolyzates, indicating the effectiveness of the SPE–HPAEC–PAD method. The carbohydrate content of hydrolyzed Mg-SSL, WBL and PMWW was also determined using the GC method. The results, presented in Table 5, show that the two methods are in good agreement. The precision of the combined hydrolysis and SPE–HPAEC–PAD method was assessed by carrying out replicate ($n = 4$) hydrolysis and subsequent carbohydrate analysis, using a sample of mill WBL. The results, presented in Table 6, show that the overall precision ranged between 2 and 7%, and the total monosaccharide result had an R.S.D. of about 3%. The precision results for mannose were not determined, since it was present below the detectable level in this particular sample.

In the case of the PMWW hydrolyzate, monosaccharides originate mainly from dissolved hemicellulose components. The unhydrolyzed PMWW sample was also analyzed, and found to contain no monosaccharides. The ability to routinely use HPAEC–PAD to determine carbohydrates in highly contaminated process liquors is due primarily to the effectiveness of the sample clean-up technique described in this work. After performing several hundred analyses of wood, pulp and process liquor samples using the same column, we have not observed any significant decrease in efficiency, and continue to use the same guard and analytical columns.

4. Conclusions

We have demonstrated that wood monosaccharides can be baseline resolved under isocratic

Table 5
Comparison of carbohydrate results for hydrolyzed Mg-SSL, WBL (pilot plant sample), PMWW, obtained using SPE–HPAEC–PAD and GC methods

Monosaccharide	Monosaccharide concentration (mg/l)					
	Mg-SSL		WBL		PMWW	
	HPAEC	GC	HPAEC	GC	HPAEC	GC
Arabinose	333	426	1005	1095	110	102
Galactose	1054	1053	1366	1294	165	141
Glucose	2023	1908	146	140	32	39
Xylose	772	782	1685	1773	18	15
Mannose	4524	4523	105	80	36	47
Total	8706	8692	4307	4382	361	344

Table 6
Overall precision obtained for replicate analysis of WBL (mill sample) hydrolyzate, using the SPE–HPAEC–PAD method

Monosaccharide	Monosaccharide concentration (mg/l)					
	Analysis No.				Mean	R.S.D. (%)
	1	2	3	4		
Arabinose	1177	1148	1161	1213	1175	2.4
Galactose	711	777	794	804	772	5.4
Glucose	40	35	40	37	38	6.5
Xylose	1410	1497	1519	1563	1497	4.3
Total	3338	3457	3514	3617	3482	3.3

All hydrolyses and analyses were performed on the same day.

conditions in less than 40 min. Very reproducible retention times, peak areas and response factors were obtained by using a post-run column flush with 350 m*M* NaOH. The PAD response was linear for each monosaccharide over the concentration range of 0.5 to 150 mg/l. The applicability of the HPAEC–PAD technique has been expanded to include the analysis of carbohydrates in process liquors through the development of a simple, inexpensive SPE technique which utilizes PVP–SAX sorbents. Carbohydrates were quantitatively recovered from pulp and process liquor hydrolyzates using the SPE technique. Carbohydrate results obtained for wood, pulp, Mg-SSL, WBL and PMWW, using HPAEC–PAD and GC methods were in excellent agreement. The overall precision of the SPE–HPAEC–PAD method for pulp and weak black liquor ranged between 2 to 7% expressed as R.S.D. of individual monosaccharide concentrations. Optimum monosaccharide yield from the three types of process liquors was demonstrated to occur at the same acid/sample ratio (1 ml 72% H_2SO_4 per 10 ml sample).

5. Acknowledgement

We thank Dr. Jean Bouchard for critically reviewing the manuscript and for his helpful comments.

6. References

[1] J.F. Saeman, W.E. Moore, R.L. Mitchell and M.A. Millett, *Tappi J.*, 37 (1954) 336.
[2] L.G. Borchardt and C.V. Piper, *Tappi J.*, 53 (1970) 257.
[3] C. Hoebler, J.L. Barry, A. David and J. Delort-Laval, *J. Agric. Food Chem.*, 37 (1989) 360.
[4] P.J. Harris, A.B. Blakeney, R.J. Henry and B.A. Stone, *J. Assoc. Off. Anal. Chem.*, 71 (1988) 272.
[5] J.T. Sweeley, W.E. Moore, R.L. Mitchell and M.A. Millett, *J. Am. Chem. Soc.*, 85 (1963) 2497.
[6] G.L. Cowie and J.I. Hedges, *Anal. Chem.*, 56 (1984) 497.
[7] J.M. MacLeod and J.V. Benko, *J. Wood Chem. Technol.*, 2 (1982) 207.
[8] R.B. Kesler, *Anal. Chem.*, 39 (1967) 1416.
[9] P.L. Van Biljon and S.P. Olivier, *J. Chromatogr.*, 473 (1989) 305.
[10] L.I. Larsson and O. Samuelson, *Svensk Papperstidn.*, 70 (1967) 571.
[11] M. Sinner, M.H. Simatupang and H.H. Dietrichs, *Wood Sci. Technol.*, 9 (1975) 307.
[12] B. Krogerus, *Paperi ja Puu*, 66 (1984) 649.
[13] G. Marko-Varga, E. Dominguez, B. Hahn-Hägerdal and L. Gorton, *Chromatographia*, 30 (1990) 591.
[14] G. Bonn, R. Pecina, E. Burtscher and O. Bobleter, *J. Chromatogr.*, 287 (1984) 215.
[15] D.W. Patrick and W.R. Kracht, *J. Chromatogr.*, 318 (1985) 269.
[16] G. Marko-Varga, E. Dominguez, B. Hahn-Hägerdal, L. Gorton, H. Irth, G.J. de Jong, R.W. Frei and U.A.Th. Brinkman, *J. Chromatogr.*, 523 (1990) 173.
[17] W.E. Karr, L.G. Cool, M.M. Merriman and D.L. Brink, *J. Wood Chem. Tech.*, 11 (1991) 447.
[18] T. Lindén and B. Hahn-Hägerdal, *Biotechnol. Tech.*, 3 (1989) 189.
[19] H. Binder, *J. Chromatogr.*, 189 (1980) 414.

[20] F.E. Wentz, A.D. Marcy and M.J. Gray, *J. Chromatogr. Sci.*, 20 (1982) 349.
[21] R.C. Pettersen, V.H. Schwandt and M.J. Effland, *J. Chromatogr. Sci.*, 22 (1984) 478.
[22] M.G. Paice, L. Jurasek and M. Desrochers, *Tappi J.*, 65 (1982) 103.
[23] D.C. Johnson and W.R. LaCourse, *Anal. Chem.*, 62 (1990) 589A.
[24] J.D. Olechno, S.R. Carter, W.T. Edwards, D.G. Gillen, R.R. Townsend, Y.C. Lee and M.R. Hardy, in T.E. Hugli (Editor), *Techniques in Protein Chemistry*, Academic Press, San Diego, CA, 1989, p. 367.
[25] D.A. Martens and W.T. Frankenberger, *Chromatographia*, 29 (1990) 7.
[26] R.D. Rocklin and C.A. Pohl, *J. Liq. Chromatogr.*, 6 (1983) 1577.
[27] W.T. Edwards, C.A. Pohl and R. Rubin, *Tappi J.*, 70 (1987) 138.
[28] R.C. Pettersen and V.H. Schwandt, *J. Wood Chem. and Tech.*, 11 (1991) 495.
[29] M. Ishihara, S. Uemura, N. Hayashi and K. Shimizu, *Biotechnol. Bioeng.*, 37 (1991) 948.
[30] D.A. Martens and W.T. Frankenberger, *Talanta*, 38 (1991) 245.
[31] D.A. Martens and W.T. Frankenberger, *J. Chromatogr.*, 546 (1991) 297.
[32] K. Koizumi, Y. Kubota, T. Tanimoto and Y. Okada, *J. Chromatogr.*, 464 (1989) 365.
[33] K. Koizumi, M. Fukuda and S. Hizukuri, *J. Chromatogr.*, 585 (1991) 233.
[34] R.J. Wicks,, M.A. Moran, L.J. Pittman and R.E. Hodson, *Appl. Environ. Microbiol.*, 57 (1991) 3135.
[35] G.O.H. Peelen, J.G.N. deJong and R.A. Wevers, *Anal. Biochem.*, 198 (1991) 334.
[36] M.R. Hardy, R.R. Townsend and Y.C. Lee, *Anal. Biochem.*, 170 (1988) 54.
[37] G.P. Reddy and C.A. Bush, *Anal. Biochem.*, 198 (1991) 278.
[38] K.W. Swallow, N.H. Low and D.R. Petrus, *J. Assoc. Off. Anal. Chem.*, 74 (1991) 341.
[39] D.R. White and W.W. Widmer, *J. Agric. Food Chem.*, 38 (1990) 1918.
[40] R.M. Pollman, *J. Assoc. Off. Anal. Chem.*, 72 (1989) 425.
[41] K.W. Swallow and N.H. Low, *J. Agric. Food Chem.*, 38 (1990) 1828.
[42] S. Mou, Q. Sun and D. Lu, *J. Chromatogr.*, 546 (1991) 289.
[43] K.A. Garleb, L.D. Bourquin and G.C. Fahey, *J. Agric. Food Chem.*, 37 (1989) 1287.
[44] S.C. Churms, *J. Chromatogr.*, 500 (1990) 555.
[45] Y.C. Lee, *Anal. Biochem.*, 189 (1990) 151.
[46] D.C. Johnson, D. Dobberpuhl, R. Roberts and P. Vandeberg, *J. Chromatogr.*, 640 (1993) 79.
[47] W. Bichard, *B.Sc. Thesis*, Concordia University, Montreal, April 1990.
[48] J.M. Hachey, V.T. Bui, Y. Tremblay, D. Houde and W.G. Mihelich, *J. Wood Chem. Technol.*, 6 (1986) 389.
[49] G.W. Sanderson and B.P.M. Perera, *Analyst*, 91 (1960) 335.
[50] C. Ciavatta, M. Govi, L.V. Antisari and P. Sequi, *J. Chromatogr.*, 509 (1990) 141.
[51] M.N. Clifford, *J. Chromatogr.*, 94 (1974) 261.

ELSEVIER

Journal of Chromatography A, 671 (1994) 351–357

JOURNAL OF CHROMATOGRAPHY A

Simultaneous determination of anions and triclosan in dentifrices by gradient ion chromatography and isocratic high-performance liquid chromatography interfaced with conductivity and ultraviolet detection

Michael P. Demkowicz*, Varsha Chauhan, David A. Stern, Fred G. Vasquez

SmithKline Beecham Consumer Brands, Analytical/Microbiology Research Department, Parsippany, NJ 07054, USA

Abstract

The simultaneous separation of fluoride, phosphates and triclosan ions (F^-, PO_4^{3-}, $P_2O_7^{4-}$, $Cl_2H_7C_{13}O_2$) in a dentifrice formulation using a coupled ion chromatography and high-performance liquid chromatography system is described. The anion species are separated from the other components of a given dentifrice formulation using a Dionex IonPac AS11 (250 × 4.0 mm) analytical column. A sodium hydroxide (200 m*M* to 100% water) gradient mobile phase is used to elute the fluoride and phosphate species from the column within 7 min using a Dionex Anion Self-Regenerating Suppressor (ASRS-I 4 mm). The separation of anions and triclosan was carried out using a two-mobile phase system that simultaneously injected a 15-μl sample into the 200 m*M* NaOH to 100% water ion chromatography gradient system as well as a 10-μl sample into the water–acetonitrile (40:60) isocratic HPLC system. The anion species are then quantitated using a conductometric detector (0–30 μS). Triclosan is separated from the other components of the dentifrice formulation using a Waters Nova-Pak C_{18}, 4 μm, 150 × 3.9 mm HPLC column. A water–acetonitrile (40:60) mobile phase is used to elute the triclosan from the column within 6 min. The triclosan analyte is then quantitated using ultraviolet detection at 280 nm and 0.005 AUFS. All analytes are quantitated using the Dionex AI-450 chromatography software program (release 3.30).

1. Introduction

The primary goal in our laboratories is to measure the components of various dentifrice formulations by classical methods. The introduction of a multicomponent sample would encompass at least three times the amount of analyst preparation and analysis time using current methodologies. The aim of this study is to develop an assay that simultaneously determines the amount of fluoride, phosphate and triclosan from a single sample preparation.

In the present paper, we propose that a union of suppressed gradient ion chromatography (IC) and reversed-phase isocratic HPLC to provide the best of both worlds, in so far as quantitation of a multicomponent dentifrice matrix is concerned.

2. Principles

Frequently IC separation involves species of widely different affinities for the stationary phase. In such a case, eluent conditions that favor the resolution of most weakly held species

* Corresponding author.

0021-9673/94/$07.00
SSDI 0021-9673(93)E1250-4

are often unsuitable for the more tightly held ions in a sample matrix [1]. These samples cannot be easily handled by isocratic methods, because of their wide k' range [2]. The ionic separation is possible only by gradient elution over a specific concentration range.

Applications to ionic analysis using conductometric single-column IC were soon demonstrated [3]. More recently, Renn and Synovec [4] improved the potential practical utility of this concept with a system that simultaneously injects separate portions of an unknown sample into two individual IC systems, operating in parallel with different eluents.

Suppressed conductometric anion chromatography has proven to be the analytical technique of choice for the determination of strong and moderately weak acid anions [5]. If a column containing sulfonated polystyrene–divinylbenzene is treated with a hydrogencarbonate anion, the fixed quaternary amine moiety is completely converted into the carbonate anion form. The anions of interest will be exchanged in an equilibrium process for the carbonate anion. The separation of the anions will be controlled by their different affinities for the stationary phase [6].

Both from a theoretical and practical standpoint it is simplest to consider a background of nearly pure water, as may be obtained with NaOH eluent in suppressed IC system [7]. Recently developed electrodialytic on-line ultrapure eluent generators and suppressors [5] can indeed attain essentially pure water as the detector background.

The application of gradient elution in HPLC with UV detection follows directly [1]. The development of HPLC and the theoretical understanding of the separation processes involved have been, in particular, dependent on the fundamental studies by Horváth *et al.* [8], Knox [9], Scott [10] and Snyder [11]. Reversed-phase systems are characterized by strong interactions between the polar mobile phase and various sample molecules.

Moreover, interactions between sample molecules and the non-polar stationary phase are weak. This effect suggests that interactions between sample and solvent molecules will mainly determine relative retention and values of α in reversed-phase separations [12]. The differences in interactive energies between non-polar solutes with the mobile phase and the differences in hydrophobic solute molecular surface area are responsible for the functional group selectivity observed in reversed-phase chromatography [13].

3. Experimental

3.1. Apparatus

An electropneumatically driven microinjector valve (Dionex, Sunnyvale, CA, USA) equipped with a 15-μl loop and connected in series to a Dual-Stack Slider Valve equipped with a 10-μl loop (Dionex) was used for sample injections (see Fig. 1). The IC system was suppressed using a Dionex Anion Self-Regenerating Suppressor (ASRS-I 4 mm) with a SRS Controller setting of 3. The Autosuppression External Water Mode

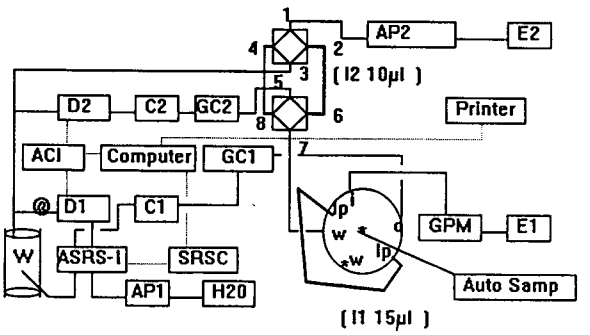

Fig. 1. Schematic of simultaneous injector system using two different columns and mobile phases. The MicroInjector Valve (MIV) and the Dual-Stacked Slider Valve (DSSV) (Dionex) are shown in the load position. AP1, AP2 = External HPLC pumps; ASRS-I = membrane suppressor; Auto Samp = Dionex automated sampler; ACI = Advanced Computer Interface; Computer = Dell system 310w/AI-450 software; C1, C2 = IonPac AS11, Nova-Pak C_{18}; D1, D2 = conductometric and UV detectors; E1, E2 = 200 m*M* NaOH and water–acetonitrile (40:60); GC1, GC2 = guard columns IonPac AG11 and Nova-Pak C_{18}; GPM = gradient pump module; I1, I2 = injector valves MIV (15 μl) and DSSV (10 μl); Printer = Digital 2100 Plus; SRSC = SRS controller; W = HPLC waste; @ = (4 mm) backpressure assembly.

was achieved using a Waters 6000A pump at a flow-rate of 2.1 ml/min. A Dionex IonPac AG11 (50 × 4.0 mm) guard column was used. The separations were carried out on a Dionex IonPac AS11 (250 × 4.0 mm). Table 1 shows the 200 m*M* NaOH to 100% water gradient profile. A gradient pump module (Dionex) was used to achieve a 3%/min gradient profile using a flow-rate of 2.0 ml/min and conductometric detection with a temperature compensation of 1.7°C. The samples were injected using an automated sampler (Dionex) with settings: Type: sample, Inj: 1, Type: loop, Mode: prop, Bleed: off, Inj/Vial: 1.

The isocratic HPLC system was achieved using a Waters 510 pump plumbed with 0.010 in. (1 in. = 2.54 cm) polyether ether ketone (PEEK) tubing (Dionex) into the Dual-Stacked Slider Valve. A Waters pre-column Guard-Pak consisting of a Nova-Pak C_{18} insert, and a Nova-Pak C_{18}, 4 μm, 60 Å, 150 × 3.9 mm analytical column was used for triclosan separations. The water–acetonitrile (40:60) eluent, at a 1.5 ml/min flow-rate, and a detection wavelength of 280 nm and 0.005 AUFS, was used. All injections were made at ambient temperature. The chromatograms were recorded and quantitated using the Dionex AI-450 chromatography software program (release 3.30).

The volumetric ware was Nalgene PMP. The pipettes were Kimax USA. The HPLC filters were 0.45-μm nylon Titan HPLC syringe type.

Table 1
Ion chromatographic gradient profile used to separate anions from dentifrice formulations

Time (min)	Flow (ml/min)	%1	%2	V5	V6
0.0	2.0	10	90	0	0
0.1	2.0	10	90	1	1
0.2	2.0	10	90	0	0
10.0	2.0	40	60	0	0
10.1	2.0	10	90	0	0
15.0	2.0	10	90	0	0

Ion chromatographic parameters: low pressure limit = 0; high pressure limit = 3000; eluent 1 = 200 m*M* NaOH; eluent 2 = 100% 18 MΩ deionized water; V5 off (0) = $PO_4^{3-}/P_2O_7^{4-}$; V5 on (1) = 15 μl; V6 off (0) = $Cl_2H_7C_{13}O_2$; V6 on (1) = 10 μl.

The centrifuge ware was Nalgene Oak Ridge (50 ml). The centrifuges used were DuPont refrigerated superspeed Servall RC-2 and Sorvall RC-5B both with an angular velocity of 13 000 rpm at 10–20°C. The vortex used was a Baxter SP mixer.

3.2. Materials

Dihydrogen disodium pyrophosphate (97.17% pure, Monsanto), triclosan (Irgasan 300, 100.1% pure, Ciba-Geigy), sodium phosphate dibasic (99.5% pure, Fisher Scientific), sodium fluoride (99.999% pure, Aldrich) were purchased commercially.

3.3. Analytical Reagents

NaOH volumetric solution (0.2 *M*, Mallinckrodt) and acetonitrile, UV grade (Burdick & Jackson) were also obtained commercially. The following dentifrice formulations were prepared by SmithKline Beecham Product and Process Development, Weybridge, UK: placebos and 80–120% of full formula.

3.4. Procedures

Preparation of standard stock solutions

Standard stock solutions were prepared to contain 80–120% (w/v) of their respective anions in 18 MΩ water. The triclosan stock solution was prepared in 100% acetonitrile. Each stock solution was diluted to a working standard stock concentration and diluted with their respective solvents and mixed thoroughly. For calibration purposes, dilute standard solutions of each analyte were prepared by stepwise dilution with a water–acetonitrile (40:60) diluent of each working standard stock solution to obtain exactly 80–120% of the full formula per 100 ml.

Preparation of tests solutions

A 10–20-g sample of dentifrice was composited, and from that a 2-g sample was accurately weighed into a 50-ml Nalgene centrifuge tube. An aliquot of 25 ml of (40:60) diluent was introduced along with 4 glass beads (4 mm) and

vortexed 4 min (speed 10) timed. The aliquots were cold centrifuged at 10–20°C for 15 min with an angular velocity of 13 000 rpm. The supernatant was quantitatively transferred into a 100-ml Nalgene PMP volumetric flask. The extraction procedure was repeated a total of three trials. The supernatants were completed to volume with the (40:60) diluent solution and mixed thoroughly on a vortex. A 1:20 dilution was performed and mixed thoroughly on a vortex. All sample and standard solutions were filtered using a 0.45-μm nylon filter.

Chromatographic separation of anions and triclosan

The separation of anions and triclosan was carried out using a two-mobile phase system that simultaneously injected a 15-μl sample into the 200 m*M* NaOH to 100% water IC gradient system as well as a 10-μl sample into the water–acetonitrile (40:60) isocratic HPLC system (see Fig. 1). The combined IC–HPLC system is described fully in the *Apparatus* section.

Calibration curves

Calibration curves were constructed from the three dilute standards of each anion and triclosan. Each concentration was injected onto the columns. Least squares regression was used to determine linearity characteristics.

Chromatographic analysis of dentifrice forms

The prepared test solutions were chromatographed three times against the constructed calibration curves.

4. Results and discussion

4.1. Chromatographic separation of anions and triclosan

To permit retention and good separation of both anions and triclosan in a single diluent preparation, an optimal water–acetonitrile diluent was selected. The extraction time was chosen at 3 times and water–acetonitrile (40:60) diluent concentration to yield 100 ± 3% recovery of both anions and triclosan. Optimization of the extraction time and diluent composition is illustrated in Table 2. The gradient optimization was reached at a concentration of 44–55 m*M* of the counterion in a mobile phase consisting of 200 m*M* NaOH to 100% water using a 3%/min gradient profile. A 50% decrease in the concentration of the counterion resulted a loss in resolution of the phosphate anions. Moreover, an increase in the gradient profile to 66% resulted in a loss of resolution of the early eluting fluoride ion.

Table 2
Analytical results of extraction time study (batch 016) to determine optimum sample extraction time using a water–acetonitrile diluent: recovery (%) *vs.* extraction trials

Analyte[a]	Recovery (%) (n = 3)			
	1 ×[b]	2 ×	3 ×	5 ×
Water–acetonitrile (50:50)				
F^-	100.26	108.99	108.65	110.34
$P_2O_7^{4-}$	105.47	110.32	107.84	108.74
$Cl_2H_7C_{13}O_2$	84.83	85.33	89.46	89.60
Water–acetonitrile (40:60)				
F^-	88.52	95.66	102.42	103.66
$P_2O_7^{4-}$	96.82	102.36	103.47	103.89
$Cl_2H_7C_{13}O2$	98.38	90.61	102.00	103.81

[a] Tube composite of separate sample masses.
[b] Number of extraction trials.

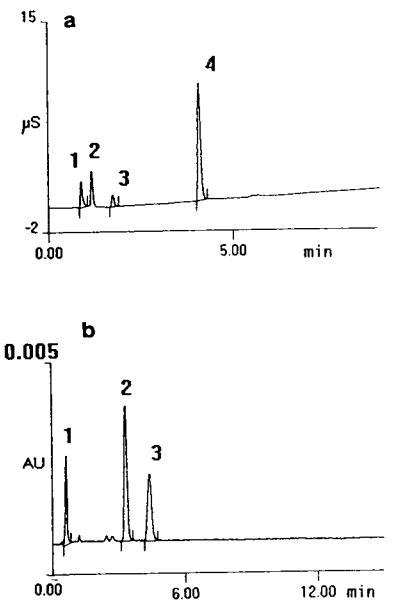

Fig. 2. (a) Representative chromatogram for identification and separation of anions within a (100%) dentifrice formulation. Peaks: 1 = F^-; 2 = unknown; 3 = PO_4^{3-}; 4 = $P_2O_7^{4-}$. (b) Representative chromatogram for identification and separation of triclosan within a (100%) dentifrice formulation. Peaks: 1 = unknown; 2 = unknown; 3 = $Cl_2H_7C_{13}O_2$. Note: chromatograms shown in each figure were obtained from a single injection.

4.2. Chromatographic separation of triclosan.

A method validated in our laboratory was modified to contain water–acetonitrile (40:60). Separation and quantitation of triclosan compared favorably to existing methodologies in our laboratory. Identification of each anion and triclosan was achieved after comparisons with relative retention times of standard dilutions of respective anions in the water–acetonitrile (40:60) diluent. Fig. 2a and b illustrates a good separation of the dentifrice formulation using the simultaneous injector system. The mean relative retention times (Table 3) obtained from six chromatograms of each anion were: 0.2324, 0.4414 and 1.0097, respectively. The mean relative retention time of triclosan was 1.0034 compared to a (100%) standard concentration as shown in Table 3.

At the optimum counterion concentration and water–organic ratio, separations of the analytes were obtained within 7 min.

4.3. Calibration curves

Table 3 shows that good linearity is accomplished for amounts of 80–120% of formula using three concentration levels.

4.4. Chromatographic analysis of anions and triclosan in some laboratory-scale dentifrice

Table 4 shows analytical results of some laboratory-scale aged dentifrice. The aged dentifrice was chosen to assess the impact of the stability indication of the developed assay. The method was found to show stability indications with the breakdown phosphate anion (PO_4^{3-}) eluting before the major phosphate component (see Fig. 2a). Proprietary constraints prohibit the declaration of amount of breakdown in the current dentifrice prototype. Moreover, the results

Table 3
Relative retention times (RRTs) of anions and triclosan and linearity of their calibration curves

Analyte	RRT	S.D. ($n = 6$)	Range (%)	R^2 [a]
F^-	0.2324[b]	0.0020	80–120	0.9913
PO_4^{3-}	0.4414[b]	0.0447	80–120	0.9960
$P_2O_7^{4-}$	1.0097[b]	0.0801	80–120	0.9977
$Cl_2H_7C_{13}O_2$	1.0034[c]	0.0024	80–120	0.9951

[a] R^2 obtained from three points.
[b] Relative to phosphate.
[c] Relative to a triclosan (100%) standard.

Table 4
Analytical results of (aged) laboratory scale dentifrice

Analyte[a]	Theory (% w/w)	Amount found (%, w/v) ($n = 3$)	Recovery (%)	R.S.D. (%)
F^-	80	78.03	97.78	1.91
	100	99.96	98.78	2.53
	120	88.21	73.51	0.37
$P_2O_7^{4-}$	80	93.48	111.38	2.32
	100	113.59	107.39	1.49
	120	143.49	94.20	0.36
$Cl_2H_7C_{13}O_2$	80	83.75	104.69	3.72
	100	107.46	107.46	0.99
	120	136.71	113.92	5.02

[a] Tube composites of separate sample masses.

found in Table 4 were calculated based upon a total amount of phosphate (PO_4^{3-} and $P_2O_7^{4-}$) recovered. Good recoveries and acceptable precision were obtained within a detection range of 80–120% of prototype formula levels.

4.5. Chromatographic analysis of anions and triclosan in a pilot batch

Table 5 shows analytical results of the pilot batch dentifrice. Good recoveries and acceptable precision were obtained at the (100%) full prototype formula level. Excipients did not show interference with the eluting anions and triclosan. Spiking the pilot production dentifrice with each analyte did not alter the relative retention time of each anion and triclosan.

5. Conclusions

The ability to extract both anions and triclosan from one sample preparation and resolve these analytes in 7 min using gradient IC coupled with isocratic HPLC has been demonstrated. This new method was found to be considerably faster than presently used methods for the determination of anions and triclosan in dentifrice formulations. The method has been shown to be stability indicating, yielding a reproducible amount of (PO_4^{3-}), within the linear range of the (PO_4^{3-}) calibration curve. Moreover, future applications as an encompassing cleaning validation method of anions and triclosan appear to show merit. Further development work will be addressed to assess method ruggedness.

Table 5
Analytical results of a pilot plant batch (016) of dentifrice containing anions and triclosan

Analyte	Theory (%, w/w)	Amount found (%, w/v) ($n = 6$)	R.S.D. (%)
F^-	100	97.72	4.40
$P_2O_7^{4-}$	100	98.15	2.74
$Cl_2H_7C_{13}O_2$	100	100.05	0.55

6. Acknowledgements

The authors are thankful to their spouses and families for their patience and understanding. We eminently appreciate the thorough review of the manuscript by Dr. E.R. Reynolds. The assistance and support from Dr. R. Soltero, A. Eggert and F. Vasquez are gratefully acknowledged. Technical assistance provided by Steve Albright of the Dionex Corporation was highly useful in the design of the injection system. The loan of chromatographic equipment from F. Roufaiel was appreciated. J. Sodano and J. Pierre of Product Development are thanked for their formulation assistance and supply of samples. We would like to thank P. Heller, R. Rivers and R. Crecco for their graphic art assistance and expertise.

7. References

[1] H. Small, in D. Hercules (Editor), *Ion Chromatography*, Plenum Press, New York, 1989, Ch. 7, p. 186, 36.

[2] L.R. Snyder, J.L. Glajch and J.J. Kirkland, in L.R. Snyder (Editor), *Practical HPLC Method Development*, Wiley, New York, 1988, Ch. 6, p. 154.

[3] S.A. Wilson, E.S. Yeung and D.R. Bobbit, *Anal. Chem.*, 56 (1984) 1457–1460.

[4] C.N. Renn and R.E. Synovec, *Anal. Chem.*, 61 (1989) 1915–1921.

[5] I. Berglund and P.K. Dasgupta, *Anal. Chem.*, 64 (1992) 3007–3012.

[6] J. Weiss, in E.L. Johnson (Editor), *Handbook of Ion Chromatography*, Dionex, Sunnyvale, CA, 1986, Ch. 3, p. 20.

[7] I. Berglund and P.K. Dasgupta, *Anal. Chem.*, 63 (1991) 2175–2183.

[8] Cs. Horváth, W. Melander and I. Molnár, *J. Chromatogr.*, 125 (1976) 129.

[9] J.H. Knox, in C.F. Simpson (Editor), *Practical High Performance Liquid Chromatography*, Heyden & Son, London, 1976.

[10] R.P.W. Scott, in C.F. Simpson (Editor), *Practical High Performance Liquid Chromatography*, Heyden & Son, London, 1976.

[11] L.R. Snyder, *Chromatogr. Rev.* 7 (1965) 1.

[12] P.C. Sadek and P.W. Carr, *J. Chromatogr. Sci.*, 21 (1983) 314.

[13] S. Ahuja, in J.D. Winefordner (Editor), *Selectivity and Detectability Optimizations in HPLC*, Wiley, New York, 1989, Ch. 6, p. 187.

ELSEVIER

Journal of Chromatography A, 671 (1994) 359–365

JOURNAL OF CHROMATOGRAPHY A

Determination of chelating agents in fertilizers by ion chromatography

Ivo Vande Gucht

Ministry of Agriculture, State Laboratory, Braamkasteelstraat 59, B 9050 Gentbrugge, Belgium

Abstract

In agronomy, chelating agents are used to complex trace elements (Fe, Mn, Zn, Cu, Co) for fertilization. An EEC directive allows the use of six chelating agents (EDTA, HEEDTA, DTPA, EDDHA, EDDHMA and EDDCHA), and requires an effective stability of at least 80%. An ion chromatographic method was developed to identify and determine the total amount of chelating agents in fertilizers. Precolumn derivatization of the metal chelates to the corresponding Fe(III) chelates is followed by elution with HNO_3–NaOAc mixture, postcolumn reaction with $HClO_4$ and UV–Vis detection at 330 nm. The method offers a specific, sensitive technique for determining EDTA, HEEDTA and DTPA in fertilizers.

1. Introduction

The feature of controlling the concentration of the free form of metal ions is fundamental in the various applications of chelating agents. Best known is the example of EDTA, which, apart from being a common laboratory reagent, is widely used, *e.g.*, in the water treatment, cleaning, power, mining, textile, food, agricultural and pharmaceutical industries.

In agronomy, chelating agents are used for micronutrient fertilization in hydroculture and in foliar and soil application. The essential plant nutritive elements in mineral fertilizers can be divided into three groups: main elements (N, P, K), secondary elements (S, Ca, Mg, Na) and trace elements or micronutrients (Fe, Mn, Zn, B, Cu, Mo, Co). Trace elements deficiencies can be overcome by fertilization with salts, oxides, hydroxides, organomineral complexes and chelates of the trace elements. Chelates offer the highest efficiency, bringing the trace element into a plant-available form at relatively low doses from the soil to the root and into the plant cells. In Europe, EEC Directive 76/116 allows chelates of the elements Fe, Mn, Zn, Cu and Co to be used as such or incorporated in mixed fertilizers. An effective degree of chelation of at least 80% is required [1].

Six chelating agents are allowed to be used for this purpose. They all belong to the class of the aminocarboxylic acids, and are commonly abbreviated as EDTA, HEEDTA, DTPA, EDDHA, EDDHMA and EDDCHA. The full names and structures of the compounds considered in this study (EDTA, HEEDTA, DTPA, EDDHA, and two related compounds DCTA and NTA) are illustrated in Fig. 1.

The concentration of these chelating agents in commercial fertilizers can range from about 0.01% to more than 50%. At low levels, the identification and determination of these compounds constitute a difficult analytical problem, especially in the presence of a complex matrix

0021-9673/94/$07.00
SSDI 0021-9673(94)00124-R

EDTA Ethylenediaminetetraacetic acid

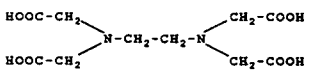

HEEDTA 2-Hydroxyethyl-ethylenediaminetriacetic acid

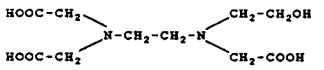

DTPA Diethylenetriaminepentaacetic acid

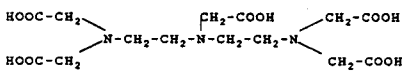

EDDHA Ethylenediamine-di-(2-hydroxyphenyl) acetic acid

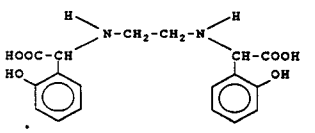

DCTA 1,2-diamino-cyclohexanetetraacetic acid

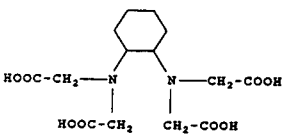

NTA Nitrilotriacetic acid

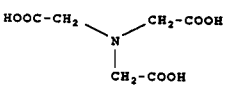

Fig. 1. Structures of some important chelating agents of the aminocarboxylic acid group [2].

with large amounts of other water-soluble substances.

Further, from an agronomic point of view, the determination of the stability of a chelate is considered to be a more important concern than the determination of the nature and the amount of a chelating agent. The lack of clear evidence about the efficiency of chelates under field conditions and the possible mobilization of heavy metals such as Cd, Ni and Pb call for a detailed study of the stability of a given chelate in fertilizer, soil and plant extracts.

The chemistry involved in the formation and stability of a chelate in complex media is characterized by a number of chemical equilibria, which can be characterized by their physical constants [3,4]. The most important equilibria, illustrated for Mn–EDTA as an example, are as follows:

(i) complexation of the metal ion by the chelating agent (stability constant K_c):

$$Mn^{2+} + EDTA^{4-} \rightleftharpoons Mn\text{–}EDTA^{2-}$$

(ii) protonation of the chelating agent (dissociation constant K_A):

$$H_4EDTA \rightleftharpoons H_3EDTA^- \rightleftharpoons H_2EDTA^{2-} \rightleftharpoons HEDTA^{3-} \rightleftharpoons EDTA^{4-}$$

(iii) oxidation–reduction of the metal ion (reduction potential E_0):

$$Mn^{2+} \rightleftharpoons Mn^{3+} \rightleftharpoons Mn^{4+}$$

(iv) hydroxylation of the metal ion:

$$Mn^{2+} \rightleftharpoons Mn(OH)^+ \rightleftharpoons Mn(OH)_2 \rightleftharpoons Mn(OH)_3^-$$

(v) precipitation of the metal ion (solubility product K_s):

$$MnO_2;\ MnCO_3;\ Mn_3(PO_4)_2;\ Mn(OH)_2$$

It is clear that the entire chelation process is considerably influenced by (1) the pH, affecting all of the above equilibria, (2) the nature of the chelating agent and the metal ion and (3) the presence of other competing metal ions and complexing or chelating agents.

As these chelates tend to form highly water-soluble ionic species, the choice of ion-exchange chromatography as an analytical method seems to be justified. Although the retention mechanism is governed by ion exchange, the complexation behaviour plays an important role, both thermodynamically and kinetically. Further, non-ionic interactions of the analytes with the stationary phase can be expected, *e.g.*, the interactions of the phenolic groups of some chelating agents with a polystyrene–divinylbenzene-based substrate.

The final objective, the separation of a complex mixture of chelates, formed by reaction of different chelating agents with different metal ions, has not been reported. Because of the complexity of the system, subdivision of the problem should be considered: the separation of different chelating agents associated with a single

metal ion; and the separation of different metal ions associated with a single chelating agent. Existing methods were considered in this respect. A standard application, developed for polyphosphates and other polyvalent complexing agents, using acidic elution and postcolumn derivatization with UV–Vis detection, offered good prospects for the separation of different chelating agents [5,6].

2. Experimental

2.1. Reagents and solutions

Eluents were prepared by dissolving or diluting analytical-reagent grade products (nitric acid, sodium acetate and potassium hydrogentartrate, all from Merck, Darmstadt, Germany) in water purified with an Elgastat UHQ system (Elga, UK) and degassed with helium. Eluents containing potassium hydrogentartrate became cloudy after a few days and were therefore replaced daily. Stock standard solutions (1 m*M*) of metal ions such as Fe(III), Mn(II), Zn(II), Cu(II) and Co(II) were prepared by dissolving high-purity salts [$Fe(NO_3)_3 \cdot 9H_2O$, $MnSO_4 \cdot H_2O$, $ZnSO_4 \cdot 7H_2O$, $CuSO_4 \cdot 5H_2O$, and $CoSO_4 \cdot 7H_2O$, all from Merck] in water. The Fe(III) solution was prepared immediately before use.

Stock standard solutions (1 m*M*) of the chelating agents EDTA, HEEDTA, DTPA, EDDHA, DCTA and NTA were prepared by dissolving the corresponding sodium salts in water or the acids in 5 m*M* NaOH using: $Na_2EDTA \cdot 2H_2O$ (Merck), $Na_3HEEDTA$ (Fluka, Buchs, Switzerland), H_5DTPA (Merck), H_4EDDHA (Sigma, St. Louis, MO, USA), $H_4DCTA \cdot H_2O$ (UCB, Brussels, Belgium) and H_3NTA (Merck).

Standard solutions of metal chelates were prepared by mixing appropriate volumes of metal ion solutions with those of chelating agents to obtain stoichiometrically balanced combinations of metal ions and chelating agents.

Samples of fertilizers were ground, sieved to 0.1 mm, extracted with water at room temperature and filtered through folded Whatman 2V filter-paper. Before injection, solutions were, if necessary, filtered again through a 0.2-μm membrane filter. Unless stated otherwise, all metal chelates were injected in concentrations of 0.01–0.1 m*M*.

2.2. Instrumentation

A Dionex Series 2003i ion chromatograph was used with a 50-μl injection loop, an isocratic pump and a UV–Vis detector with a 330-nm filter. For postcolumn derivatization an unheated reagent delivery module was used. Different 4-mm columns were used, all from Dionex. An Ion Pac AS7 separator in combination with an Ion Pac AG7 or NG1 guard column was used. The Ion Pac AS7 separator contains a 10-μm poly(styrene–divinylbenzene) (PS–DVB)-based substrate agglomerated with an aminated ion-exchange latex. Ion Pac NG1 is a PS–DVB-based reversed-phase guard column without any functional groups. The flow-rate was 0.5 ml/min. Chromatograms were recorded with a Shimadzu Series C-R5A Chromatopac integrator. For atomic absorption spectrometry, a Perkin-Elmer Series 2380 spectrometer with deuterium-arc background correction was used.

3. Results and discussion

The standard application for polyvalent complexing agents utilizes 30–70 m*M* HNO_3 as the eluent (isocratic), postcolumn derivatization with 1 g/l $Fe(NO_3)_3 \cdot 9H_2O$ in 2% $HClO_4$ and UV–Vis detection at 330 nm. The separation column used features a high capacity (80 μequiv. per column) and a relatively high hydrophobic nature, having both anion- and cation-exchange capacity [7]. With a sample containing only free chelating agents, *e.g.*, H_4EDTA, or the corresponding Na salts, the forms eluting on the column under acidic conditions ($pH \approx 1.3$) are the free, fully protonated forms [8].

Fig. 2 illustrates the separation of a mixture of the sodium salts of NTA, EDTA, HEEDTA, DTPA and EDDHA. However, when the sample contains stronger chelates such as Fe(III)–

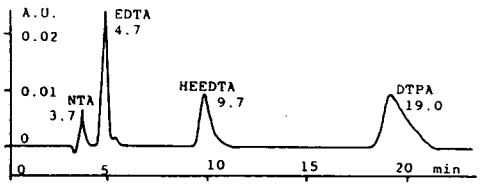

Fig. 2. Separation of the sodium salts of NTA, EDTA, HEEDTA and DTPA. Eluent, 70 m*M* HNO_3; columns, Ion Pac AS7 + guard; detection, postcolumn reaction with Fe(III)–$HClO_4$ with subsequent UV spectrophotometry at 330 nm EDDHA was not detected.

EDTA, some of which only partially dissociate, an influence of the associating metal ion on the retention time of the corresponding chelating agent can be observed, as illustrated in Fig. 3.

Table 1 shows the stability constants of some metal chelates of EDTA, HEEDTA and DTPA [2]. In an acidic environment, one would expect the sodium salt and the relatively weak EDTA complexes (Mn, Zn) to dissociate and the acid form of EDTA to elute (Fig. 3a–c). Only Fe(III) would remain complexed and elute as the less strongly retained Fe–EDTA (Fig. 3d). Cu–EDTA creates an intermediate situation, with the chelate partially dissociating during the run, giving a Cu–EDTA peak moving ahead of a

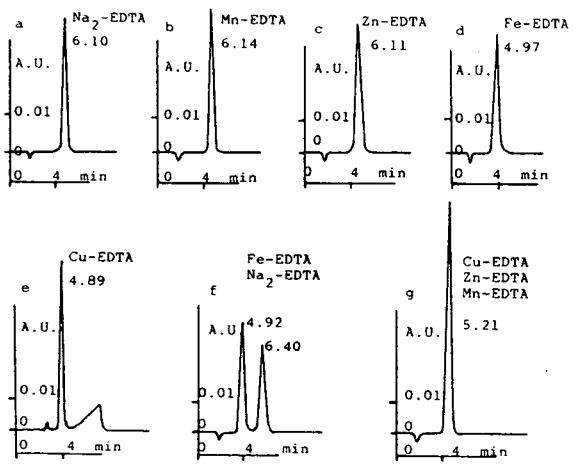

Fig. 3. Influence of the associating metal ion on the retention time of EDTA. Eluent, 50 m*M* HNO_3; columns and detection, as in Fig. 2. Injection of (a) Na_2EDTA, (b) Mn–EDTA, (c) Zn–EDTA, (d) Fe–EDTA, (e) Cu–EDTA, (f) Na_2EDTA + Fe–EDTA and (g) Cu–EDTA + Zn–EDTA + Mn–EDTA; solute concentrations 0.04 m*M*.

Table 1
Stability constants (log K_c) of different metal chelates of EDTA, HEEDTA and DTPA [3]

Metal ion	Log K_c		
	EDTA	HEEDTA	DTPA
Al^{3+}	16.3	14.3	18.6
Ba^{2+}	7.86	6.3	8.87
Ca^{2+}	10.69	8.3	10.83
Co^{2+}	16.31	14.6	19.27
Cu^{2+}	18.80	17.6	21.55
Fe^{2+}	14.32	12.3	16.5
Fe^{3+}	25.1	19.8	28.0
Mg^{2+}	8.79	7.0	9.3
Mn^{2+}	13.87	10.9	15.6
Ni^{2+}	18.62	17.3	20.32
Pb^{2+}	18.04	15.7	18.80
Sr^{2+}	8.73	6.9	9.77
Zn^{2+}	16.50	14.7	18.4

fronting peak of free EDTA (Fig. 3e). Injection of a mixture of Na_2EDTA and Fe–EDTA results in two peaks, corresponding to free EDTA and Fe–EDTA (Fig. 3f). Mixtures of Mn–EDTA, Zn–EDTA, and Cu–EDTA elute as a single peak with an average retention time, shifted toward the retention time of the most stable complex (Fig. 3g).

Subsequently, the method was modified by including a precolumn treatment of the sample with Fe(III) in an acidic medium, replacing the chelated metal ion present in the sample with Fe(III). This simple procedure permits only Fe chelates to be eluted and a single retention time to be obtained for a given chelating agent, independent of the associated metal ion. The precolumn treatment is carried out by mixing four volumes of the sample solution (concentration of chelating agents between 0.01 and 0.1 m*M*) with 1 volume of a solution of 5 g/l $Fe(NO_3)_3 \cdot 9H_2O$ in 0.15 *M* HNO_3, allowing it to react for 5 min at room temperature. The postcolumn reaction is carried out with 2% $HClO_4$, stabilizing the Fe chelates and increasing the absorbance at 330 nm.

As illustrated in Fig. 4, the influence of the eluent composition on retention, resolution and

detection was studied with mixtures of sodium salts of NTA, EDTA, HEEDTA, DTPA and EDDHA. In comparison with Fig. 2, it is clear from Fig. 4a that Fe chelates elute much faster than the corresponding free chelating agents. As generally expected, Fig. 4a–c show for DTPA as an example that with increasing pH the negative charge of the chelate also increases, causing a longer retention. The pH of all eluents was kept acidic to prevent the influence of matrix components in the fertilizers. The presence of acetate and tartrate in the eluent positively affects the selectivity and permits better resolution of EDTA, HEEDTA and DTPA (Fig. 4b–d).

The importance of non-ionic interactions of the analyte with the stationary phase was demonstrated for EDDHA and DCTA. EDDHA does not elute when both guard and separation columns are used. However, using the much shorter guard column AG7 and an eluent consisting of 50 m*M* HNO_3–50 m*M* NaOAc, Fe–EDDHA elutes as a single peak, indicating that the

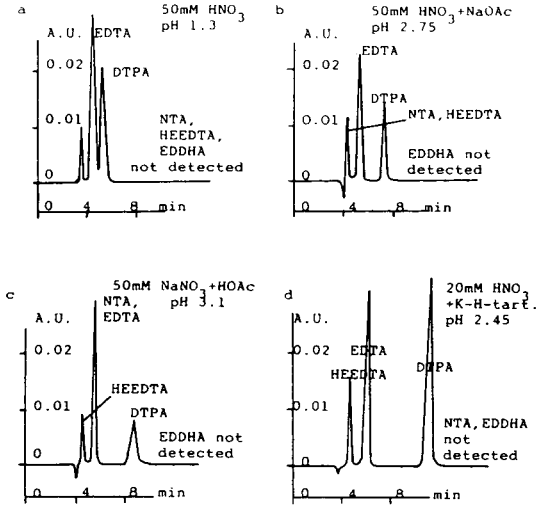

Fig. 4. Influence of eluent composition on retention, resolution and detection. Columns, as in Fig. 2, precolumn reaction of the sodium salts of NTA, EDTA, HEEDTA, DTPA and EDDHA with Fe(III)–HNO_3; postcolumn reaction with $HClO_4$ with subsequent UV spectrophotometry at 330 nm. Eluents: (a) 50 m*M* HNO_3 (pH 1.3); (b) 50 m*M* HNO_3–50 m*M* NaOAc (pH 2.75); (c) 50 m*M* $NaNO_3$–50 m*M* HOAc (pH 3.1); (d) 20 m*M* HNO_3–20 m*M* potassium hydrogentartrate (pH 2.45).

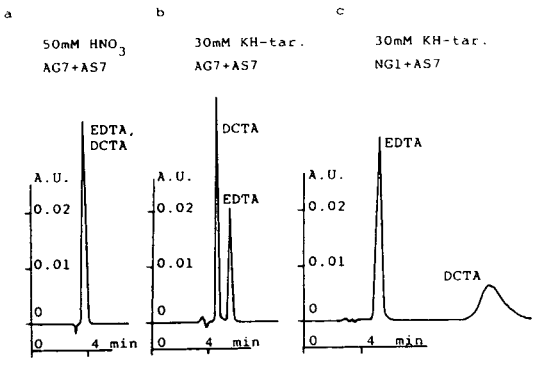

Fig. 5. Resolution of EDTA and DCTA. Precolumn reaction of the sodium salts of EDTA and DCTA with Fe(III)–HNO_3; detection, postcolumn reaction with $HClO_4$ and subsequent UV spectrophotometry at 330 nm, (a) 50 m*M* HNO_3 as the eluent and Ion Pac AS7 + guard columns as the separator; (b) 30 m*M* potassium hydrogentartrate as the eluent and Ion Pac AS7 + guard columns as the separator; (c) 30 m*M* potassium hydrogentartrate as the eluent and Ion Pac AS7 + NGl guard columns as the separator.

compound adsorbs on the substrate material due to its phenolic groups. As illustrated in Fig. 5, non-ionic interactions also determine the retention behaviour of DCTA.

The above-described method using an AS7 separator in combination with an NG1 guard column, 50 m*M* HNO_3–50 m*M* NaOAc as the eluent, precolumn treatment with Fe(III)–HNO_3, postcolumn reaction with $HClO_4$ and UV detection at 330 nm was tested to check its analytical performance. Standard solutions of EDTA, HEEDTA and DTPA with concentrations between 0.01 and 0.2 m*M* were injected and peak heights measured. Sensitivities, detection limits and correlation coefficients were derived from three calibration graphs and are given in Table 2. Table 2 also shows that, after fifteen injections of standard solutions (0.01–0.2 m*M*), the retention times do not shift significantly.

A recovery study was carried out with three commercial NPK fertilizers not containing chelated trace elements. Before extraction, the samples were spiked with three levels of EDTA, HEEDTA and DTPA, corresponding to amounts of 0.01, 0.1 and 1% (w/w), and an excess of 10% (mol Cu/mol chelating agent) of Cu(II) was added. Two fertilizers were only

Table 2
Sensitivities, detection limits, correlation coefficients and retention times of EDTA, HEEDTA and DTPA (0.01–0.2 m*M*)

Parameter	EDTA	HEEDTA	DTPA
Sensitivity (absorbance/m*M*)	0.312	0.208	0.364
Detection limit (m*M*)	0.00578	0.00659	0.00717
Correlation coefficient	0.99989	0.99986	0.99984
Retention time (min)	4.539 ± 0.109	3.977 ± 0.073	6.399 ± 0.155

Precolumn treatment with Fe(III)–HNO_3; eluent, 50 m*M* HNO_3–50 m*M* NaOAc; AS7 separation + NG1 guard columns; postcolumn reaction with $HClO_4$; UV detection at 330 nm.

spiked with EDTA and the third fertilizer was spiked with EDTA, HEEDTA and DTPA. The results are given in Table 3. Matrix components from fertilizers interfere only slightly by increasing the void volume signal, as illustrated in Fig. 6.

The method proved to be satisfactory for the determination of the total amount of EDTA, HEEDTA and DTPA in mixed fertilizers at levels down to 0.1%. In fact, the system is completely insensitive even to large amounts of chloride, nitrate, carbonate, sulphate and orthophosphate. It must be emphasized that, after repeated injections of solutions treated with excess of Fe(III), the characteristics of the separation column are irreversibly altered. Residual iron on the column leads to a decrease in sensitivity for sulphate and orthophosphate. Solutions of Mn–EDTA, Zn–EDTA, Co–EDTA and Cu–EDTA were injected onto the "contaminated" column, without precolumn treatment with Fe(III)–HNO_3. After postcolumn reaction with Fe(III)–$HClO_4$ and UV detection at 330 nm, the eluate was fractionated and the

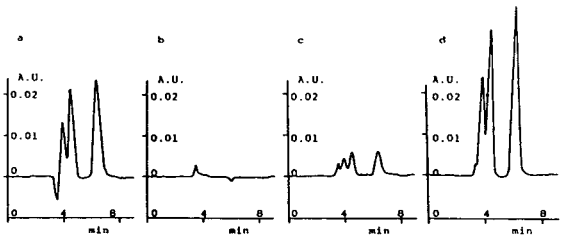

Fig. 6. Chromatograms for (a) a standard solution of HEEDTA, EDTA and DTPA (each 0.08 m*M*), (b) NPK 15.5.15 fertilizer, and the same sample spiked with (c) 0.1% (w/w) and (d) 1% (w/w) of HEEDTA, EDTA and DTPA, in the presence of an excess of Cu(II). Method: see Table 2.

Table 3
Recoveries of EDTA, HEEDTA and DTPA when added at levels of 0.01, 0.1 and 1% (w/w) to commercial fertilizers, in the presence of an excess of Cu(II)

Sample declaration	Concentration added (%, w/w)	Recovery (%)		
		EDTA	HEEDTA	DTPA
NPK 12.8.16 + 10 SO_3	0.01	97	–[a]	–[a]
	0.1	94	–[a]	–[a]
	1	114	–[a]	–[a]
NPK 9.8.18 + 15 SO_3	0.01	107	–[a]	–[a]
	0.1	95	–[a]	–[a]
	1	96	–[a]	–[a]
NPK 15.5.15	0.01	65	–[b]	137
	0.1	103	114	94
	1	103	98	109

Method: see Table 2.
[a] No spike added.
[b] Below determination limit.

collected EDTA fraction analysed by atomic absorption spectrometry. In all instances, except with Cu–EDTA, the only metal present in the collected fraction was iron. When Mn–EDTA, Zn–EDTA or Co–EDTA was injected, these metals were not recovered in the EDTA fraction, but in the void volume fraction. In spite of the acidic eluent, residual iron remains on the column, replacing manganese, zinc and cobalt from their weak complexes, letting the free metal ions run rapidly through the column.

Acknowledgement

The author thanks the staff of Dionex (Mechelen, Belgium) for providing technical advice and financial support.

References

[1] *Off. J. Eur. Commun.*, No. L 281/116 (1989) 116.
[2] L. Kaudy, J.F. Rounsaville and G. Schulz (Editors), *Ullmann's Encyclopedia of Industrial Chemistry*, Vol. A10, J.R. Hart, W.R. Grace and Co., Lexington, MA, 1987, pp. 95–99.
[3] A. Ringbom, *Complexation in Analytical Chemistry*, Wiley, New York, 1963.
[4] A. Ringbom, *Les Complexes en Chimie Analytique*, Dunod, Paris, 1967.
[5] *Dionex Application Note 44*, Dionex, Sunnyvale, CA, 1983.
[6] J. Weiss, *Handbook of Ion Chromatography*, Dionex, Sunnyvale, CA, 1986, pp. 55 and 71.
[7] *Dionex Product Selection Guide 1991*, Dionex, Sunnyvale, CA, 1991.
[8] Dionex, Mechelen, personal communications.

ELSEVIER

Journal of Chromatography A, 671 (1994) 367–374

JOURNAL OF CHROMATOGRAPHY A

Determination of trace levels of cyanamide in a novel potassium channel activator bulk drug by pulsed electrochemical detection

Jay B. Nair

Analytical Research and Development, Bristol-Myers Squibb Pharmaceutical Research Institute, New Brunswick, NJ 08903-0191, USA

Abstract

Trace amounts of cyanamide may be found in a novel potassium channel activator bulk drug. A chromatographic method is described for detecting trace levels of cyanamide as low as 1 ppm (w/w) using pulsed electrochemical detection at a silver electrode. The bulk drug is dissolved in acetonitrile–water and injected into the IC system. Cyanamide is eluted under isocratic conditions within 10 min.

1. Introduction

Trace amounts of cyanamide may be found in bulk drugs where cyanamide was used in the synthesis of the drug or one of the intermediates. In this report we show a method developed for detecting trace levels of cyanamide in a novel potassium channel activator bulk drug. A sensitive method was needed to determine levels of cyanamide in the bulk drug since cyanamide is toxic and complete removal of it was important from a process development point of view.

Cyanamide detection has been reported using a number of different techniques. A liquid chromatographic method was used to detect calcium cyanamide after pre-column derivatization to dansyl cyanamide [1]. This was used as a stability indicating assay for the analysis of calcium cyanamide in bulk material and dosage form. Cyanamide in plasma was detected selectively and sensitively using another pre-column derivatization technique with 5-(dimethylamino)naphthalene-1-sulfonyl chloride [2]. Chemical assays for cyanamide in biological fluids have been reviewed [3]. Further studies include: the spectrophotometric determination of cyanamide with pentacyanoferrates [4], a gas chromatographic method to detect cyanamide in blood plasma after extraction and derivatization with heptafluorobutyric anhydride (HFBA) [5], a reaction rate method for determining trace concentrations of cyanamide [6], use of an ion selective electrode for cyanamide [7], an infrared method to determine trace quantities of cyanamide in guanidine sulfate [8], indirect argentometry to detect cyanamide in solutions [9], analysis of cyanamide derivatives by the separation of mixtures on ion-exchange resins [10], and use of *p*-phenylenediamine hydrochloride for the spectrophotometric determination of cyanamide [11]. Many of these methods are tedious since they involve derivatization of some sort.

In this paper, a direct chromatographic method using pulsed electrochemical detection

0021-9673/94/$07.00
SSDI 0021-9673(94)00228-2

(PED), on a polymeric AS-10 anion-exchange column, is described for sensitive determination of cyanamide in a bulk drug substance.

The pulsed electrochemical detector is equipped with a pair of silver working electrodes. Silver enables selective detection of the cyanide moiety in the cyanamide molecule with extremely high sensitivity at a very low oxidation potential (+0.08 V) according to the reaction:

$$Ag^0 + (H_2NCN)^- \rightleftharpoons Ag^+(CNNH_2)^-$$

This chromatographic method with PED can monitor cyanamide down to ppm (w/w) levels in a bulk drug substance as shown in this study.

2. Experimental

2.1. Instrumentation

A Dionex gradient pump module (GPM) and eluent degas module (EDM-II) and Dionex pulsed electrochemical detector (PED-1) equipped with silver working electrodes were controlled through a Dionex interface (Dionex, Sunnyvale, CA, USA) by a Compaq Deskpro 386/25L personal computer running the AI-450 software version 3.30 (Dionex). The injector used was Hitachi autosampler Model 655A-40 (Hitachi Instruments, Danbury, CT, USA).

2.2. Reagents

Sodium hydroxide 50% (w/w) was purchased from J.T. Baker (Phillipsburg, NJ, USA). 200 m*M* Sodium Hydroxide was prepared from this solution. HPLC grade acetonitrile (MeCN) was obtained from Baxter Scientific (McGaw Park, IL, USA). Deionized water was further purified using a Millipore Milli-Q system (Millipore, Bedford, MA, USA). All mobile phases were filtered before use with 0.45-μm Nylon-66 filters (Schleicher & Schuell, Keene, NH, USA) and a solvent filtration kit (Schleicher & Schuell). Hydrochloric acid (concentrated) was purchased from J.T. Baker from which a 1-*M* solution was prepared for column clean-up. Cyanamide 50% (w/w) was obtained from Aldrich (Milwaukee, WI, USA) and was used for standard preparations.

2.3. Chromatographic system

An IonPac AS-10 anion chromatographic column with an IonPac AG-10 anion guard column (Dionex) was used. Mobile phase [MeCN–50 m*M* NaOH (1:99)] was prepared by transferring 500 ml of 200 m*M* sodium hydroxide and 20 ml acetonitrile into a 2-l volumetric flask and diluting to volume with water. The flow-rate was 1 ml/min. The column temperature was ambient. Under these conditions cyanamide elutes in under 10 min.

2.4. Detector conditions

Detection was performed with a Dionex pulsed electrochemical detector using silver electrodes. Range on the detector was 300 nC. Data sampling was done only from 0.1 to 0.78 s (one pulsing cycle is 0.88 s). After that, a positive pulse at 0.1 V and a negative sweep at −0.1 V cleaned the electrode surface.

Data collection was performed on a chart recorder (Kipp & Zonen, Delft, Netherlands) or an IBM-PS/2 computer with an advanced computer interface (Dionex) and AI-450 software (Dionex). The A1-450 software also controlled the Dionex instrument and the gradient program. Data was simultaneously collected on a Micro VAX 3400 microcomputer running VG Multichrom software version 1.8 through a VG chromserver (VG Instruments, Danvers, MA, USA).

2.5. Preparation of standards and samples

Sample solvent was prepared by separately measuring equal amounts of MeCN and water, combining them in a suitable container and mixing well. Stock solution 1 (1000 μg/ml cyanamide) was made by accurately weighing 100 mg 50% cyanamide into a 50-ml volumetric flask containing 25 ml of the sample solvent. It was diluted to volume with the sample solvent and

mixed well. From this stock solution working standard solution 1 (100 ng/ml cyanamide), working standard solution 2 (50 ng/ml cyanamide) and working standard solution 3 (15 ng/ml cyanamide) were made by appropriate dilutions with the sample solvent.

Working sample solution (5 mg/ml of the bulk drug) was prepared by transferring 50.0 mg of the bulk drug sample into a 10-ml volumetric flask. A volume of 5.0 ml of MeCN was transferred to the flask and after sample dissolution diluted to volume with water.

3. Results and discussion

Fig. 1 shows the chromatogram of the working standard solution 3 containing cyanamide at 15 ng/ml. The retention time of cyanamide is 6.99 min and the k' was calculated to be 1.33. The pulse feature of PED provides baseline stability due to the clean electrode surface resulting in better reproducibility compared to continuous DC amperometry. Fig. 2 shows the chromatogram of a blank injection (sample solvent). A very small peak is seen in the blank at the retention time of cyanamide which calculates to be less than 1 ppm (the detection limit). Fig. 3 shows the chromatogram of the bulk drug substance stored at 30°C and 75% relative humidity. Fig. 4 shows the chromatogram of a sample after the synthetic process had been optimized. The process has been optimized so that the levels of cyanamide in typical batches of the potassium channel activator are less than the detection limit (1 ppm w/w) as shown in Fig. 4.

One of the main advantages of this technique is that no sample clean up is necessary due to the selectivity. In this instance, bulk drug substance is dissolved in acetonitrile–water (50:50) and directly injected into the ion chromatography (IC) system.

The linear regression data for cyanamide is shown in Table 1. Linearity standard solutions were injected over the range of 15 to 150 ng/ml. Peak areas were used for regression analysis. Within this range, cyanamide had a linear response, with a correlation coefficient of 0.9982. A three-point calibration is used for the quantitation of cyanamide. The three standards used here cover the range of 15–100 ng/ml (3–20 ppm).

Accuracy for cyanamide was determined by spiking a batch of the bulk drug substance at various levels with cyanamide and calculating the recovery (Table 2). Spiked sample solutions were prepared by adding 0–25 ppm cyanamide to the bulk drug substance solution. The re-

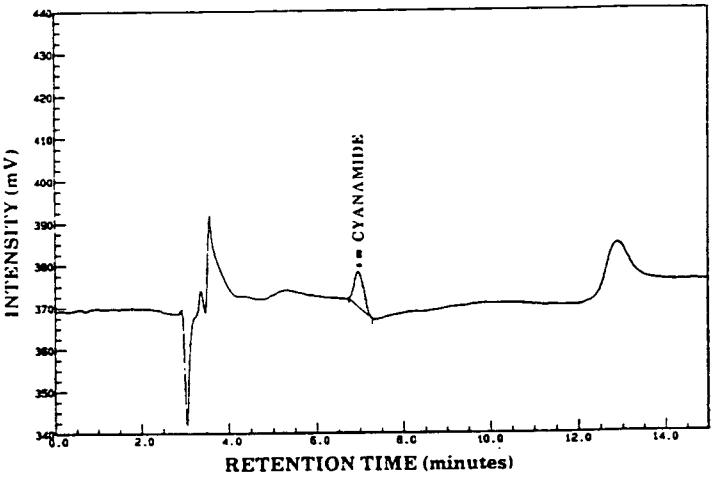

Fig. 1. Chromatogram of the working standard solution 3 showing cyanamide at 15 ng/ml (3 ppm for the drug concentration at 5 mg/ml).

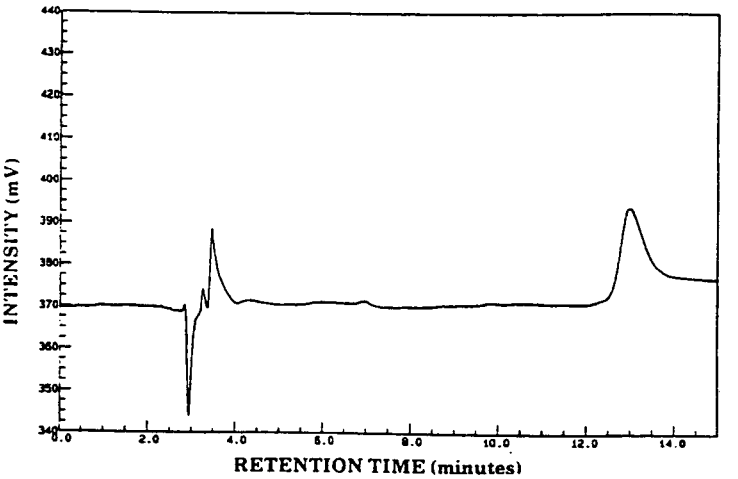

Fig. 2. Blank injection of the sample solvent, acetonitrile–water (50:50).

covery of cyanamide was determined by

$$\% \text{ Recovery} = \frac{\text{ppm found}}{\text{ppm spiked}} \cdot 100$$

The recovery of cyanamide was satisfactory. The recovery values for cyanamide spikes ranging from 3 to 25 ppm were 89 to 106%.

The precision of the system for cyanamide was determined by injecting the bulk drug substance at 5 mg/ml several times. An investigational batch containing 5 ppm (w/w) of cyanamide was used for this study. Peak areas of multiple injections of this same solution were used to calculate the precision of the system. The standard deviation was 0.25 for a mean value of 5.4 ppm and the coefficient of variation was 4.6% as shown in Table 3.

The intra-day reproducibility of the method

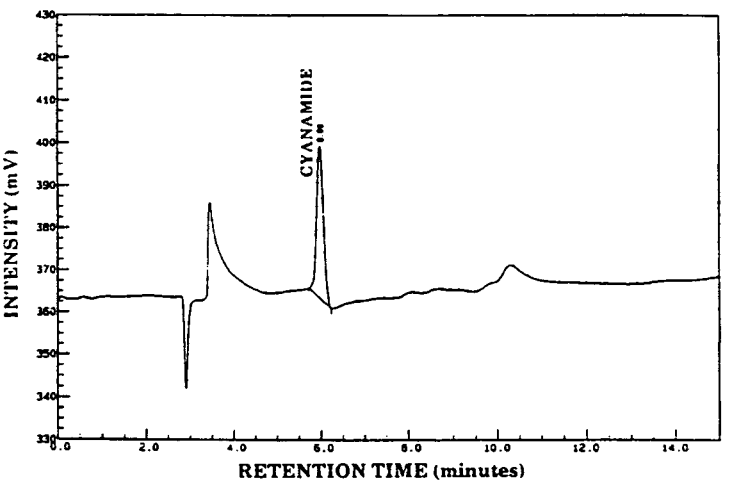

Fig. 3. Chromatogram of a batch of a highly stressed stability sample of the bulk drug substance.

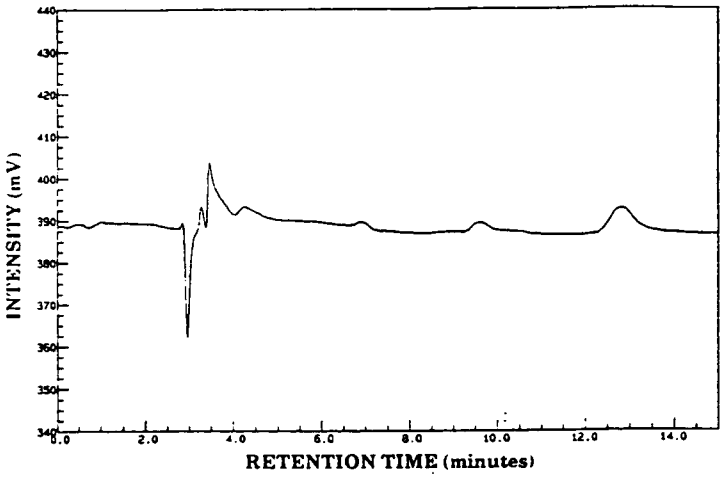

Fig. 4. A typical batch of the drug substance at the working concentration, 5 mg/ml.

Table 1
Linear regression for cyanamide

Concentration (ng/ml)	Area 1	Area 2	Mean peak area
14.99	147 460	140 702	144 081
24.99	218 601	204 770	211 686
49.85	381 401	363 189	372 295
74.78	521 410	512 321	516 866
99.70	648 182	657 579	652 881
124.6	766 612	788 738	777 676
149.6	879 904	909 206	894 555

$y = 5594x + 79\,670$; $r = 0.9982$.

Table 2
Recovery of cyanamide from the bulk drug substance

Added (ppm)	Found (ppm)	(Recovery (%)
0	<DL ($n = 4$)	–
2.99	2.76	92
4.99	5.06	101
9.98	10.62	106
14.96	15.51	104
19.95	18.82	94
24.94	22.26	89

for cyanamide was determined by weighing the bulk drug substance eight different times and analyzing the results using this method. The relative standard deviation was 6.4% for a mean value of 5 ppm and the standard deviation was 0.34. These results are shown in Table 4.

The inter-day reproducibility of the assay was demonstrated for three batches assayed on two days. Samples analyzed on day 1 gave compar-

Table 3
Precision of the system for cyanamide

Injection	Peak area	Cyanamide (ppm)
1	211 806	5.25
2	203 849	5.02
3	206 431	5.10
4	218 506	5.44
5	213 626	5.30
6	215 071	5.35
7	229 927	5.77
8	212 730	5.28
9	224 656	5.62
10	226 801	5.68
Mean	216 340	5.38
S.D.	8153	0.25
R.S.D. (%)	3.8%	4.6%

Table 4
Reproducibility of the method for cyanamide

Sample mass (mg)	Cyanamide found (ppm)		
	Injection 1	Injection 2	Mean
49.8	6.00	5.47	5.85
50.0	5.52	5.72	5.62
50.1	4.80	5.49	5.15
49.7	5.21	4.95	5.08
49.9	4.99	4.94	4.97
50.0	4.46	5.47	4.97
50.2	5.41	4.76	5.09
49.9	6.11	5.07	5.59
Mean			5.29
S.D.			0.34
R.S.D. (%)			6.4

able results on day 2, three weeks later. The results are shown in Table 5.

The stability of the spiked bulk drug substance working sample solutions (apparent pH *ca.* 5.4) also was investigated over a period of 53 h (*ca.* 2 days). No significant increase in cyanamide content was found in the sample solvent as shown in Table 6.

4. Estimation of detection limit (DL) and minimum quantifiable limit (MQL)

The detection limit (DL) and the minimum quantifiable limit (MQL) for cyanamide were estimated as a function of the standard deviation of the baseline noise and the slope of the linear regression line. The baseline noise was estimated from the standard deviation of the peak area of ten replicate injections of a batch containing *ca.* 5 ppm cyanamide (precision of the system study).

Table 5
Day-to-day reproducibility of the method

Batch number	Cyanamide (ppm)	
	Day 1	Day 2
3 138 216 823	11	11
3 138 216 727	5	4
3 138 216 427	11	11

Table 6
Stability of the bulk drug substance in the sample solvent

Period (h)	Cyanamide found (ppm)
4	11.50
7	12.30
26	13.43
29	12.54
53	13.31
	Mean = 12.62
	S.D. = 0.79
	R.S.D. = 6.26%

The DL and MQL values for cyanamide were estimated as follows:

$$\text{DL (ppm)} = \frac{3 \cdot \text{S.D.} \cdot 10^6}{S \cdot C_w}$$

$$\text{MQL (ppm)} = \frac{10 \cdot \text{S.D.} \cdot 10^6}{S \cdot C_w}$$

where: S.D. is the standard deviation of the baseline noise, estimated from the replicate injection reproducibility (area counts); 10^6 is a factor to convert to ppm; S is the sensitivity, *i.e.*, slope of the response *versus* concentration, determined from standard linearity evaluation (area counts per ng/ml); C_w is the working concentration ($5 \cdot 10^6$ ng/ml).

It has been observed that a DL of 1 ppm and a MQL of 3 ppm are reliably attainable for cyanamide, showing reasonable agreement with statistical calculations. Therefore, these values for DL and MQL are used for reporting purposes.

Fig. 5 is a chromatogram of the drug substance spiked with cyanamide at the DL (1 ppm). Fig. 6 is a chromatogram of the drug substance spiked at the MQL (3 ppm).

5. Conclusions

A highly selective ion chromatographic meth-

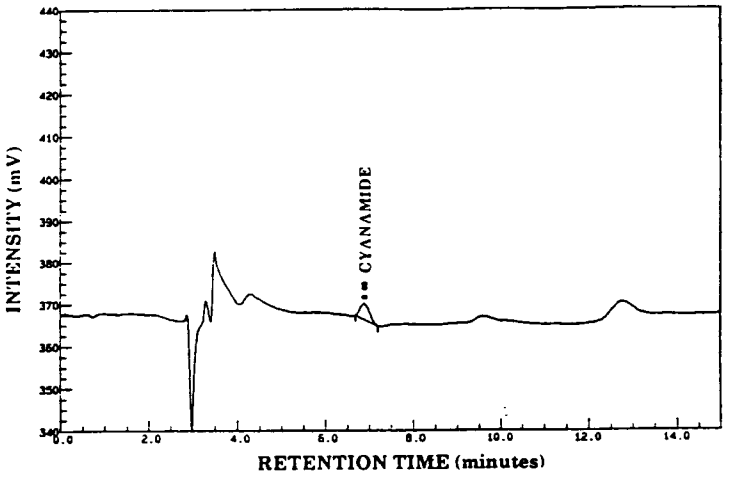

Fig. 5. Detection limit of cyanamide at 5 ng/ml (1 ppm) in the presence of the bulk drug substance at 5 mg/ml.

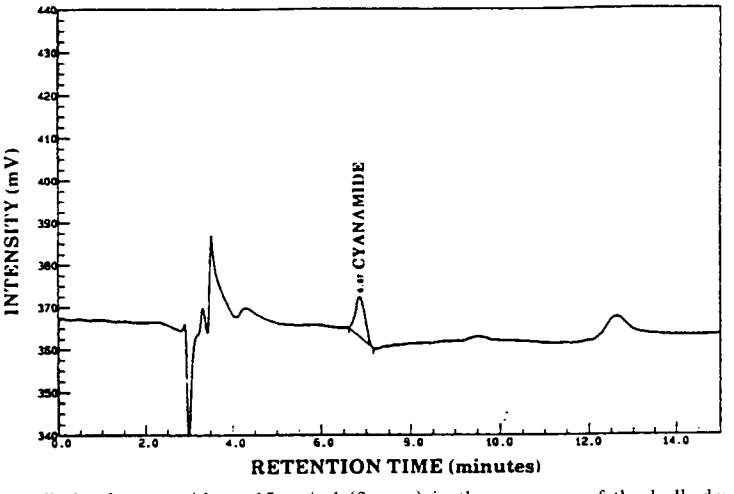

Fig. 6. Minimum quantifiable limit of cyanamide at 15 ng/ml (3 ppm) in the presence of the bulk drug substance at 5 mg/ml.

od with pulsed electrochemical detection (PED) was developed for the sensitive detection of ultratrace levels of cyanamide (1 ppm, w/w) in a novel potassium channel activator bulk drug substance.

Acknowledgement

The technical assistance of Mr. John Vargo is gratefully appreciated.

References

[1] S. Chen, A.P. Ocampo and P.J. Kucera, *J. Chromatogr.*, 558 (1991) 141.
[2] J. Prunosa, R. Obach and J.M. Valles, *J. Chromatogr.*, 377 (1986) 253.
[3] J.P. Brien and C.W. Loomis, *Alcohol. Clin. Exp. Res.*, 7 (1983) 256.
[4] I. Banyai and M.T. Beck, *Acta. Chim. Acad. Sci. Hung.*, 111 (1982) 141.
[5] C.W. Loomis and J.F. Brien, *J. Chromatogr.*, 222 (1981) 421.
[6] T.A. Nieman, F.J. Holler and C.G. Enke, *Anal. Chem.*, 48 (1976) 899.

[7] K. Toth and E. Pungor, *Hung. Sci. Instrum.*, 25 (1972) 15.
[8] T. Urbanya and A. Walter, *J. Pharm. Sci.*, 60 (1971) 1699.
[9] Z.E. Mel'chekova, *Zavod. Lab.*, 43 (1977) 1323.
[10] E.N. Boitsov, Yu.I. Mushkin and W.K. Karlik, *Zavod. Lab.*, 35 (1969) 790.
[11] T. Nakahachi, *Niigata Igakkai Zasshi*, 82 (1968) 478.

ELSEVIER

Journal of Chromatography A, 671 (1994) 375–382

JOURNAL OF CHROMATOGRAPHY A

Applications of capillary zone electrophoresis in clinical chemistry
Determination of low-molecular-mass ions in body fluids

W. Buchberger*, K. Winna, M. Turner

Department of Analytical Chemistry, Johannes-Kepler-University, A-4040 Linz, Austria

Abstract

Investigations were carried out on parameters influencing separation selectivity in the capillary zone electrophoresis of inorganic cations. Copper sulphate can be recommended as a carrier electrolyte salt for the separation of alkali and alkaline earth metal ions. Its separation selectivity is different from that of the widely used aromatic amines and it is compatible with indirect UV detection at 214 nm. The addition of organic solvents to the electrolyte results in a general increase in the migration times of divalent cations relative to monovalent cations. Ion-pairing reagents such as sodium dodecyl sulphate were found to exhibit specific effects on some ions (especially strontium and barium), but are less useful owing to interferences with the separation of alkali metal ions by sodium introduced with the ion-pairing reagent. Applications to the determination of cations relevant in clinical chemistry are demonstrated for serum samples. Further, the determination of anions in serum was investigated using chromate as electrolyte. Generally, the advantage of capillary zone electrophoresis over ion chromatography can be seen in the fact that proteins need not be removed from the sample and do not interfere with the separation of low-molecular-mass ions.

1. Introduction

The determination of inorganic cations (alkali and alkaline earth metal ions) and low-molecular-mass anions in body fluids is of considerable importance for diagnostic purposes and part of the routine tasks in clinical laboratories. Ion chromatographic methods, although capable of separating all of the relevant cations or anions in one run, have not found widespread acceptance. This may be partly due to problems with the lifetime of separation columns if proteinaceous samples such as serum or plasma are injected. Therefore, proteins should be removed before injection, but this requires additional sample preparation procedures, which can be time consuming or result in incomplete recoveries. Recently, the use of a new stationary phase with a semi-permeable surface allowed the direct injection of body fluids for the separation of anions by ion-interaction chromatography [1]. Nevertheless, problems still exist in separating early-eluting ions such as fluoride or organic acids from the proteins eluting in the void volume.

Capillary zone electrophoresis (CZE) should be capable of overcoming several of the drawbacks of chromatography. It is a highly efficient separation method for ionized species based on the combined effects of electrophoresis and electroosmosis and can handle proteinaceous

* Corresponding author.

0021-9673/94/$07.00
SSDI 0021-9673(94)00206-O

samples much better owing to the absence of a stationary phase. Denaturation and precipitation of proteins can easily be avoided by choosing a physiologically compatible carrier electrolyte. Further, this technique is likewise suited if only a limit amount of sample (*e.g.*, a few microlitres of tear fluid) is available.

This paper reports results from investigations into the applicability of CZE to the routine determination of several cations and some anions in different body fluids. Special attention was paid to the parameters affecting the separation selectivity of cations. The influence of different carrier electrolyte salts, of organic solvents and of ion-pairing reagents was investigated in detail.

2. Experimental

The CZE instrument employed was a Quanta 4000 (Waters, Milford, MA, USA) equipped with a negative and a positive high-voltage power supply and interfaced to a Hewlett-Packard Model 3359 data acquisition system. Separations were carried out using an AccuSep fused-silica capillary (52 cm effective length × 75 μm I.D.) (Waters). Injection was performed hydrostatically by elevating the sample at 10 cm for a specified time. Indirect UV detection at 214 or 254 nm was used.

The carrier electrolytes for cation separations were prepared from copper sulphate, copper chloride or imidazole (adjusted to pH 4.5 with hydrochloric acid) and the carrier electrolyte for anion separation from sodium chromate (all chemicals obtained from Merck, Darmstadt, Germany) and OFM BT Anion (obtained from Waters). The electrolytes were prepared either in water purified with a Milli-Q system (Millipore) or in water–ethylene glycol mixtures. Samples were prepared in Milli-Q-purified water.

Electroosmotic flow mobilities were determined by injecting mesityl oxide or benzyl alcohol as a neutral marker.

Reference serum samples with certified values were obtained from Nycomed (Oslo, Norway) and Behringwerke (Marburg, Germany).

3. Results and discussion

3.1. Effect of nature of carrier electrolyte on cation separation

The separation of several alkali and alkaline earth metal ions relevant for clinical analysis is hampered by the fact that some of them have almost identical mobilities (such as sodium and magnesium). Weston *et al.* [2] have shown that the employment of a complexing agent such as citric acid or α-hydroxyisobutyric acid as an additive to the carrier electrolyte can solve this problem owing to changes in the effective charge of the analyte ions on establishing complexation equilibria.

An alternative way of adjusting the separation selectivity was reported by Beck and Engelhardt [3]. They used imidazole as a carrier electrolyte instead of the more commonly used aromatic amines. In this way they claimed to be able to separate the sodium–magnesium peak pair. Unfortunately, during our experiments we were not able to confirm these results. Nevertheless, it seemed worthwhile to investigate further electrolytes with respect to different separation selectivities. The choice is restricted owing to the prerequisites of a reasonable UV absorption in order to allow indirect UV detection and also a mobility similar to that of the analyte ions. Papers on ion chromatography of cations with indirect UV detection had suggested the use of cerium(III) or copper(II) salts as mobile phases [4]. These electrolytes should also meet all the requirements of CZE. Owing to the better baseline stability at 214 nm, copper(II) was chosen for our work instead of cerium(III), although the latter has also recently been reported to be useful for several applications with indirect UV and fluorescence detection [5,6].

The behaviour of cations in a copper(II) electrolyte turned out to be dependent on the counter ion of the copper. Copper(II) chloride yielded almost the same separation selectivity as the imidazole electrolyte (which in turn gave the same separation selectivity as aromatic amines in their protonated form). Pronounced changes in migration order were observed when using cop-

Table 1
Relative migration times of cations in different carrier electrolytes (sodium = 1)

Ion	5 m*M* $CuSO_4$	5 m*M* $CuCl_2$	5 m*M* imidazole (pH 4.5)
Caesium	0.71	0.73	0.74
Rubidium	0.73	0.73	0.74
Potassium	0.76	0.76	0.80
Sodium	1.00	1.00	1.00
Barium	1.09	0.90	0.90
Strontium	1.11	0.94	0.92
Calcium	1.13	0.95	0.93
Magnesium	1.18	1.00	1.00
Lithium	1.21	1.17	1.09
Nickel	1.22	1.00	1.00
Manganese	1.23	1.01	1.00
Zinc	1.23	1.00	1.00

Conditions: voltage, 25 kV; indirect UV detection at 214 nm.

per(II) sulphate instead of copper(II) chloride. Table 1 shows the migration order (given as relative migration times normalized to the migration time of sodium) of several alkali, alkaline earth and transition metal ions.

As can be seen from Table 1, the most obvious changes occurred with the divalent cations, whose migration times were increased with respect to the monovalent ions. One might speculate on association equilibria between divalent cations and sulphate leading to a decreased effective charge and therefore longer migration times. This idea is supported by the decrease in electrophoretic mobilities, μ_{ephor} (which are the observed mobilities minus the electroosmotic mobility), of divalent cations on increasing the copper sulphate concentration (Fig. 1). An estimation of the magnitude of the interaction between the cations and sulphate can be carried out in a way analogous to the determination of dissociation constants of acids described by Cleveland *et al.* [7]. The association constant K_{ass} for a metal cation and sulphate can be found from the equation

$$\log c_{SO_4^{2-}} = \log \frac{1}{K_{ass}} - \log \frac{\mu_{ephor}}{\mu^0_{ephor} - \mu_{ephor}} \quad (1)$$

where μ^0_{ephor} is the electrophoretic mobility of the cation in an electrolyte without sulphate ions. The association constants calculated for calcium, magnesium and nickel were in the range 25–50 $mol^{-1}\ l^{-1}$. It should be remembered that these calculations give just a rough estimation of the magnitude of the interactions and, among other things, do not take into account changes in the size of the species.

3.2. Effects of organic modifier on cation separation

Work carried out earlier [8] on the separation of anions by CZE has demonstrated that the

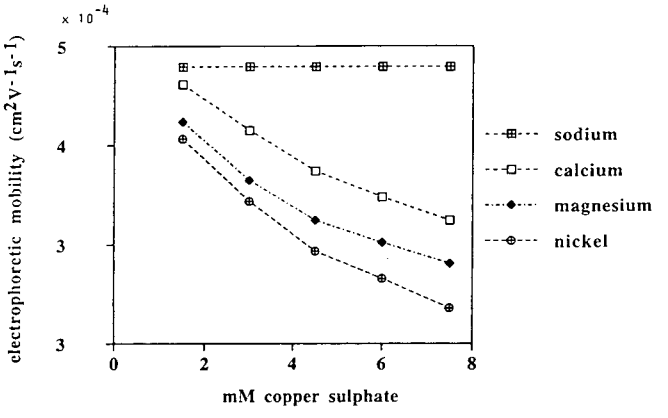

Fig. 1. Effect of copper sulphate concentration in the carrier electrolyte on the migration order of cations. Conditions: voltage, 20 kV; indirect UV detection at 214 nm.

addition of organic solvents to the carrier electrolyte can change the migration order considerably. Therefore, in a series of experiments the influence of ethylene glycol at levels up to 20% was investigated. As can be seen from the results in Fig. 2 for the copper sulphate electrolyte, there are some general trends resulting from the organic modifier, such as the increase in migration times of divalent ions relative to the migration times of the monovalent ions sodium and lithium. Similar results were obtained with the imidazole electrolyte. This effect might be attributed to the changes in the hydration of ions on addition of an organic solvent resulting in changes in migration times. Increasing the amount of organic modifier in an imidazole electrolyte up to 60% even made possible the separation of some transition metal ions, as can be seen from Fig. 3. Unfortunately, the increase

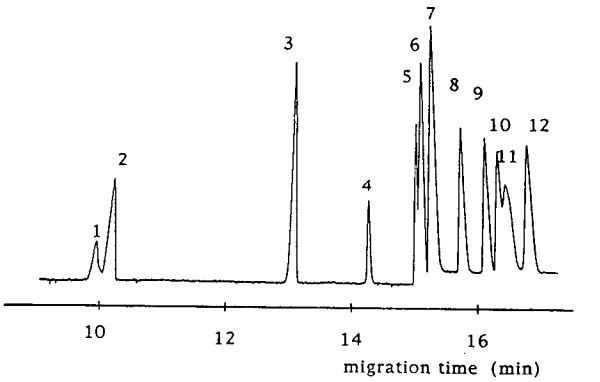

Fig. 3. Separation of a standard mixture of cations using a 5 m*M* imidazole carrier electrolyte (pH 4.5) containing 60% ethylene glycol. Peaks: 1 = rubidium; 2 = caesium, potassium; 3 = sodium; 4 = barium; 5 = strontium; 6 = calcium; 7 = magnesium; 8 = manganese; 9 = cobalt; 10 = nickel; 11 = zinc; 12 = lithium. Conditions: voltage, 20 kV; indirect UV detection at 214 nm.

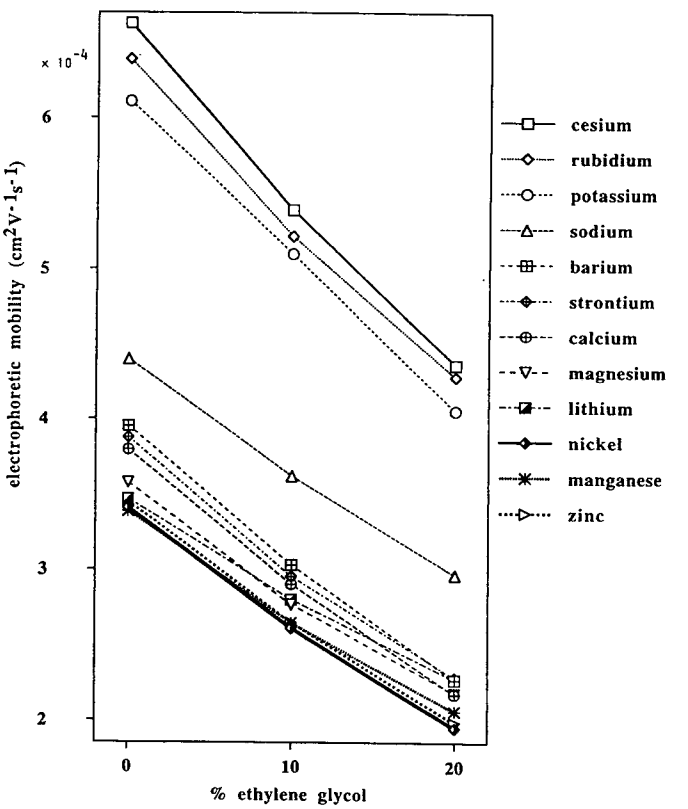

Fig. 2. Effect of ethylene glycol in the carrier electrolyte on the migration order of cations. Conditions: voltage, 20 kV; indirect UV detection at 214 nm.

in the amount of organic modifier causes a decrease in the electroosmotic flow, which was $0.96 \cdot 10^{-4}$, $0.56 \cdot 10^{-4}$ and $0.50 \cdot 10^{-4}$ cm^2 V^{-1} s^{-1} in 5 m*M* $CuSO_4$ with 0, 10 and 20% ethylene glycol, respectively. Therefore, higher voltages are recommended in order to avoid too long migration times.

3.3. *Effects of ion-pairing reagents on cation separations*

Ion-pairing reagents have been successfully applied to the optimization of anion separations, but so far this approach has not yet been used in the separation of cations. In this work, sodium dodecyl sulphate (SDS) was investigated as an ion-pairing reagent. Unfortunately, in an imidazole electrolyte even an SDS concentration as low as 0.5 m*M* leads to pronounced peak tailing. On the other hand, a copper sulphate electrolyte with up to 10 m*M* SDS resulted in well shaped peaks. As can be seen from Fig. 4, the most striking effect is the much slower migration of strontium and barium. Their migration times are considerably lower than those of several transition metal ions if an SDS concentration between 5 and 10 m*M* is used, and became even longer than that of the neutral marker. This suggests some equilibrium between these cations and SDS adsorbed on the inner surface of the capillary. The electroosmotic flow increased considerably when SDS was added to the carrier electrolyte. The electroosmotic mobilities in 5 m*M* copper sulphate were $0.96 \cdot 10^{-4}$ cm^2 V^{-1} s^{-1} without

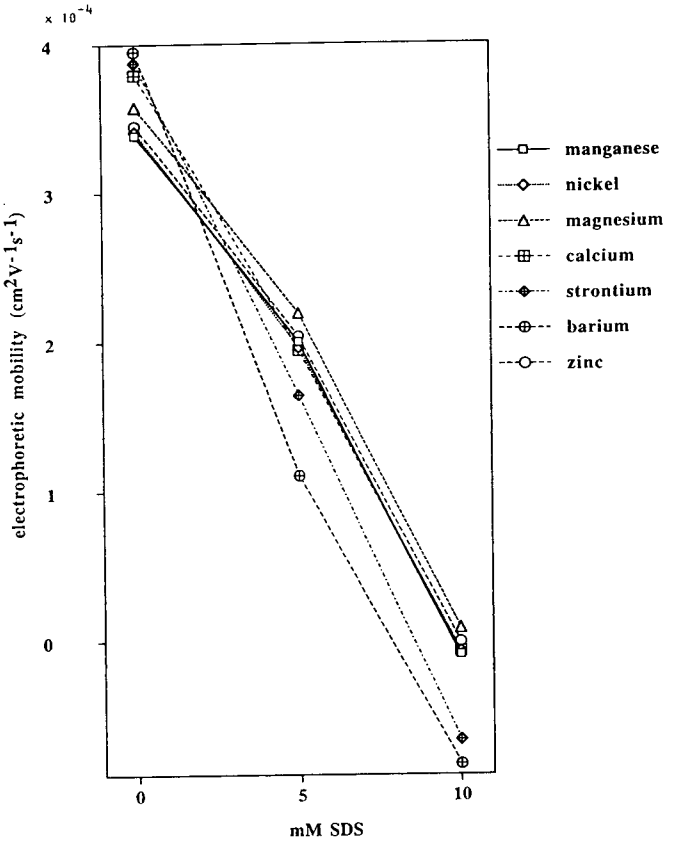

Fig. 4. Effect of sodium dodecyl sulphate in the carrier electrolyte on the migration order of cations. Conditions: voltage, 20 kV; indirect UV detection at 214 nm.

SDS and $2.65 \cdot 10^{-4}$ cm^2 V^{-1} s^{-1} with 5 or 10 m*M* SDS. Unfortunately, the presence of sodium ions from SDS in the electrolyte caused system peaks that interfered with the determination of alkali ions.

3.4. Application to samples of biological material

Biological samples such as serum may contain a high concentration of sodium (*ca.* 140 m*M* in serum). This can be expected to have adverse effects on the efficiency of the separation. Generally, the electrical conductance of the sample should be considerably lower than that of the electrolyte in order to obtain sample focusing effects called "sample stacking". Obviously, this demand cannot be met by biological samples, because their electric conductances even at a 10- or 20-fold dilution may still be equal to or higher than that of the electrolytes normally used. Fortunately, this disadvantage can be overcome by making use of "sample self-stacking" recently described by Gebauer *et al.* [9]. If there is one analyte ion in excess, all other analyte ions having lower mobilities can be focused as long as the electrolyte has a (slightly) lower mobility than all analyte ions. Copper fulfils this criterion for serum samples, as it has a mobility slightly lower than those of the alkali and alkaline earth metals of interest in serum. In addition, its mobility is still high enough to avoid tailed peaks which will occur if there is an excessive mismatch between electrolyte and analyte ions. The focusing effect can be expected not to apply to potassium, which migrates faster than sodium. Nevertheless, the results given below demonstrate that the peak shape of potassium in serum samples is still acceptable.

Considering sensitivity and sample loading, a 20-fold dilution of serum samples and an injection time of 20 s were found to be appropriate. Care must be taken to avoid exceeding the linear range for sodium. Generally, the dynamic range is limited by the concentration of the carrier electrolyte, as changes in the detector signal can be expected only as long as there are enough UV absorbing ions in the carrier. It might be assumed that 1 mol of sodium should displace 0.5 mol of copper; in fact, its transfer ratio is even lower, as analyte ions having higher electrophoretic mobilities than electrolyte ions exhibit lower transfer ratios than calculated from a one-to-one equivalent displacement [10]. The experimental data confirmed that in a 3 m*M* copper sulphate electrolyte the response for sodium is linear up to at least 250 ppm (corresponding to 5000 ppm in the sample before dilution). This covers the whole range of normal and pathological serum samples. It would even allow a lower dilution of the sample in order to increase the sensitivity for potassium, calcium and magnesium. Unfortunately, in this case the resolution decreases considerably.

For quantification purposes, an internal standard was added to the samples and to the standard solutions to correct for eventually changing injection volumes. Lithium was chosen as the internal standard, as it migrates closely after the peaks of interest and its normal concentration in biological samples is negligible.

During a series of injections for the determination of cations with a copper electrolyte, it was noticed that the migration times of all ions increased considerably from run to run. Obviously, this was due to the proteins in the samples, which tended to adsorb to the inner surface of the capillary, thereby reducing the ζ-potential and the electroosmotic flow. This problem could be overcome by flushing the capillary with 0.1 *M* sodium hydroxide solution between runs. This procedure resulted in stable migration times. No interfering peaks from proteins were observed in the electropherograms.

Fig. 5 shows the chromatogram of a serum sample. The reproducibility (relative standard deviation) for the determination of cations was *ca.* 7% for potassium, 1% for sodium, 5% for calcium and 7% for magnesium. This reproducibility might seem poor, but nevertheless could be sufficient for several routine purposes. One of the obvious advantages of CZE is its ability to handle biological samples available only in small amounts, such as tear fluid, which was also successfully analysed by this technique.

The accuracy of the mean was checked by

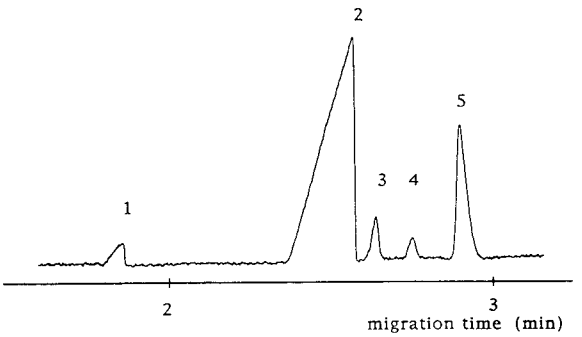

Fig. 5. Electropherogram of cations in a serum sample (1:20 dilution) using a 5 m*M* copper sulphate electrolyte. Peaks: 1 = potassium; 2 = sodium; 3 = calcium; 4 = magnesium; 5 = lithium (internal standard). Conditions: voltage, 30 kV; indirect UV detection at 214 nm.

using a reference serum with certified values. Table 2 compares the results of the CZE method and the certified values. The agreement between these data seems fairly satisfactory. In addition, it should be pointed out that calcium partly exists as a protein-bound species in serum. Obviously, the CZE method measures the total amount of calcium, which means that any bound calcium is released from proteins after injection.

Another series of experiments were carried out on the determination of anions in serum samples. Of the anions present in serum, chloride, sulphate, phosphate, carbonate acetate and lactate are in a concentration range suitable for CZE. Typical electrolytes described in the literature for the CZE of anions include chromate, phthalate and benzoate [11]. Recently, we found that Cu(II) $EDTA^{2-}$ is another electrolyte with interesting prospects for anion separations, as it can selectively detect monobasic carbonic acids in mixtures with dibasic acids. For serum samples, 5 m*M* chromate containing 0.5 m*M* OFM BT Anion as an electroosmotic flow modifier gave the best performance. Serum samples were diluted 20-fold before injection. No changes in migration times for anions in proteinaceous samples were observed (contrary to the situation for cation determinations as described above). Probably adsorption of proteins on the inner surface is suppressed by the use of the electroosmotic flow modifier, which itself adsorbs to the surface.

Table 2
Comparison of results for a serum reference sample obtained by CZE with certified values

Element	Concentration (mg l^{-1})	
	CZE	Certified value[a]
Potassium	178	174
Sodium	2915	2970
Calcium	103.5	98
Magnesium	19.1	20.1

[a] Certified values were obtained by atomic emission spectrometry.

Similarly to cation determination, an internal standard was used for quantification. Malonic acid (concentration 10 ppm), which migrates between sulphate and phosphate, turned out to be useful for this purpose. Generally, the reproducibility was less satisfactory for some of the anions owing to the occurrence of interfering negative peaks and to sensitivity problems in the case of sulphate. The accuracy of the means could not be checked as certified reference materials were not available.

In conclusion, CZE was found to be adequate for the determination of a range of cations relevant in the clinical analysis of biological samples and several anions. The most important advantage seems to be that proteins do not interfere (in contrast to ion chromatography) so that sample preparation can be kept to a minimum. More sensitive detection methods would help to overcome some of the drawbacks of the proposed methods and open up CZE to the determination of trace elements in blood, serum and similar matrices. Post-separation reaction detectors and electrochemical detectors might have some prospects with respect to sensitivity and selectivity for complex samples, but are not yet ready for routine application.

References

[1] W. Buchberger, H. Malissa and E. Mülleder, *J. Chromatogr.*, 602 (1992) 51.

[2] A. Weston, P.R. Brown, P. Jandik, W.R. Jones and A.L. Heckenberg, *J. Chromatogr.*, 593 (1992) 289.
[3] W. Beck and H. Engelhardt, *Chromatographia*, 33 (1992) 313.
[4] J.H. Sherman and N.D. Danielson, *Anal. Chem.*, 59 (1987) 490.
[5] K. Bächmann, J. Boden and I. Haumann, *J. Chromatogr.*, 626 (1992) 259.
[6] K. Bächmann, I. Haumann and T. Groh, *Fresenius' J. Anal. Chem.*, 343 (1992) 901.
[7] J.A. Cleveland, M.H. Benko, S.J. Gluck and Y.M. Walbroehl, *J. Chromatogr. A*, 652 (1993) 301.
[8] W. Buchberger and P.R. Haddad, *J. Chromatogr.*, 608 (1992) 59.
[9] P. Gebauer, W. Thormann and P. Bocek, *J. Chromatogr.*, 608 (1992) 47.
[10] M.W.F. Nielen, *J. Chromatogr.*, 588 (1991) 321.
[11] P. Jandik and W.R. Jones, *J. Chromatogr.*, 546 (1991) 431.

ELSEVIER

Journal of Chromatography A, 671 (1994) 383–387

JOURNAL OF CHROMATOGRAPHY A

Versatility of capillary electrophoresis of anions with a high-mobility chromate electrolyte

Stuart A. Oehrle

Millipore Corporation, Waters Industrial Division, 34 Maple Street, Milford, MA 01757, USA

Abstract

Capillary ion electrophoresis (Waters' trade name: Capillary Ion Analysis) is a capillary electrophoretic technique which is optimized for the rapid analysis of low-molecular-mass inorganic and organic ions. Indirect UV detection at 254 nm was used throughout. An electroosmotic flow modifier was added to the chromate electrolyte and a negative power supply was used. Analysis of anions in a variety of samples with differing matrices was investigated. Examples discussed include trace level anions in power plant water (ng/ml) and μg/ml level of anions in intermediate and concentrated sulfonated dyes. Anion analysis using this technique is rapid (less than 5 min), with little sample preparation required. The same electrolyte composition, with only minor variations, was used for all samples. Both hydrostatic mode of injection for ppm level analysis and electromigration mode of injection for trace level analysis was used.

1. Introduction

Anion analysis using a chromate, high-mobility, electrolyte with an osmotic flow modifier (OFM) has been previously shown to be a sensitive technique for the analysis of anions [1–3]. The purpose of this paper is to show examples of specific applications using this high-mobility electrolyte. OFM was added to the electrolyte as an additive that reverses the normally cathodic direction of the electroosmotic flow (EOF) that is found in fused-silica capillaries. This creates a co-electroosmotic condition that augments the mobility of the analytes.

The first example is of low-level anion analysis, part-per-billion (ppb), for sulfate and nitrate in water samples from a coal fired power plant. Current ion chromatographic (IC) techniques require extensive trace enrichment and run times of approximately 12–15 min. Capillary ion electrophoresis (CIE) (Waters' trade name: Capillary Ion Analysis, CIA) allows for fast (less than 5 min) analysis times. Electromigration was used as an injection mode since it has been shown to be a good injection mode for low level anion analysis [2]. Sodium octanesulfonate was added as well, as an electromigrative additive to improve the trace enrichment process [2]. OFM, in the hydroxide form, was added to the chromate electrolyte. The hydroxide form of the OFM was used so as to make final the working electrolyte pH more alkaline than it is in the normal bromide form.

The second set of examples is μg/ml level anion analysis of intermediate and concentrated

* Corresponding author.

0021-9673/94/$07.00
SSDI 0021-9673(93)E1134-L

sulfonated dyes. For these samples a chromate electrolyte was used as well, with OFM added in the standard Br form [4]. IC was also employed, in the analysis of the sulfonated dyes for comparison purposes.

2. Experimental

2.1. Instrumentation

The capillary electrophoresis (CE) system employed was the Quanta 4000 (Waters Chromatography Division of Millipore, Milford, MA, USA) with a negative power supply. A Hg lamp was used for indirect UV detection at 254 nm. AccuSep polyimide fused-silica capillaries of dimension 60 cm × 75 μm I.D. were used throughout. The IC system employed consisted of a 6000A pump, U6K manual injector and M431 conductivity detector (all from Waters). An IC-Pak A Anion column was used for IC analysis. A borate–gluconate mobile phase was used [4].

Data acquisition was carried out with a Waters Millennium 2010 chromatography manager with SAT/IN modules connecting the CE and IC systems to the data station with the signal polarity inverted from the CE. Detector time constant for the CE was set at 0.1 s and the data rate for the CE was 20 points/s and 1 point/s for the IC system. Collection of electropherographic and chromatographic data was initiated by a signal connection between both the CE and manual injector and the SAT/IN module.

2.2. Preparation of electrolytes

High-purity water (Milli-Q) was used to prepare all solutions (Millipore, Bedford, MA, USA). The chromate electrolyte was prepared from a concentrate containing 100 m*M* sodium chromate tetrahydrate (Fisher Scientific, Pittsburgh, PA, USA) and 0.0056 m*M* sulfuric acid (J.T. Baker, Phillipsburg, NJ, USA; Ultrex grade). OFM for reversal of the direction of the EOF was a 20 m*M* concentrate (CIA-Pak OFM anion BT) obtained from Waters. For low-level trace enrichment analysis the OFM was converted to the hydroxide form by passing the OFM through an ion-exchange resin (AG1-X8, OH form; Bio-Rad, Richmond, CA, USA). The working electrolyte for low-level analysis consisted of 7 m*M* chromate–0.7 m*M* OFM-OH. For μg/ml-level analysis OFM was added without any pretreatment [4]. The working electrolyte for standard, μg/ml-level analysis, consisted of 5 m*M* chromate–0.5 m*M* OFM-BT, pH 8.1 [5]. All working electrolytes were prepared fresh daily and degassed prior to use.

2.3. Reagents

All standard solutions were prepared by diluting 1000 μg/ml stock solutions containing the individual anions. For the CIE and IC analysis of the sulfonated dyes the same standard solutions were used. For trace-level analysis all samples and solutions were stored in pre-rinsed plastic ware. Sodium octanesulfonate (VHG Labs., Manchester, NH, USA) was added to standards and samples for trace enrichment (100 μl per 100 ml solution). To prevent contamination from handling, disposable, non-talc, gloves were worn.

2.4. System operation

Two sample carousel configurations were employed for the CE system. The 13-position carousel used 4-ml (45 × 15 mm) polypropylene Sunvials (Sunbrokers, Wilmington, NC, USA) for electrolytes and samples. The 20-position carousel used 600-μl polypropylene centrifuge tubes (Waters) for sample vials and 20-ml HDPE sample side electrolyte vials (Waters). Receiving side electrolyte vials were 20-ml glass scintillation vials (Waters) for both carousels. The 13-position carousel was used for ng/ml-level analysis since the larger sample vial size allowed for easier rinsing of the vials and minimized contamination. The 20-vial carousel was used for μg/ml-level analysis.

3. Results and discussion

3.1. Low-level analysis (ng/ml)

For the analysis of low-level anions using trace enrichment techniques a water blank must be run and the amounts adjusted for any anions present which are to be quantitated [2]. Duplicate injections of three different levels of standards ranging in value from 8–36 ng/ml was done. Correlation coefficients of 0.999, for both anions calibrated, was calculated using a linear fit. Fig. 1 is an electropherogram of an anion standard. The samples analyzed from the power plant were found to contain extremely low amounts of anions. Fig. 2 is an example electropherogram of one of the samples. At these low levels the anions were below the intercept of the calibration curve with the exception of sulfate, in Fig. 2, which was 9 ng/ml. All samples were well below the 15 ng/ml limit set by the plant. Other peaks in the electropherograms correspond to unidentified anions or small organic acids.

3.2. μg/ml level analysis of dyes

Sulfate analysis was of the most interest since it is involved in the manufacturing of the sul-

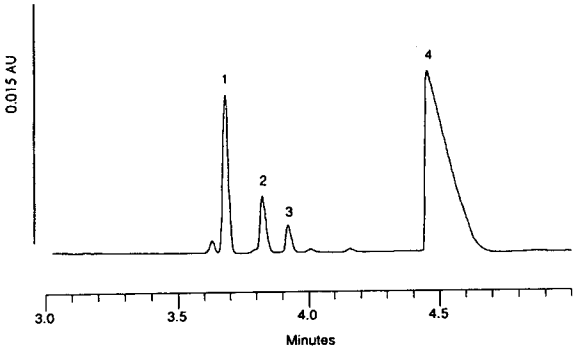

Fig. 1. Electropherogram of anion standard. CIE conditions: Fused-silica 60 cm × 75 μm I.D. capillary; voltage 15 kV (negative); 7 m*M* chromate–0.7 m*M* CIA-Pak OFM Anion (patented) OH form; indirect UV detection at 254 nm; electromigration injection (5 kV for 45 s). Peaks: 1 = chloride (contaminant); 2 = sulfate (16 ng/ml); 3 = nitrate (13 ng/ml); 4 = carbonate (contaminant).

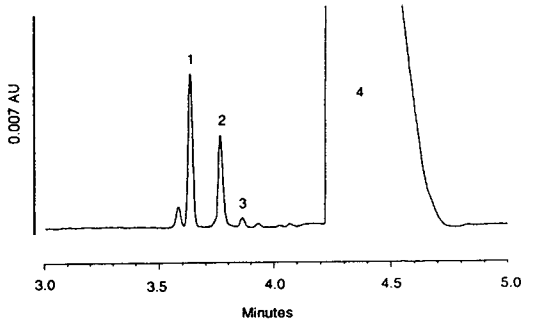

Fig. 2. Electropherogram of boiler sample (neat). CIE conditions as in Fig. 1. Peaks: 1 = chloride (not quantitated); 2 = sulfate (9 ng/ml); 3 = nitrate (< 5 ng/ml); 4 = carbonate (not quantitated).

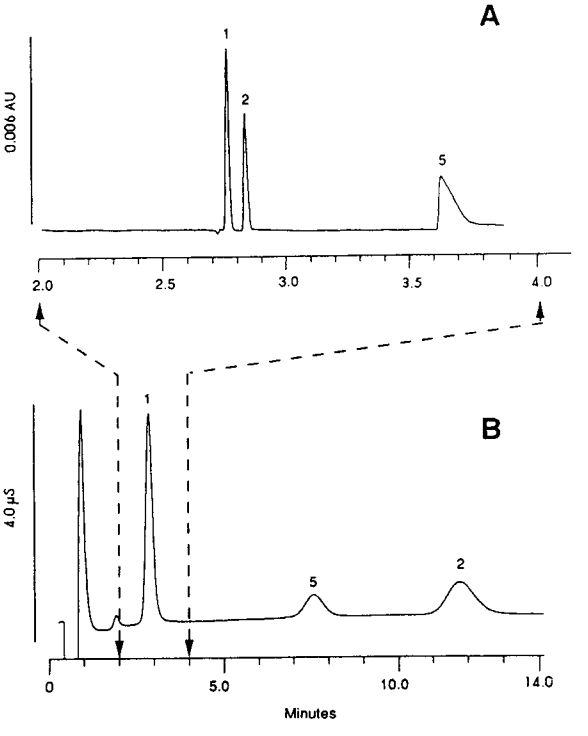

Fig. 3. 10 μg/ml chloride, sulfate and phosphate standard. (A) Electropherogram. Conditions, capillary: 60 cm × 75 μm I.D.; voltage: 18 kV (negative); 4.5 m*M* chromate–0.5 m*M* CIA-Pak OFM Anion-BT, pH 8.1; indirect UV at 254 nm; hydrostatic injection (10 cm for 30 s). (B) Chromatogram from IC system. Conditions, column: Waters IC-Pak Anion A; eluent: modified borate–gluconate, flow-rate: 1.2 ml/min, detection: conductivity. Peaks: 1 = chloride; 2 = sulfate; 5 = phosphate. One noticeable advantage of CIE is in the time of analysis as compared to IC.

fonated dyes. Other anions, chloride and phosphate, were quantitated as well for comparison purposes with IC. As mention previously, CIE offers the ability to analyze for anions fairly quickly (about 5 min). Fig. 3 exemplifies this since one CIE run can be done in less than 4 min. In this case if sulfate was the only anion of interest the run could be stopped at 3 min and the capillary purged briefly to replenish the capillary with electrolyte and another analysis started. A linear calibration curve was plotted for duplicate injection of three different levels of standards from 5–25 μg/ml. Correlation coefficients, for both IC and CIE, were 0.999 for all anions calibrated. Figs. 4 and 5 are of different in-process dyes. As can be seen in Fig. 5, CIE was able to easily detect phosphate in the blue dye sample. Table 1 shows a comparison between CIE and IC for the two samples analyzed. As can be seen the values determined from both techniques agreed quite well. One disadvantage

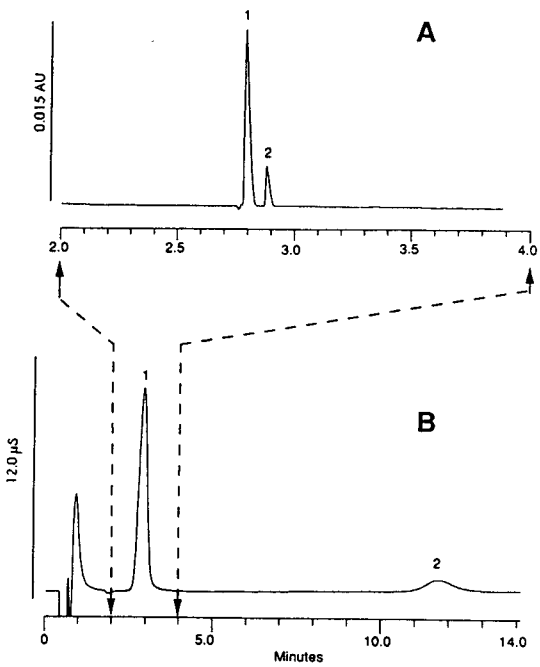

Fig. 4. Intermediate green dye. Diluted 1:50 with high-purity water. Conditions as in Fig. 3. (A) Electropherogram. (B) Chromatogram from IC. Peaks: 1 = chloride; 2 = sulfate. Amounts found listed in Table 1.

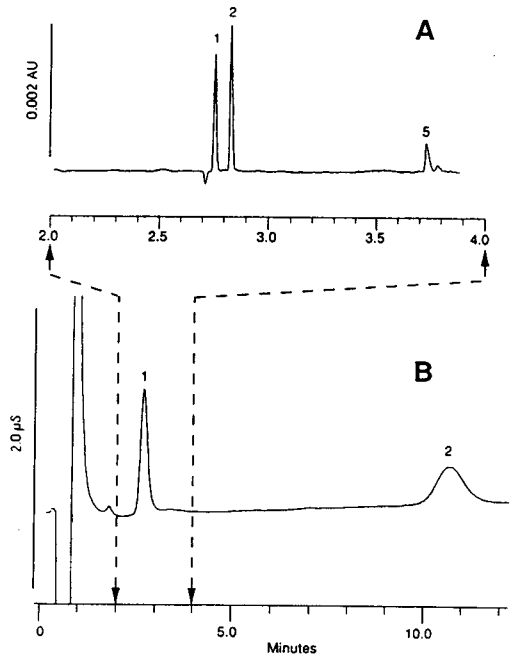

Fig. 5. Concentrated blue dye. Run neat. Conditions as in Fig. 3. (A) Electropherogram. (B) Chromatogram from IC. Peaks: 1 = chloride; 2 = sulfate; 5 = phosphate. Amounts found listed in Table 1.

of IC for the analysis of sulfonated dyes was that the dyes tended to adhere to the column causing column degradation and loss of resolution. This could be seen by the column effluent which became discolored from the dyes and remained discolored for several column volumes after the run. Even with a pre-column the analytical column still degraded quite rapidly. With CIE there was no apparent loss of efficiency over time since the capillary is hollow and the purge incorporated at the end of the run flushed the capillary with new electrolyte.

4. Conclusions

The results of this work show how CIE, using chromate electrolyte and indirect detection can be used for a variety of samples. CIE offers the advantage over IC for rapid analysis of anions as well as no noticeable sample adsorption as was seen with the sulfonated dyes on the IC column.

Table 1
Quantitative results of sulfonated dyes by CIE and IC

	Cl^-	R.S.D. (%)	SO_4^{2-}	R.S.D. (%)	HPO_4^{2-}	R.S.D. (%)
CIE (average amount in μg/ml, n = 2)						
Blue dye	2.78	0.94	4.69	0.56	0.89	1.55
Green dye	1897	0.87	503	1.32	N.D.[a]	–
IC (average amount in μg/ml, n = 2)						
Blue dye	2.64	0.67	4.33	0.03	N.D.	–
Green dye	1909	0.13	497	0.27	N.D.	–

[a] N.D. = None detected.

Work continues in our laboratory investigating additional applications for CIE. As of now, CIE offers a complementary method of analysis and in some cases a superior and less expensive means of analysis than IC.

5. Acknowledgement

The author acknowledges William R. Jones for his valuable assistance with this project and for helpful discussions.

5. References

[1] P. Jandik and W.R. Jones, *J. Chromatogr.*, 546 (1991) 431.
[2] G. Bondoux, P. Jandik and W.R. Jones, *J. Chromatogr.*, 602 (1992) 79.
[3] W.R. Jones and P. Jandik, *J. Chromatogr.*, 546 (1991) 445.
[4] A.L. Heckenberg, P.G. Alden, B.J. Wildman, J. Krol, J.P. Romano, P.E. Jackson, P. Jandik and W.R. Jones, *Waters Innovative Methods for Ion Analysis*, Millipore, Milford, MA, rev. 2.0, 1991.
[5] Waters Chromatography Division of Millipore, *US Patents*, 5104 506, 5128 055 and 5156 728 (1992).

ELSEVIER

Journal of Chromatography A, 671 (1994) 389–395

JOURNAL OF CHROMATOGRAPHY A

Application of capillary electrophoresis in atmospheric aerosols analysis: determination of inorganic and organic anions

Ewa Dabek-Zlotorzynska*, Joseph F. Dlouhy

Chemistry Division, Environmental Technology Centre, Environment Canada, 3439 River Road, Ottawa, Ontario K1A 0H3, Canada

Abstract

The usefulness of capillary electrophoresis in the analysis of inorganic and organic anions in atmospheric aerosols was investigated. Various electrolytes based on chromate, pyromellitate (PMA), phthalate and 2,6-naphthalenedicarboxylate (NDC) were tested. Two separate electrolyte systems (PMA and NDC) are recommended for determination of anions with different mobility. Results obtained by parallel analysis of sulphate by capillary electrophoresis and ion chromatography in atmospheric aerosols are presented.

1. Introduction

The measurement of the chemical composition of atmospheric aerosols has been and still is the subject of many studies using different analytical techniques and collection methods.

For the determination of inorganic anions, ion chromatography (IC) has become the technique of choice [1]. It has already reached a stage of maturity, so that its potential and limitations are by now well known. Other new techniques such as capillary electrophoresis (CE) have only been introduced in the last several years [2–5].

Capillary electrophoresis is revolutionizing separation science. CE and related techniques such as micellar electrokinetic capillary chromatography (MECC) or capillary gel electrophoresis (CGE) offer a high separation efficiency and separation speed for charged and neutral species, and great progress has been made in instrumentation and applications in recent years [6,7]. Applications include the separation of small inorganic and organic anions with indirect UV detection in many real samples [9–19]. Excellent separation efficiencies were reported with chromate, pyromellitate and other aromatic carboxylic acid salts containing electrolytes [7–21].

This study was undertaken to investigate the usefulness of CE in the analysis of inorganic and organic anions in atmospheric aerosols. Also, this study was performed to obtain independent complementary confirmation of the IC results. CE may be used as a complement to IC analysis [13,16], because the selectivity for anion separation by CE differs significantly from that obtained using anion exchange columns in IC. In order to obtain the best selectivity of CE separation, and sensitivity with indirect detection, various potential electrolytes such as chromate [8], pyromellitate (PMA) [20], phthalate [11] and 2,6-naphthalenedicarboxylate (NDC) [21] were investigated. This paper presents also results obtained by parallel analysis of sulphate in the

* Corresponding author.

0021-9673/94/$07.00
SSDI 0021-9673(94)00110-U

aqueous atmospheric aerosol extracts by CE and IC methods.

2. Experimental

2.1. Capillary electrophoresis

All CE experiments were performed with a Beckman P/ACE 2100 instrument (Fullerton, CA, USA) equipped with a multi-wavelength UV detector, an automatic sample changer, a liquid thermostated capillary cartridge (capillary 75 μm I.D. × 375 μm O.D. × 57 cm total length, 50 cm to detector) and an IBM PS/2 70 personal computer utilizing Beckman Gold System (V 7.11) software for instrument control and data collection.

Prior to use the capillary was pretreated with 0.1 *M* NaOH for 10 min, then rinsed with deionized water and the used electrolyte. To maintain good peak shapes and reproducible migration times, the capillary tube was rinsed with the running electrolyte for 1 min before the sample was injected. The capillary temperature was kept at 25 ± 0.1°C by means of a fluorocarbon liquid continuously circulating through the cartridge. Unless otherwise noted, all injections were achieved using a 10-s pressure injection technique.

All electrolyte compositions and operating conditions used in this study are presented in Table 1. The electrolytes were filtered and degassed by creating a vacuum inside the syringe.

2.2. Ion chromatography

The IC system used in this study was from Dionex (Sunnyvale, CA, USA) as described previously [22]. Separation of anions by gradient elution was performed on an IonPac-AS10 column with an IonPac-AG10 guard column. Conductivity detection was carried out using an anion self-regenerating suppressor (ASRS-I) in the recycle mode.

2.3. Reagents

All solutions were prepared with deionized water (18 MΩ cm) obtained by treating the tap water using reverse osmosis and ion exchange (Millipore, Model RO 20 and Model SuperQ).

All chemicals were purchased commercially from either Aldrich (Milwaukee, WI, USA) or Fisher Scientific (Ottawa, ON, Canada) in the highest purity available, and were used as is

Table 1
Experimental conditions for CE analysis

Conditions	Chromate (E1)	PMA [a] (E2)	Phthalate (E3)	NDC [b] (E4)
Electrolyte composition	5.0 m*M* chromate 0.5 m*M* TTAB [d] pH = 8.0	2.25 m*M* PMA 0.75 m*M* HMOH [e] 6.50 m*M* NaOH 1.60 m*M* TEA [f] pH = 7.7	5.0 m*M* KHP [c] 0.5 m*M* TTAB 1.0 m*M* boric acid pH = 5.9	2.0 m*M* NDC 0.5 m*M* TTAB 5.0 m*M* NaOH pH = 10.9
Polarity	(−)	(−)	(−)	(−)
Detection	Indirect, 254 nm	Indirect, 254 nm	Indirect, 254 nm	Indirect, 280 nm
Voltage	20 kV	30 kV	20 kV	20 kV
Injection	Pressure, 10 s	Pressure, 10 s	Pressure, 10 s	Pressure, 10 s

[a] Pyromellitic acid
[b] 2,6-Naphthalenedicarboxylic acid
[c] Potassium hydrogen phthalate
[d] Tetradecyltrimethylammonium bromide
[e] Hexamethonium hydroxide
[f] Triethanolamine

without further purification. Pyromellitate based electrolyte was obtained from Dionex.

2.4. Quantitation procedure

The CE procedures were calibrated with freshly prepared mixed standard solutions every day that samples were analyzed. The mixed anion stock solution was diluted to produce working standard solutions at four different concentrations within the range 0.2–10 μg/ml. Calibration graphs were plotted based on the linear regression analysis of the corrected peak area (peak area/migration time).

Identification of individual ions was based on the comparison of migration times of analytes with those of standard solutions. Some samples were spiked with standard solution. Ion chromatography results were also used for identification of some ions.

Detection limits were defined as three times the standard deviation of 18 replicate analyses of the standard with concentration about ten times the expected detection limit.

2.5. Filter extraction

Atmospheric aerosols collected on thin PTFE filters using virtual dichotomous samplers were obtained from the Pollution Measurement Division, Environmental Technology Centre, Environment Canada. The samplers fractionated the aerosol into two aerodynamic size ranges yielding coarse (<10 μm) and fine (<2 μm) particles.

PTFE filter collected aerosols were non-destructively analyzed by X-ray fluorescence (XRF) for fifty elements. Then, the chemical analysis of extracts of atmospheric aerosols was performed using ion chromatography [22] and capillary electrophoresis. The extraction of water soluble aerosols collected on filters was performed with 15 ml of water by sonication in an ultrasonic bath (Branson and Smithkline, Model Bransonic 42) for 30 min. Before addition of water, the filters with collected aerosols were wetted with 100 μl of isopropanol. The extracts were analyzed less than 24 h after extraction. The residue of extracts was preserved by storage at -20°C [23].

3. Results and discussion

3.1. Selection of electrolyte

One of the major aims of this work was to investigate the utility of various potential electrolytes for the determination of inorganic and organic anions in atmospheric aerosols. In this work, four electrolytes with different mobilities and with strong UV absorption were investigated.

Fig. 1 shows the four electropherograms obtained with the 14-anion mixture with tested electrolytes under conditions listed in Table 1. The chromate electrolyte shows most of the tested anions fully resolved with increasing tailing for the later peaks. Under conditions proposed by Harold *et al.* [20], the PMA electrolyte shows better resolution of bromide (Peak 1) through to oxalate (Peak 6) in comparison to the chromate electrolyte separation. However, other less mobile anions are separated at times longer than 5 min. The phthalate and NDC electrolyte separations show improved peak symmetry for less mobile anions, but fail to resolve inorganic anions.

Sensitivities of the tested methods expressed as the response (corrected peak area) per unit concentration (slope of the calibration curve) were compared. The ratio of sensitivities for the PMA, phthalate and NDC methods *vs.* the chromate method is presented in Table 2. As can be seen, a better sensitivity for inorganic anions is obtained using the PMA than the chromate based electrolyte. The NDC electrolyte shows the best sensitivity and selectivity for less mobile anions (formate through benzoate).

Table 3 summarizes the migration time and peak area precision (R.S.D.) for tested anions in a mixed standard under conditions listed in Table 1. Excellent precision of migration times was observed with the PMA and NDC based electrolytes. Precision of peak areas was better

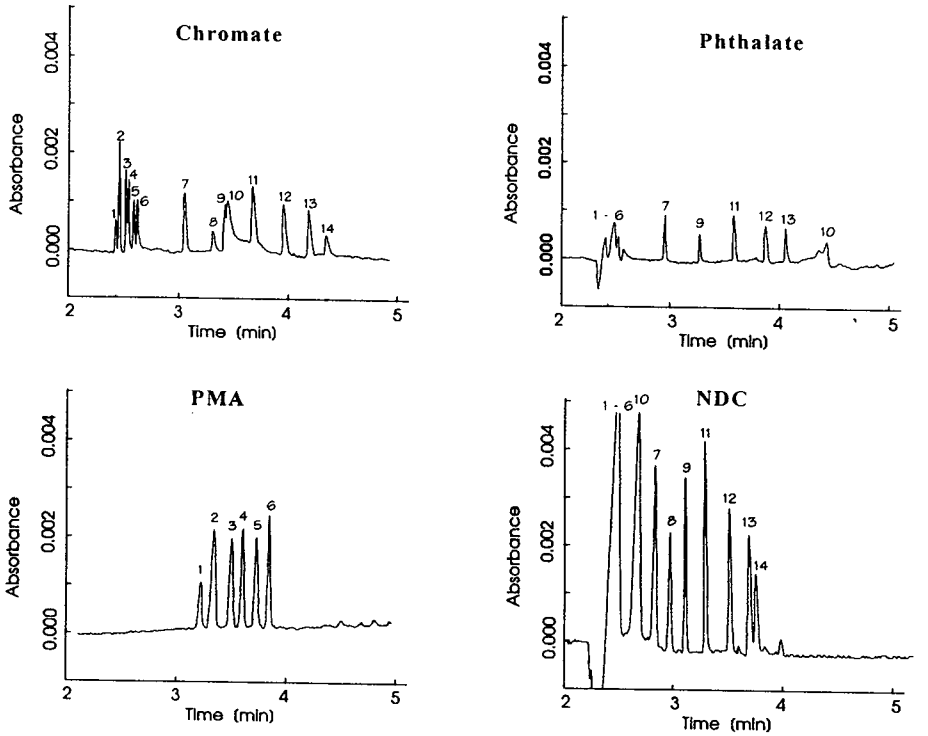

Fig. 1. Electropherograms of a 4 μg/ml anion mixed standard obtained with tested electrolyte compositions. Peaks: 1 = bromide; 2 = chloride; 3 = sulphate; 4 = nitrite; 5 = nitrate; 6 = oxalate; 7 = formate; 8 = phthalate; 9 = methanesulphonate; 10 = bicarbonate or carbonate; 11 = acetate; 12 = propionate; 13 = butyrate; 14 = benzoate. See Table 1 for more details.

Table 2
Sensitivity ratio and detection limit

Ion	Sensitivity ratio			Detection limit (ng/ml)	
	E2/E1	E3/E1	E4/E1	E2	E4 [21]
Bromide	1.72	–	–	210	–
Chloride	1.50	–	–	188	–
Sulphate	1.30	–	–	168	–
Nitrite	1.41	–	–	220	–
Nitrate	1.77	–	–	219	–
Oxalate	1.57	–	–	190	–
Formate	1.33	0.42	3.15	166	133
Acetate	–	0.52	2.14	–	102
Propionate	–	0.55	2.60	–	102
Butyrate	–	0.58	2.28	–	118

E1, E2, E3, and E4 are the chromate, PMA, phthalate and NDC based electrolytes, respectively. For more details see Table 1.

Table 3
Comparison of precision

Ion	Relative standard deviation (%) [a]					
	Migration time			Peak area		
	Chromate	PMA	NDC [21]	Chromate	PMA	NDC [21]
Bromide	0.74	0.19	–	8.80	6.17	–
Chloride	0.64	0.19	–	4.68	4.09	–
Sulphate	0.66	0.22	–	3.41	3.99	–
Nitrite	0.67	0.21	–	3.95	3.65	–
Nitrate	0.68	0.23	–	3.92	4.98	–
Oxalate	0.66	0.28	–	3.09	5.43	–
Formate	1.20	0.29	0.32	4.73	3.11	4.43
Acetate	1.27	–	0.38	5.46	–	3.42
Propionate	1.39	–	0.45	6.09	–	3.39
Butyrate	1.43	–	0.48	8.29	–	3.94

[a] Relative standard deviation from 18 replicates of anion mixed standard at concentration 4 μg/ml.

than 5% for most of the anions under investigation.

These results show that with respect to the separation ability and sensitivity, the use of two separate electrolyte systems is preferable. Major inorganic anions in aqueous extracts of coarse and fine atmospheric aerosols were determined using the PMA based electrolyte. Separation of aliphatic carboxylic acids and other organic compounds was performed with the NDC based electrolyte.

Detection limits (for a 10-s pressure injection) of anions studied with the PMA and NDC based electrolytes are listed in Table 2. It can be seen that all anions have detection limits in the ng/ml range.

3.2. Determination of anions in atmospheric aerosols

Typical electropherograms of coarse and fine atmospheric aerosol extracts are presented in Fig. 2. Coarse atmospheric aerosol particles contain chloride, sulphate and nitrate as the major ions, as reported previously [22]. Sulphate is the major ion of fine atmospheric aerosols.

Table 4
Recovery data of quality control sample

Ion	Recovery						
	Inter-laboratory median [24] (μg/ml)	Mean (%)			R.S.D. (%)		
		CE	IC		CE	IC	
			iso	gra		iso	gra
Chloride	2.135	99.79	98.85	102.92	4.38	3.19	1.41
Sulphate	8.811	104.55	99.75	107.16	1.89	2.11	1.65
Nitrate	5.301	104.13	100.70	101.32	2.21	2.59	2.16

Reported results are the mean and relative standard deviation of 14 (CE) and 4 (IC) replicates. Iso and gra are isocratic and gradient elution, respectively.

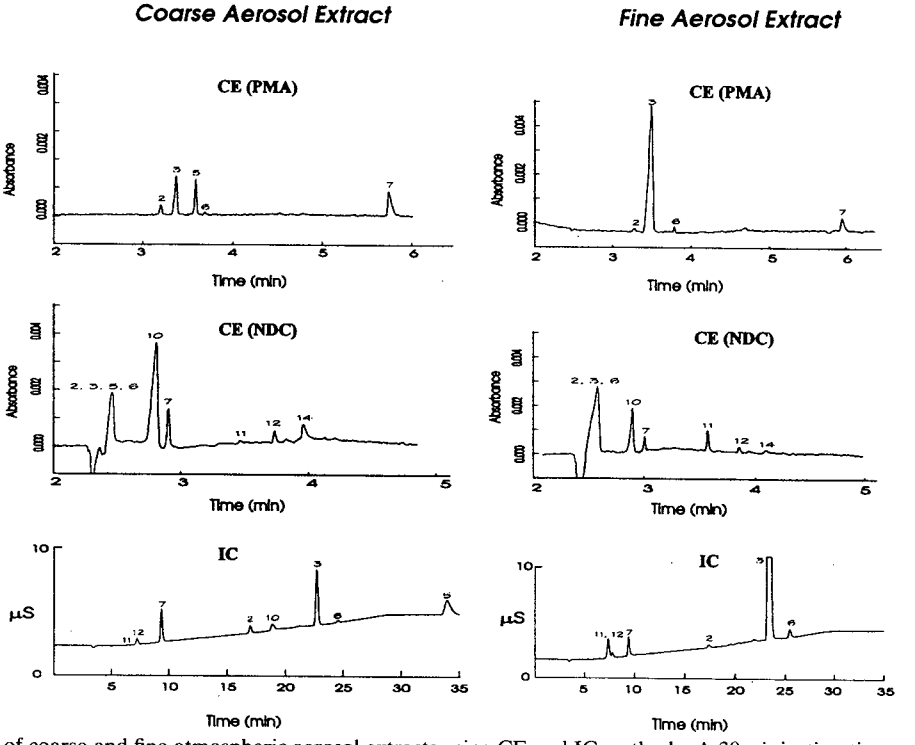

Fig. 2. Analysis of coarse and fine atmospheric aerosol extracts using CE and IC methods. A 30-s injection time was used with the PMA based electrolyte; see Table 1 for more details. Peaks are the same as in Fig. 1.

Organic anions such as formate and acetate are also present in atmospheric aerosols.

Results obtained by parallel analysis of sulphate in the extracts of atmospheric aerosols by CE and IC methods were compared. To date nearly 90 filter samples have been analyzed. Only sulphate was present in a sufficient amount to allow a quantitative comparison of results obtained by the two independent separation methods. Fig. 3 shows a high degree of correlation between CE and IC results for sulphate (CE = 0.91 IC (gradient) + 0.19, $r^2 = 0.9953$; CE = 1.03 IC (isocratic) + 0.03, $r^2 = 0.9969$). Some outliers are present. Additional studies are needed to explain these differences in measured sulphate concentrations between the two methods.

To evaluate the accuracy of CE and IC results, an external control sample was analyzed in the same manner as the samples. The recovery data for the external quality control sample presented in Table 4 agree with interlaboratory medians [24]. The analytical results are also precise as shown by the standard deviation.

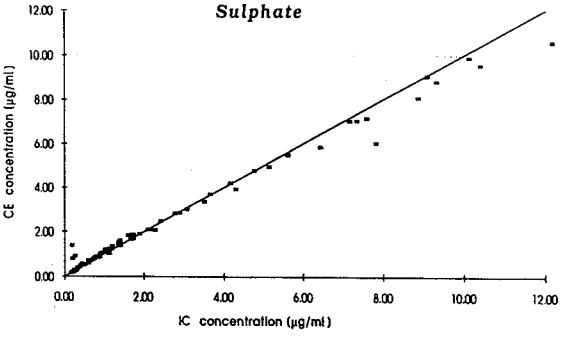

Fig. 3. Comparison of sulphate determined by CE (PMA electrolyte) *vs.* the gradient IC method. The solid line indicates the 1:1 relationship between CE and IC results.

4. Conclusions

Results of this work show that capillary electrophoresis is an effective separation method for the determination of anions in atmospheric aerosols. This technique provides highly efficient separation with high accuracy, precision, short analysis time and low reagent consumption. However, two separate electrolyte systems (PMA and NDC) are recommended for analysis of inorganic and organic anions.

Capillary electrophoresis also complements ion chromatography, the recognized method of ion analysis, and thus greatly reduces problems caused by interfering ions and allows easy peak confirmation. Work continues in this laboratory towards the adoption of CE to other types of samples of interest.

5. References

[1] P.R. Haddad and P.E. Jackson, *Ion Chromatography: Principles and Applications (Journal of Chromatography Library*, Vol. 46), Elsevier, Amsterdam, 1990.
[2] F. Mikkers, F. Everaerts and T. Verheggen, *J. Chromatogr.*, 169 (1979) 1–10.
[3] F. Mikkers, F. Everaerts and T. Verheggen, *J. Chromatogr.*, 169 (1979) 11–20.
[4] J.W. Jorgenson and K.D. Lukacs, *J. Chromatogr.*, 218 (1981) 209–261.
[5] J.W. Jorgenson and K.D. Lukacs, *Anal. Chem.*, 53 (1981) 1298–1302.
[6] W.G. Kuhr, *Anal. Chem.*, 62 (1990) 403R–414R.
[7] P. Jandik and G. Bonn, *Capillary Electrophoresis of Small Molecules and Ions*, VCH Publishers: New York, 1993.
[8] W.R. Jones and P. Jandik, *Amer. Lab.*, 22(9) (1990) 51.
[9] W.R. Jones and P. Jandik, *J. Chromatogr.*, 546 (1991) 431–443.
[10] W.R. Jones and P. Jandik, *J. Chromatogr.*, 546 (1991) 445–458.
[11] B.F. Kenney, *J. Chromatogr.*, 546 (1991) 423–430.
[12] B.J. Wildman, P.E. Jackson, W.R. Jones and P.G. Alden, *J. Chromatogr.*, 546 (1991) 459–466.
[13] J. Romano, P. Jandik, W.R. Jones and P.E. Jackson, *J. Chromatogr.*, 546 (1991) 411–421.
[14] G. Bondoux, P. Jandik and W.R. Jones, *J. Chromatogr.*, 602 (1992) 79–88.
[15] D.R. Salmon and J. Romano, *J. Chromatogr.*, 602 (1992) 219–225.
[16] K.A. Hargadon and B.R. McCord, *J. Chromatogr.*, 602 (1992) 241–247.
[17] S.C. Grocott, L.P. Jefferies, T. Bowser, J. Carnevale and P.E. Jackson, *J. Chromatogr.*, 602 (1992) 257–264.
[18] J.P. Romano and J. Krol, *J. Chromatogr.*, 640 (1993) 403–412.
[19] J.B. Nair and C.G. Izzo, *J. Chromatogr.*, 640 (1993) 445–463.
[20] M.P. Harold, M.J. Wojtusik, J. Rivello and P. Henson, *J. Chromatogr.*, 640 (1993) 463.
[21] E. Dabek-Zlotorzynska and J.F. Dlouhy, *J. Chromatogr.*, submitted for publication.
[22] E. Dabek-Zlotorzynska and J.F. Dlouhy, *J. Chromatogr.*, 640 (1993) 217–226.
[23] E. Dabek-Zlotorzynska, D. Mathieu and J.F. Dlouhy, *The Stability of Aqueous Extracts of Aerosols. Ion Chromatographic Determination of the Effects of Some Preservation Methods*, Environmental Technology Centre, Environment Canada, Ottawa, ON, Canada, 1993.
[24] N. Arafat and K.I. Aspila, *LRTAP Intercomparison Study L-33; Major Ions, Nutrients and Physical Properties in Water*, National Water Research Institute, Burlington, ON, Canada, 1993.

ELSEVIER

Journal of Chromatography A, 671 (1994) 397–402

JOURNAL OF CHROMATOGRAPHY A

Evaluation of carrier electrolytes for capillary zone electrophoresis of low-molecular-mass anions with indirect UV detection

Sarah M. Cousins, Paul R. Haddad*, Wolfgang Buchberger

Department of Chemistry, University of Tasmania, GPO Box 252C, Hobart, Tasmania 7001, Australia

Abstract

Indirect UV detection in capillary zone electrophoresis has been investigated with respect to transfer ratios for low-molecular-mass analyte anions and chromate or various aromatic carboxylic acids acting both as carrier electrolytes and detection probes. The transfer ratio can be regarded as a measure of the effectiveness by which analyte ions displace the UV-absorbing probe ions and has been found to depend on the relative mobilities of the analyte and the carrier. Highest values of transfer ratios have occurred when the carrier ion had a higher mobility than the analyte ion. This trend follows the Kohlrausch theory, but still considerable deviations between calculated and experimental data have been encountered. Consideration of the transfer ratio, the molar absorptivity of the probe and the degree of separation achieved, suggests that chromate is the best electrolyte for high-mobility inorganic anions. The results obtained enable predictions of the most suitable carrier electrolyte for various applications with indirect UV detection.

1. Introduction

In recent years, capillary zone electrophoresis (CZE) has become a highly efficient separation technique for inorganic and low-molecular-mass organic anions [1–3]. Many of these species have no or only negligible UV absorbance, so that indirect UV detection is currently the preferred detection mode. In this form of detection, a UV-absorbing species (or "probe") having the same charge as the analyte is used as electrolyte. Displacement of the probe by the migrating analyte creates a region where the concentration of the probe is less than that in the bulk electrolyte, and this forms the basis of indirect detection [4]. Optimal sensitivity can be achieved if several conditions are fulfilled. First, the detection wavelength should be such that the carrier electrolyte ion generates a UV-absorption background and the sample ion absorption is minimal. Second, the molar absorptivity of the carrier electrolyte ion should be high in order to ensure high sensitivity; the concentration of the carrier electrolyte must be high enough to ensure a high dynamic range but should be such that the background absorbance of the electrolyte falls within the linear range of the detector and is at a level where baseline noise remains low. Third, the mobility of carrier electrolyte ions should be similar to that of analyte ions in order to maintain the shape of the migrating zone as an approximately Gaussian distribution and so avoid a deterioration in resolution.

Sensitivity in indirect UV detection is gov-

* Corresponding author.

0021-9673/94/$07.00
SSDI 0021-9673(93)E1223-M

erned by the molar absorptivity of the carrier electrolyte and its charge. One might expect that the displacement of the probe ion by the migrating analyte would occur on an equivalent-per-equivalent basis. Nevertheless, investigations into quantitative aspects of indirect UV detection published by Nielen [5] show that, from the Kohlrausch theory, the change concentration (Δ[B]) of a probe ion (B) caused by an analyte concentration [A] is given by:

$$\Delta[B] = -\frac{z_A}{z_B} \cdot \frac{\mu_B[\mu_A + \mu_C]}{\mu_A[\mu_B + \mu_C]} \cdot [A] \quad (1)$$

where z is the charge of the analyte (A) and the probe (B) and μ the effective electrophoretic mobility of the analyte (A), the probe (B) and the counter-ion (C). Eq. 1 indicates that equivalent-per-equivalent displacement can be expected only if the analyte has the same mobility as the background ions. When this is not the case, sensitivity of detection will be affected to some extent.

In this paper we report the determination of transfer ratios (TR) for several carrier electrolytes commonly used for anion separation by CZE, including chromate, benzoate, phthalate, trimellitate and pyromellitate. The term "transfer ratio" as used throughout this paper is defined as the number of moles of probe ions displaced by one mole of analyte ions. The data obtained have been used to investigate the degree to which transfer ratios calculated from the Kohlrausch theory can be verified. The general pattern arising from these data should be useful for predictions of optimal carrier electrolyte compositions for various applications.

2. Experimental

2.1. Instrumentation

The CZE instrument employed was a Quanta 4000 (Waters, Milford, MA, USA) interfaced to a Maxima 820 data station (Waters). Separations were carried out using an AccuSep (Waters) fused-silica capillary (60 cm × 75 μm I.D., effective length 52 cm). Injection was performed hydrostatically by elevating the sample at 10 cm for 30 s at the cathodic side of the capillary. The run voltage was −20 kV. Indirect UV detection at 254 nm was used.

2.2. Reagents and procedures

Carrier electrolytes (5 mM) were prepared in water treated with a Millipore (Bedford, MA, USA) Milli-Q water purification apparatus using sodium chromate, benzoic acid, phthalic acid, trimellitic acid (1,2,4-benzenetricarboxylic acid) or pyromellitic acid (1,2,4,5-benzenetetracarboxylic acid). The pH was adjusted to 8.0 using sodium hydroxide or hydrochloric acid. All chemicals used were of analytical-reagent grade. OFM Anion BT (Waters) was used as an electroosmotic flow modifier in all carrier electrolytes at a concentration of 0.5 mM, except in the case of the pyromellitate electrolyte which was used in combination with 0.5 mM hexamethonium bromide (Sigma, St. Louis, MO, USA).

Relative migration times of probe anions were obtained by injecting these anions into a 5 mM phosphate buffer pH 8 and measuring migration times relative to bromide by direct UV detection at 214 nm. Molar absorptivities of the probes were determined using a Varian 5E UV–Vis–near-IR spectrophotometer with 1 cm path length quartz cells.

3. Results and discussion

3.1. Characteristics of the probe ions

At the electrolyte pH used (8.0) in this work, all of the probes are fully ionized, so that the charge varies between −1 (for benzoate) and −4 (for pyromellitate). The molar absorptivities and relative migration times (with respect to bromide) of the probe ions are listed in Table 1, which shows that chromate has the highest mobility, followed by the series of aromatic carboxylic acids arranged in order of decreasing charge. A schematic representation of the relative migration times of the probes and those of

Table 1
Experimentally determined molar absorptivities and relative migration times

Probe	Molar absorptivity ($l\,mol^{-1}\,cm^{-1}$)	Relative migration time[a]
Chromate	3180	1.000
Pyromellitate	7062	1.125
Trimellitate	7147	1.232
Phthalate	1357	1.365
Benzoate	809	1.804

[a] Measured with respect to bromide.

the analyte anions used in this study is given in Fig. 1. It can be seen that only three of the probes (chromate, pyromellitate and trimellitate) have relative migration times (and hence mobilities) which fall within the approximate range covered by the analyte anions, with the remaining two probes having significantly longer relative migration times (*i.e.* lower mobilities).

3.2. Determination of transfer ratios

The determination of transfer ratios was based on the following sequence of steps.

The first step involved the injection of the probe ions (*i.e.* chromate, benzoate, phthalate, trimellitate and pyromellitate) into a UV-transparent electrolyte, which was a phosphate buffer pH 8, using direct UV detection at 254 nm. Calibration plots (peak area *versus* molar concentration) were established for each probe and in order to account for the influence of different migration velocities on the peak area monitored by the detector, all peak areas were multiplied by the apparent velocities of the ions. These velocities were calculated from the migration times and the length of the capillary. The slopes of the calibration plots were calculated from these data and these slopes provided quantitative values for the area counts per mole of each probe.

The next step involved the injection of analyte ions (chloride, sulphate, citrate, fluoride and phosphate) using one of the probes as carrier electrolyte and indirect UV detection at 254 nm. A calibration plot of peak area of analyte ion *versus* molar concentration were prepared for each analyte ion and the slope calculated. As can be seen from Fig. 2A, the slopes for analyte ions of the same charge (which would be expected to be the same if equivalent-per-equivalent displacement of the probe occurred) differed considerably unless the areas were corrected for the varying migration velocities of the sample band. However, even after multiplication of peak areas by migration velocities some differences in slopes still remain, such as for sulphate and phosphate (see Fig. 2B). These variations must be attributed to differences in the transfer ratios of the analyte anions.

In the final step, transfer ratios were calcu-

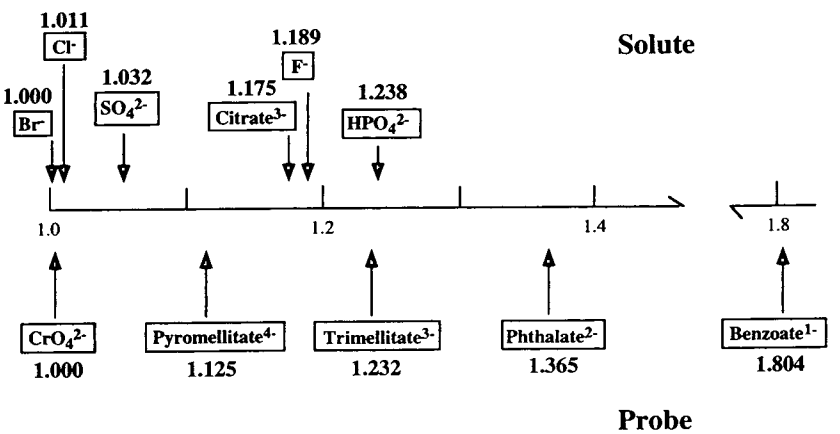

Fig. 1. Relative migration times of the probes and analyte anions used in this study.

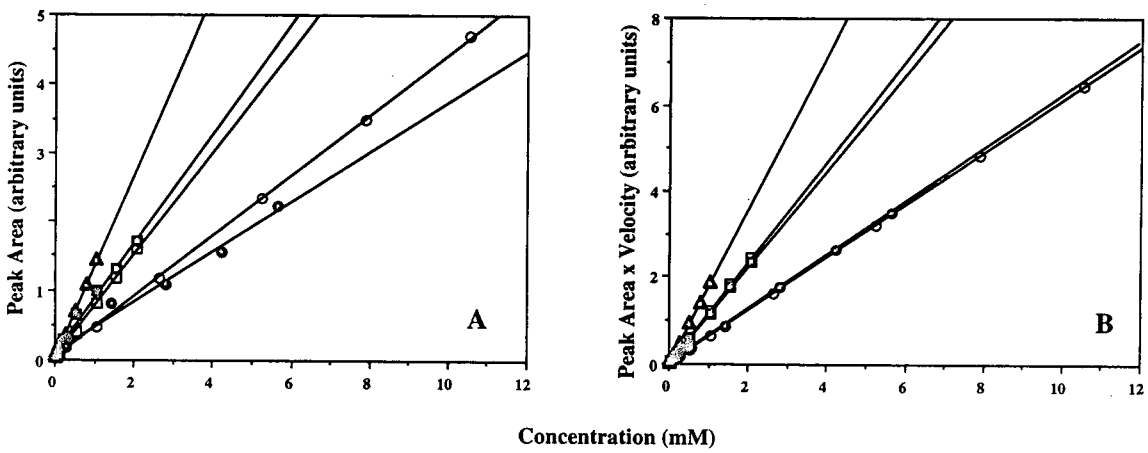

Fig. 2. Calibration plots using trimellitate as probe. (A) Without and (B) with correction for differing migration velocities of the analyte anions. ○ = Fluoride; ● = chloride; □ = sulphate; ■ = phosphate; ▲ = citrate.

lated for each analyte ion. The transfer ratio is the quotient of the slope of an analyte calibration plot and the slope of the probe calibration plot. The entire process was repeated for each probe.

Table 2 summarises the results for transfer ratios of the analyte ions using different probes. The experimentally determined transfer ratios are compared with the ratios expected on the basis of an equivalent-to-equivalent exchange

Table 2
Experimentally determined transfer ratios and comparison with calculated data

		Probe				
		Benzoate	Phthalate	Trimellitate	Pyromellitate	Chromate
Chloride	a	0.184	0.205	0.325	0.366	0.608
	b	1.000	0.500	0.333	0.250	0.500
	c	0.651	0.423			0.521
Fluoride	a	0.421	0.233	0.319	0.356	0.718
	b	1.000	0.500	0.333	0.250	0.500
	c	0.748	0.486			0.599
Sulphate	a	0.897	0.575	0.612	0.625	1.124
	b	2.000	1.000	0.667	0.500	1.000
	c	1.277	0.831			1.023
Phosphate	a	1.065	0.463	0.585	0.584	1.218
	b	2.000	1.000	0.667	0.500	1.000
	c	1.476	0.960			1.182
Citrate	a	1.629	0.614	0.931	0.593	1.756
	b	3.000	1.500	1.000	0.750	1.500
	c	2.019	1.313			1.617

a = Transfer ratios from experiment; b = transfer ratio calculated on the basis of an equivalent-to-equivalent exchange; c = transfer ratio calculated according to ref. 5.

between probe and analyte. Table 2 also includes the transfer ratios calculated from Eq. 1 [5], in which the calculations have been based on mobility data from the literature [6,7]. The experimental data follow the general trend seen in the calculated data, but the fit of the experimental data to the model is poor.

An overview of the transfer ratios and their dependencies on different probes can be achieved if the transfer ratios of the analytes are multiplied by the charge of the probes (in order to normalise variation in transfer ratios arising from the different charges of the probes) and plotted against the relative mobilities of the probes (expressed as the inverse of the relative migration times shown in Fig. 1). This plot is given in Fig. 3. Considering the two univalent analytes (chloride and fluoride), it can be seen that the transfer ratio, corrected for the charge on the probe, should ideally be unity (that is, the lowermost broken line in Fig. 3). The observed values are less than unity for benzoate and phthalate (identified as probes 1 and 2, respectively, in Fig. 3), close to unity for trimellitate (probe 3) and greater than unity for pyromellitate and chromate (probes 4 and 5, respectively). A similar pattern is evident for the two divalent analytes, sulphate and phosphate, with the transfer ratio values being less than the expected value (namely 2) for the probes of low mobility and greater than this value for the probes of higher mobility. The same can be said for the behaviour of the trivalent analyte, citrate. Whilst this trend is in general accordance with Eq. 1, the data show some anomalies. For example, the transfer ratios for chloride and fluoride are almost unity for the trimellitate probe, however its mobility is close only to that of fluoride. Other examples of such anomalies can be seen. Nevertheless, Fig. 3 demonstrates clearly that the transfer ratio of an ion generally increases as the mobility of the probes increases (provided that the charge of the probes remains the same).

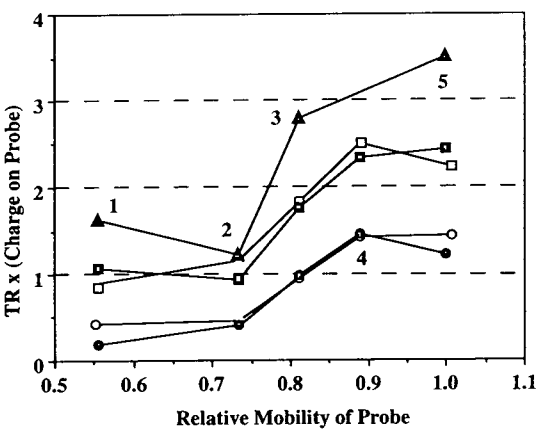

Fig. 3. Dependence of transfer ratios (multiplied by the charge on the probe) upon the relative mobility of the probe. Probes: 1 = benzoate; 2 = phthalate; 3 = trimellitate; 4 = pyromellitate; 5 = chromate. The broken lines show the theoretical values for solutes having a single, double and triple charge. Symbols as in Fig. 2.

3.3. Maximising detection sensitivity

In addition to the transfer ratio, the molar absorptivity of the probe must be taken into account if the sensitivity of indirect UV detection with different probes is to be evaluated. In Fig. 4, the observed transfer ratios multiplied by the absorptivity of the probe are plotted against the relative mobilities of the probes. The higher the value of this product, the higher the sensitivity of indirect UV detection. The fact that the transfer ratios of trimellitate, pyromellitate and chromate

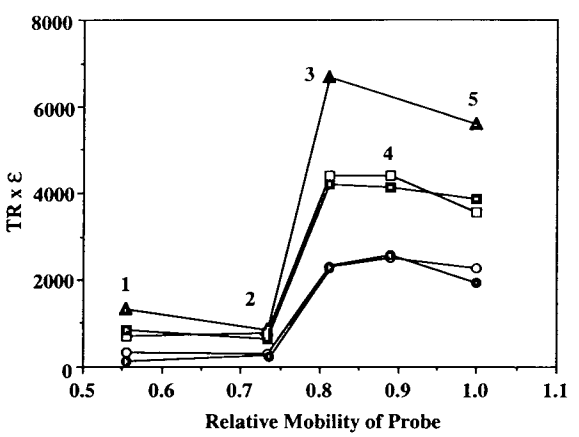

Fig. 4. Dependence of transfer ratios multiplied by the absorptivity of the probe upon the mobility of the probe. Probes: 1 = benzoate; 2 = phthalate; 3 = trimellitate; 4 = pyromellitate; 5 = chromate. Symbols as in Fig. 2.

exceed the equivalent-per-equivalent values, combined with their high molar absorptivities, suggest that these probes should be preferred to benzoate and phthalate. Fig. 2 suggests that optimal sensitivity for most analyte anions will result with trimellitate as probe.

Since the probe also acts as a background electrolyte, selection of a suitable probe must include not only the consideration of high sensitivity but also of separation efficiency. It might become necessary to compromise on sensitivity in order to obtain a desired degree of resolution between species to be separated. A comparison of the separations achieved with chromate, trimellitate and pyromellitate showed that chromate provided the best overall performance for the separation of the analyte anions used in this paper and is therefore the preferred probe, despite a small loss in sensitivity resulting from the fact that its molar absorptivity is less than that for trimellitate.

The results obtained in this paper can be used to predict suitable probes for the indirect detection of a variety of anions. For example, alkanesulphonic acids can be separated and detected using probes such as *p*-phenolsulphonate, *p*-toluenesulphonate or *p*-hydroxybenzoate. The relative migration times (with respect to bromide) of these probes in a phosphate buffer are 1.85, 2.01 and 2.06, respectively. The alkane sulphonates from ethanesulphonate to pentanesulphonate have relative migration times between 1.67 and 2.06. The use of *p*-phenolsulphonate as probe should therefore give the highest transfer ratios. However, *p*-hydroxybenzoate is likely to be the best probe on the basis that its molar absorptivity at 254 nm is much greater than that of the other two probes (ϵ of *p*-hydroxybenzoate: 10299 l mol^{-1} cm^{-1}; ϵ of *p*-phenolsulphonate: 783 l mol^{-1} cm^{-1}; ϵ of *p*-toluenesulphonate: 344 l mol^{-1} cm^{-1}).

4. References

[1] W.R. Jones and P. Jandik, *J. Chromatogr.*, 546 (1991) 445.
[2] W.R. Jones, *J. Chromatogr.*, 640 (1993) 387.
[3] M.P. Harrold, M.J. Wojtusik, J. Riviello and P. Henson, *J. Chromatogr.*, 640 (1993) 463.
[4] F. Foret, S. Fanali, L. Ossicini and P. Boček, *J. Chromatogr.*, 470 (1989) 299.
[5] M.W.F. Nielen, *J. Chromatogr.*, 588 (1991) 321.
[6] J.A. Dean (Editor), *Lange's Handbook of Chemistry*, McGraw-Hill, New York, 14th ed., 1992, p. 8.158.
[7] D.R. Lide (Editor), *Handbook of Chemistry and Physics*, CRC Press, Boca Raton, FL, 72nd ed., 1991, p. 5-96.

ELSEVIER

Journal of Chromatography A, 671 (1994) 403–410

JOURNAL OF CHROMATOGRAPHY A

Applications of capillary electrophoresis in the eye-care pharmaceutical industry

Richard R. Chadwick*, Jeff C. Hsieh, Ketan S. Resham, R. Brett Nelson

Allergan Optical, 2525 Dupont Drive, Irvine, CA 92715-2002, USA

Abstract

The speed and resolution of capillary electrophoresis (CE), combined with its low cost and low volume requirements, make it a promising method of separating eye-care pharmaceuticals and analyzing the ionic composition of tears. Capillary zone electrophoresis (CZE) offers linearity, precision, and recovery comparable to high-performance liquid chromatography (HPLC) at a fraction of its cost. In addition, CZE separates and quantitates cocoamphocarboxyglycinate in the presence of a non-ionic fatty acid amide surfactant seven times faster than HPLC. CE easily detects such cations as sodium and potassium in human tears.

1. Introduction

The eye-care pharmaceutical industry has suffered from slow, expensive analyses and the generation of large volumes of solvent waste. Capillary electrophoresis (CE) offers inherent speed, low operating costs, high resolution, and low sample volume requirements. It is an attractive alternative for the separation problems of eye-care pharmaceuticals. CE is maturing as an analytical technique [1–3], as evidenced by improvement in its quantitative capabilities [4–6], and it is finding increased use in pharmaceutical analysis [7–9]. Capillary zone electrophoresis (CZE) is particularly attractive because it can perform separations with US$ 5 columns instead of the US$ 300–800 columns that high-performance liquid chromatography (HPLC) requires for analyzing multiple types of ionic analytes.

The present work applies CE to quantitative stability assays for the analysis of active ingredients in finished products, raw materials, and ionic components in tears. The contact lens care product segment of the eye-care pharmaceutical industry includes surfactant cleaners for removing protein and lipid deposits from contact lenses, proteolytic enzyme products for removing protein deposits, and disinfecting solutions for contact lenses. These pharmaceuticals require flexible and efficient separation techniques. Additionally, studies designed to assess their ocular effect require analytical tools capable of a detailed analysis of tear constituents.

Cocoamphocarboxyglycinate (see Fig. 1) is a zwitterionic surfactant used to clean lipid and

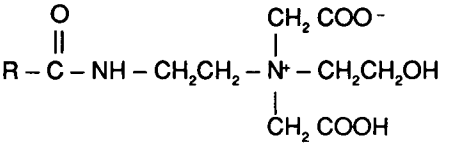

Fig. 1. The structure of cocoamphocarboxyglycinate.

* Corresponding author.

0021-9673/94/$07.00
SSDI 0021-9673(94)00086-O

protein deposits from rigid gas permeable (RGP) contact lenses in the product RESOLVE/GP® Daily Cleaner. Presently, cocoamphocarboxyglycinate is effectively analyzed in this product formulation by ion-exclusion HPLC [10]. However, the method suffers from a long cycle time due to the late elution of the non-ionic fatty acid amide surfactant in the product formulation on the ion-exclusion column (76 min). The present work utilizes CZE to separate and quantitate cocoamphocarboxyglycinate in the presence of non-ionic fatty acid amide surfactant in under 12 min, seven times faster than the existing ion-exclusion HPLC method.

A CE method was developed for the quantitative analysis of the raw material N-acetylcysteine, which is used as a mucolytic agent for aiding in the removal of protein deposits from contact lenses. The current United States Pharmacopeia (USP) method for the analysis of this compendial raw material utilizes reversed-phase HPLC [11]. CE effectively separates N-acetylcysteine from its hydrolysis product cysteine and its oxidation products cystine and N-acetylcystine (see Fig. 2) 1.5 times faster than the USP method while providing comparable precision.

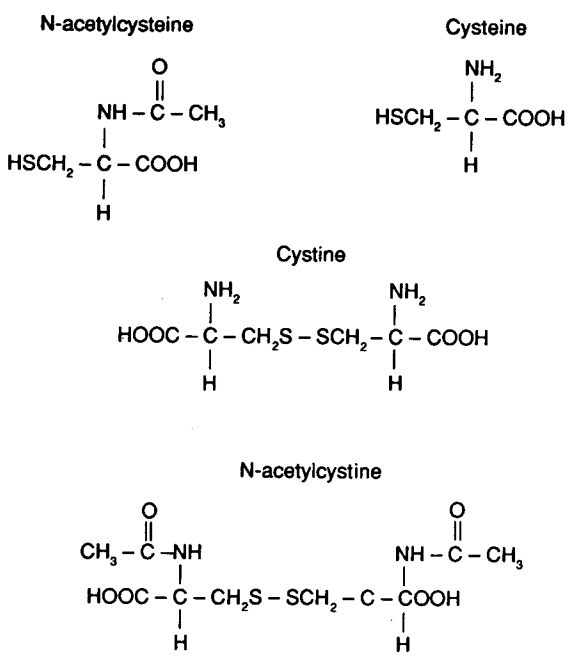

Fig. 2. The structure of N-acetylcysteine and its degradation products.

In ocular research, CE is a powerful technique for studying the composition of tears, including *in-vivo* measurements [12]. Due to the inherently low volume of the human tear, typically 6 μl [13], analysis by HPLC requires multiple tear collections to provide enough sample for analysis since a typical HPLC injection volume is 10 μl. The low sample injection volume required of CE (typically a few nl) makes this technique ideal for analyzing tear samples. Analyzing inorganic constituents of tears is important in establishing benchmarks for normal human corneal physiology. These benchmarks can help in designing products that are compatible with ocular physiology.

2. Experimental

2.1. Materials

Fused silica, polyimide coated capillary tubing (365 μm O.D. × 75 μm I.D.) was obtained from Polymicro Technologies (Phoenix, AZ, USA). ACS reagent grade sodium tetraborate decahydrate, boric acid, copper sulfate pentahydrate and formic acid (88%, w/w) were obtained from Mallinckrodt (Paris, KY, USA). ACS reagent grade sodium borate decahydrate was obtained from Aldrich (Milwaukee, WI, USA).

Cocoamphocarboxyglycinate was obtained from Rhone-Poulenc (Cranbury, NJ, USA). The non-ionic fatty acid amide surfactant was obtained from Stepan Chemical Comp. (Northfield, IL, USA). N-acetylcysteine was obtained from Diamalt/SST Corp. (Clifton, NJ, USA). Reagent grade cysteine, cystine, and benzoic acid were obtained from Sigma (St. Louis, MO, USA). HPLC grade methanol was obtained from Baxter Scientific Products (Irvine, CA, USA). Deionized water having resistivity greater than 17 MΩ · cm was obtained with a Millipore Milli-Q reagent water system (Bedford, MA, USA). N-acetylcystine was generated *in situ* from N-acetylcysteine by treatment with 3% hydrogen

peroxide. All reagents were used as received from the manufacturer.

2.2. Equipment

Electrophoresis experiments were conducted on a Dionex CES I capillary electrophoresis system obtained from Dionex (Sunnyvale, CA, USA). UV detection was employed by using 200 nm radiation for detection of cocoamphocarboxyglycinate and for N-acetylcysteine and its degradation products. For the detection of inorganic cations, indirect UV detection utilizing Cu^{2+} chromophore in the form of $CuSO_4$ at 215 nm was employed [14]. Electrophoretic data were acquired using a PE Nelson Analytical 941 analog-to-digital converter with subsequent storage on a VAX 6000 computer (Bedford, MA, USA).

2.3. Methods

Capillaries (52 cm long) were prepared by scoring the polyimide coating with a ceramic cutting tool and breaking at the scored mark. The on-column detection window was introduced onto the capillary 5 cm from the end by burning off the coating with a butane lighter. The capillary was prepared for use by flushing with 0.5 *M* NaOH under pressure of 5 p.s.i. (1 p.s.i. = 6894.76 Pa) for 3 min, followed by a 3-min rinse with deionized water. This cycle was repeated twice more. The capillary was then flushed for 15 min with the running buffer under pressure. Different running buffers were employed for each analysis and are indicated in the appropriate figures. All buffers were vacuum-filtered through a 0.45-μm Nylon-66 filter to remove particulates.

The 10 m*M* $Na_2B_4O_7$–50 m*M* H_3BO_3, pH 8.5 buffer was prepared from analytical reagent grade $Na_2B_4O_7 \cdot 10H_2O$ and H_3BO_3. The 50:50 (v/v) 10 m*M* $Na_2B_4O_7$–50 m*M* H_3BO_3/methanol buffer was prepared by mixing equal volumes of the 10 m*M* $Na_2B_4O_7$–50 m*M* H_3BO_3 buffer and the HPLC grade methanol. The 4.0 m*M* $CuSO_4$, pH 3.0 buffer was prepared from analytical reagent grade $CuSO_4 \cdot 5H_2O$ and 88% (w/w) formic acid. The pH of the buffer was adjusted to 3.0 with 1 *M* H_2SO_4.

All samples were injected with gravity injection by raising the capillary to a height of 5 cm for 10 s. For all analyses performed, the injection end of the capillary served as the anode. Different separation voltages were employed for the various separations employed. For the analysis of cocoamphocarboxyglycinate, an operating voltage of + 30 kV was employed, + 18 kV was used for the analysis of N-acetylcysteine, and + 20 kV for the analysis of inorganic ions. Peak components were identified by comparing their migration times with those of the corresponding standard for each analyte.

3. Results and discussion

3.1. Separation and quantitation of cocoamphocarboxyglycinate

Cocoamphocarboxyglycinate is a zwitterionic surfactant possessing a quaternary amine nitrogen center and two carboxylate groups (Fig. 1). The RESOLVE/GP Daily Cleaner product formulation also contains a non-ionic fatty acid amide surfactant. These two surfactants may therefore be separated by using a buffer that imparts a non-zero electrical charge to the cocoamphocarboxyglycinate.

Due to the bifunctional nature of cocoamphocarboxyglycinate, one could either lower the pH to impart a positive charge or raise the pH above the pK_a of the cocoamphocarboxyglycinate carboxylate groups to provide a net negative charge to the cocoamphocarboxyglycinate molecule. A high pH buffer approach was adopted. This avoided electrostatic attraction of the cocoamphocarboxyglycinate molecules to the negatively charged silanol sites of the capillary and the associated band tailing problems that can result from such adsorptive interactions if cocoamphocarboxyglycinate carried a positive charge [15]. Additionally, since the electroosmotic flow increases substantially at basic pH, a high pH buffer gives a rapid separation [16].

Another consideration in selecting a separation buffer for the surfactants is the propensity for these materials to stick to glass in the absence of organic solvents. This is especially true with the non-ionic fatty acid amide surfactant, which has limited solubility in pure water. With the above considerations in mind, a buffer consisting of methanol/10 m*M* $Na_2B_4O_7$–50 m*M* H_3BO_3 (50:50) with a pH of 8.5 was employed.

Fig. 3 shows a representative electropherogram obtained by diluting the RESOLVE/GP Daily Cleaner product 1:50 (v/v) in the running buffer. The neutral non-ionic fatty acid amide surfactant homologues are shown to migrate as a single peak at 4.7 min. The cocoamphocarboxyglycinate homologues appear as a cluster of 6 peaks, corresponding to the different alkyl chain homologues centered near 7.0 min. The cocoamphocarboxyglycinate separation displays an efficiency of 54 500 theoretical plates for the main peak at 7.0 min.

Despite the good cocoamphocarboxyglycinate resolution shown in Fig. 3, multiple injections of the sample revealed a deterioration of the cocoamphocarboxyglycinate resolution, and the non-ionic fatty acid amide surfactant peak showed significant tailing (Fig. 4). Dilution of the product formulation in pure methanol reduced the non-ionic fatty acid amide surfactant tailing, recovered the good cocoamphocarboxyglycinate homologue resolution as seen in Fig. 4, and maintained this good resolution for multiple repeated injections of sample.

For quantitation and precision, an internal standard consisting of benzoic acid was added to the sample. Additionally, preliminary spiked recovery studies indicated that cocoamphocarboxyglycinate recovery was lower in the presence of the non-ionic fatty acid amide surfactant, probably due to co-adsorption of these surfactants on the capillary surface. Therefore, non-ionic fatty acid amide surfactant was added to the cocoamphocarboxyglycinate standard.

Fig. 5 illustrates the lack of interference of both the benzoic acid internal standard and non-ionic fatty acid amide surfactant in the detection of cocoamphocarboxyglycinate. Neither compound exhibits any response in the region of the cocoamphocarboxyglycinate peaks. The linearity was checked from 0.03% (w/v) to 0.15% (w/v), corresponding to a range of 25% to 150% of the

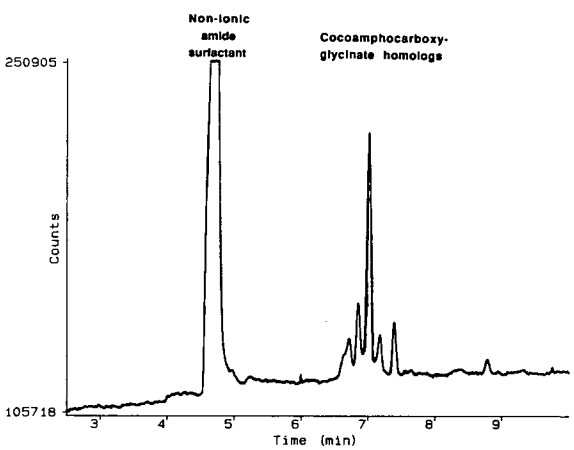

Fig. 3. Electropherogram of cocoamphocarboxyglycinate in RESOLVE/GP Daily Cleaner for contact lenses. Conditions: buffer, 50:50 (v/v) methanol/10 m*M* $Na_2B_4O_7$–50 m*M* H_3BO_3, pH 8.5; capillary, 52 cm (47 cm to detector) × 75 μm I.D.; applied voltage, +30 kV; temperature, ambient; detection, UV absorbance at 200 nm; injection, gravity, 50 mm height for 10 s. Sample concentration 0.4 mg/ml cocoamphocarboxyglycinate obtained by dilution of 1 ml of RESOLVE/GP Daily Cleaner in 50 ml methanol.

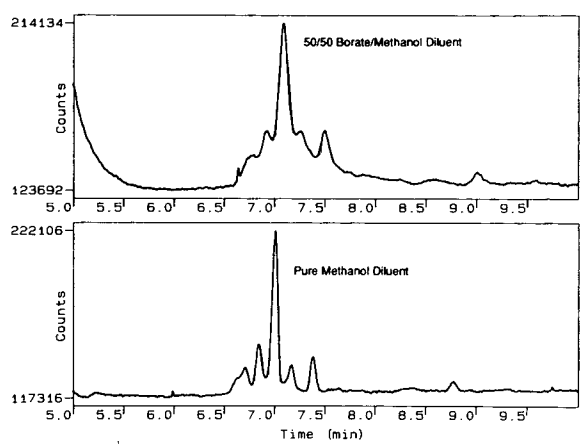

Fig. 4. Electropherogram showing the effect of sample diluent on cocoamphocarboxyglycinate resolution in RESOLVE/GP Daily Cleaner. All electrophoretic conditions as in Fig. 3. Top electropherogram: running buffer used as the diluent (1:50). Bottom electropherogram: pure methanol used as the sample diluent (1:50).

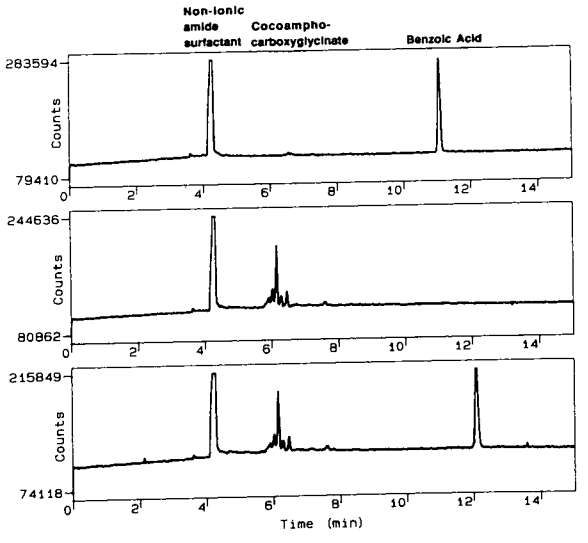

Fig. 5. Overlay of electropherograms showing lack of vehicle and internal standard interference in the analysis of cocoamphocarboxyglycinate. Top: electropherogram of product vehicle spiked with benzoic acid internal standard. Middle: full product formulation without benzoic acid internal standard added. Bottom: full product formulation spiked with benzoic acid internal standard.

label claim (2.00%, w/v) of cocoamphocarboxyglycinate in the surfactant cleaner product.

The cocoamphocarboxyglycinate quantitation data showed excellent linearity in this concentration range, as indicated by a linear correlation coefficient of 0.9995 and a y-intercept very close to zero. The precision at the target concentration of cocoamphocarboxyglycinate contained in the product is 1.5% relative standard deviation (R.S.D., ± 1 SD, $n = 4$).

The equivalence of the present CE method for the analysis of cocoamphocarboxyglycinate with the existing ion-exclusion HPLC method was demonstrated by analyzing a shared sample of RESOLVE/GP Daily Cleaner (see Table 1). Statistical t-testing of the mean cocoamphocarboxyglycinate assay values and F-testing of the standard deviations of these measurements at 95% confidence demonstrated the statistical equivalence of the data obtained by both methods.

Table 1 shows an overall performance comparison of the CE cocoamphocarboxyglycinate method and the ion-exclusion HPLC method. The CE method yields comparable linearity, precision, and accuracy to the ion-exclusion HPLC method. However, it is seven times faster and much more economical due to lower column costs and significantly lower consumption of chemicals.

3.2. Raw material analysis: N-acetylcysteine

N-acetylcysteine raw material analysis is currently performed by analytical methodology specified in the United States Pharmacopeia XXII [11], which utilizes reversed-phase HPLC. For analysis by CE, a pH 8.5 buffer was em-

Table 1
Comparison of cocoamphocarboxyglycinate analysis by CE and ion-exclusion HPLC

Parameter	CE	Ion-exclusion HPLC
Linearity, r	0.9995	0.9990
Precision, as % R.S.D. (± 1 SD, $n = 6$)	± 1.5%	± 1.6%
Recovery at 100% of product label claim (2.0% w/v corresponding to 0.04% w/v injected; ± 1 SD, $n = 6$)	100.0 ± 1.5%	100.6 ± 1.6%
Analysis time per sample	12 min	90 min
Volume mobile phase per sample	0.1 ml	50 ml
Column cost	US$ 5	US$ 800
Cocoamphocarboxyglycinate assay results for shared RESOLVE/GP Daily Cleaner sample	2.01 ± 0.03% (w/v) ± 1 SD, $n = 6$	2.03 ± 0.03% (w/v) ± 1 SD, $n = 6$

ployed. To analyze the purity of N-acetylcysteine raw material, the analytical method must be able to separate N-acetylcysteine from its degradation products: cysteine, cystine, and N-acetylcystine. Fig. 2 shows their structures and Fig. 6 displays the electropherogram of N-acetylcysteine and its degradation products. Cysteine and cystine are seen to comigrate at 3.9 min, ahead of the N-acetylcysteine peak seen at 4.6 min. The separation displays high efficiency, with approximately 41 000 theoretical plates seen for the N-acetylcysteine peak. N-acetylcystine (the disulfide dimer of N-acetylcysteine) is observed at 5.0 min.

For quantitative analysis, benzoic acid served as an internal standard and the area of the N-acetylcysteine peak was ratioed against the benzoic acid peak. Fig. 7 shows the electropherogram of N-acetylcysteine spiked with the benzoic acid internal standard. The linearity of the N-acetylcysteine CE method was tested in the concentration range of 0.3–1.6 mg/ml. Linear least-squares analysis yielded a correlation coefficient of 0.99995.

To assess the equivalence of the CE method to the USP HPLC method for N-acetylcysteine

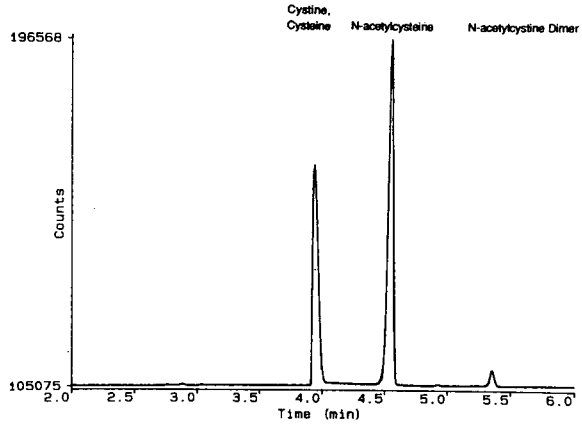

Fig. 6. Electropherogram of N-acetylcysteine and its degradation products. Conditions: buffer, 10 m*M* $Na_2B_4O_7$–50 m*M* H_3BO_3, pH 8.5. capillary, 52 cm (47 cm to detector) × 75 μm I.D.; applied voltage, +18 kV; temperature, ambient; detection, UV absorbance at 200 nm; injection, gravity, 50 mm height for 10 s. Sample concentration, 0.5 mg/ml of each component except N-acetylcystine, which appears at a concentration of approximately 0.1 mg/ml.

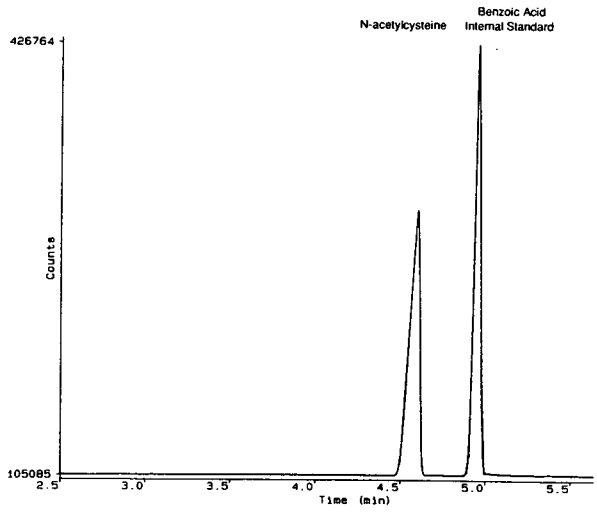

Fig. 7. Electropherogram of N-acetylcysteine with benzoic acid internal standard spiked in (all conditions as in Fig. 6).

analysis, a sample of N-acetylcysteine raw material was assayed by the two methods. Table 2 compares the assay data obtained by both methods. The mean N-acetylcysteine assay values were compared by *t*-testing at the 95% confidence interval and shown to be nearly equivalent. The CE method displayed a precision of 0.5% R.S.D. This is comparable to the HPLC assay data obtained with the USP method, and it is well within the USP guideline of $<2\%$ R.S.D.

The CE method for the analysis of N-acetylcysteine is extremely rapid and cost effective, as Table 2 shows. The CE method is three times faster and the column costs are approximately one sixtieth due to the low costs of fused silica capillaries compared to reversed-phase C_{18} HPLC columns.

3.3. CE analysis of inorganic cations in tears

Fig. 8 shows the electropherogram of a human tear sample diluted 1:24 (v/v) in deionized water. Comparison of the peaks observed for the tear electropherogram with the peaks for an inorganic cation standard containing potassium, sodium, calcium, and magnesium identifies the cation peaks in the tear electropherogram. Potassium migrates at 3.4 min in the tear sample,

Table 2
Comparison of CE USP reversed-phase HPLC methods for N-acetylcysteine raw material analysis

Parameter	CE	Reversed-phase HPLC
Precision, as % R.S.D. (±1 SD, $n = 6$)	±0.7%	±0.3%
Run time	6 min	15 min
Column cost	US$ 5	US$ 300
N-Acetylcysteine assay purity	99.6 ± 0.7% (w/w) ± 1 SD, $n = 6$	100.8 ± 0.3% (w/w) ± 1 SD, $n = 6$

followed by sodium at 5.0 min, calcium at 5.3 min, and magnesium at 5.8 min.

The efficiency of the separation as measured by the number of theoretical plates in the sodium peak displays 1200 theoretical plates for the tear sample. However, the separation has high enough efficiency to clearly separate sodium, potassium, calcium, and magnesium from one another. The relatively low number of theoretical plates seen for sodium is due mainly to sample overload.

Because the current study is preliminary, the method has not had rigorous linearity testing. However, a semi-quantitative estimate of the concentration of the various components was performed. It was based on peak area comparisons between the tear sample and the cation standard shown in Fig. 8. All the levels observed are in general agreement with values reported in the literature.

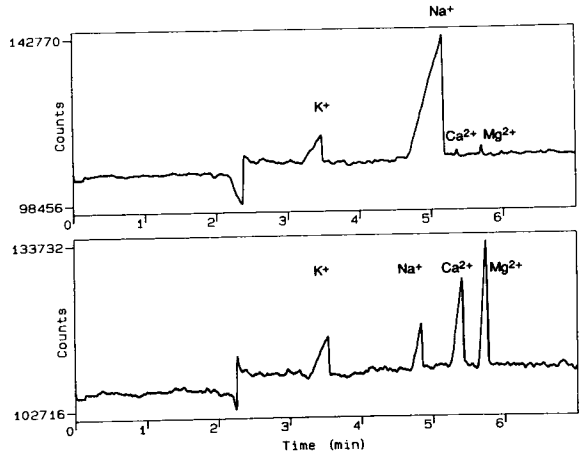

Fig. 8. Survey electropherogram of human tear sample diluted 1:20 in deionized water (top) and inorganic cation standard (bottom). Conditions: Buffer, 4 m*M* copper(II) sulfate–4 m*M* formic acid (3:6); capillary, 52 cm (47 cm to detector) × 75 μm I.D.; applied voltage, +20 kV; temperature, ambient; detection, indirect UV at 215 nm.

4. Conclusion

CE is an effective, flexible technique capable of analyzing components important to the eye-care pharmaceutical industry. The current project has demonstrated the applicability of CE to the analysis of active ingredients in product formulations, raw material analysis, and ocular research. The ability of CE to perform as a quantitative analytical technique was demonstrated by the analysis of cocoamphocarboxyglycinate in a surfactant cleaner product and by the analysis of N-acetylcysteine raw material. The precision, linearity, and accuracy were comparable to existing HPLC methods but analysis times and cost were significantly less.

CE was also shown to be a useful tool for probing the composition of inorganic cations in tears. The inherent speed, high resolution, and powerful separation mechanism of CE make it an excellent tool for separation challenges encountered by the eye-care pharmaceutical industry.

5. Acknowledgements

The author would like to thank Mr. Mossa Abdul for obtaining the comparative HPLC data and Dr. Howard Goldman for editorial assistance in preparing this manuscript.

6. References

[1] W.G. Kuhr and C.A. Monnig, *Anal. Chem.*, 64 (1992) 389R.

[2] W.G. Kuhr, *Anal. Chem.*, 62 (1990) 403R.

[3] R.A. Wallingford and A.E. Ewing, *Adv. Chromatogr.*, 29 (1989) 1.

[4] D.M. Goodall, S.J. Williams and D.K. Lloyd, *Trends Anal. Chem.*, 10 (1991) 272.

[5] E.B. Dose and G.A. Guichon, *Anal. Chem.*, 63 (1991) 1154.

[6] S.J. Williams, D.M. Goodall and K.P. Evans, *J. Chromatogr.*, 629 (1993) 379.

[7] S.R. Rabel and J.F. Stobaugh, *Pharm. Res.*, 10 (1993) 171.

[8] S. Arrowood and A.M. Hoyt, Jr., *J. Chromatogr.*, 586 (1991) 177.

[9] P.S. Dalal, P. Albuquerque and H.R. Bhagat, *Anal. Biochem.*, 211 (1993) 34.

[10] *Allergan Analytical Chemistry Development Method*, Allergan, Irvine, CA, 1988.

[11] *The United States Pharmacopeia*, Mack Publishing, Easton, PA, 22nd Revision (USP XXII), 1990.

[12] S.T. Lin, R. Dadoo, R.B. Mandell and R.N. Zare, unpublished manuscript.

[13] W. Scherz, M.G. Doane and C.H. Dohlam, *Albrecht von Graefes Arch. Klin. Exp. Opthamol.*, 192 (1974) 141.

[14] *Determination of Alkali Metals, Alkaline-Earth Metals, and Ammonium using Capillary Electrophoresis, Dionex Application Note No. 84*, Dionex, Sunnyvale, CA, 1992.

[15] R.R. Chadwick, J.C. Hsieh and R.B. Nelson, paper presented at the *Joint Meeting of FACSS XVIII and Pacific Conference, Anaheim, CA 1991*, Abstract No. 692.

[16] P.D. Grossman and J.C. Colburn, *Capillary Electrophoresis: Theory and Practice*, Academic Press, New York, 1992.

ELSEVIER

Journal of Chromatography A, 671 (1994) 411–417

JOURNAL OF CHROMATOGRAPHY A

Factors influencing trace ion analysis with preconcentration by electrostacking

Mary Jo Wojtusik*, Michael P. Harrold

Dionex Corporation, 1228 Titan Way, Sunnyvale, CA 94088, USA

Abstract

Capillary electrophoresis with indirect UV detection and electrostacking achieves low μg/l detection limits for inorganic anions and cations in various low conductivity matrices. Since this technique requires electromigration injection, parameters such as analyte electrophoretic mobility, electroosmotic flow, and sample and operating buffer ionic strength influence the amount of material that is actually injected into the capillary. These parameters are not easily controlled and are affected by such factors as injection voltage and duration, operating buffer, and operating buffer pH. The effects of these factors on sensitivity and resolution are demonstrated. The use of a novel carrier ion, dimethyldiphenylphosphonium ion, improves sensitivity for cations. Techniques for optimizing trace level determinations are also discussed.

1. Introduction

Capillary zone electrophoresis (CZE) with indirect UV detection is fast becoming a routine technique for the determination of small, inorganic ions when present at mg/l concentrations in various sample matrices. However, very few reports have dealt specifically with trace enrichment of inorganic ions to achieve μg/l detection limits [1–4]. To date, trace enrichment to enhance sensitivity in CZE has been performed using: on-line isotachophoresis (ITP) prior to CZE separation with an ITP preconcentration capillary which is then coupled to the separation capillary [1,5–8], field amplification [9,10], and electrostacking [2]. Electrostacking is an attractive technique because the isotachophoretic preconcentration step and the electrophoretic separation are performed in the same capillary [3] and can be done with unmodified, commercially available instrumentation.

To perform electrostacking, a sample of lower ionic strength than the operating buffer is injected into the capillary using an electromigration injection in which sample components migrate into the capillary under the influence of an applied electric field. The sample injected is thus biased toward ions with the highest mobilities [11,12]. When using electromigration injection, the electric field strength along the length of the capillary is not constant. The portion of the capillary filled with high resistivity, low conductance sample experiences a much higher field strength than the remainder of the capillary that contains lower resistivity, higher conductance operating buffer [11]. Since analyte velocity is directly proportional to field strength [13], analyte ions migrate rapidly to the concentration boundary between the operating buffer and the sample zone and "stack" as they slow down at the boundary interface [14]. Enrichment factors

* Corresponding author.

0021-9673/94/$07.00
SSDI 0021-9673(93)E1254-W

of several orders of magnitude from very low ionic strength samples are possible using the electrostacking technique [2,3].

To normalize the conductance of both sample and standard solutions, an isotachophoretic terminating ion, typically at low μM concentration, is added to both [3]. With normalized conductance for both sample and standard solutions, accurate quantification of analytes in low ionic strength sample matrices is possible. The terminating ion must have the same charge as the analytes of interest and must migrate slower so as not to interfere with the stacking process or the separation of the analytes. Typical terminating ions are tetrabutylammonium for cation separations and octanesulfonate for anion separations.

Since electrostacking of inorganic ions is typically performed in fused-silica capillaries, electroosmotic flow also plays a role in the trace enrichment process. For example, the movement of the concentration boundary formed by the high ionic strength operating buffer and the lower ionic strength sample is dependent on the electroosmotic flow of the entire bulk solution and is described by an average electroosmotic flow velocity [14] as opposed to a true isotachophoretic concentration boundary which moves at a constant velocity [15]. Isotachophoresis is typically performed in coated capillaries which exhibit no electroosmotic flow. Electroosmotic flow is influenced by such parameters as the nature of the operating buffer ions, operating buffer pH, and injection voltage. The extent to which these parameters affect the trace enrichment of inorganic ions using electrostacking and other factors that influence sensitivity and resolution are discussed in this paper.

2. Experimental

2.1. Equipment

The capillary electrophoresis experiments were performed with a Dionex CES-I automated system and UV detection (Dionex, Sunnyvale, CA, USA). Fused-silica capillaries (Polymicro Technologies, Phoenix, AZ, USA) of 50 μm I.D., 375 μm outer diameter (O.D.), and 50 cm total length were used. The detection window was located 5 cm from the end of the capillary. Data collection was with a Dionex AI-450 chromatography workstation using a 10-Hz sampling rate. Dionex OnGuard A cartridges in the hydroxide form were used to convert dimethyldiphenylphosphonium (DDP) iodide to DDP hydroxide, and hexamethonium bromide to hexamethonium hydroxide (HMOH).

2.2. Chemicals

Pyromellitic acid (PMA) and 2-(N-morpholino)ethanesulfonic acid (MES) were obtained from Sigma (St. Louis, MO, USA). Hexamethonium bromide (monohydrate), dimethyldiphenylphosphonium iodide, and 18-crown-6 (1,4,7,10,13,16-hexaoxacyclooctadecane) were obtained from Aldrich (Milwaukee, WI, USA). Triethanolamine and formic acid were obtained from Fluka (Ronkonkoma, NY, USA). Sodium hydroxide, 50% aqueous solution (w/w) and phosphoric acid were obtained from Fisher Scientific (Pittsburgh, PA, USA). Copper(II) sulfate (pentahydrate) was obtained from MCB (Norwood, OH, USA). Octanesulfonic acid, 0.1 *M* aqueous solution, and tetrabutylammonium hydroxide, 0.1 *M* aqueous solution, were from Dionex. All reagents were ACS or analytical reagent grade and prepared in 18 mΩ cm resistance deionized water.

In experiments where premixed operating buffers were applicable, IonPhor Anion PMA Electrolyte Buffer and IonPhor Cation Cu Electrolyte Buffer from Dionex were used.

Cation standards were obtained as 1000 mg/l ion standard solutions from Aldrich or prepared from chloride salts obtained from Fisher Scientific. Anion standards were prepared from sodium salts obtained from Fisher Scientific.

3. Results and discussion

3.1. Operating buffer pH

During electrostacking of analytes in a low ionic strength sample matrix, the pH of the

operating electrolyte can greatly effect efficiency and resolution. Fig. 1 shows a comparison of the separation of cations using an operating buffer that contains copper(II) as the carrier ion at different pH values. A carrier ion is a buffer component that has the same electrical charge and similar electrophoretic mobility as the analytes of interest. An additional requirement for indirect UV detection is that the carrier ion must also be chromophoric. At the higher pH, electroosmotic flow is faster and analyte migration times are shorter. Higher efficiencies are observed at higher pH for the earlier migrating species (Table 1) primarily because at the higher pH, the mobility of the copper(II) carrier ion is more closely matched to the mobilities of the earlier migrating analytes and band dispersion is minimized [16].

Table 1
Efficiencies for cation standards using cupric-containing operating buffer at pH 3.0 and pH 4.8

Cation	Efficiency[a]	
	pH 3.0	pH 4.8
Ammonium	2579	4454
Potassium	8351	11 695
Sodium	8442	14 511
Calcium	24 763	26 711
Magnesium	30 000	39 624
Strontium	164 404	129 051
Lithium	132 594	77 014
Barium	68 702	48 803

[a] Values were calculated using the electropherograms in Fig. 1 and peak width at $\frac{1}{2}$ height.

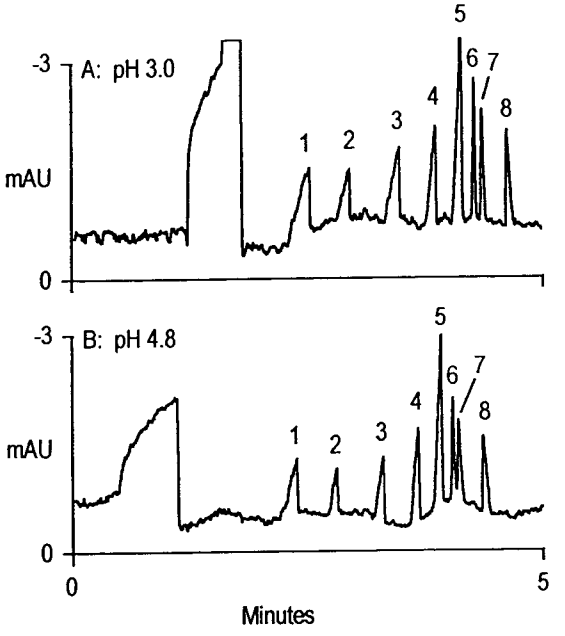

Fig. 1. Effect of operating buffer pH on efficiency. Conditions: (A) operating buffer, 4 m*M* copper(II) sulfate, 4 m*M* 18-crown-6, 4 m*M* formic acid, pH 3.0; capillary, 50 cm × 50 μm I.D. fused silica; positive polarity, detector side cathodic; constant voltage at 20 kV; injection, electromigration, 5000 V, 90 s; detection, indirect UV at 215 nm; terminating ion, 50 μ*M* tetrabutylammonium hydroxide; (B) as in A except operating buffer, 4 m*M* copper(II) sulfate, 4 m*M* 18-crown-6, pH 4.8. The large baseline disruption prior to peak 1 is likely hydronium ion. Cation standards: 1 = ammonium ion (50 μg/l); 2 = potassium (50 μg/l); 3 = sodium (50 μg/l); 4 = calcium (50 μg/l); 5 = magnesium (50 μg/l); 6 = strontium (50 μg/l); 7 = lithium (10 μg/l); 8 = barium (75 μg/l).

Another effect that may contribute to higher efficiencies of the earlier migrating analytes with the higher pH buffer is the increased electroosmotic flow as compared to the electroosmotic flow of the pH 3 buffer. With the higher electroosmotic flow, the velocity of the concentration boundary is faster and the boundary forms higher up in the capillary so that a larger area or zone of low ionic strength solution forms as compared to a lower pH buffer with slower electroosmotic velocity. The larger zone of lower conductance sample creates a larger region of higher effective electric field strength and permits more "stacking" of the analytes with higher electrophoretic mobility, since analyte velocity is increased in this region.

Hydrostatic injection of a plug of water prior to electrostacking also creates a larger, low conductance, high electric field zone [17]. In electropherogram Fig. 2A, a typical electrostacking experiment was performed in which a cation standard was injected using electromigration injection at 5000 V for 90 s. Electropherogram Fig. 2B was obtained by first injecting a plug of water using gravity injection (100 mm for 20 s) and then injecting the cation standard with electromigration injection. A significant improvement in the efficiencies of calcium through

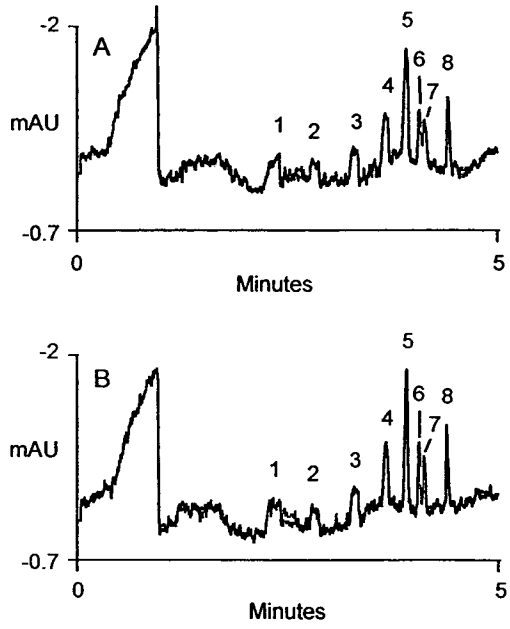

Fig. 2. Effect of water plug preinjection. Conditions: (A) as in Fig. 1A; (B) as in Fig. 1A, except first injection, water hydrostatic injection, gravity, 100 mm, 20 s; second injection, as in Fig. 1A. Cation standards: 1 = ammonium ion (5 μg/l); 2 = potassium (5 μg/l); 3 = sodium (5 μg/l); 4 = calcium (5 μg/l); 5 = magnesium (5 μg/l); 6 = strontium (5 μg/l); 7 = lithium (1 μg/l); 8 = barium (7.5 μg/l).

barium is observed. The peaks representing ammonium ion, potassium, and sodium are at or below detection limits with no improvement in efficiency. The improved efficiency has resulted in better resolution for strontium and lithium. Thus, hydrodynamic preinjection of a water plug is an effective means of improving efficiency and sensitivity for most cations. Application of this technique is obviously limited by the magnitude of the water blank.

3.2. Carrier ion

Since the carrier ion provides the UV background for indirect detection and its mobility to a large extent determines analyte peak efficiency and shape, the specific carrier ion used influences sensitivity. For example, when using dimethyldiphenylphosphonium (DDP) as the UV-absorbing carrier ion for cation separations, an improvement in detection limits is realized compared to separations obtained with a cupric carrier ion (Table 2). A representative electropherogram is shown in Fig. 3. Visual comparison of the electropherogram in Fig. 3 with the electropherograms in Fig. 1, which were ob-

Table 2
Comparison of detection limits using cupric-containing buffer and DDP-containing buffer

Cation	Detection limits (μg/l)[a]	
	Cupric-containing buffer[b]	DDP-containing buffer[c]
Ammonium	11	3
Potassium	7	2
Calcium	7	8
Sodium	9	3
Magnesium	7	1
Strontium	14	3

[a] Detection limit = (S.D.) · $t_{(s)}$ where $t_{(s)}$ for 99% single sided student's t-test distribution.
[b] Electrophoretic conditions as in Fig. 3 for pH 3.0 operating buffer.
[c] Electrophoretic conditions as in Fig. 4.

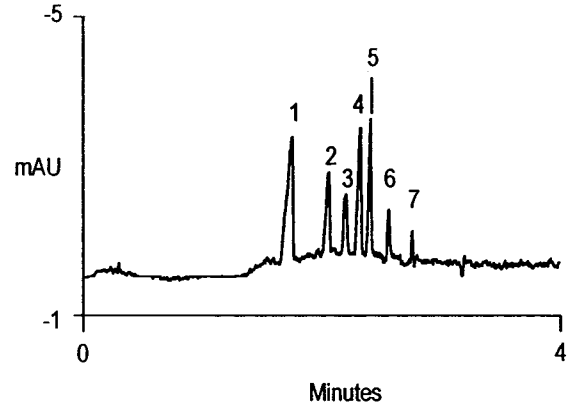

Fig. 3. Electropherogram from DDP-containing operating buffer. Conditions: operating buffer, 5 m*M* DDP hydroxide, 4 m*M* 18-crown-6, 5 m*M* MES, pH 6.0 adjusted with phosphoric acid; capillary, 50 cm × 50 μm I.D. fused silica; positive polarity, detector side cathodic; constant voltage at 25 kV; injection, electromigration, 2500 V, 45 s; terminating ion, 50 μ*M* tetrabutylammonium hydroxide. Cation standards: 1 = ammonium ion (5 μg/l); 2 = potassium (10 μg/l); 3 = calcium (10 μg/l); 4 = sodium (10 μg/l); 5 = magnesium (5 μg/l); 6 = strontium (10 μg/l); 7 = barium (10 μg/l).

tained with the cupric carrier ion, shows that the mobility of DDP is more closely matched to the mobilities of the analytes than is cupric ion at either pH 3.0 or pH 4.8. More symmetric peaks are obtained with DDP as a result of the similar mobilities. In addition, the signal-to-noise ratio is much better with DDP even with analytes present at a factor of 10 less as compared to the signal-to-noise ratio for the cupric carrier ion.

Dimethyldiphenylphosphonium is commercially available as the iodide salt. In order to obtain sensitive indirect UV detection with DDP, the iodide, which absorbs strongly at low UV wavelengths, is exchanged with hydroxide by passing DDP iodide through a hydroxide-form anion-exchange resin.

3.3. Injection voltage

Electrostacking also provides low μg/l detection limits for small inorganic anions (Table 3). However, too high of an injection voltage can adversely effect resolution of some analytes. This effect is shown in Fig. 4. The electropherograms in Fig. 4A and B were obtained using identical conditions except for the injection voltage, which was 2500 V in Fig. 4A and 5000 V in Fig. 4B. In electropherogram 4B, formate and phosphate comigrate and the baseline disruption due to carbonate is significantly earlier. The reason for this has as yet not been determined, however we postulate that at the higher injection voltage, more highly mobile hydroxide ion is concentrated in the capillary creating a localized pH change that is too high to be buffered by the electrolyte. The migration of weak acids, such as formate, phosphate, and carbonate, would be the most affected by such a pH phenomenon.

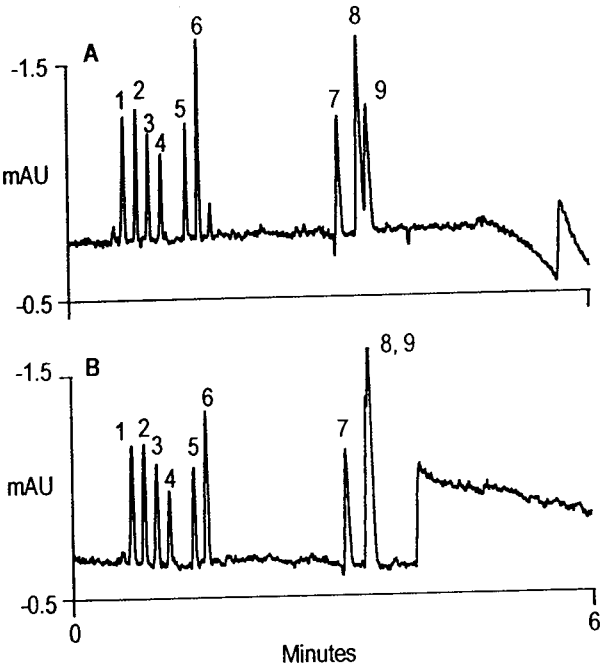

Fig. 4. Effect of injection voltage on efficiency and resolution. Conditions: (A) operating buffer, 2.25 m*M* pyromellitic acid, 6.50 m*M* sodium hydroxide, 0.75 m*M* hexamethonium hydroxide, 1.6 m*M* triethanolamine, pH 7.7; capillary, 50 cm × 50 μm I.D. fused silica; negative polarity, detector side anodic; constant voltage, 30 kV; injection, electromigration, 2500 V, 45 s; terminating ion, 50 μM octanesulfonic acid; (B) as in A except injection, electromigration, 5000 V, 45 s. Anion standards: 1 = chloride (10 μg/l); 2 = sulfate (10 μg/l); 3 = nitrite (10 μg/l); 4 = nitrate (10 μg/l); 5 = molybdate (20 μg/l); 6 = azide (20 μg/l); 7 = fluoride (5 μg/l); 8 = formate (10 μg/l); 9 = phosphate (20 μg/l).

Table 3
Detection limits for anion standards using electrostacking

Anion[a]	Detection limits (μg/l)[b]
Chloride	0.5
Sulfate	0.6
Nitrate	1.5
Fluoride	0.9
Phosphate	2.0

Electrophoretic conditions as in Fig. 5A.
[a] Anion standard concentration was 5 μg/l.
[b] Detection limit = (S.D.) · $t_{(s)}$ where $t_{(s)}$ for 99% single sided student's t test distribution.

An interesting and unexpected result is that the efficiencies observed for the peaks in electropherogram 4A in which sample was introduced using a 2500-V electromigration injection are better than the efficiencies observed when a 5000-V electromigration injection was used as in electropherogram 4B. Both electropherograms were obtained using the same separation conditions. The result indicates that less band dispersion occurs during separation if sample is

injected using a lower voltage. One possible explanation is that heat generated during injection is not dissipated during separation. A 5000-V electromigration injection would produce more heat than a 2500-V injection and would potentially result in more band dispersion.

3.4. Operating buffer impurities

The presence of trace ionic impurities, especially the analyte(s) of interest, in the operating buffer compromise accurate determination because subsequent to the electrostacking process, the impurities in the operating buffer zone that enters the capillary when the capillary is placed back in the buffer solution after injection migrate to and are separated with the individual analyte zones. In Fig. 5A, the electropherogram was obtained using an operating buffer to which had been added trace levels (10 μg/l) of bromide, chloride, sulfate, and nitrate. High purity, deionized water was injected using electromigration. An injection of water using identical conditions except that "uncontaminated" operating buffer was used is shown in Fig. 5B for comparison. As indicated by the electropherograms in Fig. 5, it is imperative that when performing electrostacking for trace anion analysis, the operating buffer be free of ionic impurities, most notably the ionic species of interest for the analysis. In addition, the presence of electroosmotic flow modifier counterions, such as bromide from hexamethonium bromide or tetradecyltrimethylammonium bromide (TTAB), or chloride from cetyltrimethylammonium chloride (CTAC), will prevent accurate determinations using electrostacking if the counterion is not removed from the operating buffer. Ionic impurities in the terminating ion solution added to the sample are also present as interferences.

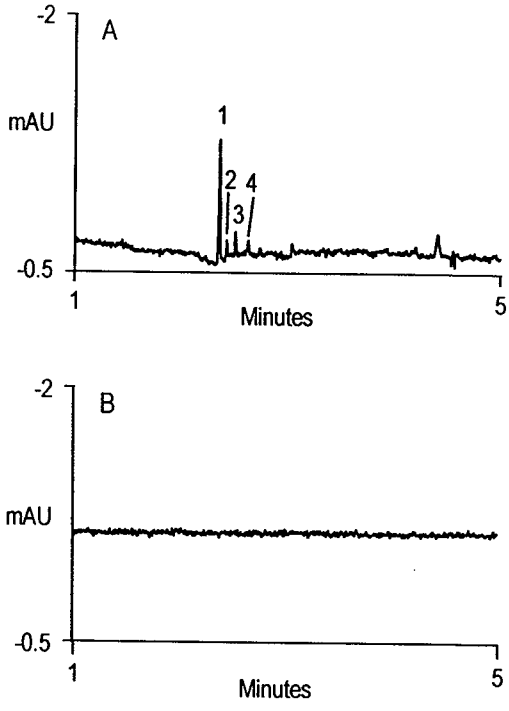

Fig. 5. Effect of trace level impurities in the operating buffer. Conditions: (A) as in Fig. 4A except 10 μg/l each of bromide, chloride, sulfate, and nitrate were added to the operating buffer; injection, water sample by electromigration, 2500 V, 45 s; No terminating ion added to the sample; (B) as in A except uncontaminated operating buffer used. Peaks: 1 = bromide; 2 = chloride; 3 = sulfate; 4 = nitrate.

4. Conclusions

Electrostacking with electromigration injection permits low μg/l level determinations of inorganic ions in low ionic strength sample matrices. Stacking can be enhanced by using conditions such as operating buffer pH, that promote formation of the concentration boundary higher up in the capillary creating a larger high electric field zone. Hydrostatic introduction of a water plug prior to electrostacking also enhances the stacking effect by creating a larger high field zone. The carrier ion, DDP, can be used for trace cation determinations as an alternative to cupric ion or chromophoric amines and provides excellent signal-to-noise ratio for trace level determinations. The resolution of weak acid anions can be adversely effected if electromigration injection voltage is too high. To ensure accurate determination when electrostacking, the operating buffer and the terminating ion solution must be free of impurities that interfere with the electrophoretic separation. By optimizing both

the electrostacking and the electrophoretic separation conditions, sensitivity for trace ions is maximized.

5. Acknowledgements

The authors thank Dr. John Statler and John Stillian for their suggestions and comments during preparation of this manuscript.

6. References

[1] F.M. Everaerts, Th.P.E.M. Verheggen and F.E.P. Mikkers, *J. Chromatogr.*, 169 (1979) 21.
[2] P. Jandik, W.R. Jones, A. Weston and P.R. Brown, *LC · GC*, 9 (1991) 634.
[3] P. Jandik and W.R. Jones, *J. Chromatogr.*, 546 (1991) 431.
[4] P.E. Jackson and P.R. Haddad, *J. Chromatogr.*, 640 (1993) 481.
[5] V. Dolnik, M. Deml and P. Bocek, *J. Chromatogr.*, 320 (1985) 89.
[6] D. Kaniansky and J. Marak, *J. Chromatogr.*, 498 (1990) 191.
[7] F. Foret, V. Sustacek and P. Bocek, *J. Microcolumn Sep.*, 2 (1990) 229.
[8] D.S. Stegehuis, U.R. Tjaden and J. van der Greef, *J. Chromatogr.*, 591 (1992) 341.
[9] R.-L. Chien and D.S. Burgi, *Anal. Chem.*, 64 (1992) 489A.
[10] R.-L. Chien and D.S. Burgi, *Anal. Chem.*, 64 (1992) 1046.
[11] J.D. Olechno, J.M.Y. Tso, J. Thayer and A. Wainwright, *Am Lab.*, December (1990) 30.
[12] X. Huang, M.J. Gordon and R. Zare, *Anal. Chem.*, 60 (1988) 375.
[13] R. Wallingford and A. Ewing, *Adv. Chromatogr.*, 29 (1989) 1.
[14] R.-L. Chien and J.C. Helmer, *Anal. Chem.*, 63 (1991) 1354.
[15] L.C. Sander, *CRC Crit. Rev. Anal. Chem.*, 18 (1987) 299.
[16] F.E.P. Mikkers, F.M. Everaerts and Th.P.E.M. Verheggen, *J. Chromatogr.*, 169 (1979) 1.
[17] R.-L. Chien, *Anal. Chem.*, 63 (1991) 2866.

ELSEVIER

Journal of Chromatography A, 671 (1994) 419–427

JOURNAL OF CHROMATOGRAPHY A

Metal ion capillary electrophoresis with direct UV detection Effect of a charged surfactant on the migration behaviour of metal chelates

A.R. Timerbaev*, O.P. Semenova, P. Jandik☆, G.K. Bonn

Department of Analytical Chemistry, Johannes Kepler University, A-4040 Linz, Austria

Abstract

The migration behaviour of anionic metal 4-(2-pyridylazo)resorcinol (PAR) and Arsenazo III complexes was investigated in capillary electrophoresis (CE) using micellar solutions of sodium dodecyl sulphate. The separation mechanism of arsenazo complexes is governed by the electrophoresis in the bulk carrier electrolyte without any observable interaction with the micellar phase. For less hydrophilic PAR complexes, the resolution can be additionally explained in terms of differential partitioning into the micelle. It was also found that ion-pair formation between anionic solutes and the cationic component of the electrophoretic buffer contributes to the retention mechanism and permits the separation of closely migrating PAR complexes. Both chelating systems have been applied to the CE separation and determination of various metal ions with enhanced selectivity and sensitivity relative to previously reported metal complexation CE techniques. Application to the analysis of complex sample matrices, containing high levels of acids and complexing agents, was demonstrated.

1. Introduction

High-performance capillary electrophoresis (CE) of metal ions after precolumn complexation is distinguished by a number of advantages in comparison with other CE methods. First, complete complexation before the separation largely eliminates interferences from complex sample matrices (*e.g.*, serum [1,2], pharmaceutical preparations [3], electroplating solutions [4] and ores [5]). Second, varying complex-forming conditions can additionally increase the selectivity of the metal analysis. Third, it is possible to separate metal ions that possess a slow rate of complexation or that are incompatible with the carrier electrolytes commonly used in CE [4,5]. When using light-absorbing chelating reagents [1,2,6,7], the sensitivity of direct spectrophotometric detection of metal ions is comparable to or better than that of CE with indirect UV detection. Further, there are no special restrictions on the types of ions that can be used in the electrophoretic buffer (a large difference in mobility of the carrier electrolyte ion and the analyte ion leads to excessive peak tailing/fronting in other CE methods).

Nevertheless, the precolumn metal complex-

* Corresponding author. On leave from Mendeleev Russian University of Chemical Technology, Moscow, Russian Federation.

☆ Present address: Sarasep Inc., Santa Clara, CA 95054, USA.

0021-9673/94/$07.00
SSDI 0021-9673(93)E0055-Y

ation technique still lags behind other CE methods in some analytical characteristics, most conspicuously in the number of cations that can be simultaneously determined. In our opinion, further progress in this respect could depend on the application of micellar buffer systems. The separation principle of micellar CE [or micellar electrokinetic chromatography (MEKC)] is based on two mechanisms, micellar solubilization and electrokinetic migration, and this provides a wider option in optimization and additional possibilities for the enhancement of the separation selectivity [8,9]. In addition, micellar CE is not limited to electrically charged solutes so that its applicability can be extended to neutral metal chelates, as illustrated by Saitoh *et al.* [10,11], who separated metal acetylacetonato complexes in micellar solutions of sodium dodecyl sulphate (SDS). A few MEKC separations of negatively charged metal chelates have been reported [12–14], but with a limited number of separated metals and long analysis times. In a recent paper [15], we attempted to improve the resolution for metal complexes of 8-hydroxyquinoline-5-sulphonic acid (HQS) using SDS as a charged surfactant, but were able to observe only a minor effect of the micellar partitioning on mobility differences (probably because of the comparatively low hydrophobicity of the solutes).

This paper presents results from a continuation of our investigations on the CE of metal complexes in micellar electrophoretic systems. We studied the utility of 4-(2-pyridylazo)resorcinol (PAR) and Arsenazo III as chelating reagents that form intensely coloured, highly stable chelates with a wide variety of metal ions. Attention was also given to a comparison of the resolving powers attainable in pure and micellar CE systems. By using the effective mobility as a migration parameter, the influence of micellar solubilization was established. Also discussed are the common features in the migration behaviour of the complexes. Conclusions about the separation mechanism are presented along with a discussion of the analytical potential of the method.

2. Experimental

2.1. Chemicals

4-(2-Pyridylazo)resorcinol (PAR) and Arsenazo III [disodium salt of 2,7-bis(2-arsonophenylazo)-1,8-dihydroxynapthalenedisulphonic acid] were purchased from Merck (Darmstadt, Germany) and Aldrich Chemie (Steinheim, Germany), respectively, and used as a $5 \cdot 10^{-3}$ *M* stock solution in 0.01 *M* sodium tetraborate. Standard solutions of metal ions were prepared from the nitrates, except for vanadium, zirconium, tin and uranium, which were ammonium metavanadate, zirconium oxychloride, tin dioxide and uranyl acetate, at a concentration $2 \cdot 10^{-3}$ *M* in 0.01 *M* HNO_3. Sodium dodecyl sulphate (SDS) from Serva (Heidelberg, Germany) was dissolved in the corresponding buffer. Buffer solutions were prepared from sodium tetraborate or by mixing sodium (or ammonium) monohydrogenphosphate and dihydrogenphosphate in appropriate ratios. The pH values indicated below were measured after addition of SDS. The carrier electrolytes also contained an appropriate amount of a chelating reagent (usually $1 \cdot 10^{-4}$ *M*). All chemicals were of analytical-reagent grade and all solutions were prepared using doubly distilled water.

Metal complexes were prepared by direct mixing of metal and reagent standard solutions before the injection, unless stated otherwise.

2.2. Apparatus and procedure

Analyses were performed on Waters (Milford, MA, USA) Quanta 4000 and Applied Biosystems (San Jose, CA, USA) Model 270A CE systems equipped with a positive high-voltage power supply and fused-silica capillaries of 75 μm I.D. Detection was carried out by on-column spectrophotometric measurements at specified wavelengths. Electropherograms were recorded and processed with a Hewlett-Packard Model 3359 data acquisition system. Samples were introduced into the capillary at the anodic side by hydrostatic injections from a height of 10 cm

(Quanta 4000) or by applying a vacuum at a pressure of 16.9 kPa (Model 270A) for a specified time. To ensure day-to-day reproducibility of migration times, especially in the experiments with surfactant-rich electrolyte concentrations, the capillary was washed with 0.01 *M* NaOH for 30 min before the work.

The electroosmotic flow (EOF) velocity (or migration time of the bulk eluent) was determined from the migration time of acetone added to a sample. The effective mobility, μ_{eff}, was calculated as the difference between the observed mobility, μ_{ob}, and electroosmotic mobility, μ_{eo}, and expressed as negative values because it is opposed to the latter. Capacity factors, k', were calculated according to $k' = (t - t_0)/t_0$, where t and t_0 are the migration time of a solute and neutral marker, respectively. Such calculations are not affected by uncertainties in the electrophoretic mobility of the micelles and the true ionic electrophoretic mobility of the complexes.

2.3. Sample preparation

An accurately weighed amount of a zirconium ceramic (85% ZrO_2, 10% Nb_2O_5, 5% Ta_2O_5) was melted with 3 g of NaF and 4.5 g of H_3BO_3 in a platinum crucible, heating at 1000°C for 30 min. The melt was treated with a requisite amount (*ca.* 60 ml) of concentrated H_2SO_4 and the mixture was heated at 120°C until the solid was completely decomposed (*ca.* 1 h). The solution was cooled and then diluted to 250 ml with 10% tartaric acid. A 1-ml portion of the resulting solution was used for injection after filtering this solution through a PTFE membrane syringe filter and mixing with an equal volume of Arsenazo III standard solution. The corresponding blank solutions were prepared similarly, but without the addition of ceramic.

The same procedure was used to prepare zirconium and tantalum standard solutions from the corresponding oxides, whereas niobium oxide was dissolved by melting with $K_2S_2O_7$ followed by treatment with H_2SO_4 and tartaric acid.

3. Results and discussion

3.1. Pyridylazoresorcinolates

Saitoh *et al.* [12] were the first to demonstrate the feasibility of resolving transition metal ions in form of PAR complexes using micellar CE. They reported a 30-min separation of cobalt (III), chromium(III), nickel(II) and iron(III) chelates in a silica capillary with a 20 m*M* SDS micellar buffer. Later, the same group obtained good efficiency and a short analysis time (within 6 min) for the separation of PAR and its complexes with Co(III), Fe(II), Ni(II) and V(V) in a CE system without a micellar phase [7]. Both CE techniques demonstrated separations of only a limited number of metal ions, especially in comparison with metal CE analysis based on partial in-capillary complexation [9]. Based on this, the aim of the present study was also to achieve an improved peak capacity for separations of metal–PAR complexes with no decrease in analysis times.

In the initial experiment, borate electrophoretic buffers were tested to evaluate the effect of different concentrations of SDS. The buffers were prepared with increasing amount of the surfactant in sodium tetraborate solution without further pH adjustments (the effect of SDS concentration on the pH was limited to 0.05 unit). As can be seen in Table 1, the results are essentially the same as those obtained previously for metal–HQS complexes [15]. The effective mobilities of PAR complexes and their relative migration velocities calculated from the differences in k' values are largely unaffected by the surfactant concentration. As the complexes exist as doubly charged species under the alkaline conditions employed (Fig. 1, $n = 2$; according to the acid dissociation constants [7,12] both 1-hydroxy groups of PAR ligands are fully deprotonated at pH 9.0), strong repulsion between anionic solutes on the one hand and negatively charged head groups of micelles on the other probably suppresses any partitioning processes. Therefore, the increased migration times observed in the presence of micelles are solely a

Table 1
Effective mobilities and capacity factors of metal–PAR complexes at different concentrations of SDS in the borate electrophoretic buffer

Complex	SDS (mmol/l)					
	0		50		150	
	$\mu_{eff} \times 10^5$ ($cm^2/V \cdot s$)	k'	$\mu_{eff} \times 10^5$ ($cm^2/V \cdot s$)	k'	$\mu_{eff} \times 10^5$ ($cm^2/V \cdot s$)	k'
Cu(II)	27.1	0.60	26.7	0.76	27.0	0.81
Fe(III)	27.9	0.61	27.5	0.72	27.9	0.83
Ni(II)	27.8	0.62	27.6	0.73	26.7	0.78
Zn(II)	28.4	0.63	28.9	0.75	–	–
PAR	23.0	0.45	24.8	0.58	26.4	0.76

Capillary, 35/42 cm × 75 μm I.D.; pH, 9.0; voltage, 15 kV.

result of the decreased EOF velocity, changing from $73.6 \cdot 10^{-5}$ $cm^2/V \cdot s$ under normal CE conditions to $63.6 \cdot 10^{-5}$ $cm^2/V \cdot s$ and then $60.8 \cdot 10^{-5}$ $cm^2/V \cdot s$ at 50 and 150 m*M* SDS, respectively. Only the free chelating reagent, which is singly charged in this pH range, showed a lower effective mobility (along with a higher retention relative to the complexes) with increasing SDS concentration. This behaviour may have been related to the effect of micellar solubilization.

As the resolution of closely related complexes was not improved by changing the surfactant concentration alone, it was decided to continue to investigate the micellar CE behaviour with phosphate carrier electrolytes. The electropherograms shown in Fig. 2 illustrate the influence of compositional buffer changes on the resolution of a test mixture of five complexes. For a phosphate buffer at pH 8.0, the migration time remains almost unchanged at constant micellized SDS concentration, whereas the resolution was slightly improved (*cf.*, electropherograms a and b). However, the choice of metal counter ion in the carrier electrolyte influences the separation selectivity more drastically. When disodium hydrogenphosphate was replaced with diammonium hydrogenphosphate, which resulted in the replacement of about 28% of the

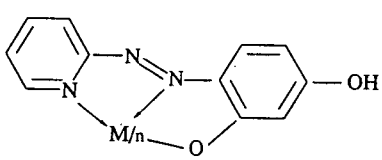

Fig. 1. Structure of metal–PAR complexes.

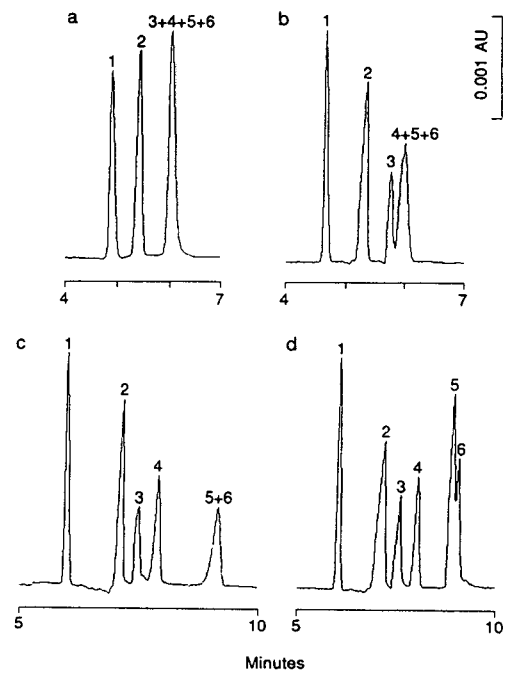

Fig. 2. Electropherograms of metal–PAR complexes with different micellar carrier electrolytes: (a) $Na_2B_4O_7$; (b) Na_2HPO_4–NaH_2PO_4; (c) $(NH_4)_2HPO_4$–NaH_2PO_4; (d) $(NH_4)_2HPO_4$–$NH_4H_2PO_4$. All buffers were 10 m*M* and contained 50 m*M* SDS and $1 \cdot 10^{-4}$ *M* PAR. Capillary, 35/42 cm × 75 μm I.D.; voltage, 15 kV; injection, 10 s (hydrostatic); detection, 254 nm. Peaks: 1 = Co(III); 2 = PAR; 3 = Cu(II); 4 = Ni(II); 5 = Fe(III); 6 = Zn(II).

Table 2
Effect of metal counter ion of the phosphate electrophoretic buffer on effective mobilities of metal–PAR complexes

Complex	$\mu_{eff} \times 10^5$ ($cm^2/V \cdot s$)		
	Na_2HPO_4–NaH_2PO_4	$(NH_4)_2HPO_4$–NaH_2PO_4	$(NH_4)_2HPO_4$–$NH_4H_2PO_4$
Co(III)	21.7	22.9	23.6
Cu(II)	28.4	30.7	30.7
Fe(III)	29.6	35.9	35.1
Ni(II)	29.6	32.2	32.2
PAR	26.2	29.4	29.3

Capillary, 35/42 cm × 75 μm I.D.; SDS, 50 mmol/l; pH, 8.0; voltage, 15 kV.

sodium ions in the micellar buffer, the effective mobilities were decreased, as can be seen from the results of Table 2. Referring to Fig. 2, this leads to complete resolution of copper, nickel and iron (or zinc) complexes; however, the latter two still co-migrates. In a buffer containing both components as ammonium salts, the peaks of iron and zinc were partially resolved, although the μ_{eff} values remained virtually unchanged (see Table 2).

As expected, these data can be well explained in terms of ion-pair formation between the solute and the cationic component of the electrophoretic buffer. Ammonium ion acting as a stronger ion-pairing cation than sodium ion decreases the negative charge of the complexes through ion association and thereby diminishes the electrostatic repulsion, facilitating the incorporation of paired complexes by the micelle. Nevertheless, the elution order for the complexes is not different from that in a pure CE migration system. This seems to indicate that the electrophoresis predominates over the interaction with the micelle in the migration behaviour even with SDS–ammonium salts present in buffer solutions. Phosphate buffers of lower pH were found to be less suitable for separation as the migration times appeared to be longer (owing to the decreased EOF) without any significant change in selectivity. Further experiments were therefore conducted with the buffer consisting of $(NH_4)_2HPO_4$–$NH_4H_2PO_4$ (pH 8.0).

Based on the aforementioned results, we decided to study further the micellar effect on the optimum separation of PAR complexes. Increasing the surfactant concentration in an optimized buffer electrolyte system produced a gradual decrease in the migration velocities of solutes. In this experiment, the concentration of SDS was increased in several steps up to 150 m*M*. The decrease in migration velocities was considered to be a result of cooperative effects of changes in the phase ratio and electroosmotic mobility (due to changes in viscosity and ionic strength). Together with longer run times, we were able to observe that the resolution was enhanced. Therefore, an SDS concentration of 75 m*M* in the buffer, providing the separation of most of the complexes under consideration within 10 min, was concluded to be optimum.

Fig. 3 displays an electropherogram showing the optimized separation of a nine-component metal ion mixture. Metals that form PAR complexes less stable than that of cadmium (manganese, alkaline earths, etc.) could not be detected under the experimental conditions used. The vanadium (V)–PAR complex migrated very close to the copper chelate, whereas La(III), Zr(IV), Sn(IV) and U(VI) complexes exhibited

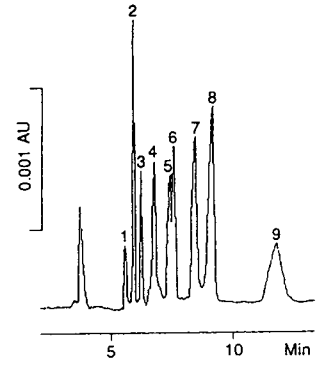

Fig. 3. Micellar CE separation of metal chelates of PAR. Capillary, 42/50 cm × 75 mm I.D.; carrier electrolyte, 10 m*M* ammonium phosphate buffer containing 75 m*M* SDS and $1 \cdot 10^{-4}$ *M* PAR (pH 8.0); voltage, 15 kV; injection, 30 s (hydrostatic); detection, 254 nm. Metals (mol/l): 1 = Cr(III) ($2.4 \cdot 10^{-4}$); 2 = Co(II) ($6 \cdot 10^{-5}$); 3 = Cu(II) ($8 \cdot 10^{-5}$); 4 = Pb(II) ($8 \cdot 10^{-5}$); 5 = Ni(II) ($8 \cdot 10^{-5}$); 6 = Fe(II) ($8 \cdot 10^{-5}$); 7 = Zn(II) ($1.6 \cdot 10^{-4}$); 8 = Fe(III) ($8 \cdot 10^{-5}$); 9 = Cd(II) ($2.4 \cdot 10^{-4}$). The first-migrating peak belongs to acetone.

broad and asymmetric peaks with smaller peak heights. The formation of the chromium(III) complex requires the use of triethanolamine as an auxilary ligand for acceleration of complexation; we followed the procedure described in ref. 16 after a minor alteration of the conditions (high contents of triethanolamine affect the migration times). It should be noted that by varying the reagent-to-metal ratio in the injected sample solution one can attain a decrease in the PAR peak intensity until its complete disappearance. Of practical importance also is the possibility of differentiating between different oxidation states of iron.

Further optimization of analytical performance of the PAR chelating system was directed towards detectability enhancement. CE systems from two different manufacturers were utilized for these experiments (see Experimental). When the detection of complexes is accomplished in the visible spectral range, a general increase in sensitivity will be expected. Limits of detection, defined as three times the baseline noise, are summarized in Table 3. Injections of the same duration correspond to *ca.* five times higher injected volumes with the Model 270A (with due regard to differences in capillary length). Therefore, for the purposes of comparison, the corresponding detection limits were evaluated in an 8-nl injection volume. As can be seen, increased peak intensities and a smaller background signal when the detection wavelength was fixed at 500 nm resulted in substantially better performance than UV detection performed on the Quanta 4000. An illustrative electropherogram showing a peak near the limit of detection for the cobalt–PAR chelate is presented in Fig. 4.

Table 3
Detection limits (mol/l) of metal ions as PAR complexes

Metal ion	Detection wavelength (nm)	
	254[a]	500[b]
Co(II)	$8 \cdot 10^{-7}$	$1 \cdot 10^{-7}$
Cu(II)	$2 \cdot 10^{-6}$	$6 \cdot 10^{-7}$
Fe(III)	$4 \cdot 10^{-6}$	$9 \cdot 10^{-7}$
Ni(II)	$3 \cdot 10^{-6}$	$1 \cdot 10^{-6}$
Zn(II)	$2.4 \cdot 10^{-5}$	$8 \cdot 10^{-7}$

[a] Quanta 4000; injection time, 5 s (*ca.* 8 nl).
[b] Model 270A; evaluated in an 8-nl injection volume.

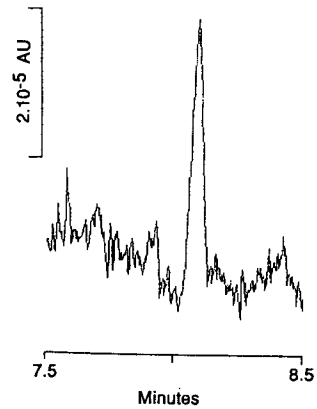

Fig. 4. Detectability of cobalt–PAR complex ($1 \cdot 10^{-7}$ *M*) near the detection limit. Capillary, 43/63 cm × 75 μm I.D.; voltage, 20 kV; injection 5 s (vacuum); detection, 500 nm. Carrier electrolyte as in Fig. 3.

3.2. Complexes of Arsenazo III

Initial studies were carried out with the borate buffer systems shown in Table 4. Also given in Table 4 are the migration characteristics of various metal chelates and the reagent. Their comparison with the corresponding data for PAR complexes (see Table 1) indicates that metal–Arsenazo III complexes exhibited far larger retentions under both normal and micellar CE conditions. This is thought to be a result of their higher electrophoretic mobility. This observation is in accord with the higher charge of complexes containing several ionizable groups that do not participate in complexation (Fig. 5); according to data on the acid ionization of Arsenazo III [17], at pH 9 both sulphonic and arsonic groups are ionized (one completely and the other partially). The capability of this reagent to form complexes with a 1:1 and 2:1 metal-to-ligand stoichiometry also favours a higher electrophoretic mobility. Nevertheless, we always observed the migration of Arsenazo III complexes towards the cathode (the detection side). Correspondingly, the electroosmotic velocity must have been always high-

Table 4
Effective mobilities and capacity factors of metal–Arsenazo III complexes in different borate carrier electrolytes

Complex	Borate buffer		Borate buffer + $1 \cdot 10^{-4}$ *M* Arsenazo III		Borate buffer + $1 \cdot 10^{-4}$ *M* Arsenazo III + 50 m*M* SDS		Borate buffer + $1 \cdot 10^{-4}$ *M* Arsenazo III + 100 m*M* SDS	
	$\mu_{eff} \times 10^5$ ($cm^2/V \cdot s$)	k'	$\mu_{eff} \times 10^5$ ($cm^2/V \cdot s$)	k'	$\mu_{eff} \times 10^5$ ($cm^2/V \cdot s$)	k'	$\mu_{eff} \times 10^5$ ($cm^2/V \cdot s$)	k'
Cu(II)	43.1	1.59	44.7	1.45	42.2	1.63	41.4	1.78
Fe(III)	44.8	1.62	46.1	1.52	44.6	1.83	43.1	1.95
La(III)	41.2	1.29	41.0	1.15	42.2	1.55	39.7	1.48
Pb(II)	–	–	–	–	43.0	1.58	40.6	1.64
Arsenazo III	45.7	1.68	46.8	1.66	45.3	1.88	43.9	2.02

Capillary, 42/50 cm × 75 μm I.D.; pH, 9.0; voltage, 15 kV.

er than the electrophoretic velocity of any of the solutes employed.

The second distinctive feature of the discussed chelating system is the formation of metal complexes under more acidic conditions. As shown below, this permits the applicability of metal complexation CE to be extended to highly acidic samples (*e.g.*, after decomposition with mineral acids). In fact, the optimum complexation required a slight change in the procedure, that is, addition of nitric acid to the metal solution in a 1:1 ratio before mixing with the reagent solution.

The micellar CE behaviour of Arsenazo III complexes with respect to the surfactant concentration was studied also for ammonium phosphate electrolytes. The addition of SDS gave rise to an enhanced retention but this effect was evidently caused by the corresponding changes in the electroosmotic mobility. Typical results in terms of μ_{eff} *versus* surfactant concentration are depicted in Fig. 6. It can be seen from these profiles that as the SDS concentration was varied between 25 and 100 m*M*, the effective mobilities increased. This phenomenon is believed to be attributable to changes in the true ionic mobility of the analytes with the parameter studied. As would be expected from the highly acidic nature of the ligand's sulphonic and arsonic groups, the effective mobilities are insensitive to pH in the range more suitable for counter–electroosmotic migration [9] (we particularly investigated the pH range 6.5–8 in an attempt to improve the resolution). Therefore, as with HQS complexes [15], the dependence of charge on pH could not be exploited to obtain better micellar CE separations.

Taking into account the higher charge of Arsenazo III complexes, it is unlikely that they are solubilized by the anionic SDS micelle owing to electrostatic repulsion. In addition, the small dimensions make micelles less suitable for the solubilization of large aggregates such as these complexes. Consequently, unlike PAR complexes, they migrated due to the electrophoresis of

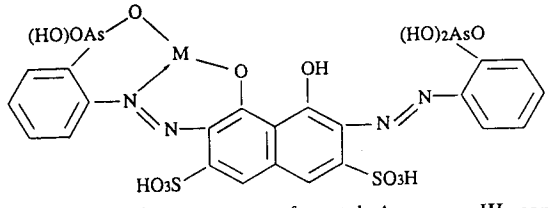

Fig. 5. Molecular structure of metal–Arsenazo III complexes.

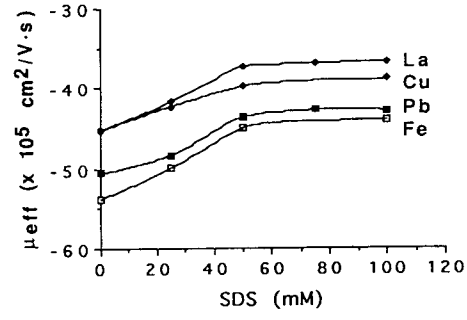

Fig. 6. Effective mobility of metal–Arsenazo III complexes as a function of surfactant concentration. Carrier electrolyte, 10 m*M* $(NH_4)_2HPO_4$–$NH_4H_2PO_4$ containing $1 \cdot 10^{-4}$ *M* Arsenazo III (pH 8.0). Other conditions as in Table 4.

the solute itself without any interaction with the micellar phase. When using micellar buffer solutions, the separations become longer and less efficient without any observable increase in selectivity. Fig. 7 distinctly shows the superiority of the resolving power of CE with no surfactant in the electrophoretic buffer. Also, the presence of SDS was found to affect adversely the detectability (note also the appearance of an additional negative excursion from the baseline).

On the basis of the above results, non-micellar CE with a phosphate buffer of pH 7.0 was chosen as the optimum migrating system. We also investigated CE separations of other metals not shown in Fig. 7 under same conditions. Rare earth complexes co-migrated with that of lanthanum, whereas the zirconium complex had a mobility close to that of the iron chelate; in the presence of tartaric acid both niobium and tantalum formed mixed-ligand complexes [17] that probably led to large irregularities in their retention behaviour (see below); nickel, chromium and molybdenium complexes produced badly asymmetric peaks; no migration of zinc, manganese, vanadium, bismuth and alkaline earth metal complexes was observed.

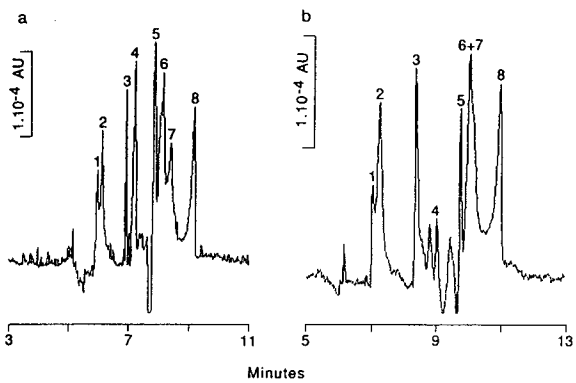

Fig. 7. Comparison between (a) pure CE and (b) micellar CE performance for metal–Arsenazo III complexes. Capillary, 42/50 cm × 75 μm I.D.; carrier electrolyte, (a) 10 m*M* $(NH_4)_2HPO_4$–$NH_4H_2PO_4$ containing $1 \cdot 10^{-4}$ *M* arsenazo III (pH 8.0); (b) same as (a) + 50 m*M* SDS; voltage, 20 kV; injection, 2 s (hydrostatic); detection, 254 nm. Peaks: 1 = Ce(III); 2 = La(III); 3 = U(VI); 4 = Cu(II); 5 = Arsenazo III; 6 = Pb(II); 7 = Co(II); 8 = Fe(III). Concentration of all metals $1.5 \cdot 10^{-4}$ *M*, except La ($3 \cdot 10^{-4}$ *M*) and U ($7.5 \cdot 10^{-5}$ *M*).

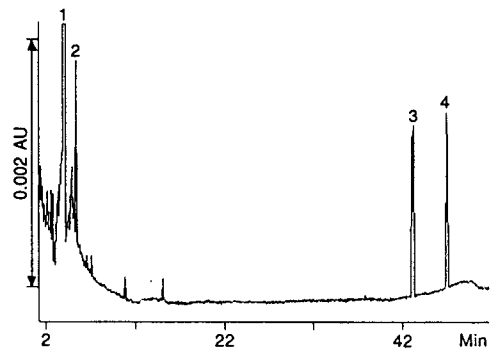

Fig. 8. CE analysis of a zirconium ceramic. Voltage, 28 kV; injection, 15 s. Other conditions as in Fig. 7a. Peaks: 1 = Arsenazo III; 2 = zirconium (196 ppm); 3 = niobium (23 ppm); 4 = tantalum (23.5 ppm).

Evaluation of the applicability of the Arsenazo III chelating system to real samples was performed with the analysis of zirconium ceramics containing niobium and tantalum as alloying additives. The baseline-resolved separation of all metallic constituents of the sample was achieved under the optimum separation conditions outlined (Fig. 8). Owing to the large differences in migration times, zirconium as a main component did not interfere with the detection of niobium and tantalum. For practioners of CE, it is also important to note that the only treatment of the analysed solution consisted in dilution and filtration (for additional details, see Experimental).

4. Conclusions

It has been shown that micellar electrophoretic systems can be applied to the CE separation of negatively charged metal complexes provided that these complexes possess a hydrophobic nature so as to be solubilized by anionic SDS micelles. With PAR complexes, both the electrophoretic mobility and micellar partitioning contribute to their separation; the latter seemingly has a smaller effect. The cationic component of the carrier electrolyte (*e.g.*, ammonium) can act as an ion-pairing counter ion and help to overcome electrostatic repulsion between anionic solutes and negatively charged head groups of the micelle. This alters the relative contribution

of partitioning processes and leads to an improvement in resolution.

As demonstrated above, it is more difficult to manipulate the retention behaviour of highly ionized solutes, *e.g.*, metal–Arsenazo III complexes. The limited capacity of micellar CE with respect to these chelates is also consistent with the larger size of the molecules making solubilization more difficult. In consequence, their separation is not influenced by variations in the SDS concentration and is based exclusively on differences in electrophoretic mobility. The same observation is valid for other metal complexes with "hydrophilic" ionizable groups, such as 5-sulphohydroxyquinolinates [15] and N-methyl-N-2-sulphoethyldithiocarbamates, currently under investigation in our laboratory. On the other hand, metal–Arsenazo III complexes demonstrate the impressive selectivity in the non-micellar CE mode that provides good separations for a variety of metal ions.

In conclusion, the chelating systems described here show promise regarding the expansion of the analytical potential of metal complexation CE toward the achievement of multi-element separations with good detectability. Possibilities of further improvements still exist and will be explored in future work. Immunity of CE based on precolumn complexation to complex sample matrices, which are currently impossible to analyse by using present CE methodology, is especially attractive. Therefore, this method will well complement traditional approaches to the separation and determination of metal ions by CE.

5. Acknowledgements

Financial support by the Austrian Ministry of Science and Research through grant No 45.270/-46a/93 is gratefully appreciated. We gratefully acknowledge the help of E. Radda of the Applied Biosystems Division of Perkin-Elmer in assessing the injected volumes. We also thank A. Jerschow, Johannes Kepler University, for assistance during the sample preparation.

6. References

[1] S. Motomizu, S. Nishimura, Y. Obata and H. Tanaka, *Anal. Sci.*, 7 (1991) 253.
[2] S. Motomizu, M. Oshima, S. Matsuda, Y. Obata and H. Tanaka, *Anal. Sci.*, 8 (1992) 619.
[3] A.R. Timerbaev, W. Buchberger, O.P. Semenova and G. Bonn, in A. Dyer, M.J. Hudson and P.A. Williams (Editors), *Ion Exchange Processes: Advances and Applications*, Royal Society of Chemistry, Cambridge, 1993, p. 111.
[4] W. Buchberger, O.P. Semenova and A.R. Timerbaev, *J. High Resolut. Chromatogr.*, 16 (1993) 153.
[5] M. Aguilar, A. Farran and M. Martinez, *J. Chromatogr.*, 635 (1993) 127.
[6] A.R. Timerbaev, W. Buchberger, O.P. Semenova and G. Bonn, *J. Chromatogr.*, 630 (1993) 379.
[7] M. Iki, H. Hoshino and T. Yotsuyanagi, *Chem. Lett.*, (1993) 701.
[8] J. Vindevogel and P. Sandra, *Introduction to Micellar Electrokinetic Chromatography*, Hüthig, Heidelberg, 1992.
[9] P. Jandik and G.K. Bonn, *Capillary Electrophoresis of Small Molecules and Ions*, VCH, New York, 1993.
[10] K. Saitoh, C. Kiyohara and N. Suzuki, *J. High Resolut. Chromatogr.*, 14 (1991) 245.
[11] K. Saitoh, C. Kiyohara and N. Suzuki, *Anal. Sci.*, 7 (1991) 269.
[12] T. Saitoh, H. Hoshino and T. Yotsuyanagi, *J. Chromatogr.*, 469 (1989) 175.
[13] T. Saitoh, H. Hoshino and T. Yotsuyanagi, *Anal. Sci.*, 7 (1991) 495.
[14] T. Saitoh, N. Ojima, H. Hoshino and T. Yotsuyanagi, *Mikrochim. Acta*, 106 (1992) 91.
[15] A.R. Timerbaev, O.P. Semenova and G. Bonn, *Chromatographia*, 37 (1993) 497.
[16] H. Hoshino and T. Yotsuyanagi, *Anal. Chem.*, 57 (1985) 625.
[17] S.B. Savvin, *Organic Reagents of Arsenazo III Type*, Atomizdat, Moscow, 1971 (in Russian).

ELSEVIER

Journal of Chromatography A, 671 (1994) 429–435

JOURNAL OF CHROMATOGRAPHY A

New electrolyte systems for the determination of metal cations by capillary zone electrophoresis

Youchun Shi, James S. Fritz*

Department of Chemistry and Ames Laboratory, US Department of Energy, Iowa State University, Ames, IA 50011, USA

Abstract

Many +1 and +2 metal cations can be separated efficiently by CZE using lactic acid as a complexing reagent. Addition of a crown ether, as well as lactic acid, permits the separation of K^+ and NH_4^+ in addition to the ions previously separated. The problem of determining trace amounts of metal ions in the presence of a very high concentration of another metal ion was also addressed. For example, a large Na^+ peak (1000 ppm, w/w) covers up the peaks of Ca^{2+}, Mg^{2+}, Sr^{2+} and Ba^{2+} (1 ppm each). However, addition of increasing concentrations of methanol to the electrolyte permits complete resolution of Ca^{2+} and Mg^{2+} from the Na^+. Further addition of a crown ether moves Sr^{2+} and Ba^{2+} to longer migration times and permits resolution of these ions as well. Separation of metal cations with slower complexation kinetics is possible under conditions where only the free metal ions are present. Aluminum(III) and vanadium(IV), along with several other metal ions, were separated at pH 3.2 using nicotinamide as a buffer component and as a reagent for indirect detection.

1. Introduction

The art and science of separation of metal cations continues to develop at a fast pace. Indirect detection by means of a chromogenic cation [1,2] (often called a visualization reagent) is quite common, although suppressed conductivity [3] and electrochemical detection [4] have recently been used for some inorganic cations. It has become quite common to include a weak complexing reagent in the electrolyte to enhance the separation of cations with very similar electrophoretic mobilities. Several authors have reported excellent separations based on these principles [5–13]. In a recent publication we reported the separation of 27 metal cations in only 6.0 min using lactic acid as an auxiliary complexing reagent [13]. However, it was not possible to resolve the potassium and ammonium peaks from one another.

In the present work an electrolyte containing both lactic acid and a crown ether was used to separate 16 of the most commonly determined metal ions. The effect of methanol on this system was also investigated. Quantitative aspects of the separations were studied and the problem of determining trace metal ions in the presence of a high concentration of another cation was addressed. An uncomplexing electrolyte system is also introduced here.

2. Experimental

A Waters Quanta 4000 capillary electrophoresis system (Millipore Waters, Milford, MA, USA), equipped with a positive power supply was employed to separate metal cations and generate all electropherograms. Polyamide-

* Corresponding author.

0021-9673/94/$07.00
SSDI 0021-9673(93)E1263-Y

coated, fused-silica capillaries (Polymicro Technology, Phoenix, AZ, USA), were 60 cm in length with an I.D. of 75 μm and a distance of 52.5 cm from the point of injection to the window of on column detection. Indirect UV detection was employed at 214 nm or 254 nm. A voltage of 15 to 30 kV was applied for separations. The time of hydrodynamic injection was 30 or 40 s for most separations. A Servogor 120 flatbed recorder (Goerz Instruments, Austria) was used to plot electropherograms. The chart speed was set at 3 cm/min for all electropherograms presented in this paper.

All standards and electrolytes were prepared with analytical-reagent grade chemicals and 18 MΩ deionized waters by a Barnstead Nanopure II system (Sybron Barnstead, Boston, MA, USA).

Lactate buffers were mixed with lactic acid (J.T. Baker, Phillipsburg, NJ, USA), 4-methylbenzylamine (Fluka, Ronkonkoma, NY, USA), methanol (Fisher Scientific, Fair Lawn, NJ, USA) and 18-crown-6 (Aldrich, Milwaukee, WI, USA). The 4-methylbenzylamine was used as the protonated cation for indirect detection of the sample cations and for pH-adjustment. This reagent is identical to Waters UV-Cat 1 which is patented for use as an indirect detection reagent in capillary zone electrophoresis [14].

The uncomplexing buffer was prepared with nicotinamide (Sigma, St. Louis, MO, USA) and other modifiers. Formic acid (Aldrich, Milwaukee, WI, USA) was used to adjust pH.

3. Results and discussion

3.1. Electrolytes containing lactic acid and a crown ether

Lactic acid makes possible the separation of metal ions with almost identical mobilities by complexing the individual metal ions to varying degrees. The divalent transition metal ions and the lanthanides are two examples. However, NH_4^+ and K^+ cations also have virtually identical mobilities and are not complexed by lactic acid. Previous investigators found that ammonium and potassium ions can be separated by CZE if a suitable crown ether is incorporated into the electrolyte [15–18]. The K^+ ion is selectively complexed and its mobility is reduced just enough to permit a good separation.

We found that an electrolyte solution containing both lactic acid (11 m*M*) and a crown ether (2.6 m*M* 18-crown-6) will permit an excellent electrophoretic separation of 16 metal ions, including NH_4^+ and K^+ (Fig. 1). The electrolyte also contained 7.5 m*M* 4-methylbenzylamine as an indirect detection coion. Separations in which 12-crown-4 or 15-crown-5 was used in place of 18-crown-6 failed to separate NH_4^+ and K^+.

Incorporation of 18-crown-6 into the electrolyte containing lactic acid affects the migration of several metal ions other than K^+ and NH_4^+. The crown ether increases the migration time of Sr^{2+} by 15%, Pb^{2+} by 18% and Ba^{2+} by 35%, apparently by complexation to form a bulkier, less mobile species. The effect of 18-crown-6 on the migration times of metal ions, compared to lactic acid alone, is summarized in Table 1.

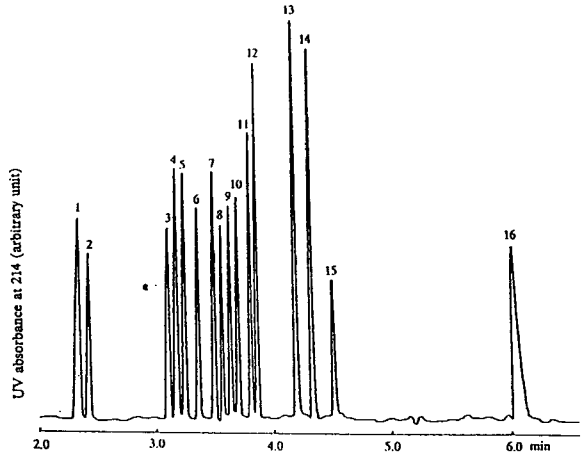

Fig. 1. Separation of 16 common metal ions and ammonium. Electrolyte, 11 m*M* lactic acid, 2.6 m*M* 18-crown-6, 7.5 m*M* 4-methylbenzylamine, 8% methanol, pH 4.3; applied voltage, 30 kV; injection time, 30 s. Peaks: 1 = NH_4^+ (5 ppm); 2 = K^+ (5 ppm); 3 = Na^+ (3 ppm); 4 = Ca^{2+} (3 ppm); 5 = Sr^{2+} (5 ppm); 6 = Mg^{2+} (1.5 ppm); 7 = Mn^{2+} (3.2 ppm); 8 = Ba^{2+} (5 ppm); 9 = Cd^{2+} (4 ppm); 10 = Fe^{2+} (3.2 ppm); 11 = Li^+ (0.8 ppm); 12 = Co^{2+} (3.2 ppm); 13 = Ni^{2+} (3.2 ppm); 14 = Zn^{2+} (3.2 ppm); 15 = Pb^{2+} (5 ppm); 16 = Cu^{2+} (4 ppm).

Table 1
Effect of 2.6 m*M* 18-crown-6 on the migration times (t_M) of metal ions in electrolyte also containing 11 m*M* lactic acid, 7.5 m*M* 4-methylbenzylamine and 8% methanol, buffered to pH 4.3

Ion	Lactic acid, t_M (min)	Lactic acid + 18-crown-6, t_M (min)	t_M increase (%)
NH_4^+	2.33	2.37	1.7
K^+	2.33	2.54	9.0
Ba^{2+}	2.78	3.75	35
Sr^{2+}	2.96	3.41	15
Na^+	3.05	3.14	3.0
Ca^{2+}	3.12	3.22	3.2
Mg^{2+}	3.28	3.43	4.6
Mn^{2+}	3.42	3.54	3.5
Cd^{2+}	3.55	3.68	3.7
Li^+	3.70	3.85	4.1
Co^{2+}	3.81	3.95	3.7
Pb^{2+}	4.08	4.81	18
Ni^{2+}	4.15	4.44	7.0
Zn^{2+}	4.30	4.62	7.4
Cu^{2+}	5.96	6.20	4.0

3.2. *Effect of methanol*

Several investigators have studied the effect of organic solvents on CZE [13,19–21]. Acetophenone was used as a neutral marker to measure the electroosmotic mobility as a function of methanol content in the electrolyte. The electroosmotic mobility decreases in a non-linear manner, as shown in Fig. 2. The electrophoretic mobility decreases almost linearly as the percentage of methanol in the electrolyte is increased (Fig. 3). The sum of these effects is a non-linear increase in migration times of the metal ions (Fig. 4). In general, methanol in the electrolyte improves the separation of metal ions having adjacent migration times.

3.3. *Effect of a high Na^+ concentration*

One of the shortcomings of CZE is that ion peaks become very broad at higher concentrations. We investigated the determination of 1 ppm each of Mg^{2+}, Ca^{2+}, Sr^{2+} and Ba^{2+} in the presence of 75 ppm of Na^+. Fig. 5 shows that

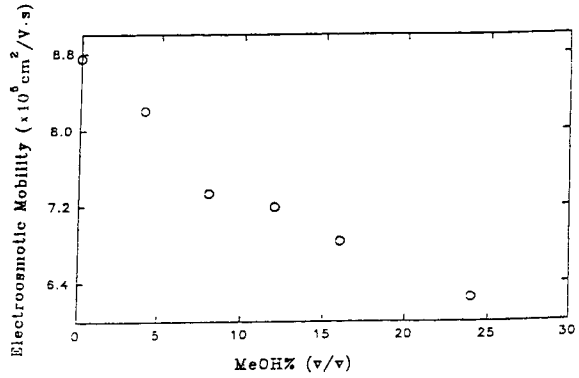

Fig. 2. Change of electroosmotic mobility with methanol as a buffer modifier. Electrolyte, 15 m*M* lactic acid, 10 m*M* 4-methylbenzylamine, 0–24% (v/v) methanol, pH 4.3; applied voltage, 20 kV; injection time, 30 s; neutral marker, acetophenone.

only Mg^{2+} can be separated from this concentration in 8% methanol, and only Mg^{2+} and Ca^{2+} can be determined in 16% methanol or 32% methanol. However if 18-crown-6 is added to the electrolyte, the migration times of Sr^{2+} and Ba^{2+} are slowed sufficiently that all four of the trace metal ions can be determined (Fig. 6). By lowering the applied voltage and reducing the injection time from 30 s to 6 s, 1 ppm of each of the four trace metal ions can be determined in the presence of 1000 ppm of sodium (Fig. 7).

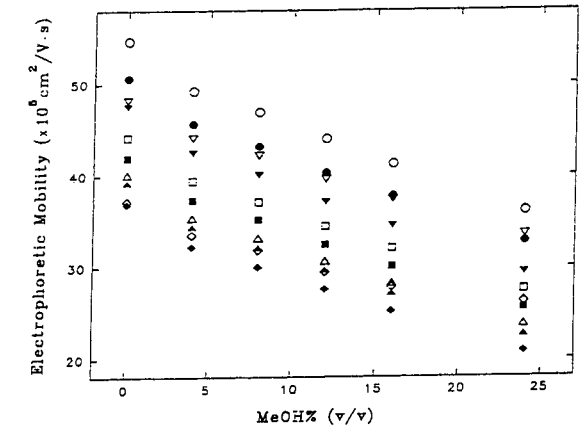

Fig. 3. Change of electrophoretic mobility with methanol as a buffer modifier. Conditions as in Fig. 2. ○ = Ba; ● = Sr; ▽ = Na; ▼ = Ca; □ = Mg; ■ = Mn; △ = Cd; ▲ = Fe; ◇ = Li; ◆ = Co.

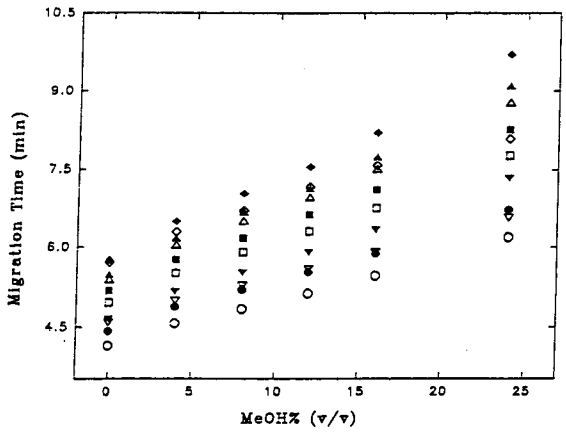

Fig. 4. Change of migration time with methanol as a buffer modifier. Conditions as in Fig. 2. Symbols as in Fig. 3.

3.4. Calibration plots

Known concentrations of each of the metal ions were separated under the conditions used in Fig. 1 to test the quantitative aspects. Lithium(I)

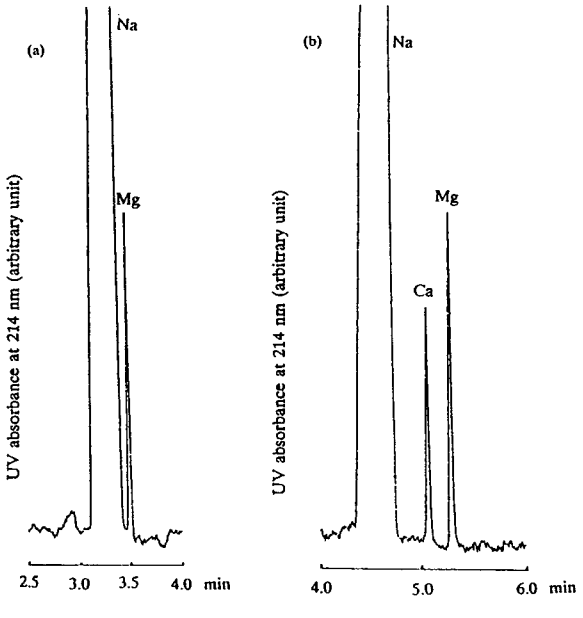

Fig. 5. Effect of methanol in the separation of 75 ppm Na^+ and 1 ppm Mg^{2+}, Ca^{2+}, Sr^{2+} and Ba^{2+}. Electrolyte, 15 m*M* lactic acid, 10 m*M* 4-methylbenzylamine, pH 4.3, (a) 8% (v/v) methanol; (b) 32% (v/v) methanol; applied voltage, 30 kV; injection time, 30 s.

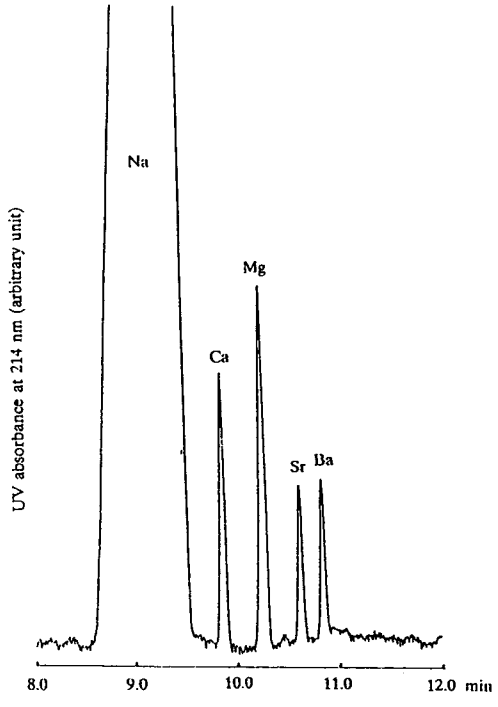

Fig. 6. Effect of 18-crown-6 in the separation of 75 ppm Na^+ and 1 ppm Mg^{2+}, Ca^{2+}, Sr^{2+} and Ba^{2+}. Electrolyte, 15 m*M* lactic acid, 10 m*M* 4-methylbenzylamine, 32% (v/v) methanol, 3.0 m*M* 18-crown-6, pH 4.3; applied voltage, 15 kV; injection time, 30 s.

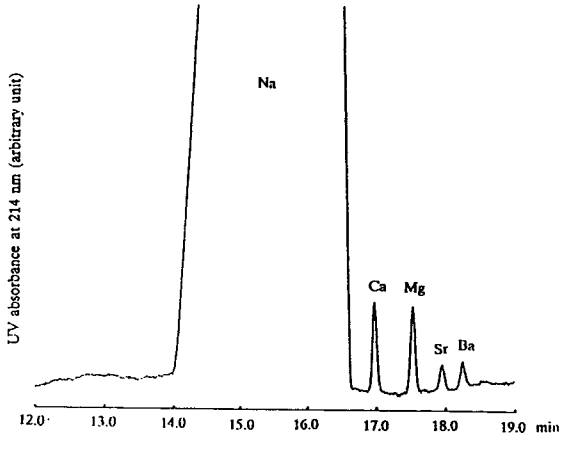

Fig. 7. Separation of 1 ppm Mg^{2+}, Ca^{2+}, Sr^{2+} and Ba^{2+} from 1000 ppm Na^+. Electrolyte conditions same as Fig. 6; applied voltage, 10 kV; injection time, 6 s.

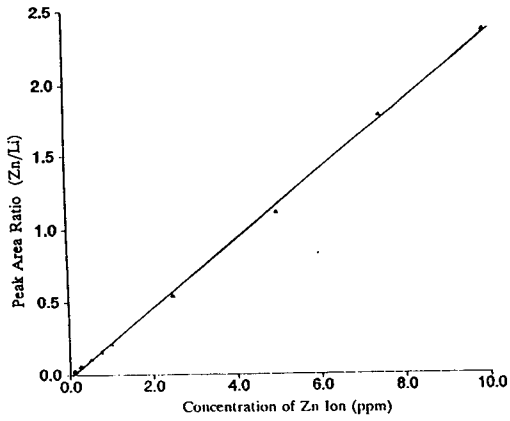

Fig. 8. Calibration plot of Zn^{2+} using Li^{+} as an internal standard. Electrolyte, 15 m*M* lactic acid, 10 m*M* 4-methylbenzylamine, 0.6 m*M* 18-crown-6, 10% (v/v) methanol, pH 4.3; applied voltage, 20 kV; injection time changing with the concentration of Zn^{2+} standard solution, 60 s for 0.10 ppm and 0.25 ppm, 30 s for 0.50 ppm to 2.5 ppm, 15 s for 5.0 ppm, 15 s for 5.0 ppm, 11 s for 7.5 ppm, 8 s for 10.0 ppm; internal standard concentration, 0.2 ppm Li^{+} in 0.10 ppm or 0.25 ppm Zn^{2+} solution, 1.0 ppm Li^{+} in 0.5 or higher concentration of Zn^{2+} solution.

was selected as an internal standard. As might be expected plots of peak height against concentrations were unsatisfactory over the range of 1 to 10 ppm. However, a plot of peak area (relative to that of Li^{+}) *vs.* concentration gave a linear plot over a 100-fold change in concentration (0.1 to 10 ppm). A typical plot (Fig. 8) shows linearity over the entire range. Slopes and correlation coefficients are listed in Table 2.

Table 2
Slopes and correlation coefficients of calibration plot for quantitative analysis of several metal cations

Ion	Slope (1/ppm)	Correlation coefficient
Sr^{2+}	0.159	0.9983
Mg^{2+}	0.560	0.9992
Mn^{2+}	0.241	0.9989
Co^{2+}	0.277	0.9995
Zn^{2+}	0.236	0.9995

Electrolyte, 15 m*M* lactic acid, 10 m*M* 4-methylbenzylamine, 0.6 m*M* 18-crown-6, 10% MeOH, pH 4.3; applied voltage, 20 kV; injection time, 8–60 s. The concentration of all metal ion standards is from 0.1 ppm to 10.0 ppm.

3.5. Separation efficiency

The electrophoretic peaks were examined with a recorder chart speed of 10 cm/min to spread out the individual peaks and facilitate measurement of peak width. The plate number (N) widely used in chromatography was calculated for Zn^{2+}, which was one of the better shaped peaks. Mikkers *et al.* [22,23] have previously explained why peak efficiency in CZE decreases with increasing sample load. At 1 ppm, the calculated value of N was *ca.* 365 000, which would indicate very efficient electrophoretic behavior. However, the calculated plate number dropped drastically as the amount of Zn^{2+} injected was increased (Fig. 9). A somewhat similar decrease in plate number with increasing amounts of sample ions was noted in a recent paper [3].

3.6. Separation of uncomplexed metal cations

Hydroxyisobutyric acid (HIBA) and lactic acid have been used extensively to separate groups of metal ions that have almost identical mobilities, such as the divalent transition metal ions and the trivalent lanthanides. Metal ions are complexed to varying degrees, resulting in differences in the

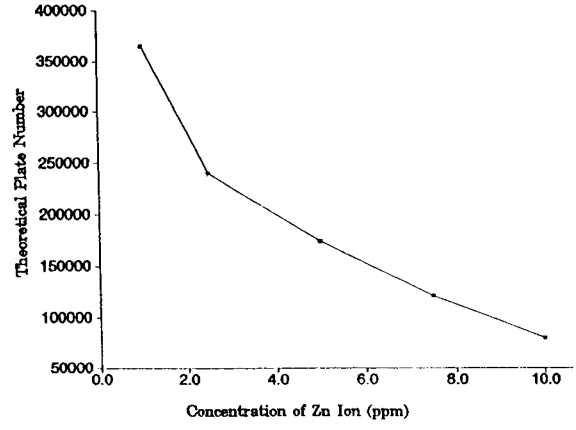

Fig. 9. Change of theoretical plate number with analyte concentration. Same electrolyte condition and applied voltage as described in Fig. 8; injection time, 15 s. Theoretical plate number calculated using $(t_M/\sigma)^2$, where t_M = the migration time and $\sigma = 2.35\ W_{1/2}$ which is the half width of a peak.

overall rates of movement of the various metal ions. The zone of each element contains the free metal cation in equilibrium with one or more metal-ligand species. In the separation of the lanthanides with lactic acid as the ligand, the migration time has been shown to be a linear function of $\bar{n}$, the average number of ligands attached to the lanthanide [13]. It will be seen that the equilibria between the free metal ion and the several complexed species must be quite fast in order to maintain a tight, compact zone. If the equilibria are not rapid, the different species would move at different rates and the zone for an element would become very diffuse.

In the lactic acid system no peak could be obtained for ions such as Al(III) and Fe(III). This could be due to their complexation kinetics. We therefore decided to study the separation of metal ions by CZE under conditions where only free, uncomplexed ions would be present. To avoid complications from hydrolysis of metal ions, a very acidic pH was chosen.

Attempts were made to separate metal ions such as Cu^{2+} and Cr^{3+}, which have a reasonable absorbance in the UV spectral range. Using buffers such like protonated β-alanine (pK_a = 3.6)–β-alanine or formic acid (pK_a = 3.75)–formate, Cu^{2+}, Cr^{3+}, UO_2^{2+} and VO^{2+} were separated and directly detected at 214 nm. However, the detection sensitivity was rather poor. The absorbance of many other metal ions is so low that direct detection is not feasible. The situation becomes even worse if only a few detection wavelengths are available on the instrument.

For these reasons indirect detection is the better choice for multi-element detection with high sensitivity. In practice, not all buffer systems are suitable for the indirect detection. The baseline was very noisy and no metal ion peaks could be discerned with β-alanine or formate as the buffer and 4-methylbenzylamine or phenylethylamine as the UV-visualizing agent. However, good peaks were obtained at pH 3.2 with nicotinamide (pK_a = 3.3) as the UV-visualizing coion, and formate as the counterion.

Fig. 10a shows a separation of several metal ions at pH 3.2 using 8.0 m*M* nicotinamide–formate buffer. It is now possible to obtain good

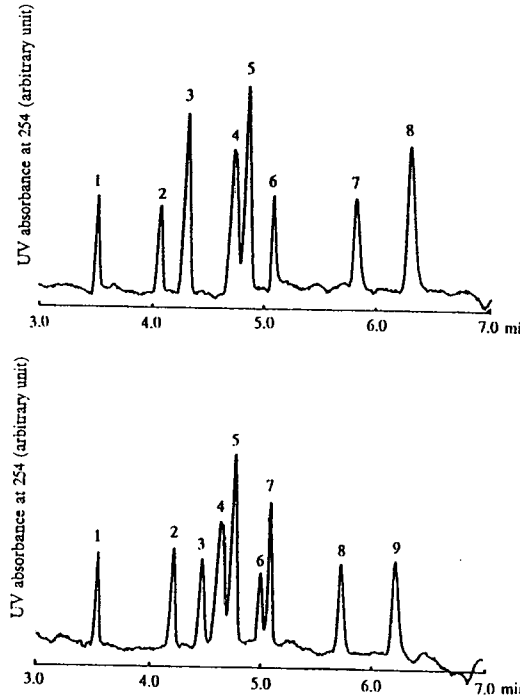

Fig. 10. (a) Separation of a sample standard mixture using an uncomplexing electrolyte. Electrolyte, 8 m*M* nicotinamide, pH 3.2 adjusted with formic acid; applied voltage, 25 kV; injection time, 40 s. Peaks: 1 = K^+ (1.5 ppm); 2 = Ba^{2+} (1.5 ppm); 3 = Sr^{2+} (1.5 ppm) and Ca^{2+} (0.8 ppm); 4 = Mg^{2+} (0.5 ppm) and Na^+ (0.8 ppm); 5 = Al^{3+} (0.8 ppm); 6 = Cu^{2+} (0.8 ppm); 7 = Li^+ (0.2 ppm); 8 = VO^{2+} (2.0 ppm). (b) Separation of the same sample standard mixture using an uncomplexing electrolyte with 18-crown-6. Electrolyte, 8 m*M* nicotinamide, 0.6 m*M* 18-crown-6, pH 3.2 adjusted with formic acid; applied voltage, 25 kV; injection time, 40 s. Peaks: 1 = K^+ (1.5 ppm); 2 = Ca^{2+} (0.8 ppm); 3 = Sr^{2+} (1.5 ppm); 4 = Mg^{2+} (0.5 ppm) and Na^+ (0.8 ppm); 5 = Al^{3+} (0.8 ppm); 6 = Cu^{2+} (0.8 ppm); 7 = Ba^{2+} (1.5 ppm); 8 = Li^+ (0.2 ppm); 0 = VO^{2+} (2.0 ppm).

peaks for Al^{3+} and VO^{2+}. In other experiments good peaks were obtained for UO_2^{2+}, Cr^{3+} and Ag^+.

In Fig. 10a Ca^{2+} and Sr^{2+} co-migrate (peak 3) and Mg^{2+} and Na^+ co-migrate in peak 4. The separation was repeated under the same conditions but with 0.6 m*M* 18-crown-6 also added to the electrolyte (Fig. 10b). The crown ether lengthened the migration times of Sr^{2+} and Ba^{2+} so that separation of Ca^{2+} and Sr^{2+} was obtained.

The separation of Al^{3+} was tried under the

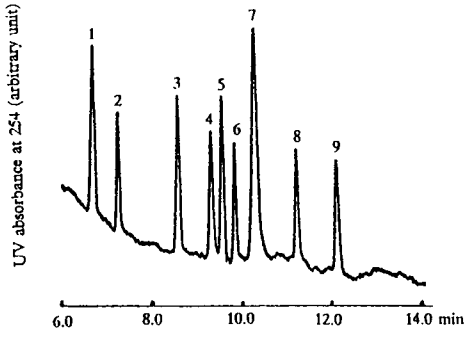

Fig. 11. Electropherogram of a standard mixture with nine common cations using a nicotinamide electrolyte. Electrolyte, 8 m*M* nicotinamide, 12% methanol, 0.95 m*M* 18-crown-6, pH 3.2 adjusted with formic acid; applied voltage, 25 kV; injection time, 40 s. Peaks: $1 = NH_4^+$ (1.5 ppm); $2 = K^+$ (1.5 ppm); $3 = Ca^{2+}$ (1.0 ppm); $4 = Na^+$ (1.0 ppm); $5 = Mg^{2+}$ (0.5 ppm); $6 = Sr^{2+}$ (1.0 ppm); $7 = Al^{3+}$ (1.0 ppm); $8 = Ba^{2+}$ (1.0 ppm); $9 = Li^+$ (0.2 ppm).

same conditions as used for the separation shown in Fig. 10b but with lactic acid added to the electrolyte. No Al^{3+} peak was found, suggesting that the kinetics of forming and dissociating the Al^{3+}–lactate complex may be slow. The crown ether in the electrolyte probably does not complex Al^{3+}.

By adjusting slightly the concentrations of nicotinamide and crown ether, and by adding methanol to the electrolyte, it was possible to completely resolve a mixture containing Mg^{2+}, Al^{3+}, the alkaline earths and the first three alkali metal ions (Fig. 11).

4. Acknowledgements

We wish to thank Waters Division of Millipore for their gift of the Waters Quanta 4000 CE system and associated chemicals. We also thank Andrea Weston and Peter Jandik for valuable technical assistance in the initial stages of this research.

Ames Laboratory is operated for the US Department of Energy under Contract No. W-7405-Eng-82. This work was supported by the Director of Energy Research, Office of Basic Energy Sciences.

References

[1] E. Yeung and W.K. Kuhr, *Anal. Chem.*, 63 (1991) 275A.
[2] F. Foret, S. Fanali, L. Ossicini and P. Boček, *J. Chromatogr.*, 470 (1989) 299.
[3] N. Avdalovic, C.A. Pohl, R.D. Rocklin and J.R. Stillian, *Anal. Chem.*, 65 (1993) 1470.
[4] W. Lu, R.M. Cassidy and A.S. Baranski, *J. Chromatogr.*, 640 (1993) 433.
[5] F. Foret, S. Fanali, A. Nardi and P. Boček, *Electrophoresis*, 11 (1990) 780.
[6] A. Weston, P.R. Brown, A.L. Heckenberg, P. Jandik and W.R. Jones, *J. Chromatogr.*, 602 (1992) 249.
[7] A. Weston, P.R. Brown, P. Jandik, W.R. Jones and A.L. Heckenberg, *J. Chromatogr.*, 593 (1992) 289.
[8] P. Jandik, W.R. Jones, A. Weston and P.R. Brown, *LC·GC*, 9 (1991) 634.
[9] X. Huang and R.M. Zare, *Anal. Chem.*, 63 (1991) 2193.
[10] M. Chen and R.M. Cassidy, *J. Chromatogr.*, 602 (1992) 227.
[11] W.R. Jones, P. Jandik and R. Pfeifer, *Am. Lab.*, May (1991) 40.
[12] M. Chen and R.M. Cassidy, *J. Chromatogr.*, 640 (1993) 473.
[13] Y. Shi and J.S. Fritz, *J. Chromatogr.*, 640 (1993) 473.
[14] W.R. Jones, P. Jandik, M. Merion and A. Weston, *US Pat.*, 5 156 724 (1992); *US Pat.*, 5 128 005 (1992).
[15] M. Tazaki, M. Takagi and K. Ueno, *Chem. Lett.*, (1984) 203.
[16] F.S. Stover, *J. Chromatogr.*, 289 (1984) 203.
[17] K. Fukushi and K. Hiro, *J. Chromatogr.*, 523 (1990).
[18] K. Bächmann, J. Boden and I. Haumann, *J. Chromatogr.*, 626 (1992) 259.
[19] S. Fujiwara and S. Honda, *Anal. Chem.*, 59 (1987) 487.
[20] B.B. Van Orman, G.G. Liversidge, G.L. McIntire, T.M. Olefirowicz and A.G. Ewing, *J. Microcol. Sep.*, 2 (1990) 176.
[21] C. Schwer and E. Kenndler, *Anal. Chem.*, 63 (1991) 1801.
[22] F.E. Mikkers, F.M. Everaerts and Th.P.E.M. Verheggen, *J. Chromatogr.*, 169 (1979) 1.
[23] F.E. Mikkers, F.M. Everaerts and Th.P.E.M. Verheggen, *J. Chromatogr.*, 169 (1979) 11.

ELSEVIER

Journal of Chromatography A, 671 (1994) 437–443

JOURNAL OF CHROMATOGRAPHY A

Studies on the determination of inorganic anions by capillary electrophoresis

Nancy J. Benz, James S. Fritz*

Department of Chemistry and Ames Laboratory, Iowa State University, Ames, IA 50011, USA

Abstract

In order to separate anions effectively it is usually necessary to eliminate or reverse the direction of electroosmotic flow (EOF) resulting from attraction of cations to the negatively charged surface of a silica capillary. Previous workers have accomplished this by adding a quaternary ammonium salt (Q^+) as an EOF "modifier". Under typical experimental conditions, a concentration of $Q^+ > 0.25$ mM is required to reverse the EOF direction. Addition of a low percentage of 1-butanol to the aqueous electrolyte was found to reduce the EOF. A combination of butanol and a very low concentration of Q^+ (typically 0.03 mM) was found to be particularly effective in controlling EOF and in giving effective separations of complex mixtures of anions. The probable mechanism of the butanol-Q^+ effect is discussed.

1. Introduction

Capillary electrophoresis (CE) has become an efficient technique for separating inorganic and organic anions. Several separations of inorganic and short-chain organic acid anions have been reported using UV detection [1–5]. Conductivity detection has also been used successfully for these separations [6,7].

In conventional CE using a fused-silica capillary, the electroosmotic flow (EOF) is toward the cathode where detection is performed. Anions, however, have electrophoretic mobilities toward the anode. Only anions having mobilities with magnitudes less than that of the EOF are detected with this configuration. Thus, it is necessary to eliminate or reverse the direction of the EOF for most anion separations.

There are several ways to control EOF. These include altering the buffer pH [8–10] or the electrolyte composition by adding surfactants [6,11,12] or organic solvents [10,13,14]. Other methods include coating the inner capillary walls [15–17] or applying an external electric field [18–20]. Several studies of the effects of these parameters on anion separations have been published [21–23].

The most common method used to reverse the EOF for anion separations is to add a quaternary ammonium salt to the electrolyte solution. The positively charged compound is electrostatically attracted to the ionized capillary wall, thus creating a net positive charge on the wall. With the use of a negative power supply, all anions are detected at the anode.

In HPLC, Morris and Fritz [24] found that chromatographic behavior of polar compounds can be dramatically modified by use of a suitable mobile phase additive. A concentration of 4–5% 1-butanol in water was found to be particularly useful. A dynamic equilibrium of butanol exists

* Corresponding author.

0021-9673/94/$07.00
SSDI 0021-9673(93)E1179-4

between the mobile phase and the resin, thus coating the resin with a thin film of butanol.

It was thought that a similar effect was likely to occur in CE. Again, a dynamic equilibrium of butanol is expected between the aqueous electrolyte and the walls of the silica capillary. Several anion separations have been reported which use electrolyte solutions with organic solvent additives [2,22,23]. Most of these studies have been limited to low-molecular-mass solvents such as methanol, ethanol and acetonitrile.

In the present work, it is shown that a combination of low concentrations of a quaternary ammonium salt and 1-butanol added to the electrolyte solution affects anion separations. EOF can be controlled more easily when butanol is present and excellent anion separations are possible.

2. Experimental

The CE system used for all experiments was the Waters Quanta 4000 (Waters Chromatography Division of Millipore, Milford, MA, USA). Fused-silica capillaries (Polymicro Technology, Phoenix, AZ, USA) with lengths of 70 cm and inner diameters of 75 μm were used. At 62.5 cm from the injection end of the capillary, the polyimide coating was burned off to create a detection window.

New capillaries were conditioned by rinsing with 1 *M* NaOH for approximately 1 h, followed by a 15-min rinse with deionized water. A 5-min rinse with NaOH, followed by a 5-min rinse of deionized water was used to wash the capillaries at the start of each day and between runs with different electrolyte solutions.

Electrokinetic sampling was used with a sample voltage of 10 kV for 5 s (unless otherwise specified) or the hydrostatic sampling mode was used with a sampling time of 20 s and height of 10 cm. The capillary was purged with electrolyte solution for 2 min before each run. All separations were carried out at room temperature. The negative or positive power supply was used at 30 kV for each experiment.

On-column indirect UV detection at 254 nm was used for all separations of inorganic and short-chain organic acid anions. The electrolyte solutions for these separations contained 5 m*M* sodium chromate as the visualization reagent. Direct UV detection at 254 nm was used for the separation of the aromatic organic acid anions.

All solutions were prepared using deionized water from a Barnstead Nanopure II system (Sybron Barnstead, Boston, MA, USA). All reagents and solvents used were reagent grade. Stock solutions of the inorganic anions were prepared from their corresponding sodium salts. Stock solutions of the organic acids were prepared from the organic acid and the pH raised to form the anion. The chromate electrolyte solutions were prepared from a stock solution of 100 m*M* sodium chromate (Fisher Scientific, Fair Lawn, NJ, USA). The borate buffer solutions were prepared from a stock solution of 20 m*M* sodium tetraborate decahydrate (Fisher Scientific). A 20 m*M* stock solution of OFM Anion-BT, a proprietary reagent from Waters Chromatography Division of Millipore, identified as $R(CH_3)_3N^+Br^-$, where R is a long-chain alkyl group [25], was used as the quaternary ammonium salt. All alcohols used were obtained from Aldrich (Milwaukee, WI, USA). Adjustments of pH were made with dilute solutions of reagent grade HCl or NaOH.

3. Effect of Q^+ on EOF

Separation of inorganic and short-chain organic acid anions by CE requires the reversal or elimination of EOF. A proprietary reagent developed by Waters, OFM Anion-BT (which will be referred to as Q^+), was used in our work as an EOF modifier. When there is no Q^+ present in a 5 m*M* chromate electrolyte solution and a negative power supply is used, the EOF is strong and toward the cathode. However, as increasing amounts of Q^+ are added to the electrolyte solution, the magnitude of the EOF to the cathode is decreased until its direction is eventually reversed to the anode. As the concentration of Q^+ in the electrolyte solution is increased, the charge on the capillary wall becomes less nega-

tive before obtaining a net positive charge. A dynamic equilibrium is likely to exist between the Q^+ on the surface of the capillary wall and the Q^+ in the electrolyte solution.

Fairly high concentrations of Q^+ (*e.g.* 0.5 m*M*) have been used successfully for several applications [2–5]. However, these concentrations of Q^+ in the electrolyte solution may result in a build-up of Q^+ on the capillary from run to run thus making it necessary to clean the capillary more often. Hydrophobic alkyl ammonium salts, such as Q^+, also have limited solubility and may form insoluble pairs with some electrolyte components [23,26]. Therefore, a lower concentration of Q^+ in the electrolyte solution may be beneficial for the analysis of some samples.

4. Effect of organic solvents on EOF

Buchberger and Haddad [22] studied the effect of up to 30% methanol, acetonitrile, tetrahydrofuran, acetone and ethylene glycol on the migration order of ten different anions. They noted a general increase in migration times owing to: (1) a decrease in conductivity resulting in a lower current, and (2) a decrease in the amount of Q^+ adsorbed on the inner capillary wall, resulting in lower EOF to the anode.

If a low concentration (*e.g.* <0.05 m*M*) of Q^+ is used in the electrolyte solution with a negative power supply, the EOF is still in the opposite direction to the electrophoretic flow of the sample anions. This results in very long migration times.

Addition of alcohols such as methanol, ethanol, 1-propanol, 1-butanol and 1- and 2-pentanol decrease the EOF toward the cathode, thus resulting in faster migration times. However, even high concentrations (*e.g.* 20%) of methanol, ethanol and 1-propanol do not result in satisfactory decreases in migration times. Low concentrations of butanol (3–5%) and pentanol (1–2%) result in significant decreases in migration times. Anions that had migration times of *ca.* 30 min when a low concentration of Q^+ was used as the lone additive to the electrolyte solution showed migration times of *ca.* 3 min when a low concentration of butanol or pentanol was added to the electrolyte solution. Since pentanol had limited solubility in the aqueous electrolyte solution and less controllable effects on the EOF, 1-butanol was chosen as the most promising alcohol to use as an EOF modifier.

5. Effect of 1-butanol on EOF

The effect of 1-butanol on the EOF was studied by measuring the EOF at increasing butanol concentrations. The EOF was measured using a positive power supply, a 5 m*M* chromate electrolyte solution at pH 8.0, and deionized water as the neutral marker. Electrolyte solutions containing greater than 8% butanol were not studied due to solubility limitations of butanol in the aqueous solution. Fig. 1 shows the effect of increasing butanol concentrations on the EOF. The EOF coefficient was calculated from the expression $\mu_{eo} = (LL_d)/(Vt)$, where L = capillary length (cm), L_d = capillary length from injection to detector (cm), V = applied voltage (Vs) and t = time (s). Although butanol does not reverse the EOF, there is a significant decrease in the EOF to the cathode as the concentration of butanol is increased. This effect is due in part to the butanol adsorbing to the capillary surface, thus cancelling the effect of the covered ionized groups on the EOF. It is likely that a dynamic equilibrium is established between the butanol in solution and the butanol on the capillary surface.

6. Effect of Q^+ and butanol on EOF

Since neither a low concentration of Q^+ or butanol alone reversed the EOF, a combination of the two modifiers was investigated. Fig. 2 shows the effect of increasing Q^+ concentrations on the EOF in electrolyte solutions containing 0, 3 or 5% butanol. The EOF direction is reversed at a much lower concentration of Q^+ when butanol is added to the electrolyte solution.

Three possible mechanisms were considered to explain the observed results. (1) Ion interaction

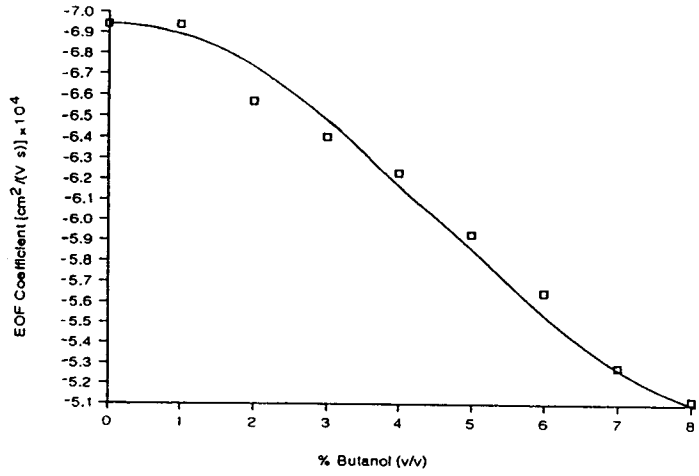

Fig. 1. Variation of EOF coefficient *versus* percentage 1-butanol added to an electrolyte solution of 5 m*M* chromate at pH 8.0. Negative coefficients indicate flow toward the cathode.

between the Q^+ and the analyte anions is unlikely to occur in the solution phase because of the very low concentrations of Q^+ (<0.1 m*M*) being used. Furthermore, the relative migration times of several anions studied were unchanged when the concentration of Q^+ was varied from 0.03 to 0.1 m*M*. (2) Formation of a micelle was ruled out because the concentration of Q^+ in the electrolyte solution was far below the critical micelle concentration [27]. (3) The most plausible mechanism is one in which both butanol and Q^+ are adsorbed on the capillary surface by a dynamic equilibrium. The adsorbed butanol would shift the Q^+ equilibrium so that the surface achieves a net positive charge at a significantly lower Q^+ concentration. This mechanism is supported by the work of Scott and Simpson [28] on the distribution of several solvents including butanol between an aqueous phase and a reversed phase silica surface. They concluded that a dynamic equilibrium exists in which there is a monolayer coating of butanol on the surface.

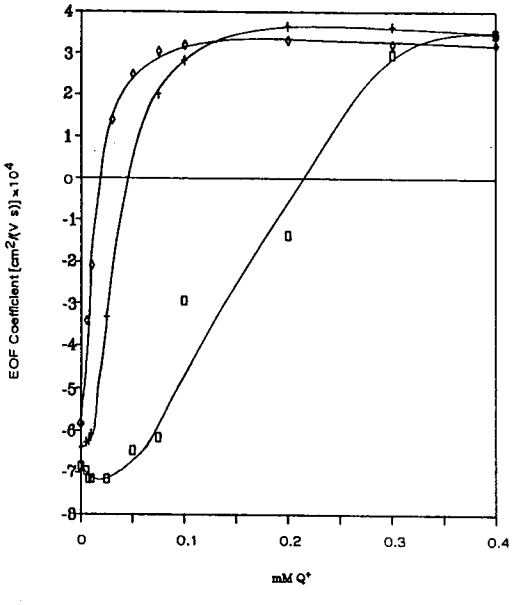

Fig. 2. EOF coefficient as a function of concentration of Q^+ added to electrolyte solutions of 5 m*M* chromate at pH 8.0 containing 0 (□), 3 (+) or 5% (◇) 1-butanol. Negative coefficients indicate flow toward the cathode.

The effect of using low concentrations of both Q^+ and butanol is more impressive when actual CE separations are viewed. Fig. 3A shows an attempted separation of an anion mixture using 0.075 m*M* Q^+ in an aqueous electrolyte solution containing 5 m*M* chromate at pH 8.0. Migration of the anions was so slow that only the first few anions had appeared after an hour. Using the

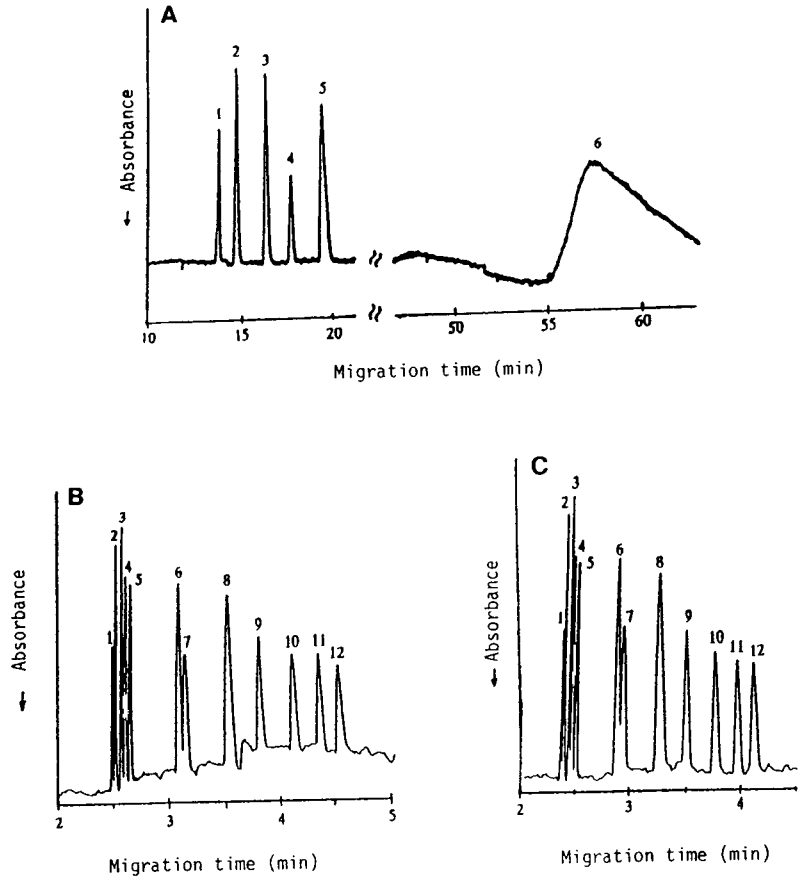

Fig. 3. Separation of inorganic and short-chain organic acid anions using varying concentrations of 1-butanol. Peaks: 1 = Br^- (5 ppm, w/w); 2 = Cl^- (5 ppm); 3 = SO_4^{2-} (6 ppm); 4 = NO_2^- (7 ppm); 5 = NO_3^- (8 ppm); 6 = F^- (8 ppm); 7 = $HCOO^-$ (10 ppm); 8 = CO_3^{2-} (7 ppm); 9 = acetate (10 ppm); 10 = propionate (10 ppm); 11 = butyrate (10 ppm); 12 = valerate (10 ppm). (A) Electrolyte: 5 m*M* chromate, 0.075 m*M* Q^+, pH 8.0; applied voltage: −30 kV, current: 23 μA, electromigration injection 6 s/10 kV. (B) Electrolyte: 5 m*M* chromate, 0.075 m*M* Q^+, 3% 1-butanol, pH 8.0; applied voltage: −30 kV, current: 21 μA, electromigration injection 6 s/10 kV. (C) Electrolyte: 5 m*M* chromate, 0.075 m*M* Q^+, 5% 1-butanol, pH 8.0; applied voltage: −30 kV, current: 21 μA, electromigration injection 10 s/10 kV.

same experimental conditions except for the addition of 3% butanol to the electrolyte solution, an excellent separation (Fig. 3B) was obtained in less than 5 min. The separation (Fig. 3C) observed when 5% butanol was added was even faster.

Several anions were separated using a combination of low concentrations of Q^+ and butanol. A typical separation of some of these anions using 0.03 m*M* Q^+ and 4% butanol is shown in Fig. 4. Without butanol, a much higher concentration of Q^+ was required to obtain a comparable separation.

Several aromatic carboxylic acid anions were separated using conditions similar to those used previously (Fig. 5). Direct UV detection at 254 nm was used for these anions along with a borate buffer solution. Separation of this mixture was also attempted using the positive power supply and a borate buffer solution with no additives. Under these conditions, the EOF was toward the cathode with the electrophoretic mobilities of the

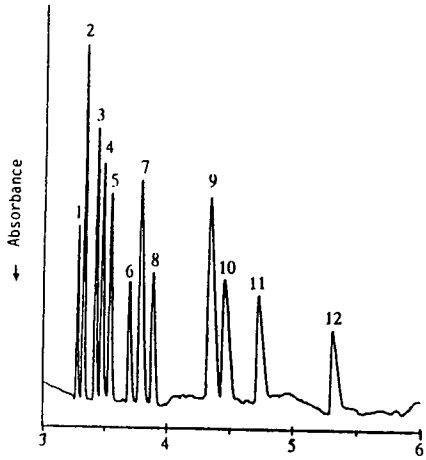

Fig. 4. Separation of inorganic anions. Electrolyte: 5 m*M* chromate, 0.03 m*M* Q^+, 4% 1-butanol, pH 8.0; applied voltage: −30 kV, current: 23 μA, electromigration injection 5 s/10 kV. Peaks: 1 = Br^- (5 ppm); 2 = Cl^- (5 ppm); 3 = SO_4^{2-} (6 ppm); 4 = NO_2^- (7 ppm); 5 = NO_3^- (7 ppm); 6 = MoO_4^{2-} (10 ppm); 7 = N_3^- (10 ppm); 8 = ClO_3^- (8 ppm); 9 = F^- (8 ppm); 10 = $HCOO^-$ (8 ppm); 11 = ClO_2^- (8 ppm); 12 = CO_3^{2-} (7 ppm).

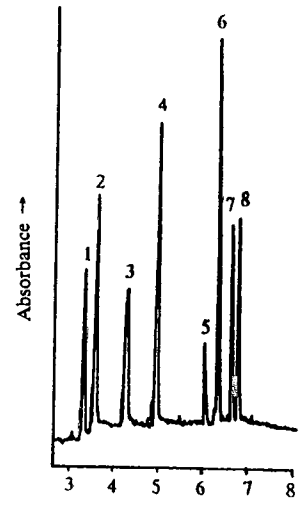

Fig. 5. Separation of aromatic organic acid anions. Electrolyte: 1 m*M* borate, 0.03 m*M* Q^+, 4% 1-butanol, pH 8.5; applied voltage: −30 kV, current: 5.2 μA, hydrostatic injection: 20 s. Peaks: 1 = 1,2,4,5-benzenetetracarboxylate ($5.9 \cdot 10^{-5}$ *M*); 2 = 1,2,4-benzenetricarboxylate ($7.2 \cdot 10^{-5}$ *M*); 3 = 3-nitrophthalate ($7.1 \cdot 10^{-5}$ *M*); 4 = 2,4-dihydroxybenzoate ($6.5 \cdot 10^{-5}$ *M*); 5 = benzoate ($1.2 \cdot 10^{-4}$ *M*); 6 = 4-nitrobenzoate ($4.8 \cdot 10^{-4}$ *M*); 7 = 3,5-diaminobenzoate ($6.6 \cdot 10^{-5}$ *M*); 8 = 1,2-napthoquinone-4-sulfonic acid ($4.2 \cdot 10^{-5}$ *M*).

anions in the opposite direction. The separation was unsuccessful, resulting in poor resolution of the less mobile anions and long migration times for the most mobile anions.

7. Conclusions

The combination of low concentrations of 1-butanol and a quaternary ammonium reagent in aqueous solutions is an excellent way to modify EOF in the CE separation of anions. Coating the capillary surface by a dynamic equilibrium involving butanol and Q^+ is an attractive alternative to other methods that have been proposed for adjusting EOF. Separations using this system are less noisy and more reproducible.

8. Acknowledgements

We wish to thank Waters Chromatography Division of Millipore for their gift of the Waters Quanta 4000 CE instrument and associated chemicals and supplies. We also thank Andrea Weston and Petr Jandik for valuable technical assistance in the initial stages of this research.

Ames Laboratory is operated for the US Department of Energy under Contract No. W-7405-Eng-82. This work was supported by the Director of Energy Research, Office of Basic Energy Sciences.

9. References

[1] P. Jandik and W.R. Jones, *J. Chromatogr.*, 546 (1991) 431.
[2] J. Romano, P. Jandik, W.R. Jones and P.E. Jackson, *J. Chromatogr.*, 546 (1991) 411.
[3] B.F. Kenney, *J. Chromatogr.*, 546 (1991) 423.
[4] W.R. Jones and P. Jandik, *J. Chromatogr.*, 608 (1992) 385.
[5] G. Bondoux, P. Jandik and W.R. Jones, *J. Chromatogr.*, 602 (1992) 79.

[6] X. Huang, J.A. Luckey, M.J. Gordon and R.N. Zare, *Anal. Chem.*, 61 (1989) 766.
[7] N. Avdalovic, C.A. Pohl, R.D. Rocklin and J.R. Stillian, *Anal. Chem.*, 65 (1993) 1470.
[8] W.J. Lambert and D.L. Middleton, *Anal. Chem.*, 62 (1990) 1585.
[9] K.D. Lukacs and J.W. Jorgenson, *J. High Resolut. Chromatogr. Chromatogr. Commun.*, 8 (1985) 407.
[10] C. Schwer and E. Kenndler, *Anal. Chem.*, 63 (1991) 1801.
[11] T. Tsuda, *J. High Resolut. Chromatogr. Chromatogr. Commun.*, 10 (1987) 622.
[12] T. Kaneta, S. Tanaka and H. Yoshida, *J. Chromatogr.*, 538 (1991) 385.
[13] S. Fujiwara and S. Honda, *Anal. Chem.*, 59 (1987) 487.
[14] B.B. VanOrman, G.G. Liversidge, G.L. McIntire, T.M. Olefirowicz and A.G. Ewing, *J. Microcol. Sep.*, 2 (1990) 176.
[15] S. Hjertén, *J. Chromatogr.*, 347 (1985) 191.
[16] J.T. Smith and Z. El Rassi, *Electrophoresis*, 14 (1993) 396.
[17] G.J.M. Bruin, J.P. Chang, R.H. Kuhlman, K. Zegers, J.C. Kraak and H. Poppe, *J. Chromatogr.*, 471 (1989) 429.
[18] C.S. Lee, D. McManigill, C.T. Wu and B. Patel, *Anal. Chem.*, 63 (1991) 1519.
[19] M.A. Hayes and A.G. Ewing, *Anal. Chem.*, 64 (1992) 512.
[20] M.A. Hayes, I. Kheterpal and A.G. Ewing, *Anal. Chem.* 65 (1993) 27.
[21] W.R. Jones and P. Jandik, *J. Chromatogr.*, 546 (1991) 445.
[22] W. Buchberger and P.R. Haddad, *J. Chromatogr.*, 608 (1992) 59.
[23] M.P. Harrold, M.J. Wojtusik, J. Riviello and P. Henson, *J. Chromatogr.*, 640 (1993) 463.
[24] J.B. Morris and J.S. Fritz, unpublished results.
[25] W.R. Jones, P. Jandik and M. Merion, *US Pat.*, 5 104 506 (1992).
[26] E. Jungerman (Editor), *Cationic Surfactants*, Armour-Dial, Chicago, IL, 1969.
[27] P. Mukerjee and K.J. Mysels (Editors), *Critical Micelle Concentrations of Aqueous Surfactant Systems*, National Standard Reference Data Series–National Bureau of Standards 36 (NSRDS-NBS36) United States Dept. of Commerce, Government Printing Office, Washington, DC, 1970.
[28] R.P.W. Scott and C.F. Simpson, *Faraday Symp. Chem. Soc.*, 15 (1980) 69.

ELSEVIER

Journal of Chromatography A, 671 (1994) 445–451

JOURNAL OF CHROMATOGRAPHY A

Determination of inorganic sulfate in detergent products by capillary electrophoresis

James M. Jordan*, R. Laura Moese, R. Johnson-Watts, D. Edward Burton

The Procter and Gamble Company, 6060 Center Hill Avenue, Cincinnati, OH 45224, USA

Abstract

We have been able to show that capillary electrophoresis (CE) can be used for the rapid determination of sulfate in granular detergents. With this method, an aqueous solution of the detergent (5 g/l) is prepared and a small, filtered (0.2 μm) portion is used for the assay. The total analysis time per sample by CE is less than 15 min using duplicate injections, with 2-min washes between each injection. The analytical method and a comparison of results between CE and gravimetric determinations, will be discussed. Sodium sulfate was quantitated by CE and by a $BaCl_2$ gravimetric method using 26 different granular detergents with levels ranging from 2 to 40% Na_2SO_4. A least squares fit of the gravimetric data plotted *versus* the CE data resulted in $r^2 = 0.991$, $m = 0.92 \pm 0.02$ and $b = -0.41 \pm 0.24$ (SEE = 0.864), where m = slope, b = y-intercept, and SEE = standard error of estimate. Day-to-day CE results varied by less than 1.0% Na_2SO_4. Within a given day, results from replicate samples varied typically by less than 0.5% Na_2SO_4. The optimum linear range for this method is between 10 to 100 μg/ml, even though the response is linear up to and beyond 180 μg/ml. Sulfate concentrations above 100 μg/ml result in poor resolution for samples with multiple ions.

1. Introduction

This paper describes the use of a technique for the determination of low-molecular-mass ionic analytes by capillary electrophoresis (CE), using indirect ultraviolet detection. In particular, we have selected an approach developed for the determination of small inorganic anions using an electrolyte composed of chromate and a quaternary amine electroosmotic flow modifier to affect separation, as first reported by Jones and Jandik in 1990 [1,2]. This approach has proven successful especially for the determination of anions in complex samples such as Kraft black liquors in the pulp and paper industry [3], bulk pharmaceuticals and their synthetic intermediates [4] and prenatal vitamin formulations [5].

Since laundry detergents also represent complex mixtures of organic and inorganic components, this same approach was selected for determining sulfate. Laundry detergents typically include surfactants (anionic, cationic, non-ionic and/or amphoteric), organic chelating agents (*i.e.* EDTA), oxidizing agents (*i.e.* sodium perborate), optical brighteners, enzymes, water/solvents and inorganic salts such as sodium carbonate, sulfate, chloride, silicate and borax. The quantitation of sodium sulfate in detergent products can be a long and tedious process using well known gravimetric determinations. The usual approach for quantitating sulfate in detergent products is by a gravimetric method using barium chloride [6,7], which can require 3 to 4 days per sample to complete, depending on how easily the samples can be vacuum filtered.

Although ion chromatography may be consid-

* Corresponding author.

0021-9673/94/$07.00
SSDI 0021-9673(93)E1117-I

ered as an alternative to gravimetric methods, the cost involved in personnel training and instrument maintenance is a serious consideration, and still some preparation is needed for detergent samples. We were interested in determining if CE would provide us a fast and simple means for the rapid quantitation of sulfate, thereby providing a significant improvement in our lab's productivity.

2. Experimental

2.1. Instrumentation

A Quanta 4000 CE system (Waters Chromatography Division of Millipore, Milford, MA, USA) equipped with a 60 cm × 75 μm I.D. fused-silica capillary (Waters AccuSep CE capillary assembly), a Hg lamp with 254-nm filters and negative power supply was employed for all experiments. Data acquisition and processing was performed using a Waters 860 Chromatography Data System on a MicroVax 3100 Computer (Digital Equipment Corp., Maynard, MA, USA). A Waters Laboratory Acquisition and Communications/Environment (LAC/E) module was used to connect the data system and CE instrument over Ethernet and is interfaced with the host computer for data archiving and processing. The LAC/E module receives the analog signal from the CE instrument through a Waters SAT/IN (Satellite Interface) module, which is an A/D converter. The CE instrument detector output is connected directly to the SAT/IN module with inverted signal polarity. The CE detector time constant was set at 0.1 s with a data acquisition rate of 20 Hz. Data collection was initiated by a signal cable connection between the Quanta 4000 and the SAT/IN module.

2.2. Reagents

Sodium chromate tetrahydrate (analytical-reagent grade), Ultrex and reagent-grade sulfuric acid were obtained from J.T. Baker (Phillipsburg, NJ, USA). Sodium sulfate, 99.99 + % pure, sodium hydroxide, potassium hydroxide and barium chloride were obtained from Aldrich (Milwaukee, WI, USA). A bromide standard solution (500 μg/ml) was obtained from HACH Co. (Loveland, CO, USA). Waters CIA-Pak OFM Anion-BT solution was obtained as a 20 m*M* concentrate from the Waters Division of Millipore. Purified water (18 MΩ) was obtained using a Millipore Milli-Q Plus water purification system (Bedford, MA, USA) and this water was used for preparing all solutions.

2.3. Solutions

Electrolyte solutions were prepared daily, filtered using a 0.45-μm Millipore membrane (type HV) disposable syringe filter, and degassed with a Waters solvent clarification kit. Solutions of 100 m*M* KOH were used for pre-conditioning the capillary daily. A chromate electrolyte concentrate was prepared by adding to a 1-l volumetric flask, 500 ml Milli-Q water, 23.41 g sodium chromate tetrahydrate and 68 ml of 10 m*M* sulfuric acid (prepared by diluting 560 μl of concentrated sulfuric acid to 1 l using Milli-Q water). This concentrate may be stored in volumetric or sealed glass container for up to 1 year and will make 20 l of electrolyte. The working electrolyte solution was prepared by diluting 5 ml of the Waters OFM Anion-BT solution [8] and 7 ml of the electrolyte chromate concentrate to 100 ml. This results in a 5 m*M* chromate and 0.5 m*M* OFM electrolyte. The pH of the electrolyte may be adjusted as necessary to pH 8.0 with 100 m*M* NaOH.

Sulfate quantitation was based on external standard calibration. The sulfate standard solutions of 10, 30, 70 and 100 μg/ml were prepared from dilutions of a 4000 μg/ml concentrated standard. Duplicate injections at each level were used to calibrate the system.

The presence of bromide in the electrolyte, which is introduced by the OFM, causes a "dip" in the baseline at the migration time corresponding to bromide [9]. This could potentially interfere with the quantitation of chloride and sulfate so we have used a bromide diluent to eliminate this problem. The bromide standard

solution is used to prepare the diluent for the final dilution step of the samples. The diluent was prepared by diluting 30 ml of the 500 μg/ml standard solution to 1 l. This results in approximately a 15 μg/ml bromide spike in the samples.

The granular detergent samples should be riffled and ground before usage to ensure representative samples are taken. Sample solutions were prepared by dissolving 5 g of a detergent sample in 1 l of Milli-Q water. If the sample was known to have less than 5% sodium sulfate, 300 μl of the 500 μg/ml bromide stock was diluted to 10 ml using the sample solution (5 g/l) as diluent. For samples having more than 5% sodium sulfate, 1.0 ml of the sample solution was diluted to 10 ml using the 15 μg/ml bromide diluent. A small portion of the spiked sample solution was then filtered using a disposable 5 ml syringe and a 0.2-μm Gelman Ion Chromatography Acrodiscs (Ann Arbor, MI, USA) filter before being placed in the sample tray.

2.4. Gravimetric procedure

The gravimetric procedure [7] for determining inorganic sulfate in laundry detergents is basically comprised of four steps: (1) alcohol separation, (2) removal of soluble silicates, (3) precipitation of sulfate with barium chloride and (4) weigh dry precipitate. For the alcohol separation, a 5-g sample of detergent was dissolved in hot ethanol and digested on a steam bath. Then the inorganic fraction was collected by vacuum filtration. This fraction was washed with concentrated hydrochloric acid, followed by evaporation to dryness and was repeated for a total of three iterations. The silicate was then separated by vacuum filtration. The filtrate was then diluted, and an aliquot taken and heated to boiling. At this point barium chloride was added to precipitate the sulfate. The precipitate was then separated by vacuum filtration and dried in a furnace.

2.5. Electrophoretic conditions

Waters capillary ion electrophoresis (Waters' trade name: Capillary Ion Analysis) Method N-601 for general anions was used without modification [10]. The conditions used were 20 kV run voltage, hydrostatic injection at 10 cm height for 30 s, 254 nm detection, 0.1 s time constant, negative detector polarity, ambient temperature, 60 cm × 75 μm I.D. fused-silica capillary and 5 min run time.

3. Results and discussion

Initial work with the CE method involved determination of the linear dynamic range for the quantitation of sulfate using standard solutions. Sulfate concentrations of 4, 10, 20, 30, 40, 50, 60, 70, 80, 90, 100, 120, 140 and 180 μg/ml were run with triplicate injections at each level. A least squares fit of the data through a zero intercept was linear over the entire range with $r^2 = 0.9985$ and $m = 300$. A linear least squares fit with a non-zero intercept returned values of $r^2 = 0.9994$, $m = 292 \pm 2.0$ and $b = 789 \pm 177$ (SEE = 379), where m = slope, b = y-intercept, and SEE = standard error of estimate. The working range was selected to be between 10–100 μg/ml since resolution of the sulfate and chloride peaks begins to seriously deteriorate at levels approaching 100 μg/ml. Typical calibration curves over this range have a correlation coefficient of $r^2 = 0.9994$.

To compare results from CE and gravimetric sulfate determinations, 26 laundry detergent samples with sulfate levels ranging from 2 to 40% were used for both methods. A typical electropherogram for a detergent sample is shown in Fig. 1. In this figure, the bromide spike

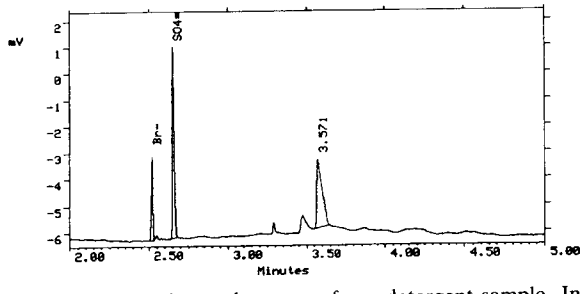

Fig. 1. Typical electropherogram for a detergent sample. In this figure, the bromide spike is readily identified and well separated from the sulfate peak, which represents approximately 20 μg/ml sulfate.

is readily identified and well separated from the sulfate peak, which represents approximately 20 μg/ml sulfate. The CE results for laundry detergent samples are summarized in Table 1. Compact and regular detergents refer to different types of detergent formulations. Typically, absolute day-to-day results varied by less than 0.5% Na_2SO_4 by CE, and by not more than 2.0%. Replicate hydrostatic injections of the same sample typically varied by less than 0.05%. The day-to-day variability for some of these samples can be directly tied to particular detergent formulations for which it was difficult to obtain representative samples. To determine within-day variability, seven detergent samples were run in duplicate and the results are summarized in Table 2. As shown by the data, duplicate samples varied typically by less than 0.5% Na_2SO_4 within a given day.

Gravimetric results are given in Table 3. Since the gravimetric determination is so labor intensive, typically only one sample is ever run for a sulfate determination. Duplicate gravimetric determinations are rarely performed on a daily basis unless some problem with a detergent formulation mass balance is identified. As seen by these results, gravimetric determinations can vary substantially, and this approach is very dependent on the skill of the analyst. Overall, the gravimetric method is very reliable, and results typically vary by less than 1% Na_2SO_4. A correlation plot of the % Na_2SO_4 determined by the CE and gravimetric methods is shown in Fig. 2. A least squares fit of the data results in $r^2 = 0.991$, $m = 0.92 \pm 0.02$ and $b = -0.41 \pm 0.24$ (SEE = 0.864). Examples of differences for several of the samples are given in Table 4 for comparison. As shown by the correlation plot,

Table 1
Summary of CE results for day-to-day determinations of % sodium sulfate in 26 granular detergent products

Description	Day-to-day results, % Na_2SO_4	Average result, % Na_2SO_4	S.D.
Compact granule	2.0, 1.6, 1.7, 1.7	1.7	0.2
Compact granule	1.9, 2.1, 2.1	2.0	0.1
Compact granule	2.2, 2.2, 2.3	2.2	0.1
Compact granule	2.2, 2.2, 2.3	2.3	0.1
Compact granule	2.2, 2.4, 2.3	2.3	0.1
Compact granule	2.1, 2.9, 2.9, 2.5	2.6	0.5
Compact granule	2.6, 3.1, 3.1	2.9	0.3
Compact granule	2.9, 3.3	3.1	0.3
Compact granule	3.2, 3.6, 3.8	3.5	0.3
Compact granule	3.7, 3.8	3.8	0.1
Compact granule	4.0, 5.1, 4.0	4.4	0.6
Compact granule	4.8, 5.0	4.9	0.2
Compact granule	5.6, 4.3	5.3	0.2
Compact granule	5.7, 5.9	5.8	0.1
Compact granule	6.3, 6.3, 6.3	6.3	0.0
Compact granule	6.5, 6.5	6.5	0.0
Compact granule	6.7, 6.9	6.8	0.1
Compact granule	7.5, 7.1	7.3	0.3
Compact granule	8.7, 9.1	8.9	0.3
Compact granule	12.1, 13.1	12.6	0.7
Regular granule	13.5, 12.0, 12.7	12.7	0.8
Regular granule	16.4, 16.4, 16.7, 16.6, 16.2	16.5	0.1
Regular granule	18.7, 19.0	18.9	0.2
Regular granule	20.3, 19.7	20.0	0.4
Regular granule	22.8, 24.7	23.7	1.4
Regular granule	37.3, 36.7	37.0	0.4

Table 2
Summary of duplicate CE results for within-day determinations of % sodium sulfate in seven granular detergent products

Description	Within-day results, % Na_2SO_4	Average, % Na_2SO_4	S.D.
Regular granule	16.43, 16.66	16.55	0.16
Compact granule	5.59, 4.55	5.07	0.74
Compact granule	5.43, 4.82	5.13	0.43
Compact granule	2.07, 2.25	2.16	0.13
Compact granule	2.91, 2.86	2.89	0.04
Compact granule	2.51, 2.60	2.56	0.06
Compact granule	7.21, 7.50	7.36	0.20

Table 3
Summary of gravimetric results for day-to-day determinations of % sodium sulfate in 26 granular detergent products

Description	Day-to-day gravimetric results, % Na_2SO_4	Average, % Na_2SO_4	S.D.
Compact granule	2.6, 1.9	2.2	0.4
Compact granule	2.8, 2.6	2.7	0.2
Compact granule	2.8, 2.6	2.7	0.2
Compact granule	2.9, 2.9	2.9	0.0
Compact granule	1.9, 2.8	2.3	0.6
Compact granule	4.3, 3.1	3.7	0.8
Compact granule	3.9, 3.3	3.6	0.4
Compact granule	3.3, 3.5	3.4	0.1
Compact granule	4.3, 2.6	3.5	1.2
Compact granule	5.1, 1.4	3.2	2.6
Compact granule	5.9, 5.8	5.9	0.1
Compact granule	5.1, 4.9, 1.8, 4.9, 5.5, 5.5	4.6	1.4
Compact granule	7.1, 6.2	6.7	0.6
Compact granule	7.9, 7.5, 6.8, 7.6	7.4	0.4
Compact granule	8.3, 8.8	8.6	0.4
Compact granule	8.2, 8.5	8.3	0.2
Compact granule	8.8, 8.0	8.4	0.6
Compact granule	8.3, 9.3	8.8	0.7
Compact granule	9.5, 9.5	9.5	0.0
Regular granule	13.9	13.9	
Regular granule	15.6, 15.6	15.6	0.0
Regular granule	16.9, 17.2, 17.3, 16.3, 18.1, 17.8, 16.8	17.2	0.6
Regular granule	22.1	22.1	
Regular granule	23.5, 23.5	23.5	0.0
Regular granule	24.0, 23.6	23.8	0.3
Regular granule	40.4	40.4	

CE results tend to be slightly lower than gravimetric results. The absolute difference between CE and gravimetric results ranged from 0 to 3.5% Na_2SO_4, and typically varied by 1.0% or less. This small difference was judged to be insignificant for our purposes.

4. Conclusions

CE provides an easier and accurate means for quantitating sulfate in detergent products with equivalent results to the gravimetric procedure. The major advantages of CE are speed, simplici-

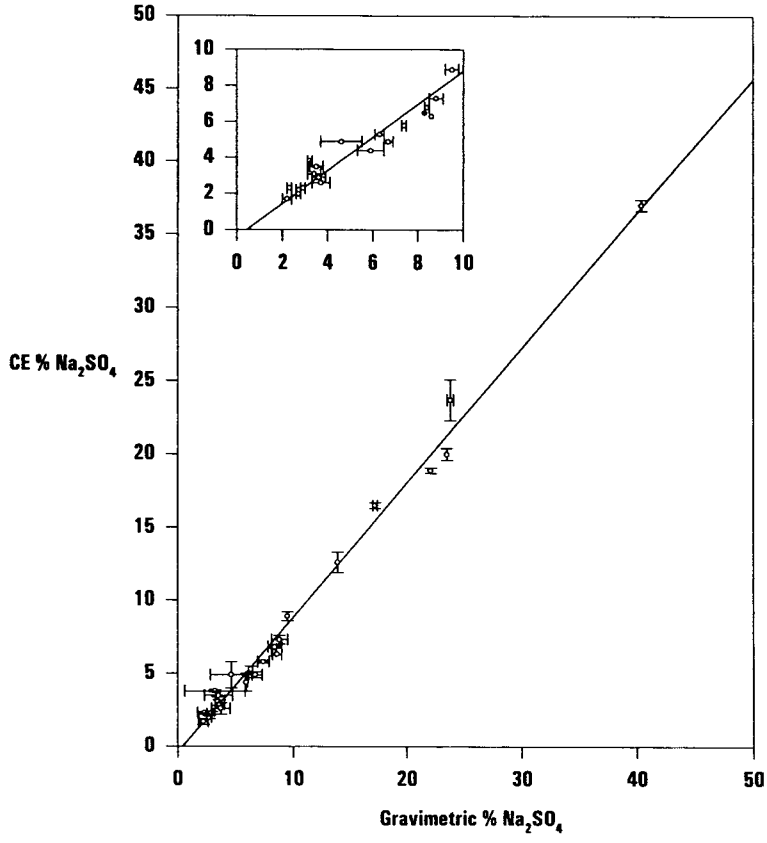

Fig. 2. Correlation plot for sulfate determinations by CE and gravimetric methods. A least squares fit of the data results in $r^2 = 0.991$, $m = 0.92 \pm 0.02$ and $b = -0.41 \pm 0.24$ (SEE = 0.864).

Table 4
Summary of CE and gravimetric results for the determination of Na_2SO_4 in seven different granular detergents and the calculated difference between methods

Sample	Gravimetric results, % Na_2SO_4			CE results, % Na_2SO_4			Difference (gravimetric − CE), % Na_2SO_4
	$\bar{x}$	S.D.	n	$\bar{x}$	S.D.	n	
Regular granule	17.2	0.2	7	16.5	0.1	4	0.7
Compact granule	4.6	1.4	6	4.5	1.0	3	0.1
Compact granule	7.4	0.5	4	5.8	0.1	2	1.6
Compact granule	9.5	0.0	2	8.9	0.3	2	0.6
Compact granule	3.2	2.6	2	3.8	0.1	2	−0.6
Compact granule	8.4	0.6	2	6.8	0.1	2	1.6

ty, significant time savings and minimal consumption of reagents. Because of the simplicity and speed of the CE method, duplicate samples can be easily run to check results or to get quick answers. An added benefit not discussed in the text of the paper is the potential to quantitate sulfate and chloride simultaneously by CE. Other anions such as sulfite, nitrate, orthophosphate and carbonate can also be identified in the same run, and in some cases quantitated.

5. References

[1] W.R. Jones and P. Jandik, *Am. Lab*, 22(9) (1990) 51.
[2] W.R. Jones and P. Jandik, M. Merion and A. Weston, *US Pat.*, 5 128 005 (1992).
[3] D.R. Salomon and J. Romano, *J. Chromatogr.*, 602 (1992) 219.
[4] J.B. Nair and C.G. Izzo, *J. Chromatogr.*, 640 (1993) 445.
[5] M.E. Swartz, *J. Chromatogr.*, 640 (1993) 441.
[6] B.M. Milwidsky and D.M. Gabriel, *Detergent Analysis, A Handbook for Cost-effective Quality Control*, Halsted Press, Division of Wiley, New York, 1982.
[7] W.W. Scott and N.H. Furman (Editor), *Standard Methods of Chemical Analysis*, Van Nostrand, Princeton, NJ, 1958.
[8] W.R. Jones, P. Jandik and M. Merion, *US Pat.*, 5 104 506 (1992).
[9] M.P. Harrold, M.J. Wojtusik, J. Riviello and P. Henson, *J. Chromatogr.*, 640 (1993) 463.
[10] A.L. Heckenberg, P.G. Alden, B.J. Krol, J.P. Romano, P.E. Jackson, P. Jandik and W.R. Jones, *Waters Innovative Methods for Ion Analysis, Manual No. 22340*, Waters Division of Millipore, Milford, MA, Rev. 1.0, 1989.

Author Index

Vol. 671, Nos. 1 + 2

Journal of Chromatography A

NEWS SECTION

INTERNATIONAL ION CHROMATOGRAPHY SYMPOSIUM 1993, BALTIMORE, MD, SEPTEMBER 12–15, 1993

Fig. 1. Scientific Committee: front row (from left to right), Paul Haddad, University of Tasmania; Richard Cassidy, University of Saskatchewan; Hamish Small, HSR; James Fritz, Iowa State University; back row (from left to right), Corrado Sarzanini, University of Turin; John Stillian, Dionex Corp.; John Lamb, Brigham Young University; Donald Pietrzyk, University of Iowa; Gabriella Schmuckler, Israel Institute of Technology; Douglas Gjerde, Sarasep Inc.; William Jones, Waters Chromatography; Wolfgang Buchberger, Johannes Keppler University.

Fig. 2. Richard Cassidy (right), Program Chairman, congratulates IC Award Winner Dan Lee (left) of Hamilton Company.

Directory of Capillary Electrophoresis

(TrAC Supplement No. 1)

©1994 Paperback 156 pages Price:Dfl.137.00(US$ 70.00)

detail from page 33

423 27 7784
ctrophoresis
nucleotides, nucle-

general instrumenta-

nosis; DNA sequenc-

Karger Barry L., Professor
Northeastern University
Barnett Institute
341 Mugar Hall
360 Huntington Avenue
Boston, MA 02115
USA
Tel: 617 437 2867; Fax: 617 437 2855
Techniques: isotachophoresis, capillary zone el
trophoresis, capillary gel electrophoresis,

- **Containing over 450 V.I.P.s Worldwide**
- **Including Complete Addresses, Fax and Phone Numbers, and E-Mail Addresses (where available)**
- **Giving Techniques, Applications and Research Topics**
- **Providing an Extensive Subject Index**

This directory of researchers in capillary electrophoresis not only contains the names and addresses of most leading scientists in this rapidly developing field. The papers in this area that each listed scientist considers as his or her most significant contribution are given. A geographical index with techniques and application areas shows who is doing what in each country. Instrument manufacturers and suppliers are also listed on a country by country basis, along with the products or services they offer.

The editors have endeavoured to collect together, in this one source, information on who's who and the major research trends in the field of capillary electrophoresis.

detail from page 82

	Isotachophoresis	Capillary zone electr	Capillary gel electro	Electrokinetic capill	Capillary isoelectric	Proteins/peptides, a	Pharmaceuticals/dr	Nucleic acids, nucle	
Germany (cont'd)									
Engelhardt Heinz, Professor	☐	■	☐	■	☐	■	■	☐	I
Frey Rolf W.	■	■	☐	■	■	■	■	■	I
Gaus Hans-Joachim	☐	■	☐	■	☐	■	■	■	[
Gilges Martin	☐	■	☐	☐	☐	■	☐	☐	[
Grune Tilman, Dr.	☐	■	☐	☐	☐	☐	☐	■	[
Hebenbrock Kirstin A., Dr.	☐	☐	■	☐	☐	■	☐	■	[
Heiger David, Dr.	☐	■	■	■	☐	■	■	■	[
Karger Achim E., Dr.	☐	☐	■	■	☐	☐	■	■	[
Kleiböhmer Wolfgang, Dr.	☐	■	☐	■	☐	☐	☐	☐	I
Lucas Kurt, Dr.	■	■	■	■	■	■	■	■	[

ORDER FORM

Please send this form to your regular supplier or to:

Elsevier Science B.V.
Attn. Eugene P.M. Wijnhoven
P.O. Box 330, 1000 AH Amsterdam The Netherlands
Fax: +31 (20) 586 2845

☐ **Yes,** Please send me a copy of **Directory of Capillary Electrophoresis**

☐ Please charge my credit card:
☐ Eurocard ☐ Mastercard ☐ American Express ☐ VISA ☐ Access

Card number: _____ Expiry Date: _____

Vat registration number: _____ Signature: _____

Name: _____

Address: _____

US$ prices are valid only for the USA & Canada and are subject to exchange rate fluctuations; in all other countries the Dutch guilder price (Dfl.) is definitive. Customers in the European Union should add the appropriate VAT rate applicable in their country to the price(s). Books are sent postfree if prepaid.

PUBLICATION SCHEDULE FOR THE 1994 SUBSCRIPTION

Journal of Chromatography A and *Journal of Chromatography B: Biomedical Applications*

MONTH	1993	J	F	M	A	M	J	
Journal of Chromatography A	652–657	658/1 658/2 659/1 659/2	660/1 + 2 661/1 + 2 662/1 662/2	663/1 663/2 664/1	664/2 665/1 665/2 666/1 + 2 667/1 + 2	668/1 668/2 669/1 + 2	670/1 + 2 671/1 + 2 672/1	The publication schedule for further issues will be published later.
Bibliography Section				681/1			681/2	
Journal of Chromatography B: Biomedical Applications		652/1	652/2 653/1	653/2 654/1	654/2 655/1	655/2	656/1 656/2	

INFORMATION FOR AUTHORS

(Detailed *Instructions to Authors* were published in *J. Chromatogr. A*, Vol. 657, pp. 463–469. A free reprint can be obtained by application to the publisher, Elsevier Science B.V., P.O. Box 330, 1000 AH Amsterdam, Netherlands.)

Types of Contributions. The following types of papers are published: Regular research papers (full-length papers), Review articles, Short Communications and Discussions. Short Communications are usually descriptions of short investigations, or they can report minor technical improvements of previously published procedures; they reflect the same quality of research as full-length papers, but should preferably not exceed five printed pages. Discussions (one or two pages) should explain, amplify, correct or otherwise comment substantively upon an article recently published in the journal. For Review articles, see inside front cover under Submission of Papers.

Submission. Every paper must be accompanied by a letter from the senior author, stating that he/she is submitting the paper for publication in the *Journal of Chromatography A* or *B*.

Manuscripts. Manuscripts should be typed in **double spacing** on consecutively numbered pages of uniform size. The manuscript should be preceded by a sheet of manuscript paper carrying the title of the paper and the name and full postal address of the person to whom the proofs are to be sent. As a rule, papers should be divided into sections, headed by a caption (*e.g.*, Abstract, Introduction, Experimental, Results, Discussion, etc.) All illustrations, photographs, tables, etc., should be on separate sheets.

Abstract. All articles should have an abstract of 50–100 words which clearly and briefly indicates what is new, different and significant. No references should be given.

Introduction. Every paper must have a concise introduction mentioning what has been done before on the topic described, and stating clearly what is new in the paper now submitted.

Experimental conditions should preferably be given on a *separate* sheet, headed "Conditions". These conditions will, if appropriate, be printed in a block, directly following the heading "Experimental".

Illustrations. The figures should be submitted in a form suitable for reproduction, drawn in Indian ink on drawing or tracing paper. Each illustration should have a caption, all the *captions* being typed (with double spacing) together on a *separate sheet*. If structures are given in the text, the original drawings should be provided. Coloured illustrations are reproduced at the author's expense, the cost being determined by the number of pages and by the number of colours needed. The written permission of the author and publisher must be obtained for the use of any figure already published. Its source must be indicated in the legend.

References. References should be numbered in the order in which they are cited in the text, and listed in numerical sequence on a separate sheet at the end of the article. Please check a recent issue for the layout of the reference list. Abbreviations for the titles of journals should follow the system used by *Chemical Abstracts*. Articles not yet published should be given as "in press" (journal should be specified), "submitted for publication" (journal should be specified), "in preparation" or "personal communication".

Vols. 1–651 of the *Journal of Chromatography*; *Journal of Chromatography, Biomedical Applications* and *Journal of Chromatography, Symposium Volumes* should be cited as *J. Chromatogr.* From Vol. 652 on, *Journal of Chromatography A* (incl. Symposium Volumes) should be cited as *J. Chromatogr. A* and *Journal of Chromatography B: Biomedical Applications* as *J. Chromatogr. B.*

Dispatch. Before sending the manuscript to the Editor please check that the envelope contains four copies of the paper complete with references, captions and figures. One of the sets of figures must be the originals suitable for direct reproduction. Please also ensure that permission to publish has been obtained from your institute.

Proofs. One set of proofs will be sent to the author to be carefully checked for printer's errors. Corrections must be restricted to instances in which the proof is at variance with the manuscript.

Reprints. Fifty reprints will be supplied free of charge. Additional reprints can be ordered by the authors. An order form containing price quotations will be sent to the authors together with the proofs of their article.

SIMPLY POWERFUL

Introducing the New DX 500 Ion Chromatography Systems

Whether you're exploring new methods or facing a backlog of routine samples, the DX 500 meets all your IC application requirements.

It's that simple.

Compact, interlocking modules make it easy to configure exactly the DX 500 system you want. And whichever modules you select, uniform front panels put control at your fingertips for fast, accurate set-up and operation.

As for performance, no-compromise, precise, pulseless pumps help you achieve ideal gradient and isocratic flow. State-of-the-art conductivity, electrochemical, and optical detectors provide the ultimate in detection limits.

Even full PC-based system control is straightforward. Built-in PC-to-module communications create a unified environment for high-speed digital data transfer, real-time monitoring, and intuitive system control. Powerful PeakNet™ workstations simplify networking and automation with trouble-free software that has *true* Windows™ look, feel, and behavior.

And the entire DX 500 system—from sample injection to data management—comes with the Dionex Customer Satisfaction Guarantee. A of which makes choosing the right IC syste for your application much simpler.

For a free brochure on the DX 500 IC Sys call **1-800-723-1161** today. (Outside the U.S., contact your local Dionex sales representati

DIONEX

BETTER SEPARATIONS
THROUGH BETTER CHEMISTRY

Dionex Corporation, P.O. Box 3603, Sunnyvale, CA 94088-3603 (408) 737-0700 **Belgium**, Dionex N.V., (015) 203800 **Canada**, Dionex Canada Ltd., (416) 855-2551 **France**, Dionex S.A., (1) 39 46 08 40
Germany, Dionex GmbH, (06126) 991-0 **Italy**, Dionex S.r.l., (06) 30895454 **Japan**, Nippon Dionex K.K., (06) 885-1213 **The Netherlands**, Dionex B.V., (076) 714800 **United Kingdom**, Dionex (UK) Ltd., (0276) 691722